Scientific and Technical Aerospace Reports

Volume 37
December 6, 1999

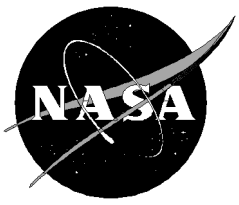

National Aeronautics and Space Administration
Langley Research Center

Scientific and Technical Information Program Office

The NASA STI Program Office . . . in Profile

Since its founding, NASA has been dedicated to the advancement of aeronautics and space science. The NASA Scientific and Technical Information (STI) Program Office plays a key part in helping NASA maintain this important role.

The NASA STI Program Office is operated by Langley Research Center, the lead center for NASA's scientific and technical information. The NASA STI Program Office provides access to the NASA STI Database, the largest collection of aeronautical and space science STI in the world. The Program Office is also NASA's institutional mechanism for disseminating the results of its research and development activities. These results are published by NASA in the NASA STI Report Series, which includes the following report types:

- TECHNICAL PUBLICATION. Reports of completed research or a major significant phase of research that present the results of NASA programs and include extensive data or theoretical analysis. Includes compilations of significant scientific and technical data and information deemed to be of continuing reference value. NASA's counterpart of peer-reviewed formal professional papers but has less stringent limitations on manuscript length and extent of graphic presentations.

- TECHNICAL MEMORANDUM. Scientific and technical findings that are preliminary or of specialized interest, e.g., quick release reports, working papers, and bibliographies that contain minimal annotation. Does not contain extensive analysis.

- CONTRACTOR REPORT. Scientific and technical findings by NASA-sponsored contractors and grantees.

- CONFERENCE PUBLICATION. Collected papers from scientific and technical conferences, symposia, seminars, or other meetings sponsored or cosponsored by NASA.

- SPECIAL PUBLICATION. Scientific, technical, or historical information from NASA programs, projects, and missions, often concerned with subjects having substantial public interest.

- TECHNICAL TRANSLATION. English-language translations of foreign scientific and technical material pertinent to NASA's mission.

Specialized services that complement the STI Program Office's diverse offerings include creating custom thesauri, building customized databases, organizing and publishing research results . . . even providing videos.

For more information about the NASA STI Program Office, see the following:

- Access the NASA STI Program Home Page at ***http://www.sti.nasa.gov***

- E-mail your question via the Internet to help@sti.nasa.gov

- Fax your question to the NASA STI Help Desk at (301) 621-0134

- Telephone the NASA STI Help Desk at (301) 621-0390

- Write to:
  NASA STI Help Desk
  NASA Center for AeroSpace Information
  7121 Standard Drive
  Hanover, MD 21076-1320

Introduction

Scientific and Technical Aerospace Reports (STAR) is an electronic abstract journal, listing citations with abstracts for aerospace-related reports obtained from worldwide sources. It is electronically published biweekly and announces documents that have recently been entered into the NASA Scientific and Technical Information (STI) Database. The documents are of the following types:

- NASA, NASA contractor, and NASA grantee reports;
- Reports issued by other U.S. Government agencies, domestic and foreign institutions, universities, and private firms;
- Translations in report form;
- NASA-owned patents and patent applications
- Other U.S. Government agency and foreign patents and patent applications
- Domestic and foreign dissertations and theses.

Also included are two indexes, Subject Term and Personal Author. The Subject Term Index is generated from the *NASA Thesaurus* terms associated and listed with each document.

STAR subject coverage includes all aspects of aeronautics and space research and development, supporting basic and applied research, and applications. Aerospace aspects of Earth resources, energy development, conservation, oceanography, environmental protection, urban transportation, and other topics of high national priority are also covered.

Abstracts in *STAR* are categorized by 10 major subject divisions that are divided further into 76 specific subject categories. The subject divisions and categories are listed in the Table of Contents together with a note for each that defines its scope and provides any cross-references.

SCAN Goes Electronic!

If you have electronic mail or if you can access the Internet, you can view biweekly issues of *SCAN* from your desktop absolutely free!

Electronic SCAN takes advantage of computer technology to inform you of the latest worldwide, aerospace-related, scientific and technical information that has been published.

No more waiting while the paper copy is printed and mailed to you. You can view *Electronic SCAN* the same day it is released—up to 191 topics to browse at your leisure. When you locate a publication of interest, you can print the announcement. You can also go back to the *Electronic SCAN* home page and follow the ordering instructions to quickly receive the full document.

Start your access to *Electronic SCAN* today. Over 1,000 announcements of new reports, books, conference proceedings, journal articles...and more—available to your computer every two weeks.

Timely
Flexible
Complete
FREE!

For Internet access to *E-SCAN*, use any of the following addresses:

http://www.sti.nasa.gov
ftp.sti.nasa.gov
gopher.sti.nasa.gov

To receive a free subscription, send e-mail for complete information about the service first. Enter **scan@sti.nasa.gov** on the address line. Leave the subject and message areas blank and send. You will receive a reply in minutes.

Then simply determine the SCAN topics you wish to receive and send a second e-mail to **listserv@sti.nasa.gov**. Leave the subject line blank and enter a subscribe command, denoting which topic you want and your name in the message area, formatted as follows:

Subscribe SCAN–02–01 Jane Doe

For additional information, e-mail a message to **help@sti.nasa.gov**.

Phone: (301) 621-0390

Fax: (301) 621-0134

Write: NASA STI Help Desk
NASA Center for AeroSpace Information
7121 Standard Drive
Hanover, MD 21076-1320

Looking just for *Aerospace Medicine and Biology* reports?

Although hard copy distribution has been discontinued, you can still receive these vital announcements through your *E-SCAN* subscription. Just **Subscribe SCAN-AEROMED Jane Doe** in the message area of your e-mail to **listserv@sti.nasa.gov**.

Table of Contents

Subject Divisions

Document citations are grouped first by the following divisions. Select a division title to view the category-level Table of Contents.

A. Aeronautics
B. Astronautics
C. Chemistry and Materials
D. Engineering
E. Geosciences
F. Life Sciences
G. Mathematical and Computer Sciences
H. Physics
I. Social Sciences
J. Space Sciences
K. General

Indexes

Two indexes are available. You may use the find command under the tools menu while viewing the PDF file for direct match searching on any text string. You may also select either of the two indexes provided for searching on *NASA Thesaurus* subject terms and personal author names.

Subject Term Index
Personal Author Index

Document Availability

Select **Availability Info** for important information about NASA Scientific and Technical Information (STI) Program Office products and services, including registration with the NASA Center for AeroSpace Information (CASI) for access to the NASA CASI TRS (Technical Report Server), and availability and pricing information for cited documents.

Subject Categories of the Division A. Aeronautics

Select a category to view the collection of records cited. N.A. means no abstracts in that category.

01 Aeronautics (General) 1

02 Aerodynamics 1

Includes aerodynamics of bodies, combinations, wings, rotors, and control surfaces; and internal flow in ducts and turbomachinery. For related information, see also *34 Fluid Mechanics and Heat Transfer.*

03 Air Transportation and Safety 2

Includes passenger and cargo air transport operations; and aircraft accidents. For related information, see also *16 Space Transportation* and *85 Urban Technology and Transportation.*

04 Aircraft Communications and Navigation 7

Includes digital and voice communication with aircraft; air navigation systems (satellite and ground based); and air traffic control. For related information, see also *17 Space Communications, Spacecraft Communications, Command and Tracking* and *32 Communications Radar.*

05 Aircraft Design, Testing and Performance 10

Includes aircraft simulation technology. For related information, see also *18 Spacecraft Design, Testing and Performance* and *39 Structural Mechanics*. For land transportation vehicles, see *85 Urban Technology and Transportation*.

06 Aircraft Instrumentation 12

Includes cockpit and cabin display devices; and flight instruments. For related information, see also *19 Spacecraft Instrumentation* and *35 Instrumentation and Photography.*

07 Aircraft Propulsion and Power 13

Includes prime propulsion systems and systems components, e.g., gas turbine engines and compressors; and onboard auxiliary power plants for aircraft. For related information, see also *20 Spacecraft Propulsion and Power*, *28 Propellants and Fuels*, and *44 Energy Production and Conversion*.

08 Aircraft Stability and Control 21

Includes aircraft handling qualities; piloting; flight controls; and autopilots. For related information, see also *05 Aircraft Design, Testing and Performance*.

09 Research and Support Facilities (Air) 22

Includes airports, hangars and runways; aircraft repair and overhaul facilities; wind tunnels; shock tubes; and aircraft engine test stands. For related information, see also *14 Ground Support Systems and Facilities (Space).*

Subject Categories of the Division B. Astronautics

Select a category to view the collection of records cited. N.A. means no abstracts in that category.

12 Astronautics (General) 26

For extraterrestrial exploration, see *91 Lunar and Planetary Exploration*.

13 Astrodynamics N.A.

Includes powered and free-flight trajectories; and orbital and launching dynamics.

14 Ground Support Systems and Facilities (Space) 28

Includes launch complexes, research and production facilities; ground support equipment, e.g., mobile transporters; and simulators. *For related information, see also 09 Research and Support Facilities (Air).*

15 Launch Vehicles and Space Vehicles 28

Includes boosters; operating problems of launch/space vehicle systems; and reusable vehicles. For related information, see also *20 Spacecraft Propulsion and Power.*

16 Space Transportation 30

Includes passenger and cargo space transportation, e.g., shuttle operations; and space rescue techniques. For related information, see also *03 Air Transportation and Safety* and *18 Spacecraft Design, Testing and Performance*. For space suits, see *54 Man/System Technology and Life Support*.

17 Space Communications, Spacecraft Communications, Command and Tracking N.A.

Includes telemetry; space communication networks; astronavigation and guidance; and radio blackout. For related information, see also *04 Aircraft Communications and Navigation* and *32 Communications and Radar.*

18 Spacecraft Design, Testing and Performance 31

Includes satellites; space platforms; space stations; spacecraft systems and components such as thermal and environmental controls; and attitude controls. For life support systems, see *54 Man/System Technology and Life Support*. For related information, see also *05 Aircraft Design, Testing and Performance*, *39 Structural Mechanics, and 16 Space Transportation*.

19 Spacecraft Instrumentation 35

For related information, see also *06 Aircraft Instrumentation* and *35 Instrumentation and Photography.*

20 Spacecraft Propulsion and Power 37

Includes main propulsion systems and components, e.g., rocket engines; and spacecraft auxiliary power sources. For related information, see also *07 Aircraft Propulsion and Power*, *28 Propellants and Fuels*, *44 Energy Production and Conversion*, and *15 Launch Vehicles and Space Vehicles*.

Subject Categories of the Division C. Chemistry and Materials

Select a category to view the collection of records cited. N.A. means no abstracts in that category.

23 Chemistry and Materials (General) 43

24 Composite Materials 44

Includes physical, chemical, and mechanical properties of laminates and other composite materials. For ceramic materials see *27 Nonmetallic Materials*.

25 Inorganic and Physical Chemistry 47

Includes chemical analysis, e.g., chromatography; combustion theory; electrochemistry; and photochemistry. For related information see also *77 Thermodynamics and Statistical Physics*.

26 Metallic Materials 53

Includes physical, chemical, and mechanical properties of metals, e.g., corrosion; and metallurgy.

27 Nonmetallic Materials 56

Includes physical, chemical, and mechanical properties of plastics, elastomers, lubricants, polymers, textiles, adhesives, and ceramic materials. For composite materials see *24 Composite Materials.*

28 Propellants and Fuels 60

Includes rocket propellants, igniters and oxidizers; their storage and handling procedures; and aircraft fuels. For related information see also *07 Aircraft Propulsion and Power, 20 Spacecraft Propulsion and Power*, and *44 Energy Production and Conversion*.

29 Materials Processing 68

Includes space-based development of products and processes for commercial application. For biological materials see *55 Space Biology.*

Subject Categories of the Division D. Engineering

Select a category to view the collection of records cited. N.A. means no abstracts in that category.

31 Engineering (General) 70

Includes vacuum technology; control engineering; display engineering; cryogenics; and fire prevention.

32 Communications and Radar 72

Includes radar; land and global communications; communications theory; and optical communications. For related information see also *04 Aircraft Communications and Navigation* and *17 Space Communications, Spacecraft Communications, Command and Tracking*. For search and rescue see 03 Air Transportation and Safety, and *16 Space Transportation*.

33 Electronics and Electrical Engineering 80

Includes test equipment and maintainability; components, e.g., tunnel diodes and transistors; microminiaturization; and integrated circuitry. For related information see also *60 Computer Operations and Hardware* and *76 Solid-State Physics*.

34 Fluid Mechanics and Heat Transfer 85

Includes boundary layers; hydrodynamics; fluidics; mass transfer and ablation cooling. For related information see also *02 Aerodynamics* and *77 Thermodynamics and Statistical Physics.*

35 Instrumentation and Photography 91

Includes remote sensors; measuring instruments and gauges; detectors; cameras and photographic supplies; and holography. For aerial photography see *43 Earth Resources and Remote Sensing*. For related information see also *06 Aircraft Instrumentation* and *19 Spacecraft Instrumentation*.

36 Lasers and Masers 97

Includes parametric amplifiers. For related information see also *76 Solid-State Physics*.

37 Mechanical Engineering 97

Includes auxiliary systems (nonpower); machine elements and processes; and mechanical equipment.

38 Quality Assurance and Reliability 100

Includes product sampling procedures and techniques; and quality control.

39 Structural Mechanics 101

Includes structural element design and weight analysis; fatigue; and thermal stress. For applications see *05 Aircraft Design, Testing and Performance* and *18 Spacecraft Design, Testing and Performance*.

Subject Categories of the Division E. Geosciences

Select a category to view the collection of records cited. N.A. means no abstracts in that category.

42 Geosciences (General) 104

43 Earth Resources and Remote Sensing 106

Includes remote sensing of earth resources by aircraft and spacecraft; photogrammetry; and aerial photography. For instrumentation see *35 Instrumentation and Photography.*

44 Energy Production and Conversion 113

Includes specific energy conversion systems, e.g., fuel cells; global sources of energy; geophysical conversion; and windpower. For related information see also *07 Aircraft Propulsion and Power*, *20 Spacecraft Propulsion and Power*, and *28 Propellants and Fuels*.

45 Environment Pollution 115

Includes atmospheric, noise, thermal, and water pollution.

46 Geophysics 129

Includes aeronomy; upper and lower atmosphere studies; ionospheric and magnetospheric physics; and geomagnetism. For space radiation see *93 Space Radiation*.

47 Meteorology and Climatology 151

Includes weather forecasting and modification.

48 Oceanography 214

Includes biological, dynamic, and physical oceanography; and marine resources. For related information see also *43 Earth Resources and Remote Sensing*.

Subject Categories of the Division F. Life Sciences

Select a category to view the collection of records cited. N.A. means no abstracts in that category.

51 Life Sciences (General) 216

52 Aerospace Medicine 218

Includes physiological factors; biological effects of radiation; and effects of weightlessness on man and animals.

53 Behavioral Sciences 224

Includes psychological factors; individual and group behavior; crew training and evaluation; and psychiatric research.

54 Man/System Technology and Life Support 225

Includes human engineering; biotechnology; and space suits and protective clothing. For related information see also *16 Space Transportation.*

55 Space Biology N.A.

Includes exobiology; planetary biology; and extraterrestrial life.

Subject Categories of the Division G. Mathematical and Computer Sciences

Select a category to view the collection of records cited. N.A. means no abstracts in that category.

59 Mathematical and Computer Sciences (General) 226

60 Computer Operations and Hardware 229

Includes hardware for computer graphics, firmware, and data processing. For components see *33 Electronics and Electrical Engineering*.

61 Computer Programming and Software 230

Includes computer programs, routines, algorithms, and specific applications, e.g., CAD/CAM.

62 Computer Systems 237

Includes computer networks and special application computer systems.

63 Cybernetics 238

Includes feedback and control theory, artificial intelligence, robotics and expert systems. For related information see also *54 Man/System Technology and Life Support.*

64 Numerical Analysis 240

Includes iteration, difference equations, and numerical approximation.

65 Statistics and Probability 241

Includes data sampling and smoothing; Monte Carlo method; and stochastic processes.

66 Systems Analysis 242

Includes mathematical modeling; network analysis; and operations research.

67 Theoretical Mathematics 242

Includes topology and number theory.

Subject Categories of the Division H. Physics

Select a category to view the collection of records cited. N.A. means no abstracts in that category.

70 Physics (General) 243

For precision time and time interval (PTTI) see *35 Instrumentation and Photography;* for geophysics, astrophysics or solar physics see *46 Geophysics, 90 Astrophysics,* or *92 Solar Physics*.

71 Acoustics 244

Includes sound generation, transmission, and attenuation. For noise pollution see *45 Environment Pollution.*

72 Atomic and Molecular Physics 249

Includes atomic structure, electron properties, and molecular spectra.

73 Nuclear and High-Energy Physics 257

Includes elementary and nuclear particles; and reactor theory. For space radiation see *93 Space Radiation.*

74 Optics 258

Includes light phenomena and optical devices. For lasers see *36 Lasers and Masers*.

75 Plasma Physics 262

Includes magnetohydrodynamics and plasma fusion. For ionospheric plasmas see *46 Geophysics.* For space plasmas see *90 Astrophysics*.

76 Solid-State Physics 269

Includes superconductivity. For related information see also *33 Electronics and Electrical Engineering* and *36 Lasers and Masers*.

77 Thermodynamics and Statistical Physics 276

Includes quantum mechanics; theoretical physics; and Bose and Fermi statistics. For related information see also *25 Inorganic and Physical Chemistry* and *34 Fluid Mechanics and Heat Transfer.*

Subject Categories of the Division I. Social Sciences

Select a category to view the collection of records cited. N.A. means no abstracts in that category.

80 Social Sciences (General) 276

Includes educational matters.

81 Administration and Management 278

Includes management planning and research.

82 Documentation and Information Science 279

Includes information management; information storage and retrieval technology; technical writing; graphic arts; and micrography. For computer documentation see *61 Computer Programming and Software*.

83 Economics and Cost Analysis 282

Includes cost effectiveness studies.

84 Law, Political Science and Space Policy 283

Includes NASA appropriation hearings; aviation law; space law and policy; international law; international cooperation; and patent policy.

85 Urban Technology and Transportation 285

Includes applications of space technology to urban problems; technology transfer; technology assessment; and surface and mass transportation. For related information see *03 Air Transportation and Safety, 16 Space Transportation*, and *44 Energy Production and Conversion.*

Subject Categories of the Division J. Space Sciences

Select a category to view the collection of records cited. N.A. means no abstracts in that category.

88 Space Sciences (General) 287

89 Astronomy 287

Includes radio, gamma-ray, and infrared astronomy; and astrometry.

90 Astrophysics 295

Includes cosmology; celestial mechanics; space plasmas; and interstellar and interplanetary gases and dust. For related information see also *75 Plasma Physics*.

91 Lunar and Planetary Exploration 300

Includes planetology; and manned and unmanned flights. For spacecraft design or space stations see *18 Spacecraft Design, Testing and Performance*.

92 Solar Physics 303

Includes solar activity, solar flares, solar radiation and sunspots. For related information see also *93 Space Radiation.*

93 Space Radiation 307

Includes cosmic radiation; and inner and outer earth's radiation belts. For biological effects of radiation see *52 Aerospace Medicine*. For theory see *73 Nuclear and High-Energy Physics.*

Subject Categories of the Division K. General

Select a category to view the collection of records cited. N.A. means no abstracts in that category.

99 General 311

Includes aeronautical, astronautical, and space science related histories, biographies, and pertinent reports too broad for categorization; histories or broad overviews of NASA programs.

Document Availability Information

The mission of the NASA Scientific and Technical (STI) Program Office is to quickly, efficiently, and cost-effectively provide the NASA community with desktop access to STI produced by NASA and the world's aerospace industry and academia. In addition, we will provide the aerospace industry, academia, and the taxpayer access to the intellectual scientific and technical output and achievements of NASA.

Eligibility and Registration for NASA STI Products and Services

The NASA STI Program offers a wide variety of products and services to achieve its mission. Your affiliation with NASA determines the level and type of services provided by the NASA STI Program. To assure that appropriate level of services are provided, NASA STI users are requested to register at the NASA Center for AeroSpace Information (CASI). Please contact NASA CASI in one of the following ways:

E-mail:	help@sti.nasa.gov
Fax:	301-621-0134
Phone:	301-621-0390
Mail:	ATTN: Registration Services NASA Center for AeroSpace Information 7121 Standard Drive Hanover, MD 21076-1320

Limited Reproducibility

In the database citations, a note of limited reproducibility appears if there are factors affecting the reproducibility of more than 20 percent of the document. These factors include faint or broken type, color photographs, black and white photographs, foldouts, dot matrix print, or some other factor that limits the reproducibility of the document. This notation also appears on the microfiche header.

NASA Patents and Patent Applications

Patents and patent applications owned by NASA are announced in the STI Database. Printed copies of patents (which are not microfiched) are available for purchase from the U.S. Patent and Trademark Office.

When ordering patents, the U.S. Patent Number should be used, and payment must be remitted in advance, by money order or check payable to the Commissioner of Patents and Trademarks. Prepaid purchase coupons for ordering are also available from the U.S. Patent and Trademark Office.

NASA patent application specifications are sold in both paper copy and microfiche by the NASA Center for AeroSpace Information (CASI). The document ID number should be used in ordering either paper copy or microfiche from CASI.

The patents and patent applications announced in the STI Database are owned by NASA and are available for royalty-free licensing. Requests for licensing terms and further information should be addressed to:

National Aeronautics and Space Administration
Associate General Counsel for Intellectual Property
Code GP
Washington, DC 20546-0001

Sources for Documents

One or more sources from which a document announced in the STI Database is available to the public is ordinarily given on the last line of the citation. The most commonly indicated sources and their acronyms or abbreviations are listed below, with an Addresses of Organizations list near the back of this section. If the publication is available from a source other than those listed, the publisher and his address will be displayed on the availability line or in combination with the corporate source.

Avail: NASA CASI. Sold by the NASA Center for AeroSpace Information. Prices for hard copy (HC) and microfiche (MF) are indicated by a price code following the letters HC or MF in the citation. Current values are given in the NASA CASI Price Code Table near the end of this section.

Note on Ordering Documents: When ordering publications from NASA CASI, use the document ID number or other report number. It is also advisable to cite the title and other bibliographic identification.

Avail: SOD (or GPO). Sold by the Superintendent of Documents, U.S. Government Printing Office, in hard copy.

Avail: BLL (formerly NLL): British Library Lending Division, Boston Spa, Wetherby, Yorkshire, England. Photocopies available from this organization at the price shown. (If none is given, inquiry should be addressed to the BLL.)

Avail: DOE Depository Libraries. Organizations in U.S. cities and abroad that maintain collections of Department of Energy reports, usually in microfiche form, are listed in Energy Research Abstracts. Services available from the DOE and its depositories are described in a booklet, *DOE Technical Information Center—Its Functions and Services* (TID-4660), which may be obtained without charge from the DOE Technical Information Center.

Avail: ESDU. Pricing information on specific data, computer programs, and details on ESDU International topic categories can be obtained from ESDU International.

Avail: Fachinformationszentrum Karlsruhe. Gesellschaft für wissenschaftlich-technische Information mbH 76344 Eggenstein-Leopoldshafen, Germany.

Avail: HMSO. Publications of Her Majesty's Stationery Office are sold in the U.S. by Pendragon House, Inc. (PHI), Redwood City, CA. The U.S. price (including a service and mailing charge) is given, or a conversion table may be obtained from PHI.

Avail: Issuing Activity, or Corporate Author, or no indication of availability. Inquiries as to the availability of these documents should be addressed to the organization shown in the citation as the corporate author of the document.

Avail: NASA Public Document Rooms. Documents so indicated may be examined at or purchased from the National Aeronautics and Space Administration (JBD-4), Public Documents Room (Room 1H23), Washington, DC 20546-0001, or public document rooms located at NASA installations, and the NASA Pasadena Office at the Jet Propulsion Laboratory.

Avail: NTIS. Sold by the National Technical Information Service. Initially distributed microfiche under the NTIS SRIM (Selected Research in Microfiche) are available. For information concerning this service, consult the NTIS Subscription Section, Springfield, VA 22161.

Avail: Univ. Microfilms. Documents so indicated are dissertations selected from Dissertation Abstracts and are sold by University Microfilms as xerographic copy (HC) and microfilm. All requests should cite the author and the Order Number as they appear in the citation.

Avail: US Patent and Trademark Office. Sold by Commissioner of Patents and Trademarks, U.S. Patent and Trademark Office, at the standard price of $1.50 each, postage free.

Avail: (US Sales Only). These foreign documents are available to users within the United States from the National Technical Information Service (NTIS). They are available to users outside the United States through the International Nuclear Information Service (INlS) representative in their country, or by applying directly to the issuing organization.

Avail: USGS. Originals of many reports from the U.S. Geological Survey, which may contain color illustrations, or otherwise may not have the quality of illustrations preserved in the microfiche or facsimile reproduction, may be examined by the public at the libraries of the USGS field offices whose addresses are listed on the Addresses of Organizations page. The libraries may be queried concerning the availability of specific documents and the possible utilization of local copying services, such as color reproduction.

Addresses of Organizations

British Library Lending Division
Boston Spa, Wetherby, Yorkshire
England

Commissioner of Patents and Trademarks
U.S. Patent and Trademark Office
Washington, DC 20231

Department of Energy
Technical Information Center
P.O. Box 62
Oak Ridge, TN 37830

European Space Agency–
Information Retrieval Service ESRIN
Via Galileo Galilei
00044 Frascati (Rome) Italy

ESDU International
27 Corsham Street
London
N1 6UA
England

Fachinformationszentrum Karlsruhe
Gesellschaft für wissenschaftlich–technische
Information mbH
76344 Eggenstein–Leopoldshafen, Germany

Her Majesty's Stationery Office
P.O. Box 569, S.E. 1
London, England

NASA Center for AeroSpace Information
7121 Standard Drive
Hanover, MD 21076-1320

(NASA STI Lead Center)
National Aeronautics and Space Administration
Scientific and Technical Information Program Office
Langley Research Center – MS157
Hampton, VA 23681

National Technical Information Service
5285 Port Royal Road
Springfield, VA 22161

Pendragon House, Inc.
899 Broadway Avenue
Redwood City, CA 94063

Superintendent of Documents
U.S. Government Printing Office
Washington, DC 20402

University Microfilms
A Xerox Company
300 North Zeeb Road
Ann Arbor, MI 48106

University Microfilms, Ltd.
Tylers Green
London, England

U.S. Geological Survey Library National Center
MS 950
12201 Sunrise Valley Drive
Reston, VA 22092

U.S. Geological Survey Library
2255 North Gemini Drive
Flagstaff, AZ 86001

U.S. Geological Survey
345 Middlefield Road
Menlo Park, CA 94025

U.S. Geological Survey Library
Box 25046
Denver Federal Center, MS914
Denver, CO 80225

NASA CASI Price Code Table

(Effective July 1, 1998)

Code	U.S., Canada, & Mexico	Foreign
A01	$ 8.00	$ 16.00
A02	12.00	24.00
A03	23.00	46.00
A04	25.50	51.00
A05	27.00	54.00
A06	29.50	59.00
A07	33.00	66.00
A08	36.00	72.00
A09	41.00	82.00
A10	44.00	88.00
A11	47.00	94.00
A12	51.00	102.00
A13	54.00	108.00
A14	56.00	112.00
A15	58.00	116.00
A16	60.00	120.00
A17	62.00	124.00
A18	65.50	131.00
A19	67.50	135.00
A20	69.50	139.00
A21	71.50	143.00
A22	77.00	154.00
A23	79.00	158.00
A24	81.00	162.00
A25	83.00	166.00
A99	Contact NASA CASI	

Code	U.S., Canada, & Mexico	Foreign
E01	$101.00	$202.00
E02	109.50	219.00
E03	119.50	238.00
E04	128.50	257.00
E05	138.00	276.00
E06	146.50	293.00
E07	156.00	312.00
E08	165.50	331.00
E09	174.00	348.00
E10	183.50	367.00
E11	193.00	386.00
E12	201.00	402.00
E13	210.50	421.00
E14	220.00	440.00
E15	229.50	459.00
E16	238.00	476.00
E17	247.50	495.00
E18	257.00	514.00
E19	265.50	531.00
E20	275.00	550.00
E21	284.50	569.00
E22	293.00	586.00
E23	302.50	605.00
E24	312.00	624.00
E99	Contact NASA CASI	

Payment Options

All orders must be prepaid unless you are registered for invoicing or have a deposit account with the NASA CASI. Payment can be made by VISA, MasterCard, American Express, or Diner's Club credit card. Checks or money orders must be in U.S. currency and made payable to "NASA Center for AeroSpace Information." To register, please request a registration form through the NASA STI Help Desk at the numbers or addresses below.

Handling fee per item is $1.50 domestic delivery to any location in the United States and $9.00 foreign delivery to Canada, Mexico, and other foreign locations. Video orders incur an additional $2.00 handling fee per title.

The fee for shipping the safest and fastest way via Federal Express is in addition to the regular handling fee explained above—$5.00 domestic per item, $27.00 foreign for the first 1-3 items, $9.00 for each additional item.

Return Policy

The NASA Center for AeroSpace Information will replace or make full refund on items you have requested if we have made an error in your order, if the item is defective, or if it was received in damaged condition, and you contact CASI within 30 days of your original request.

NASA Center for AeroSpace Information
7121 Standard Drive
Hanover, MD 21076-1320

E-mail: help@sti.nasa.gov
Fax: (301) 621-0134
Phone: (301) 621-0390

Rev. 7/98

Federal Depository Library Program

In order to provide the general public with greater access to U.S. Government publications, Congress established the Federal Depository Library Program under the Government Printing Office (GPO), with 53 regional depositories responsible for permanent retention of material, inter-library loan, and reference services. At least one copy of nearly every NASA and NASA-sponsored publication, either in printed or microfiche format, is received and retained by the 53 regional depositories. A list of the Federal Regional Depository Libraries, arranged alphabetically by state, appears at the very end of this section. These libraries are not sales outlets. A local library can contact a regional depository to help locate specific reports, or direct contact may be made by an individual.

Public Collection of NASA Documents

An extensive collection of NASA and NASA-sponsored publications is maintained by the British Library Lending Division, Boston Spa, Wetherby, Yorkshire, England for public access. The British Library Lending Division also has available many of the non-NASA publications cited in the STI Database. European requesters may purchase facsimile copy or microfiche of NASA and NASA-sponsored documents FIZ–Fachinformation Karlsruhe–Bibliographic Service, D-76344 Eggenstein-Leopoldshafen, Germany and TIB–Technische Informationsbibliothek, P.O. Box 60 80, D-30080 Hannover, Germany.

Submitting Documents

All users of this abstract service are urged to forward reports to be considered for announcement in the STI Database. This will aid NASA in its efforts to provide the fullest possible coverage of all scientific and technical publications that might support aeronautics and space research and development. If you have prepared relevant reports (other than those you will transmit to NASA, DOD, or DOE through the usual contract- or grant-reporting channels), please send them for consideration to:

ATTN: Acquisitions Specialist
NASA Center for AeroSpace Information
7121 Standard Drive
Hanover, MD 21076-1320.

Reprints of journal articles, book chapters, and conference papers are also welcome.

You may specify a particular source to be included in a report announcement if you wish; otherwise the report will be placed on a public sale at the NASA Center for AeroSpace Information. Copyrighted publications will be announced but not distributed or sold.

Federal Regional Depository Libraries

ALABAMA

AUBURN UNIV. AT MONTGOMERY LIBRARY
Documents Dept.
7300 University Dr.
Montgomery, AL 36117–3596
(205) 244–3650 Fax: (205) 244–0678

UNIV. OF ALABAMA
Amelia Gayle Gorgas Library
Govt. Documents
P.O. Box 870266
Tuscaloosa, AL 35487–0266
(205) 348–6046 Fax: (205) 348–0760

ARIZONA

DEPT. OF LIBRARY, ARCHIVES, AND PUBLIC RECORDS
Research Division
Third Floor, State Capitol
1700 West Washington
Phoenix, AZ 85007
(602) 542–3701 Fax: (602) 542–4400

ARKANSAS

ARKANSAS STATE LIBRARY
State Library Service Section
Documents Service Section
One Capitol Mall
Little Rock, AR 72201–1014
(501) 682–2053 Fax: (501) 682–1529

CALIFORNIA

CALIFORNIA STATE LIBRARY
Govt. Publications Section
P.O. Box 942837 – 914 Capitol Mall
Sacramento, CA 94337–0091
(916) 654–0069 Fax: (916) 654–0241

COLORADO

UNIV. OF COLORADO – BOULDER
Libraries – Govt. Publications
Campus Box 184
Boulder, CO 80309–0184
(303) 492–8834 Fax: (303) 492–1881

DENVER PUBLIC LIBRARY
Govt. Publications Dept. BSG
1357 Broadway
Denver, CO 80203–2165
(303) 640–8846 Fax: (303) 640–8817

CONNECTICUT

CONNECTICUT STATE LIBRARY
231 Capitol Avenue
Hartford, CT 06106
(203) 566–4971 Fax: (203) 566–3322

FLORIDA

UNIV. OF FLORIDA LIBRARIES
Documents Dept.
240 Library West
Gainesville, FL 32611–2048
(904) 392–0366 Fax: (904) 392–7251

GEORGIA

UNIV. OF GEORGIA LIBRARIES
Govt. Documents Dept.
Jackson Street
Athens, GA 30602–1645
(706) 542–8949 Fax: (706) 542–4144

HAWAII

UNIV. OF HAWAII
Hamilton Library
Govt. Documents Collection
2550 The Mall
Honolulu, HI 96822
(808) 948–8230 Fax: (808) 956–5968

IDAHO

UNIV. OF IDAHO LIBRARY
Documents Section
Rayburn Street
Moscow, ID 83844–2353
(208) 885–6344 Fax: (208) 885–6817

ILLINOIS

ILLINOIS STATE LIBRARY
Federal Documents Dept.
300 South Second Street
Springfield, IL 62701–1796
(217) 782–7596 Fax: (217) 782–6437

INDIANA

INDIANA STATE LIBRARY
Serials/Documents Section
140 North Senate Avenue
Indianapolis, IN 46204–2296
(317) 232–3679 Fax: (317) 232–3728

IOWA

UNIV. OF IOWA LIBRARIES
Govt. Publications
Washington & Madison Streets
Iowa City, IA 52242–1166
(319) 335–5926 Fax: (319) 335–5900

KANSAS

UNIV. OF KANSAS
Govt. Documents & Maps Library
6001 Malott Hall
Lawrence, KS 66045–2800
(913) 864–4660 Fax: (913) 864–3855

KENTUCKY

UNIV. OF KENTUCKY
King Library South
Govt. Publications/Maps Dept.
Patterson Drive
Lexington, KY 40506–0039
(606) 257–3139 Fax: (606) 257–3139

LOUISIANA

LOUISIANA STATE UNIV.
Middleton Library
Govt. Documents Dept.
Baton Rouge, LA 70803–3312
(504) 388–2570 Fax: (504) 388–6992

LOUISIANA TECHNICAL UNIV.
Prescott Memorial Library
Govt. Documents Dept.
Ruston, LA 71272–0046
(318) 257–4962 Fax: (318) 257–2447

MAINE

UNIV. OF MAINE
Raymond H. Fogler Library
Govt. Documents Dept.
Orono, ME 04469–5729
(207) 581–1673 Fax: (207) 581–1653

MARYLAND

UNIV. OF MARYLAND – COLLEGE PARK
McKeldin Library
Govt. Documents/Maps Unit
College Park, MD 20742
(301) 405–9165 Fax: (301) 314–9416

MASSACHUSETTS

BOSTON PUBLIC LIBRARY
Govt. Documents
666 Boylston Street
Boston, MA 02117–0286
(617) 536–5400, ext. 226
Fax: (617) 536–7758

MICHIGAN

DETROIT PUBLIC LIBRARY
5201 Woodward Avenue
Detroit, MI 48202–4093
(313) 833–1025 Fax: (313) 833–0156

LIBRARY OF MICHIGAN
Govt. Documents Unit
P.O. Box 30007
717 West Allegan Street
Lansing, MI 48909
(517) 373–1300 Fax: (517) 373–3381

MINNESOTA

UNIV. OF MINNESOTA
Govt. Publications
409 Wilson Library
309 19th Avenue South
Minneapolis, MN 55455
(612) 624–5073 Fax: (612) 626–9353

MISSISSIPPI

UNIV. OF MISSISSIPPI
J.D. Williams Library
106 Old Gym Bldg.
University, MS 38677
(601) 232–5857 Fax: (601) 232–7465

MISSOURI

UNIV. OF MISSOURI – COLUMBIA
106B Ellis Library
Govt. Documents Sect.
Columbia, MO 65201–5149
(314) 882–6733 Fax: (314) 882–8044

MONTANA

UNIV. OF MONTANA
Mansfield Library
Documents Division
Missoula, MT 59812–1195
(406) 243–6700 Fax: (406) 243–2060

NEBRASKA

UNIV. OF NEBRASKA – LINCOLN
D.L. Love Memorial Library
Lincoln, NE 68588–0410
(402) 472–2562 Fax: (402) 472–5131

NEVADA

THE UNIV. OF NEVADA LIBRARIES
Business and Govt. Information Center
Reno, NV 89557–0044
(702) 784–6579 Fax: (702) 784–1751

NEW JERSEY

NEWARK PUBLIC LIBRARY
Science Div. – Public Access
P.O. Box 630
Five Washington Street
Newark, NJ 07101–7812
(201) 733–7782 Fax: (201) 733–5648

NEW MEXICO

UNIV. OF NEW MEXICO
General Library
Govt. Information Dept.
Albuquerque, NM 87131–1466
(505) 277–5441 Fax: (505) 277–6019

NEW MEXICO STATE LIBRARY
325 Don Gaspar Avenue
Santa Fe, NM 87503
(505) 827–3824 Fax: (505) 827–3888

NEW YORK

NEW YORK STATE LIBRARY
Cultural Education Center
Documents/Gift & Exchange Section
Empire State Plaza
Albany, NY 12230–0001
(518) 474–5355 Fax: (518) 474–5786

NORTH CAROLINA

UNIV. OF NORTH CAROLINA – CHAPEL HILL
Walter Royal Davis Library
CB 3912, Reference Dept.
Chapel Hill, NC 27514–8890
(919) 962–1151 Fax: (919) 962–4451

NORTH DAKOTA

NORTH DAKOTA STATE UNIV. LIB.
Documents
P.O. Box 5599
Fargo, ND 58105–5599
(701) 237–8886 Fax: (701) 237–7138

UNIV. OF NORTH DAKOTA
Chester Fritz Library
University Station
P.O. Box 9000 – Centennial and University Avenue
Grand Forks, ND 58202–9000
(701) 777–4632 Fax: (701) 777–3319

OHIO

STATE LIBRARY OF OHIO
Documents Dept.
65 South Front Street
Columbus, OH 43215–4163
(614) 644–7051 Fax: (614) 752–9178

OKLAHOMA

OKLAHOMA DEPT. OF LIBRARIES
U.S. Govt. Information Division
200 Northeast 18th Street
Oklahoma City, OK 73105–3298
(405) 521–2502, ext. 253
Fax: (405) 525–7804

OKLAHOMA STATE UNIV.
Edmon Low Library
Stillwater, OK 74078–0375
(405) 744–6546 Fax: (405) 744–5183

OREGON

PORTLAND STATE UNIV.
Branford P. Millar Library
934 Southwest Harrison
Portland, OR 97207–1151
(503) 725–4123 Fax: (503) 725–4524

PENNSYLVANIA

STATE LIBRARY OF PENN.
Govt. Publications Section
116 Walnut & Commonwealth Ave.
Harrisburg, PA 17105–1601
(717) 787–3752 Fax: (717) 783–2070

SOUTH CAROLINA

CLEMSON UNIV.
Robert Muldrow Cooper Library
Public Documents Unit
P.O. Box 343001
Clemson, SC 29634–3001
(803) 656–5174 Fax: (803) 656–3025

UNIV. OF SOUTH CAROLINA
Thomas Cooper Library
Green and Sumter Streets
Columbia, SC 29208
(803) 777–4841 Fax: (803) 777–9503

TENNESSEE

UNIV. OF MEMPHIS LIBRARIES
Govt. Publications Dept.
Memphis, TN 38152–0001
(901) 678–2206 Fax: (901) 678–2511

TEXAS

TEXAS STATE LIBRARY
United States Documents
P.O. Box 12927 – 1201 Brazos
Austin, TX 78701–0001
(512) 463–5455 Fax: (512) 463–5436

TEXAS TECH. UNIV. LIBRARIES
Documents Dept.
Lubbock, TX 79409–0002
(806) 742–2282 Fax: (806) 742–1920

UTAH

UTAH STATE UNIV.
Merrill Library Documents Dept.
Logan, UT 84322–3000
(801) 797–2678 Fax: (801) 797–2677

VIRGINIA

UNIV. OF VIRGINIA
Alderman Library
Govt. Documents
University Ave. & McCormick Rd.
Charlottesville, VA 22903–2498
(804) 824–3133 Fax: (804) 924–4337

WASHINGTON

WASHINGTON STATE LIBRARY
Govt. Publications
P.O. Box 42478
16th and Water Streets
Olympia, WA 98504–2478
(206) 753–4027 Fax: (206) 586–7575

WEST VIRGINIA

WEST VIRGINIA UNIV. LIBRARY
Govt. Documents Section
P.O. Box 6069 – 1549 University Ave.
Morgantown, WV 26506–6069
(304) 293–3051 Fax: (304) 293–6638

WISCONSIN

ST. HIST. SOC. OF WISCONSIN LIBRARY
Govt. Publication Section
816 State Street
Madison, WI 53706
(608) 264–6525 Fax: (608) 264–6520

MILWAUKEE PUBLIC LIBRARY
Documents Division
814 West Wisconsin Avenue
Milwaukee, WI 53233
(414) 286–3073 Fax: (414) 286–8074

Typical Report Citation and Abstract

❶ **19970001126** NASA Langley Research Center, Hampton, VA USA
❷ **Water Tunnel Flow Visualization Study Through Poststall of 12 Novel Planform Shapes**
❸ Gatlin, Gregory M., NASA Langley Research Center, USA Neuhart, Dan H., Lockheed Engineering and Sciences Co., USA;
❹ Mar. 1996; 130p; In English
❺ Contract(s)/Grant(s): RTOP 505-68-70-04
❻ Report No(s): NASA-TM-4663; NAS 1.15:4663; L-17418; No Copyright; Avail: CASI; A07, Hardcopy; A02, Microfiche
❼ To determine the flow field characteristics of 12 planform geometries, a flow visualization investigation was conducted in the Langley 16- by 24-Inch Water Tunnel. Concepts studied included flat plate representations of diamond wings, twin bodies, double wings, cutout wing configurations, and serrated forebodies. The off-surface flow patterns were identified by injecting colored dyes from the model surface into the free-stream flow. These dyes generally were injected so that the localized vortical flow patterns were visualized. Photographs were obtained for angles of attack ranging from 10' to 50', and all investigations were conducted at a test section speed of 0.25 ft per sec. Results from the investigation indicate that the formation of strong vortices on highly swept forebodies can improve poststall lift characteristics; however, the asymmetric bursting of these vortices could produce substantial control problems. A wing cutout was found to significantly alter the position of the forebody vortex on the wing by shifting the vortex inboard. Serrated forebodies were found to effectively generate multiple vortices over the configuration. Vortices from 65' swept forebody serrations tended to roll together, while vortices from 40' swept serrations were more effective in generating additional lift caused by their more independent nature.
❽ Author
❾ *Water Tunnel Tests; Flow Visualization; Flow Distribution; Free Flow; Planforms; Wing Profiles; Aerodynamic Configurations*

Key

1. Document ID Number; Corporate Source
2. Title
3. Author(s) and Affiliation(s)
4. Publication Date
5. Contract/Grant Number(s)
6. Report Number(s); Availability and Price Codes
7. Abstract
8. Abstract Author
9. Subject Terms

SCIENTIFIC AND TECHNICAL AEROSPACE REPORTS

A Biweekly Publication of the National Aeronautics and Space Administration

VOLUME 37, DECEMBER 6, 1999

01
AERONAUTICS (GENERAL)

19990107410 Federal Aviation Administration, Washington, DC USA
Aeronautical Information Publication, USA of America, Fifteenth Edition
Jan. 28, 1999; 642p; In English
Report No.(s): PB99-124372; No Copyright; Avail: CASI; A99, Hardcopy; A06, Microfiche

Topics discussed include the following: National Regulations and Requirements; Tables and Codes; Services; and Charges for Aerodromes/Heliports and Air Navigation Services.

NTIS

Air Navigation; Airports; Regulations; Air Transportation; Heliports; Aircraft Landing

19990111540 Nebraska Univ., Aviation Inst., Omaha, NE USA
Journal of Air Transportation World Wide, Volume 4
Bowen, Brent D., Editor, Nebraska Univ., USA; Kabashkin, Igor, Editor, Riga Aviation Univ., Latvia; 1999; ISSN 1093-8826; 172p; In English; See also 19990111541 through 19990111548; Copyright; Avail: Issuing Activity, Hardcopy

The Journal of Air Transportation World Wide's (JATWW) mission is to provide the global community immediate key resource information in all areas of air transportation. The goal of the Journal is to be recognized as the preeminent scholarly journal in the aeronautical aspects of transportation. As an international and interdisciplinary journal, the JATWW will provide a forum for peer-reviewed articles in all areas of aviation and space transportation research, policy, theory, case study, practice, and issues. While maintaining a broad scope, a focal point of the journal will be in the area of aviation administration and policy. Derived from text

Air Transportation; Space Transportation

02
AERODYNAMICS

Includes aerodynamics of bodies, combinations, wings, rotors, and control surfaces; and internal flow in ducts and turbomachinery. For related information see also 34 Fluid Mechanics and Heat Transfer.

19990110582 NASA Dryden Flight Research Center, Edwards, CA USA
Adaptive Wing Camber Optimization: A Periodic Perturbation Approach
Espana, Martin, NASA Dryden Flight Research Center, USA; Gilyard, Glenn, NASA Dryden Flight Research Center, USA; Automatic Control in Aerospace; September 1994, pp. 35-40; In English; Aerospace Control, 12-16 Sep. 1994, Palo Alto, CA, USA; Sponsored by International Federation of Automatic Control, Unknown
Report No.(s): H-1998; No Copyright; Avail: CASI; A02, Hardcopy; A01, Microfiche

Available redundancy among aircraft control surfaces allows for effective wing camber modifications. As shown in the past, this fact can be used to improve aircraft performance. to date, however, algorithm developments for in-flight camber optimization have been limited. This paper presents a perturbational approach for cruise optimization through in-flight camber adaptation. The method uses, as a performance index, an indirect measurement of the instantaneous net thrust. As such, the actual performance

improvement comes from the integrated effects of airframe and engine. The algorithm, whose design and robustness properties are discussed, is demonstrated on the NASA Dryden B-720 flight simulator.
Author
Adaptive Control; Optimization; Wing Camber; Perturbation; Drag; Control Surfaces; Flight Simulators; Transport Aircraft

19990111704 Arizona State Univ., Dept. of Mechanical and Aerospace Engineering, Tempe, AZ USA
Swept-Wing Receptivity Studies Using Distributed Roughness ***Final Report, 1 Jun. 1997 - 31 Oct. 1999***
Saric, William S., Arizona State Univ., USA; October 1999; 15p; In English
Contract(s)/Grant(s): NAG1-1925; No Copyright; Avail: CASI; A03, Hardcopy; A01, Microfiche

Transition to turbulence in swept-wing flows has resisted correlation with linear theory because of its sensitivity to freestream conditions and 3-D roughness and because one of the principal instability modes quickly 'becomes nonlinear. In the face of such a formidable problem, two rather long-term fundamental efforts have been underway at DLR Gottinberg and Arizona State University that address swept-wing transition. These efforts have been recently reviewed by Bippes (1997) and Reibert and Saric (1997). Thus, the present work is a continuation of a series of studies on swept-wing boundary layers which have led to a better understanding of the transition process. In particular, we have taken advantage of the sensitivity to 3-D roughness and the modal nature of the instability in order to propose a particular control strategy. Complementing the two aforementioned reviews, general reviews of the swept-wing transition problem are found in Arnal (1997) and Kachanov (1996). Other recent reviews include Reshotko (t997), Crouch (1997), and Herbert (1997a,b). The failure of linear theory is discussed in Reed et al. (1996). The historical work is found in Reed and Sar-ic (1989). The basic idea is that the combination of sweep and chordwise pressure gradient within the boundary layer creates a velocity component perpendicular to the inviscid streamline. This crossflow profile is inflectional and exhibits both traveling and stationary unstable waves called crossflow vortices that are (approximately) aligned along the inviscid streamlines. Under conditions of low freestream turbulence levels, the dominant crossflow wave is stationary (Reibert and Saric t997) while moderate to high turbulence levels initiate dominant traveling waves (Dehle and Bippes 1996; Bippes 1997). 'Me mechanism is relatively insensitive to sound and 2-D surface roughness (Radeztsky et al. 1993) but very sensitive to 3-D roughness near the attachment line. We concentrate our work on low-turbulence freestream flows and stationary crossflow waves. Although the v' and w' components of the disturbances are very small, by convecting streamwise momentum in the wall-normal direction, they produce 0(l) changes inu'.Thus the mean flow is highly distorted with localized inflection points. Transition is then triggered by a high-frequency secondary instability of the distorted mean profile.
Author
Vortices; Turbulence; Traveling Waves; Surface Roughness; Low Turbulence; Inviscid Flow; Boundary Layers

03
AIR TRANSPORTATION AND SAFETY

Includes passenger and cargo air transport operations; and aircraft accidents. For related information see also 16 Space Transportation and 85 Urban Technology and Transportation.

19990107328 NASA Langley Research Center, Hampton, VA USA
Flight Data Reduction of Wake Velocity Measurements Using an Instrumented OV-10 Airplane
Vicroy, Dan D., NASA Langley Research Center, USA; Stuever, Robert A., NASA Langley Research Center, USA; Stewart, Eric C., NASA Langley Research Center, USA; Rivers, Robert A., NASA Langley Research Center, USA; September 1999; 66p; In English
Contract(s)/Grant(s): RTOP 538-04-11-12
Report No.(s): NASA/TM-1999-209552; NAS 1.15:209552; L-17892; No Copyright; Avail: CASI; A04, Hardcopy; A01, Microfiche

A series of flight tests to measure the wake of a Lockheed C- 130 airplane and the accompanying atmospheric state have been conducted. A specially instrumented North American Rockwell OV-10 airplane was used to measure the wake and atmospheric conditions. An integrated database has been compiled for wake characterization and validation of wake vortex computational models. This paper describes the wake- measurement flight-data reduction process.
Author
Flight Tests; Wakes; Velocity Measurement; Mathematical Models; Procedures

19990110063 Royal Aeronautical Society, London, UK

Flight Safety- A Total Commitment

Flight Safety- A Total Commitment Proceedings; 1998; 73p; In English, Feb. 3, 1998, London, UK; See also 19990110064 through 19990110070; ISBN 1-85768-0197; Copyright; Avail: Issuing Activity (Royal Aeronautical Society, 4 Hamilton Place, London, W1V 0BQ, UK); US Sales Only, Hardcopy, Microfiche

Contents include the following: a global view of flight safety concerns; type certification on new design concepts-SST (airworthiness requirements and new technology); service through safety-implications for flight crew training; train, inspect and audit - is there any other way?; flight safety in business aviation; maintaining existing ATC safety levels whilst responding to the demands of increasing traffic; and the investigation of accidents and incidents and lessons to be learned.

CASI

Aircraft Reliability; Flight Safety; Flight Training

19990110064 International Federation of Air Line Pilot Associations, Chertsey, UK

A global view of flight safety concerns

McInnis, R. J. (Ron), International Federation of Air Line Pilot Associations, UK; Flight Safety- A Total Commitment; 1998; 8p; In English; See also 19990110063; Copyright; Avail: Issuing Activity (Royal Aeronautical Society, 4 Hamilton Place, London, W1V 0BQ, London, UK); US Sales Only, Hardcopy, Microfiche

Globalisation has become a commonplace word in the aviation industry. This paper examines the current safety concerns of the international pilot community and the trend for global airlines in the ever-increasing air traffic scenario. If the current increase in air traffic and its accident rate continues the industry could face a major accident every week in 10 years' time. Several areas of the world are recognized as being safety deficient; the reasons for these deficiencies are examined, together with graphic examples of accidents and incidents. An effective safety reporting system is called for one which can provide feedback without fear of prosecutions or job losses for those providing the reports. There still exists in some States the situation where the agency that makes the rules not also enforces them but also investigates the accidents. This is in direct contravention of the ICAO guidelines. The paper ends with a practical solution on what can be done to provide positive answers to the problems.

Author

Flight Safety; Feedback; Commercial Aircraft; Airline Operations; Air Traffic

19990110065 Royal Aeronautical Society, London, UK

Type certification on new design concepts-SST

Baker, P. P., Royal Aeronautical Society, UK; 1998; 28p; In English; See also 19990110063; Copyright; Avail: Issuing Activity (Royal Aeronautical Society, 4 Hamilton Place, London, W1V 0BQ, UK); US Sales Only, Hardcopy, Microfiche

Keeping up to date with aircraft development is an imperative requirement for the Certification Authorities if they are not to lose credibility and if a comparable, if not improved, level of safety is to be maintained. In the case of Concorde it is thought this objective was achieved. However, safety is always balanced between cost and practicability and Concorde was fortunate in having been publicly funded throughout. It is ,perhaps, interesting to speculate if such an elaborate set of requirements would have emerged had the aircraft been manufactured privately. Certainly Government Institutional support was 'heavy' and the Certification Authorities were clearly encouraged to act similarly and in fact were 'used' to not only monitor, but also to approve, the early flight test programme, something which is not their usual role. As is well known the project was not cheap. It should be remembered that Certification Authorities are funded differently. Some, like the CAA, charge for their services and have to 'pay their way'. Others, like the FAA, are paid for by the tax payer (and ticket purchaser) and have to meet an annual fixed budget. The current trend to standardise requirements is applauded, naturally, not least by the manufactures and purchasers of aircraft, who stand to gain the most. Agreement on common standards, however, inevitably leads to compromise, and where funding is a problem, ready acceptance of the work of others - the net result can mean that safety is the loser. Setting a rigorous standard in one comparatively small body is much easier than applying a world wide universal set of rules with a world wide set of vested interests to go with them. It is hard to say that an accident should never have happend, since it is an accident. Nevertheless, such a description seems to suit a number of recent accidents to new 'equipment'. There certainly is no room for complacency and the combination of new technology and the desire to compromise standards could be an unfortunate one.

Author

Aircraft Design; Flight Tests; Safety

19990110066 British Midland Airways, London, UK

Service through safety - Implications for flight crew training

Harris, D. H. R., British Midland Airways, UK; 1998; 2p; In English; See also 19990110063; Copyright; Avail: Issuing Activity

(Royal Aeronautical Society, 4 Hamilton Place, London, W1V 0BQ, UK); US Sales Only, Hardcopy, Microfiche

Aviation is a very complex and changing environment. One of the possible problems that we have to recognize is that of culture, the culture of the operators and of the passengers. The challenge facing the trainer is to increase the level of awareness of crews during the different phases of flight. It is widely accepted that the most critical phases of flight are the take-off and lending. The investigation of incidents and accidents frequently points to crew error, in one form or other, as being a key factor. What we must never lose sight of is that this must only be achieved through a safe operating environment.

Derived from text

Safety; Flight Training; Flight Crews; Errors; Services

19990110067 Civil Aviation Authority, Flight Operations Standards, London, UK

'Train, inspect and audit' - Is there any other way?

Carver, T., Civil Aviation Authority, UK; 1998; 7p; In English; See also 19990110063; Copyright; Avail: Issuing Activity (Royal Aeronatical Society, 4 Hamilton Place, London, W1V 0BQ, UK); US Sales Only, Hardcopy, Microfiche

Is there anything new for us in aviation safety? What is changing to affect aviation? Is there any need to chang what we do to ensure safe air transport? This paper will consider some of these changes and their impact, arguing that, whereas external events may chang our technology, the human resource which is still central to our industry, remains constant in its failings which affect air safety whether operating with pilotless aircraft or skillfully handled bi-plane. The paper will consider air safety and commerce as a combination in a total commitment of engineer, pilot, operator and regulator, and will continue the argument to show that air safety can be maintained and enhanced mainly by concentration on Training, Inspecting and Auditing. It will conclude that no single element of the aviation industry can abrogate or delegate to any other element, all of its activities and responsibilities under any one of the three headings.

Author

Aircraft Safety; Education; Flight Safety; Human Resources; Regulators

19990110068 Civil Aviation Authority, London, UK

Flight safety in business aviation

Robinson, J. B., Civil Aviation Authority, UK; 1998; 6p; In English; See also 19990110063; Copyright; Avail: Issuing Activity (Royal Aeronatical Society, 4 Hamilton Place, London, W1V 0BQ, UK); US Sales Only, Hardcopy, Microfiche

Business Aviation has an essential role in the commercial, financial and industrial viability of the World. It provides governments. corporations and companies with a flexible. secure service to any destination world-wide without the problems associated with travel by the rigid network of the scheduled airlines. Due to the steady increase in the demand by the public for air travel. and despite the great advance in information technology and communications, the need for Business Aviation is increasing which is born out by the demand for and introduction of very long range business jet aircraft. to meet this demand Business Aviation has to achieve the highest standards of flying operations in aviation in an evermore crowded environment and with new technology which is not always user-friendly. At times resources are stretched to then limits and it is beholden to the Business Aviation community to ensure that it achieves its tasks with the utmost safety. A first look at the safety record for Business Aviation appears to show that all-is-well and that it is one of the safest means of transport in the World. but there are specific areas that do need attention if the number of accidents/incidents is to be reduced and, hopefully eliminated. .

Author

Airline Operations; Commercial Aircraft; Flight Safety; Jet Aircraft; Viability

19990110069 Board of Trade, London, UK

Maintaining existing ATC safety levels whilst responding to the demands of increasing traffic

Ennis, George, Board of Trade, UK; 1998; 6p; In English; See also 19990110063; Copyright; Avail: Issuing Activity (Royal Aeronatical Society, 4 Hamilton Place, London, W1V 0BQ, UK); US Sales Only, Hardcopy, Microfiche

This paper explains how NATS plans to maintain or reduce the overall number of ATC induced safety incidents regardless of the rate of traffic growth. It summarizes the current air traffic situation in Europe and explains NATS' approach to managing safety. It highlights a current safety issue and illustrates how NATS is improving safety year-on-year, in particular how human factor issues are being addressed. The paper examines future ATC developments in terms of the technology and the new operating concepts needed to enhance capacity, safely and cost effectively, in line with growing demand.

Author

Air Traffic Control; Safety; Incidence

19990110070 Department of Transport, Air Accidents Investigation Branch, Farnborough, UK

The investigation of accidents and incidents and lessons to be learned

Whidborne, Richard StJ, Department of Transport, UK; 1998; 14p; In English; See also 19990110063; Copyright; Avail: Issuing Activity (Royal Aeronatical Society, 4 Hamilton Place, London, W1V 0BQ, UK); US Sales Only, Hardcopy, Microfiche

The paper discusses the investigation of accidents and incidents from the perspective of a government investigation body. The attitudes of different parties towards a major occurrence, and their objectives, are discussed before describing some aspects of the methodology used in investigation. The lessons to be learned are described in terms of a 'product' which comprises the identification of safety deficiencies and consequent recommendations. The closure of recommendations by recipients is discussed in terms of acceptance and implementation by the regulatory authorities.

Author

Accident Investigation; Incidence

19990111541 Belgrade Univ., Yugoslavia

Determining Usability Versus Cost and Yields of a Regional Transport

Gvozdenovic, Slobodan, Belgrade Univ., Yugoslavia; Journal of Air Transportation World Wide; 1999; Volume 4, No. 2, pp. 1-21; In English; See also 19990111540; Copyright; Avail: Issuing Activity, Hardcopy

Regional transports are designed to operate on air networks having the basic characteristics of short trip distances and low density passengers/cargo, i.e. small numbers of passengers per flight. Regional transports passenger capacity is from 10 to 100 seats and operate on routes from 350 to 1000 nautical miles (nm). In order to meet passenger requirements providing low fares and high or required number of frequencies, airlines must constantly monitor operational costs and keep them low. It is obvious that costs of operating aircraft must be lower than yield obtained by transporting passengers and cargo. The requirement to achieve favorable yield/cost ratio must provide the answer to the question of which aircraft will best meet a specific air network (Simpson, 1972). An air network is defined by the number of services, the trip distance of each service, and the number of flights (frequencies) per day and week.

Derived from text

Airline Operations; Operating Costs; Air Cargo; Civil Aviation; Commercial Aircraft; Passengers

19990111542 University of Southern Georgia, Statesboro, GA USA

Outsourcing as an Airline Strategy

Rutner, Stephen M., University of Southern Georgia, USA; Brown, John H., University of Southern Georgia, USA; Journal of Air Transportation World Wide; 1999; Volume 4, No. 2, pp. 22-31; In English; See also 19990111540; Copyright; Avail: Issuing Activity, Hardcopy

Since the deregulation of the airline industry, carriers have searched for any method to improve their competitive position. At the same time, there has been a growth in the use of Third Party Logistics throughout corporate America. This paper presents an overview of the Third Party Logistics system of outsourcing and insourcing within the airline industry. This discussion generated a number of propositions, possible future scenarios and opportunities for empirical testing.

Author

Airline Operations; Air Transportation

19990111543 Jordan Univ. of Science and Technology, Irbid, Jordan

Stochastic Modeling of Airlines' Scheduled Services Revenue

Hamed, M. M., Jordan Univ. of Science and Technology, Jordan; Journal of Air Transportation World Wide; 1999; Volume 4, No. 2, pp. 32-48; In English; See also 19990111540; Copyright; Avail: Issuing Activity, Hardcopy

Airlines' revenue generated from scheduled services account for the major share in the total revenue. As such, predicting airlines' total scheduled services revenue is of great importance both to the governments (in case of national airlines) and private airlines. This importance stems from the need to formulate future airline strategic management policies, determine government subsidy levels, and formulate governmental air transportation policies. The prediction of the airlines' total scheduled services revenue is dealt with in this paper. Four key components of airline's scheduled services are considered. These include revenues generated from passenger, cargo, mail, and excess baggage. by addressing the revenue generated from each schedule service separately, air transportation planners and designers are able to enhance their ability to formulate specific strategies for each component. Estimation results clearly indicate that the four stochastic processes (scheduled services components) are represented

by different Box-Jenkins ARIMA models. The results demonstrate the appropriateness of the developed models and their ability to provide air transportation planners with future information vital to the planning and design processes.
Author
Air Transportation; Airline Operations; Schedules; Services; Revenue; Stochastic Processes; Regression Analysis; Econometrics; Time Series Analysis

19990111545 Cranfield Univ., Bedford, UK
The Effect of Corporate Influence in the Short Haul Business Travel Market
Mason, Keith J., Cranfield Univ., UK; Journal of Air Transportation World Wide; 1999; Volume 4, No. 2, pp. 66-83; In English; See also 19990111540; Copyright; Avail: Issuing Activity, Hardcopy

The importance of corporate involvement in the decision making process for business related air travel is being increasingly recognised in the literature. Business travellers consume air services (i.e. they take airline flights), however; they may not be the principal decision-maker in the purchase. Also it is the organization that employs the traveller that incurs die cost for air travel. Consequently this research addresses the relationship between the traveller and the employing organisation in the purchase of air travel. In this paper traveller opinions on their corporate travel policy are evaluated using a Likert summated rating scale. The benefits sought, by the traveller, from the air service are also investigated and these benefits are used to segment the short haul business air travel market in the EU. Changes in the market for short haul business travel since the full liberalisation of the aviation market in-the EU are evaluated by comparing the data to an earlier study of similar travellers in 1992.
Author
Air Transportation; Airline Operations; Short Haul Aircraft; Passenger Aircraft; Passengers

19990111546 Cranfield Univ., Bedford, UK
The Role of Capital Productivity in British Airways' Financial Recovery
Morrell, Peter, Cranfield Univ., UK; Journal of Air Transportation World Wide; 1999; Volume 4, No. 2, pp. 84-99; In English; See also 19990111540; Copyright; Avail: Issuing Activity, Hardcopy

British Airways (BA) was privatised in 1987, but its financial recovery occurred a number of years earlier. This recovery was sustained throughout the early 1990s economic recession, a period when few major airlines were operating profitably. This paper examines the role of productivity developments at British Airways from the early 1980s through 1996. The emphasis is on capital productivity and investment, but changes in capital intensity and labour productivity are also evaluated. Various measures are considered for both capital and labour productivity: outputs are measured in available tonne-kms (ATKS) and revenue tonne-kms (RTKs), with the former preferred over the latter two measures, after adjustment for work performed by BA for others. Capital inputs are measured in equivalent lease costs adjusted to constant prices with a different treatment of flight and ground equipment or assets. Labour inputs are derived from total payroll costs deflated by a UK wage price index. The airline made considerable capital investments over the period and at the same time went through two major processes of labour restructuring. This resulted in a gradual increase in capital intensity, relative high labour productivity growth, but poor capital productivity performance. However, capital investment played an important role in the airline's sustained labour and total factor productivity over the whole period.
Author
Airline Operations; Operating Costs; Labor; Productivity

19990111548 Directorate General of Civil Aviation, The Hague, Netherlands
Benchmark Airport Charges
deWit, A., Directorate General of Civil Aviation, Netherlands; Cohn, N., Hague Consulting Group, Netherlands; Journal of Air Transportation World Wide; 1999; Volume 4, No. 2, pp. 121-144; In English; See also 19990111540; Copyright; Avail: Issuing Activity, Hardcopy

The Netherlands Directorate General of Civil Aviation (DGCA) commissioned Hague Consulting Group (HCG) to complete a benchmark study of airport charges at twenty eight airports in Europe and around the world, based on 1996 charges. This study followed previous DGCA research on the topic but included more airports in much more detail. The main purpose of this new benchmark study was to provide insight into the levels and types of airport charges worldwide and into recent changes in airport charge policy and structure. This paper describes the 1996 analysis. It is intended that this work be repeated every year in order to follow developing trends and provide the most up-to-date information possible.
Author
Airports; Policies; Trends; Trend Analysis

19990111692 National Air and Space Museum, Washington, DC USA
Fifty Years of Transatlantic Fight
Smith, Richard K., National Air and Space Museum, USA; 1969; In English; 6th; Annual Meeting and Technical Display, 20-24 Oct. 1969, Anaheim, CA, USA; Sponsored by American Inst. of Aeronautics and Astronautics, USA
Report No.(s): AIAA Paper 69-1044; Copyright; Avail: Issuing Activity, Hardcopy

The history of transatlantic flight can be divided into seven periods. They are not all distinct in time; during the first twenty years they overlap to a considerable extent. But for convenience they may be summarized L (1) the great flights, 1919-1924; (2) the barnstorming, 1926-1938; (3) the heyday of the airship, 1919-1937; (4) the dawn of commercial airplane operations, 1935-1939; (5) World War II; (6) the post-war airs crew period, 1945-1957; and (7) the first generation of the jet era, 1958-1969. Derived from text

Commercial Aircraft; Transoceanic Flight; Histories

19990113073 Federal Aviation Administration, Washington, DC USA
Notices to Airmen Domestic/International, May 20, 1999
May 20, 1999; 290p
Report No.(s): PB99-153736; No Copyright; Avail: CASI; A13, Hardcopy; A03, Microfiche

Table of Contents: Airway Notams; Airports, Facilities, and Procedural Notams; General FDC Notams; Part 95 Revisions to Minimum En Route IFR Altitudes and Changeover Points; International Notices to Airmen; Graphic Notices (General Information; Special Military Operations; Major Sporting amd/or Entertainment Events; Northeast USA; Southeast USA; East Central United States; South Central USA; North Central USA; Northwest USA; Southwest USA; and Alaska/Hawaii).
NTIS

Air Navigation; Airports; National Airspace System; Charts

19990113078 National Transportation Safety Board, Washington, DC USA
National Transportation Safety Board Transportation Initial Decisions and Orders and Board Opinions and Orders Adopted and Issued during the Month of May 1999
May 1999; 366p
Report No.(s): PB99-916705; NTSB/IDBOO-99/05; No Copyright; Avail: CASI; A16, Hardcopy; A03, Microfiche

This publication contains all Judge Initial Decisions and Board Opinions and Orders in Safety and Seaman Enforcement Cases for May 1999.
NTIS

Air Transportation; Accident Prevention; Safety Management

04
AIRCRAFT COMMUNICATIONS AND NAVIGATION

Includes digital and voice communication with aircraft; air navigation systems (satellite and ground based); and air traffic control. For related information see also 17 Space Communications, Spacecraft Communications, Command and Tracking and 32 Communications and Radar.

19990106584 NASA Goddard Space Flight Center, Greenbelt, MD USA
Tracking the Relative Motion of Four Space Payloads Launched From a Sub-Orbital NASA Rocket
Martel, Hugh, Waypoint Consulting, Inc., Canada; Bull, Barton, NASA Goddard Space Flight Center, USA; [1999]; 6p; In English; ION GPS '99, 1999, Nashville, TN, USA; No Copyright; Avail: CASI; A02, Hardcopy; A01, Microfiche

One problem, which is comparatively new in the field of GPS applications, is the determination of the relative trajectories of space vehicles. Applications include the docking of spacecraft, collision avoidance in the area of space stations, and trajectory reconstruction of multiple payloads. The required precision in any of these applications will vary, according to the requirements of the task and abilities of GPS to cope with the environment and the dynamics. This paper describes the post-mission reconstruction of the relative trajectories of four GPS receivers attached to four payloads jettisoned from a rocket in a sub-orbital NASA science mission. It is shown that the sub-decimetre level were achieved with single frequency GPS receivers.
Author

Global Positioning System; Receivers; Orbit Determination; Position Indicators; Spacecraft Tracking

19990108577 NASA Goddard Space Flight Center, Greenbelt, MD USA

Testing of the International Space Station and X-38 Crew Return Vehicle GPS Receiver ***Final Report***

Simpson, James, NASA Goddard Space Flight Center, USA; Campbell, Chip, NASA Goddard Space Flight Center, USA; Carpenter, Russell, NASA Goddard Space Flight Center, USA; Davis, Ed, NASA Goddard Space Flight Center, USA; Kizhner, Semion, NASA Goddard Space Flight Center, USA; Lightsey, E. Glenn, Texas Univ., USA; Davis, George, Orbital Sciences Corp., USA; Jackson, Larry, Orbital Sciences Corp., USA; [1999]; 10p; In English; GPS Conference, 14-17 Sep. 1999, Nashville, TN, USA; No Copyright; Avail: CASI; A02, Hardcopy; A01, Microfiche

This paper discusses the process and results of the performance testing of the GPS receiver planned for use on the International Space Station (ISS) and the X-38 Crew Return Vehicle (CRV). The receiver is a Force-19 unit manufactured by Trimble Navigation and modified in software by the NASA Goddard Space Flight Center (GSFC) to perform navigation and attitude determination in space. The receiver is the primary source of navigation and attitude information for ISS and CRV. Engineers at GSFC have developed and tested the new receiver with a Global Simulation Systems Ltd (GSS) GPS Signal Generator (GPSSG). This paper documents the unique aspects of ground testing a GPS receiver that is designed for use in space. A discussion of the design of tests using the GPSSG, documentation, data capture, data analysis, and lessons learned will precede an overview of the performance of the new receiver. A description of the challenges that were overcome during this testing exercise will be presented. Results from testing show that the receiver will be within or near the specifications for ISS attitude and navigation performance. The process for verifying other requirements such as Time to First Fix, Time to First Attitude, selection/deselection of a specific GPS satellite vehicles (SV), minimum signal strength while still obtaining attitude and navigation, navigation and attitude output coverage, GPS week rollover, and Y2K requirements are also given in this paper.

Author

Global Positioning System; Navigation; Guidance (Motion); Navigation Satellites; Receivers; Signal Generators

19990108579 NASA Goddard Space Flight Center, Greenbelt, MD USA

Pre-Flight Testing of Spaceborne GPS Receivers Using a GPS Constellation Simulator

Kizhner, Semion, NASA Goddard Space Flight Center, USA; Davis, Edward, NASA Goddard Space Flight Center, USA; Alonso, Roberto, Argentine Space Agency, Argentina; [1999]; 11p; In English; ION GPS 1999 Conference, 14-17 Sep. 1999, Nashville, TN, USA; No Copyright; Avail: CASI; A03, Hardcopy; A01, Microfiche

The NASA Goddard Space Flight Center (GSFC) Global Positioning System (GPS) applications test facility has been established within the GSFC Guidance Navigation and Control Center. The GPS test facility is currently housing the Global Simulation Systems Inc. (GSSI) STR2760 GPS satellite 40-channel attitude simulator and a STR4760 12-channel navigation simulator. The facility also contains a few other resources such as an atomic time standard test bed, a rooftop antenna platform and a radome. It provides a new capability for high dynamics GPS simulations of space flight that is unique within the aerospace community. The GPS facility provides a critical element for the development and testing of GPS based technologies i.e. position, attitude and precise time determination used on-board a spacecraft, suborbital rocket or balloon. The GPS simulator system is configured in a transportable rack and is available for GPS component development as well as for component, spacecraft subsystem and system level testing at spacecraft integration and test sites. The GPS facility has been operational since early 1996 and has been utilized by space flight projects carrying GPS experiments, such as the OrbView-2 and the Argentine SAC-A spacecrafts. The SAC-A pre-flight test data obtained by using the STR2760 simulator and the comparison with preliminary analysis of the GPS data from SAC-A telemetry are summarized. This paper describes pre-flight tests and simulations used to support a unique spaceborne GPS experiment. The GPS experiment mission objectives and the test program are described, as well as the GPS test facility configuration needed to verify experiment feasibility. Some operational and critical issues inherent in GPS receiver pre-flight tests and simulations using this GPS simulator, and test methodology are described. Simulation and flight data are presented. A complete program of pre-flight testing of spaceborne GPS receivers using a GPS constellation simulator is detailed.

Author

Flight Simulation; Flight Tests; Global Positioning System; Guidance (Motion); Navigation; Navigation Satellites

19990110307 Civil Aeromedical Inst., Oklahoma City, OK USA

Controller Teamwork Evaluation and Assessment Methodology: A Scenario Calibration Study ***Final Report***

Bailey, Larry L., Civil Aeromedical Inst., USA; Broach, Dana M., Civil Aeromedical Inst., USA; Thompson, Richard C., Civil Aeromedical Inst., USA; Enos, Robert J., Civil Aeromedical Inst., USA; October 1999; 22p; In English

Contract(s)/Grant(s): AM-B-98-HRR-172

Report No.(s): DOT/FAA/AM/99/24; No Copyright; Avail: CASI; A03, Hardcopy; A01, Microfiche

A low cost air traffic control (ATC) multi-sector training platform was developed to simulate radar-based air traffic control tasks. The purpose of the training device was to provide a vehicle for delivering ATC training on teamwork. However, before training could be delivered it was first necessary to develop training scenarios that would place participants under a specific amount of work. The results of the scenario calibration study reported in this paper suggest that the three scenarios can be viewed as representing low, medium, and high workload conditions based on the performance of 31 four-person teams. Statistically significant performance differences were observed across all three scenarios based on the percentage of aircraft that reached their destination within the allotted time, the amount of aircraft delay, the number of safety errors, and participants' perceptions of their workload.

Author

Air Traffic Control; Training Devices; Low Cost; Evaluation; Fabrication; Calibrating

19990110320 NASA Goddard Space Flight Center, Greenbelt, MD USA

GPS Ocean Reflection Experiment on Spartan 251

Garrison, James L, NASA Goddard Space Flight Center, USA; Russo, Angela, NASA Goddard Space Flight Center, USA; Mickler, Dave, Colorado Univ., USA; Armatys, Michael, Colorado Univ., USA; Ferebee, Melvin J., NASA Langley Research Center, USA; [1999]; 39p; In English; 10N GPS 1999, 4 Sep. 1999, Nashville, TN, USA; No Copyright; Avail: CASI; A03, Hardcopy; A01, Microfiche

It has recently been demonstrated that the GPS signal which has reflected from the ocean surface contains useful geophysical data from which the sea surface wind speed and other parameters can be extracted. This can be used for remote sensing, similar to present day use of radar altimeters or scatterometers, but with significantly smaller instrumentation because of the utilization of the existing GPS broadcast signal for illumination. Several campaigns of aircraft experimentation have been completed demonstrating this technique and reflected GPS data has been reliably collected from 25 km altitude on a balloon. However, there has not yet been a demonstration that the reflected GPS signal can be detected from orbit with sufficient signal to noise ratio (SNR) to make useful remote sensing measurements. A technology demonstration experiment was planned for a Space Shuttle flight in the late 2000 using the Spartan 251 recoverable carrier. This experiment would also have been the first flight validation of the PiVoT GPS receiver developed in house at the Goddard Space Flight Center. The "open-architecture" design of this receiver would allow the software modifications to be made which control code-correlator spacing to map out the shape of the reflected signal waveform, which is the most basic data product generated by this instrumentation. A moderate gain left-hand circularly polarized antenna, constructed from an array of off-the-shelf hemispherical antennas was to be used to give approximately 3 to 6 dB of additional gain. Preliminary SNR predictions have been done indicating that this antenna would offer sufficient gain to record waveform measurements. A system level description of the experiment instrumentation, including the receiver, antenna and data storage and retrieval will be given. The visibility of GPS reflections over the mission duration of several hours will be studied, including the effects of the limited beamwidth of the antenna. Spartan 251 has now been postponed with the earliest opportunity in the year 2002. The results of this study however, have been 2 used to further the define the requirements and expected performance of reflected GPS receivers in orbit. Several other space flight opportunities are being considered based upon this new information.

Author

Global Positioning System; Wind Velocity; Waveforms; Remote Sensing; Ocean Surface; Data Storage

19990111573 NASA Pasadena Office, CA USA

Methods and Apparatus for Reducing Multipath Signal Error Using Deconvolution

Kumar, Rajendra, Inventor, Jet Propulsion Lab., California Inst. of Tech., USA; Lau, Kenneth H., Inventor, Jet Propulsion Lab., California Inst. of Tech., USA; Jun. 29, 1999; In English

Patent Info.: Filed 16 Jan. 1997; NASA-Case-NPO-19602-1-CU; US-Patent-5,918,161; US-Patent-Appl-SN-786356; No Copyright; Avail: US Patent and Trademark Office, Hardcopy

A deconvolution approach to adaptive signal processing has been applied to the elimination of signal multipath errors as embodied in one preferred embodiment in a global positioning system receiver. The method and receiver of the present invention estimates then compensates for multipath effects in a comprehensive manner. Application of deconvolution, along with other adaptive identification and estimation techniques, results in completely novel GPS (Global Positioning System) receiver architecture.

Author

Signal Processing; Errors; Multipath Transmission

19990111743 NASA Langley Research Center, Hampton, VA USA

Investigation of Measurement Errors in Doppler Global Velocimetry

Meyers, James F., NASA Langley Research Center, USA; Lee, Joseph W., NASA Langley Research Center, USA; 1999; 14p; In English; World Aviation Congress and Exposition, 19-21 Oct. 1999, San Francisco, CA, USA; Sponsored by Society of Automotive Engineers, Inc., USA

Report No.(s): SAE-1999-01-5599; Copyright; Avail: Issuing Activity, Hardcopy

While the initial development phase of Doppler Global Velocimetry (DGV) has been successfully completed, there remains a critical next phase to be conducted, namely the determination of an error budget to provide quantitative bounds for measurements obtained by this technology. This paper describes a laboratory investigation that consisted of a detailed interrogation of potential error sources to determine their contribution to the overall DGV error budget. A few sources of error were obvious; e.g., Iodine vapor absorption lines, optical systems, and camera characteristics. However, additional non-obvious sources were also discovered; e.g., laser frequency and single-frequency stability, media scattering characteristics, and interference fringes. This paper describes each identified error source, its effect on the overall error budget, and where possible, corrective procedures to reduce or eliminate its effect.

Author

Error Analysis; Instrument Errors; Velocity Measurement

05
AIRCRAFT DESIGN, TESTING AND PERFORMANCE

Includes aircraft simulation technology. For related information see also 18 Spacecraft Design, Testing and Performance and 39 Structural Mechanics. For land transportation vehicles see 85 Urban Technology and Transportation.

19990110584 NASA Dryden Flight Research Center, Edwards, CA USA

Design Challenges Encountered in a Propulsion-Controlled Aircraft Flight Test Program

Maine, Trindel, NASA Dryden Flight Research Center, USA; Burken, John, NASA Dryden Flight Research Center, USA; Burcham, Frank, NASA Dryden Flight Research Center, USA; Schaefer, Peter, University of Southern California, USA; June 1994; 19p; In English; 30th; Joint Propulsion, 27-29 Jun. 1994, Indianapolis, IN, USA; Sponsored by American Inst. of Aeronautics and Astronautics, USA

Contract(s)/Grant(s): RTOP 505-68-33

Report No.(s): H-2000; AIAA Paper 94-3359; Copyright Waived; Avail: CASI; A03, Hardcopy; A01, Microfiche

The NASA Dryden Flight Research Center conducted flight tests of a propulsion-controlled aircraft system on an F-15 airplane. This system was designed to explore the feasibility of providing safe emergency landing capability using only the engines to provide flight control in the event of a catastrophic loss of conventional flight controls. Control laws were designed to control the flightpath and bank angle using only commands to the throttles. Although the program was highly successful, this paper highlights some of the challenges associated with using engine thrust as a control effector. These challenges include slow engine response time, poorly modeled nonlinear engine dynamics, unmodeled inlet-airframe interactions, and difficulties with ground effect and gust rejection. Flight and simulation data illustrate these difficulties.

Author

Flight Tests; Design Analysis; Propulsion; Flight Control; Control Equipment; Ground Effect (Aerodynamics); Simulation; Thrust

19990110637 McDonnell-Douglas Aerospace, Long Beach, CA USA

Suppressor Nozzle Impact on Aircraft Performance and Design

Mortlock, Alan K., McDonnell-Douglas Aerospace, USA; First NASA/Industry High Speed Research Program Nozzle Symposium; September 1999, pp. 32-1 - 32-7; In English; See also 19990110605; No Copyright; Avail: CASI; A02, Hardcopy; A10, Microfiche

The exhaust nozzle performance of the HSCT engine is an extremely sensitive design parameter for determining the aircraft size to perform to a mission requirement. The acoustic and thrust performance required during takeoff and climb can determine engine size and consequently effect overall aircraft mission performance. During supersonic cruise the noise suppression devices must be stowed in a manner to prevent leakage or blockage in order to achieve the best efficient nozzle conditions.

Author

Sensitivity; Noise Reduction; Design Analysis; Acoustic Properties

19990110676 NASA Dryden Flight Research Center, Edwards, CA USA

A Flying Qualities Study of Longitudinal Long-Term Dynamics of Hypersonic Planes

Cox, Timothy H., NASA Dryden Flight Research Center, USA; Sachs, G., Technische Univ., Germany; Knoll, A., Technische Univ., Germany; Stich, R., Technische Univ., Germany; 19950401; 26p; In English; 6th; International Aerospace Planes and Hypersonics Technologies, 3-7 Apr. 1995, Chattanooga, TN, USA; Sponsored by American Inst. of Aeronautics and Astronautics, USA

Contract(s)/Grant(s): RTOP 466-70-64

Report No.(s): NASA/TM-1999-104308; NAS 1.15:104308; H-2034; No Copyright; Avail: CASI; A03, Hardcopy; A01, Microfiche

The NASA Dryden Flight Research Center and the Technical University of Munich are cooperating in a research program to assess the impact of unstable long-term dynamics on the flying qualities of planes in hypersonic flight. These flying qualities issues are being investigated with a dedicated flight simulator for hypersonic vehicles located at NASA Dryden. Several NASA research pilots have flown the simulator through well defined steady-level turns with varying phugoid and height mode instabilities. The data collected include Pilot ratings and comments, performance measurements, and Pilot workload measurements. The results presented in this paper include design guidelines for height and Phugoid mode instabilities, an evaluation of the tapping method used to measure pilot workload, a discussion of techniques developed by the pilots to control large instabilities, and a discussion of how flying qualities of unstable long-term dynamics influence control Power design requirements.

Author

Flight Characteristics; Hypersonic Aircraft; Oscillations; Longitudinal Stability; Aircraft Stability; Controllability; Longitudinal Control; Flight Simulation

19990111717 California Univ., School of Engineering and Applied Science, Los Angeles, CA USA

Characterization of Materials Degradation due to Corrosion and Fatigue in Aerospace Structures ***Final Report, 15 Apr. 1993 - 14 Oct. 1998***

Mai, A. K.; Yang, J. M.; Ono, K.; May 13, 1999; 17p; In English

Contract(s)/Grant(s): F49620-93-1-0320; AF Proj. 3484

Report No.(s): AD-A364745; No Copyright; Avail: CASI; A03, Hardcopy; A01, Microfiche

Research was carried out in two related areas: (1) the degradation in the load carrying capacity of the structural components, and (2) nondestructive evaluation (NDE) for characterization of the degradation. In the first topic, the effect of pitting corrosion on the strength of aircraft grade aluminum alloys was studied through laboratory tensile and fatigue tests and theoretical modeling. The probability of failure in the presence of multiple pits was found to be strongly affected by certain parameters of the pit distribution. The effect of fatigue and dynamic loading on structural (polymer matrix as well as metal matrix) composites was also studied both theoretically and experimentally. Certain metal matrix composites were found to perform poorly under transverse loads due to stress concentration effects at fiber-matrix debond edges and at microcracks within the interfacial layers. In the second topic, four relatively new ultrasonic NDE techniques were developed. In the first, a guided wave based technique for detecting hidden corrosion sites in aluminum lap joints was developed. This technique has the potential to improve the effectiveness and efficiency of lap joint inspection significantly. Another technique based on a dual transducer pitch-catch arrangement was developed that can be used for cost-effective characterization of composite laminates. A third technique based on dual contact transducers was introduced for the monitoring of the stiffness degradation of composites during fatigue loading. In the fourth technique a guided wave based acoustic emission method was developed for monitoring micro crack growth from corrosion sites in aluminum and from impact load sites in composites. This technique has the potential for use in detecting the presence of hidden corrosion sites at an early stage of their development in metallic aircraft structures and to monitor impact damage in composite aircraft structures.

DTIC

Composite Materials; Composite Structures; Fatigue Tests

19990113114 Army Research Lab., Hampton, VA USA

Evaluation of the Grasshopper Unmanned Aerial Vehicle ***Final Report***

Wilbur, Matthew L., Army Research Lab., USA; October 1999; 20p; In English

Contract(s)/Grant(s): 62211/A47B

Report No.(s): VTD-NR-99-05; No Copyright; Avail: CASI; A03, Hardcopy; A01, Microfiche

This report details the evaluation of small-scale UAV to benefit United States military forces: The future may prove that a Grasshopper-class vehicle like this one is an excellent platform for reconnaissance and surveillance. However, the feasibility of

such a UAV powered by off-the-shelf brushless electric motors and controllers typically used in 'hobby-class' vehicles is minimal at this time due to the technology status of the motors, controllers, and batteries. The motors and the motor controllers utilized during this test program were incapable of converting enough electrical power to generate sufficient thrust to lift a 10 lb vehicle. Based on the results of this program it is clear that if a motor and propeller were identified that could generate sufficient thrust, the battery weight required to drive the system would easily exceed the gross weight of the vehicle. Based on the results of this test effort the following conclusions have been reached: 1)The out-of-ground effect flight condition is the design driver of a Grasshopper-class flight vehicle. A UAV with sufficient thrust to operate out-of-ground effect will easily support in-ground effect flight. 2) The propeller/duct design of this baseline Grasshopper design does not provide an increase in thrust production over that generated by an unducted propeller. Further development of this vehicle will require careful attention to the propeller duct coupling effect. 3) A maximum out-of-ground effect thrust o approximately 1.9 lb is attainable using current technology brushless electric motor/controller systems. This appears to be the upper limit regardless of the propeller design used. 4) The maximum thrust-per-power value, a measure of the efficiency of a motor and propeller is nearly the same regardless of the propeller design used. 5) The primary contributor to poor thrust capability is the lack of sufficient power delivery and/or rotational speed to the propeller -- affected primarily by the motor/controller characteristics.
Author
Evaluation; Pilotless Aircraft; Surveillance; Flight Conditions; Flight Tests

06
AIRCRAFT INSTRUMENTATION

Includes cockpit and cabin display devices; and flight instruments. For related information see also 19 Spacecraft Instrumentation and 35 Instrumentation and Photography.

19990107391 NASA Marshall Space Flight Center, Huntsville, AL USA
1999 Digital Avionics Highlights
Polites, Michael E., NASA Marshall Space Flight Center, USA; [1999]; 1p; In English; No Copyright; Avail: Issuing Activity, Hardcopy; Abstract Only

This article summarizes the highlights of recent events and developments in guidance, navigation, and control in space, aircraft, and weapons. This article is about 1,200 words long. Information for the article was collected from other NASA Centers, DoD, and industry. All information was previously cleared by the originating organizations. Information for the article was also gathered from Aviation Week and Space Technology, and similar sources.
Author
Guidance (Motion); Navigation; Spacecraft Control; Flight Control; Weapons

19990110310 NASA Dryden Flight Research Center, Edwards, CA USA
Flush Airdata Sensing (FADS) System Calibration Procedures and Results for Blunt Forebodies
Cobleigh, Brent R., NASA Dryden Flight Research Center, USA; Whitmore, Stephen A., NASA Dryden Flight Research Center, USA; Haering, Edward A., Jr., NASA Dryden Flight Research Center, USA; Borrer, Jerry, NASA Johnson Space Center, USA; Roback, V. Eric, NASA Langley Research Center, USA; November 1999; 34p; In English; 9th; International Space Planes and Hypersonic Systems and Technologies, 1-5 Nov. 1999, Norfolk, VA, USA
Contract(s)/Grant(s): RTOP 242-33-02-00-23
Report No.(s): NASA/TP-1999-209012; NAS 1.60:209012; H-2379; AIAA Paper 99-4816; No Copyright; Avail: CASI; A03, Hardcopy; A01, Microfiche

Blunt-forebody pressure data are used to study the behavior of the NASA Dryden Flight Research Center flush airdata sensing (FADS) pressure model and solution algorithm. The model relates surface pressure measurements to the airdata state. Spliced from the potential flow solution for uniform flow over a sphere and the modified Newtonian impact theory, the model was shown to apply to a wide range of blunt-forebody shapes and Mach numbers. Calibrations of a sphere, spherical cones, a Rankine half body, and the F-14, F/A-18, X-33, X-34, and X-38 configurations are shown. The three calibration parameters are well-behaved from Mach 0.25 to Mach 5.0, an angle-of-attack range extending to greater than 30 deg, and an angle-of-sideslip range extending to greater than 15 deg. Contrary to the sharp calibration changes found on traditional pitot-static systems at transonic speeds, the FADS calibrations are smooth, monotonic functions of Mach number and effective angles of attack and sideslip. Because the FADS calibration is sensitive to pressure port location, detailed measurements of the actual pressure port locations on the flight

vehicle are required and the wind-tunnel calibration model should have pressure ports in similar locations. The procedure for calibrating a FADS system is outlined.
Author
Calibrating; Detection; Forebodies; Mathematical Models; Pressure Measurement

07
AIRCRAFT PROPULSION AND POWER

Includes prime propulsion systems and systems components, e.g., gas turbine engines and compressors; and onboard auxiliary power plants for aircraft. For related information see also 20 Spacecraft Propulsion and Power, 28 Propellants and Fuels, and 44 Energy Production and Conversion.

19990107334 NASA Dryden Flight Research Center, Edwards, CA USA
Inlet Flow Characteristics During Rapid Maneuvers for an F/A-18A Airplane
Steenken, William G., General Electric Co., USA; Williams, John G., General Electric Co., USA; Walsh, Kevin R., NASA Dryden Flight Research Center, USA; October 1999; 224p; In English
Contract(s)/Grant(s): NAS3-26617; RTOP 505-68-30
Report No.(s): NASA/TM-1999-206587; H-2371; NAS 1.15:206587; No Copyright; Avail: CASI; A10, Hardcopy; A03, Microfiche

The F404-GE-400 engine powered F/A-18A High Alpha Research Vehicle (HARV) was used to examine the characteristics of inlet airflow during rapid aircraft maneuvers. A study of the degree of similarity between inlet data obtained during rapid aircraft maneuvers and inlet data obtained at steady aerodynamic attitudes was conducted at the maximum engine airflow of approximately 145 IBM/sec using a computer model that was generated from inlet data obtained during steady aerodynamic maneuvers. Results show that rapid-maneuver inlet recoveries agreed very well with the recoveries obtained at equivalent stabilized angle-of-attack conditions. The peak dynamic circumferential distortion values obtained during rapid maneuvers agreed within 0.01 units of distortion over the 10 - 38 degree angle of attack range with the values obtained during steady aerodynamic maneuvers while similar agreement was found for the peak dynamic radial distortion values up to 29 degrees angle-of-attack. Exceedences of the rapid-maneuver peak dynamic circumferential distortion values relative to the peak distortion model values at steady attitudes occurred only at low or negative angles of attack and were inconsequential from an engine-stability assessment point of view. The results of this study validate the current industry practice of testing at steady aerodynamic conditions to characterize inlet recovery and peak dynamic distortion levels.
Author
Air Flow; Air Intakes; Flow Characteristics; Research Aircraft; Intake Systems; Inlet Flow

19990109093 NASA Glenn Research Center, Cleveland, OH USA
The Effect of Air Preheat at Atmospheric Pressure on the Formation of NO(x) in the Quick-Mix Sections of an Axially Staged Combustor
Vardakas, M. A., California Univ., USA; Leong, M. Y., California Univ., USA; Brouwer, J., California Univ., USA; Samuelsen, G. S., California Univ., USA; Holdeman, J. D., NASA Glenn Research Center, USA; September 1999; 28p; In English; Original contains color illustrations
Contract(s)/Grant(s): NCC3-412; RTOP 537-02-20
Report No.(s): NASA/TM-1999-209431; E-11872; NAS 1.15:209431; No Copyright; Avail: CASI; A03, Hardcopy; A01, Microfiche

The Rich-burn/Quick-mix/Lean-burn (RQL) combustor concept has been proposed to minimize the formation of nitrogen oxides (NO(x)) in gas turbine systems. The success of this combustor strategy is dependent upon the efficiency of the mixing section bridging the fuel-rich and fuel-lean stages. Note that although these results were obtained from an experiment designed to study an RQL mixer, the link between mixing and NOx signatures is considerably broader than this application, in that the need to understand this link exists in most advanced combustors. The experiment reported herein was designed to study the effects of inlet air temperature on NO(x) formation in a mixing section. The results indicate that NO(x) emission is increased for all preheated cases compared to non-preheated cases. When comparing the various mixing modules, the affect of jet penetration is important, as this determines where NO(x) concentrations peak, and affects overall NO(x) production. Although jet air comprises

70 percent of the total airflow, the impact that jet air preheat has on overall NO(x) emissions is small compared to preheating both main and jet air flow.
Author
Atmospheric Pressure; Nitrogen Oxides; Jet Mixing Flow; Gas Pressure; Combustion Chambers; Gas Heating

19990110574 Rockwell International Corp., Los Angeles Aircraft Div., Los Angeles, CA USA
B-1 AFT Nacelle Flow Visualization Study
Celniker, Robert, Rockwell International Corp., USA; January 1975; 40p; In English
Contract(s)/Grant(s): NAS4-2182
Report No.(s): NASA/CR-1999-127493; NAS 1.26:127493; NA-74-626; No Copyright; Avail: CASI; A03, Hardcopy; A01, Microfiche

A 2-month program was conducted to perform engineering evaluation and design tasks to prepare for visualization and photography of the airflow along the aft portion of the B-1 nacelles and nozzles during flight test. Several methods of visualizing the flow were investigated and compared with respect to cost, impact of the device on the flow patterns, suitability for use in the flight environment, and operability throughout the flight. Data were based on a literature search and discussions with the test personnel. Tufts were selected as the flow visualization device in preference to several other devices studied. A tuft installation pattern has been prepared for the right-hand aft nacelle area of B-1 air vehicle No.2. Flight research programs to develop flow visualization devices other than tufts for use in future testing are recommended. A design study was conducted to select a suitable motion picture camera, to select the camera location, and to prepare engineering drawings sufficient to permit installation of the camera. Ten locations on the air vehicle were evaluated before the selection of the location in the horizontal stabilizer actuator fairing. The considerations included cost, camera angle, available volume, environmental control, flutter impact, and interference with antennas or other instrumentation.
Author
B-1 Aircraft; Nacelles; Flow Visualization; Flight Tests; High Speed Photography; Cameras

19990110605 NASA Glenn Research Center, Cleveland, OH USA
First NASA/Industry High Speed Research Program Nozzle Symposium
Long–Davis, Mary Jo, NASA Glenn Research Center, USA; First NASA/Industry High Speed Research Program Nozzle Symposium; September 1999; 788p; In English; 1st, 17-22 Nov. 1992, Cleveland, OH, USA; See also 19990110606 through 19990110643; Original contains color illustrations
Contract(s)/Grant(s): RTOP 537-05-23
Report No.(s): NASA/CP-1999-209423; E-11937; NAS 1.55:209423; No Copyright; Avail: CASI; A99, Hardcopy; A10, Microfiche

The First High Speed Research (HSR) Nozzle Symposium was hosted by NASA Lewis Research Center on November 17-19, 1992 in Cleveland, Ohio, and was sponsored by the HSR Source Noise Working Group. The purpose of this symposium was to provide a national forum for the government, industry, and university participants in the program to present and discuss important low noise nozzle research results and technology issues related to the development of appropriate nozzles for a commercially viable, environmentally compatible, U.S. High-Speed Civil Transport. The HSR Phase I research program was initiated in FY90 and is approaching the first major milestone (end of FY92) relative to an initial FAR 36 Stage 3 nozzle noise assessment. Significant research results relative to that milestone were presented. The opening session provided a brief overview of the Program and status of the Phase H plan. The next five sessions were technically oriented and highlighted recent significant analytical and experimental accomplishments. The last Session included a panel discussion by the Session Chairs, summarizing the progress seen to date and discussing issues relative to further advances in technology necessary to achieve the Program Goals. Attendance at the Symposium was by invitation only and included only industry, academic, and government participants who are actively involved in the High-Speed Research Program. The technology presented in this meeting is considered commercially sensitive.
Author
Conferences; Low Noise; Nozzle Design; Nozzle Flow; Nozzle Efficiency; Technology Assessment

19990110606 General Electric Co., Aircraft Engines, Cincinnati, OH USA
Aero-Performance and Aero-Mixing Tests of 2D-CD Mixer/Ejector Nozzles, Part 1, Aero-Performance Tests
Askew, J. W., General Electric Co., USA; Yetter, J., General Electric Co., USA; First NASA/Industry High Speed Research Program Nozzle Symposium; September 1999, pp. 3-1 - 3-22; In English; See also 19990110605; No Copyright; Avail: CASI; A03, Hardcopy; A10, Microfiche

The four objectives of the aerodynamic performance test of two-dimensional mixer/ejector nozzles: (1) Establish Aerodynamic Performance Characteristics and Design Criteria of 2D Suppressor Ejector Nozzles For Trade Studies At Take-Off Flight Conditions. (2) Quantify The Effects of Key Geometric And Aerodynamic Variables On Performance. (3) Test and Evaluate Geometric Parameter Variants Consistent With Those of Acoustic Test (e.g. Suppressor Area Ratio). and (4) Obtain Detailed Data That Can Be Used Later For Verifying And Validating CFD Codes For Performance Prediction of 2D Suppressor Ejector Nozzles. Derived from text

Aerodynamic Characteristics; Design Analysis; Performance Tests; Performance Prediction; Data Acquisition

19990110607 General Electric Co., Aircraft Engines, Cincinnati, OH USA

Aero-Performance and Aero-Mixing Tests of 2D-CD Mixer/Ejector Nozzles, Part 2, Sample of Aero-Mixing Test Data and Inference

Mengle, V. G., General Electric Co., USA; Shin, H–W., General Electric Co., USA; Askew, J. W., General Electric Co., USA; Whitfield, C. E., General Electric Co., USA; First NASA/Industry High Speed Research Program Nozzle Symposium; September 1999, pp. 3-23 - 3-35; In English; See also 19990110605; No Copyright; Avail: CASI; A03, Hardcopy; A10, Microfiche

The tests on suppressor/ejector nozzle models conducted in G.E.'s Aerodynamic Research Laboratory (ARL) are supposed to complement the aero-performance tests, reported in Part 1, and the acoustic tests soon to be conducted in G.E.'s Cell 41. In particular, the tests were done with the above three objectives in mind, namely, to improve the understanding of internal and external fluid-dynamics of such nozzles, its aerodynamic characteristics (chute and ram drag etc.) and, to a lesser extent, CFD-code validation. In this brief paper, however, we focus only on the first objective, namely, a better understanding of the flow-field in terms of the internal mixing process and internal shock structures. Moreover, due to brevity of presentation only a limited amount of data is shown to give a flavor of the test results and, hence, only limited conclusions are drawn.

Author

Performance Tests; Performance Prediction; Nozzle Design; Two Dimensional Models; Suppressors; Ejectors

19990110608 General Electric Co., Aircraft Engines, Cincinnati, OH USA

Acoustic and Aero-Mixing Tests of Fluid Shield Nozzles, Part 1, Acoustics

Salikuddin, M., General Electric Co., USA; Brausch, J., General Electric Co., USA; Mengle, V., General Electric Co., USA; First NASA/Industry High Speed Research Program Nozzle Symposium; September 1999, pp. 4-1 - 4-19; In English; See also 19990110605; No Copyright; Avail: CASI; A03, Hardcopy; A10, Microfiche

Environmental acceptability and economic viability are crucial issues in the development of the next generation HSCT (High Speed Civil Transport). Low noise exhaust nozzle technology has significant impact on both these issues. The exhaust system design that meets FAR 36 Stage 3 takeoff acoustic requirements and provides high levels of cruise and transonic performance and adequate takeoff performance at an acceptable weight is essential to the success of any HSCT program.

Author

Acceptability; Economics; Exhaust Nozzles; Exhaust Systems; Low Noise

19990110609 General Electric Co., Aircraft Engines, Cincinnati, OH USA

Acoustic and Aero-Mixing Tests of Fluid Shield Nozzles, Part 2, 2D-Fluid-Shield Nozzle Aero-Mixing Tests

Mengle, V. G., General Electric Co., USA; Shin, H–W., General Electric Co., USA; Whitfield, C., General Electric Co., USA; Wisler, S., General Electric Co., USA; Askew, J., General Electric Co., USA; First NASA/Industry High Speed Research Program Nozzle Symposium; September 1999, pp. 4-21 - 4-28; In English; See also 19990110605; No Copyright; Avail: CASI; A02, Hardcopy; A10, Microfiche

The objective of the fluid-shield nozzle aero-mixing tests being conducted in GE's Aerodynamic Research Laboratory (AR) is to complement the acoustic tests done on such nozzles in GE's Cell 41. The focus is to help understand the fluid-dynamics and the aero-dynamics of such nozzles to improve their performance. In particular, we need a better understanding of: (a) the three-dimensional shock-structures that produce shock-associated noise, (b) the mixing process between the shield-flow, the core-flow, and the ambient flow which affects the fluid-shield evolution and acoustic efficiency, and (c) the pressure distributions on the chutes and the plug which affect the drag. The models in the ARL tests were, however, "two-dimensional" or rectangular in nature and the above figure shows the baseline model layout. It is similar to an if unwrapped" sector of the original round fluid-shield model used in Cell 41 and may also help in the design of future generation 2D fluid-shield nozzles. Shadowgraphs, laser velocimetry, and static pressure tap measurements were the primary tools used and planar laser sheet is planned to be used

in the near future for flow visualization. The LV-system used, namely two-focus laser (L2F), is briefly described in the previous paper. This paper gives a flavor of typical tests results and insights obtained about flows in such nozzles.
Derived from text
Acoustic Measurement; Performance Tests; Aerodynamic Noise; Pressure Measurement; Nozzle Efficiency

19990110610 General Electric Co., Aircraft Engines, Cincinnati, OH USA
GE/Boeing Acoustic Test Axisymmetric Mixer/Ejector Nozzle
Brown, W. H., General Electric Co., USA; Brausch, J. F., General Electric Co., USA; First NASA/Industry High Speed Research Program Nozzle Symposium; September 1999, pp. 5-1 - 5-14; In English; See also 19990110605; No Copyright; Avail: CASI; A03, Hardcopy; A10, Microfiche

Previous studies suggest that the keys to reducing the noise of heated jets are (1) reducing the shear velocity between the jet and the ambient and (2) absorbing as much of the mixing noise as possible before it can propagate to the farfield. Reducing the shear velocity is accomplished in the AMEN concept by the use of suppressor nozzles and ejectors. In the AMEN concept, the ejector entrains ambient air which is mixed with the engine air to reduce the overall velocity. The AMEN nozzle employs a suppressor area ratio greater than previous studies in an attempt to reduce the mixed jet velocity and obtain high levels of noise suppression at high jet velocities. Treatment of the ejector surface further enhances the acoustic performance by absorbing mixing noise before it can propagate to the ground. The suppressor nozzle itself serves two functions: (1) it enhances mixing by providing more shear area between the engine flow and entrained air, and (2) it reduces the characteristic dimension of the nozzle so that the wavelengths of the mixing noise are reduced. The use of a plug provides more surface for acoustic treatment as well as the possibility of using porosity to reduce shock noise within the ejector by wave cancellation off the plug surface. The efficacy of bulk absorbers at two different densities and of two plug surface porosities was evaluated both statically and in simulated flight with both flush and scoop inlets.
Derived from text
Mixers; Ejectors; Nozzle Design; Nozzle Efficiency; Acoustic Properties; Noise Reduction

19990110611 NASA Lewis Research Center, Cleveland, OH USA
Pratt & Whitney Two Dimensional HSR Nozzle Test in the NASA Lewis 9- by 15- Foot Low Speed Wind Tunnel: Aerodynamic Results
Wolter, John D., NASA Lewis Research Center, USA; Jones, Christopher W., Pratt and Whitney Aircraft, USA; First NASA/Industry High Speed Research Program Nozzle Symposium; September 1999, pp. 6-1 - 6-19; In English; See also 19990110605; No Copyright; Avail: CASI; A03, Hardcopy; A10, Microfiche

This paper discusses a test that was conducted jointly by Pratt & Whitney Aircraft Engines and NASA Lewis Research Center. The test was conducted in NASA's 9- by 15-Foot Low Speed Wind Tunnel (9x15 LSWT). The test setup, methods, and aerodynamic results of this test are discussed. Acoustical results are discussed in a separate paper by J. Bridges and J. Marino.
Author
Performance Tests; Two Dimensional Models; Nozzle Geometry

19990110612 NASA Lewis Research Center, Cleveland, OH USA
Pratt & Whitney 2D Model in LeRC 9 ft x 15 ft Acoustics
Bridges, James, NASA Lewis Research Center, USA; Marino, Jodilyn, Pratt and Whitney Aircraft, USA; First NASA/Industry High Speed Research Program Nozzle Symposium; September 1999, pp. 7-1 - 7-21; In English; See also 19990110605; No Copyright; Avail: CASI; A03, Hardcopy; A10, Microfiche

The theory of mixer-ejectors for noise suppression is illustrated in this cartoon. Since jet noise SPL scales as velocity to the eighth power and diameter squared, increasing the jet diameter while lowering its velocity and keeping thrust constant decreases the noise. However, in supersonic craft, the drag penalty for increasing diameter at supersonic cruise makes this option very expensive. One would like to have a large engine during takeoff which could be shrunk during cruise. The retractable ejector is such an expandable engine. If the mixer flow can be expanded to the size of the ejector exit, the noise generated downstream of the ejector will be much less than the small diameter mixer nozzle alone. of course, this also requires that the noise created in expanding the flow to fill the ejector be absorbed by a liner in the ejector walls so that none of this noise is heard. Since this mixing of internal hot gas and external cold air must take place in as short a distance as possible, the mixer must be very effective and therefore probably much noisier than a simple nozzle.
Derived from text
Jet Aircraft Noise; Mixers; Noise Reduction; Two Dimensional Models

19990110613 Boeing Co., Seattle, WA USA

Test Results Boeing NFM Nozzle in LSAF

Nihart, G. L., Boeing Co., USA; First NASA/Industry High Speed Research Program Nozzle Symposium; September 1999, pp. 8-1 - 8-14; In English; See also 19990110605; No Copyright; Avail: CASI; A03, Hardcopy; A10, Microfiche

The 1990 test nozzle was based on a design designated the Near-Fully Mixed (NFM) nozzle. The key features of this nozzle are: (1) 12 aspiration chutes that stay in the flow at all operating conditions. (2) Hinged flaps that change the primary nozzle throat area and expansion ratio. and (3) The flaps close off the aspiration flow at the cruise condition.

Author

Performance Tests; Nozzle Efficiency; Nozzle Design

19990110614 NASA Lewis Research Center, Cleveland, OH USA

Supersonic Jet Mixing Enhancement due to Natural and Induced Screech

Rice, E. J., NASA Lewis Research Center, USA; Raman, G., Sverdrup Technology, Inc., USA; First NASA/Industry High Speed Research Program Nozzle Symposium; September 1999, pp. 9-1 - 9-15; In English; See also 19990110605; No Copyright; Avail: CASI; A03, Hardcopy; A10, Microfiche

Outline of presentation are: (1) Review of experimental apparatus. (2) Effect of natural screech of jet mixing; converging nozzle, underexpanded jet and converging-diverging nozzle, design pressure.(3) Effect of induced screech on jet mixing: produced by paddles in shear layers, similar to edge tones, and converging-diverging nozzle, design pressure. (4) Effect of paddles on near-field jet noise. and (5) Concluding remarks.

Author

Screech Tones; Convergent-Divergent Nozzles; Jet Aircraft Noise; Jet Mixing Flow; Nozzle Design; Combustion Stability

19990110615 NASA Lewis Research Center, Cleveland, OH USA

Mixing Enhancement in Supersonic Jets by Delta-Tabs

Zaman, K. B. M. Q., NASA Lewis Research Center, USA; First NASA/Industry High Speed Research Program Nozzle Symposium; September 1999, pp. 10-1 - 10-19; In English; See also 19990110605; No Copyright; Avail: CASI; A03, Hardcopy; A10, Microfiche

The investigation includes carry out fundamental experiments studying mechanisms of effect: (1) experiments on subsonic and supersonic jets to assess influence of compressibility, (2) parametric study on tab geometry to optimize effect for given flow blockage (this effort led to ”delta-tab”), (3) quantify mixing enhancement in the jet, and (4) analyze mechanism of streamwise vorticity generation.

Author

Compressibility; Experimentation; Subsonic Flow; Supersonic Jet Flow; Vorticity

19990110616 Georgia Inst. of Tech., Atlanta, GA USA

Vibrating Splitter Insert to Enhance Mixing and Reduce Supersonic Jet Noise

Ahuja, Krish K., Georgia Inst. of Tech., USA; First NASA/Industry High Speed Research Program Nozzle Symposium; September 1999, pp. 11-1 - 11-26; In English; See also 19990110605; No Copyright; Avail: CASI; A03, Hardcopy; A10, Microfiche

A number of concepts of reducing supersonic jet noise have recently been tested using small-scale nozzles at Georgia Tech Research Institute by the author. One of them included a coaxial rectangular nozzle. Both nozzles had an equivalent diameter of 2 inches. This configuration provides considerable reduction in noise and also some control on the noise directivity. (See DGLR/AIAA 92-02-127: ”Supersonic Jet Noise Reduction by Coaxial Rectangular Nozzles,” by K. K. Ahuja, J. Manes, and K. Massey.) It is shown in this presentation, that the inner nozzle can be replaced by splitter plates (inserts) that provide even further noise reduction at supersonic conditions through enhanced mixing.

Author

Noise Reduction; Supersonic Jet Flow; Nozzle Design

19990110618 University of Southern California, Dept. of Aerospace Engineering, Los Angeles, CA USA

Application of a Flip-Flop Nozzle on Plume Mixing Enhancement

Schreck, Stefan, University of Southern California, USA; Michaelian, Mark, University of Southern California, USA; Ho, Chih–Ming, California Univ., USA; First NASA/Industry High Speed Research Program Nozzle Symposium; September 1999, pp. 13-1 - 13-15; In English; See also 19990110605

Contract(s)/Grant(s): NAG1-1096; No Copyright; Avail: CASI; A03, Hardcopy; A10, Microfiche

Mach wave radiation is a major source of noise in high speed jets. It is created by turbulent eddies which travel at supersonic speed within the shear layer of the jet. Downstream of the potential core, the convection speed of the eddies decays and noise production is reduced. Once the convection speeds drops below the speed of sound, eddy Mach wave radiation ceases. Mach wave radiation may be reduced by shortening the core length of the jet. This requires a faster growth of the shear layer, i.e. enhanced mixing in the jet. We investigated the possibility of mixing enhancement by the excitation of the instability waves in a supersonic rectangular jet.
Author
Flip-Flops; Nozzle Design; Augmentation; Electromagnetic Radiation; Mach Number; Sound Waves; Supersonic Jet Flow; Vortices

19990110619 NASA Langley Research Center, Hampton, VA USA
Effect of Swirl on Noise from a High Aspect Ratio Rectangular Nozzle
Ponton, M. K., NASA Langley Research Center, USA; Seiner, J. M., NASA Langley Research Center, USA; Mitchell, L. K., NASA Langley Research Center, USA; First NASA/Industry High Speed Research Program Nozzle Symposium; September 1999, pp. 14-1 - 14-15; In English; See also 19990110605; No Copyright; Avail: CASI; A03, Hardcopy; A10, Microfiche

Based on extensive work performed by Dr. Thomas H. Sobota (Advanced Projects Research Incorporated (APRI)) on swirling flows in circular-to-rectangular transition sections, a model assembly was designed and fabricated in support of a Phase 1 Small Business Innovation Research Contract between the NASA-Langley Research Center and APRI. This assembly was acoustically tested as part of this Phase 1 effort, the goal being to determine whether the controlled introduction of axial vorticity could affect the various noise generation mechanisms present in an underexpanded supersonic rectangular jet.
Author
Fabrication; Design Analysis; Models; Acoustic Sounding; Performance Tests; Ductile-Brittle Transition

19990110620 NASA Langley Research Center, Hampton, VA USA
Application Focused Schlieren to Nozzle Ejector Flowfields
Mitchell, L. Kerry, NASA Langley Research Center, USA; Ponton, Michael K., NASA Langley Research Center, USA; Seiner, John M., NASA Langley Research Center, USA; Manning, James C., NASA Langley Research Center, USA; Jansen, Bernard J., Lockheed Engineering and Sciences Co., USA; Lagen, Nicholas T., Lockheed Engineering and Sciences Co., USA; First NASA/Industry High Speed Research Program Nozzle Symposium; September 1999, pp. 15-1 - 15-14; In English; See also 19990110605; No Copyright; Avail: CASI; A03, Hardcopy; A10, Microfiche

The motivation of the testing was to reduce noise generated by eddy Mach wave emission via enhanced mixing in the jet plume. This was to be accomplished through the use of an ejector shroud, which would bring in cooler ambient fluid to mix with the hotter jet flow. In addition, the contour of the mixer, with its chutes and lobes, would accentuate the merging of the outer and inner flows. The objective of the focused schlieren work was to characterize the mixing performance inside of the ejector. Using flow visualization allowed this to be accomplished in a non-intrusive manner.
Author
Flow Distribution; Jet Flow; Noise Reduction; Nonintrusive Measurement; Plumes; Performance Tests

19990110621 NASA Lewis Research Center, Cleveland, OH USA
PARC Analysis of the NASA/GE 2D NRA Mixer/Ejector Nozzle
DeBonis, J. R., NASA Lewis Research Center, USA; First NASA/Industry High Speed Research Program Nozzle Symposium; September 1999, pp. 16-1 - 16-32; In English; See also 19990110605; No Copyright; Avail: CASI; A03, Hardcopy; A10, Microfiche

Interest in developing a new generation supersonic transport has increased in the past several years. Current projections indicate this aircraft would cruise at approximately Mach 2.4, have a range of 5000 nautical miles and carry at least 250 passengers. A large market for such an aircraft will exist in the next century due to a predicted doubling of the demand for long range air transportation by the end of the century and the growing influence of the Pacific Rim nations. Such a proposed aircraft could more than halve the flying time from Los Angeles to Tokyo. However, before a new economically feasible supersonic transport can be built, many key technologies must be developed. Among these technologies is noise suppression. Propulsion systems for a supersonic transport using current technology would exceed acceptable noise levels. All new aircraft must satisfy FAR 36 Stage III noise regulations. The largest area of concern is the noise generated during takeoff. A concerted effort under NASA's High Speed Research (HSR) program has begun to address the problem of noise suppression. One of the most promising concepts being

studied in the area of noise suppression is the mixer/ejector nozzle. This study analyzes a typical noise suppressing mixer ejector nozzle at take off conditions, using a Full Navier-Stokes (FNS) computational fluid dynamics (CFD) code.
Author
Ejectors; Mixers; Noise Intensity; Noise Reduction; Propulsion System Configurations; Supersonic Transports

19990110622 United Technologies Research Center, East Hartford, CT USA
Analysis of a Second Generation Mixer-Ejector Exhaust System
Barber, T. J., United Technologies Research Center, USA; LaBarre, R. E., United Technologies Research Center, USA; Chiappetta, L. M., United Technologies Research Center, USA; First NASA/Industry High Speed Research Program Nozzle Symposium; September 1999, pp. 17-1 - 17-35; In English; See also 19990110605; Original contains color illustrations; No Copyright; Avail: CASI; A03, Hardcopy; A10, Microfiche

Analysis Background, Grid Generation Approach, Navier-Stokes Analysis Approach, and Discussion of Results are outlined. This presentation will describe previous approaches for analyzing mixer-type nozzle geometries. A key reason preventing a complete numerical solution has been short-coming in grid generation. A new grid generation procedure will be described and Navier-Stokes solutions obtained using such a grid will be presented. Finally, comparisons with experimental data measured in the NASA Lewis RC 9 by 12 tunnel will be presented.
Author
Systems Analysis; Grid Generation (Mathematics); Exhaust Systems; Ejectors

19990110623 NASA Lewis Research Center, Cleveland, OH USA
PAR Analysis of HSR Nozzles
Georgiadis, Nicholas J., NASA Lewis Research Center, USA; First NASA/Industry High Speed Research Program Nozzle Symposium; September 1999, pp. 18-1 - 18-21; In English; See also 19990110605; No Copyright; Avail: CASI; A03, Hardcopy; A10, Microfiche

Only recently has computational fluid dynamics (CFD) been relied upon to predict the flow details of advanced nozzle concepts. Computer hardware technology and flow solving techniques are advancing rapidly and CFD is now being used to analyze such complex flows. Validation studies are needed to assess the accuracy, reliability, and cost of such CFD analyses. At NASA Lewis, the PARC2D/3D full Navier-Stokes (FNS) codes are being applied to HSR-type nozzles. This report presents the results of two such PARC FNS analyses. The first is an analysis of the Pratt and Whitney 2D mixer-ejector nozzle, conducted by Dr. Yunho Choi (formerly of Sverdrup Technology-NASA Lewis Group). The second is an analysis of NASA-Langley's axisymmetric single flow plug nozzle, conducted by the author.
Author
Axisymmetric Flow; Plug Nozzles; Computer Programs; Nozzle Design

19990110624 Science Applications International Corp., Fort Washington, PA USA
Status on Numerical Computation of Supersonic Jet Plumes
Dash, Sanford M., Science Applications International Corp., USA; First NASA/Industry High Speed Research Program Nozzle Symposium; September 1999, pp. 19-1 - 19-45; In English; See also 19990110605; No Copyright; Avail: CASI; A03, Hardcopy; A10, Microfiche

This paper will provide an overview of our status to predict the structure of supersonic jet plumes as relevant to noise suppression research for the High-Speed Civil Transport (HSCT) program. Topics to be discussed will include: the CFD codes utilized; advances made in turbulence modeling; an ability to analyze complex flows; and, the present utility of unsteady flow simulations.
Author
Supersonic Jet Flow; Plumes; Noise Reduction; Simulation; Turbulence Models

19990110625 Ohio State Univ., Columbus, OH USA
Analysis of Numerical Methods for Application to Jet Noise Problems
Scott, J. N., Ohio State Univ., USA; First NASA/Industry High Speed Research Program Nozzle Symposium; September 1999, pp. 20-1 - 20-24; In English; See also 19990110605; No Copyright; Avail: CASI; A03, Hardcopy; A10, Microfiche

Contents include the following: (1) Review results of Navier-Stokes solutions of unsteady jet flow. (2) Analysis of numerical methods using solutions of model problems. (3) Stability and accuracy analysis: viscous Burgers equation. and (4) Propagation of acoustic disturbances: linearized Euler equations.
Derived from text
Numerical Analysis; Jet Aircraft Noise; Unsteady Flow; Accuracy

19990110638 NASA Lewis Research Center, Cleveland, OH USA
Assessment of Integrated Nozzle Performance
Lambert, H. H., NASA Lewis Research Center, USA; Mizukami, M., NASA Lewis Research Center, USA; First NASA/Industry High Speed Research Program Nozzle Symposium; September 1999, pp. 33-1 - 33-19; In English; See also 19990110605; No Copyright; Avail: CASI; A03, Hardcopy; A10, Microfiche

This presentation highlights the activities that researchers at the NASA Lewis Research Center (LeRC) have been and will be involved in to assess integrated nozzle performance. Three different test activities are discussed. First, the results of the Propulsion Airframe Integration for High Speed Research 1 (PAIHSR1) study are presented. The PAIHSR1 experiment was conducted in the LeRC 9 ft x l5 ft wind tunnel from December 1991 to January 1992. Second, an overview of the proposed Mixer/ejector Inlet Distortion Study (MIDIS-E) is presented. The objective of MIDIS-E is to assess the effects of applying discrete disturbances to the ejector inlet flow on the acoustic and aero-performance of a mixer/ejector nozzle. Finally, an overview of the High-Lift Engine Aero-acoustic Technology (HEAT) test is presented. The HEAT test is a cooperative effort between the propulsion system and high-lift device research communities to assess wing/nozzle integration effects. The experiment is scheduled for FY94 in the NASA Ames Research Center (ARC) 40 ft x 80 ft Low Speed Wind Tunnel (LSWT).
Author
Acoustic Properties; Aerodynamic Noise; Engine Tests; High Temperature Tests; Inlet Flow; Nozzle Efficiency; Experimentation

19990110639 NASA Langley Research Center, Hampton, VA USA
High Temperature Acoustic Liner Technology
Parrott, Tony L., NASA Langley Research Center, USA; Jones, Michael G., Lockheed Engineering and Sciences Co., USA; Posey, Joe W., NASA Langley Research Center, USA; First NASA/Industry High Speed Research Program Nozzle Symposium; September 1999, pp. 34-1 - 34-17; In English; See also 19990110605; No Copyright; Avail: CASI; A03, Hardcopy; A10, Microfiche

This paper describes work currently in progress at Langley on liner concepts that employ structures that may be suitable for broadband exhaust noise attenuation in high speed flow environments and at elevated temperatures characteristic of HSCT applications. Because such liners will need to provide about 10 dB suppression over a 2 to 3 octave frequency range, conventional single-degree-of-freedom resonant structures will not suffice. Bulk absorbers have the needed broadband absorption characteristic; however, at lower frequencies they tend to be inefficient.
Author
Noise Reduction; High Speed; Broadband; Exhaust Nozzles; High Temperature

19990110640 NASA Lewis Research Center, Cleveland, OH USA
Exhaust Nozzle Materials Development for the High Speed Civil Transport
Grady, J. E., NASA Lewis Research Center, USA; First NASA/Industry High Speed Research Program Nozzle Symposium; September 1999, pp. 35-1 - 35-21; In English; See also 19990110605; No Copyright; Avail: CASI; A03, Hardcopy; A10, Microfiche

The USA has embarked on a national effort to develop the technology necessary to produce a Mach 2.4 High Speed Civil Transport (HSCT) for entry into service by the year 2005. The viability of this aircraft is contingent upon its meeting both economic and environmental requirements. Two engine components have been identified as critical to the environmental acceptability of the HSCT. These include a combustor with significantly lower emissions than are feasible with current technology, and a lightweight exhaust nozzle that meets community noise standards. The Enabling Propulsion Materials (EPM) program will develop the advanced structural materials, materials fabrication processes, structural analysis and life prediction tools for the HSCT combustor and low noise exhaust nozzle. This is being accomplished through the coordinated efforts of the NASA Lewis Research Center, General Electric Aircraft Engines and Pratt & Whitney. The mission of the EPM Exhaust Nozzle Team is to develop and demonstrate this technology by the year 1999 to enable its timely incorporation into HSCT propulsion systems.
Author
Technology Assessment; Aircraft Engines; Engine Design; Combustion Chambers; Exhaust Nozzles; Fabrication; Propulsion System Performance

19990110693 DYNACS Engineering Co., Inc., Brook Park, OH USA

SiC/SiC Leading Edge Turbine Airfoil Tested Under Simulated Gas Turbine Conditions ***Final Report***

Robinson, R. Craig, DYNACS Engineering Co., Inc., USA; Hatton, Kenneth S., AlliedSignal Composites, Inc., USA; September 1999; 16p; In English; 23rd; Composites, Materials and Structures, 25-29 Jan. 1999, Cocoa Beach, FL, USA; Sponsored by American Ceramic Society, USA

Contract(s)/Grant(s): SAA3-145; RTOP 505-23-2F

Report No.(s): NASA/CR-1999-209314; E-11919; NAS 1.26:209314; No Copyright; Avail: CASI; A03, Hardcopy; A01, Microfiche

Silicon-based ceramics have been proposed as component materials for use in gas turbine engine hot-sections. A high pressure burner rig was used to expose both a baseline metal airfoil and ceramic matrix composite leading edge airfoil to typical gas turbine conditions to comparatively evaluate the material response at high temperatures. to eliminate many of the concerns related to an entirely ceramic, rotating airfoil, this study has focused on equipping a stationary metal airfoil with a ceramic leading edge insert to demonstrate the feasibility and benefits of such a configuration. Here, the idea was to allow the SiC/SiC composite to be integrated as the airfoil's leading edge, operating in a "free-floating" or unrestrained manner. and provide temperature relief to the metal blade underneath. The test included cycling the airfoils between simulated idle, lift, and cruise flight conditions. In addition, the airfoils were air-cooled, uniquely instrumented, and exposed to the same internal and external conditions, which included gas temperatures in excess of 1370 C (2500 F). Results show the leading edge insert remained structurally intact after 200 simulated flight cycles with only a slightly oxidized surface. The instrumentation clearly suggested a significant reduction (approximately 600 F) in internal metal temperatures as a result of the ceramic leading edge. The object of this testing was to validate the design and analysis done by Materials Research and Design of Rosemont, PA and to determine the feasibility of this design for the intended application.

Author

Silicon; Leading Edges; Airfoils; Gas Turbine Engines; Design Analysis

08
AIRCRAFT STABILITY AND CONTROL

Includes aircraft handling qualities; piloting; flight controls; and autopilots. For related information see also 05 Aircraft Design, Testing and Performance.

19990110571 National Aerospace Lab., Tokyo, Japan

Anti-Symmetric Mode Flutter of Winged Reentry Space Vehicle

Kanda, A., National Aerospace Lab., Japan; Ueda, T., National Aerospace Lab., Japan; December 1997; 30p; In Japanese

Report No.(s): PB99--127722; NAL/TR-1342; Copyright Waived; Avail: Issuing Activity (Natl Technical Information Service (NTIS)), Microfiche

The reentry winged space vehicle 'HOPE' projects is proceeding. HOPE has a tip-fin wing which forms a non-planar wing. Anti-symmetric mode flutter experiments were conducted on a similar configuration model to HOPE by using the sting supporting system in which the rolling mode can be controlled in a transonic wind tunnel (NAL). Several flutter points have been obtained for a single model. The results of the experiments and those of the analysis by DPM (Doublet-Point Method) are compared. The comparison shows good agreement in the subsonic region. In the supersonic region, however, the experimental flutter speed rise considerably, making the analytical results conservative. It has a tendency to agree again as the Mach number increases.

NTIS

Flutter Analysis; Reentry Vehicles; Aerodynamic Forces; Wing Profiles; Wind Tunnel Tests; Transonic Flow; Hope Aerospace Plane

19990111735 NASA Langley Research Center, Hampton, VA USA

Advanced Aerodynamic Control Effectors

Wood, Richard M., NASA Langley Research Center, USA; Bauer, Steven X. S., NASA Langley Research Center, USA; 1998; 14p; In English; 1999 World Aviation Congress, 19-21 Oct. 1999, San Francisco, CA, USA; Sponsored by Society of Automotive Engineers, Inc.

Report No.(s): SAE-1999-01-5619; Copyright; Avail: Issuing Activity, Hardcopy

A 1990 research program that focused on the development of advanced aerodynamic control effectors (AACE) for military aircraft has been reviewed and summarized. Data are presented for advanced planform, flow control, and surface contouring technologies. The data show significant increases in lift, reductions in drag, and increased control power, compared to typical

aerodynamic designs. The results presented also highlighted the importance of planform selection in the design of a control effector suite. Planform data showed that dramatic increases in lift (> 25%) can be achieved with multiple wings and a sawtooth forebody. Passive porosity and micro drag generator control effector data showed control power levels exceeding that available from typical effectors (moving surfaces). Application of an advanced planform to a tailless concept showed benefits of similar magnitude as those observed in the generic studies.
Author
Aerodynamics; Control Equipment; Planforms; End Effectors

09
RESEARCH AND SUPPORT FACILITIES (AIR)

Includes airports, hangars and runways; aircraft repair and overhaul facilities; wind tunnels; shock tubes; and aircraft engine test stands. For related information see also 14 Ground Support Systems and Facilities (Space).

19990109636 Institute for Human Factors TNO, Soesterberg, Netherlands
The Use of Simulators for Training and Instruction ***Interim Report Het gebruik van simulatoren voor training en instructie***
Verstegen, D. M. L., Institute for Human Factors TNO, Netherlands; Barnard, Y. F., Institute for Human Factors TNO, Netherlands; van Rooij, J. C. G. M., Institute for Human Factors TNO, Netherlands; Apr. 12, 1999; 64p; In English
Contract(s)/Grant(s): B98-052; TNO Proj. 730.1
Report No.(s): TD-99-0029; TM-99-B0003; Copyright; Avail: Issuing Activity, Hardcopy

Advanced Learning Systems, such as simulators, have great potential for education. Simulators can provide opportunities for training when learning tasks on the real system is impossible, too dangerous or too expensive. Furthermore, it is possible to build in instructional facilities, e.g. to provide feedback and to register performance (automatically), which are usually not available on the real system. The difficulty level of exercises can be controlled and adapted to the needs of individual students. The current use of training simulators is described, in the form of an analysis of the results of field visits to 39 military training simulators. The results show that the possibilities of simulators are at present not used to their full extent. Especially facilities for instructor support, for feedback, assessment and performance registration, are often poor or lacking. Apparently, not much attention and resources are spent on the design of instructional facilities. It is argued that specifications for training simulators should be derived from the training objectives it should cover, i.e. the tasks that will be trained with it. Issues that should be addressed include: simulator coverage, integration in overall training, adaptation to target groups of trainees and to the needs of individual trainees, instruction, guidance and feedback, assessment of trainees, quality assurance and evaluation of training, adaptation of training and/or scenarios, instructor support and lay down specifications and the specification process. Further research will be oriented towards methodologies to develop training simulator specifications.
Author
Training Simulators; Learning; Education; Training Evaluation

19990109651 Institute for Human Factors TNO, Soesterberg, Netherlands
Effects of Asymmetric Delays on Task Performance in Networked Simulators ***Interim Report Effecten van Asymmetrische Vertragingen op de Taakprestatie in Genetwerkte Simulatoren***
deVries, S. C., Institute for Human Factors TNO, Netherlands; Kappe, B., Institute for Human Factors TNO, Netherlands; Aug. 19, 1999; 42p; In English
Contract(s)/Grant(s): A96/KL/354; TNO Proj. 730.3
Report No.(s): TD-99-0333; TNO-TM-99-A056; Copyright; Avail: Issuing Activity, Hardcopy

Distributed Interactive Simulation (DIS) is a collection of protocols used to connect various simulators. DIS is not free of complications because those simulators may be quite heterogeneous and geographically dispersed. Important are the effects of delays, which are encountered in several ways in the context of DIS. Also notable are the effects of the low update rate. A preceding experiment examined how the effects of delays within and between simulators influenced the group performance resulting in guidelines which specified maximum allowable delays. The current experiment was performed to answer questions around non-linear interactions between internal and external delays found in the preceding experiment. A consequence of these interactions might be that the performance of combinations of fast and slow simulators could be disproportionally determined by the level of the slower simulators. Additionally, using an improved version of the experiment, the implications of a mathematical model were studied. This study suggested that a certain amount of internal delay may be beneficial in the presence of external delays. The results of the experiment showed that the performance of a heterogeneous ensemble of simulators is not worse than the performance of a homogeneous ensemble with comparable internal delays. All performance measures depended linearly on

the delay values and no interaction between the factors internal and external delay was found. The report concludes with a few modified guidelines.
Author
Asymmetry; Distributed Interactive Simulation; Mathematical Models; Simulators

19990109657 Institute for Human Factors TNO, Soesterberg, Netherlands
The Specification of Training Simulators and Other Advanced Training Means ***Final Report De Specificatie van Geavanceerde Onderwijsleermiddelen***
Verstegen, D. M. L., Institute for Human Factors TNO, Netherlands; Barnard, Y. F., Institute for Human Factors TNO, Netherlands; vanRooij, J. C. G. M., Institute for Human Factors TNO, Netherlands; Jun. 07, 1999; 42p; In Dutch
Contract(s)/Grant(s): A98/KL/368; TNO Proj. 730.3
Report No.(s): TD-99-0050; TNO-TM-99-A044; Copyright; Avail: Issuing Activity, Hardcopy

More and more the Royal Netherlands Army uses advanced training means, such as Computer Based Training, simulations and simulators. The specification, development and/or acquisition of these training systems is, however, a bottleneck. Existing procedures and guidelines are not specifically oriented toward these advanced training system, and do not offer sufficient support in this area. The goal of this project is to identify suitable methods and tools and to integrate them in the organizational structure and the current acquisition procedures. This report describes the results of the first phase of the project: the current acquisition process is analysed and problems are identified. Subsequently a number of existing methods and tools for support in this area are described and evaluated: MASTER, BOOT, COMAID, ELSTAR (all results of TNO projects), the commercial software package Designer's Edge and GOOS, the tool that is currently used by the Royal Netherlands Army to develop syllabi. None of these methods and tools fulfills all the criteria. They offer support for specific domains or for parts of the acquisition process, but they are still isolated and are -except for GOOS- not yet used by the Royal Netherlands Army. In the subsequent workpackages of this project we will try to integrate some of these methods and tools, and to combine their strengths to provide sufficient support for the specification and acquisition of advanced training means. At this moment the lack of support is most evident in the first phase of the acquisition process, where a needs statement has to be written and a first estimation of the costs has to be made in order to claim budget. Therefore, we will focus on this phase initially.
Author
Training Simulators; Specifications; Education; Applications Programs (Computers)

19990110470 NYMA, Inc., Brook Park, OH USA
Flow Quality Measurements in an Aerodynamic Model of NASA Lewis' Icing Research Tunnel ***Final Report***
Canacci, Victor A., NYMA, Inc., USA; Gonsalez, Jose C., NYMA, Inc., USA; January 1999; 20p; In English; 31st; Joint Propulsion, 10-12 Jul. 1995, San Diego, CA, USA; Sponsored by American Inst. of Aeronautics and Astronautics, USA
Contract(s)/Grant(s): NAS3-27186; RTOP 523-91-13
Report No.(s): NASA/CR-1999-202353; E-10790; NAS 1.26:202353; No Copyright; Avail: CASI; A03, Hardcopy; A01, Microfiche

As part of an on-going effort to improve the aerodynamic flow characteristics of the Icing Research Tunnel (IRT), a C, C, modular scale model of the facility was fabricated. This 1/10th-scale model was used to gain further understanding of the C C, flow characteristics in the IRT. The model was outfitted with instrumentation and data acquisition systems to determine pressures, velocities, and flow angles in the settling chamber and test section. Parametric flow quality studies involving L, the insertion and removal of a model of the IRT's distinctive heat exchanger (cooler) and/or of a honeycomb in the settling chamber were performed. These experiments illustrate the resulting improvement or degradation in flow quality.
Author
Aerodynamic Characteristics; Honeycomb Structures; Ice Formation; Heat Exchangers; Flow Characteristics; Degradation; Coolers

19990110575 NASA Ames Research Center, Moffett Field, CA USA
Overview of the NASA AMES-Dryden Integrated Test Facility
Mackall, Dale, NASA Ames Research Center, USA; McBride, David, NASA Ames Research Center, USA; Cohen, Dorothea, NASA Ames Research Center, USA; May 1990; 17p; In English; 36th ASD/TMD Proceedings, 7-10 May 1990, Denver, CO, USA
Contract(s)/Grant(s): RTOP 505-68-27
Report No.(s): NASA/TM-1999-101720; NAS 1.15:101720; H-1596; No Copyright; Avail: CASI; A03, Hardcopy; A01, Microfiche

The Integrated Test Facility (ITF), being built at the NASA Ames Research Center's Dryden Flight Research Facility (ADFRF), will provide new real-time test capabilities for emerging research aircraft. An overview of the ITF and the real-time systems being developed to operate this unique facility are outlined in this paper. The ITF will reduce flight test risk by minimizing the difference between the flight- and ground-test environments. The ground-test environment is provided by combining real-time flight simulation with the actual aircraft. The generic capabilities of the ITF real-time systems, the real-time data recording, and the remotely augmented vehicle (RAV) monitoring system will be discussed. The benefits of applying simulation to aircraft-in-the-loop testing and RAV monitoring system capabilities to the X-29A flight research program will also be discussed.
Author
Computerized Simulation; Test Facilities; Data Recording; Ground Tests; Flight Simulators; Flight Simulation; X-29 Aircraft; Real Time Operation

19990110641 NASA Lewis Research Center, Cleveland, OH USA
LeRC NATR Free-Jet Development
Long–Davis, M., NASA Lewis Research Center, USA; Cooper, B. A., NASA Lewis Research Center, USA; First NASA/Industry High Speed Research Program Nozzle Symposium; September 1999, pp. 36-1 - 36-23; In English; See also 19990110605; No Copyright; Avail: CASI; A03, Hardcopy; A10, Microfiche

The Nozzle Acoustic Test Rig (NATR) was developed to provide additional test capabilities at Lewis needed to meet HSR program goals. The NATR is a large f ree-jet facility (free-jet diameter = 53 in.) with a design Mach number of 0.3. It is located inside a geodesic dome, adjacent to the existing Powered Lift Facility (PLF). The NATR allows nozzle concepts to be acoustically assessed for far-field (approximately 50 feet) noise characteristics under conditions simulating forward flight. An ejector concept was identified as a means of supplying the required airflow for this free-jet facility. The primary stream is supplied through a circular array of choked nozzles and the resulting low pressure in the constant, annular- area mixing section causes a "pumping" action that entrains the secondary stream. The mixed flow expands through an annular diffuser and into a plenum chamber. Once inside the plenum, the flow passes over a honeycomb/screen combination intended to remove large disturbances and provide uniform flow. The flow accelerates through an elliptical contraction section where it achieves a free-jet Mach number of up to 0.3.
Author
Noise Measurement; Simulation; Research Facilities; Fabrication; Honeycomb Structures; Air Flow

19990111450 Kyushu Univ., Faculty of Engineering, Fukuoka, Japan
Technology Reports of Kyushu University, Volume 71
Nov. 06, 1998; ISSN 0023-2718; 56p; In Japanese; See also 19990111451 through 19990111452; No Copyright; Avail: CASI; A04, Hardcopy; A01, Microfiche

Contents include the following: A study of the catalytically stabilized thermal reactor. Supersonic combustion wind tunnel facility.
CASI
Research; Catalytic Activity; Supersonic Combustion

19990111452 Kyushu Univ., Faculty of Engineering, Fukuoka, Japan
Supersonic Combustion Wind Tunnel Facility
Inokuchi, Yuzo, Kyushu Univ., Japan; Sumi, Takahiro, Kyushu Univ., Japan; Mito, Ryousuke, Kyushu Univ., Japan; Murakami, Tsutomu, Kyushu Univ., Japan; Gonda, Hiroyuki, Kyushu Univ., Japan; Matsumoto, Kentaro, Kyushu Univ., Japan; Yamasaki, Nobuhiko, Kyushu Univ., Japan; Namba, Masanobu, Kyushu Univ., Japan; Technology Reports of Kyushu University; Nov. 06, 1998; Volume 71, No. 6, pp. 567-574; In Japanese; See also 19990111450; No Copyright; Avail: CASI; A02, Hardcopy; A01, Microfiche

The paper presents an overview. design strategy, details of components and performance of the newly built supersonic combustion wind tunnel. This blowdown type wind tunnel has a vitiation heater to simulate the scramjet engine combustor. Total temperature, total pressure and static pressure measured at the test section are 1300 K, 0.04 MPa, and 0.04 MPa. respectively. The mach number calculated from the measured total/static pressure ratio is 2.0, which equals exactly to the design value. Non-uniformities of measured pressure and temperature are within 5% of their space-mean value, which can be regarded as uniform enough for the supersonic combustion experimental research. The wind tunnel is capable of realizing a steady state operation of 10 seconds required for PLIF measurement of supersonic combustion field.
Author
Blowdown Wind Tunnels; Design Analysis; Performance Prediction

19990111544 University of Southern Illinois, Carbondale, IL USA

Planning for New Primary Airports in the USA: A Survey of Metropolitan Planning Organizations

NewMeyer, David A., University of Southern Illinois, USA; Journal of Air Transportation World Wide; 1999; Volume 4, No. 2, pp. 49-65; In English; See also 19990111540; Copyright; Avail: Issuing Activity, Hardcopy

Airport congestion at primary airports in major metropolitan areas was analyzed in a report prepared by the Transportation Research Board (TRB) in 1990. Taking the top twenty-three most congested airports from this study, a questionnaire was prepared and sent to the metropolitan planning organizations (MPOS) for twenty of the twenty-three metropolitan areas represented in the TRB study. The questionnaire focused on the role of the MPOs in planning for new primary airports in the USA, including questions about the status of the most recent MPO airport system plan, whether or not the latest plan recommends a new primary airport, and whether or not any other entities in the MPO areas are recommending new primary airports. The results indicated that 44.4 percent of the eighteen respondent MPOs have airport system plans that are five years old or older. Also, only two of the respondent MPOs have recommended a new primary airport in their latest regional airport system plan and only one of these two is a common recommendation in the Federal Aviation Administration's National Plan of Integrated Airport System.
Author

Air Traffic; Airports; Airport Planning

19990111547 Directorate General of Civil Aviation, The Hague, Netherlands

The Integrated Airport Competition Model, 1998

Veldhuis, J., Directorate General of Civil Aviation, Netherlands; Essers, I., Directorate General of Civil Aviation, Netherlands; Bakker, D., Hague Consulting Group, Netherlands; Cohn, N., Hague Consulting Group, Netherlands; Kroes, E., Hague Consulting Group, Netherlands; Journal of Air Transportation World Wide; 1999; Volume 4, No. 2, pp. 100-120; In English; See also 19990111540; Copyright; Avail: Issuing Activity, Hardcopy

This paper addresses recent model development by the Directorate General of Civil Aviation (DGCA) and Hague Consulting Group (HCG) concerning long-distance travel. Long-distance travel demand is growing very quickly and raising a great deal of economic and policy issues. There is increasing competition among the main Western European airports, and smaller, regional airports are fighting for market share. New modes of transport, such as high speed rail, are also coming into the picture and affect the mode split for medium distance transport within Europe. Developments such as these are demanding the attention of policy makers and a tool is required for their analysis. For DGCA, Hague Consulting Group has developed a model system to provide answers to the policy questions posed by these expected trends, and to identify areas where policy makers can influence the traveller choices. The development of this model system, the Integrated Airport Competition Model/integraal Luchthaven Competitie Model (ILCM), began in 1992. Since that time the sub-models, input data and user interface have been expanded, updated and improved. HCG and DGCA have transformed the ILCM from a prototype into an operational forecasting tool.
Author

Airports; Competition; Models

19990111718 General Accounting Office, Resources, Community and Economic Development Div., Washington, DC USA

General Aviation Airports: Oversight and Funding

Anderson, John H., Jr; Jun. 09, 1999; 12p; In English; Testimony Before the Subcommittee on Aviation, Committee on Transportation and Infrastructure, House of Representatives.

Report No.(s): AD-A364752; GAO/T-RCED-99-214; No Copyright; Avail: CASI; A03, Hardcopy; A01, Microfiche

All Federal Aviation Administration (FAA) field offices rely primarily on third-party complaints to identify airports' noncompliance with allowable uses. Only 4 of FAA's 23 field offices monitor general aviation airports to ensure that they comply with federal requirements to use airport land only for airport purposes. to do this, these four field offices rely on the airports' self-certifications that they are in compliance. Relying on airports' self-certifications and third-party complaints is not sufficient. Without monitoring, airports' unauthorized use of land has gone uncorrected-in some cases for over a decade. For example, airport land has been inappropriately used for mobile home parks; little league baseball fields; dog pounds; duck-hunting blinds; and city police, fire, and vehicle maintenance facilities. Unauthorized land use has resulted in the loss or diversion of millions of dollars in airport revenues from general aviation airports, which are typically owned by local governments. In some cases, increased risks to aviation safety also resulted. For example, FAA determined that birds attracted by an unauthorized landfill on an airport posed a possible danger to aircraft. If and when FAA becomes aware that an airport is not complying, ft has a variety of statutory and administrative alternatives. However, FAA has generally chosen not to use them, preferring to address noncompliance through

negotiation and settlement, an approach that has not always been effective in resolving airports' noncompliance. Our report included recommendations designed to address these problems.
DTIC
Airports; Federal Budgets; Grants; Investments

12
ASTRONAUTICS (GENERAL)

For extraterrestrial exploration see 91 Lunar and Planetary Exploration.

19990107361 Alpha Technology, Huntsville, AL USA
Human Mars Mission: SEP Architecture Crew Taxi Propulsion Stage Study and Design and Technology for Reaction and Control System, Part 1 ***Final Report, 7 May - 30 Sep. 1999***
Young, Archie, Alpha Technology, USA; Oct. 07, 1999; 47p; In English
Contract(s)/Grant(s): NASA Order H-28653-D; No Copyright; Avail: CASI; A03, Hardcopy; A01, Microfiche

The Mars exploration is a candidate pathway to expand human presence and useful activities in the solar system. There are several propulsion system options being considered to place the Mars payload on its inter-planetary transfer trajectory. One propulsion option is the use of Solar Electric Propulsion (SEP) to spiral out with the Mars payload from an initial Low Earth Orbit (LEO) to an elliptical High Earth Orbit (HEO). This report, presented in annotated facing page format, describes the work completed on the design of a crew taxi propulsion stage used in conjunction with the SEP. Transportation system/mission analysis topics covered in this report include sub-system analysis, trajectory profile description, mass performance and crew taxi stage sizing, stage configuration, stage cost, and Trans-Mars Injection (TMI) launch window. The high efficiency of SEP is used to provide the major part of the TMI propulsion maneuver. Orbital energy is continuously added over a period of approximately twelve months. The SEP and Mars payload follow a spiral trajectory from an initial LEO to a final elliptical HEO. A small chemical stage is then used to provide the final part of the TMI. The now unloaded SEP returns to LEO to repeat another spiral trajectory with payload to HEO. The spiral phase of the SEP's trajectory takes several months to reach HEO, thus significantly increasing the exposure time of the crew to zero-gravity. In order to minimize the long zero-gravity effects, a high thrust chemical stage delivers the crew to the SEP's HEO. The crew rendezvous with the Mars payload in HEO. After a checkout period the Mars payload with the crew is injected onto a Trans-Mars Trajectory by a small chemical stage.
Author
Mars Exploration; Systems Analysis; Design Analysis; Technology Assessment; Checkout; Solar Electric Propulsion; Weightlessness

19990110322 Arizona Univ., Space Engineering Research Center, Tucson, AZ USA
In-Situ Resource Utilization for Economical Space Missions ***Final Report***
Ramohalli, Kumar, Arizona Univ., USA; 1999; 18p; In English
Contract(s)/Grant(s): NAG1-1825; NAGW-1332; No Copyright; Avail: CASI; A03, Hardcopy; A01, Microfiche

This paper presents some recent developments in the technologies of ISRU with the specific intention of cost reductions in space missions. Recognizing that a certain level of technology maturation is necessary before the mission designers will seriously consider any technology, the hypothesis is made that the overall cost-index is inversely proportional to the TRL. Also recognizing that the cost is directly proportional to the mass at launch, the cost-index is identified as the ratio of the launch mass to the TRL. Whether this cost-index is the true measure of the overall mission cost is arguable; however, the relative costs of comparable technologies can be readily assessed by applying identical rules of such an evaluation. As one example of this approach, Mars Sample Return (MSR) is studied, and nine competing technologies are evaluated for the key Mars Ascent Vehicle (MAV). It is found that the technology of oxygen production through the dissociation of atmospheric carbon dioxide can be a key technology. In addition to reporting upon this technology briefly, one innovative application that significantly enhances the science capabilities of a rover is discussed.
Author
Technology Utilization; Gas Dissociation; Oxygen Production

19990111575 NASA Langley Research Center, Hampton, VA USA
Predicting Mission Success in Small Satellite Missions
Saunders, Mark, NASA Langley Research Center, USA; Richie, Wayne R., NASA Langley Research Center, USA; Moore, Arlene, NASA Langley Research Center, USA; Rogers, John, NASA Langley Research Center, USA; 19991008; 12p; In English;

50th; Small Satellite Missions, 4-8 Oct. 1999, Amsterdam, Netherlands
Report No.(s): IAF-99-IAA.11.2.05; No Copyright; Avail: Issuing Activity, Hardcopy

In our global society with its increasing international competition and tighter financial resources, governments, commercial entities and other organizations are becoming critically aware of the need to ensure that space missions can be achieved on time and within budget. This has become particularly true for the National Aeronautics and Space Administration's (NASA) Office of Space Science (OSS) which has developed their Discovery and Explorer programs to meet this need. As technologies advance, space missions are becoming smaller and more capable than their predecessors. The ability to predict the mission success of these small satellite missions is critical to the continued achievement of NASA science mission objectives. The NASA Office of Space Science, in cooperation with the NASA Langley Research Center, has implemented a process to predict the likely success of missions proposed to its Discovery and Explorer Programs. This process is becoming the basis for predicting mission success in many other NASA programs as well. This paper describes the process, methodology, tools and synthesis techniques used to predict mission success for this class of mission.
Author
NASA Programs; Space Missions; Small Scientific Satellites

19990111599 NASA Goddard Space Flight Center, Greenbelt, MD USA
Autonomous Command Operations of the WIRE Spacecraft
Walyus, Keith, NASA Goddard Space Flight Center, USA; Prior, Mike, NASA Goddard Space Flight Center, USA; Saylor, Richard, NASA Goddard Space Flight Center, USA; [1999]; 1p; In English; 3rd; Reducing the Cost of Spacecraft Ground Systems and Operations; No Copyright; Avail: Issuing Activity, Hardcopy; Abstract Only

This paper presents operational innovations which will be introduced on NASA's Wide Field Infrared Explorer (WIRE) mission. These innovations include an end-to-end design architecture for an autonomous commanding capability for the uplink of command loads during unattended station contacts. The WIRE mission is the fifth and final mission of NASA's Goddard Space Flight Center Small Explorer (SMEX) series to be launched in March of 1999. Its primary mission is the targeting of deep space fields using an ultra-cooled infrared telescope. Due to its mission design WIRE command loads are large (approximately 40 Kbytes per 24 hours) and must be performed daily. to reduce the cost of mission operations support that would be required in order to uplink command loads, the WIRE Flight Operations Team has implemented all autonomous command loading capability. This capability allows completely unattended operations over a typical two-day weekend period. The key factors driving design and implementation of this capability were: 1) integration with already existing ground system autonomous capabilities and systems, 2) the desire to evolve autonomous operations capabilities based upon previous SMEX operations experience - specifically the TRACE mission, 3) integration with ground station operations - both autonomous and man-tended, 4) low cost and quick implementation, and 5) end-to-end system robustness. A trade-off study was performed to examine these factors in light of the low-cost, higher-risk SMEX mission philosophy. The study concluded that a STOL (Spacecraft Test and Operations Language) based script, highly integrated with other scripts used to perform autonomous operations, was best suited given the budget and goals of the mission. Each of these factors is discussed in addition to use of the TRACE mission as a testbed for autonomous commanding prior to implementation on WIRE. The capabilities implemented on the WIRE mission are an example of a low-cost, robust, and efficient method for autonomous command loading when implemented with other autonomous features of the ground system. They call be used as a design and implementation template by other missions interested in evolving toward autonomous and lower cost operations. Additionally, the WIRE spacecraft will be used as an operational testbed upon completion of its nominal mission later in 1999. One idea being studied is advanced on-board modeling. Advanced on-board modeling techniques will be used to more efficiently display the spacecraft state. This health and safety information could be used by engineers on the ground or could be used by tile spacecraft for its own assessments. Additionally, this same state information could also be input into the event-driven scheduling system, as the scheduling system will need to assess the spacecraft state before undertaking a new activity. Advanced modeling techniques are being evaluated for a number of NASA missions including The Next Generation Space Telescope (NGST), which is scheduled to launch in 2007.
Author
Architecture (Computers); Autonomy; End-to-End Data Systems; Infrared Radiation; Infrared Telescopes; Mission Planning

19990111703 NASA Marshall Space Flight Center, Huntsville, AL USA
A Plasma Drag Hypervelocity Particle Accelerator (HYPER)
Best, Steve R., NASA Marshall Space Flight Center, USA; Rose, M. Frank, NASA Marshall Space Flight Center, USA; [1998]; 1p; In English; 1998 Hypervelocity Impact, 17 Nov. 1998, Huntsville, AL, USA; Copyright; Avail: Issuing Activity, Hardcopy; Abstract Only

Current debris models are able to predict the growth of the space debris problem and suggest that spacecraft must employ armor or bumper shields for some orbital altitudes now and that the problem will become worse as a function of time. The practical upper limit to the velocity distribution is on the order of 40 km/s and is associated with the natural environment. The velocity distribution of the man-made component peaks at 9-10 km/s with maximum velocity in the 14-16 km/s range. Experience in space has verified that the ”high probability of impact” particles are in the microgram to milligram range. These particles can have very significant effects on coatings, insulators, and thin metallic layers. The surface of thick materials becomes pitted and the local debris component is enhanced by ejecta from the impact events. In this paper, the HYPER facility is described which produces a reasonable simulation of the man-made space debris spectrum in a controlled environment. The facility capability is discussed in terms of drive geometry, energetics, velocity distribution, diagnostics, and projectile/debris loading. The facility has been used to study impact phenomena on Space Station Freedom’s solar array structure, the calibration of space debris collectors, other solar array materials, potential structural materials for use in space, electrical breakdown in the space environment, and as a means of clarifying or duplicating the impact phenomena on surfaces which have been exposed in space.
Author
Hypervelocity Guns; Plasma Accelerators; Particle Accelerators; Space Debris

14
GROUND SUPPORT SYSTEMS AND FACILITIES (SPACE)

Includes launch complexes, research and production facilities; ground support equipment; e.g., mobile transporters; and simulators. For related information see also 09 Research and Support Facilities (Air).

19990111521 NASA Goddard Space Flight Center, Greenbelt, MD USA
Enabling High Performance Reconfigurable Ground Data Processing Systems
Hines, Tonjua M., NASA Goddard Space Flight Center, USA; deFigueiredo, Marco Aurelio, Stingher Gaffarian Technologies, Inc., USA; 1998; 1p; In English; SCD II FOZ DO IGUASSU, 11 Feb. 1998, Brazil
Contract(s)/Grant(s): 28-0001-5; No Copyright; Avail: Issuing Activity, Hardcopy; Abstract Only

The deployment of high data rate instruments onboard satellites with direct broadcast capability demands the implementation of powerful ground data processing systems. Conversely, to enable the widespread usage of direct broadcast data and the generation of subsequent data products, low cost data processing systems must be available. Reconfigurable computers based on Field Programmable Gate Arrays (FPGA) enable the implementation of ground data processing systems that lead to higher performance and lower cost while keeping a high degree of programmability and maintainability. This paper presents the conceptualization of the MODIS Adaptive Level One Accelerator (ALOA), a prototype under construction at NASA’s Goddard Space Flight Center. The ALOA is a computer workstation augmented by a reconfigurable computer. The system will calibrate and geographically locate data from the EOS-AM1 MODerate resolution Imaging Spectroradiometer (MODIS) instrument at near real-time data rates.
Author
Data Processing Equipment; Calibrating; Cost Reduction; Data Acquisition; Low Cost; Workstations

15
LAUNCH VEHICLES AND SPACE VEHICLES

Includes boosters; operating problems of launch/space vehicle systems; and reusable vehicles. For related information see also 20 Spacecraft Propulsion and Power.

19990107378 NASA Marshall Space Flight Center, Huntsville, AL USA
Applied Virtual Reality in Reusable Launch Vehicle Design, Operations Development, and Training
Hale, Joseph P., NASA Marshall Space Flight Center, USA; [1997]; 1p; In English; Autofact ’97, 3-7 Nov. 1997, Detroit, MI, USA; No Copyright; Avail: CASI; A01, Hardcopy; A01, Microfiche; Abstract Only; Abstract Only

Application of Virtual Reality (VR) technology offers much promise to enhance and accelerate the development of Reusable Launch Vehicle (RLV) infrastructure and operations while simultaneously reducing developmental and operational costs. One of the primary cost areas in the RLV concept that is receiving special attention is maintenance and refurbishment operations. To produce and operate a cost effective RLV, turnaround cost must be minimized. Designing for maintainability is a necessary requirement in developing RLVs. VR can provide cost effective methods to design and evaluate components and systems for maintenance and refurbishment operations. The National Aeronautics and Space Administration (NASA)/Marshall Space Flight

Center (MSFC) is beginning to utilize VR for design, operations development, and design analysis for RLVs. A VR applications program has been under development at NASA/MSFC since 1989. The objectives of the MSFC VR Applications Program are to develop, assess, validate, and utilize VR in hardware development, operations development and support, mission operations training and science training. The NASA/MSFC VR capability has also been utilized in several applications. These include: 1) the assessment of the design of the late Space Station Freedom Payload Control Area (PCA), the control room from which onboard payload operations are managed; 2) a viewing analysis of the Tethered Satellite System's (TSS) "end-of-reel" tether marking options; 3) development of a virtual mockup of the International Space Welding Experiment for science viewing analyses from the Shuttle Remote Manipulator System elbow camera and as a trainer for ground controllers; and 4) teleoperations using VR. This presentation will give a general overview of the MSFC VR Applications Program and describe the use of VR in design analyses, operations development, and training for RLVs.
Author
NASA Programs; Research and Development; Design Analysis; Reusable Launch Vehicles; Training Devices; Virtual Reality; Computer Aided Design; Human-Computer Interface; Cost Reduction; Production Costs

19990110585 Aero Thermo Technology, Inc., Huntsville, AL USA
Launch Vehicle Design Process Description and Training Formulation ***Final Report, 23 Apr. - 15 Aug. 1999***
Atherton, James, Aero Thermo Technology, Inc., USA; Morris, Charles, Aero Thermo Technology, Inc., USA; Settle, Gray, Aero Thermo Technology, Inc., USA; Teal, Marion, Aero Thermo Technology, Inc., USA; Schuerer, Paul, Aero Thermo Technology, Inc., USA; Blair, James, Aero Thermo Technology, Inc., USA; Ryan, Robert, Aero Thermo Technology, Inc., USA; Schutzenhofer, Luke, Aero Thermo Technology, Inc., USA; Aug. 31, 1999; 86p; In English; Original contains color illustrations
Contract(s)/Grant(s): NASA Order H-30968-D
Report No.(s): NASA/CR-1999-209751; NAS 1.26:209751; No Copyright; Avail: CASI; A05, Hardcopy; A01, Microfiche

A primary NASA priority is to reduce the cost and improve the effectiveness of launching payloads into space. As a consequence, significant improvements are being sought in the effectiveness, cost, and schedule of the launch vehicle design process. In order to provide a basis for understanding and improving the current design process, a model has been developed for this complex, interactive process, as reported in the references. This model requires further expansion in some specific design functions. Also, a training course for less-experienced engineers is needed to provide understanding of the process, to provide guidance for its effective implementation, and to provide a basis for major improvements in launch vehicle design process technology. The objective of this activity is to expand the description of the design process to include all pertinent design functions, and to develop a detailed outline of a training course on the design process for launch vehicles for use in educating engineers whose experience with the process has been minimal. Building on a previously-developed partial design process description, parallel sections have been written for the Avionics Design Function, the Materials Design Function, and the Manufacturing Design Function. Upon inclusion of these results, the total process description will be released as a NASA TP. The design function sections herein include descriptions of the design function responsibilities, interfaces, interactive processes, decisions (gates), and tasks. Associated figures include design function planes, gates, and tasks, along with other pertinent graphics. Also included is an expanded discussion of how the design process is divided, or compartmentalized, into manageable parts to achieve efficient and effective design. A detailed outline for an intensive two-day course on the launch vehicle design process has been developed herein, and is available for further expansion. The course is in an interactive lecture/workshop format to engage the participants in active learning. The course addresses the breadth and depth of the process, requirements, phases, participants, multidisciplinary aspects, tasks, critical elements,as well as providing guidance from previous lessons learned. The participants are led to develop their own understanding of the current process and how it can be improved. Included are course objectives and a session-by-session outline of course content. Also included is an initial identification of visual aid requirements.
Author
Design Analysis; Payloads; Cost Reduction; Effectiveness; Training Analysis; Management Planning

19990111698 NASA Marshall Space Flight Center, Huntsville, AL USA
Design of a Low Cost Avionics System for Launch Vehicles
Crawford, Kevin, NASA Marshall Space Flight Center, USA; Wallace, Shawn, NASA Marshall Space Flight Center, USA; Jan. 28, 1998; In English; Digital Avionics, 31 Oct. - 6 Nov. 1998, Seattle, WA, USA; Copyright; Avail: Issuing Activity, Hardcopy, Microfiche

Marshall Space Flight Center has long been one of the leaders in development of propulsion systems. Due to current launch vehicle costs, Marshall Space Flight Centers (MSFC) Advanced Space Transportation Program (ASTP) office has emphasized the development of low cost launch vehicles. The Bantam launch vehicle is one of the primary programs that has low cost as a requirement. One of the driving factors for a low cost launch vehicle is a low cost avionics system. This paper will summarize

MSFC's Astrionics Laboratories efforts in designing a low cost avionics system. MSFC has done Phase A avionics system design and has been working with various contractors on a Phase B preliminary avionics design. Deriving the major requirements, trade studies and cost drivers are some of the topics to be discussed.
Author
Systems Engineering; Avionics; Launch Vehicles; Aircraft Design

19990113117 Starcraft Boosters, Inc., Houston, TX USA
The StarBooster System: A Cargo Aircraft for Space ***Final Report, 3 Sep. - 29 Oct. 1999***
Davis, Hubert P., Starcraft Boosters, Inc., USA; Dula, Arthur M., Starcraft Boosters, Inc., USA; McLaughlin, Don, Starcraft Boosters, Inc., USA; Frassanito, John, Starcraft Boosters, Inc., USA; Andrews, Jason, Editor, Starcraft Boosters, Inc., USA; Oct. 27, 1999; 69p; In English
Contract(s)/Grant(s): NASA Order H-30550-D
Report No.(s): SBI-1999-001A; No Copyright; Avail: CASI; A04, Hardcopy; A01, Microfiche

Starcraft Boosters has developed a different approach for lowering the cost of access to space. We propose developing a new aircraft that will house an existing expendable rocket stage. This vehicle, termed StarBooster, will be the first stage of a family of launch vehicles. by combining these elements, we believe we can reduce the cost and risk of fielding a new partially reusable launch system. This report summarizes the work performed on the StarBooster concept since the company's inception in 1996. Detailed analyses are on-going and future reports will focus on the maturation of the vehicle and system design.
Derived from text
Booster Rocket Engines; Reusable Launch Vehicles; Propulsion System Performance; Space Transportation

16
SPACE TRANSPORTATION

Includes passenger and cargo space transportation, e.g., shuttle operations; and space rescue techniques. for related information see also 03 Air Transportation and Safety and 18 Spacecraft Design, Testing and Performance. For space suits see 54 Man/System Technology and Life Support

19990106574 NASA Goddard Space Flight Center, Greenbelt, MD USA
Testing of the International Space Station and X-38 Crew Return Vehicle GPS Receiver ***Final Report***
Simpson, James, NASA Goddard Space Flight Center, USA; Campbell, Chip, NASA Goddard Space Flight Center, USA; Carpenter, Russell, NASA Goddard Space Flight Center, USA; Davis, Ed, NASA Goddard Space Flight Center, USA; Kizhner, Semion, NASA Goddard Space Flight Center, USA; Lightsey, E. Glenn, Texas Univ., USA; Davis, George, Orbital Sciences Corp., USA; Jackson, Larry, Orbital Sciences Corp., USA; [1999]; 5p; In English; ION GPS Conference, 14-17 Sep. 1999, Nashville, TN, USA; No Copyright; Avail: CASI; A01, Hardcopy; A01, Microfiche

This paper discusses the process and results of the performance testing of the GPS receiver planned for use on the International Space Station (ISS) and the X-38 Crew Return Vehicle (CRV). The receiver is a Force-19 unit manufactured by Trimble Navigation and Modified in software by the NASA Goddard Space Flight Center (GSFC) to perform navigation and attitude determination in space. The receiver is the primary source of navigation and attitude information for ISS and CRV. Engineers at GSFC have developed and tested the new receiver with a Global Simulation Systems Ltd (GSS) GPS Signal Generator (GPSSG). This paper documents the unique aspects of ground testing a GPS receiver that is designed for use in space. A discussion of the design and tests using the GPSSG, documentation, data capture, data analysis, and lessons learned will precede an overview of the performance of the new receiver. A description of the challenges of that were overcome during this testing exercise will be presented. Results from testing show that the receiver will be within or near the specifications for ISS attitude and navigation performance. The process for verifying other requirements such as Time to First Fix, Time to First Attitude, selection/deselection of a specific GPS satellite vehicles (SV), minimum signal strength while still obtaining attitude and navigation, navigation and attitude output coverage, GPS week rollover, and Y2K requirements are also given in this paper.
Author
Ground Tests; Performance Tests; International Space Station; X-38 Crew Return Vehicle; Global Positioning System; Receivers

19990107335 NASA Kennedy Space Center, Cocoa Beach, FL USA
Debris/Ice/TPS Assessment and Integrated Photo Analysis of Shuttle Mission STS-93 ***Final Report, 18-28 Jul. 1999***
Katnik, Gregory N., NASA Kennedy Space Center, USA; September 1999; 160p; In English; Original contains color illustrations
Contract(s)/Grant(s): OMRS00U0

Report No.(s): NASA/TM-1999-208555; NAS 1.15:208555; No Copyright; Avail: CASI; A08, Hardcopy; A02, Microfiche

A debris/ice/thermal protection system assessment and integrated photographic analysis was conducted for Shuttle mission STS-93. Debris inspections of the flight elements and launch pad were performed before and after launch. Icing conditions on the External Tank were assessed by the use of computer programs and infrared scanned data during cryogenic loading of the vehicle, followed by on-pad visual inspection. High speed photography of the launch was analyzed to identify ice/debris sources and evaluate potential vehicle damage and/or in-flight anomalies. This report documents the ice/debris/thermal protection system conditions and integrated photographic analysis findings of Space Shuttle mission STS-93 and the resulting effect on the Space Shuttle Program.

Author

Debris; Ice; Ice Formation; Ice Prevention; Thermal Protection

19990113195 NASA Marshall Space Flight Center, Huntsville, AL USA

NASA X-34 Technology in Motion

Beech, Geoffrey, NASA Marshall Space Flight Center, USA; Chandler, Kristie, NASA Marshall Space Flight Center, USA; [1997]; 1p; In English; Deneb Simulation, 29 Sep. - 3 Oct. 1997, Troy, MI, USA; Copyright; Avail: Issuing Activity; Abstract Only, Hardcopy, Microfiche

The X-34 technology development program is a joint industry/government project to develop, test, and operate a small, fully-reusable hypersonic flight vehicle. The objective is to demonstrate key technologies and operating concepts applicable to future reusable launch vehicles. Integrated in the vehicle are various systems to assure successful completion of mission objectives, including the Main Propulsion System (MPS). NASA-Marshall Space Flight Center (MSFC) is responsible for developing the X-34's MPS including the design and complete build package for the propulsion system components. The X-34 will be powered by the Fastrac Engine, which is currently in design and development at NASA-MSFC. Fastrac is a single-stage main engine, which burns a mixture of liquid oxygen (LOX) and kerosene(RP-1). The interface between the MPS and Fastrac engine are critical for proper system operation and technologies applicable to future reusable launch vehicles. Deneb's IGRIP software package with the Dynamic analysis option provided a key tool for conducting studies critical to this interface as well as a mechanism to drive the design of the LOX and RP-1 feedlines. Kinematic models were created for the Fastrac Engine and the feedlines for various design concepts. Based on the kinematic simulation within Envision, design and joint limits were verified and system interference controlled. It was also critical to the program to evaluate the effect of dynamic loads visually, providing a verification tool for dynamic analysis and in some cases uncovering areas that had not been considered. Deneb's software put the X-34 technology in motion and has been a key factor in facilitating the strenuous design schedule.

Author

X-34 Reusable Launch Vehicle; Software Engineering; Design Analysis; Aircraft Industry; Computer Aided Design

18
SPACECRAFT DESIGN, TESTING AND PERFORMANCE

Includes satellites; space platforms; space stations; spacecraft systems and components such as thermal and environmental controls; and attitude controls. For life support systems see 54 Man/System Technology and Life Support. For related information see also 05 Aircraft Design, Testing and Performance, 39 Structural Mechanics, and 16 Space Transportation.

19990107381 NASA Marshall Space Flight Center, Huntsville, AL USA

Electrodynamic Tethers for Spacecraft Propulsion

Johnson, Les, NASA Marshall Space Flight Center, USA; Estes, Robert D., Smithsonian Astrophysical Observatory, USA; Lorenzini, Enrico, Smithsonian Astrophysical Observatory, USA; Martinez–Sanchez, Manuel, Massachusetts Inst. of Tech., USA; Sanmartin, Juan, Madrid Polytechnic Univ., Spain; Vas, Irwin, Boeing Defense and Space Group, USA; [1998]; 1p; In English; 36th; Aerospace Sciences, 12-15 Jan. 1998, Reno, NV, USA; No Copyright; Avail: Issuing Activity, Hardcopy

Relatively short electrodynamic tethers can use solar power to 'push' against a planetary magnetic field to achieve propulsion without the expenditure of propellant. The groundwork has been laid for this type of propulsion. NASA began developing tether technology for space applications in the 1960's. Important recent milestones include retrieval of a tether in space (TSS-1, 1992), successful deployment of a 20-km-long tether in space (SEDS-1, 1993), and operation of an electrodynamic tether with tether current driven in both directions-power and thrust modes (PMG, 1993). The planned Propulsive Small Expendable Deployer System (ProSEDS) experiment will demonstrate electrodynamic tether thrust during its flight in early 2000. ProSEDS will use the flight-proven Small Expendable Deployer System (SEDS) to deploy a 5 km bare copper tether from a Delta II upper stage to achieve approximately 0.4 N drag thrust, thus deorbiting the stage. The experiment will use a predominantly 'bare' tether for

current collection in lieu of the endmass collector and insulated tether approach used on previous missions. Theory and ground-based plasma chamber testing indicate that the bare tether is a highly-efficient current collector. The flight experiment is a precursor to utilization of the technology on the International Space Station for reboost application and the more ambitious electrodynamic tether upper stage demonstration mission which will be capable of orbit raising, lowering and inclination changes - all using electrodynamic thrust. In addition, the use of this type of propulsion may be attractive for future missions at Jupiter and any other planetary body with a magnetosphere.
Author
Spacecraft Propulsion; Electrodynamics; Tethering; Orbital Rendezvous; Tetherlines; Rendezvous Guidance; Rendezvous Spacecraft; Spacecraft Docking

19990108555 NASA Goddard Space Flight Center, Greenbelt, MD USA
The Implementation of Satellite Control System Software Using Object Oriented Design
Anderson, Mark O., NASA Goddard Space Flight Center, USA; Reid, Mark, NASA Goddard Space Flight Center, USA; Drury, Derek, Hammers Co., USA; Hansell, William, Hammers Co., USA; Phillips, Tom, Hammers Co., USA; 1998; 1p; In English; 12th; Small Satellites, 31 Aug. 1998, Logan, UT, USA; Sponsored by Utah State Univ., USA; Copyright; Avail: Issuing Activity, Hardcopy; Abstract Only

NASA established the Small Explorer (SMEX) program in 1988 to provide frequent opportunities for highly focused and relatively inexpensive space science missions that can be launched into low earth orbit by small expendable vehicles. The development schedule for each SMEX spacecraft was three years from start to launch. The SMEX program has produced five satellites; Solar Anomalous and Magnetospheric Particle Explorer (SAMPEX), Fast Auroral Snapshot Explorer (FAST), Submillimeter Wave Astronomy Satellite (SWAS), Transition Region and Coronal Explorer (TRACE) and Wide-Field Infrared Explorer (WIRE). SAMPEX and FAST are on-orbit, TRACE is scheduled to be launched in April of 1998, WIRE is scheduled to be launched in September of 1998, and SWAS is scheduled to be launched in January of 1999. In each of these missions, the Attitude Control System (ACS) software was written using a modular procedural design. Current program goals require complete spacecraft development within 18 months. This requirement has increased pressure to write reusable flight software. Object-Oriented Design (OOD) offers the constructs for developing an application that only needs modification for mission unique requirements. This paper describes the OOD that was used to develop the SMEX-Lite ACS software. The SMEX-Lite ACS is three-axis controlled, momentum stabilized, and is capable of performing sub-arc-minute pointing. The paper first describes the high level requirements which governed the architecture of the SMEX-Lite ACS software. Next, the context in which the software resides is explained. The paper describes the benefits of encapsulation, inheritance and polymorphism with respect to the implementation of an ACS software system. This paper will discuss the design of several software components that comprise the ACS software. Specifically, Object-Oriented designs are presented for sensor data processing, attitude control, attitude determination and failure detection. The paper addresses the benefits of the OOD versus a conventional procedural design. The final discussion in this paper will address the establishment of the ACS Foundation Class (AFC) Library. The AFC is a large software repository, requiring a minimal amount of code modifications to produce ACS software for future projects, saving production time and costs.
Author
Applications Programs (Computers); Computer Programs; Object-Oriented Programming; Software Development Tools; Software Engineering; Software Reuse; Software Reliability; Systems Engineering

19990108570 NYMA, Inc., Hampton, VA USA
An Initial Strategy for Commercial Industry Awareness of the International Space Station
Jorgensen, Catherine A., NYMA, Inc., USA; October 1999; 13p; In English
Contract(s)/Grant(s): NAS1-96013; RTOP 953-20-00-01
Report No.(s): NASA/CR-1999-209686; NAS 1.26:209686; RAB.001CR; No Copyright; Avail: CASI; A03, Hardcopy; A01, Microfiche

While plans are being developed to utilize the ISS for scientific research, and human and microgravity experiments, it is time to consider the future of the ISS as a world-wide commercial marketplace developed from a government owned, operated and controlled facility. Commercial industry will be able to seize this opportunity to utilize the ISS as a unique manufacturing platform and engineering testbed for advanced technology. NASA has begun the strategic planning of the evolution and commercialization of the ISS. The Pre-Planned Program Improvement (P3I) Working Group at NASA is assessing the future ISS needs and technology plans to enhance ISS performance. Some of these enhancements will allow the accommodation of commercial applications and the Human Exploration and Development of Space mission support. As this information develops, it is essential to disseminate this information to commercial industry, targeting not only the private and public space sector but also the non-aerospace commercial industries. An approach is presented for early distribution of this information via the ISS Evolution

Data book that includes ISS baseline system information, baseline utilization and operations plans, advanced technologies, future utilization opportunities, ISS evolution and Design Reference Missions (DRM). This information source and tool can be used as catalyst in the commercial world for the generation of ideas and options to enhance the current capabilities of the ISS.
Author
International Space Station; Management Planning; Manufacturing; Commercialization; Commerce

19990109162 Science Applications International Corp., Huntsville, AL USA
LDEF Satellite Radiation Analyses ***Final Report, May 1992 - Dec. 1995***
Armstrong, T. W., Science Applications International Corp., USA; Colborn, B. L., Science Applications International Corp., USA; Mar. 01, 1996; 56p; In English
Contract(s)/Grant(s): NAS8-39386
Report No.(s): NASA/CR-1999-209737; NAS 1.26:209737; SAIC-TN-96040; No Copyright; Avail: CASI; A04, Hardcopy; A01, Microfiche

Model calculations and analyses have been carried out to compare with several sets of data (dose, induced radioactivity in various experiment samples and spacecraft components, fission foil measurements, and LET spectra) from passive radiation dosimetry on the Long Duration Exposure Facility (LDEF) satellite, which was recovered after almost six years in space. The calculations and data comparisons are used to estimate the accuracy of current models and methods for predicting the ionizing radiation environment in low earth orbit. The emphasis is on checking the accuracy of trapped proton flux and anisotropy models.
Author
Long Duration Exposure Facility; Spaceborne Experiments; Ionizing Radiation; Radioactivity

19990109648 Instituto Nacional de Pesquisas Espacias, Sao Jose dos Campos, Brazil
Digital Simulation, with Sensors in the Loop, of Attitude Control Systems of Artificial Satellites ***Simulacao Digital, com Sensores na Malha, de Sistemas de Controle de Atitude de Satelites Artificiais***
deAraujoTredinnick, Patricia Trindade, Instituto Nacional de Pesquisas Espacias, Brazil; 1999; 176p; In Portuguese
Report No.(s): INPE-7175-TDI/677; No Copyright; Avail: CASI; A09, Hardcopy; A02, Microfiche

This work discusses and implements the digital simulation, with a 3 axis dynamic simulator and its angle sensors in the loop, of attitude control systems of artificial satellites. It has as application the first brazilian Scientific Applications Satellite - (SACI-1) which uses an autonomous attitude control system and will be spin stabilized with active spin rate, spin axis and precession control through magnetic torque coils interacting with the geomagnetic field. The work: 1) uses a three axis dynamic simulator and its angle sensors, an interface PC-C and its drivers, command and drive routines of the dynamic simulator, precise time routines, and the stand-alone simulation of Prudencio modified by us; 2) verifies and characterizes the tools that are used; 3) investigates some forms of estimating the spin rate; and 4) compares the stand-alone simulation of Prud6ncio modified by us, with the simulation done in this work. Based on that, we conclude that it is possible to substitute a software model by the corresponding hardware in the loop that, in our in case, was a dynamic simulator with its three axis angle sensors.
Author
Scientific Satellites; Simulators; Magnetic Coils; Digital Simulation; Automatic Control

19990110570 National Aerospace Lab., Tokyo, Japan
Ground Effects Obtained from Flight Tests of ALFLEX
Okada, N., National Aerospace Lab., Japan; Suito, T., National Aerospace Lab., Japan; December 1997; 20p; In Japanese
Report No.(s): PB99--127714; NAL-TR-1344; Copyright Waived; Avail: Issuing Activity (Natl Technical Information Service (NTIS)), Microfiche

The ALFLEX (Automatic Landing FLight EXperiment) vehicle is a 37% scale model of a future reentry vehicle. HOPE (H-II Orbiting Plane), and was developed for investigating the horizontal landing capability of the HOPE. The flight experiment was carried out at the Woomera Airfield in South Australia in 1996. Landing trials of the ALFLEX were realized by releasing the vehicle hung by a cable from a helicopter. After the release, the vehicle autonomously made path capture, equilibrium gliding on a -30 deg flight path, flare and touch-down on a runway. During the development phase, ground effects had been considered as key issues that affect the landing performance, and wind tunnel tests for predicting the ground effects had been carried out. For the purpose of validating the potential of the wind tunnel data for future designs, ground effect characteristics derived from the flight data and comparison with the wind tunnel data are given in this paper.
NTIS
Hope Aerospace Plane; Reentry Vehicles; Ground Effect (Aerodynamics); Flight Tests; Automatic Landing Control; Wind Tunnel Tests; Scale Models; Aircraft Landing

19990110587 Instituto Nacional de Pesquisas Espacias, Sao Jose dos Campos, Brazil

Discrete-Time Attitude Control of Artificial Satellites with Flexible Appendages ***Controle Discreto da Atitude de Satelites Artificiais com Apendices Flexiveis***

daCostaTredinnick, Marcelo Ricardo Alves, Instituto Nacional de Pesquisas Espacias, Brazil; 1999; 266p; In Portuguese

Report No.(s): INPE-7179-TDI/680; No Copyright; Avail: CASI; A12, Hardcopy; A03, Microfiche

This work discusses and simulates the discrete-time control of artificial satellites with flexible appendages, and its stability in function of growing sampling periods. Due to mission needs the dimensions of the appendages tend to increase becoming more flexible. As a result, it is important to investigate the effects of digital characteristics such as sampling period, delays (in inputs, processing and outputs) and amplitude quantization on it. In this work only the sampling period effects are investigated. The discrete-time PD controller design is done considering aspects such as the aliasing and the hidden oscillations. The PD controller is tested with 2 plants: an harmonic oscillation, and a model of the China-Brazil Earth Resources Satellite - (CBERS-1), comparing the analog PD, with standard discrete-time PD obtained by classic s-z mappings (Tustin and Schneider) and by a new s-z mapping proposed in this work, using the same simulation conditions (control gains, etc.). The Jury stability criterion, root-loci, transient and steady state responses with those plants were used to analyze their performances. Some many stabilization methods were inferred. The new method has shown the best performance amongst the approaches tested.

Author

Discrete Functions; Time Dependence; Artificial Satellites; Controllers; Stabilization; Simulation; Stability; Attitude Control

19990110691 NASA Goddard Space Flight Center, Greenbelt, MD USA

1999 NSREC Short Course: Proton Effects and Test Issues for Satellite Designers: Displacement Effects, Section 4

Marshall, Cheryl J., NASA Goddard Space Flight Center, USA; Marshall, Paul W., NASA Goddard Space Flight Center, USA; [1999]; 50p; In English, 12-17 Jul. 1999, Norfolk, VA, USA; Sponsored by Institute for Electrical and Electronic Engineers; No Copyright; Avail: CASI; A03, Hardcopy; A01, Microfiche

This portion of the Short Course is divided into two segments to separately address the two major proton-related effects confronting satellite designers: ionization effects and displacement damage effects. While both of these topics are deeply rooted in ”traditional” descriptions of space radiation effects, there are several factors at play to cause renewed concern for satellite systems being designed today. For example, emphasis on Commercial Off-The-Shelf (COTS) technologies in both commercial and government systems increases both Total Ionizing Dose (TID) and Single Event Effect (SEE) concerns. Scaling trends exacerbate the problems, especially with regard to SEEs where protons can dominate soft error rates and even cause destructive failure. In addition, proton-induced displacement damage at fluences encountered in natural space environments can cause degradation in modern bipolar circuitry as well as in many emerging electronic and opto-electronic technologies.

Author

Protons; Radiation Dosage; Radiation Effects; Ionization; Failure; Damage; Circuits

19990110700 NASA Marshall Space Flight Center, Huntsville, AL USA

EXPRESS Rack Overview

Sledd, Annette M., NASA Marshall Space Flight Center, USA; Mueller, Charles W., NASA Marshall Space Flight Center, USA; [1999]; 1p; In English; 37th; 37th Aerospace Sciences, 11-14 Jan. 1999, Reno, NV, USA; Sponsored by American Inst. of Aeronautics and Astronautics, USA

Report No.(s): AIAA Paper 99-0313; Copyright; Avail: Issuing Activity, Hardcopy; Abstract Only

The EXpedite the PRocessing of Experiments to Space Station or EXPRESS Rack System, was developed to provide Space Station accommodations for small, subrack payloads. The EXPRESS Rack accepts Space Shuttle middeck locker type payloads and International Subrack Interface Standard (ISIS) Drawer payloads, allowing previously flown payloads an opportunity to transition to the International Space Station. The EXPRESS Rack provides power, data, command and control, video, water cooling, air cooling, vacuum exhaust, and Nitrogen supply to payloads. The EXPRESS Rack system also includes transportation racks to transport payloads to and from the Space Station, Suitcase Simulators to allow a payload developer to verify power and data interfaces at the development site, Functional Checkout Units to allow Payload checkout at KSC prior to launch, and trainer racks for the astronauts to learn how to operate the EXPRESS Racks prior to flight. Standard hardware and software interfaces provided by the EXPRESS Rack simplify the analytical and physical integration processes, and facilitates simpler ISS payload development. The EXPRESS Rack has also formed the basis for the U.S. Life Sciences payload racks on Space Station.

Author

International Space Station; Space Station Payloads; Space Shuttle Payloads; Space Vehicle Checkout Program; Checkout

19990110711 NASA Goddard Space Flight Center, Greenbelt, MD USA

Spacecraft Attitude Representations

Markley, F. Landis, NASA Goddard Space Flight Center, USA; [1999]; 19p, 27 Oct. 1999, Aalborg, Denmark; No Copyright; Avail: CASI; A03, Hardcopy; A01, Microfiche

The direction cosine matrix or attitude matrix is the most fundamental representation of the attitude, but it is very inefficient: It has six redundant parameters, it is difficult to enforce the six (orthogonality) constraints. the four-component quaternion representation is very convenient: it has only one redundant parameter, it is easy to enforce the normalization constraint, the attitude matrix is a homogeneous quadratic function of q, quaternion kinematics are bilinear in q and m. Euler angles are extensively used: they often have a physical interpretation, they provide a natural description of some spacecraft motions (COBE, MAP), but kinematics and attitude matrix involve trigonometric functions, ”gimbal lock” for certain values of the angles. Other minimum (three-parameter) representations: Gibbs vector is infinite for 180 deg rotations, but useful for analysis, Modified Rodrigues Parameters are nonsingular, no trig functions, Rotation vector phi is nonsingular, but requires trig functions.

Author

Attitude (Inclination); Vectors (Mathematics)

19990113094 NASA Marshall Space Flight Center, Huntsville, AL USA

Development Approach for the Accommodation of Materials Science Research for the Materials Science Research Facility on the International Space Station

Schaefer, D. A., NASA Marshall Space Flight Center, USA; Cobb, S. D., NASA Marshall Space Flight Center, USA; Szofran, F. R., NASA Marshall Space Flight Center, USA; 2000; 3p; In English; Space Technology and Application, 30 Jan. - 3 Feb. 2000, Albuquerque, NM, USA; No Copyright; Avail: Issuing Activity, Hardcopy

The Materials Science Research Facility (MSRF) is a modular facility comprised of autonomous Materials Science Research Racks (MSRR’s) for research in the microgravity environment afforded by the International Space Station (ISS). The initial MSRF concept consists of three Materials Science Research Racks (MSRR-1, MSRR-2, and MSRR-3) which will be developed for a phased deployment beginning on the third Utilization Flight (UF-3). The facility will house materials processing apparatus and common subsystems required for operating each device. Each MSRR is a stand alone autonomous rack and will be comprised of either on-orbit replaceable Experiment Modules, Module Inserts, investigation unique apparatus, and/or multiuser generic processing apparatus. Each MSRR will support a wide range of materials science themes in the NASA research program and will use the ISS Active Rack Isolation System (ARIS). MSRF is being developed for the USA Laboratory Module and will provide the apparatus for satisfying near-term and long-range Materials Science Discipline goals and objectives.

Author

Microgravity; Research Facilities; Materials Science; Commerce Lab; Space Commercialization; Mission Planning

19
SPACECRAFT INSTRUMENTATION

For related information see also 06 Aircraft Instrumentation and 35 Instrumentation and Photography.

19990106566 NASA Goddard Space Flight Center, Greenbelt, MD USA

Detector Assembly and the Ultralow-Temperature Refrigerator for XRS

Porter, F. S., NASA Goddard Space Flight Center, USA; Dipirro, M. J., NASA Goddard Space Flight Center, USA; Kelley, R. L., NASA Goddard Space Flight Center, USA; Pham, T., NASA Goddard Space Flight Center, USA; Stahle, C. K., NASA Goddard Space Flight Center, USA; Szymkowiak, A. E., NASA Goddard Space Flight Center, USA; Tuttle, J. G., NASA Goddard Space Flight Center, USA; Audley, M. D., NASA Goddard Space Flight Center, USA; Gendraau, K. C., NASA Goddard Space Flight Center, USA; Brekosky, R. P., NASA Goddard Space Flight Center, USA; Gysax, J. D., NASA Goddard Space Flight Center, USA; [1999]; 1p; In English, 18-23 Jul. 1999, Denver, CO, USA; Sponsored by International Society for Optical Engineering, USA; No Copyright; Avail: Issuing Activity, Hardcopy; Abstract Only

The X-ray spectrometer (XRS) on the Japanese Astro-E Spacecraft is the first ultra low temperature space borne instrument. The system utilizes a 900g Ferric Ammonium Alum (FAA) Adiabatic Demagnetization Refrigerator (ADR) with a helium-3 gas gap heat switch to cool the detector assembly to 0.060K. The system operates in a ”single shot” configuration allowing the system to remain at its operating temperature for about 40 hours in the lab. The on-orbit performance is expected to be about 35 hours with a 97% duty cycle. The detector assembly for XRS consists of a 32 channel microcalorimeter array

bias electronics, thermometry, and an anti-coincidence detector that are attached to the cold stage of the ADR. to thermally Isolate the detector system from the superfluid helium reservoir, the detector system is suspended by Kevlar cords and electrical connection in made by L30, 17-micron diameter, tensioned NbTi leads. The detectors are read out in a source-follower arrangement using FET amplifiers operating at 130K mounted in multiply-thermally-isolated assemblies that also use Kevlar and stainless steel wiring. The design and thermal performance of this system will be discussed and compared to the theoretical limits.

Author

Japanese Spacecraft; X Ray Spectrometers; Cryogenic Temperature; Temperature Effects; Temperature Measurement; Temperature Measuring Instruments; Demagnetization; Magnetic Fields; Magnetic Cooling; Refrigerators

19990107397 Swedish Inst. of Space Physics, Kiruna, Sweden

The Ion Mass Imager on the Planet-B Spacecraft

Norberg, O., Swedish Inst. of Space Physics, Sweden; Yamauchi, M., Swedish Inst. of Space Physics, Sweden; Lundin, R., Swedish Inst. of Space Physics, Sweden; Olsen, S., Swedish Inst. of Space Physics, Sweden; Borg, H., Swedish Inst. of Space Physics, Sweden; Barabash, S., Swedish Inst. of Space Physics, Sweden; Hirahara, M., Rikkyo Univ., Japan; Mukai, T., Tokyo Univ., Japan; Hayakawa, H., Tokyo Univ., Japan; Earth Planets Space; 1998; Volume 50, pp. 199-205; In English; Copyright; Avail: Issuing Activity, Hardcopy

The Ion Mass Imager (IMI) is a light-weight ion mass composition instrument for the Japanese Planet-B mission to be launched to Mars in 1998. The objective of the Planet-B mission is to study the Martian environment with emphasis on the upper atmosphere interaction with the solar wind. IMI measures positive ions with energies between 10 eV/q and 35 keV/q and with a mass resolution_high enough to resolve the most important ion species (H(+), He(++), He(+), O(++), O+, 02+). The instrument has a 360 degree field-of-view aperture and uses the spacecraft spin to cover almost the full unit sphere to obtain three-dimensional distribution functions every 4 s (half a spacecraft spin period). Particles are energy-filtered by a spherical electrostatic analyzer, and then mass-analysed by the magnetic separation method. The ions hit a microchannel plate assembly with a position sensitive anode divided into 32 mass channels. Together with 16 angular sectors, this system ”imagcs” the direction of motion and mass of ions. A pre- acceleration voltage of 0-4000 V is used to select the mass range, e.g., modes optimized for light ions (up to O(+)) and heavy ions (O(+) to charged dust grains). A loss-less data compression algorithm is used in the in-flight processing software to optimize the amount of data that can be returned from Mars.

Author

Apertures; Field of View; Mars Environment; Nozomi Mars Orbiter; Positive Ions; Mars Atmosphere; Mass Spectrometers; Ion Optics

19990110531 Environmental and Life Support Technology, Inc., Parker, CO USA

Miniature Electroanalytical Platform for Monitoring Metals and Organics Aboard Spacecraft

Jolly, Clifford D., Environmental and Life Support Technology, Inc., USA; Aug. 26, 1999; 79p; In English; Diskette: 1 3.5-inch DSHD diskette

Contract(s)/Grant(s): NAS9-99004

Report No.(s): NONP-NASA-DK-1999112316; No Copyright; Avail: CASI; A05, Hardcopy; A01, Microfiche; A02, Diskette

The project was to define electroanalytical methods for spacecraft applications. In Phase 1 the primary analyte used to demonstrate the electroanalytical techniques was biocidal silver in potable water. The objectives were to develop a method that shows essentially linear response throughout the measurement range required for spacecraft operation, shows acceptable repeatability (estimated +/- 10%), a lower limit of detection of 25 ppb, and uses materials that are safe for the spacecraft cabin environment. Based 6n.the Phase I work, these objectives are achievable. The method was tested in the presence of potential interferences, and only copper had a significant effect as an interferant to the silver analysis. The method was shown to be applicable to analysis of nickel and copper A pre-prototype silver analyzer was fabricated as a proof- of-concept for the technology.

Author

Technology Utilization; Prototypes; Miniaturization; Fabrication; Cabin Atmospheres

20
SPACECRAFT PROPULSION AND POWER

Includes main propulsion systems and components, e.g., rocket engines; and spacecraft auxiliary power sources. For related information see also 07 Aircraft Propulsion and Power, 28 Propellants and Fuels, 44 Energy Production and Conversion, and 15 Launch Vehicles and Space Vehicles.

19990106559 NASA Dryden Flight Research Center, Edwards, CA USA

Propellant Feed System Leak Detection: Lessons Learned From the Linear Aerospike SR-71 Experiment (LASRE)

Hass, Neal, NASA Dryden Flight Research Center, USA; Mizukami, Masashi, NASA Dryden Flight Research Center, USA; Neal, Bradford A., NASA Dryden Flight Research Center, USA; St. John, Clinton, NASA Dryden Flight Research Center, USA; Beil, Robert J., NASA Kennedy Space Center, USA; Griffin, Timothy P., Dynacs Engineering Co., Inc., USA; November 1999; 37p; In English; 9th; International Space Planes and Hypersonic Systems, 1-5 Nov. 1999, Norfolk, VA, USA; Sponsored by American Inst. of Aeronautics and Astronautics, USA

Contract(s)/Grant(s): RTOP 243-33-02

Report No.(s): NASA/TM-1999-206590; NAS 1.15:206590; H-2378; Copyright Waived; Avail: CASI; A03, Hardcopy; A01, Microfiche

This paper presents pertinent results and assessment of propellant feed system leak detection as applied to the Linear Aerospike SR-71 Experiment (LASRE) program flown at the NASA Dryden Flight Research Center, Edwards, California. The LASRE was a flight test of an aerospike rocket engine using liquid oxygen and high-pressure gaseous hydrogen as propellants. The flight safety of the crew and the experiment demanded proven technologies and techniques that could detect leaks and assess the integrity of hazardous propellant feed systems. Point source detection and systematic detection were used. Point source detection was adequate for catching gross leakage from components of the propellant feed systems, but insufficient for clearing LASRE to levels of acceptability. Systematic detection, which used high-resolution instrumentation to evaluate the health of the system within a closed volume, provided a better means for assessing leak hazards. Oxygen sensors detected a leak rate of approximately 0.04 cubic inches per second of liquid oxygen. Pressure sensor data revealed speculated cryogenic boiloff through the fittings of the oxygen system, but location of the source(s) was indeterminable. Ultimately, LASRE was cancelled because leak detection techniques were unable to verify that oxygen levels could be maintained below flammability limits.

Author

Leakage; Aerospike Engines; Gas Detectors; Pressure Sensors; Feed Systems; Flight Tests

19990108597 NASA Dryden Flight Research Center, Edwards,CA USA

Evaluation of the Linear Aerospike SR-71 Experiment (LASRE) Oxygen Sensor

Ennix, Kimberly A., NASA Dryden Flight Research Center, USA; Corpening, Griffin P., NASA Dryden Flight Research Center, USA; Jarvis, Michele, NASA Dryden Flight Research Center, USA; Chiles, Harry R., NASA Dryden Flight Research Center, USA; November 1999; 22p; In English; 9th; Space Planes and Hypersonic Systems, 1-5 Nov. 1999, Norfolk, VA, USA; Sponsored by American Inst. of Aeronautics and Astronautics, USA; Original contains color illustration

Contract(s)/Grant(s): RTOP 529-31-44

Report No.(s): NASA/TM-1999-206589; H-2377; NAS 1.15:206589; Copyright Waived; Avail: CASI; A03, Hardcopy; A01, Microfiche

The Linear Aerospike SR-71 Experiment (LASRE) was a propulsion flight experiment for advanced space vehicles such as the X-33 and reusable launch vehicle. A linear aerospike rocket engine was integrated into a semi-span of an X-33-like lifting body shape (model), and carried on top of an SR-71 aircraft at NASA Dryden Flight Research Center. Because no flight data existed for aerospike nozzles, the primary objective of the LASRE flight experiment was to evaluate flight effects on the engine performance over a range of altitudes and Mach numbers. Because it contained a large quantity of energy in the form of fuel, oxidizer, hypergolics, and gases at very high pressures, the LASRE propulsion system posed a major hazard for fire or explosion. Therefore, a propulsion-hazard mitigation system was created for LASRE that included a nitrogen purge system. Oxygen sensors were a critical part of the nitrogen purge system because they measured purge operation and effectiveness. Because the available oxygen sensors were not designed for flight testing, a laboratory study investigated oxygen-sensor characteristics and accuracy over a range of altitudes and oxygen concentrations. Laboratory test data made it possible to properly calibrate the sensors for flight. Such data also provided a more accurate error prediction than the manufacturer's specification. This predictive accuracy increased confidence in the sensor output during critical phases of the flight. This paper presents the findings of this laboratory test.

Author

Aerospike Engines; Oxygen; SR-71 Aircraft; Gas Detectors; Propulsion System Configurations

19990110107 Naval Health Research Center, Toxicology Detachment, San Diego, CA USA

The Neurobehavioral Toxicity of JP-8, JP-5 and JP-4 Jet Fuels

Nordholm, A. F., Naval Health Research Center, USA; Ritchie, G. D., Geo-Centers, Inc., USA; Malcolm, W., ManTech Environmental Technology, Inc., USA; Carpenter, R. L., Naval Health Research Center, USA; Rossi, John, III, Naval Health Research Center, USA; Still, K. R., Naval Health Research Center, USA; JANNAF 28th Propellant Development and Characterization Subcommittee and 17th Safety and Environmental Protection Subcommitte Joint Meeting; April 1999; Volume 1, pp. 197-213; In English; See also 19990110087; No Copyright; Avail: CPIA, 10630 Little Patuxent Pkwy., Suite 202, Columbia, MD 21044-3200 HC, Hardcopy

(U) Groups of Sprague-Dawley rats (n = 32) were exposed by whole body inhalation methods to JP-8 (1.0 mg/L +/- 10%) or JP-5 (1.2 mg/L +/- 10%) vapor for 6 hr/day, 5 days/wk, for 6 wk, to JP-4 (2.0 mg/L +/- 10%; n = 16) vapor for 6 hr/day for 14 consecutive days; or to appropriate room air control conditions. The concentrations were selected to represent real world vapor exposures that might be experienced by the operational military. Following conclusion of the exposures, rats were rested for 14-65 days, then were evaluated for persisting neurobehavioral deficits with a battery of tests selected from the Neurobehavioral Toxicity Assessment Battery (NTAB) for their presumed ability to identify, performance deficits similar to those previously identified in chronically exposed European jet engine workers. NTAB tests utilized included: Forelimb Grip Strength (FGS), evaluating muscle strength; General Locomotor Activity (GLA); Forced Treadmill (FT), measuring physical fatigue; Tail Flick Response (TFR), evaluating nociception; Acoustic Startle Response/Prepulse Inhibition (ASR/PPI), quantifying auditory brainstem function and inhibition; Passive Avoidance (PA), evaluating short-term memory; Porsolt Forced Swim test (PFST), measuring emotional depression; Morris Water Maze (MWM), quantifying spatial localization and short term memory; Appetitive Reinforcer Approach Sensitization (ARAS), evaluating central nervous system (CNS) sensitization and dopaminergic function, and Conspecific Approach (CA), evaluating social behavior. Following sacrifice, regional CNS tissues were evaluated for changes, from air controls, in levels of neurotransmitters and major metabolites.

Author

JP-4 Jet Fuel; JP-5 Jet Fuel; JP-8 Jet Fuel; Hydrocarbons; Toxicity; Military Technology

19990110312 Lockheed Martin Astronautics, Huntsville, AL USA

Study on the Modifications Required to Re-Engine the Lockheed D-21 Drone ***Final Report***

Oct. 22, 1999; 153p; In English

Contract(s)/Grant(s): NASA Order H-31409-D; No Copyright; Avail: CASI; A08, Hardcopy; A02, Microfiche

This report was prepared by Lockheed Martin (LM). The purpose of this 45 day study contract was to investigate the feasibility of using the D-21 as a Rocket Based Combined Cycle engine test-bed. The new NASA engine is entitled "Demonstration of Rocket Combined Cycle Operations (DRACO)". Four objectives were defined and modification study provide an estimation of the: (1) mudified vehicle performance; (2) required engine performance; (3) required vehicle modification; and (4) modification cost and schedule.

Derived from text

Research; Feasibility Analysis; Engine Tests; Revisions

19990110316 NASA Marshall Space Flight Center, Huntsville, AL USA

Antimatter Requirements and Energy Costs for Near-Term Propulsion Applications

Schmidt, G. R., NASA Marshall Space Flight Center, USA; Gerrish, H. P., NASA Marshall Space Flight Center, USA; Martin, J. J., NASA Marshall Space Flight Center, USA; Smith, G. A., Pennsylvania State Univ., USA; Meyer, K. J., Pennsylvania State Univ., USA; [1999]; 23p; In English; No Copyright; Avail: CASI; A03, Hardcopy; A01, Microfiche

The superior energy density of antimatter annihilation has often been pointed to as the ultimate source of energy for propulsion. However, the limited capacity and very low efficiency of present-day antiproton production methods suggest that antimatter may be too costly to consider for near-term propulsion applications. We address this issue by assessing the antimatter requirements for six different types of propulsion concepts, including two in which antiprotons are used to drive energy release from combined fission/fusion. These requirements are compared against the capacity of both the current antimatter production infrastructure and the improved capabilities that could exist within the early part of next century. Results show that although it may be impractical to consider systems that rely on antimatter as the sole source of propulsive energy, the requirements for propulsion based on antimatter-assisted fission/fusion do fall within projected near-term production capabilities. In fact, a new facility designed solely for antiproton production but based on existing technology could feasibly support interstellar precursor missions and omniplanetary spaceflight with antimatter costs ranging up to $6.4 million per mission.

Author

Annihilation Reactions; Antimatter; Antiprotons; Propulsion

19990110663 Alabama Univ., Propulsion Research Center, Huntsville, AL USA

Space Solar Power Technical Interchange Meeting 2: SSP TIM 2

Sanders, Jim, Alabama Univ., USA; Hawk, Clark W., Alabama Univ., USA; Dec. 22, 1998; 28p; In English

Contract(s)/Grant(s): NAS8-97095; NASA Order H-30192-D; No Copyright; Avail: CASI; A03, Hardcopy; A01, Microfiche

The 2nd Space Solar Power Technical Interchange Meeting (SSP TIM 2) was conducted September 21st through 24th with the first part consisting of a Plenary session. The summary results of this Plenary session are contained in part one of this report. The attendees were then organized into Working Breakout Sessions and Integrated Product Team (IPT) Sessions for the purpose of conducting in-depth discussions in specific topic areas and developing a consensus as to appropriate study plans and actions to be taken. The Second part covers the Plenary Summary Session, which contains the summary results of the Working Breakout Sessions and IPT Sessions. The appendix contains the list of attendees. The ob'jective was to provide an update for the study teams and develop plans for subsequent study activities. This SSP TIM 2 was initiated and the results reported electronically over the Internet. The International Space Station (ISS) could provide the following opportunities for conducting research and technology (R&T) which are applicable to SSP: (1) Automation and Robotics, (2) Advanced Power Generation, (3) Advanced Power Management & Distribution (PMAD), (4) Communications Systems and Networks, (5) Energy Storage, (6) In Space Propulsion (ISP), (7) Structural Dynamics and Control, and Assembly and (8) Wireless Power Transmission.

Author

Propulsion; Technology Transfer; Solar Generators; Solar Energy Conversion; Space Commercialization

19990110664 NASA Marshall Space Flight Center, Huntsville, AL USA

Magnetic Flux Compression Using Detonation Plasma Armatures and Superconductor Stators: Integrated Propulsion and Power Applications

Litchford, Ron, NASA Marshall Space Flight Center, USA; Robertson, Tony, NASA Marshall Space Flight Center, USA; Hawk, Clark, Alabama Univ., USA; Turner, Matt, Alabama Univ., USA; Koelfgen, Syri, Alabama Univ., USA; 1999; In English; 10th; Advanced Space Propulsion, 5-8 Apr. 1999, Huntsville, AL, USA; Sponsored by NASA, USA; Copyright; Avail: Issuing Activity, Hardcopy

This presentation discusses the use of magnetic flux compression for space flight applications as a propulsion and other power applications. The qualities of this technology that make it suitable for spaceflight propulsion and power, are that it has high power density, it can give multimegawatt energy bursts, and terawatt power bursts, it can produce the pulse power for low impedance dense plasma devices (e.g., pulse fusion drivers), and it can produce direct thrust. The issues of a metal vs plasma armature are discussed, and the requirements for high energy output, and fast pulse rise time requires a high speed armature. The plasma armature enables repetitive firing capabilities. The issues concerning the high temperature superconductor stator are also discussed. The concept of the radial mode pulse power generator is described. The proposed research strategy combines the use of computational modeling (i.e., magnetohydrodynamic computations, and finite element modeling) and laboratory experiments to create a demonstration device.

CASI

Magnetic Flux; Plasmas (Physics); Superconductors (Materials); Armatures; Dense Plasmas; Stators; Pulse Generators; Electromagnetic Propulsion; Plasma Propulsion; Magnetoplasmadynamics

19990110674 NASA Marshall Space Flight Center, Huntsville, AL USA

Microstructure and Mechanical Properties of Vacuum Plasma Sprayed Cu-8Cr-4Nb

Holmes, Richard, NASA Marshall Space Flight Center, USA; Ellis, David, NASA Lewis Research Center, USA; McKechnie, Timothy, Plasma Processes, USA; Hickman, Robert, Plasma Processes, USA; Feb. 25, 1997; In English; 10th; Advanced Propulsion Research, 5-9 Apr. 1999, Huntsville, AL, USA; Sponsored by Jet Propulsion Lab., California Inst. of Tech., USA

Contract(s)/Grant(s): NAS8-97240; Copyright; Avail: Issuing Activity, Hardcopy, Microfiche

This paper compares the tensile properties of Cu-8Cr-4Nb material produced by VPS to material previously produced by extrusion. The microstructure of the VPS material is also presented. The combustion chamber liner of rocket motors represents an extreme materials application. The liner hot wall is exposed to a 2760 C (5000 F) flame while the cold side is exposed to cryogenic hydrogen liquid. Materials for use in the combustion chamber liner require a combination of high temperature strength, creep resistance, and low cycle fatigue resistance along with high thermal conductivity. The hot side is also subject to localized cycles between reducing and oxidizing environments that degrade the liner by a process called blanching. A new Cu-8 at.% Cr-4 at% Nb (Cu-8Cr-4Nb) alloy has been developed at NASA Lewis Research Center as a replacement for the currently used alloy, NARloy-z (Cu-3 wt.% Ag-0.5 wt.% Zr). The alloy is strengthened by a fine dispersion of Cr2Nb particles. The alloy has better mechanical properties than NARloy-Z while retaining most of the thermal conductivity of pure copper. The alloy has been successfully consolidated by extrusion and hot isostatic pressing (HIPing). However, vacuum plasma spraying (VPS) offers

several advantages over prior consolidation methods. VPS can produce a near net shape piece with the profile of the liner. In addition, oxidation resistant and thermal barrier coatings can be incorporated as an integral part of the liner hot wall during the VPS deposition. The low oxygen VPS Cu-8Cr-4Nb exhibits a higher strength than Cu-8Cr-4Nb produced by extrusion at elevated temperatures and a comparable strength at room temperature. Moduli and ductility were not significantly different. However, the ability to produce parts to near-net shape and maintain the good elevated temperature tensile properties of the extruded Cu-8Cr-4Nb makes VPS an attractive processing method for fabricating rocket engine combustion liners.
Derived from text
Plasma Spraying; Copper Alloys; Refractory Metal Alloys; Heat Resistant Alloys; Rocket Linings; Tensile Strength; Chromium Alloys

19990110675 Smithsonian Astrophysical Observatory, Cambridge, MA USA
Electrodynamic Thrust Performance for Space Solar Satellite Applications ***Final Report, 16 Nov. 1998 - 31 May 1999***
Estes, Robert D., Smithsonian Astrophysical Observatory, USA; June 1999; 8p; In English
Contract(s)/Grant(s): NASA Order H -29923-D; No Copyright; Avail: CASI; A02, Hardcopy; A01, Microfiche

The use of spinning tethers to transfer payloads from low earth orbit (LEO) to geosynchronous earth orbit (GEO) has previously been considered for payload masses up to 4000 kg (4 MT). The construction of the solar power station requires a transfer of 22,568 MT per year from LEO to GEO. This is envisioned to be carried out in payload units of 20 MT or 40 MT, which implies a frequency of 1188 or 594 flights per year, respectively. We could say from the outset that the use of spinning tethers for such large payloads at such high launch frequencies does not appear promising. This is inherent in the principles of spinning tether transfer, which we will briefly sketch below. Somewhat different scenarios are possible, but the basic physics remains the same. We consider only a single stage from LEO to GTO tether system, since the complexity involved in phasing the launches, docking, and spinups for a two-stage system for so many payloads rules out a two-stage system, in our opinion. The payload must first be launched to LEO, where it docks with the tether launch platform and is connected to the tether. The tether (tens of kilometers long) is then deployed with the payload upward. In order to give the payload the velocity necessary to launch it into a geosynchronous transfer orbit (GTO), i.e., to impart the required Av, the tethered system must be spun up about the center of mass of the tether-platform-payload system. The two end masses (platform and payload) are driven to rotate about the center of mass of the tethered system. Both the final rotational velocity and the phasing of the tether spin have to be controlled so that payload is in the vertically up position at the perigee of the LEO and with the velocity required to achieve the GTO when it is released at that point. Upon release, the payload then goes into GTO, where it again requires an acceleration to reach GEO (circularization of the orbit). The platform goes into a lower orbit, from which it must be raised in order to be at the proper LEO for docking with another payload. For this scheme to make sense at all, the platform must be envisioned as having a solar powered electrical thrust system to regain LEO and to spin up the tethered system. Similarly, solar powered electrical propulsion would be used to circularize the orbit to GEO.
Derived from text
Thrust; Electrodynamics; Technology Utilization; Payloads; Geosynchronous Orbits; Launching; Low Earth Orbits; Propulsion

19990110680 NASA Marshall Space Flight Center, Huntsville, AL USA
Technical Challenges for Next Generation Liquid Rocket Engine Nozzles
Clinton, R. G., Jr., NASA Marshall Space Flight Center, USA; Eckel, Andy, NASA Lewis Research Center, USA; Self, Kennt, Air Force Research Lab., USA; Rhemer, Chris, Rhemer, Chris, USA; Winans, Dick, Boeing/Rocketdyne, USA; Martinez, Joe, Air Force Research Lab., USA; Lawrence, Tim, NASA Marshall Space Flight Center, USA; Marchol, Paul, Aerojet, USA; [1998]; 1p; In English; National Space and Missile Materials Symposium, 19-22 Oct. 1998, Colorado Springs, CO, USA; Copyright; Avail: Issuing Activity, Hardcopy; Abstract Only

Next generation launch and propulsion systems face significant challenges of providing increased performance at lower cost with shorter development cycles. The use of existing materials in new application areas and the development and application of ”advanced” material systems are enabling for the achievement of these aggressive goals. An area which offers substantial opportunity to decrease liquid rocket engine systems weight, and thus provide a measure of increased performance, is the nozzle. This presentation will examine the technical issues and showstoppers limiting the application of alternate materials to liquid rocket engine nozzles and identify the key material systems which have the potential for high payoff relative to the forcing functions of cost and performance (weight). Existing nozzle material development projects will be cited and opportunities for future joint partnerships to address these materials and processes challenges will be addressed. The presentation will include overviews of activities in low cost ablative nozzles, ceramic matrix composite cooled and uncooled nozzles, and advanced metallics.
Author
Liquid Propellant Rocket Engines; Propulsion System Performance; Rocket Nozzles; Nozzle Design; Engine Design

19990111460 Hampton Univ., Dept. of Computer Science, VA USA

Parallelization of Rocket Engine System Software (PRESS)

Cezzar, Ruknet, Hampton Univ., USA; HBCUs/OMUs Research Conference Agenda and Abstracts; August 1999, pp. 13; In English; See also 19990111455; No Copyright; Avail: Issuing Activity, Hardcopy; Abstract Only

The principal aim is to assess parallelization requirements for FORTRAN based software packages developed as part of Rocket Engine Numeric Simulator (RENS) project. During the first-year, Two-Dimensional Kinetics (TDK), a very large package was studied. During the second-year, we analyzed turbine and pump design packages TURBDES/PUMPDES. During the third year, we have worked on integrating the GASP subsystems into the TURBDES/ PUMPDES using the driver code RESSAP (Rocket Engine System Sizing end Analysis Program). In our final report, dated October 18, 1999, we showed how RESSAP code can run over a local network using Message Passing Interface (MPI) facilities. As discussed in previous progress reports, after experimenting with distributed computations over UNIX based local networks using standard public-domain tools MPI or PVM (Parallel Virtual Machine), the next step is distributed computing over heterogenous, UNIX or NT based, intranets and over the Internet. For this purpose, an evolving set of standards called COmmon Object Request Broker Architecture (CORBA) is the most appropriate tool. While supporting object-oriented languages and applications through standard Interface Definition Language (IDL), there is a possibility of support for FORTRAN based applications through C++ wrappers. Otherwise, through process reengineering, various rocket engine design software tools can be converted to an object-oriented format thereby allowing the use of CORBA facilities. At present, the two popular vendor offerings based on CORBA standards are Iona's OrbixWeb and Visigenic's VisiBroker. Since VisiBroker have been chosen for Netscape browser support and incorporates Java, it is a useful tool for the internet, as well. Indeed, VisiBroker is sometimes also referred to as CORBA+JAVA. Recently there has been a rapid progress in the evolution of CORBA in supporting distributed computing. Some of these developments have been discussed in our final report for the PRESS project which is currently on its one-year no-cost extension period. The accompanying 15-minute presentation will through some light into such developments. Meanwhile, we are currently in the process of acquiring an integration and optimization tool from Enginous Software, Inc. This package is called I-Sight and is a promising one for integrating RENS FORTRAN based code for more efficient use and sharing. If, by the time of the presentation, we are able to purchase and install I-Signt on our NT server, we will provide a description of its capabilities and promise for RENS software as part of the presentation.

Author

Applications Programs (Computers); Object-Oriented Programming; Rocket Engine Design; Rocket Engines; Simulators; Systems Analysis; Models; Computer Aided Design; Design Analysis; Engine Design

19990111462 Howard Univ., Dept. of Electrical Engineering, Washington, DC USA

Aerospace Power System Load Shedding with Reliability Constraint

Momoh, James A., Howard Univ., USA; Zhu, Jizhong, Howard Univ., USA; Kaddah, Sahar, S., Howard Univ., USA; HBCUs/OMUs Research Conference Agenda and Abstracts; August 1999, pp. 15; In English; See also 19990111455; No Copyright; Avail: Issuing Activity, Hardcopy; Abstract Only

Aerospace power system automation requires adequate power to meet critical load functions during known and uncertain system conditions. The uncertainties in load, network change cause system disturbance which could lead to changes in system congestion margin and reliability. The curtailment of load should adequately include value, location and cost while at the same time include reliability and congestion margin. Under this project Howard University research team and the NASA mentor have designed a scheme which uses an Everett optimization method for load shedding without solving optimization with "stationary point" The load shed and generation control are determined by using reliability index LOLP, EUE to validate system control before a control option is done. The integrated scheme consists of five modules: (1) The expected congestion margin during high power demand or during minimum generation schedule or system violations. (2) Reliability of system or component needed prior in determining the load shedding scheme, and determination of risk assessment during system operation. (3) Determination of options needed for mitigating System Vulnerability, these options include generation rescheduling, running system at a risk and load curtailment. (4) Determination of strategy for load curtailment for coordinating system conditions and available control. (5) Cost Benefit analysis. The scheme is tested using a benchmark NASA system consisting of generators, loads and network. The scheduled loads are prioritized and the corresponding reliability indices are provided. The scheme will assist power management on board the space station.

Author

Aerospace Systems; Critical Loading; Systems Engineering; Optimization; Control Systems Design; Concurrent Engineering; Network Control

19990111481 Tuskegee Inst., AL USA

Sputtering Erosion in the Ion Thruster

Ray, Pradosh, Tuskegee Inst., USA; Shutthanandan, V., Tuskegee Inst., USA; HBCUs/OMUs Research Conference Agenda and Abstracts; August 1999, pp. 35; In English; See also 19990111455; No Copyright; Avail: Issuing Activity, Hardcopy; Abstract Only

An experimental study is described to measure the sputtering yield at low ion energies. Molybdenum was sputtered with 100 eV xenon ions using a new set-up. An ion gun was used to generate the ion beam. The residual gas pressure was approximately 1 x10(exp -9) Torr. The ion beam current was in the range of 0.65 micro A at an operational pressure of 1 x10(exp-5) Torr. The sputtered atoms were collected on two thin, 12.5-mm wide aluminum strips positioned in mutually orthogonal directions. These strips were mounted on a collector plate which formed a semi-circle of 15 mm radius around the position where the ion beam focused on the target surface. The amount of sputtered materials deposited on these aluminum foils were determined by Rutherford backscattering spectrometry (RBS) as a function of angle of ejection. The differential sputtering yields obtained from RBS measurements were subsequently converted into absolute sputtering yield.

Author

Erosion; Ion Beams; Sputtering

19990113116 Ceramic Composites, Inc., Millersville, MD USA

Oxidation Resitant HfC-TaC Rocket Thruster for High Performance Propellants ***Final Report***

Patterson, Mark, Ceramic Composites, Inc., USA; Aug. 26, 1999; 25p; In English

Contract(s)/Grant(s): NAS3-27272; No Copyright; Avail: CASI; A03, Hardcopy; A01, Microfiche

The purpose of this reasearch effort was to develop high temperature, oxidation resistant thrusters which would lessen the thruster cooling requirements, resulting in increased performance and longer life for onboard propulsion systems for spacecraft. This research effort focussed on developing ceramic matrix composites (CMCs) for this application, and specifically investigated the use of HfC stabilized with TaC. This material composition can potentially operate in a stoichiometric oxygen to hydrogen ratio at a temperature of 5000 deg F (2760 deg C) in a radiatively cooled mode. Various compositions of Hafnium Carbide (HfC) and Tantalum Carbide (TaC) were deposited by chemical vapor deposition (CVD) and tested, in an attempt to identify the composition which offered the best oxidation resistance. Although it was identified that small amounts of TaC appeared to offer improved oxidation resistance over HfC alone, an optimal composition was not identified. A 251bf thruster was fabricated from a novel CMC sandwich construction with a HfC-TaC matrix, and survived two test firings, each of 5 seconds before a failure in the injector caused the run to be aborted. It was not possible to control the relative stoichiometry of the HfC and TaC composition throughout the reactor due to the large difference in the thermodynamics of the HfC and TaC formation from their respective chlorides. This also resulted in an inability to infiltrate TaC into the preform under the experimental conditions investigated. Other material compositions were fabricated and tested and two material systems; HfC-SiC functionally graded to C(sub f)/C and Re functionally graded to C(sub f)/C were selected for further testing. These functionally graded composites have use in a number of propulsion applications presently of interest to NASA and the defense industry. Their ability to withstand extremely hostile thermal environments and the light-weight and high-strength exhibited from the C(sub f)/C composite make these materials particularly suited for these applications. In the Phase III which is presently underway, Re functionally graded to C(sub f)/C is being further developed and tested for application in the thrust cells for the Linear Aerospike Engine for the X33 and RLV.

Derived from text

Ceramic Matrix Composites; Oxidation Resistance; Tantalum Carbides; Solid Propellant Rocket Engines; Hafnium Carbides; Propulsion System Performance; Refractory Materials

19990113121 NASA Dryden Flight Research Center, Edwards, CA USA

Evaluation of the Linear Aerospike SR-71 Experiment (LASRE) Oxygen Sensor

Ennix, Kimberly A., NASA Dryden Flight Research Center, USA; Corpening, Griffin P., NASA Dryden Flight Research Center, USA; Jarvis, Michele, NASA Dryden Flight Research Center, USA; Chiles, Harry R., NASA Dryden Flight Research Center, USA; November 1999; 24p; In English; 9th; 9th International Space Planes and Hypersonic Systems, 1-5 Nov. 1999, Norfolk, VA, USA

Contract(s)/Grant(s): RTOP 529-31-44-00-32

Report No.(s): NASA/TM-1999-206589; NAS 1.15:206589; H-2377; No Copyright; Avail: CASI; A03, Hardcopy; A01, Microfiche

The Linear Aerospike SR-71 Experiment (LASRE) was a propulsion flight experiment for advanced space vehicles such as the X-33 and reusable launch vehicle. A linear aerospike rocket engine was integrated into a semi-span of an X-33-like lifting body shape (model), and carried on top of an SR-71 aircraft at NASA Dryden Flight Research Center. Because no flight data

existed for aerospike nozzles, the primary objective of the LASRE flight experiment was to evaluate flight effects on the engine performance over a range of altitudes and Mach numbers. Because it contained a large quantity of energy in the form of fuel, oxidizer, hypergolics, and gases at very high pressures, the LASRE propulsion system posed a major hazard for fire or explosion. Therefore, a propulsion-hazard mitigation system was created for LASRE that included a nitrogen purge system. Oxygen sensors were a critical part of the nitrogen purge system because they measured purge operation and effectiveness. Because the available oxygen sensors were not designed for flight testing, a laboratory study investigated oxygen-sensor characteristics and accuracy over a range of altitudes and oxygen concentrations. Laboratory test data made it possible to properly calibrate the sensors for flight. Such data also provided a more accurate error prediction than the manufacturer's specification. This predictive accuracy increased confidence in the sensor output during critical phases of the flight. This paper presents the findings of this laboratory test.

Author

Aerospike Engines; Liquid Nitrogen; Gas Detectors; Oxygen Analyzers; Purging

23
CHEMISTRY AND MATERIALS (GENERAL)

19990108478 NASA Marshall Space Flight Center, Huntsville, AL USA

Materials Selection and Their Characteristics as Used in Rapid Prototyping

Cooper, K., NASA Marshall Space Flight Center, USA; Salvail, P., IIT Research Inst., USA; Vesely, E., IIT Research Inst., USA; Wells, D.; [1999]; 1p; In English; Investment Casting Institute Technology meeting, 31 Oct. - 3 Nov. 1999, San Francisco, CA, USA; No Copyright; Avail: Issuing Activity, Hardcopy; Abstract Only

NASA's Marshall Space Flight Center (MSFC) conducted a program to evaluate six technologies used in Rapid Prototyping (RP) to produce investment casting patterns. In this paper, RP refers to the collective additive fabrication technologies known as Solid Free-Form Fabrication. Such technologies are being used with increasing frequency in manufacturing applications, due in part to their rapidly expanding capabilities to fabricate models from many types of materials. This study used ABS plastic, polycarbonate, TrueForm PM6, epoxy resin, paper, starch, and wax. The baseline model was a semi-complex prototype fuel pump housing, intended for use in the X-33 reusable launch vehicle. All models were shelled in a production- grade colloidal silica ceramic. Primary coats were zircon-base flour with zircon backup, while secondary coats were silica grains with a tabular alumina backup. Each model was shelled in an identical manner, using the same atmospheric conditions and drying times, as well as the same number of layers. Bake-outs and firing cycles were consistent with the leach ability of each material. Preheat and bath temperatures were also kept consistent. All molds were cast in vacuum using a hydrogen-resistant superalloy (NASA- 23) that was developed in-house. The final technical evaluation included detailed measurements of the model and the final casting, in order to determine any dimensional changes caused by different pattern materials, as well as documentation of all defects and any obvious refractory/model reactions. Prototype production costs were estimated for each method and taken into consideration during trade-off analysis.

Author

Aluminum Oxides; Ceramics; Defects; Epoxy Resins; Heat Resistant Alloys; Investment Casting; Polycarbonates; Silicon Dioxide; Mechanical Properties

19990110566 Department of Energy, Washington, DC USA

New synthesis of TATB process development studies

Schmidt, R. D., Department of Energy, USA; Mitchell, A. R., Department of Energy, USA; Pagoria, P. F., Department of Energy, USA; Apr. 01, 1998; 14p; In English; 29th; ICT, USA

Report No.(s): DE98-058330; UCRL-JC-130089; CONF-980696; No Copyright; Avail: Department of Energy Information Bridge, Microfiche

We described a new synthesis of 1,3,5-triamino- 2,4,6-trinitrobenzene (TATB) in 1996 at the 27th International Annual Conference of ICT. 1,1,1- trialkylhydrazinium salts are highly reactive reagents which aminate nitroaromatic compounds through vicarious nucleophilic substitution (VNS) of hydrogen. Our new VNS synthesis potentially affords an inexpensive and a more environmentally benign preparation of TATB. We describe in this report our progress in scaling up the synthesis of TATB from the laboratory to the pilot plant. We discuss structure and control of impurities, changes in yield/quality with reaction conditions,

choice of solvents, workup and product isolation, safety, and environmental considerations. Particle size characterizations as well as small-scale safety and performance testing are also discussed.
NTIS
Reaction Kinetics; Synthesis (Chemistry); TATB

24
COMPOSITE MATERIALS

Includes physical, chemical, and mechanical properties of laminates and other composite materials. For ceramic materials see 27 Nonmetallic Materials.

19990108574 NASA Lewis Research Center, Cleveland, OH USA
Method for Forming Fiber Reinforced Composite Bodies with Graded Composition and Stress Zones
Singh, Mrityunjay, Inventor, NASA Lewis Research Center, USA; Levine, Stanley R., Inventor, NASA Lewis Research Center, USA; Smialek, James A., Inventor, NASA Lewis Research Center, USA; Aug. 31, 1999; In English
Patent Info.: Filed 30 Dec. 1997; NASA-Case-LEW-16221-1; US-Patent-5,945,166; US-Patent-Appl-SN-001584; No Copyright; Avail: US Patent and Trademark Office, Hardcopy

A near-net, complex shaped ceramic fiber reinforced silicon carbide based composite bodies with graded compositions and stress zones is disclosed. To provide the composite a fiber preform is first fabricated and an interphase is applied by chemical vapor infiltration, sol-gel or polymer processes. This first body is further infiltrated with a polymer mixture containing carbon, and/or silicon carbide, and additional oxide, carbide, or nitride phases forming a second body. One side of the second body is spray coated or infiltrated with slurries containing high thermal expansion and oxidation resistant. crack sealant phases and the other side of this second body is coated with low expansion phase materials to form a third body. This third body consisting of porous carbonaceous matrix surrounding the previously applied interphase materials, is then infiltrated with molten silicon or molten silicon-refractory metal alloys to form a fourth body. The resulting fourth body comprises dense composites consisting of fibers with the desired interphase which are surrounded by silicon carbide and other second phases materials at the outer and inner surfaces comprising material of silicon, germanium, refractory metal suicides, borides, carbides, oxides, and combinations thereof The resulting composite fourth body has different compositional patterns from one side to the other.
Author
Fiber Composites; Composite Structures; Reinforcing Materials; Metal Working; Forming Techniques; Reinforcing Fibers

19990110662 Florida Inst. of Tech., Aerospace Engineering Program, Melbourne, FL USA
Delamination Modeling of Composites for Improved Crash Analysis, *1 May 1998 - 19 May 1999*
Fleming, David C., Florida Inst. of Tech., USA; 1999; 75p; In English
Contract(s)/Grant(s): NAG1-2061; No Copyright; Avail: CASI; A04, Hardcopy; A01, Microfiche

Finite element crash modeling of composite structures is limited by the inability of current commercial crash codes to accurately model delamination growth. Efforts are made to implement and assess delamination modeling techniques using a current finite element crash code, MSC/DYTRAN. Three methods are evaluated, including a straightforward method based on monitoring forces in elements or constraints representing an interface; a cohesive fracture model proposed in the literature; and the virtual crack closure technique commonly used in fracture mechanics. Results are compared with dynamic double cantilever beam test data from the literature. Examples show that it is possible to accurately model delamination propagation in this case. However, the computational demands required for accurate solution are great and reliable property data may not be available to support general crash modeling efforts. Additional examples are modeled including an impact-loaded beam, damage initiation in laminated crushing specimens, and a scaled aircraft subfloor structures in which composite sandwich structures are used as energy-absorbing elements. These examples illustrate some of the difficulties in modeling delamination as part of a finite element crash analysis.
Author
Composite Structures; Crashes; Delaminating; Finite Element Method; Impact Damage; Mathematical Models; Crashworthiness

19990110679 NASA Marshall Space Flight Center, Huntsville, AL USA
Key Issues for Aerospace Applications of Ceramic Matrix Composites
Clinton, R. G., Jr., NASA Marshall Space Flight Center, USA; Levine, S. R., NASA Lewis Research Center, USA; [1998]; 1p; In English; Pacific Coast Regional Meeting, 22-24 Oct. 1998, Irvine, CA, USA; Sponsored by American Ceramic Society, USA;

Copyright; Avail: Issuing Activity, Hardcopy; Abstract Only

Ceramic matrix composites (CMC) offer significant advantages for future aerospace applications including turbine engine and liquid rocket engine components, thermal protection systems, and ”hot structures”. Key characteristics which establish ceramic matrix composites as attractive and often enabling choices are strength retention at high temperatures and reduced weight relative to currently used metallics. However, due to the immaturity of this class of materials which is further compounded by the lack of experience with CMC’s in the aerospace industry, there are significant challenges involved in the development and implementation of ceramic matrix composites into aerospace systems. Some of the more critical challenges are attachment and load transfer methodologies; manufacturing techniques, particularly scale up to large and thick section components; operational environment resistance; damage tolerance; durability; repair techniques; reproducibility; database availability; and the lack of validated design and analysis tools. The presentation will examine the technical issues confronting the application of ceramic matrix composites to aerospace systems and identify the key material systems having potential for substantial payoff relative to the primary requirements of light weight and reduced cost for future systems. Current programs and future research opportunities will be described in the presentation which will focus on materials and processes issues.

Author

Aerospace Engineering; Structural Engineering; Ceramic Matrix Composites; Composite Structures; Engine Parts; Turbine Engines; Liquid Propellant Rocket Engines

19990111456 Atlanta Univ., GA USA

Long Term Durability of Polymer Matrix Composites for High Temperature Applications

Badir, Ashraf, Atlanta Univ., USA; Shonkwiler, Brian, Atlanta Univ., USA; HBCUs/OMUs Research Conference Agenda and Abstracts; August 1999, pp. 9; In English; See also 19990111455; No Copyright; Avail: Issuing Activity, Hardcopy; Abstract Only

The objective of this research is to identify the mechanisms of damage in tension-tension, fatigue of unidirectional T650-35 carbon fiber/AMB-21 polyimide laminates. AMB-21 is a polymer developed by NASA GRC as a noncarcinogenic environmentally friendly polyimide. An experimental study was conducted to investigate the mechanical behavior of the unidirectional T650-35/AMB-21 polymer composite system and the AMB-21 resin matrix. Quasi-static tensile and fatigue properties were examined. Accomplishments included successful fatigue testing with tabbed dog-bone shaped specimen in which failure occurred away from the tabs. The data obtained will help in assessing replacement of PMR-15 with AMB-21 as a matrix for high temperature applications. Fatigue experiments at room temperature and high temperature (230 C) have been conducted for several unidirectional dog bone samples at a level of maximum stress, S(sub max) = (0.70 - 0 90) sigma(sub ult), with R(sub sigma) = 0.1 (sigma(sub min)/sigma(sub max)). The S(sub max) values were based on the average ultimate tensile strength, sigma(sub ult), obtained from the static tensile test (234xl0(exp 3) psi at room temperature and 195xl0(exp 3) psi at 230C). A cyclic load frequency of 10 Hz with a sinusoidal command waveform was employed. All high temperature tests were conducted under isothermal conditions. A test fixture made of aluminum machined into two matching halves was used Each half of the fixture contained resistance heater rods. Heat from the fixture was transferred to the test specimen through direct contact of fixture and specimen along the entire length of the fixture and across the entire width of the specimen. The fatigue life diagram for tension-tension loading of the unidirectional T650-35/AMB21 laminates was determined. The axes of the diagram are strain arid logarithm of the load cycles to failure. Although fatigue testing is done under controlled load, the variable on the vertical axis of the diagram is the maximum strain attained in the first load cycle. The significance of the maximum strain is that this quantity represents the state of damage reached in the first load cycle and it is reasonable to expect trial any progression of damage in subsequent load cycles will be determined by this state of damage. Furthermore the two extreme states in fatigue, i.e., the static failure and the fatigue limit, are given generically in terms of strain.

Author

Cyclic Loads; Failure; Fatigue Tests; High Temperature Tests; Loads (Forces); Polymer Matrix Composites; Tensile Properties; Thermodynamic Properties; Thermal Fatigue

19990111471 NASA Glenn Research Center, Cleveland, OH USA

Aerothermo-Structural Analysis of Low Cost Composite Nozzle/Inlet Components

Shivakumar, Kuwigai, North Carolina Agricultural and Technical State Univ., USA; Challa, Preeli, North Carolina Agricultural and Technical State Univ., USA; Sree, Dave, Tuskegee Inst., USA; Reddy, D., NASA Glenn Research Center, USA; HBCUs/OMUs Research Conference Agenda and Abstracts; August 1999, pp. 25; In English; See also 19990111455; No Copyright; Avail: Issuing Activity, Hardcopy; Abstract Only

This research is a cooperative effort among the Turbomachinery and Propulsion Division of NASA Glenn, CCMR of NC A&T State University, and the Tuskegee University. The NC A&T is the lead center and Tuskegee University is the participating institution. Objectives of the research were to develop an integrated aerodynamic, thermal and structural analysis code for design

of aircraft engine components, such as, nozzles and inlets made of textile composites; conduct design studies on typical inlets for hypersonic transportation vehicles and setup standards test examples and finally manufacture a scaled down composite inlet. These objectives are accomplished through the following seven tasks: (1) identify the relevant public domain codes for all three types of analysis; (2) evaluate the codes for the accuracy of results and computational efficiency; (3) develop aero-thermal and thermal structural mapping algorithms; (4) integrate all the codes into one single code; (5) write a graphical user interface to improve the user friendliness of the code; (6) conduct test studies for rocket based combined-cycle engine inlet; and finally (7) fabricate a demonstration inlet model using textile preform composites. Tasks one, two and six are being pursued. Selected and evaluated NPARC for flow field analysis, CSTEM for in-depth thermal analysis of inlets and nozzles and FRAC3D for stress analysis. These codes have been independently verified for accuracy and performance. In addition, graphical user interface based on micromechanics analysis for laminated as well as textile composites was developed. Demonstration of this code will be made at the conference. A rocket based combined cycle engine was selected for test studies. Flow field analysis of various inlet geometries were studied. Integration of codes is being continued. The codes developed are being applied to a candidate example of trailblazer engine proposed for space transportation. A successful development of the code will provide a simpler, faster and user-friendly tool for conducting design studies of aircraft and spacecraft engines, applicable in high speed civil transport and space missions.

Author

Aerothermodynamics; Aircraft Design; Algorithms; Composite Materials; Engine Parts; Micromechanics; Structural Analysis; Textiles; Thermal Analysis

19990111538 NASA Glenn Research Center, Cleveland, OH USA

Quantifying Uncertainties in the Thermo-Mechanical Properties of Particulate Reinforced Composites

Mital, Subodh K., Toledo Univ., USA; Murthy, Pappu L. N., NASA Glenn Research Center, USA; June 1999; 18p; In English

Contract(s)/Grant(s): NCC3-524; RTOP 523-21-13

Report No.(s): NASA/TM-1999-209174; E-11681; NAS 1.15:209174; No Copyright; Avail: CASI; A03, Hardcopy; A01, Microfiche

The present paper reports results from a computational simulation of probabilistic particulate reinforced composite behavior. The approach consists use of simplified micromechanics of particulate reinforced composites together with a Fast Probability Integration (FPI) technique. Sample results are presented for a Al/SiC(sub p)(silicon carbide particles in aluminum matrix) composite. The probability density functions for composite moduli, thermal expansion coefficient and thermal conductivities along with their sensitivity factors are computed. The effect of different assumed distributions and the effect of reducing scatter in constituent properties on the thermal expansion coefficient are also evaluated. The variations in the constituent properties that directly effect these composite properties are accounted for by assumed probabilistic distributions. The results show that the present technique provides valuable information about the scatter in composite properties and sensitivity factors, which are useful to test or design engineers.

Author

Numerical Analysis; Computation; Particulate Reinforced Composites; Thermal Expansion; Mechanical Properties

19990111588 NASA Langley Research Center, Hampton, VA USA

Method of Fabricating Chopped-Fiber Composite Piston

Rivers, H. Kevin, Inventor, NASA Langley Research Center, USA; Ransone, Philip O., Inventor, NASA Langley Research Center, USA; Northam, G. Burton, Inventor, NASA Langley Research Center, USA; Sep. 07, 1999; In English; Provisional US-Patent-Appl-SN-012930, filed 6 Mar. 1996

Patent Info.: Filed 5 Mar. 1997; NASA-Case-LAR-15643-1; US-Patent-5,948,330; US-Patent-Appl-SN-816403; US-Patent-Appl-SN-012930; No Copyright; Avail: US Patent and Trademark Office, Hardcopy

A three-dimensional piston molding is fabricated from a mixture of chopped, carbon tow filaments of variable length, which are prepregged with carbonaceous organic resins and/or pitches and molded by conventional molding processes into a near net shape, to form a carbon-fiber reinforced organic-matrix composite part. Continuous reinforcement in the form of carbon-carbon composite tapes or pieces of fabric can be also laid in the mold before or during the charging of the mold with the chopped-fiber mixture, to enhance the strength in the crown and wrist-pin areas. The molded chopped-fiber reinforced organic-matrix composite parts are then pyrolized in an inert atmosphere, to convert the organic matrix materials to carbon. These pyrolized parts are then densified by reimpregnation with resins or pitches, which are subsequently carbonized. Densification is also accomplished by direct infiltration with carbon by vapor deposition processes. Once the desired density has been achieved, the piston molds are

machined to final piston dimensions, and piston ring grooves are added. to prevent oxidation and/or to seal the piston surface or near surface, the chopped-fiber piston is coated with ceramic and/or metallic sealants: and/or coated with a catalyst.
Author
Fabrication; Fiber Composites; Pistons; Molds

19990113120 Massachusetts Inst. of Tech., Cambridge, MA USA
Mechanism-based Modeling of Long-term Degradation
McManus, H. L., Massachusetts Inst. of Tech., USA; Foch, B. J., Space Systems/Loral, USA; Cunningham, R. A., Boeing Co., USA; Proceedings of the 3rd International Conference on Progress in Durability Analysis of Composite Systems; 1998, pp. 63-70; In English; 3rd; Progress in Durability Analysis of Composite Systems, 14-17 Sep. 1997, Blacksburg, VA, USA
Contract(s)/Grant(s): NAG3-2054; ISBN 90-5410-960-2; Copyright; Avail: Issuing Activity, Hardcopy

The use of composites in high temperature, long lifetime applications requires a basic understanding of composite degradation mechanisms, advances in analytical capabilities, and accurate accelerated and scaled tests. to advance all of these goals, models are proposed based on a variety of fundamental material mechanisms. Thermal, oxygen, and moisture diffusion, chemical reactions, composite micromechanics; modified laminated plate theory, and future mechanics based damage models are used. All models attempt to stay as simple and fundamental as possible. All are coupled, so that interactions between various effects are modeled implicitly. Ongoing efforts at MIT are reviewed here, with some reference to other work, but no attempt is made to do a comprehensive review. Mechanism based models are yielding understanding of the mechanisms behind observed degradation phenomena, are helping to design accelerated tests, and are the first steps towards a predictive capability.
Author
Mechanical Properties; Durability; Micromechanics; Mathematical Models; Structural Analysis; Thermal Degradation

25
INORGANIC AND PHYSICAL CHEMISTRY

Includes chemical analysis, e.g., chromatography; combustion theory; electrochemistry; and photochemistry. For related information see also 77 Thermodynamics and Statistical Physics.

19990106564 Alabama Univ., Center for Microgravity and Materials Research, Huntsville, AL USA
Temperature Dependence of Diffusivities in Liquid Elements (LMD) ***Final Report, 3 Feb. 1993 - 31 May 1998***
Banish, R. Michael, Alabama Univ., USA; Rosenberger, Franz, Alabama Univ., USA; May 1998; 47p; In English
Contract(s)/Grant(s): NAS8-39716; NCC8-99
Report No.(s): NASA/CR-1999-209738; NAS 1.26:209738; No Copyright; Avail: CASI; A03, Hardcopy; A01, Microfiche

This research was to advance the understanding of diffusion mechanisms in liquid metals and alloys through accurate diffusivity measurements over a wide range of temperatures, including the proximity of the materials melting points. Specifically, it was driven towards developing a methodology (and subsequent flight hardware) to enable several diffusion coefficient measurements (i.e., at several different temperatures) to be performed using a single sample. The Liquid Metal Diffusion (LMD) was funded as a Flight Definition Project in February 1993 in response to NRA 91-OSSA-20 (Microgravity Science and Applications Division). The Science Concept Review for LAID was held during April 1994. In January 1995 we were informed that we had failed this review and the project was change to ground-based activities only. A new proposal was submitted for the next NRA addressing the panels concerns. As part of NASA's Risk Mitigation program, a scaled-down version of the hardware was funded in July of 1995 for a flight opportunity utilizing experiment on the Microgravity Isolation Mount. This experiment was to determine the self-diffusivity of indium at 185 C. The LMD was transferred to the Mir Space Station in STS-81 and returned on STS-84 (January - May 1997). Three, out of five, self-diffusion data sets were returned. A description of this experiment/hardware is included below. This summary is only intended to give the reader an overview of the results obtained for the tasks outlined in the original proposal. Research that was not published is explained in more detail. At the end of this report is a list of refereed publications and invited talks that were given as a result of this work. The reader is directed to these for further details. Attachment: Real-time diffusivity measurements in liquids at several temperatures with one sample, On the insensitivity of liquid diffusivity measurements to deviations from 1D transport, and Numerical simulations of the convective contamination of diffusivity measurements in liquids.
Derived from text
Temperature Dependence; Liquid Metals; Diffusion Coefficient; Research; Diffusivity; Convection; Fluid Mechanics

19990107326 Kyushu Univ., Graduate School of Engineering, Fukuoka, Japan

Monte Carlo Simulation of the Three-Dimensional XY Model with Bilinear-Biquadratic Exchange Interaction II

Nagata, Hideki, Kyushu Univ., Japan; Tanaka, Akinori, Kyushu Univ., Japan; Muraoka, Yoshinori, Kyushu Univ., Japan; Idogaki, Toshihiro, Kyushu Univ., Japan; Technology Reports of Kyushu University; July 1999; ISSN 0023-2718; Volume 72, No. 4, pp. 361-368; In Japanese; No Copyright; Avail: CASI; A02, Hardcopy; A01, Microfiche

The three-dimensional XY model with bilinear and biquadratic exchange interaction, J and J', has been studied by Monte Carlo simulation. From the detailed analysis of the histogram for the order parameter distribution and of the Binder parameter, the successive pbase transition found for 0 is less than J/J' </= 0.35 between quadrupole and dipole ordering can be characterized as a first order type. The finite size scaling analysis gives a precise estimate of the critical exponent gamma and nu for the continuous phase transition from paramagnetic to quadrupole or (dipole–quadrupole) ordered phase, and suggests that the present system belongs to the same universality class with the conventional XY model which includes no biquadratic exchange interaction J'.

Author

Monte Carlo Method; Computerized Simulation

19990107343 Sandia National Labs., Albuquerque, NM USA

Reactions and Diffusion During Annealing-Induced H(+) Generation in SOI Buried Oxides; Microelectronics Engineering

Devine, R. A. B.; Fleetwood, D. M.; Vanheusden, K.; Warren, W. L.; Jun. 07, 1999; 4p; In English

Report No.(s): DE00-007451; SAND99-1430J; No Copyright; Avail: Department of Energy Information Bridge, Hardcopy

We report experimental results suggesting that mobile protons are generated at strained Si-O-Si bonds near the Si/SiO interface during annealing in forming gas. Our data further suggest that the presence of the top Si layer plays a crucial role in the mobile generation process. Finally, we show that the diffusion of the reactive species presumably towards the generation sites occurs laterally along the buried oxide layer, and can be impeded significantly due to the presence of trapping sites in the buried oxide.

NTIS

Silicon Oxides; Hydrogen Ions; Experimentation; Data Acquisition; Annealing; Diffusion

19990109047 California Univ., Mechanical and Aerospace Engineering Dept., Los Angeles, CA USA

Ignition Delay Associated with a Strained Strip

Gerk, T. J., California Univ., USA; Karagozian, A. R., California Univ., USA; 1996, pp. 1095-1102; In English; 26th; Combustion, 1996, Pittsburgh, PA, USA

Contract(s)/Grant(s): N00014-93-I-1383; NCC2-374; Copyright; Avail: Issuing Activity, Hardcopy, Microfiche

Ignition processes associated with two adjacent fuel-oxidizer interferences bounding a strained fuel strip are explored here using single-step activation energy asymptotics. Calculations are made for constant as well as temporally decaying strain fields. There possible models of ignition are determined: one in which the two interfaces ignite independently as diffusion flames; one in which the two interfaces ignite dependently and in which ignition occurs to form a single , premixed flame at very high strain rates before ignition is completely prevented. In contrast to a single, isolated interface in which ignition can be prevented by overmatching heat production with heat convection due to strain, ignition of a strained fuel strip can also be prevented if the finite extend of fuel is diluted by oxidizer more quickly than heat production can cause a positive feedback thermal runaway. These behaviors are dependent on the relative sizes of timescales associated with species and heat diffusion, with convection due to strain, and with the chemical reaction. The result here indicate that adjacent, strained species interfaces may ignite quite differently in nature from ignition of a single, strained intrface and that their interdependence should be considered as the interfaces are brought closer together in complex strain fields. Critical strain rates leading to complete ignition delay are found to be considerably smaller for the fuel strip than those for single interfaces as the fuel strip is made thin in comparison to diffusion and chemical length scales.

Author

Ignition; Delay; Positive Feedback; Diffusion Length; Chemical Reactions

19990109094 AeroChem Research Labs., Inc., Princeton, NJ USA

Interaction of Burning Metal Particles ***Final Report, 1 Jul. 1996 - 31 Aug. 1999***

Dreizin, Edward L., AeroChem Research Labs., Inc., USA; Berman, Charles H., AeroChem Research Labs., Inc., USA; Hoffmann, Vern K., AeroChem Research Labs., Inc., USA; Aug. 31, 1999; 85p; In English

Contract(s)/Grant(s): NAS3-96017

Report No.(s): TP-579; No Copyright; Avail: CASI; A05, Hardcopy; A01, Microfiche

Physical characteristics of the combustion of metal particle groups have been addressed in this research. The combustion behavior and interaction effects of multiple metal particles has been studied using a microgravity environment, which presents a unique opportunity to create an ”aerosol” consisting of relatively large particles, i.e., 50-300 m diameter. Combustion behavior of such an aerosol could be examined using methods adopted from well-developed single particle combustion research. The experiment included fluidizing relatively large (order of 100 m diameter) uniform metal particles under microgravity and igniting such an ”aerosol” using a hot wire igniter. The flame propagation and details of individual particle combustion and particle interaction have been studied using a high speed movie and video-imaging with cameras coupled with microscope lenses to resolve individual particles. Interference filters were used to separate characteristic metal and metal oxide radiation bands from the thermal black body radiation. Recorded flame images were digitized and various image processing techniques including flame position tracking, color separation, and pixel by pixel image comparison were employed to understand the processes occurring in the burning aerosol. The development of individual particle flames, merging or separation, and extinguishment as well as induced particle motion have been analyzed to identify the mechanisms governing these processes. Size distribution, morphology, and elemental compositions of combustion products were characterized and used to link the observed in this project aerosol combustion phenomena with the recently expanded mechanism of single metal particle combustion.

Author

Chemical Composition; Combustion Physics; Combustion Products; Igniters; Image Processing; Metal Combustion; Metal Particles; Particle Interactions; Size Distribution

19990110072 Flinders Univ., Dept. of Physics, Adelaide, Australia

The Development of Electron Momentum Spectroscopy

McCarthy, Ian E., Flinders Univ., Australia; Australian Journal of Physics; 1998; Volume 51, No. 4, pp. 593-607; In English; See also 19990110071; Copyright; Avail: Issuing Activity (Australian Journal of Physics, P.O. Box 1139, 150 Oxford St., Collingwood, Victoria 3066, Australia), Hardcopy, Microfiche

Electron momentum spectroscopy measures relative differential cross sections as a function of recoil momentum for energy-resolved states of the ion in a kinematically-complete electron- impact ionisation experiment. The experiment is done in a kinematic range where correct cross sections are obtained by simple reaction approximations. It amounts to a measurement of orbital momentum densities and coefficients describing electron correlations in the ion for most ion states of a gas target. Certain ion states give information about ground-state correlations. For a solid target it amounts to a measurement of the energy-momentum density of occupied electron bands.

Author

Electron Spectroscopy; Scattering Cross Sections; Ionized Gases; Kinetic Energy

19990110073 Australian National Univ., Atomic and Molecular Physics Lab., Canberra, Australia

Recent Developments in Electron Momentum Spectroscopy of Solids

Vos, Maarten, Australian National Univ., Australia; Australian Journal of Physics; 1998; Volume 51, No. 4, pp. 609-618; In English; See also 19990110071; Copyright; Avail: Issuing Activity (Australian Journal of Physics, P.O. Box 1139, 150 Oxford St., Collingwood, Victoria 3066, Australia), Hardcopy, Microfiche

With the advent of two-dimensional electron detection, electron momentum spectroscopy of solids evolved from a spectroscopy in its infancy to a new, viable technique, looking for its place in solid state physics. Here I give an overview of the first sets of experiments, the evolution of the interpretation of these experiments and possible future directions.

Author

Electron Spectroscopy; Momentum; Technology Assessment

19990110074 Tsinghua Univ., EMS Lab., Bejing, China

Progress of Electron Momentum Spectroscopy in China

Chen, X. J., Tsinghua Univ., China; Australian Journal of Physics; 1998; Volume 51, No. 4, pp. 619-632; In English; See also 19990110071; Copyright; Avail: Issuing Activity (Australian Journal of Physics, P.O. Box 1139, 150 Oxford St., Collingwood, Victoria 3066, Australia), Hardcopy, Microfiche

Developments in the application of electron momentum spectroscopy (EMS) in China are described. Particular attention will focus on our progress in applying various generation EMS spectrometers to atomic and molecular targets of interest. Results from these experiments are presented.

Author

Electron Spectroscopy; Momentum; Progress

19990110083 Australian National Univ., Research School of Physical Sciences and Engineering, Canberra, Australia

Future Directions in Electron Momentum Spectroscopy of Matter

Weigold, Erich, Australian National Univ., Australia; Australian Journal of Physics; 1998; Volume 51, No. 4, pp. 751-761; In English; Past Achievements and Future Directions in Electron Momentum Spectroscopy on Atoms, Molecules and Solids, Nov. 1997, Adelaide, Australia; See also 19990110071; Copyright; Avail: Issuing Activity (Australian Journal of Physics, P.O. Box 1139, 150 Oxford St., Collingwood, Victoria 3066, Australia), Hardcopy, Microfiche

The development of coincidence spectrometers with multivariable detection techniques, higher energy kinematics, monochromated and spin-polarized electron sources, will usher in a new generation of electron momentum spectroscopy revealing new electronic phenomena in atoms, molecules and solids. This will be enhanced by developments in target preparation, such as spin polarised, oriented and aligned atoms and molecules, radicals, surfaces and strongly correlated systems in condensed matter.

Author

Electron Spectroscopy; Momentum; Condensed Matter Physics

19990110112 Naval Surface Warfare Center, Indian Head, MD USA

BuNENA Wastewater Treatment Summary

Marx, W. J., Naval Surface Warfare Center, USA; Simms, B., Naval Surface Warfare Center, USA; JANNAF 28th Propellant Development and Characterization Subcommittee and 17th Safety and Environmental Protection Subcommitte Joint Meeting; April 1999; Volume 1, pp. 267-275; In English; See also 19990110087; No Copyright; Avail: CPIA, 10630 Little Patuxent Pkwy., Suite 202, Columbia, MD 21044-3200 HC, Hardcopy

NSWC, IHDIV has been tasked with the development of a commercially viable process for the production of n-butyl nitratoethylnitramine (BuNENA). As part of this effort, the Environmental Technology Branch was tasked to develop a process for treatment of the wastewater streams generated by this process. This report outlines the basic BuNENA wastewater treatment system and the lessons learned during the development of the process. The process developed for treating this wastewater incorporates three basic wastewater treatment techniques, neutralization and settling, activated carbon filtration, and biological treatment. Each technique is designed to remove a characteristic or constituent that would prevent the water from being discharged to local surface waters. The pH of the water prior to treatment makes it a corrosive characteristic hazardous waste. The BuNENA and acetate concentrations make the water present a toxicity and Biological Oxygen Demand (BOD) problem that would not be allowed under our current NPDES permit. by the end of this project, 15 batches of wastewater were successfully treated, for a total of approximately 16,000 gallons. 25 drums of spent carbon, and 45 gallons of BuNENA rich liquid organic waste were generated from this process. Consumed during this time were 5,000 lbs. of activated carbon, 11,300 lbs. sodium hydroxide, and 800 lbs. sodium carbonate. This report also includes a revised cost estimate for treating this wastewater and a summary of the data collected during the treatment of the wastewater.

Author

Waste Water; Water Treatment; Toxicity; Biochemical Oxygen Demand; Water Pollution; Waste Treatment

19990110115 Primex Aerospace Co., Redmond, WA USA

Detection of Silicon Contamination in Hydrazine

Wucherer, E. J., Primex Aerospace Co., USA; Christofferson, S. S., Primex Aerospace Co., USA; JANNAF 28th Propellant Development and Characterization Subcommittee and 17th Safety and Environmental Protection Subcommitte Joint Meeting; April 1999; Volume 1, pp. 289-299; In English; See also 19990110087; No Copyright; Avail: CPIA, 10630 Little Patuxent Pkwy., Suite 202, Columbia, MD 21044-3200 HC, Hardcopy

The silicon contamination level in hydrazine was monitored as part of an elastomer compatibility program. The initial test method utilized graphite furnace atomic absorption spectroscopy (GFAAS) to monitor the silicon content (along with calcium and zinc). Discrepancies in the observed versus predicted values of silicon contamination led us to suspect the accuracy of the GFAAS result. Subsequently, samples were reanalyzed by inductively coupled plasma - mass spectroscopy (ICP-MS), flame AAS and ICP-optical emission spectroscopy (ICP-OES). Flame AAS and ICP-OES were found to deliver consistent values of silicon contamination in the ppm range while GFAAS and ICP-MS values were variable and significantly lower. Proposed explanations of the discrepancies will be presented.

Author

Silicon; Contamination; Hydrazines

19990110301 Department of Energy, Office of Energy Research, Washington, DC USA

Influence of surface defects and local structure on acid/base properties and oxidation pathways over metal oxide surfaces ***Final Report, Jun. 1990 - Jan. 1997***

Cox, D. F., Department of Energy, USA; Dec. 31, 1997; 19p; In English

Report No.(s): DE99-000026; DOE/ER/14129-T1; No Copyright; Avail: Department of Energy Information Bridge, Microfiche

This final report covers work done during project period one and project period two. All the work in project period one was focused on the selective oxidation of oxygenated hydrocarbons over the SnO2(110) single crystal surface. In project period two, the emphasis was on the acid/base properties of SnO(110) as well as two different Cu2O single crystal surfaces. Prior to the summary of results, a description of these different surfaces is given as background information. Results are described for the dissociation and reaction of Bronsted acids (methanol, formic acid, water, formaldehyde, acetone, propene, acetic acid, and carbon monoxide). Results from project period two include: ammonia adsorption, CO2 adsorption, propene adsorption and oxidation, with tin oxides; complimentary work with copper oxides; and STM investigations.

NTIS

Metal Oxides; Surface Defects; Crystal Surfaces; Tin Oxides; Copper Oxides; Oxidation

19990110568 National Inst. of Standards and Technology, Building and Fire Research Lab., Gaithersburg, MD USA

Molecular Level Design of Fire Retardants and Suppressants

Nyden, M. R., National Inst. of Standards and Technology, USA; January 1999; 42p; In English

Report No.(s): PB98--148406; NISTIR-6275; No Copyright; Avail: Issuing Activity (Natl Technical Information Service (NTIS)), Microfiche

The various methods that comprise the field of molecular modeling are reviewed in the context of their potential for application to the molecular level design of new fire retardants and suppressants. The capabilities of these techniques are demonstrated by performing calculations on systems ranging in molecular complexity from small gas phase molecules to polymers. As a consequence of its fundamental basis, molecular modeling can be used to predict the properties of new materials in ways that macroscopic models cannot and, thereby, offers an unrivaled potential for computer aided molecular design. The purpose of this paper therefore, to provide a meaningful introduction to the field with an emphasis on how these techniques can be applied to the design and development of fire retardants and suppressants.

NTIS

Flame Retardants; Computer Aided Design; Polymers; Molecular Gases; Suppressors

19990110572 Department of Energy, Office of Energy Research, Washington, DC USA

Identification and temporal behavior of radical intermediates formed during the combustion and pyrolysis of gaseous fuels: Kinetic pathways to soot formation ***Final Report, 1 Ju. 1994 - 30 Jun. 1997***

Kern, R. D., Department of Energy, USA; Sep. 30, 1998; 19p; In English

Report No.(s): DE99-001092; DOE/ER/13400-18; No Copyright; Avail: Department of Energy Information Bridge, Microfiche

The authors have developed software in-house to automate the processing of peak heights recorded from the shock tube: time-of-flight mass spectrometer (TOF) experiments in a format suitable for the modeling programs and have performed numerous ab initio calculations to provide energy barrier values and thermodynamic data for several key reactions in various reaction mechanisms. Each of the studies described here has contributed to the understanding of the detailed kinetics of the reactions of acyclic fuels, the thermal decompositions of aromatic ring compounds, the shock tube techniques dedicated to combustion science problems, and the role of theoretical chemistry in providing essential thermodynamic and kinetics information necessary for constructing plausible reaction mechanisms. The knowledge derived from these investigations is applicable not only to the area of pre-particle soot formation chemistry, but also to various incineration and coal pyrolysis problems.

NTIS

Fuels; Combustion; Pyrolysis; Reaction Kinetics; Soot

19990110692 Georgia Inst. of Tech., School of Earth and Atmospheric Sciences, Atlanta, GA USA

The Measurement of Sulfur Oxidation Products and Their Role in Homogeneous Nucleation ***Final Report, 1 Jul. 1997 - 30 Jun. 1999***

Eisele, F. L., Georgia Inst. of Tech., USA; 1999; 50p; In English

Contract(s)/Grant(s): NAG5-6383; GT Proj. G35-W91; No Copyright; Avail: CASI; A03, Hardcopy; A01, Microfiche

An improved version of a transverse ion source was developed which uses selected ion chemical ionization mass spectrometry techniques inside of a particle nucleation flow tube. These new techniques are very unique, in that the chemical

ionization is done inside of the flow tube rather than by having to remove the compounds and clusters of interest which are lost on first contact,with any surfaces. The transverse source is also unique because it allows the ion reaction time to be varied over more than an order of magnitude, which in turn makes possible the separation of ion induced cluster growth from the charging of preexisting molecular clusters. As a result of combining these unique capabilities, the first ever measurements of prenucleation molecular clusters were performed. These clusters are the intermediate stage of growth in the gas-to-particle conversion process. This new technique provides a means of observing clusters containing 2, 3, 4, ... and up to about 8 sulfuric acid molecules, where the critical cluster size under these measurement conditions was about 4 or 5. Thus, the nucleation process can now be directly observed and even growth beyond the critical cluster size can be investigated. The details of this investigation are discussed in a recently submitted paper, which is included as Appendix A. Measurements of the diffusion coefficient of sulfuric acid and sulfuric acid clustered with a water molecule have also been performed. The measurements are also discussed in more detail in another recently submitted paper which is included as Appendix B. The empirical results discussed in both of these papers provide a critical test of present nucleation theories. They also provide new hope for resolving many of the huge discrepancies between field observation and model prediction of particle nucleation. The second part of the research conducted under this project was directed towards the development of new chemical ionization techniques for measuring sulfur oxidation products.

Derived from text

Sulfuric Acid; Ion Sources; Nucleation; Reaction Time; Oxidation; Molecular Clusters

19990110713 Colorado Univ., Mechanical Engineering Dept., Boulder, CO USA

Combustion of Metals in Reduced-Gravity and Extra Terrestrial Environments

Branch, M.C., Colorado Univ., USA; Abbud–Madrid, A., Colorado Univ., USA; Daily, J. W., Colorado Univ., USA; Sep. 15, 1999; 7p; In English

Contract(s)/Grant(s): NAG3-2220

Report No.(s): CCER-99-06; No Copyright; Avail: CASI; A02, Hardcopy; A01, Microfiche

The combustion of metals is a field with important practical applications in rocket propellants, high-temperature flames, and material synthesis. Also, the safe operation of metal containers in high-pressure oxygen systems and with cryogenic fuels and oxidizers remains an important concern in industry. The increasing use of metallic components in spacecraft and space structures has also raised concerns about their flammability properties and fire suppression mechanisms. In addition, recent efforts to embark on unmanned and manned planetary exploration, such as on Mars, have also renewed the interest in metal/carbon-dioxide combustion as an effective in situ resource utilization technology. In spite of these practical applications, the understanding of the combustion properties of metals remains far behind that of the most commonly used fuels such as hydrocarbons. The lack of understanding is due to the many problems unique to metal- oxidizer reactions such as: low-temperature surface oxidation prior to ignition, heterogeneous reactions, very high combustion temperatures, product condensation, high emissivity of products, and multi-phase interactions. Very few analytical models (all neglecting the influence of gravity) have been developed to predict the burning characteristics and the flame structure details. Several experimental studies attempting to validate these models have used small metal particles to recreate gravity-free conditions. The high emissivity of the flames, rapid reaction, and intermittent explosions experienced by these particles have made the gathering of any useful information on burning rates and flame structure very difficult. The use of a reduced gravity environment is needed to clarify some of the complex interactions among the phenomena described above. First, the elimination of the intrusive buoyant flows that plague all combustion phenomena is of paramount importance in metal reactions due to the much higher temperatures reached during combustion. Second, a low-gravity environment is absolutely essential to remove the destructive effect of gravity on the shape of a molten metal droplet in order to study a spherically symmetric condition with large bulk samples. The larger size of the spherical metal droplet and the longer burning times available in reduced gravity extend the spatial and temporal dimensions to permit careful probing of the flame structure and dynamics. Third, the influence of the radiative heat transfer from the solid oxides can be studied more carefully by generating a stagnant spherical shell of condensed products undisturbed by buoyancy.

Derived from text

Gravitational Effects; Mathematical Models; Metal Combustion; Burning Rate; Combustion Physics; Radiative Heat Transfer

26
METALLIC MATERIALS

Includes physical, chemical, and mechanical properties of metals, e.g., corrosion; and metallurgy.

19990107330 Boeing Co., Rocketdyne Div., Canoga Park, CA USA
Effects of Internal and External Hydrogen on Inconel 718
Walter, R. J., Boeing Co., USA; Frandsen, J. D., Boeing Co., USA; [1999]; 1p; In English; TMS 1999 Fall Meeting, 31 Oct. - 4 Nov. 1999, Cincinnati, OH, USA; Sponsored by ASM International, USA
Contract(s)/Grant(s): NAS8-27980; No Copyright; Avail: Issuing Activity, Hardcopy; Abstract Only

Internal hydrogen embrittlement (IHE) and hydrogen environment embrittlement (HEE) tensile and bend crack growth tests were performed on Inconel 718. For the IHE tests, the specimens were precharged to approximately 90 ppm hydrogen by exposure to 34.5 MPa H2 at 650 C. The HEE tests were performed in 34.5 MPa H2. Parameters evaluated were test temperature, strain rate for smooth and notch specimen geometries. The strain rate effect was very significant at ambient temperature for both IHE and HEE and decreased with increasing temperatures. For IHE, the strain rate effect was neglible at 260'C, and for HEE the strain rate effect was neglible at 400 C. At low temperatures, IHE was more severe than HEE, and at high temperatures HEE was more severe than IHE with a cross over temperature about 350 C. At 350 C, the equilibrium hydrogen concentration in Inconel 718 is about 50% lower than the hydrogen content of the precharged IHE specimens. Dislocation hydrogen sweeping of surface absorbed hydrogen was the likely transport mechanism for increasing the hydrogen concentration in the HEE tests sufficiently to produce the same degree of embrittlement as that of the more highly hydrogen charged IHE specimens. The main IHE fracture characteristic was formation of large, brittle flat facets, which decreased with increasing test temperature. The IHE fracture matrix surrounding the large facets ranged between brittle fine faceted to microvoid ductility depending upon strain rate, specimen geometry as well as temperature. The HEE fractures were characteristically fine featured, transgranular and brittle with a significant portion forming a "saw tooth" crystallographic pattern. Both IHE and HEE fractures were predominantly along the {1 1 1) slip and twin boundaries. With respect to embrittlement mechanism, it was postulated that dislocation hydrogen sweeping and hydrogen enhanced localized plasticity were active in HEE and IHE for concentrating hydrogen along (1 1 1) slip and twin planes. Final brittle failure occurred by hydrogen induced planer decohesion.
Author
Hydrogen; Hydrogen Embrittlement; Brittleness; Ductility; Inconel (Trademark); Iron Alloys; Steels

19990107355 Sandia National Labs., Albuquerque, NM USA
Tensile Creep Properties of the 50Au-50Cu Braze Alloy
Stephens, J. J.; May 28, 1999; 13p; In English; Symposium to Honor Julia Weertman, 1-4 Nov. 19999, Cincinnati, OH, USA; Sponsored by Department of Energy, USA
Report No.(s): DE00-007143; SAND99-0758C; No Copyright; Avail: Department of Energy Information Bridge, Hardcopy

The 50Au-50CU (wt.%) alloy is a solid-solution strengthened braze alloy used extensively in conventional, hermetic metal/ceramic brazing applications where low vapor pressure is a requirement. Typical metal/ceramic base materials would be Kovar(TM) alloy and metallized and Ni-plated 94% alumina ceramic. The elevated temperature mechanical properties are important for permitting FEA evaluation of residual stresses in metal/ceramic brazes given specific geometries and braze cooldown profiles. For material with an atomic composition of 76.084 at.% CL 23.916 Au (i.e., on the Cu-rich side of Cu3Au) that was annealed for 2 hr. at 750 C and water quenched a Garofalo sin(h) equation was found to adequately characterize the minimum strain rate data over the temperature mnge 450-850 C. At lower temperatures (250 arid 350 C), a conventional power law equation was found to characterize the data. For samples held long periods of time at 375 C (96 hrs.) and slowly cooled to room temperature, a slight strengthening reaction was observed: with the stress necessary to reach the same strain rate increasing by about 15% above the baseline annealed and quenched data. X-ray deffiction indicates that the 96 hr at 375 C + slow cool condition does indeed order. The microhardness of the ordered samples indicates a value of 94.5 VHN, compared to 93.7 VHN for the baseline annealed and quenched (disordered FCC) samples. From a brazing perspective, the relative sluggishness of this ordering reaction does not appear to pose a problem for braze joints cooled at reasonable rates following brazing.
NTIS
Brazing; Gold Alloys; Copper Alloys; Tensile Properties; Mechanical Properties; Soldered Joints

19990110476 Department of Energy, Washington, DC USA
Ab initio calculation of tight-binding parameters
McMahan, A. K., Department of Energy, USA; Klepeis, J. E., Department of Energy, USA; Dec. 01, 1997; 15p; In English; Sponsored by Materials Research Society, USA

Report No.(s): DE98-057442; UCRL-JC-127710; No Copyright; Avail: Department of Energy Information Bridge, Microfiche

We calculate ab initio values of tight-binding parameters for the f- electron metal Ce and various phases of Si, from local-density functional one- electron Hamiltonian and overlap matrix elements. Our approach allows us to unambiguously test the validity of the common minimal basis and two-center approximations as well as to determine the degree of transferability of both nonorthogonal and orthogonal hopping parameters in the cases considered.

NTIS

Cesium; Silicon; Binding Energy; Electrons

19990110519 Department of Energy, Office of Financial Management and Controller, Washington, DC USA

Interfacial electronic charge transfer and density of states in short period Cu/Cr multilayers

Bello, A. F., Department of Energy, USA; VanBuuren, T., Department of Energy, USA; Kepesis, J. E., Department of Energy, USA; Barbee, T. W., Department of Energy, USA; Apr. 01, 1998; 9p; In English; Sponsored by Materials Research Society, USA

Report No.(s): DE98-057688; UCRL-JC-130780; No Copyright; Avail: Department of Energy Information Bridge, Microfiche

Nanometer period metallic multilayers are ideal structures to investigate electronic phenomena at interfaces between metal films since interfacial atoms comprise a large atomic fraction of the samples. The multilayers studied were fabricated by magnetron sputtering and consist of bilayers from 1.9 mn to 3.3 mn. X-ray diffraction, cross-section TEM and plan-view TEM show the Cu layers to have a BCC structure Cu in contrast to its equilibrium FCC structure. The electronic structure of the Cu and the Cr layers in several samples of thin Cu/Cr multilayers were studied using x-ray absorption spectroscopy (XAS). Total electron yield was measured and used to study the white lines at the Cu L(sub 2) and L(sub 3) absorption edges. The white lines at the Cu absorption edges are strongly related to the unoccupied d-orbitals and are used to calculate the amount of charge transfer between the Cr and Cu atoms in interfaces. Analysis of the Cu white lines show a charge transfer of 0.026 electrons/interfacial Cu atom to the interfacial Cr atoms. In the Cu XAS spectra we also observe a van Hove singularity between the L(sub 2) and L(sub 3) absorption edges as expected from the structural analysis. The absorption spectra are compared to partial density of states obtained from a full-potential linear muffin-tin orbital calculation. The calculations confirm the presence of charge transfer and indicate that it is localized to the first two interfacial layers in both Cu and Cr.

NTIS

Copper; Chromium; Electron Transfer; Magnetron Sputtering; Metal Films; Fabrication

19990110567 Department of Energy, Office of Civilian Radioactive Waste Management, Washington, DC USA

Stress corrosion cracking of Fe-Ni-Cr-Mo, Ni-Cr-Mo and Ti alloys in 90 C acidic brine

Roy, A. K., Department of Energy, USA; Fleming, D. L., Department of Energy, USA; Lum, B. Y., Department of Energy, USA; Nov. 01, 1997; 9p; In English; Corrosion '98, 1998, USA

Report No.(s): DE98-058331; UCRL-JC-128477; No Copyright; Avail: Department of Energy Information Bridge, Microfiche

Susceptibility to stress corrosion cracking (SCC) of candidate materials for the inner container of the multi-barrier nuclear waste package was evaluated by using wedge-loaded precracked double-cantilever-beam (DCB) specimens in deaerated acidic brine (pH at 2.70) at 90 deg C. Materials tested include Alloys 825, G-30, C-4, 625 and C-22; and Ti Grade-12. Duplicate specimen of each material was loaded at different initial stress intensity factor (K) values ranging between 23 and 46 ksi/in. Both metallography and compliance method were used to determine the final crack length. The final stress intensity for SCC (K(sup ISCC)) was computed from the measured final wedge load and the average crack length. The results indicate that in general, the final crack length measured by metallography and compliance was very close to each other, thus, providing very similar K(sup ISCC) values. While tests are still ongoing, the preliminary results suggest that, compared to other five alloys tested, Alloy 825 may exhibit the maximum tendency to SCC.

NTIS

Stress Corrosion Cracking; Alloys; Radioactive Materials; Crack Propagation; Titanium Alloys; Iron Alloys; Chromium Alloys; Molybdenum Alloys; Brines

19990111466 Louisiana State Univ., Dept. of Mechanical Engineering, Baton Rouge, LA USA

Microstructure and Numerical Analysis of Hot Forging of Duplex Titanium Aluminide

Abernathy, M. C., Louisiana State Univ., USA; Raman, A., Louisiana State Univ., USA; Mirshams, R. A., Southern Univ., USA; Wereczak, A., Oak Ridge National Lab., USA; HBCUs/OMUs Research Conference Agenda and Abstracts; August 1999, pp. 19; In English; See also 19990111455; No Copyright; Avail: Issuing Activity, Hardcopy; Abstract Only

Gamma titanium aluminide is an attractive material for high temperature engine components in the aerospace, aeronautical, and automobile industries. Hot forging process is one of the major manufacturing processes for production of turbine blades and other engine components. Integration of microstructure characteristics in the hot forging process has been investigated by different

researchers. This paper is going to report our investigation on the mathematical integration of microstructure characteristics and evolution in the flow stress relationship during hot forging of titanium aluminide. Sandstrom and Lagneborg model and numerical analysis approach by Pietrzyk were used in this analysis. Titanium aluminide with a composition of 46-50 at%. Al and a duplex microstructure was used for verification of the model. Compression tests were conducted in the temperature range- between 950-1100C and strain rates of 0.001 0.1 per second. Metallographical examination indicated microstructural changes in the original duplex morphology due to dynamic recovery, recrystallization, and grain growth. Experimental stress-strain relationships for different conditions used for verification of the simulated curves.
Author
Compression Tests; Microstructure; Numerical Analysis; Titanium Aluminides; Hot Working; Forging; Metal Working

19990111495 Department of Energy, Washington, DC USA
Integration of adaptive process control with computational simulation for spin-forming
Raboin, P., Department of Energy, USA; Mar. 10, 1998; 23p; In English
Report No.(s): DE98-057742; UCRL-ID-130211; No Copyright; Avail: Department of Energy Information Bridge, Microfiche
Improvements in spin-forming capabilities through upgrades to a metrology and machine control system and advances in numerical simulation techniques were studied in a two year project funded by Laboratory Directed Research and Development (LDRD) at Lawrence Livermore National Laboratory. Numerical analyses were benchmarked with spin-forming experiments and computational speeds increased sufficiently to now permit actual part forming simulations. Extensive modeling activities examined the simulation speeds and capabilities of several metal forming computer codes for modeling flat plate and cylindrical spin-forming geometries. Shape memory research created the first numerical model to describe this highly unusual deformation behavior in Uranium alloys. A spin-forming metrology assessment led to sensor and data acquisition improvements that will facilitate future process accuracy enhancements, such as a metrology frame. Finally, software improvements (SmartCAM) to the manufacturing process numerically integrate the part models to the spin-forming process and to computational simulations.
NTIS
Process Control (Industry); Uranium Alloys; Finite Element Method; Metal Working; Forming Techniques; Flat Plates; Adaptive Control; Shape Memory Alloys

19990111496 Department of Energy, Office of Civilian Radioactive Waste Management, Washington, DC USA
First increment of second specimen results to performance assessment-long term corrosion
Wang, F., Department of Energy, USA; Jan. 01, 1998; 131p; In English
Report No.(s): DE98-057730; UCRL-ID-129830; No Copyright; Avail: Department of Energy Information Bridge, Microfiche
In this correspondence, we report the 6 month corrosion data of corrosion resistant alloys (alloys 825, C22 and C4, and Ti Gr 12 and Ti Gr 16, and Inconel 625) and one year data of corrosion-allowance materials (A387 Gr22, A516 Gr55, and A27 Gr70-40), intermediate resistance alloys (Monel 400 and CDA 715) and corrosion resistant materials (alloys C22 and 625 only).
NTIS
Corrosion Resistance; Alloys; Corrosion

19990111501 Kinki Univ., Faculty of Engineering, Hiroshima, Japan
Improvement of Fatigue Strength in High Performance Carburized and Shot-Peened Steels
Hatate, Minoru, Kinki Univ., Japan; Hamasaka, Naoji, Komatsu Ltd., Japan; Shiota, Toshio, Kinki Univ., Japan; Research Reports of the Faculty of Engineering, Kinki University; 1993; ISSN 0386-491X, No. 27, pp. 63-72; In Japanese; Copyright; Avail: Issuing Activity, Hardcopy, Microfiche
The effects of carburizing process and shot peening on the surface layer properties of carburized steels had been investigated in order to improve fatigue strength of ordinary carburized steels, and high performance carburized and shot peened steels developed. Lowering the Si, Mn and Cr contents in steel makes the depth of the grain boundary oxidation shallow in the condition of the N2-base carburizing with low CO2 concentration. In case of using high Mo and Ni-low Si and Mn-0.5%Cr case-hardening steel, utilizing shot peening treatment makes it possible significant increase the residual compressive stress and surface hardness because the retained austenite is transformed into martensite, the so-called stress induced martensite. Therefore, shot-peened test pieces with the lowered depth of the grain boundary oxidation exhibited the rotating bending fatigue limit 1.57 times of that of ordinary carburized steel.
Derived from text
Steels; Carburizing; Shot Peening; Surface Layers; Carbon Dioxide Concentration; Hardening (Materials); Residual Stress

19990113143 Swedish Inst. for Metals Research, Stockholm, Sweden
Influence of Weld Bead Width on Fatigue Properties of Laser Welds
Meurling, F.; 1999; 38p; In English
Report No.(s): PB99-173841; IM-1999-004; SIMR/R-1999/004-SE; No Copyright; Avail: CASI; A01, Microfiche; A03, Hardcopy

The aim of the present study was to observe the influence of the weld bead width on the fatigue properties of laser welds. The weld appearance and geometry depends upon many factors and by controlling these parameters it is possible to increase the welding speed. However this may imply a decrease in weld bead width which in turn may influence the fatigue properties of the weld.
NTIS
Welded Joints; Beads; Laser Welding; Fatigue (Materials); Width

27
NONMETALLIC MATERIALS

Includes physical, chemical, and mechanical properties of plastics, elastomers, lubricants, polymers, textiles, adhesives, and ceramic materials. For composite materials see 24 Composite Materials.

19990107354 Sandia National Labs., Albuquerque, NM USA
Growth Kinetics and Modeling of Direct Oxynitride Growth with NO-O2 Gas Mixtures
Everist, S.; Nelson, J.; Sharangpani, R.; Smith, P. M.; Tay, S. P.; May 03, 1999; 6p; In English; 195th, 2-6 May 1999, Seattle, WA, USA; Sponsored by Electrochemical Society, USA
Report No.(s): DE00-007196; SAND99-1008C; No Copyright; Avail: Department of Energy Information Bridge, Hardcopy

We have modeled growth kinetics of oxynitrides grown in NO-O2 gas mixtures from first principles using modified Deal-Grove equations. Retardation of oxygen diffusion through the nitrided dielectric was assumed to be the dominant growth-limiting step. The model was validated against experimentally obtained curves with good agreement. Excellent uniformity, which exceeded expected values, was observed.
NTIS
Deposition; Dielectrics; Oxynitrides; Gas Mixtures

19990107358 Department of Energy, Kansas City, MO USA
Automated Image Processing System for Concrete Evaluation
Baumgart, C. W., Department of Energy, USA; Cave, S. P., Department of Energy, USA; Linder, K. E., Department of Energy, USA; Nov. 23, 1998; 4p; In English; ANNIE '98: Artificial Neural Networks in Engineering, 1 Nov. 1998, Saint Louis, MO, USA; Sponsored by Department of Energy, USA
Report No.(s): DE00-001881; KCP-613-6111; No Copyright; Avail: Department of Energy Information Bridge, Hardcopy

AlliedSignal Federal Manufacturing & Technologies (FM&T) was asked to perform a proof-of-concept study for the Missouri Highway and Transportation Department (MHTD), Research Division, in June 1997. The goal of this proof-of-concept study was to ascertain if automated scanning and imaging techniques might be applied effectively to the problem of concrete evaluation. In the current evaluation process, a concrete sample core is manually scanned under a microscope. Voids (or air spaces) within the concrete are then detected visually by a human operator by incrementing the sample under the cross-hairs of a microscope and by counting the number of 'pixels' which fall within a void. Automation of the scanning and image analysis processes is desired to improve the speed of the scanning process, to improve evaluation consistency, and to reduce operator fatigue. An initial, proof-of-concept image analysis approach was successfully developed and demonstrated using acquired black and white imagery of concrete samples. In this paper, the automated scanning and image capture system currently under development will be described and the image processing approach developed for the proof-of-concept study will be demonstrated. A development update and plans for future enhancements are also presented.
NTIS
Concretes; Nondestructive Tests; Image Processing; Imagery; Highways

19990108573 NASA Lewis Research Center, Cleveland, OH USA
Elemental Metals or Oxides Distributed on a Carbon Substrate or Self-Supported and the Manufacturing Process Using Graphite Oxide as Template
Hung, Ching–Chen, Inventor, NASA Lewis Research Center, USA; Sep. 07, 1999; In English; Division of US-Patent-Appl-SN-833107, filed 4 Apr. 1997

Patent Info.: Filed 5 Nov. 1998; NASA-Case-LEW-16221-1; US-Patent-5,948,475; US-Patent-Appl-SN-186831; US-Patent-Appl-SN-833107; No Copyright; Avail: US Patent and Trademark Office, Hardcopy

A process for providing elemental metals or metal oxides distributed on a carbon substrate or self-supported utilizing graphite oxide as a percursor. The graphite oxide is exposed to one or more metal chlorides to form an intermediary product comprising carbon, metal, chloride, and oxygen. This intermediary product can be further processed by direct exposure to carbonate solutions to form a second intermediary product comprising carbon, metal carbonate, and oxygen. Either intermediary product may be further processed: a) in air to produce metal oxide; b) in an inert environment to produce metal oxide on carbon substrate; c) in a reducing environment to produce elemental metal distributed on carbon substrate. The product generally takes the shape of the carbon precursor.

Author

Metal Oxides; Carbon; Substrates; Graphite

19990108598 NASA Marshall Space Flight Center, Huntsville, AL USA

Pressure Effect in ZnO Films Using Off-Axis Sputtering Deposition

Zhu, Shen, Universities Space Research Association, USA; Su, C.–H., NASA Marshall Space Flight Center, USA; Lehoczky, S. L., NASA Marshall Space Flight Center, USA; Peters, P., NASA Marshall Space Flight Center, USA; George, M. A., Alabama Univ., USA; [1999]; 1p; In English; No Copyright; Avail: Issuing Activity, Hardcopy; Abstract Only

ZnO films are deposited on (0001) sapphire, (001) Si and quartz substrates using the off-axis reactive magnetron sputtering deposition. Based on film thickness measurements, three transport regions of sputtered particles are observed when films are deposited in the pressure regions of 5 mtorr - 150 mtorr. X-ray diffraction, scanning probes microscopy, and electrical measurements are also used to characterize these films. The full width at half maximum of theta rocking curves for epitaxial films is less than 0.5 deg. In textured films, it rises to several degrees. The epitaxial films deposited at high pressure reveal a flat surface with some hexagonal facets. The density of hexagonal facets decreases when the growth pressure is reduced. The resistivity of these epitaxial films also depends on the growth pressures. A relationship between the pressure effects and film properties are discussed.

Author

Pressure Effects; Zinc Oxides; Film Thickness; Deposition; Sapphire; Substrates; Electrical Measurement

19990109132 NASA Marshall Space Flight Center, Huntsville, AL USA

Electrical Field Effects in Phthalocyanine Film Growth by Vapor Deposition

Banks, Curtis E., NASA Marshall Space Flight Center, USA; Zhu, Shen, Universities Space Research Association, USA; Frazier, Donald O., NASA Marshall Space Flight Center, USA; Penn, Benjamin, NASA Marshall Space Flight Center, USA; Abdeldayem, Hossin, Universities Space Research Association, USA; Hicks, Roslin, NASA Marshall Space Flight Center, USA; Sarkisov, Sergey, Alabama A & M Univ., USA; [1999]; 1p; In English; Optical Science, Engineering and Instrumentation, 17-23 Jul. 1999, Denver, CO, USA; Sponsored by International Society for Optical Engineering, USA; Copyright; Avail: Issuing Activity, Hardcopy; Abstract Only

Phthalocyanine, an organic material, is a very good candidate for non-linear optical application, such as high-speed switching and optical storage devices. Phthalocyanine films have been synthesized by vapor deposition on quartz substrates. Some substrates were coated with a very thin gold film for introducing electrical field. These films have been characterized by surface morphology, material structure, chemical and thermal stability, non-linear optical parameters, and electrical behaviors. The films have excellent chemical and optical stability. However, the surface of these films grown without electrical field shows flower-like morphology. When films are deposited under an electrical field (an aligned structure is revealed on the surface. A comparison of the optical and electrical properties and the growth mechanism for these films grown with and without an electrical field will be discussed.

Author

Electric Fields; Thin Films; Phthalocyanin; Organic Materials; Coatings; Quartz; Substrates

19990109144 NASA Langley Research Center, Hampton, VA USA

Method of Preparing Polymers with Low Melt Viscosity

Jensen, Brian J., Inventor, NASA Langley Research Center, USA; Oct. 12, 1999; In English; Division of US-Patent-Appl-SN-666793, filed 18 Jun. 1996 which is a continued-in-part of abandoned US-Patent-Appl-SN-622176, filed 5 Mar. 1996

Patent Info.: Filed 5 Jun. 1998; NASA-Case-LAR-15534-3; US-Patent-5,964,687; US-Patent-Appl-SN-092515; US-Patent-Appl-SN-666793; US-Patent-Appl-SN-622176; No Copyright; Avail: US Patent and Trademark Office, Hardcopy

This invention is an improvement in standard polymerization procedures, i.e., addition-type and step-growth type polymerization, wherein monomers are reacted to form a growing polymer chain. The improvement includes employ- ing an effective amount of a trifunctional monomer (such as a trifunctional amine, anhydride, or phenol) in the polymerization procedure to form a mixture of polymeric materials consisting of branced polymers, star-shaped polymers, and linear polymers. This mixture of polymeric materials has a lower melt temperature and a lower melt viscosity than corresponding linear polymeric materials of equivalent molecular weight.
Official Gazette of the U.S. Patent and Trademark Office
Procedures; Polymerization; Polymers; Viscosity

19990109662 Aerospace Corp., Engineering and Technology Group, El Segundo, CA USA
FTIR Study of Consolidation and Crystallization of Sol-Gel Deposited PZT Films
Lipeles, R. A., Aerospace Corp., USA; Sep. 15, 1991; 12p; In English
Contract(s)/Grant(s): F04701-88-C-0089
Report No.(s): ATR-91(8308)-3; No Copyright; Avail: CASI; A03, Hardcopy; A01, Microfiche

Specular reflectance Fourier transform infrared spectroscopy (FTIR) was used to characterize the thermal processing of lead zirconate titanate (PZT) films spin cast on platinum films. The removal of organics during consolidation was measured by the disappearance of O-H, C-H, and C-O absorption bands. Conversion of metal-alkoxide bonds (M-OR) in the gel to ZrO6 and TiO6 octahedra in the perovskite lattice during sintering was evident from the emergence of the absorption band at 540/ cm. The results indicate that FITR can be used to follow the progress of thermal treatment of PZT films and provide an effective diagnostic technique to optimize processing conditions.
Author
Infrared Spectroscopy; Fourier Transformation; Crystallization; Sol-Gel Processes; Lead Zirconate Titanates; Temperature Effects

19990110102 Dynacs Engineering Co., Inc., Cocoa Beach, FL USA
FTIR Study of Vapor Offgassing from Orbiter Tile Re-Waterproofing Materials
Mattson, C. B., Dynacs Engineering Co., Inc., USA; JANNAF 28th Propellant Development and Characterization Subcommittee and 17th Safety and Environmental Protection Subcommitte Joint Meeting; April 1999; Volume 1, pp. 145-151; In English; See also 19990110087
Contract(s)/Grant(s): NAS10-98001; No Copyright; Avail: CPIA, 10630 Little Patuxent Pkwy., Suite 202, Columbia, MD 21044-3200 HC, Hardcopy

The work presented in this paper was performed to identify and quantify the offgassing behavior of alternative re-waterproofmg materials under investigation for application to Shuttle Orbiter Thermal Protection System (TPS) tile and blanket materials. The purpose was to determine whether the new materials would cause a problem with the operational analysis of residual vapors using the current portable vapor analyzer, a Miran 203. The materials investigated were limited to dimethylethoxysilane (DMES) and proposed solvent selected as suitable for use in re-waterproofing Orbiter TPS. The solvent was selected in another phase of the overall project. Obiter TPS tiles were injected with the re-waterproofing materials under constant conditions of temperature, relative humidity and air flow. The vapor concentrations of offgassing materials were monitored using Fourier Transform Infrared (FTIR) multi-component analysis, and with the Miran 203 instruments. The procedure was to record the time dependent concentrations of offgassing materials as analyzed by the FTIR, and the time response of the Miran 203 to the materials under consideration. The FTIR was calibrated for vapor phase DMES, tetramethyldisiloxane (TMDS), ethanol and the hydrocarbon solvents to be used to dilute the DMES for application to the TPS tile. The Miran 203 was calibrated for the operational measurement of DMES airborne vapors. The FTIR data, shows for the first time that the principal product which offgases from the tile after the first hour is not DMES, but TMDS and ethanol. The Miran 203 response to TMDS is the primary reading after the re-waterproofing operation is completed. The operational use of the Miran 203 to measure DMES vapors after re-waterproofmg operations has been responding to TMDS. The results of this study suggest that the historical complaints that have contributed to the low threshold limit value (TLV) for DMES concentrations, as read with the Miran 203, are actually based on instrumental responses to TMDS, for which no other toxicology information is available at this time. While there is some interference, the use of the tested hydrocarbon solvents does not adversely affect the response of the Miran 203.
Author
Infrared Spectra; Vapors; Offgassing; Tiles; Waterproofing

19990110471 Department of Energy, Office of Financial Management and Controller, Washington, DC USA

Characterizing and modeling the apparent anomalous behavior of resistivity in Cr-Si-O thin films

Jankowski, A. F., Department of Energy, USA; Mar. 01, 1998; 17p; In English; Thin Solid Films (TSF) and Surface and Coatings Technology (SCT), USA; Sponsored by American Vacuum Society, USA

Report No.(s): DE98-054784; UCRL-JC-130073; No Copyright; Avail: Department of Energy Information Bridge, Microfiche

The Cr-Si-O material system is of interest for use as a thin film resistor. The films are sputter deposited onto conducting substrates from metal oxide compacts using a reactive gas mixture. the cermet films composition range from 50 to 100 vol.% SiO2 as determined from elemental measurements of the Cr, Si and O content. In a wide range of resistivities from 10(exp 1) to 10 (exp 14) omega-cm measured through the film thickness, an apparent anomalous behavior is found with the Cr, Si and O composition. The anomaly can be deducted to a discontinuous variation of resistivity with film composition near 80 vol.% SiO2. The film microstructure is characterized as a distribution of conducting metal-silicide particles within an insulating matrix. The effective medium theory is used to predict the variation of conductivity and successfully models the anomalous resistivity behavior.

NTIS

Cermets; Thin Films; Electrical Resistivity; Metal Oxides; Chromium; Silicon; Oxygen

19990111458 Florida Agricultural and Mechanical Univ., Dept. of Electrical Engineering, Tallahassee, FL USA

Plasma-Enhanced Pulsed Laser Deposition of Boron Nitride Thin Films for Alphavoltaic Device Applications

Poindexter, E., Jr., Florida Agricultural and Mechanical Univ., USA; Pelt, J. S., Florida Agricultural and Mechanical Univ., USA; Ramsey, M. E., Florida Agricultural and Mechanical Univ., USA; Magana, R., Florida Agricultural and Mechanical Univ., USA; Durbin, Steve M., Florida Agricultural and Mechanical Univ., USA; HBCUs/OMUs Research Conference Agenda and Abstracts; August 1999, pp. 11; In English; See also 19990111455; No Copyright; Avail: Issuing Activity, Hardcopy; Abstract Only

The concept of generating low-level currents in the micro- to milliamp range using high-energy particles in conjunction with a photovoltaic device was successfully demonstrated over two decades ago using silicon-based solar cell technology Unfortunately, device lifetime was severely limited due to the cumulative effects of radiation-induced damage. We have proposed using cubic boron nitride and related ultrawide bandgap semiconductor materials as the basis for an ”alphavoltaic” device, since the bandgap energy of the semiconductor is irrelevant in radioisotope applications where the incident energy averages several hundred keV to several MeV. Our approach is the development of an enhanced pulsed laser deposition technique, where active nitrogen is supplied using an inductively coupled RF plasma source identical to that used to grow high quality GaN LEDs by molecular beam epitaxy. The boron of aluminum is supplied by ablating a suitable target with a KrF excimer laser at energy densities in the range of 0.3 to 3 J/sq cm. Lattice-matched polycrystalline diamond substrates are used as opposed to silicon, which although most commonly used, presents a considerable lattice mismatch. Results of in-situ reflection high-energy electron diffraction (RHEED), and post-growth analysis using scanning electron microscopy (SEM), atomic force microscopy (AFM), x-ray diffraction, x-ray photoelectron spectroscopy (XPS), Raman spectroscopy and Fourier transform infrared spectroscopy (FTIR) will be presented.

Author

Boron Nitrides; Polycrystals; Pulsed Laser Deposition; Semiconductors (Materials); Solar Cells; Thin Films

19990111459 Grambling State Univ., Dept. of Chemistry, LA USA

Polymerizable Monomer Reactants: Modified Polyimides

Hubbard, Danny E., Grambling State Univ., USA; Reaves, Shawn, Grambling State Univ., USA; HBCUs/OMUs Research Conference Agenda and Abstracts; August 1999, pp. 12; In English; See also 19990111455; No Copyright; Avail: Issuing Activity, Hardcopy; Abstract Only

Our research investigation focuses on the preparation of polyimides. Reaction of dianhydrides (e.g., 3,3’, 4,4’-benzophenonetetracarboxylic dianhydride), with a diamine based monomer, produces a polymer which is expected to be of potential use in high temperature (polymer) applications. The monomers of interest in this study are proposed to exhibit significant advantages in the area of flowered energy requirements during the mold process of these polymers. The resulting modified polyimides are being studied using Differential Scanning Calorimetry (DSC) and Thermal Gravimetric Analysis (TGA). Once thermal characterization has been completed on the modified polyimides our investigation extends to aging and rheological profiles, including dynamic mechanical analysis. At this point in our study we present the results of the thermal data and aging studies of the materials.

Author

Anhydrides; Diamines; Monomers; Polyimides; Temperature Effects

19990111696 NASA Marshall Space Flight Center, Huntsville, AL USA

Z-Scan Measurements on Au/SiO2 Composite Films

Bender, Matthew W., NASA Marshall Space Flight Center, USA; Smith, David D., NASA Marshall Space Flight Center, USA; Xiao, Rongfu, Hong Kong Univ. of Science and Technology, Hong Kong; Sarkisov, Sergei, Alabama A & M Univ., USA; Gregory, Don A., Alabama Univ., USA; Boyd, Robert W., Rochester Univ., USA; 1998; In English; Nonlinear Optics, 10-14 Aug. 1998, Princeville, Kauai, HI, USA; Copyright; Avail: Issuing Activity, Hardcopy, Microfiche

Z-Scan measurements were performed on Au/SiO2 composite films produced by a co-sputtering technique and compared with effective medium theories which consider the full complex nature of chi(3).

Author

Silicon Dioxide; Scanners; Gold; Silicon Films

19990113149 ARCADIS Geraghty and Miller, Inc., Research Triangle Park, NC USA

Evaluation of Low-VOC Latex Paints

Chang, J. C. S.; Fortmann, R. C.; Roache, N. F.; Lao, H. C.; 1999; 10p; In English

Report No.(s): PB99-171522; No Copyright; Avail: CASI; A02, Hardcopy; A01, Microfiche

The paper gives results of an evaluation of four commercially available low-VOC (volatile organic compound) latex paints as substitutes for conventional latex paints by assessing both their emission characteristics and their performance as coatings. Bulk analysis indicated that the VOC contents of all four paints are considerably lower than those of conventional latex paints. Low-VOC emissions were confirmed by small chamber emission tests. However, significant emissions of several aldehydes, especially formaldehyde, were detected from two of the paints. ASTM methods were used to evaluate the hiding power, scrubbability, washability, dry to touch, and yellowing index. The results indicated that one of the low-VOC paints tested showed performance equivalent or superior to that of a widely used conventional latex paint used as a control. It was concluded that low-VOC latex paint can be a viable option to replace conventional latex paints for prevention of indoor air pollution. However, paints marketed as 'low-VOC' may still have significant emissions of some individual VOCs, and some may not have performance characteristics matching those of conventional latex paints.

NTIS

Latex; Paints; Indoor Air Pollution; Air Sampling; Air Quality; Pollution Control; Pollution Monitoring

28
PROPELLANTS AND FUELS

Includes rocket propellants, igniters, and oxidizers; their storage and handling procedures; and aircraft fuels. For related information see also 07 Aircraft Propulsion and Power, 20 Spacecraft Propulsion and Power, and 44 Energy Production and Conversion.

19990110087 Johns Hopkins Univ., Chemical Propulsion Information Agency, Columbia, MD USA

JANNAF 28th Propellant Development and Characterization Subcommittee and 17th Safety and Environmental Protection Subcommittee Joint Meeting, Volume 1, *21 Mar. 1998 - 26 Apr. 1999*

Cocchiaro, James E., Editor, Johns Hopkins Univ., USA; Mulder, Edwin J., Editor, Johns Hopkins Univ., USA; Gomez–Knight, Sylvia J., Editor, Johns Hopkins Univ., USA; April 1999; 398p; In English; 28th; 17th; Propellant Development and Characterization Subcommittee, 26-30 Apr. 1999, San Diego, CA, San Diego, CA, USA, USA; Sponsored by NASA, USA; See also 19990110088 through 19990110120

Contract(s)/Grant(s): SPO700-97-D-4004

Report No.(s): CPIA-Publ-687-Vol-1; No Copyright; Avail: CPIA, 10630 Little Patuxent Pkwy., Suite 202, Columbia, MD 21044-3200 HC, Hardcopy

This volume contains 37 unclassified/unlimited-distribution technical papers that were presented at the JANNAF 28th Propellant Development & Characterization Subcommittee (PDCS) and 17th Safety & Environmental Protection Subcommittee (S&EPS) Joint Meeting, held 26-30 April 1999 at the Town & Country Hotel and the Naval Submarine Base, San Diego, California. Volume II contains 29 unclassified/limited-distribution papers that were presented at the 28th PDCS and 17th S&EPS Joint Meeting. Volume III contains a classified paper that was presented at the 28th PDCS Meeting on 27 April 1999. Topics covered in PDCS sessions include: solid propellant rheology; solid propellant surveillance and aging; propellant process engineering; new solid propellant ingredients and formulation development; reduced toxicity liquid propellants; characterization of hypergolic propellants; and solid propellant chemical analysis methods. Topics covered in S&EPS sessions include: space launch range safety; liquid propellant hazards; vapor detection methods for toxic propellant vapors and other hazardous gases;

toxicity of propellants, ingredients, and propellant combustion products; personal protective equipment for toxic liquid propellants; and demilitarization/treatment of energetic material wastes.
Author
Environment Protection; Air Pollution; Environmental Monitoring; Safety

19990110088 AmDyne Corp., Huntsville, AL USA
Rheology as the Cause of Propellant Heterogeneity in Solid Rocket Motors
Morgan, R. E., AmDyne Corp., USA; JANNAF 28th Propellant Development and Characterization Subcommittee and 17th Safety and Environmental Protection Subcommitte Joint Meeting; April 1999; Volume 1, pp. 1-7; In English; See also 19990110087; No Copyright; Avail: CPIA, 10630 Little Patuxent Pkwy., Suite 202, Columbia, MD 21044-3200 HC, Hardcopy

It has been known since 1980 that there can be locations in a solid rocket motor where there is a deviation in the ballistic and mechanical properties from the bulk property baseline values. Ballisticians have variously called this ”BARF” (Ballistic Anomaly Rate Factor), ”Hump Effect”, or ”Rainbow Effect”. While it was established early on that propellant casting methods influenced this effect, the exact cause or mechanism has yet to be explained. This paper summarizes recent discoveries that point to complex rheological behavior as the key to understanding this phenomenon. A theory is advanced to predict the maximum possible deviation from bulk properties based on the theoretical maximum packing fraction of the solids content. Practical advice and a plan of attack is given for propellant formulators, ballisticians, and mechanical property analysts to predict and quantify propellant heterogeneity and its resulting effect on rocket motor safety and reliability.
Author
Rheology; Propellants; Heterogeneity; Solid Propellant Rocket Engines

19990110089 AmDyne Corp., Huntsville, AL USA
Statistical Reproducibility of Ground Ammonium Perchlorate
Morgan, R. E., AmDyne Corp., USA; JANNAF 28th Propellant Development and Characterization Subcommittee and 17th Safety and Environmental Protection Subcommitte Joint Meeting; April 1999; Volume 1, pp. 9-15; In English; See also 19990110087; No Copyright; Avail: CPIA, 10630 Little Patuxent Pkwy., Suite 202, Columbia, MD 21044-3200 HC, Hardcopy

A nominal 16 to 20 micrometer grind of ammonium perchlorate is a common component of solid propellant formulations. This paper examines the reproducibility of a statistically significant number of grinds made over a two-year period on a production line. The time period includes two mill rebuilds and should give an excellent sample for determining the normal variation seen in this size material. The computer program PSIZE is used to calculate the particle size statistics for each grind. The role of bivariate analysis is demonstrated and the overall distribution is shown to closely follow a well-known empirical equation. The different causes of variability are briefly described and their importance on the overall particle size reproducibility is stressed. This information may be useful to propellant formulators to use as an estimate for the variability of new oxidizers.
Author
Ammonium Perchlorates; Solid Rocket Propellants; Composite Propellants

19990110090 NASA White Sands Test Facility, NM USA
Sensitized Liquid Hydrazine Detonation Studies
Rathgeber, K. A., Allied-Signal Technical Services Corp., USA; Keddy, C. P., Allied-Signal Technical Services Corp., USA; Bunker, R. L., NASA White Sands Test Facility, USA; JANNAF 28th Propellant Development and Characterization Subcommittee and 17th Safety and Environmental Protection Subcommitte Joint Meeting; April 1999; Volume 1, pp. 17-26; In English; See also 19990110087; No Copyright; Avail: CPIA, 10630 Little Patuxent Pkwy., Suite 202, Columbia, MD 21044-3200 HC, Hardcopy

Vapor-phase hydrazine (N2H4) is known to be very sensitive to detonation while liquid hydrazine is very insensitive to detonation, theoretically requiring extremely high pressures to induce initiation. A review of literature on solid and liquid explosives shows that when pure explosive substances are infiltrated with gas cavities, voids, and/or different phase contaminants, the energy or shock pressure necessary to induce detonation can decrease by an order of magnitude. Tests were conducted with liquid hydrazine in a modified card-gap configuration. Sensitization was attempted by bubbling helium gas through and/or suspending ceramic microspheres in the liquid. The hydrazine was subjected to the shock pressure from a 2 lb (0.9 kg) Composition C-4 explosive charge. The hydrazine was contained in a 4 in. (10.2 cm) diameter stainless steel cylinder with a 122 in(sup 3) (2 L) volume and sealed with a polyethylene cap. Blast pressures from the events were recorded by 63 high speed pressure transducers located on three radial legs extending from 4 to 115 ft (1.2 to 35.1 in) from ground zero. Comparison of the neat

hydrazine and water baseline tests with the ”sensitized” hydrazine tests indicates the liquid hydrazine did not detonate under these conditions.
Author
Hydrazines; Detonation; Liquid Rocket Propellants

19990110091 ACTA, Inc., Torrance, CA USA
Application of Risk Analyses to Explosive Siting Issues
Haber, Jerold M., ACTA, Inc., USA; JANNAF 28th Propellant Development and Characterization Subcommittee and 17th Safety and Environmental Protection Subcommitte Joint Meeting; April 1999; Volume 1, pp. 27-37; In English; See also 19990110087 Contract(s)/Grant(s): F04684-97-C-0001; No Copyright; Avail: CPIA, 10630 Little Patuxent Pkwy., Suite 202, Columbia, MD 21044-3200 HC, Hardcopy

Both Vandenberg Air Force Base and Cape Canaveral Air Station have been primary Air Force launch sites for many years. Over the years, the increasing size and complexity of space boosters has resulted in additional real estate for support facilities and to assure the safety of surrounding Air Force buildings and adjacent communities. For many years, the standard approach to protecting against explosive hazards has been siting based on Quantity-Distance (QD) circles. This approach has been assumed to be a conservative method of assuring personnel safety. In recent years, the number of cases requiring waivers to the QD regulations has grown rapidly. to address this situation the DoD Explosive Safety Board formed the Risk Based Explosive Safety Criteria Team (RBESCT) to investigate the feasibility of risk based methods. As part of this investigation, the team chairman postulated a hypothetical problem involving several potential explosive sites (PES’s) and several exposed sites (ES’s), all sited at the QD limits. A combination of existing public domain algorithms and new algorithms developed under the sponsorship of the Safety Offices of the 30th and 45th Space Wings of the Air Force were used to quantify the risks of casualty and fatality for the hypothetical problem. Individual risk, collective risk, and catastrophic risk were quantified for two injury levels - casualties and fatalities. Risk based QD circles were quantified for several PES-ES pairs. Finally, the effectiveness of several types of risk mitigating actions was evaluated.
Author
Risk; Decision Theory; Safety; Safety Management

19990110092 Jet Propulsion Lab., California Inst. of Tech., Pasadena, CA USA
A Comparison of Two Different Approaches to Hydrazine Loading of Spacecraft: The Use of SCAPE and Alternative Approaches
Houseman, John, Jet Propulsion Lab., California Inst. of Tech., USA; Patzold, Jack D., Jet Propulsion Lab., California Inst. of Tech., USA; Jackson, Julie R., Jet Propulsion Lab., California Inst. of Tech., USA; Brown, Pamela R., Jet Propulsion Lab., California Inst. of Tech., USA; JANNAF 28th Propellant Development and Characterization Subcommittee and 17th Safety and Environmental Protection Subcommitte Joint Meeting; April 1999; Volume 1, pp. 39-51; In English; See also 19990110087; No Copyright; Avail: CPIA, 10630 Little Patuxent Pkwy., Suite 202, Columbia, MD 21044-3200 HC, Hardcopy

The loading of spacecraft with Hydrazine type fuels has long been recognized as a hazardous operation. This has led to safety strategies that include the use of SCAPE protective suits for personnel. The use of SCAPE suits have an excellent safety record, however there are associated drawbacks. Drawbacks include the high cost of maintaining and cleaning the suits, reduced mobility and dexterity when wearing the suits, the requirement for extensive specialized health and safety training, and the need to rotate personnel every two hours. A study was undertaken to look at procedures and/or equipment to eliminate or reduce the time spent in SCAPE-type operations. The major conclusions are drawn from observations of the loading of the JPL/NASA spacecraft Deep Space One (DS1) at KSC and the loading of a commercial communications satellite by Motorola at Vandenberg AF Base. The DS1 operations require extensive use of SCAPE suits, while the Motorola operation uses only SPLASH attire with a two-man team on standby in SCAPE. The Motorola team used very different loading equipment and procedures based on an integrated approach involving the propellant supplier. Overall, the Motorola approach was very clean, much faster and simpler than the DS1 procedure. The DS1 spacecraft used a bladder in the propellant tank, whereas the Motorola spacecraft used a Propellant Management Device (PMD). The Motorola approach cannot be used for tanks with bladders. to overcome this problem, some new procedures and new equipment are proposed to enable tanks with bladders to be loaded without using SCAPE, using a modified Motorola approach. Overall, it appears feasible to adopt the non-SCAPE approach while maintaining a very high degree of safety and reliability.
Author
Hydrazines; Fuels; Liquid Rocket Propellants

19990110093 NASA White Sands Test Facility, NM USA

Reactivities of Precision Cleaning Solvents with Hypergolic Propellants

Davis, Dennis D., Allied-Signal Technical Services Corp., USA; Delgado, Rafael H., Allied-Signal Technical Services Corp., USA; Williams, James H., NASA White Sands Test Facility, USA; JANNAF 28th Propellant Development and Characterization Subcommittee and 17th Safety and Environmental Protection Subcommitte Joint Meeting; April 1999; Volume 1, pp. 53-58; In English; See also 19990110087; No Copyright; Avail: CPIA, 10630 Little Patuxent Pkwy., Suite 202, Columbia, MD 21044-3200 HC, Hardcopy

The reactivities of several selected halogenated precision cleaning solvents with hypergolic propellants has been determined by analysis of the rates of formation of halide ion decomposition products. The solvents were Asahiklin AK 225, Asahiklin AK 225 AES, HFE 7100, HFE 7100 DE, Vertrel XF, Vertrel MCA, Vertrel MCA Plus, 1,1,2-trichloro-1,2,2-trifluoroethane (CFC-113), and trans-1,2-dichloroethylene (DCE). The propellants were hydrazine (HZ), monomethylhydrazine (MMH), and mixed oxides of nitrogen (MON-3). The Vertrel solvents showed significant reactivity with HZ. All of the solvents except DCE exhibited significant reactivity with MMH, particularly HFE 7100 DE and CFC-113. HFE 7100 DE, Vertrel MCA, and Vertrel MCA Plus also showed significant reactivity with MON-3 oxidizer.

Author

Reaction Kinetics; Chemical Reactions; Reactivity; Cleaning; Cleaners; Solvents; Trichloroethylene

19990110096 Johns Hopkins Univ., Chemical Propulsion Information Agency, Columbia, MD USA

DoD Explosives Safety Standards for Energetic Liquids Program: Proposed Standards

Cocchiaro, James E., Johns Hopkins Univ., USA; Ward, Jerry M., Department of Defense Explosives Safety Board, USA; JANNAF 28th Propellant Development and Characterization Subcommittee and 17th Safety and Environmental Protection Subcommitte Joint Meeting; April 1999; Volume 1, pp. 81-95; In English; See also 19990110087; No Copyright; Avail: CPIA, 10630 Little Patuxent Pkwy., Suite 202, Columbia, MD 21044-3200 HC, Hardcopy

The Department of Defense Explosives Safety Board (DDESB) is sponsoring the DoD Explosives Safety Standards for Energetic Liquids Program to study issues and develop revised safety standards concerning explosives equivalence, compatibility mixing, and quantity-distance (Q-D) criteria for liquid propellants and related energetic liquids. Energetic Liquid has been defined as - a liquid, slurry, or gel, consisting of or containing an explosive, oxidizer, fuel, or combination of the above, that may undergo, contribute to, or cause rapid exothermic decomposition (thermal explosion), deflagration, or detonation. Fundamental to the program are tasks to 1) review energetic liquid accident and realistic large-scale test data, and 2) to review other guidelines used in the commercial sector for application to energetic liquids. Data generated in these activities is forming the basis for proposed revisions to current standards. In addition, an interagency advisory board, the Liquid Propellants Working Group (LPWG), has been established to provide oversight in the assessment of available information with respect to historical and operational requirements, and ultimately to deliberate on the formulation of recommendations. Rationale for the program as well as technical information developed from the accident and test review, with respect to hazards controlling quantity-distance criteria for energetic liquids, have been reviewed in previous JANNAF and DDESB conferences. This paper provides the current text for a proposed draft change to DoD 6055.9-STD ”DoD Ammunition and Explosives Safety Standards” concerning the hazard classification and associated Q-D criteria for energetic liquids. The reader should note that the proposal is subject to voting approval of the DDESB, and thus does not yet represent official DoD policy. The proposed text is subject to change at any time.

Author

Explosives; Ammunition; Explosions; Hazardous Materials; Safety; Safety Management

19990110097 Alliant Techsystems, Inc., Allegany Ballistics Lab., Rocket Center, WV USA

Lead-Free Ballistic Modifiers for Minimum Signature Propellants

Shanholtz, C. E., Alliant Techsystems, Inc., USA; Whiteman, J. M., Alliant Techsystems, Inc., USA; JANNAF 28th Propellant Development and Characterization Subcommittee and 17th Safety and Environmental Protection Subcommitte Joint Meeting; April 1999; Volume 1, pp. 97-101; In English; See also 19990110087; No Copyright; Avail: CPIA, 10630 Little Patuxent Pkwy., Suite 202, Columbia, MD 21044-3200 HC, Hardcopy

Replacements for lead-based ballistic modifiers were sought to reduce the toxicity of the exhaust products of minimum signature propellants. The American Conference of Government Industrial Hygienist (ACGIH) threshold limit values were used to select transition metal compounds for evaluation. Compounds of acceptable transition metals were subjected to modified Taliani testing for compatibility with nitrate esters. Those compounds found to be compatible were evaluated for effect on

propellant burn rate in simple propellant formulations. Fully formulated propellants were prepared with the best low toxicity ballistic modifier candidates. Bismuth subsalicylate and bismuth citrate were found to produce very good ballistic modification. Author

Solid Rocket Propellants; Lead Compounds; Burning Rate; Solid Propellant Combustion; Solid Propellant Rocket Engines

19990110106 Air Force Research Lab., HEST, Wright-Patterson AFB, OH USA

Review of JP-10 Toxicity Studies and Potential Health Effects

Mattie, David R., Air Force Research Lab., USA; Yu, Kyung O., Air Force Research Lab., USA; JANNAF 28th Propellant Development and Characterization Subcommittee and 17th Safety and Environmental Protection Subcommitte Joint Meeting; April 1999; Volume 1, pp. 193-196; In English; See also 19990110087; No Copyright; Avail: CPIA, 10630 Little Patuxent Pkwy., Suite 202, Columbia, MD 21044-3200 HC, Hardcopy

JP-10 is the exo-isomer of tetrahydrodicyclopentadiene. A number of toxicity studies have been conducted for JP-10. Toxicity data for JP-10 will be presented from acute, genotoxic, reproductive, metabolism, emergency exposure limits, repeated dose rangefinder and chronic/carcinogenic studies. An interim standard was proposed in 1983 at 25 ppm as an 8 hour TWA. However, formal exposure limits have not been established for JP-10. The current data and interim standard should be reviewed and a process established to determine a formal standard for JP-10.

Author

Environment Effects; Exposure; Atmospheric Effects; Atmospheric Chemistry; Chemical Composition; Toxicity; Health

19990110108 Air Force Research Lab., HEST, Wright-Patterson AFB, OH USA

Toxicity of Rocket Fuels: Comparison of Hydrogen Peroxide with Current Propellants

Mattie, David R., Air Force Research Lab., USA; JANNAF 28th Propellant Development and Characterization Subcommittee and 17th Safety and Environmental Protection Subcommitte Joint Meeting; April 1999; Volume 1, pp. 215-218; In English; See also 19990110087; No Copyright; Avail: CPIA, 10630 Little Patuxent Pkwy., Suite 202, Columbia, MD 21044-3200 HC, Hardcopy

The toxicity of hydrogen peroxide and current exposure limits will be presented in this paper. Toxicity data and exposure limits will also be presented for unleaded gasoline, kerosene and hydrazine. The toxicity of hydrogen peroxide will be compared to gasoline, which is universally known and used by everyone as a fuel. The toxicity of hydrogen peroxide will also be compared to kerosene, one of the first propellants, and to hydrazine, which is very toxic and a candidate for replacement by a less toxic compound.

Author

Toxicity; Rocket Propellants; Fuels; Hydrogen Peroxide

19990110109 NASA White Sands Test Facility, NM USA

Permeation Resistance of Chlorinated Polyethylene Against Hydrazine Fuels

Waller, J. M., Allied-Signal Technical Services Corp., USA; Williams, J. H., NASA White Sands Test Facility, USA; JANNAF 28th Propellant Development and Characterization Subcommittee and 17th Safety and Environmental Protection Subcommitte Joint Meeting; April 1999; Volume 1, pp. 219-228; In English; See also 19990110087; No Copyright; Avail: CPIA, 10630 Little Patuxent Pkwy., Suite 202, Columbia, MD 21044-3200 HC, Hardcopy

The permeation resistance of chlorinated polyethylene (CPE) used in chemical protective clothing against the aerospace fuels hydrazine, monomethylhydrazine (MMH), and uns-dimethylhydrazine (UDMH) was determined by measuring breakthrough times and time-averaged vapor transmission rates using an ASTM F 739 permeation cell. Two exposure scenarios were simulated: a 2 hour (h) fuel vapor exposure, and a liquid fuel ”splash” followed by a 2 h vapor exposure. to simulate internal suit pressure during operation, a positive differential pressure of 0.3 in. water (75 Pa) on the collection side of the permeation apparatus was used. Breakthrough was observed after exposure to liquid MMH, and to vapor and liquid UDMH. No breakthrough was observed after exposure to vapor and liquid hydrazine, or vapor MMH. A model was then used to calculate propellant concentrations inside a totally encapsulating chemical protective suit based on the ASTM permeation data obtained in the present study. Concentrations were calculated under conditions of fixed vapor transmission rate, variable breathing air flow rate, and variable splash exposure area. Calculations showed that the maximum allowable permeation rates of hydrazine fuels through CPE were of the order of 0.05 to 0.08 ng sq cm/min for encapsulating suits with low breathing air flow rates (of the order of 5 scfm or 140 L/min). Above these permeation rates, the 10 parts per billion (ppb) threshold limit value time - weighted average could be exceeded for chemical

protective suits having a CPE torso. to evaluate suit performance at ppb level concentrations, use of a sensitive analytical method such as cation exchange high performance liquid chromatography with amperometric detection was found to be essential.
Author
Permeating; Chlorination; Polyethylenes; Hydrazines; Liquid Rocket Propellants; Liquid Fuels

19990110110 Thiokol Propulsion, Brigham City, UT USA
Summary of Thiokol Propulsion's Recovery, Reclamation and Reuse (R3) Demilitarization Activities
Munson, W. O., Thiokol Propulsion, USA; Larsen, S. B., Thiokol Propulsion, USA; JANNAF 28th Propellant Development and Characterization Subcommittee and 17th Safety and Environmental Protection Subcommitte Joint Meeting; April 1999; Volume 1, pp. 235-242; In English; See also 19990110087; No Copyright; Avail: CPIA, 10630 Little Patuxent Pkwy., Suite 202, Columbia, MD 21044-3200 HC, Hardcopy

Thiokol's approach to demilitarization of rocket motors, ordnance, and energetic materials has been (and is) to look at reuse technologies first. We have several ongoing programs where this philosophy is applied. These programs range from converting Russian liquid rocket fuel into commercial chemicals to utilization of solid propellants in commercial mining explosives. We recently implemented a closed-loop system in our water washout facility to clean the water sufficiently for reuse and, in the process, recover ammonium perchlorate for commercial applications. The logic path used to select a technology and product is focused on the practicality of the process from a cost and marketability standpoint. There is a hierarchy of decisions that range from use of the item for its original purpose to open burn or open detonation.
Author
Reclamation; Recycling; Regeneration (Engineering); Waste Management; Recoverability; Reuse

19990110114 NASA White Sands Test Facility, NM USA
Electrochemical Measurement of Atmospheric Corrosion
DeArmond, Anna H., Allied-Signal Technical Services Corp., USA; Davis, Dennis D., Allied-Signal Technical Services Corp., USA; Beeson, Harold D., NASA White Sands Test Facility, USA; JANNAF 28th Propellant Development and Characterization Subcommittee and 17th Safety and Environmental Protection Subcommitte Joint Meeting; April 1999; Volume 1, pp. 283-288; In English; See also 19990110087; No Copyright; Avail: CPIA, 10630 Little Patuxent Pkwy., Suite 202, Columbia, MD 21044-3200 HC, Hardcopy

Corrosion of Shuttle thruster components in atmospheres containing high concentrations of nitrogen tetroxide (NTO) and water is an important issue in ground operations of bipropellant systems in humid locations. Measurements of the corrosivities of NTO-containing atmospheres and the responses of different materials to these atmospheres have been accomplished using an electrochemical sensor. The sensor is composed of alternating aluminum/titanium strips separated by thin insulating layers. Under high humidity conditions a thin film of water covers the surface of the sensor. Added NTO vapor reacts with the water film to form a conductive medium and establishes a galvanic cell. The current from this cell can be integrated with respect to time and related to the corrosion activity. The surface layer formed from humid air/NTO reacts in the same way as an aqueous solution of nitric acid. Nitric acid is generally considered an important agent in NTO corrosion situations. The aluminum/titanium sensor is unresponsive to dry air, responds slightly to humid air (> 75% RH), and responds strongly to the combination of humid air and NTO. The sensor response is a power function (n = 2) of the NTO concentration. The sensor does not respond to NTO in dry air. The response of other materials in this type of sensor is related to position of the material in a galvanic series in aqueous nitric acid. The concept and operation of this electrochemical corrosion measurement is being applied to other corrosive atmospheric contaminants such as hydrogen chloride, hydrogen fluoride, sulfur dioxide, and acidic aerosols.
Author
Electrochemical Corrosion; Meteorology; Nitrogen Tetroxide; Water; Ground Operational Support System; Liquid Rocket Propellants

19990110116 ENSCO, Inc., Vandenberg AFB, CA USA
Physical and Thermodynamic Properties of Hypergolic Propellants: A Review and Update
Arnold, S. L., ENSCO, Inc., USA; JANNAF 28th Propellant Development and Characterization Subcommittee and 17th Safety and Environmental Protection Subcommitte Joint Meeting; April 1999; Volume 1, pp. 301-310; In English; See also 19990110087; No Copyright; Avail: CPIA, 10630 Little Patuxent Pkwy., Suite 202, Columbia, MD 21044-3200 HC, Hardcopy

Significant errors and omissions were found in some of the reported literature values for nitrogen tetroxide, monomethylhydrazine, and Aerozine-50. The methods used to try and resolve some of these errors included (1) a comparison of various literature values, including an assessment of data quality, to determine whether reported values were measured or estimated, (2) a derivation of temperature dependent correlation coefficients and validation with independent measurements

(where sufficient measured data were available), and (3) an estimation of the missing parameters using modern techniques such as the method of corresponding states or group contribution methods. Utilizing these methods resulted in a validated set of properties (many as functions temperature) for hypergolic propellants, which are suitable for environmental modeling applications and more general engineering calculations. The complete parameter set is provided, along with references and examples illustrating the above methods. Also, mixing rules, pseudo-critical properties, and mixture properties are provided for a nominal composition Aerozine-50 mixture.
Author
Chemical Properties; Thermodynamic Properties; Propellant Properties; Hypergolic Rocket Propellants; Nitrogen Tetroxide

19990110117 Deutsche Gold- und Silber-Scheideanstalt-Huels Corp., Allendale, NJ USA
Practical Experiences with High Test Hydrogen Peroxide
Feigenbaum, Harold N., Deutsche Gold- und Silber-Scheideanstalt-Huels Corp., USA; Nimmerfroh, Norbert, Deutsche Gold- und Silber-Scheideanstalt-Huels Corp., USA; Walzer, Egon, Deutsche Gold- und Silber-Scheideanstalt-Huels A.G., Germany; JANNAF 28th Propellant Development and Characterization Subcommittee and 17th Safety and Environmental Protection Subcommitte Joint Meeting; April 1999; Volume 1, pp. 311-319; In English; See also 19990110087; No Copyright; Avail: CPIA, 10630 Little Patuxent Pkwy., Suite 202, Columbia, MD 21044-3200 HC, Hardcopy

High test hydrogen peroxide is experiencing renewed interest from the aerospace community as a storable and non-toxic alternative to other liquid chemical oxidizers used in propulsion systems. The chemical and physical properties of high concentration hydrogen peroxide are reviewed from the perspective of a long-time basic manufacturer and marketer of this material.
Author
Hydrogen Peroxide; Rocket Oxidizers; High Energy Oxidizers; Liquid Oxidizers

19990110118 Naval Surface Warfare Center, Indian Head, MD USA
Characterization of Nitrocellulose Fibers in AA-2 Propellant by Polarized Light Microscopy
Renner, Rolf H., Naval Surface Warfare Center, USA; Nauflett, George W., Naval Surface Warfare Center, USA; JANNAF 28th Propellant Development and Characterization Subcommittee and 17th Safety and Environmental Protection Subcommitte Joint Meeting; April 1999; Volume 1, pp. 341-349; In English; See also 19990110087; No Copyright; Avail: CPIA, 10630 Little Patuxent Pkwy., Suite 202, Columbia, MD 21044-3200 HC, Hardcopy

Nitrocellulose fibers were counted using polarized light microscopy in six MK 90 propellant grains taken from grain lots that exhibited various levels of combustion stability as verified during Lot Acceptance Testing (LAT) of MK 66 Rocket Motors. The fiber counts obtained for the six grains, two were marked low and four were marked high combustion stability, were compared with 1985 and 1992 grains that were taken from grain lots which passed and did not pass LAT, using the same method. The 1985 and 1992 MK 90 grains with 20 or fewer fiber count were taken from grain lots that had acceptable LAT. The physical and chemical characteristics of the current 1998 propellant are vastly different from that manufactured in 1985 and 1992. Polarized light microscopy studies indicate that at one stage during the manufacture cycle, the fiber count of the 1998 samples were about the same as the acceptable 1985 and 1992 lots, but that additional processing has further plasticized the NC fibers; the 1998 samples have an average count of less than 1 unplasticized fiber.
Author
Cellulose Nitrate; Fibers; Propellant Grains; Solid Rocket Propellants; Rocket Engines

19990110119 Naval Surface Warfare Center, Indian Head, MD USA
Characterization of Ballistic Modifier LC-12-15 in AA-2 Propellant
Renner, Rolf H., Naval Surface Warfare Center, USA; Nauflett, George W., Naval Surface Warfare Center, USA; JANNAF 28th Propellant Development and Characterization Subcommittee and 17th Safety and Environmental Protection Subcommitte Joint Meeting; April 1999; Volume 1, pp. 351-363; In English; See also 19990110087; No Copyright; Avail: CPIA, 10630 Little Patuxent Pkwy., Suite 202, Columbia, MD 21044-3200 HC, Hardcopy

This paper describes a newly developed method for the measurement of LC-12-15 particles in AA-2 propellant by light microscopy techniques. This work was performed as part of the investigation of failures of MK 66 Rocket Motors during Lot Acceptance Testing (LAT) due to combustion instability. A review of the methods used to characterize LC-12-15 was made to provide background and baseline data relating to the current problem. Microscopy is the technique of choice because of the fact that light microscopy (LM) can directly measure the size and distribution of LC-12-15 particles in AA-2 propellant. LM was also used to characterize neat LC-12-15 powder. Six 1998 samples of recent MK 90 propellant grains were analyzed and compared with previous 1992 AA-2 propellant that served as the baseline for purposes of comparison. Acceptable AA-2 propellant, based

on a comparison with the 1992 data base using the new procedure for particle counting, was shown to have no particles larger than 10 micrometers, a maximum of 3 particles in the 6 to 10 micrometers size range, and no more than 80 particles in the 3 to 5 micrometers size range. Recommendations are made for use of LM procedures to compliment the newly implemented Microtrac method for LC-12-15 particle size measurement.
Author
Propellant Grains; Solid Rocket Propellants; Powder (Particles); Particle Size Distribution; Rocket Engines

19990110120 Naval Surface Warfare Center, Indian Head, MD USA
The Effects of Moisture and Temperature Cycling on the Ballistic Properties of Composite Rocket Propellants
Caulder, S. M., Naval Surface Warfare Center, USA; Hernandez, E., Naval Surface Warfare Center, USA; JANNAF 28th Propellant Development and Characterization Subcommittee and 17th Safety and Environmental Protection Subcommitte Joint Meeting; April 1999; Volume 1, pp. 365-376; In English; See also 19990110087; No Copyright; Avail: CPIA, 10630 Little Patuxent Pkwy., Suite 202, Columbia, MD 21044-3200 HC, Hardcopy

Zero time and ten year aged in-service ammonium perchlorate/carboxyl-terminated polybutadiene (AP/CTPB) composite M-270 catapult propellant samples were examined using scanning electron microscopy (SEM) and energy dispersive x-ray microanalysis (EDX). The chemical and morphological changes in the in-service aged propellant were compared to the zero time propellant standards. A discussion of chemical and physical changes as a function of age is discussed.
Author
Moisture; Temperature Effects; Ballistics; Composite Propellants; Solid Rocket Propellants; Ammonium Perchlorates

19990110592 Department of Energy, Assistant Secretary for Energy Efficiency and Renewable Energy, Washington, DC USA
Implementation of alternative bio-based fuels in aviation: The Clean Airports Program
Shauck, M. E., Department of Energy, USA; Zanin, M. G., Department of Energy, USA; Dec. 31, 1997; 8p; In English; 3rd; Biomass Conference of the Americas, USA
Report No.(s): DE99-001104; No Copyright; Avail: Department of Energy Information Bridge, Microfiche

The Renewable Aviation Fuels Development Center at Baylor University in Waco, Texas, was designated, in March 1996, by the US Department of Energy (US DOE) as the national coordinator of the Clean Airports Program. This program, a spin-off of the Clean Cities Program, was initiated to increase the use of alternative fuels in aviation. There are two major fuels used in aviation today, the current piston engine aviation gasoline, and the current turbine engine fuel. The environmental impact of each of these fuels is significant. Aviation Gasoline (100LL), currently used in the General Aviation piston engine fleet, contributes 100% of the emissions containing lead in the USA today. In the case of the turbine engine fuel (Jet fuel), there are two major environmental impacts to be considered: the local, in the vicinity of the airports, and the global impact on climate change. The Clean Airports Program was established to promote the use of clean burning fuels in order to achieve and maintain clean air at and in the vicinities of airports through the use of alternative fuel- powered air and ground transportation vehicles.
NTIS
Jet Engine Fuels; Environment Effects; Substitutes; Clean Fuels; Climate Change; Airports

19990110593 Department of Energy, Assistant Secretary for Energy Efficiency and Renewable Energy, Washington, DC USA
Certification of the Cessna 152 on 100% ethanol
Shauck, M. E., Department of Energy, USA; Zanin, M. G., Department of Energy, USA; Dec. 31, 1997; 6p; In English; Aerospace Congress '97, 1997, USA
Report No.(s): DE99-001105; No Copyright; Avail: Department of Energy Information Bridge, Microfiche

In June 1996, the Renewable Aviation Fuels Development Center (RAFDC) at Baylor University in Waco, Texas, received a Supplemental Type Certificate (STC) for the use of 100% ethanol as a fuel for the Cessna 152, the most popular training aircraft in the world. This is the first certification granted by the Federal Aviation Administration (FAA) for a non-petroleum fuel. Certification of an aircraft on a new fuel requires a certification of the engine followed by a certification of the airframe/engine combination. This paper will describe the FAA airframe certification procedure, the tests required and their outcome using ethanol as an aviation fuel in a Cessna 152.
NTIS
Ethyl Alcohol; Aircraft Fuels; Substitutes; Certification

29
MATERIALS PROCESSING

Includes space-based development of products and processes for commercial applications. For biological materials see 55 Space Biology.

19990106576 NASA Marshall Space Flight Center, Huntsville, AL USA
An Overview of the Thermal Challenges of Designing Microgravity Furnaces
Westra, Douglas G., NASA Marshall Space Flight Center, USA; [1999]; 1p; In English; Thermal and Fluids Analysis Workshop, 13-17 Sep. 1999, Huntsville, AL, USA; No Copyright; Avail: Issuing Activity, Hardcopy; Abstract Only

In the last few years, Marshall Space Flight Center has become heavily involved in a wide variety of microgravity projects that require furnaces, with hot zone temperatures ranging from 300 C to 2300 C, requirements for isothermal and gradient processing, and both semi-conductor and metal materials. On these types of projects, the thermal engineer is a key player in the design process. These furnaces present unique challenges to the thermal designer. One challenge is designing a sample containment system that achieves dual containment, yet allows a high radial heat flux. Another challenge is providing a high axial gradient but a very low radial gradient. These furnaces also present unique challenges to the thermal analyst. First, there are several orders of magnitude difference in the size of the thermal ”conductors” between various parts of the model. A second challenge is providing high fidelity in the sample model, and connecting the sample with the rest of the furnace model, yet maintaining some sanity in the number of total nodes in the model. The purpose of this paper is to present an overview of the challenges involved in designing and analyzing microgravity furnaces and how some of these challenges have been overcome. The thermal analysis tools presently used to analyze microgravity furnaces and how they have been applied will be explained. Challenges for the future and a description of future analysis tools will be given.
Author
Microgravity; Furnaces; Design Analysis

19990106577 NASA Marshall Space Flight Center, Huntsville, AL USA
Viscosity Measurement using Drop Coalescence in Microgravity
Antar, Basil N., Tennessee Univ. Space Inst., USA; Ethridge, Edwin, NASA Marshall Space Flight Center, USA; Maxwell, Daniel, Tennessee Univ. Space Inst., USA; [1999]; 1p; In English; Annual Microgravity Science and Space Symposium, 13 Jan. 2000, Reno, NV, USA; No Copyright; Avail: Issuing Activity, Hardcopy; Abstract Only

We present in here details of a new method, using drop coalescence, for application in microgravity environment for determining the viscosity of highly viscous undercooled liquids. The method has the advantage of eliminating heterogeneous nucleation at container walls caused by crystallization of undercooled liquids during processing. Also, due to the rapidity of the measurement, homogeneous nucleation would be avoided. The technique relies on both a highly accurate solution to the Navier-Stokes equations as well as on data gathered from experiments conducted in near zero gravity environment. The liquid viscosity is determined by allowing the computed free surface shape relaxation time to be adjusted in response to the measured free surface velocity of two coalescing drops. Results are presented from two validation experiments of the method which were conducted recently on board the NASA KC-135 aircraft. In these tests the viscosity of a highly viscous liquid, such as glycerine at different temperatures, was determined to reasonable accuracy using the liquid coalescence method. The experiments measured the free surface velocity of two glycerine drops coalescing under the action of surface tension alone in low gravity environment using high speed photography. The free surface velocity was then compared with the computed values obtained from different viscosity values. The results of these experiments were found to agree reasonably well with the calculated values.
Author
Coalescing; Viscosity; Microgravity; Weightlessness

19990106579 NASA Marshall Space Flight Center, Huntsville, AL USA
Zero Gravity Cryogenic Vent System Concepts for Upper Stages
Flachbart, Robin H., NASA Marshall Space Flight Center, USA; Holt, James B., NASA Marshall Space Flight Center, USA; Hastings, Leon J., NASA Marshall Space Flight Center, USA; [1999]; 1p; In English; 1999 Thermal and Fluids Workshop, 13-17 Sep. 1999, Huntsville, AL, USA; No Copyright; Avail: Issuing Activity, Hardcopy; Abstract Only

The capability to vent in zero gravity without resettling is a technology need that involves practically all uses of sub-critical cryogenics in space. Venting without resettling would extend cryogenic orbital transfer vehicle capabilities. However, the lack of definition regarding liquid/ullage orientation coupled with the somewhat random nature of the thermal stratification and resulting pressure rise rates, lead to significant technical challenges. Typically a zero gravity vent concept, termed a thermodynamic vent system (TVS), consists of a tank mixer to destratify the propellant, combined with a Joule-Thomson (J-T)

valve to extract thermal energy from the propellant. Marshall Space Flight Center's (MSFC's) Multipurpose Hydrogen Test Bed (MHTB) was used to test both spray bar and axial jet TVS concepts. The axial jet system consists of a recirculation pump heat exchanger unit. The spray bar system consists of a recirculation pump, a parallel flow concentric tube, heat exchanger, and a spray bar positioned close to the longitudinal axis of the tank. The operation of both concepts is similar. In the mixing mode, the recirculation pump withdraws liquid from the tank and sprays it into the tank liquid, ullage, and exposed tank surfaces. When energy is required. a small portion of the recirculated liquid is passed sequentially through the J-T expansion valve, the heat exchanger, and is vented overboard. The vented vapor cools the circulated bulk fluid, thereby removing thermal energy and reducing tank pressure. The pump operates alone, cycling on and off, to destratify the tank liquid and ullage until the liquid vapor pressure reaches the lower set point. At that point. the J-T valve begins to cycle on and off with the pump. Thus, for short duration missions, only the mixer may operate, thus minimizing or even eliminating, boil-off losses.
Author
Cryogenics; Orbit Transfer Vehicles; Venting; Weightlessness; Test Stands; Rocket Test Facilities

19990107784 NASA Marshall Space Flight Center, Huntsville, AL USA
Characterization of the Heat Extraction Capability of a Compliant, Sliding, Thermal Interface for Use in a High Temperature, Vacuum Microgravity Furnace
Bellomy–Ezell, Jenny, Sverdrup Technology, Inc., USA; Farmer, Jeff, NASA Marshall Space Flight Center, USA; Breeding, Shawn, Tec-Masters, Inc., USA; Spivey, Reggie, Tec-Masters, Inc., USA; [1999]; 2p; In English; 10th; Thermal and Fluids Analysis Workshop, 13-17 Sep. 1999, Huntsville, AL, USA; No Copyright; Avail: Issuing Activity, Hardcopy; Abstract Only

Much of the material science gained in microgravity research requires processing a sample in a high performance furnace. One such furnace currently being designed is the Quench Module Insert (QMI). The Principle Investigators, for whom the furnace is proposed, require high temperature gradients in their cylindrical samples to achieve the science objectives. One of the components critical to achieving high sample axial temperature gradients in the Quench Module Insert is a high performance cold zone to extract the heat from the sample. This cold zone employs a compliant, sliding thermal interface based on a Vel-Therm felt. This felt provides a conductive path between the Sample Cartridge Assembly (SCA) exterior surface and the interior surface of the water cooled chill block while allowing movement of the sample relative to the chill block. The Vel-Therm felt is composed of long polymer-based fibers affixed to a thin flexible substrate layer. The fibers are oriented perpendicular to this substrate giving the felt the appearance of a velvet fabric. The Vel-Therm felt heat extraction capability was quantified in earlier tests performed in an inert gas environment. The current activity, described in this paper, is intended to characterize the extraction capability of Vel-Therm felt in a vacuum environment similar to the QMI environment. This testing is necessary to quantify the thermal performance of the Vel-Therm felt and the sensitivity of that performance to key variables. The data derived from these tests will be incorporated into the current thermal models to improve the quality of the models and reduce uncertainty of the analytical results. In addition, the data will be used to help select the appropriate Vel-Therm felt and set proper operating limits as well as assess the performance range of the furnace. The objective of this test is to measure the heat extraction rate of the Vel-Therm felt as specified by the effective heat transfer coefficient. Therefore, the test setup was designed to force the bulk of the heat transfer through the area where the Vel-Therm felt was applied. A heat source, consisting of a ceramic heating element encased in a Copper (Cu) housing is mounted on four isolated support rods. A 6-layer molybdenum radiation shield is used to insulate against heat loss from the heater and prevent heat exchange between the hot and cold sides of the test apparatus. The Vel-Therm felt is affixed to the surface of the cold sink, a water-cooled Cu chill block. An adjustable plate supports and isolates the cold sink from above and is used to control the amount of the deflection of the Vel- Therm when in contact with the Cu heating element housing. The primary means of establishing the power being conducted through the felt is to measure the energy being transferred to the water passing through the chill block. Analysis was performed to support the assumption that the source and sink surfaces were approximately isothermal under the specific test conditions. As a check on the amount of power passing through the felt, the power supplied to the heater was also measured. Thermocouples were strategically located throughout the test apparatus for measurement purposes. A bell jar was lowered over the assembly to impose vacuum conditions. Currently, variables tested have been fiber compression and fiber type and surface temperatures (both the hot and cold side temperatures are hypothesized to be important to the performance of the Vel-Therm.) Selected runs were repeated to ensure consistency and repeatability. Results obtained thus far reveal that Vel-Therm performance is significantly degraded by fibers being exposed to high compression. It also shows that performance is somewhat negatively impacted by previous compression, thereby, raising the question of repeatability. In addition, early results show a significant dependence on temperature. A computer aided mathematical analysis of the test setup is ongoing. The results will be correlated to actual results. The correlation will examine such details as parasitic loses, conduction down the power leads and many other concerns.
Author
Heat Transfer; Furnaces; Design Analysis; Diagnosis; Heat Transfer Coefficients; Experiment Design; High Temperature

19990111477 Tennessee State Univ., Dept. of Mechanical Engineering, Nashville, TN USA

The Design of Particle Melting in Flow Flight Module (PMF) for Microgravity Tests

Jiang, Jie, Tennessee State Univ., USA; Siddiqui, A. A., Tennessee State Univ., USA; Stewart, Christopher, Tennessee State Univ., USA; Tao, Yong, X., Tennessee State Univ., USA; HBCUs/OMUs Research Conference Agenda and Abstracts; August 1999, pp. 31; In English; See also 19990111455; No Copyright; Avail: Issuing Activity, Hardcopy; Abstract Only

To prepare for a flight test under microgravity conditions onboard KC-135, an experimental flight module is designed. The investigation is to be conducted to study the melting characteristics of a packed bed under conditions of absence of buoyancy effects. The newly designed apparatus is a closed type flow system, unlike the earlier version that is an open channel apparatus and mainly for the ground tests. The test section consists of packed bed consists of ice grains of an initially uniform, flat-rectangular parallelepiped shape, and is initially saturated with still liquid. As the liquid flows though the bed, the solid grains melt. The downstream of the packed bed is bounded by a perforate plate through which liquid can flow while the ice particles are retained. From the digital video images the local packed bed thickness is measured under control flow rate and the melting rate can be determined from the image analysis. The temperature distribution along the horizontal direction and vertical direction is measured using 16 thermocouples. An infrared camera is mounted to sense the liquid-ice mixture temperature distribution on the boundary through a sapphire window. The supply water temperature and flow rate are controlled through a heat exchanger and a flow regulator, respectively. In order to meet the requirement for flight tests, a mechanical structure and impact analysis and an electrical power analysis are conducted.

Author

Flow Velocity; Melting; Microgravity; Test Chambers; Fluid Management

31
ENGINEERING (GENERAL)

Includes vacuum technology; control engineering; display engineering; cryogenics; and fire prevention.

19990107348 Sandia National Labs., Albuquerque, NM USA

Prediction of Tungsten CMP Pad Life Using Blanket Removal Rate Data and Endpoint Data Obtained from Process Temperature and Carrier Motor Current Measurements

Hetherington, D. L.; Stein, D. J.; May 14, 1999; 8p; In English; Microelectronics Manufacturing Technologies, 19-21 May 1999, Edinburgh, Scotland, USA; Sponsored by International Society for Optical Engineering, USA

Report No.(s): DE00-007242; SAND99-1181C; No Copyright; Avail: Department of Energy Information Bridge, Hardcopy

Several techniques to predict pad failure during tungsten CMP were investigated for a specific consumable set. These techniques include blanket polish rate measurements and metrics derived from two endpoint detection schemes. Blanket polish rate decreased significantly near pad failure. Metrics from the thermal endpoint technique included change in peak temperature, change in the time to reach peak temperature, and the change in the slope of the temperature trace just prior to peak temperature all as a function of pad life. Average carrier motor current before endpoint was also investigated. Changes in these metrics were observed however these changes, excluding time to peak process temperature, were either not consistent between pads or too noisy to be reliable predictors of pad failure.

NTIS

Polishing; Service Life; Predictions; Chemical Reactions; Mechanical Measurement

19990108795 Ljubljana Univ., Faculty of Electrical Engineering, Yugoslavia

Electrotechnical Review, Volume 66 ***Elektrotehniski Vestnik, Letnik 66***

Zajc, Baldomir, Editor, Ljubljana Univ., Yugoslavia; Solina, Franc, Editor, Ljubljana Univ., Yugoslavia; 1999; ISSN 0013-5852; 80p; In English; In Slovene; See also 19990108796 through 19990108802; No Copyright; Avail: CASI; A05, Hardcopy; A01, Microfiche

Contents include the following: A reconfigurable system for prototyping of image processing algorithm. Lyapunov exponents for a harmonically forces Van der Pol oscillator with a non-linear restoring force. Transferable belief model in fault diagnosis of industrial processes, On determination of the generator share in a selected load. Fault identification in a power system element based on protective relay operation signals, New conductors for efficient overhead transmission lines. and Current reference determination in parallel active power filters.

CASI

Transmission Lines; Algorithms; Oscillators; Loads (Forces); Image Processing; Conductors; Periodicals

19990110297 Department of Energy, Assistant Secretary for Energy Efficiency and Renewable Energy, Washington, DC USA
Indirect sensing technique for diesel fuel quantity control ***Progress Report, 1 Jul - 30 Sep. 1998***
MacCarley, C. A., Department of Energy, USA; Oct. 22, 1998; 4p; In English
Report No.(s): DE99-000051; DOE/CE/15583-T2; No Copyright; Avail: Department of Energy Information Bridge, Microfiche

The project has focused on a retrofit product suitable for installation on existing mechanically-governed diesel engines. Included in this potential market are almost all diesel-powered passenger cars and light trucks manufactured prior to the introduction of the most recent clean diesel engines equipped with particulate traps and electronic controls. Also included are heavy-duty trucks, transit vehicles, school buses, and agricultural equipment. This system is intended to prevent existing diesel engines from overfueling to the point of visible particulate emissions (smoke), while allowing maximum smoke-limited torque under all operating conditions. The system employs a microcontroller and a specialized exhaust particulate emission sensor to continuously generate and update an adaptive throttle-limit map. This map specifies a maximum allowable throttle position as a function of engine speed and coolant temperature. For mechanically regulated fuel injection systems, the throttle position limit is mechanized via a linear position actuator attached to the fuel injection pump. For electronically regulated injection systems, this limit is mechanized by interception and modification of the electronic throttle input to the system.
NTIS
Diesel Engines; Exhaust Emission; Fuel Injection; Diesel Fuels; Exhaust Gases

19990110666 New York Academy of Sciences, New York, NY USA
Innovation at Risk: The Future of America's Research - Intensive Industries
Morrison, J. Ian, Institute for the Future, USA; Pietersen, William G., Institute for the Future, USA; Science, Technology, and the Economic Future; [1998], pp. 87-92; In English; ISBN 1-57331-147-2; Copyright; Avail: Issuing Activity, Hardcopy

The new reality of the global marketplace is that you are not competitive unless you are globally competitive. The correlation between innovation, competitiveness, and growth is direct and relentless. America has enjoyed high rates of innovation, and hence competitiveness, because it has traditionally been among the world's leaders in R&D spending. That is changing, and the implications for the future are not pleasant.
Derived from text
Economic Development; Economic Analysis; Research and Development

19990110697 NASA Goddard Space Flight Center, Greenbelt, MD USA
Superpolishing and Precision Metrology on a Metal Mandrel and Replicated Segments for Constellation-X
Content, D., NASA Goddard Space Flight Center, USA; Saha, T., NASA Goddard Space Flight Center, USA; Petre, R., NASA Goddard Space Flight Center, USA; Lyons, J. J., III, NASA Goddard Space Flight Center, USA; Wright, G., NASA Goddard Space Flight Center, USA; Zaniewski, J., NASA Goddard Space Flight Center, USA; Chan, K. W., NASA Goddard Space Flight Center, USA; May 20, 1999; 12p; In English, Jul. 1999, Unknown; Sponsored by International Society for Optical Engineering; No Copyright; Avail: Issuing Activity, Hardcopy

We have superpolished a diamond-turned aluminum mandrel (coated with electroless Ni) to an axial roughness of 0.34 nm rms. The mandrel is made to the Astro-E secondary mirror design for the 81st shell. Precision metrology at 100 mm to submicron scales has established the power spectral density of the mandrel and ultralightweight gold coated replicated segments. Predicted image quality of a set of optimally aligned replicated segments of this and a matching primary is substantially improved as compared to the flight mirrors for Astro-E. This approach using metal mandrels, superpolishing, and replicated ultralightweight foil mirrors, may represent a cost-effective approach to meeting the 15 arcsec half-energy width and weight requirements for the Constellation-X mission. Descriptions of the polishing apparatus, the precision metrology instruments, and the surface data analysis are presented. The general methods described are applicable to precision optics for both normal incidence and grazing incidence optics.
Author
Metrology; Mandrels; Metal Polishing; Segmented Mirrors; X Ray Optics; X Ray Telescopes

19990113152 National Inst. of Standards and Technology, Building and Fire Research Lab., Gaithersburg, MD USA
Next Generation Fire Suppression Technology Program (NGP): Technical Highlights 1998
Gann, R. G.; Aug. 1999; 20p; In English
Report No.(s): PB99-159857; NISTIR-6366; No Copyright; Avail: CASI; A03, Hardcopy; A01, Microfiche

The Department of Defense (DOD) is entering the third year of its Next Generation Fire Suppression Technology Program (NGP). The NGP goal is to demonstrate, by 2005, retrofitable, economically feasible, environmentally acceptable and user-safe processes, techniques, and fluids that meet the operational requirements currently satisfied by halon 1301 systems in aircraft,

ships, land combat vehicles, and critical mission support facilities. The potential fire locations for which alternatives to halon 1301 are sought include aircraft engine nacelles, dry bays, cargo bays, and fuel tanks; ground vehicle crew compartments; and shipboard machinery spaces and storage compartments. The hazards to be avoided include harm to people, thermal damage, post-fire corrosion, loss of visibility, and overpressure. Successful candidates must thus do well in: fire suppression efficiency and reignition quenching, ozone depletion potential (ODP), global warming potential (GWP), atmospheric lifetime, suppressant residue level, electrical conductivity, metals non-corrosivity and polymeric materials compatibility, long-term storage stability, low toxicity of the chemical and its combustion and decomposition products, speed of dispersion, safety and occupational health requirements.
NTIS
Fires; Hazards; Fire Prevention

19990113184 Ryan Aeronautical Co., Marine Systems, San Diego, CA USA
Selection of a Propulsion System for a Wet Submersible
Shackford, R. W., Ryan Aeronautical Co., USA; 1968; In English; 4th; Propulsion Joint Specialist, 10-14 Jun. 1968, Cleveland, OH, USA; Sponsored by American Inst. of Aeronautics and Astronautics, USA
Report No.(s): AIAA Paper 68-621; Copyright; Avail: Issuing Activity, Hardcopy

This paper will discuss the various parameters that must be considered in the design of a wet submersible propulsion system. These parameters will include, but not be limited to: depth, range, speed, human tolerance, volume, weight, safety, reliability, maintainability, and material requirements. These basic parameters analyses will lead to an establishment of criteria for selection of: power source, methods of inter-connection materials, environmental protection, speed reducers, motor, speed control, and propeller. The paper will demonstrate a method of selection of hardware to meet the design criteria.
Author
Design Analysis; Propulsion; Selection; Submerged Bodies; Underwater Engineering; Underwater Propulsion; Drag; Propulsion System Performance; Propulsion System Configurations; Electric Batteries

32
COMMUNICATIONS AND RADAR

Includes radar; land and global communications; communications theory; and optical communications. For related information see also 04 Aircraft Communications and Navigation and 17 Space Communications, Spacecraft Communications, Command and Tracking. For search and rescue see 03 Air Transportation and Safety, and 16 Space Transportation.

19990106557 NASA Langley Research Center, Hampton, VA USA
Method and System for Producing Images of an Object
Katzberg, Stephen J., Inventor, NASA Langley Research Center, USA; Garrison, James L., Jr., Inventor, NASA Langley Research Center, USA; Sep. 07, 1999; In English
Patent Info.: Filed 6 Jan. 1998; NASA-Case-LAR-15538-1; US-Patent-5,949,364; US-Patent-Appl-SN-003247; No Copyright; Avail: US Patent and Trademark Office, Hardcopy

A method and system are provided to produce images of an object. A receiving station is positioned in view of a range-coded signal emitting satellite and the object. The receiving station is sensitive to direct transmission of the range-coded signal and reflections of the range-coded signal from the object. Both range from the receiving station to the object and a Doppler frequency shift history between the receiving station and the object is determined using the direct transmission and reflections of the range-coded signal. An image is formed using the two-dimensional record provided by the range and the Doppler frequency shift history.
Official Gazette of the U.S. Patent and Trademark Office
Signal Reflection; Doppler Effect; Imaging Techniques

19990106561 Smithsonian Astrophysical Observatory, Cambridge, MA USA
Investigation of EM Emissions by the Electrodynamic Tether, Inclusive of an Observational Program (EMET) ***Final Report***
Estes, Robert D., Smithsonian Astrophysical Observatory, USA; October 1998; 100p; In English
Contract(s)/Grant(s): NAS8-36809
Report No.(s): NASA/CR-1999-209571; NAS 1.26:209571; No Copyright; Avail: CASI; A05, Hardcopy; A02, Microfiche

Our TSS-1/R investigation, which we shall refer to as EMET in this report, was an integral part of the effort by the TSS-1/R Investigators' Working Group (IWG) to come to an understanding of the complex interaction between the tethered satellite system and the ionosphere. All of the space-borne experiments were designed to collect data relevant to the local interaction. Only the ground- based experiments, EMET and its Italian counterpart Observations on the Earth's Surface of Electromagnetic Emissions (OESEE), held out any hope of characterizing the long range effects of the interaction. This was to be done by detecting electromagnetic waves generated by the system in the ionosphere, assuming the signal reached the Earth's surface with sufficient amplitude. As the type of plasma waves excited to carry charge away from the charge-exchange regions of the system at each end of the tether is one of the theoretical points about which there is greatest disagreement, a definitive identification of tether-generated waves could mark significant progress in the so-called current closure problem of electrodynamic tethers. Dr. Mario Grossi of the Smithsonian Astrophysical Observatory (SAO) initiated the investigation, and his experience in the field of ULF-ELF waves and their detection was invaluable throughout its course. Rice University had the responsibility of setting up the EMET ULF-VLF ground stations under a subcontract from SAO. Principal Investigator (PI) for the Rice effort was Prof. William E. Gordon, who was primary observer at the Arecibo Observatory during TSS-LR. Dr. Steve Noble handled major day-to-day operations, training, and planning for the ground-based measurements. Dr. James McCoy of NASA JSC, a member of the Mona/Arecibo team, was pilot for the numerous flights ferrying personnel and equipment between Puerto Rico and Mona Island. Final responsibility for the measurements rested with SAO, and the activities of field personnel and SAO investigators were closely co-ordinated during the mission. Dr. Enrico Lorenzini of SAO served as the eyes, ears, and brain of EMET in the Science Operations Area and PI table during the mission, whenever the PI was absent during the round-the-clock mission operations. The Rice University final report to SAO, which is included as an Appendix, contains details of the remote sites, means of communication, sensors, etc., as well as the affiliations of personnel involved in the data-gathering effort.
Derived from text
Astrophysics; Detection; Electromagnetic Radiation; Extremely Low Frequencies; Plasma Waves; Tethering; Tetherlines

19990107360 NASA Marshall Space Flight Center, Huntsville, AL USA
Sensitivity Analysis of ProSEDS (Propulsive Small Expendable Deployer System) Data Communication System
Park, Nohpill, Oklahoma State Univ., USA; Reagan, Shawn, NASA Marshall Space Flight Center, USA; Franks, Greg, NASA Marshall Space Flight Center, USA; Jones, William G., NASA Marshall Space Flight Center, USA; [1999]; 18p; In English; 8th; VLSI Symposium, 20-21 Oct. 1999, Albuquerque, NM, USA; No Copyright; Avail: CASI; A03, Hardcopy; A01, Microfiche

This paper discusses analytical approaches to evaluating performance of Spacecraft On-Board Computing systems, thereby ultimately achieving a reliable spacecraft data communications systems. The sensitivity analysis approach of memory system on the ProSEDS (Propulsive Small Expendable Deployer System) as a part of its data communication system will be investigated. Also, general issues and possible approaches to reliable Spacecraft On-Board Interconnection Network and Processor Array will be shown. The performance issues of a spacecraft on-board computing systems such as sensitivity, throughput, delay and reliability will be introduced and discussed.
Author
Sensitivity; Memory (Computers); Computers

19990109081 NASA Goddard Space Flight Center, Greenbelt, MD USA
Snow Crystal Orientation Effects on the Scattering of Passive Microwave Radiation
Foster, J. L., NASA Goddard Space Flight Center, USA; Barton, J. S., General Sciences Corp., USA; Chang, A. T. C., NASA Goddard Space Flight Center, USA; Hall, D. K., NASA Goddard Space Flight Center, USA; [1999]; 41p; In English; No Copyright; Avail: CASI; A03, Hardcopy; A01, Microfiche

For this study, consideration is given to the role crystal orientation plays in scattering and absorbing microwave radiation. A discrete dipole scattering model is used to measure the passive microwave radiation, at two polarizations (horizontal and vertical), scattered by snow crystals oriented in random and non random positions, having various sizes (ranging between 1 micrometers to 10,000 micrometers in radius), and shapes (including spheroids, cylinders, hexagons). The model results demonstrate that for the crystal sizes typically found in a snowpack, crystal orientation is insignificant compared to crystal size in terms of scattering microwave energy in the 8,100 gm (37 GHz) region of the spectrum. Therefore, the assumption used in radiative transfer approaches, where snow crystals are modeled as randomly oriented spheres, is adequate to account for the transfer of microwave energy emanating from the ground and passing through a snowpack.
Author
Snow Cover; Snow; Ice; Crystals; Orientation; Polarization (Spin Alignment)

19990109153 Exploration Physics International, Milford, NH USA

A Versatile Planetary Radio Science Microreceiver ***Final Report, 8 Oct. 1996 - 7 Oct. 1999***

Fry, Craig D., Exploration Physics International, USA; Rosenberg, T. J., Maryland Univ., USA; Oct. 26, 1999; 31p; In English

Contract(s)/Grant(s): NASw-96019

Report No.(s): C96-01AR03; No Copyright; Avail: CASI; A03, Hardcopy; A01, Microfiche

We have developed a low-power. programmable radio "microreceiver" that combines the functionality of two science instruments: a Relative Ionospheric Opacity Meter (riometer) and a swept-frequency, VTF/HF radio spectrometer. The radio receiver, calibration noise source, data acquisition and processing, and command and control functions are all contained on a single circuit board. This design is suitable for miniaturizing as a complete flight instrument. Several of the subsystems were implemented in a field-programmable gate array (FPGA), including the receiver detector, the control logic, and the data acquisition and processing blocks. Considerable efforts were made to reduce the power consumption of the instrument, and eliminate or minimize RF noise and spurious emissions generated by the receiver's digital circuitry. A prototype instrument was deployed at McMurdo Station, Antarctica, and operated in parallel with a traditional riometer instrument for approximately three weeks. The attached paper (accepted for publication by Radio Science) describes in detail the microreceiver theory of operation, performance specifications and test results.

Author

Control Systems Design; Control Theory; Sequential Control; Radio Receivers; Functional Design Specifications; Riometers; Remote Sensing; Mars Atmosphere; Planetary Ionospheres; Ionosondes

19990109161 NASA Goddard Space Flight Center, Greenbelt, MD USA

Potential Application of the Surface Reference Technique Over Land at Large Incidence Angle

Tian, L., Universities Space Research Association, USA; Heymsfield, G. M., NASA Goddard Space Flight Center, USA; Bidwell, S. W., NASA Goddard Space Flight Center, USA; [1999]; 5p; In English; 29th; Radar Meteorology, Jul. 1999, Montreal, Canada; Sponsored by American Meteorology Society, USA; No Copyright; Avail: CASI; A01, Hardcopy; A01, Microfiche

Airborne meteorological radars typically operate at attenuating wavelengths. Correction for attenuation along the propagation path, therefore, is required to retrieve reflectivity factor for accurate estimation of the rainfall rate. The surface reference technique (SRT) to correct the observed reflectivity for the effects of attenuation has been developed for down-looking radars (Meneghini et al.,1983). The SRT algorithm uses the radar cross section of the ocean surface as a means of estimating the path integrated attenuation. In the SRT an initial value is determined for the radar cross section of a rain-free area in relatively close proximity to the rain cloud. During subsequent observations of precipitation any decrease in the observed surface cross section from the reference value is assumed to be a result of the two-way attenuation along the propagation path (PIA). The PIA for each beam is then used as a limiting condition in an attenuation correction algorithm (Iguchi and Meneghini, 1994).

Derived from text

Reflectance; Radar Cross Sections; Attenuation; Algorithms; Airborne Radar

19990109653 Institute for Human Factors TNO, Soesterberg, Netherlands

Information Operations: Threats to the Effective Use of Information in Command and Control ***Final Report Information Operations: Dreigingen voor het Effectief Gebruiken van Informatie in Command en Control***

vander Kleij, R., Institute for Human Factors TNO, Netherlands; Griffioen–Young, H. J., Institute for Human Factors TNO, Netherlands; Luijf, H. A. M., Institute for Human Factors TNO, Netherlands; Klaver, M. H. A., Institute for Human Factors TNO, Netherlands; 19990621; 27p; In English

Contract(s)/Grant(s): A99/CO/312; TNO Proj. 731.2/1

Report No.(s): TD99-0323; TNO-TM-A049; Copyright; Avail: Issuing Activity, Hardcopy

Due to procedural changes in the armed forces, the reliance on information and communication technology grows ever greater. Unfortunately, this reliance on computer-based informational systems poses new informational threats to the military. This report offers, in addition to a description of the Command and Control (C2) process, a discussion of defensive and offensive Information Operations, and the way they can affect information, information-based processes, and communication and information systems (CIS). A generic C2 model is presented that is used in discussing issues of making effective use of new information means while avoiding human factors pitfalls like micro-management, fixation on the current battle, information overload, and transfer of intent in a much stronger way than ever before. Also, several offensive Information Operations means as for instance deception, disturbance and/or delay of information flows, information overload, increased uncertainty (e.g., by affecting integrity) and Psychological Operations that can be used to influence the adversary's information flow are discussed.

It is concluded that the true main target of an offensive Information Operations campaign - apart from information gathering operations - is not the specific systems that are actually attacked, but rather the adversary's decision-making process.
Author
Human Factors Engineering; Information Systems; Armed Forces; Computer Techniques

19990109655 Physics and Electronics Lab. TNO, The Hague, Netherlands
Calculation of Excitation-Factors for the APAR-Antenna for Deterministic Nulling, Using the Conjugate Gradient Method
Betjes, P. N., Physics and Electronics Lab. TNO, Netherlands; June 1999; 47p; In English; Original contains color illustrations
Contract(s)/Grant(s): A95/KM/663; TNO Proj. 24727
Report No.(s): TD99-0226; TNO-FEL-99-A140; Copyright; Avail: Issuing Activity, Hardcopy

A phased array radar like APAR allows easy manipulation of the antenna radiation pattern. by introducing proper excitations the sensitivity for disturbances like jamming and multipath may be reduced. In this report, the calculation of excitation factors for a number of desired radiation patterns is described. Attempts are made to adapt both sum and difference patterns to suppress resp. jammers in a small sector in the main beam, jammers in a larger sector outside the main beam and multipath effects. It is concluded that, with the used software, suppressing jammers inside and outside the main beam can be realised to a certain extent, but adaptations of the phase which are needed for reduction of the effect of multipath are not feasible. Shortcomings in the calculated excitations lay in the fact that the prescribed field is given only on a limited number of discrete points and that full freedom of the excitation factors is assumed.
Author
Computation; Excitons; Antenna Radiation Patterns; Jamming; Phased Arrays

19990110315 New Mexico State Univ., Klipsch School of Electrical and Computer Engineering, Las Cruces, NM USA
Bandwidth-Efficient Parallel and Serial Concatenated Codes for QPSK Modulation: Consideration for the CCSDS Near-Earth Standard
Ryan, William E., Arizona Univ., USA; Acikel, Omer, New Mexico State Univ., USA; Sep. 14, 1999; 19p; In English
Report No.(s): NMSU-ECE-99-013; No Copyright; Avail: CASI; A03, Hardcopy; A01, Microfiche

Parallel concatenated convolutional codes (PCCCS) with iterative decoding, also called "turbo codes," were first presented to the coding community at the 1993 International Conference on Communications. These codes achieved a bit error rate of 10(exp -5) at an unprecedented 0.7 dB from the Shannon limit, thus gaining the full attention of the coding community. Since that time, there has been a flurry of research activity on both parallel and serial concatenated convolutional codes (SCCCs), on related codes, and on various iterative decoders. The current document focuses on bandwidth-efficient PCCCs and SCCCs for QPSK (or BPSK) signaling. The purpose of this document is to provide an informative overview of these codes for CCSDS Panel 1A members to facilitate their consideration for the near-earth CCSDS standard. In particular, our goal is to highlight the advantages of turbo-coded QPSK over competing schemes.
Author
Parallel Processing (Computers); Binary Phase Shift Keying; Bit Error Rate

19990110564 Professional Eloquence, Orange, CA USA
Me and My Visuals
Kulda, Richard J., Professional Eloquence, USA; [1970]; 1p; In English; 5; 5th; Thermophysics, 29 Jun. - 1 Jul., 1970, Los Angeles, CA, Los Angeles, CA, USA, USA; Sponsored by American Inst. of Aeronautics and Astronautics, USA
Report No.(s): AIAA Paper 70-816; Copyright; Avail: Issuing Activity, Hardcopy

The visuals you use in your technical presentations contain the most important information you will try to transfer to your audience. Poor visuals make you look like a bumbler and give the audience the feeling that you don't really care whether they understand or not. to know what to show, you must decide what you want the visual to do for the audience. Some guidelines are given. Learning about visuals is primarily a visual experience. This paper is less a paper than it is a summary of verbal remarks made during the presentation at the AIAA 5th Thermophysic Conference and is intended as an aid to recall rather than as a self contained essay.
Author
Visual Aids; Display Devices; Imagery; Images

19990110588 Instituto Nacional de Pesquisas Espacias, Sao Jose dos Campos, Brazil

Development of a Phase Correction System to the Ionospheric Radar of Sao Luis do Maranhao

Denardini, Clezio Marcos, Instituto Nacional de Pesquisas Espacias, Brazil; 1999; 142p; In Portuguese; Original contains color illustrations

Report No.(s): INPE-7174-TDI/676; No Copyright; Avail: CASI; A07, Hardcopy; A02, Microfiche

This dissertation will present details of the development and construction of the phase correction unit, which was successfully implemented, with the help of the participating technical staff and collaboration with other scientific groups. it is needed for efficient functioning of the transmitting system it is required to achieve phase stabilisation and correct phase relationship of the signals transmitted by the different antennas. The unit was tested with the radar at "Scio Luis" when its successful operation was conducted during an operational and observational campaign in August 1998. During this campaign the first data on the dynamics of electrojet irregularities were registered with a resolution of 6s in time and 2.6 km in height resolution. The data collected during a few days of the campaign are now being analysed. Preliminary results of analysis of some data are presented in this thesis. The analysis software utilises Fast Fourier (FFT) technique to extract the Doppler frequency of the electrojet irregularity echoes, and hence their velocities, at a large number of height bins, that can be adjusted to cover height regions of specific interest, for electrojet or plasma bubble investigations. It also provides the integrated spectral power at each height, which permits plots of RTI (Range Time Intensity) maps as a function of local time. Analysis done for 31 August, which was a magnetically disturbed day, shows large variation in electrojet intensity. Such variations are found to be associated with fluctuations in the Auroral Electrojet (AE), Equatorial Electrojet (EEJ) magnetic field intensities and in the Dst indices. Also the height of the electrojet irregularities on this day appears to show a minimum near local midday. Detailed analyses are under way.

Author

Theses; Design Analysis; Fabrication; Signal Transmission; Equatorial Electrojet; Time Dependence

19990110594 North Dakota State Univ., Fargo, ND USA

TEL8 Telecommunications Network: A Pooled Fund Study for Transportation Videoconferencing ***Interim Report, Jul. 1994 - Dec. 1997***

Benson, D. E., North Dakota State Univ., USA; June 1998; 26p; In English

Report No.(s): PB99--128522; No Copyright; Avail: Issuing Activity (Natl Technical Information Service (NTIS)), Microfiche

The document provides a summary of the development of a telecommunications network dedicated to transportation. The network was initially establshed as a satellite-based videoconference system among state DOTs and transportation research universities in FHWA Region 8. The report details the development of transportation-related programming and training for the network as well as the technological evolution of the system.

NTIS

Teleconferencing; Communication Networks; Satellite Communication

19990111473 NASA Glenn Research Center, Cleveland, OH USA

ACTS Ka-band Propagation Research in a Spatially Diversified Network with Two USAT Ground Stations

Kalu, Alex, Savannah State Coll., USA; Acousta, R., NASA Glenn Research Center, USA; Durand, S., Florida Solar Energy Center, USA; Emrich, Carol, Florida Solar Energy Center, USA; Ventre, G., Florida Solar Energy Center, USA; Wilson, W., Florida Solar Energy Center, USA; HBCUs/OMUs Research Conference Agenda and Abstracts; August 1999, pp. 27; In English; See also 19990111455; No Copyright; Avail: Issuing Activity, Hardcopy; Abstract Only

Congestion in the radio spectrum below 18 GHz is stimulating greater interest in the Ka (20/30 GHz) frequency band. Transmission at these shorter wavelengths is greatly influenced by rain resulting in signal attenuation and decreased link availability. The size and projected cost of Ultra Small Aperture Terminals (USATS) make site diversity methodology attractive for rain fade compensation. Separation distances between terminals must be small to be of interest commercially. This study measures diversity gain at a separation distance is less than 5 km and investigates utilization of S-band weather radar reflectivity in predicting diversity gain. Two USAT ground stations, separated by 2.43 km for spatial diversity, received a continuous Ka-band tone sent from NASA Glenn Research Center via the Advanced Communications Technology Satellite (ACTS) steerable antenna beam. Received signal power and rainfall were measured, and Weather Surveillance Radar-1998 Doppler (WSR-88D) data were obtained as a measure of precipitation along the USAT-to-ACTS slant path. Signal attenuation was compared for the two sites, and diversity gain was calculated for fades measured on eleven days. Correlation of WSR-88D S-band reflectivity with measured Ka-band attenuation consisted of locating radar volume elements along each slant path, converting reflectivity to Ka-band attenuation with rain rate calculation as an intermediate step. Specific attenuation for each associated path segment was summed, resulting in total attenuation along the slant path. Derived Ka-band attenuation did not correlate closely with empirical data (r = 0.239), but a measured signal fade could be matched with an increase in radar reflectivity in all fade events. Applying a low pass

filter to radar reflectivity prior to deriving Ka-band attenuation improved the correlation between measured and derived signal attenuation (r = 0.733). Results indicate that site diversity at small separation distances is a viable means of rain fade compensation, and that existing models underestimate diversity gain for a subtropical climate such as Florida. Also, filtered WSR-88D reflectivity can be used for optimizing diversity terminal placement by comparing derived Ka- band attenuation between the diversity sites.
Author
Extremely High Frequencies; Ground Stations; Rain; Signal Fading; Superhigh Frequencies; Radio Frequency Interference; Attenuation; Ground Effect (Communications)

19990111474 NASA Glenn Research Center, Cleveland, OH USA
Acceptance Testing of a Satellite SCADA Photovoltaic-Diesel Hybrid System
Kalu, Alex, Savannah State Coll., USA; Acosta, R., NASA Glenn Research Center, USA; Durand, S., Florida Solar Energy Center, USA; Emrich, Carol, Florida Solar Energy Center, USA; Ventre, G., Florida Solar Energy Center, USA; Wilson, W., Florida Solar Energy Center, USA; HBCUs/OMUs Research Conference Agenda and Abstracts; August 1999, pp. 28; In English; See also 19990111455; No Copyright; Avail: Issuing Activity, Hardcopy; Abstract Only

Savannah State University (SSU) and the Florida Solar Energy Center (FSEC) have been participating in the NASA Advanced Communications Technology Satellite (ACTS) program for the last five years. This program was designed by NASA to help maintain U.S. leadership in commercial space communications by funding high-risk research, and to flight-test next-generation digital satellite components. Launched in 1993, ACTS is an U.S. government funded technology test-bed that incorporates high power Ka-band transponders, small spot beams, and on-board digital storage and switching technology. Associated with the spacecraft, is a prototype satellite control center that supports various application experiments. The SSU/FSEC application experiment is to developing a Photovoltaic-Diesel Hybrid Power system complete with satellite Supervisory Control and Data Acquisition (SCADA). The hybrid system was design to demonstrate the feasibility of using SCADA to maintain and operate remote village power systems. This configuration would enable experts at a central location to provide technical assistance to local technicians while they acquire a measure of proficiency with the hybrid system operation and maintenance. Upon full mastery of the technology, similar SCADA arrangement are planned to remotely monitor and control constellation of hybrid systems scattered overlarge rural areas. Two Orion Energy APEX-1000 hybrid systems were delivered in 1998, one was installed at SSU in eastern Georgia and the other was installed at FSEC in Central Florida. The project was designed to: (1) evaluate the performance of ACTS in a SCADA arrangement, (2) monitor the health and performance of all major hybrid subsystems, (3) investigate load control and battery charging strategies to maximize battery capacity and lifetime, and (4) develop satellite communication protocol. Preliminary results indicate that the hybrid design is suitable for satellite Supervisory Control and Data Acquisition. A modification to the controller software has produced a robust communication link capable of real time control and long term data collection.
Author
ACTS; Communication Networks; Data Acquisition; Photovoltaic Conversion; Rural Areas; Satellite Communication; Space Communication

19990111475 NASA Glenn Research Center, Cleveland, OH USA
PV-Diesel Hybrid SCADA Experiment Network Design
Kalu, Alex, Savannah State Coll., USA; Durand, S., Florida Solar Energy Center, USA; Emrich, Carol, Florida Solar Energy Center, USA; Ventre, G., Florida Solar Energy Center, USA; Wilson, W., Florida Solar Energy Center, USA; Acosta, R., NASA Glenn Research Center, USA; HBCUs/OMUs Research Conference Agenda and Abstracts; August 1999, pp. 29; In English; See also 19990111455; No Copyright; Avail: Issuing Activity, Hardcopy; Abstract Only

The essential features of an experimental network for renewable power system satellite based supervisory, control and data acquisition (SCADA) are communication links, controllers, diagnostic equipment and a hybrid power system. Required components for implementing the network consist of two satellite ground stations, to satellite modems, two 486 PCs, two telephone receivers, two telephone modems, two analog telephone lines, one digital telephone line, a hybrid-power system equipped with controller and a satellite spacecraft. In the technology verification experiment (TVE) conducted by Savannah State University and Florida Solar Energy Center, the renewable energy hybrid system is the Apex-1000 Mini-Hybrid which is equipped with NGC3188 for user interface and remote control and the NGC2010 for monitoring and basic control tasks. This power system is connected to a satellite modem via a smart interface, RS232. Commands are sent to the power system control unit through a control PC designed as PC1. PC1 is thus connected to a satellite model through RS232. A second PC, designated PC2, the diagnostic PC is connected to both satellite modems via separate analog telephone lines for checking modems'health. PC2 is also connected to PC1 via a telephone line. Due to the unavailability of a second ground station for the ACTS, one ground station is

used to serve both the sending and receiving functions in this experiment. Signal is sent from the control PC to the Hybrid system at a frequency f(sub 1), different from f(sub 2), the signal from the hybrid system to the control PC. f(sub l) and f(sub 2) are sufficiently separated to avoid interference.
Author
Communication Networks; Control Equipment; Ground Stations; Satellite Control; Photovoltaic Conversion; Network Control

19990111570 New Mexico State Univ., Klipsch School of Electrical and Computer Engineering, Las Cruces, NM USA
Performance of High Rate Turbo Codes Employing the Soft-Output Viterbi Algorithm (SOVA)
Ryan, William E., Arizona Univ., USA; Ghrayeb, Ali, Arizona Univ., USA; Oct. 20, 1999; 16p; In English
Report No.(s): NMSU-ECE-99-008; No Copyright; Avail: CASI; A03, Hardcopy; A01, Microfiche

We examine the performance of the iterative soft-output Viterbi algorithm (SOVA) for high rate turbo codes on an additive white Gaussian noise (AWGN) channel and compare its performance to that of the APP algorithm. Code rates of the form k(sub 0)/ k(sub 0) + 1 (k(sub 0) = 4, 8, 16, 32, and 64) are considered. In our simulations, we show that the SOVA algorithm yields a bit error probability (P(sub b) performance that is only about 0.7 dB inferior to the performance of the APP algorithm and about 1.7 dB from the capacity limit at P(sub b) = 10(exp -5). We also examine SOVA performance as a function of the number of iterations and a parameter we call the reliability depth.
Author
Algorithms; Reliability; Error Analysis; White Noise

19990111653 NASA Marshall Space Flight Center, Huntsville, AL USA
The Process of Science Communications at NASA/Marshall Space Flight Center
Horack, John M., Florida Univ., USA; Treise, Deborah, Florida Univ., USA; [1998]; 1p; In English; New Millennium Magnetosphere Conference, 27 Oct. 1998, Guntersville, AL, USA; Copyright; Avail: Issuing Activity, Hardcopy; Abstract Only

The communication of new scientific knowledge and understanding is an integral component of science research, essential for its continued survival. Like any learning-based activity, science cannot continue without communication between and among peers so that skeptical inquiry and learning can take place. This communication provides necessary organic support to maintain the development of new knowledge and technology. However, communication beyond the peer-community is becoming equally critical for science to survive as an enterprise into the 21st century. Therefore, scientists not only have a 'noble responsibility' to advance and communicate scientific knowledge and understanding to audiences within and beyond the peer-community, but their fulfillment of this responsibility is necessary to maintain the survival of the science enterprise. Despite the critical importance of communication to the viability of science, the skills required to perform effective science communications historically have not been taught as a part of the training of scientist, and the culture of science is often averse to significant communication beyond the peer community. Thus scientists can find themselves ill equipped and uncomfortable with the requirements of their job in the new millennium.
Author
Communication; Information Flow; Information Transfer; Technology Transfer

19990113070 National Telecommunications and Information Administration, Inst. for Telecommunication Sciences, Boulder, CO USA
Spectrum Measurements for an RF-Driven Lighting Device
Dalke, R. A.; Raush, P. J.; Sanders, F. H.; Ratzloff, J. M.; May 1999; 68p; In English
Report No.(s): PB99-156606; NTIA-99-266; No Copyright; Avail: CASI; A04, Hardcopy; A01, Microfiche

New lighting devices that emit radio frequencies are bing developed for commercial use. Since such devices may interfere with communication systems that utilize the radio spectrum, it is essential that the emission characteristics be carefully analyzed. This report describes the spectral emission characteristics of a radio frequency (nominally 2.5 MHz) driven lighting device that is under development for commercial use in the U.S. A combination of near field measurement techniques and a theoretical model were used to determine emitted field levels. This report presents the results of the measurements and details measurement and analysis methods used to determine the emissions spectrum. The results presented include the theoretical model of the radio frequency source that can be used to predict spectral emissions of arrays of such lighting devices.
NTIS
Radio Frequency Interference; Field Strength; Transmission Efficiency; Illuminating

19990113096 Helsinki Univ. of Technology, Radio Lab., Espoo Finland
HUT Radio Laboratory Research and Education 1998
Raeisaenen, A.; Lindberg, S.; Apr. 1999; 40p; In English
Report No.(s): PB99-159188; Copyright; Avail: National Technical Information Service (NTIS), Microfiche

Research and teaching activities of the Radio Laboratory in 1998 are described. In May the Radio Laboratory together with Millilab organized an international conference 'Millimetere Wave Technology and Applications: Antennas, Circuits and Systems', which attracted more than 160 participants. Also in May, Professor Antii Raisanen received the EIS Award 1998 from the Association of Electronics Engineers in Finland. On July 1, Dr. Pertti Vainikainen started asa full professor of radio engineering after appointment by President of Finland, Mr. Martti Ahtisaari. year 1998 was also a good year in education: 2 Doctor degrees, 5 Licentiate degrees and 13 Diploma degrees were awarded to the students of the Radio Laboratory.
NTIS
Radio Transmission; Mobile Communication Systems; Communication Satellites; Radio Communication; Telecommunication; Research and Development

19990113104 Technische Hogeschool Twente, Centre for Telematics and Information Technology, Enschede, Netherlands
Simulator and Analyzer for Wireless for MAC Protocols
Linnenbank, G. R. J.; 1999; 68p; In English
Report No.(s): PB99-176075; CTIT-TR-97-25; Copyright; Avail: National Technical Information Service (NTIS), Hardcopy

Recently, many multiple-access (MAC) protocols have been or are being proposed for wireless networks. As most of these multiple-access protocols are designed for specific applications (such as telephony) and analyzed accordingly, the results can not always be adapted to situations with differently behaving users. Wireless MAC protocols for data communication are not straight forward to analyze. to quickly make a reliable judgement of the usability of a multiple-access protocol for certain situations, the authors designed a simulator that makes it simple to implement the protocol and test it in different configurations and with differently behaving users. The simulator generates a large amount of quantitative analysis information and traces. To analyze te trace efficiently and effectively the authors also built an analyzer that presents the results generated by the simulator in a user friendly format allowing the user to easily perform a qualitative analysis.
NTIS
Simulators; Protocol (Computers); Multiple Access; Network Analysis; Computerized Simulation; Wireless Communication

19990113105 Technische Hogeschool Twente, Centre for Telematics and Information Technology, Enschede, Netherlands
Design and Implementation of an ATM Performance Measurement Tool
Jonk, K. J.; 1999; 88p; In English
Report No.(s): PB99-175994; CTIT-TR-97-34; Copyright; Avail: National Technical Information Service (NTIS), Hardcopy

This thesis describes the design and implementation of an ATM high speed performance measurement tool, called the ATM CellGrabber. The ATM CellGrabber is a tool that was designed to the special needs of ongoing research at the University of Twente, because commercial ATM analyzers besides being very expensive, offer very limited capabilities for certain research tasks. The design and implementation of the hardware and the software interface of the ATM CellGrabber were the core part of this assignment and are described in this thesis. The design and implementation of the driver- and application-software for the ATM CellGrabber are the subjects of a separate assignment and will be described in a future thesis, scheduled for March 1998. The prototype of the ATM CellGrabber that is described in this thesis satisfies a number of the twenty requirements, that were set up as part of this assignment. Implemented in this prototype of the ATM CellGrabber is all of the required functionality: cell extraction from SDH/SONET-streams at 155 Mbits/s; time stamping of the extracted cells; filtering of the extracted cells based on ATM header bits, and storage of long streams of the filtered cells.
NTIS
Asynchronous Transfer Mode; Computer Networks; Communication Networks

19990113107 Technische Hogeschool Twente, Centre for Telematics and Information Technology, Enschede, Netherlands
Hybrid Importance Sampling Estimation of Consecutive Cell Loss Probability
deBoer, P. T.; Nicola, V. F.; 1999; ISSN 1381-3625; 26p; In English
Report No.(s): PB99-175903; CTIT-TR-97-27; No Copyright; Avail: CASI; A01, Microfiche; A03, Hardcopy

In this paper the authors present two hybrid methods to estimate the probability of consecutive cell loss (CCL) in M/G/1/k queuing models of cell-based communications systems (e.g., ATM). Both methods make use of an explicit expression for the CCL probability in terms of other well-defined probabilities that can be determined separately. In the first method, some of these probabilities are estimated using importance sampling, while others are approximated by analytic results that hold asymptotically,

for large k. In the second method, all probabilities are estimated separately using simulations; asymptotically efficient importance sampling procedures are proposed and used to estimate small probabilities.
NTIS
Losses; Probability Theory

19990113141 National Defence Research Establishment, Dept. of Command and Control Warfare Technology, Linkoeping, Sweden
Data Transmission Using Combat Radio ***Filoeverfloering med Taktisk Radio***
Frostemark, T.; Norrby, M.; Jul. 1998; 110p; In Swedish
Report No.(s): PB99-174021; FOA-R-98-00780-504-SE; No Copyright; Avail: National Technical Information Service (NTIS), Hardcopy

The thesis discusses problems and drawbacks concerning wireless communication over a tactical internet. Different kinds of bulk data transfer protocols are being analyzed and evaluated. The protocol ETFTP has also been implemented by RFC 1986. The main purpose of this document is to use it as an up-to-date report within the area of using and developing commercial radio based internet technology in defense forces, mainly represented by CECOM (US Army Communications-Electronics Command). The document is part of the Swedish Defence Forces attempt to acquire knowledge about problems and possibilities with this technology.
NTIS
Data Transmission; Communication Equipment; Wireless Communication; Combat; Radio Communication; Radio Transmission

19990113151 National Inst. of Standards and Technology, Electronics and Electrical Engineering Lab., Boulder, CO USA
Metrology for Radio-Frequency Technology: A Bibliography of NIST Publications
Lyons, R. M.; Aug. 1999; 154p
Report No.(s): PB99-168213; NISTIR-5084; No Copyright; Avail: CASI; A08, Hardcopy; A02, Microfiche

This bibliography lists the publications by the staff of the Radio-Frequency Technology Division, formerly the Electromagnetic Fields Division, of the National Institute of Standards and Technology for the period January 1970 through July 1999. It supersedes NISTIR 5075, which listed the publications of the Electromagnetic Fields Division from January 1970 through July 1997. Selected earlier publications from the Division's predecessor organizations are included.
NTIS
Metrology; Radio Frequencies; Bibliographies

33
ELECTRONICS AND ELECTRICAL ENGINEERING

Includes test equipment and maintainability; components, e.g., tunnel diodes and transistors; microminiaturization; and integrated circuitry. For related information see also 60 Computer Operations and Hardware and 76 Solid-State Physics.

19990108799 Ljubljana Univ., Faculty of Electrical Engineering, Yugoslavia
On Determination of the Generator Share in a Selected Load ***Dolocanje Deleza Moci Generatorjev v Porabnikovem Odjemu***
Gubina, Ferdinand, Ljubljana Univ., Yugoslavia; Grgic, David, Ljubljana Univ., Yugoslavia; Electrotechnical Review; 1999; Volume 66, No. 2, pp. 120-124; In Slovene; See also 19990108795; No Copyright; Avail: CASI; A01, Hardcopy; A01, Microfiche

In the paper, a new approach to determination of the share of particular generator production in the loud demand is presented. The new method is based on power flow directions and can be utilized for both, active and reactive powers. It is exact, simple and easy to understand. Moreover, only a set of affected area data is needed for its calculation. Because of that, the share factors are named local generation distribution factors. The new method is based on a search algorithm. It searches for the power flow directions, thus matrix calculations are not required. Local generation distribution factors are calculated for lines connected to power source buses first. Power source buses are defined as buses where all injected powers to the connected lines are positive. A local generation distribution factor for line connected to a selected source bus equals 1 for the generation connected to this source bus and 0 for all other generators in the system following this scheme, local generation distribution factors for all other lines can he calculated. The calculation order is important since local generation distribution factors for all lines supplying a bus, which supplies a particular line of our interest, have to be determined beforehand. Let's say that bus i supplies a line of interest. If local generation distribution factors for all lines supplying bus i are known, then it can be calculated to what degree the bus i is supplied from any particular generator in the system. The results yield local generation distribution factors for all buses in the power system. They can be interpreted as a share of a particular generator in the load demand on this bus. The values of the local generation

distribution factors are always between zero and one. The main advantage of the new proposed method as compared to, other methods is that it can be used for both, active and reactive powers. The new algorithm offers low computing times and is suitable for parallel processing as well. The new tool has been tested on the Slovenian power system. The results show that, in general, the consumers are supplied from the nearest power plants and not necessarily from power plants where they buy electrical energy. With other words, the new tool confirms the fact that the power flows according to the physical rather than economic rules. This should be taken into account in operation of deregulated power systems since it indicates the source of monopoly in the power.system.
Author
Procedures; Loads (Forces); Electricity; Algorithms; Electric Generators

19990108800 Ljubljana Univ., Faculty of Electrical Engineering, Yugoslavia
Fault Identification in a Power System Element Based on Protective Relay Operation Signals ***Identifikacija Okvare Elementa Elektroenergetskega Sistems s Signali Delovanja Zascitnih Relejev***
Babnik , Tadeja, Ljubljana Univ., Yugoslavia; Gubina, Ferdinand, Ljubljana Univ., Yugoslavia; Electrotechnical Review; 1999; Volume 66, No. 2, pp. 125-130; In Slovene; See also 19990108795; No Copyright; Avail: CASI; A02, Hardcopy; A01, Microfiche

Disturbance in a power system generates a lot of data, which could be used to assess its nature and required response of the power system operator. The protection signals offer the possibility to identify the type ot fault, which could serve to assure an adequate power system control. For the purpose a simple method of fast identification of faults from the available protective relay signals has been developed. The new method is based on functional relations of different faults and corresponding protection relays operation. The procedure identifies faults by inversion of the basic signal-fault relation matrix of relay operation and faults. The procedure normalizes the results in order to be comparable to the probability evaluation. The method has been tested on different element protection configurations to show its efficacy. Typical results are presented in the paper.
Author
Fault Detection; Power Lines; Protection

19990108801 Maribor Univ., Faculty of Electrical Engineering, Maribor, Slovenia
New Conductors for Efficient Overhead Transmission Lines ***Novi Vodniki za Povecanje Ucinkovitosti Nadzemnih***
Jakl, Franc, Maribor Univ., Slovenia; Bakic, Kresimir, Milan Vidmar Electric Power Research Inst., Slovenia; Electrotechnical Review; 1999; Volume 66, No. 2, pp. 131-143; In Slovene; See also 19990108795; No Copyright; Avail: CASI; A03, Hardcopy; A01, Microfiche

The paper reviews the state-of-the-art in the area of conductions for overhead transmission lines designed with new materials enabling a more effective use of overhead transmission lines. Improved metallurgical and construction features allow for technical solutions qualifying the lines for higher specific transmission capabilities and operating temperatures, better aerodynamic performances, minimized rate of noise, decreased magnetic losses, etc. The Electric Supply Industry is nowadays under strong pressure exerted by the public, in particular the environmental advocators insisting on environment friendly technical solutions for overhead transmission lines in terms of minimisation of environmental impacts (electromagnetic fields, noise and visual harmonization with the environment) and spatial requirements. Obtaining permits for new overhead transmission line corridors is therefore quite uncertain and a lot of time consuming procedure. Consequently, in the overhead transmission line technique in the area of conductors and earth wire there is a strong tendency towards introducing such new materials and Construction designs that would assure a better use of the space as compared to former solutions. Conductors designed according to the most recent technologies, for instances ”black” and ”hot” conductors, allow for a considerably higher thermal stressing of overhead transmission lines at the investment cost that is not significantly higher than the one for classical conductors. Also, even at high thermal stressing invar core based conductors exhibit relatively small mechanical extensions as compared with classical conductors. Worthwhile to be mentioned is the GAP-type of such advanced conductors. In their coating they use a high temperature resistant alloy and have in their core a high quality invar wire whose transition point temperature is equal the ambient temperature what is considerably lower than the one of the classical type. The important contribution of these conductors are smaller sags throughout the overall temperature range as opposed to the classical conductor type. An intensive research has recently been investigate in the world aimed at a compacted design of conductors, the main advantage being, in particular, improved mechanical, electrical, thermal and aerodynamic properties. The round shaped smooth external surface of the new conductor type has a favourable effect on the air circulation in the conductor immediate vicinity reflecting itself in better coefficients (”Drag Coefficient”) of the aerodynamic wind effects. This in particular holds for instances of the high wind speed above 30 m/s. Other types of conductors that should also be mentioned are the Low-Wind-Pressure conductors, Low-Wind-Noise conductors, and Low-Magnetic Loss conductors. All these conductors which are designed according to the latest state-of-the-art achievements belong to the group of environment friendly designs. Also, owing to their improved aerodynamic features their

effect on mechanical stressing of steel constructions has been decreased and their noise level and energy losses have been minimised. These are properties that are being in particular highly appreciated in the construction of ultra high voltage lines of I000 kV and above.
Author
Conductors; Coating; Construction; Electrical Properties; Energy Dissipation; Heat Resistant Alloys; Nickel Alloys; Optimization; Transmission Lines; Wire

19990108802 Ljubljana Univ., Faculty of Electrical Engineering, Yugoslavia
Current reference Determination in Parallel Active Power Filters ***Ugotavljanje Tokovne Reference pri Paralelnih Aktivnih Mocnostnih Filtrih***
Nedeljkovic, David, Ljubljana Univ., Yugoslavia; Nastran, Janez, Ljubljana Univ., Yugoslavia; Electrotechnical Review; 1999; Volume 66, No. 2, pp. 144-152; In Slovene; See also 19990108795; No Copyright; Avail: CASI; A03, Hardcopy; A01, Microfiche

Pollution of the supply network by the reactive power has many undesired effects, especially harmonic distortion. The reactive power (the fundamental reactive power and/or the harmonic distortion) can be successfully reduced by a parallel active power filter. Currents, enforced into the filter branch, have to compensate reactive currents, required by the load. Consequently, line currents should be sinusoidal. Several methods for the filter current reference determination have been developed. The methods can be evaluated by many criteria. One of the most important ones is dynamics, i.e the response of the filter current reference to the load variation. An integrative method relies upon the load current active fundamental calculation, where the appropriate Fourier coefficient is updated once per cycle. Special efforts are required to avoid problems, resulting from synchronization to the network. A hybrid method is based on the analogue determination of the load current fundamental and phase shift measurement. Although simple to process, the method is very sensitive to disturbances, especially those due to synchronization. An improved integrative method calculates the corresponding Fourier coefficient continuously. Thus, synchronization problems are reduced and dynamics is improved. Methods which are based on the theory of instantaneous reactive power can be due to their nature applied only in three-phase systems. Minimizing the line currents, the reference has an immediate response, yet line reference currents are not necessarily sinusoidal. Applying low-pass filters, as shown in the Akagi's method, line currents become sinusoidal with no special synchronization. A controller method for the filter current reference determination is based on managing the flow of active power from the supply network by a controller. Its dynamics is acceptable, hut synchronization has to be performed. Dynamics of the presented methods is shown. The hybrid method has the slowest response, although it refreshes Fourier coefficient A twice a cycle. The reason for it is the very analogue filter. Pure minimization of line currents can generate non-sinusoidal line currents. It is important to observe the active power in the filter branch. The fact is that the active filter power has to cover only the losses in the filter branch as the filter capacitor voltage has to be controlled by correcting the active supply power. In practice, this control affects the line current reference and its dynamics.
Author
Capacitors; Controllers; Dynamic Response; Electric Potential; Line Current; Low Pass Filters; Synchronism

19990110296 Department of Energy, Office of Energy Research, Washington, DC USA
Pulse propagation in inhomogeneous optical waveguides ***Final Report, 15 Sep. 1992 - 14 Mar. 1996***
Menyuk, C. R., Department of Energy, USA; Aug. 17, 1998; 16p; In English
Report No.(s): DE99-000052; DOE/ER/14090-6; No Copyright; Avail: Department of Energy Information Bridge, Microfiche

Accomplishments include two Ph.D. dissertations, twenty-six archival journal publications that have appeared in print, six articles that have appeared in conference or summer school proceedings, sixteen regular conference presentations, and eleven invited conference presentations. A complete record of the publications and presentations may be found in Sec. II.E. The areas in which the author has been working--randomly varying optical fiber birefringence, passively modelocked lasers, and quasi-phase matched second harmonic generation--are all still of great current interest. Recent progress in soliton transmission has been nothing short of outstanding with the recent achievement of single channel 15 Gbit/sec, nearly error-free transmission over 35,000 km. At the same time, remarkable progress with the presently used NRZ (non-return- to-zero) transmission mode makes it less clear that solitons will ultimately be used. The author has contributed in important respects to all these areas. In long-distance transmission systems, the length scale on which the birefringence varies randomly (30--100 m) is short compared to the nonlinear and dispersive scale lengths (100--1,000 km). Consequently, it is crucial to understand and characterize this randomly varying birefringence when studying long-distance evolution in optical fibers. That has been done in a series of studies that has also led to the proposal of a numerical scheme for modeling these systems that should be orders of magnitude faster than the schemes presently being used. In the studies of the fiber ring and figure-8 lasers, the author proposed that nonlinear polarization rotation is the mechanism responsible for fast saturable absorption in the fiber ring lasers--a result that was later verified experimentally. He also explored a new approach to determining the conditions for modelocking and self-starting in these lasers

that uses the computer to determine the linear stability of both the pulsed and cw solutions. In all this work, the author has worked closely with leading experimentalists and their groups. Section 2 of this report describes in more detail some of the specific accomplishments.
NTIS
Waveguides; Wave Propagation; Optical Fibers; Optical Waveguides; Fiber Lasers; Conferences

19990110590 NASA Langley Research Center, Hampton, VA USA
Temperature Control of Avalanche Photodiode Using Thermoelectric Cooler
Refaat, Tamer F., Old Dominion Univ., USA; Luck, William S., Jr., NASA Langley Research Center, USA; DeYoung, Russell J., NASA Langley Research Center, USA; October 1999; 22p; In English
Contract(s)/Grant(s): RTOP 622-63-13-70
Report No.(s): NASA/TM-1999-209689; NAS 1.15:209689; L-17906; No Copyright; Avail: CASI; A03, Hardcopy; A01, Microfiche

Avalanche photodiodes (APDS) are quantum optical detectors that are used for visible and near infrared optical detection applications. Although APDs are compact, rugged, and have an internal gain mechanism that is suitable for low light intensity; their responsivity, and therefore their output, is strongly dependent on the device temperature. Thermoelectric coolers (TEC) offers a suitable solution to this problem. A TEC is a solid state cooling device, which can be controlled by changing its current. TECs are compact and rugged, and they can precisely control the temperature to within 0.1 C with more than a 150 C temperature gradient between its surfaces. In this Memorandum, a proportional integral (PI) temperature controller for APDs using a TEC is discussed. The controller is compact and can successfully cool the APD to almost 0 C in an ambient temperature environment of up to 27 C.
Author
Temperature Control; Avalanche Diodes; Photodiodes; Infrared Detectors; Solid State Devices

19990110668 New York Academy of Sciences, New York, NY USA
Getting from Then to Now: A Brief History of the Electric Vehicle
Wouk, Victor, Wouk (Victor) Associates, USA; Science, Technology, and the Economic Future; [1998], pp. 61-64; In English; ISBN 1-57331-147-2; Copyright; Avail: Issuing Activity, Hardcopy

Electric vehicles were among the first automotive innovations in the United Sates. In fact, they even came complete with flower pots to decorate the door posts! Ironically, the early electric vehicles were put out of business by an electric device--the electric starter. The automotive owner no longer needed a crank and a set of well-developed upper body muscles to start the engine. Voila! The automotive age.
Derived from text
Automobiles; Electric Motor Vehicles

19990110669 New York Academy of Sciences, New York, NY USA
Electric Vehicles and The Automotive Industry: The Implications of Emission Mandates
Stempel, Robert C., Energy Conversion Devices, Inc., USA; Science, Technology, and the Economic Future; [1998], pp. 55-60; In English; ISBN 1-57331-147-2; Copyright; Avail: Issuing Activity, Hardcopy

Battery-powered electric vehicles will become a key part of the nation's transportation system. Electric vehicles are quiet, fun to drive, pollution free, convenient, and require little or no maintenance. But the reason that electric vehicles are now emerging as a potential force in the automotive marketplace is not due to automotive innovation, but rather to technological innovation in the electronic and information systems industries.
Derived from text
Electric Batteries; Energy Storage; Transportation; Electric Automobiles

19990110708 New York Academy of Sciences, New York, NY USA
Electric Vehicles: Opportunity or Problem?
Bell, Robert A., Consolidated Edison Co. of New York, Inc., USA; Science, Technology, and the Economic Future; [1998], pp. 49-54; In English; ISBN 1-57331-147-2; Copyright; Avail: Issuing Activity, Hardcopy

Nothing is ever simple. Innovations often present both opportunities for change and improvement and problems for existing relationships and societal priorities. Electric vehicles, and the various means for encouraging their use, are no exception.
Derived from text
Electric Motor Vehicles; Research Vehicles; Roadway Powered Vehicles; Test Vehicles

19990111463 Howard Univ., Electrical Engineering Dept., Washington, DC USA

Experimental Evaluation of Motor Drive Technologies for Future Aerospace Applications

Rubaai, Ahmed, Howard Univ., USA; Ricketts, Daniel, Howard Univ., USA; HBCUs/OMUs Research Conference Agenda and Abstracts; August 1999, pp. 16; In English; See also 19990111455; No Copyright; Avail: Issuing Activity, Hardcopy; Abstract Only

This study presents the design and experiment of a hybrid fuzzy control scheme for a high performance brushless dc drive system. Both the designs of the fuzzy controller and its integration with the proportional-integral (PI) in a global control scheme are discussed. The principle of the proposed control scheme is that to use a PI controller, which performs satisfactory in most cases, while keeping in the background a fuzzy controller, which, is ready to take over the PI controller when severe perturbations occur. Performance of the hybrid fuzzy-PI controller is evaluated through a laboratory implementation. The laboratory implementation is based on a linguistic fuzzy controller whose design is derived from the expert knowledge during disturbed phases. Experimental results have shown excellent tracking performance of the hybrid control system, and have convincingly demonstrated the usefulness of the hybrid fuzzy controller in high performance drives with uncertainties. The proposed controller is designed and implemented in the laboratory and its effectiveness in tracking application is verified. The entire system is built and tested in the laboratory by using off-the-shelf components and software. The research study also discusses both the designs of the fuzzy controller and its integration with the PI in global control system. Results from online implementation are presented.
Author

Aerospace Engineering; Controllers; Fuzzy Systems; Automatic Control

19990111480 NASA Glenn Research Center, Cleveland, OH USA

Copper-Based OHMIC Contracts for the Si/SiGe Heterojunction Bipolar Transistor Structure

Das, Kalyan, Tuskegee Inst., USA; Hall, Harvey, Tuskegee Inst., USA; HBCUs/OMUs Research Conference Agenda and Abstracts; August 1999, pp. 34; In English; See also 19990111455; No Copyright; Avail: Issuing Activity, Hardcopy; Abstract Only

Silicon based heterojunction bipolar transistors (HBT) with SiGe base are potentially important devices for high-speed and high-frequency microelectronics. These devices are particularly attractive as they can be fabricated using standard Si processing technology. However, in order to realize the full potential of devices fabricated in this material system, it is essential to be able to form low resistance ohmic contacts using low thermal budget process steps and have full compatibility with VLSI/ULSI processing. Therefore, a study was conducted in order to better understand the contact formation and to develop optimized low resistance contacts to layers with doping densities corresponding to the p-type SiGe base and n-type Si emitter regions of the HBTS. These as-grown doped layers were implanted with BF(sub 2) up to 1 X 10(exp 16)/CM(exp 2) and As up to 5 x 10(exp 15)/CM2, both at 30 keV for the p-type SiGe base and n-type Si emitter layers, respectively, in order to produce a low sheet resistance surface layer. Standard transfer length method (TLM) contact pads on both p and n type layers were deposited using an e-beam evaporated trilayer structure of Ti/CufTi/Al (25)A/1500A/250A/1000A). The TLM pads were delineated by a photoresist lift-off procedure. These contacts in the as-deposited state were ohmic, with specific contact resistances for the highest implant doses of the order of 10(exp -7) ohm-CM2 and lower.
Author

Bipolar Transistors; Doped Crystals; Fabrication; Heterojunction Devices; Heterojunctions; Microelectronics; Silicon Transistors; Copper

19990113090 NASA Goddard Space Flight Center, Greenbelt, MD USA

Logic Design Pathology and Space Flight Electronics

Katz, Richard B., NASA Goddard Space Flight Center, USA; Barto, Rod L., Spacecraft Digital Electronics, USA; Erickson, Ken, Jet Propulsion Lab., California Inst. of Tech., USA; 1999; 77p; In English; MAPLD '99, 1999, USA; No Copyright; Avail: CASI; A05, Hardcopy; A01, Microfiche

This paper presents a look at logic design from early in the US Space Program and examines faults in recent logic designs. Most examples are based on flight hardware failures and analysis of new tools and techniques. The paper is presented in viewgraph form.
Derived from text

Systems Analysis; Space Programs; System Failures; Logic Design; Spacecraft Electronic Equipment

34
FLUID MECHANICS AND HEAT TRANSFER

Includes boundary layers; hydrodynamics; fluidics; mass transfer; and ablation cooling. For related information see also 02 Aerodynamics and 77 Thermodynamics and Statistical Physics.

19990106575 NASA Marshall Space Flight Center, Huntsville, AL USA
Optimization of a GO2/GH2 Impinging Injector Element
Tucker, P. Kevin, NASA Marshall Space Flight Center, USA; Shyy, Wei, Florida Univ., USA; Vaidyanathan, Rajkumar, Florida Univ., USA; [1999]; 1p; In English; Thermal and Fluids Analysis Workshop, 13-17 Sep. 1999, Huntsville, AL, USA; No Copyright; Avail: Issuing Activity, Hardcopy; Abstract Only

An existing injector optimization methodology, method i, is used to investigate optimal design points for a GO2/GH2 impinging injector element. The impinging element, an F-O-F triplet, is optimized in terms of such relevant design variables as fuel pressure drop, DELTA-P(sub f), oxidizer pressure drop, DELTA-P(sub o), combustor length, L(sub comb), and impingement angle, alpha, for a given mixture ratio and chamber pressure.
Derived from text
Optimization; Impingement; Injectors

19990106609 Kyushu Univ., Graduate School of Engineering, Fukuoka, Japan
PIV Measurements of Subsonic Flows Around Biconvex Blade and Cylinder
Toshimitsu, Kazu, Kyushu Univ., Japan; Ogawa, Tetsuaki, Kyushu Univ., Japan; Yamasaki, Nobuhiko, Kyushu Univ., Japan; Namba, Masanobu, Kyushu Univ., Japan; Technology Reports of Kyushu University; July 1999; ISSN 0023-2718; Volume 72, No. 4, pp. 377-383; In Japanese; No Copyright; Avail: CASI; A02, Hardcopy; A01, Microfiche

This paper presents the quantitative comparison of particle image velocimetry (PIV) measurements and finite element method (FEM) analyses of the steady flow around a biconvex blade with 20% thickness, and the qualitative PIV flow visualization of the strong turbulent flows around a cylinder at Reynolds number 1.0 x 10(exp 5). In the former comparison, the maximum velocity of PIV is 6.5% smaller than that of the numerical calculation of the inviscid FEM. This difference is caused by the effect of boundary layers along the blade surfaces from mid-chord to trailing edge. In the latter case, we can qualitatively observe Karman vortices and its vorticities in the wake region by means of a combined seeding equipment. As the results, the PIV system is useful for us to measure the steady flow velocities and observe the unsteady flow.
Author
Particle Image Velocimetry; Subsonic Flow; Convexity; Finite Element Method; Cylindrical Bodies; Turbine Blades

19990107325 Kyushu Univ., Graduate School of Engineering, Fukuoka, Japan
Critical Heat Flux for Binary Mixtures at High Pressures in Tubes
Ohno, Masaki, Kyushu Univ., Japan; Mori, Hideo, Kyushu Univ., Japan; Yoshida, Suguru, Kyushu Univ., Japan; Technology Reports of Kyushu University; July 1999; ISSN 0023-2718; Volume 72, No. 4, pp. 369-375; In Japanese; No Copyright; Avail: CASI; A02, Hardcopy; A01, Microfiche

Experimental data were obtained on critical heat flux for boiling nonazeotropic binary mixtures of HCFC-22/CFC-114 and HFC-32/HFC-134a flowing upward in a vertical tube and HFC-32/HFC-134a flowing in a horizontal tube at high subcritical pressures. When vapor-liquid density ratio was constant, the critical heat flux of the mixtures changed linearly with the mole fraction of the component, and the critical boiling number remained almost constant independently of the component mole fraction. The mixtures showed no peculiar difference from pure fluids in the characteristic of the critical heat flux. The critical heat fluxes for the mixtures could be predicted from the correlations valid for pure fluids by using the properties of the mixture for both vertical and horizontal tubes.
Author
Heat Flux; Binary Mixtures; High Pressure

19990108479 Institute for Computer Applications in Science and Engineering, Hampton, VA USA
Towards Understanding the Mechanism of Receptivity and Bypass Dynamics in Laminar Boundary Layers ***Final Report***
Lasseigne, D. G., Institute for Computer Applications in Science and Engineering, USA; Criminale, W. O., Institute for Computer Applications in Science and Engineering, USA; Joslin, R. D., NASA Langley Research Center, USA; Jackson, T. L., Institute for Computer Applications in Science and Engineering, USA; September 1999; 32p; In English
Contract(s)/Grant(s): NAS1-97046; RTOP 505-90-52-01

Report No.(s): NASA/CR-1999-209553; NAS 1.26:209553; ICASE-99-37; No Copyright; Avail: CASI; A03, Hardcopy; A01, Microfiche

Three problems concerning laminar-turbulent transition are addressed by solving a series of initial value problems. The first problem is the calculation of resonance within the continuous spectrum of the Blasius boundary layer. The second is calculation of the growth of Tollmien-Schlichting waves that are a direct result of disturbances that only lie outside of the boundary layer. And, the third problem is the calculation of non-parallel effects. Together, these problems represent a unified approach to the study of freestream disturbance effects that could lead to transition. Solutions to the temporal, initial-value problem with an inhomogeneous forcing term imposed upon the flow is sought. By solving a series of problems, it is shown that: A transient disturbance lying completely outside of the boundary layer can lead to the growth of an unstable Tollmien-Schlichting wave. A resonance with the continuous spectrum leads to strong amplification that may provide a mechanism for bypass transition once nonlinear effects are considered. A disturbance with a very weak unstable Tollmien-Schlichting wave can lead to a much stronger Tollmien-Schlichting wave downstream, if the original disturbance has a significant portion of its energy in the continuum modes. Author

Boundary Layer Transition; Laminar Boundary Layer; Turbulent Boundary Layer; Blasius Flow; Turbulent Flow; Tollmien-Schlichting Waves

19990109088 NASA Marshall Space Flight Center, Huntsville, AL USA

The Influence of Static and Rotating Magnetic Fields on Heat and Mass Transfer in Silicon Floating Zones

Croell, Arne, NASA Marshall Space Flight Center, USA; Dold, P., NASA Marshall Space Flight Center, USA; Kaiser, Th., NASA Marshall Space Flight Center, USA; Szofran, Frank, NASA Marshall Space Flight Center, USA; Benz, K. W., NASA Marshall Space Flight Center, USA; [1999]; 1p; In English

Contract(s)/Grant(s): NCC8-66; No Copyright; Avail: Issuing Activity, Hardcopy; Abstract Only

Hear and mass transfer in float-zone processing are strongly influenced by convective flows in the zone. They are caused by buoyancy convection, thermocapillary (Marangoni) convection, or artificial sources such as rotation and radio frequency heating. Flows in conducting melts can be controlled by the use of magnetic fields, either by damping fluid motion with static fields or by generating a def@ned flow with rotating fields. The possibilities of using static and rotating magnetic fields in silicon floating-zone growth have been investigated by experiments in axial static fields up to ST and in transverse rotating magnetic fields up to 7.S mT. Static fields of a few 100 MT already suppress most striations but are detrimental to the radial segregation by introducing a coring effect. A complete suppression of dopant striations caused by time-dependent thermocapillary convection and a reduction of the coring to insignificant values, combined with a shift of the axial segregation profile towards a more diffusion-limited case, is possible with static fields ? 1T. However, under certain conditions the use of high axial magnetic fields can lead to the appearance of a new type of pronounced dopant striations, caused by thermoelec:romagnetic convection. The use of a transverse rotating magnetic field influences the microscopic segregation at quite low inductions, of the order of a few mT. The field shifts time-dependent flows and the resulting striation patterns from a broad range of low frequencies at high amplitudes to a few high frequencies at low amplitudes

Author

Magnetic Fields; Heat Transfer; Mass Transfer; Float Zones; Convective Flow

19990109146 NASA Ames Research Center, Moffett Field, CA USA

Evaporative Cooling Membrane Device

Lomax, Curtis, Inventor, NASA Ames Research Center, USA; Moskito, John, Inventor, NASA Ames Research Center, USA; Sep. 07, 1999; In English

Patent Info.: Filed 25 Feb. 1998; NASA-Case-ARC-14176-1-LE; US-Patent-5,946,931; US-Patent-Appl-SN-030101; No Copyright; Avail: US Patent and Trademark Office, Hardcopy

An evaporative cooling membrane device is disclosed having a flat or pleated plate housing with an enclosed bottom and an exposed top that is covered with at least one sheet of hydrophobic porous material having a thin thickness so as to serve as a membrane. The hydrophobic porous material has pores with predetermined dimensions so as to resist any fluid in its liquid state from passing therethrough but to allow passage of the fluid in its vapor state, thereby, causing the evaporation of the fluid and the cooling of the remaining fluid. The fluid has a predetermined flow rate. The evaporative cooling membrane device has a channel which is sized in cooperation with the predetermined flow rate of the fluid so as to produce laminar flow therein. The evaporative cooling membrane device provides for the convenient control of the evaporation rates of the circulating fluid by adjusting the flow rates of the laminar flowing fluid.

Author

Evaporative Cooling; Membranes

19990110569 National Aerospace Lab., Tokyo, Japan

Drop Behavior in Acoustic Standing Waves

Kamimura, H., National Aerospace Lab., Japan; Yamanaka, T., National Aerospace Lab., Japan; October 1997; 28p; In Japanese
Report No.(s): PB99--127706; NAL-TR-1337; Copyright Waived; Avail: Issuing Activity (Natl Technical Information Service (NTIS)), Microfiche

In this report, an equation for multi-lobed waves is shown. The wave equation is first derived on the assumption that the acoustic radiation pressure around a drop is constant. Then the effects of the deformed drop on the radiation pressure surrounding the drop are considered. In addition, the equation for the relationship between the radiation pressure and a drop that becomes oblate due to the radiation pressure is obtained. The two equations are compared with the results of both ground experience and flight experience and it is shown that good agreement exists between the theoretical prediction and the experimental results.
NTIS

Standing Waves; Radiation Pressure; Pressure Drop; Sound Waves

19990110591 Department of Energy, Office of Energy Research, Washington, DC USA

Thermal radiation and conduction in microscale structures ***Final Report***

Tien, C. L., Department of Energy, USA; Sep. 02, 1998; 11p; In English
Report No.(s): DE99-001095; DOE/ER/14287-T3; No Copyright; Avail: Department of Energy Information Bridge, Microfiche

The general objective of the current research program is to achieve a better understanding of the fundamental mechanisms of thermal radiation and heat conduction in microscale structures commonly encountered in engineering applications. Specifically, the program includes both experimental and analytical investigations of radiative heat transfer in microstructures, conductive heat transfer in micro devices, and short-pulse laser material interactions. Future work is planned to apply the knowledge of microscale heat transfer gained in this project to developing thermal insulating aerogel materials, thermal design schemes for quantum well lasers, and short-pulse laser micro-fabrication techniques. A listing of publications by Chang-Lin Tien is included.
NTIS

Thermal Radiation; Conductive Heat Transfer; Quantum Well Lasers; Microstructure; Laser Materials

19990110617 McDonnell-Douglas Aerospace, Saint Louis, MO USA

Techniques for Mixing Enhancements in Supersonic Shear Layers

Kibens, V., McDonnell-Douglas Aerospace, USA; Joshi, M. C., McDonnell-Douglas Aerospace, USA; Parekh, D. E., McDonnell-Douglas Aerospace, USA; Glezer, A., Georgia Inst. of Tech., USA; Krothapalli, A., Florida State Univ., USA; Rogers, C. B., Tufts Univ., USA; First NASA/Industry High Speed Research Program Nozzle Symposium; September 1999, pp. 12-1 - 12-12; In English; See also 19990110605; No Copyright; Avail: CASI; A03, Hardcopy; A10, Microfiche

The flow exited from a rectangular, converging-diverging nozzle, with a design Mach number M = 1.47, an exit aspect ratio of 2:1, and the longer dimension equal to 33.8 mm. The nozzle flow exited onto a curved surface bounded by transparent side walls made of Plexiglas. The channel turned the flow by 90 degrees. The wall curvature started at the nozzle exit, and consisted of a section of circular arc, followed by a straight section of length equal to one radius of turning curvature. The straight section was added to avoid major channel termination effects. Four curved channels were tested, with radii R 10.2, 15.2, 20.32, and 30.5cm. The test apparatus also included a straight channel with no curvature, and unconstrained wall jets on a flat and curved plate. The primary conclusion from this work is that curved shear layers generated at supersonic pressure ratios exhibit vigorous LSS development, which denotes increased mixing of the supersonic and subsonic streams. This effect contrasts with supersonic flow in a straight channel, for which no LSS development occurs.Wedge-shaped actuator elements made of high strength aluminum alloy were driven at a 5 kHz resonance frequency by attached piezoelectric wafers.The mixing data indicates that the streamwise vortices improve both large-scale and small-scale mixing. The acoustic results show that streamwise vortices are effective at reducing the overall sound pressure level for polar angle less than 60 deg but increase noise slightly at angles around 90 deg.
Derived from text

Supersonic Flow; Shear Layers; Actuators; Aspect Ratio; Piezoelectricity; Polymethyl Methacrylate; Pressure Ratio; Sound Pressure; Technology Assessment; Multiphase Flow

19990111468 City Coll. of the City Univ. of New York, Dept. of Mechanical Engineering, NY USA

High Resolution Experiments of Compressible Turbulence Interacting with Shock Waves

Andreopoulos, Yiannis, City Coll. of the City Univ. of New York, USA; Agui, Juan, City Coll. of the City Univ. of New York, USA; HBCUs/OMUs Research Conference Agenda and Abstracts; August 1999, pp. 21; In English; See also 19990111455; No Copyright; Avail: Issuing Activity, Hardcopy; Abstract Only

The interaction of turbulent jet with a traveling shock wave has been investigated experimentally in a high resolution large scale shock tube facility. A jet facility has been designed and tested which can supply a flow with a Mach number of 0.9 through a 7.0 mm internal diameter tube exhausting along the center line of the shock tube. Two test flow configurations have been used in these experiments. In the first one, the jet was flowing in the same direction as the traveling shock wave. In the second configuration, the shock was traveling in the opposite direction to that of the jet. Helium, air and Krypton gases were used in the jet flows in an effort to generate barocilnic vorticity through a nonalignment of density and pressure gradients. Extensive flow visualization studies were carried out by using a pulsed planar laser sheet generated by a ND:YAG laser. The captured images show that the interaction is very complex. A stenosis of the jet has been observed to take place in the near field as a result of the sudden. imposition of the pressure behind the shock which is followed by a "wake like" vortex. The field far from the jet exit is characterized by increased turbulence activities. Substantial more mixing has been observed in the case of a Helium jet than in the case of a Krypton jet, as a result of the difference in the generation of additional baroclinic vorticity.
Author
Flow Visualization; Fluid Flow; Transonic Speed; Turbulent Jets; Vorticity

19990111469 City Coll. of the City Univ. of New York, Dept. of Chemical Engineering, NY USA
Surfactant Facilitated Spreading of Aqueous Drops of Hydrophobic Surfaces
Kumar, Nitin, City Coll. of the City Univ. of New York, USA; Couzis, Alex, City Coll. of the City Univ. of New York, USA; Maldarelli, Charles, City Coll. of the City Univ. of New York, USA; HBCUs/OMUs Research Conference Agenda and Abstracts; August 1999, pp. 22; In English; See also 19990111455; No Copyright; Avail: Issuing Activity, Hardcopy; Abstract Only

An aqueous phase does not wet a hydrophobic surface. When an aqueous drop is placed on such a surface, the liquid subtends a large contact angle with the solid. The capillary force derived from the large angle either prevents the drop from moving, or causes it to move very slowly before coming to rest. In either case, the wetted area at equilibrium is minimal. Existing or potential microgravity technologies such as contact film cooling, mold filling and coating processes often require aqueous phases to spread in a rapid and complete manner over solid surfaces. These surfaces are usually hydrophilic so that they are readily wet by water. However, in the normal course of operation, contaminant hydrophobic can be deposited patchwise on the surface. Surfactants facilitate the wetting of water on hydrophobic surfaces by adsorbing on the water/air and hydrophobic solid/water interfaces and lowering the surface tensions of these interfaces. The tension reductions decrease the contact angle, which increases the rate of spreading and the equilibrium wetted area. Hydrocarbon surfactants (i.e. amphiphiles with a hydrophobic moiety consisting of an extended string of methylene-CH 2-groups attached to a polar group) are capable of reducing the contact angles on surfaces which are not very hydrophobic, but do not reduce significantly the contact angles of the very hydrophobic surfaces such as parafilm polyethylene or self assembled monolayers.Trisiloxane surfactants (amphiphiles with a compact hydrophobe consisting of methyl groups linked to a trisiloxane backbone (((CH3)3)Si-O-Si-O-Si(CH3)3) and an extended ethoxylate (-(OCH2CH 2)n-) polar group with seven or eight units can significantly reduce the contact angle of water on a very hydrophobic surface and cause rapid and complete (or nearly complete) spreading. The overall goal of the research described in this proposal is to develop and verify a theory for how trisiloxanes cause superspreading, and then use this knowledge as a guide to developing more general hydrocarbon based surfactant systems which superspread. In this presentation, we will present the results of our infrared spectroscopy study on the adsorption of surfactants at a model hydrophobic surface fabricated by the self assembly of octadecyl trichlorosilane (OTS) at the oxidized silicon surface. Fourier Transform Infrared spectroscopy in attenuated total reflection mode (FTIR/ATR) allows us to follow the structure of water at the hydrophobic solid/water interface by monitoring the molecular vibration assigned to the 0-H stretching modes. As the hydrogen bonding structure of the water at the interface changes, the band shape and intensity changes. We contrast the adsorption of a superspreading trisiloxane and a polyethoxylated surfactant which does not superspread. We find a significant decrease in the intensity of the 0-H stretching band in the case of the trisiloxane as it adsorbs indicating a restructuring of interfacial water, while no such change is observed for the ethoxylate. The restructuring of the water may indicate that the hydrophobic groups of the trisiloxanes are forming a hydrophobic domain adjacent to the OTS layer. As this rearrangement removes the hydrophobic groups from water, it is of low energy and may account for the significant reduction in the solid/liquid tension which underlies superspreading. In the case of the ethoxylate, the absence of water restructuring may indicate that their hydrophobic
Author
Surfactants; Water; Wetting; Moisture Resistance; Silicon Compounds; Siloxanes; Polysiloxanes; Spreading

19990111476 Tennessee State Univ., Dept. of Mechanical Engineering, Nashville, TN USA
Three-Dimensional Numerical Simulation of Convective Melting of Solid Particles in a Fluid
Hao, Y. L., Tennessee State Univ., USA; Tao, Yong, X., Tennessee State Univ., USA; HBCUs/OMUs Research Conference

Agenda and Abstracts; August 1999, pp. 30; In English; See also 19990111455; No Copyright; Avail: Issuing Activity, Hardcopy; Abstract Only

The understanding of the phase-change characteristics for two-phase flows is important for the safety of space applications and the need for an increased number of applications in material processing. When a medium consists of packed or dispersed particles melt in a flowing fluid, at least three distinctive features arise: (1) Particles experience a full range of size variation due to phase change and collision; i.e., from initially large size to eventually diminishing within the melting zone; (2) there is momentum exchange between particles and fluid due to slip velocity and particle collision; (3) heat transfer from fluid to particles and is strongly influenced by flow characteristics, specific interfacial areas. The coupled heat, mass and momentum transfer mechanism during convective melting is further complicated due to the presence of the Earth gravity field. The density difference between fluid and particles causes the melting particles either to float to the fluid surface or settle down to the bottom of the fluid field. The resulted individual particle motion is then interacting with that from adjacent particles through collision. This makes prediction of melting rate under nonthermal equilibrium conditions very complex. Possible experiments under microgravity may give a way to study such complex phenomena by eliminating gravity related effects. to be able to perform such a task, it is important to identify the main governing parameters for complete description of convective melting processes. A physical model of two-phase flow and heat-mass transfer with the phase changes based on the theory of interacting continua is proposed. This model is proposed to simplify some aspects of the phenomena as mentioned above for a general three-dimensional application. All terms in the conservation equations are analyzed, and the constitutive equations are presented. A closed set of governing equations describing the convective melting of solid particles in a fluid is obtained. The generalized numerical method is developed for the solution of this kind set of governing equations for a three-dimensional melting case. In this case the medium consists of packed or dispersed particles that are melting in a flowing fluid. Preliminary calculation shows that the result is reasonable.
Author

Gravitation; Heat Transfer; Melting; Particle Collisions; Three Dimensional Models; Two Phase Flow; Mathematical Models; Convection

19990111482 Tuskegee Inst., Mechanical Engineering Dept., AL USA

Characterization of Flow Behind the Fan of a Turbofan Engine

Sree, Dave, Tuskegee Inst., USA; HBCUs/OMUs Research Conference Agenda and Abstracts; August 1999, pp. 36; In English; See also 19990111455; No Copyright; Avail: Issuing Activity, Hardcopy; Abstract Only

The research grant was awarded to perform analysis of experimental data obtained from hot-wire measurements behind the fan of turbofan engine models. The experiments of were conducted at NASA Glenn Research Center. FORTRAN codes have been developed to analyze the data for flow characterization. Results obtained from the data analysis include estimates of mean and turbulent velocities, correlation and spectral functions, and turbulence scales at various locations downstream of the fan. Codes have also been developed to obtain wave number-frequency spectra from two-point measurement data from which estimates of integral scales as a function of frequency can be obtained. The codes have been tested against some known results and they are found to be satisfactory. The results obtained from the data analysis codes will be helpful for determining the turbulence characteristics of the flow and for understanding how the fan wake flow contributes to the broad band noise produced by the engines. The results might also give insights into how the fan blades and/or stator vanes can be redesigned to reduce engine noise. Furthermore, the results obtained from data analysis of the experimental data can provide valuable input to validate the computer codes developed to predict the flow field and hence the noise produced by the engine models.
Author

Flow Distribution; Noise Reduction; Turbofan Engines; Turbulence; Turbofans

19990111515 Electric Power Research Inst., Palo Alto, CA USA

Fluid-damping-controlled instability of tubes in crossflow

Chen, S. S., Electric Power Research Inst., USA; Cai, Y., Electric Power Research Inst., USA; Ikantiah, G. S., Electric Power Research Inst., USA; Nov. 30, 1997; 61p; In English; International Mechanical Engineering Congress and Expo, USA; Sponsored by Department of Energy, USA

Report No.(s): DE97-008664; ANL/ET/CP-92179; No Copyright; Avail: Department of Energy Information Bridge, Microfiche

A mathematical model for fluid damping controlled instability of tubes presented in this paper is based on the unsteady flow theory. Motion dependent fluid forces are measured in a water channel. From the measured fluid forces, fluid stiffness and fluid damping coefficients, are calculated as a function of reduced flow velocity, oscillation amplitude, and Reynolds number. Once these coefficients are known, the mathematical model can be applied to predict structural instability due to fluid damping. Many cases are considered: single tube, twin tubes, tube row, triangular array, and square arrays. The results show the instability regions

based on the fluid damping coefficients and provide the answers to a series of questions on fluid elastic instability of tube arrays in crossflow.
NTIS
Cross Flow; Mathematical Models; Fluid-Solid Interactions; Flow Theory; Unsteady Flow; Damping

19990111593 Louisiana State Univ., Mechanical Engineering Dept., Baton Rouge, LA USA
Large Eddy Simulations and Turbulence Modeling for Film Cooling ***Final Report, 1994-1997***
Acharya, Sumanta, Louisiana State Univ., USA; September 1999; 138p; In English; Original contains color illustrations
Contract(s)/Grant(s): NAG3-1641; RTOP 538-12-10
Report No.(s): NASA/CR-1999-209310; NAS 1.26:209310; E-11859; No Copyright; Avail: CASI; A07, Hardcopy; A02, Microfiche

The objective of the research is to perform Direct Numerical Simulations (DNS) and Large Eddy Simulations (LES) for film cooling process, and to evaluate and improve advanced forms of the two equation turbulence models for turbine blade surface flow analysis. The DNS/LES were used to resolve the large eddies within the flow field near the coolant jet location. The work involved code development and applications of the codes developed to the film cooling problems. Five different codes were developed and utilized to perform this research. This report presented a summary of the development of the codes and their applications to analyze the turbulence properties at locations near coolant injection holes.
Author
Large Eddy Simulation; Turbulence Models; Film Cooling; Research; Mathematical Models

19990111706 Southampton Univ., Fluid Dynamics and Acoustics Group, UK
Gradient Projection Methods for Boundary Layer Transition Control
Tutty, O. R., Southampton Univ., UK; Hackenberg, P., Southampton Univ., UK; Nelson, P. A., Southampton Univ., UK; August 1999; 32p; In English
Report No.(s): ISVR-TR-284; Copyright; Avail: Issuing Activity, Hardcopy

In recent years there has been increasing interest in the control of boundary-layer transition through the use of surface suction. Here the use is considered of multiple suction panels to delay transition for cases with or without a pressure gradient imposed by the external inviscid flow. The aim is to maintain transition at a desired location with minimum cost, defined as the sum of squares of the individual suction flow rates, through an automatic adaptive feedback control loop which regulates the suction flow rates by solving a constrained optimisation problem. Numerically, two-dimensional boundary layer flow was calculated using an interactive formulation and linear stability theory was used to calculate the spatial growth rates of Tollmen-Schlichting waves, with the location of transition predicted via the e(sup N) method. The optimisation strategy was then used to update the suction flow rates. It was found that when the problem is well specified, i.e. an appropriate transition position is used, the method quickly converges. However, for at least, one case it was found that there no single optimum solution within the numerical tolerance of the method. Further, for a different problem, there are regions between the maximum and minimum transition position which are not accessible, and other positions for which a solution exist but to which the solution algorithm cannot converge as they occur at a discontinuity in the relationship between the transition position and the suction flow rates. Such difficulties could also occur in other suction optimisation formulations, and when using different solution algorithms.
Author
Boundary Layer Transition; Two Dimensional Boundary Layer; Algorithms; Automatic Control; Flow Velocity

19990111736 NASA Langley Research Center, Hampton, VA USA
Numerical Analysis of Convection/Transpiration Cooling
Glass, David E., NASA Langley Research Center, USA; Dilley, Arthur D., NYMA, Inc., USA; Kelly, H. Neale, Analytical Services and Materials, Inc., USA; 1999; 10p; In English; 9th; 3rd; Space Planes and Hypersonic Systems and Technologies, 1-5 Nov. 1999, Norfolk, VA, Norfolk, VA, USA, USA
Contract(s)/Grant(s): F33657-93C-2227
Report No.(s): AIAA Papers 99-4911; Copyright Waived; Avail: CASI; A02, Hardcopy; A01, Microfiche

An innovative concept utilizing the natural porosity of refractory-composite materials and hydrogen coolant to provide CONvective and TRANspiration (CONTRAN) cooling and oxidation protection has been numerically studied for surfaces exposed to a high heat flux, high temperature environment such as hypersonic vehicle engine combustor walls. A boundary layer code and a porous media finite difference code were utilized to analyze the effect of convection and transpiration cooling on surface heat flux and temperature. The boundary layer code determined that transpiration flow is able to provide blocking of the surface heat flux only if it is above a minimum level due to heat addition from combustion of the hydrogen transpirant. The porous

media analysis indicated that cooling of the surface is attained with coolant flow rates that are in the same range as those required for blocking, indicating that a coupled analysis would be beneficial.
Author
Numerical Analysis; Convection; Convective Heat Transfer; Sweat Cooling

19990111738 NASA Marshall Space Flight Center, Huntsville, AL USA
The Geophysical Fluid Flow Cell Experiment
Hart, J. E., Colorado Univ., USA; Ohlsen, D., Colorado Univ., USA; Kittleman, S., Colorado Univ., USA; Borhani, N., Colorado Univ., USA; Leslie, F., NASA Marshall Space Flight Center, USA; Miller, T., NASA Marshall Space Flight Center, USA; September 1999; 112p; In English; Original contains color illustrations
Contract(s)/Grant(s): NAS8-31958
Report No.(s): NASA/TP-1999-209576; M-938; NAS 1.60:209576; No Copyright; Avail: CASI; A06, Hardcopy; A02, Microfiche

The Geophysical Fluid Flow Cell (GFFC) experiment performed visualizations of thermal convection in a rotating differentially heated spherical shell of fluid. In these experiments dielectric polarization forces are used to generate a radially directed buoyancy force. This enables the laboratory simulation of a number of geophysically and astrophysically important situations in which sphericity and rotation both impose strong constraints on global scale fluid motions. During USML-2 a large set of experiments with spherically symmetric heating were carried out. These enabled the determination of critical points for the transition to various forms of nonaxisymmetric convection and, for highly turbulent flows, the transition latitudes separating the different modes of motion. This paper presents a first analysis of these experiments as well as data on the general performance of the instrument during the USML-2 flight.
Author
Free Convection; Fluid Flow; Turbulent Flow; Experimentation

35
INSTRUMENTATION AND PHOTOGRAPHY

Includes remote sensors; measuring instruments and gages; detectors; cameras and photographic supplies; and holography. For aerial photography see 43 Earth Resources and Remote Sensing. For related information see also 06 Aircraft Instrumentation, and 19 Space Instrumentation.

19990106558 NASA Langley Research Center, Hampton, VA USA
Cryogenic High Pressure Sensor Module
Chapman, John J., Inventor, NASA Langley Research Center, USA; Shams, Qamar A., Inventor, NASA Langley Research Center, USA; Powers, William T., Inventor, NASA Langley Research Center, USA; Sep. 21, 1999; In English; Division of US-Patent-Appl-SN-778065, filed 10 Dec. 1996 which is a continuation of US-Patent-Appl-SN-681245, filed 22 Jul. 1996
Patent Info.: Filed 18 Dec. 1997; NASA-Case-LAR-15280-3-SB; US-Patent-5,955,678; US-Patent-Appl-SN-992972; US-Patent-Appl-SN-778065; US-Patent-Appl-SN-681245; No Copyright; Avail: US Patent and Trademark Office, Hardcopy

A pressure sensor is provided for cryogenic, high pressure applications. A highly doped silicon piezoresistive pressure sensor is bonded to a silicon substrate in an absolute pressure sensing configuration. The absolute pressure sensor is bonded to an aluminum nitride substrate. Aluminum nitride has appropriate coefficient of thermal expansion for use with highly doped silicon at cryogenic temperatures. A group of sensors, either two sensors on two substrates or four sensors on a single substrate are packaged in a pressure vessel.
Official Gazette of the U.S. Patent and Trademark Office
Pressure Sensors; Cryogenic Temperature; Pressure Vessels; Aluminum Nitrides

19990107336 Swedish Defence Research Establishment, Div. of Sensor Technology, Linkoeping, Sweden
Fabry-Perot Grating Interferometer in Polarization-Maintaining Fiber ***Fabry-Perot Gitter Interferometer i Polarisationsbevarande Fiber***
Hamlin, Susanne, Swedish Defence Research Establishment, Sweden; Apr. 1999; 84p; In English
Report No.(s): PB99-173189; FOA-R-99-01101-409-SE; No Copyright; Avail: CASI; A01, Microfiche; A05, Hardcopy

In this work Fabry-Perot grating interferometers in polarization-maintaining fibers are experimentally investigated. The interferometer phase is changed either by stretching the fibers or by scanning the wavelength. The transmission properties as a function of strain and wavelength are measured and compared to theoretical functions. The plane of polarization of the input light

is rotated and the output light is analyzed with respect to intensity and polarization. Due to birefringence, in ordinary single mode fibers the transmission functions of the interferometer becomes degenerated which makes phase demodulation complicated. In this report it is shown that one way to solve the problem is to write the gratings in polarization-maintaining (PM) fibers. It is shown that if linearly polarized light is sent into one principal axis of the PM fiber an unwanted mode in the other principal direction as large as 3% of the main mode may appear and give rise to interference. In the gratings, energy from both modes may couple into the other which results in interference. The effects of birefringence and coupling between two polarization modes are illustrated. NTIS

Fabry-Perot Interferometers; Linear Polarization; Polarized Light

19990107383 NASA Goddard Space Flight Center, Greenbelt, MD USA

The XRS Low Temperature Cryogenic System: Ground Performance Test Results

Breon, Susan, NASA Goddard Space Flight Center, USA; Sirron, Peter, NASA Goddard Space Flight Center, USA; Boyle, Robert, NASA Goddard Space Flight Center, USA; Canavan, Ed, NASA Goddard Space Flight Center, USA; DiPirro, Michael, NASA Goddard Space Flight Center, USA; Serlemitsos, Aristides, NASA Goddard Space Flight Center, USA; Tuttle, James, NASA Goddard Space Flight Center, USA; Whitehouse, Paul, NASA Goddard Space Flight Center, USA; 1998; 1p; In English; 1998 Space Cryogenics, 20-21 Jul. 1998, Noordwijk, Netherlands; Copyright; Avail: Issuing Activity, Hardcopy; Abstract Only

The X-Ray Spectrometer (XRS) instrument is part of the Astro-E mission scheduled to launch early in 2000. Its cryogenic system is required to cool a 32-element square array of x-ray microcalorimeters to 60-65 mK over a mission lifetime of at least 2 years. This is accomplished using an adiabatic demagnetization refrigerator (ADR) contained within a two-stage superfluid helium/solid neon cooler. Goddard Space Flight Center is providing the ADR and helium dewar. The flight system was assembled in Sept. 1997 and subjected to extensive thermal performance tests. This paper presents test results at both the system and component levels. In addition, results of the low temperature topoff performed in Japan with the engineering unit neon and helium dewars are discussed.

Author

Calorimeters; Cryogenic Equipment; Magnetic Cooling; Performance Tests; X Ray Spectrometers; Cryogenics

19990108571 NASA Langley Research Center, Hampton, VA USA

Solid State Carbon Monoxide Sensor

Upchurch, Billy T., Inventor, NASA Langley Research Center, USA; Wood, George M., Inventor, NASA Langley Research Center, USA; Schryer, David R., Inventor, NASA Langley Research Center, USA; Leighty, Bradley D., Inventor, NASA Langley Research Center, USA; Oglesby, Donald M., Inventor, NASA Langley Research Center, USA; Kielin, Erik J., Inventor, NASA Langley Research Center, USA; Brown, Kenneth G., Inventor, NASA Langley Research Center, USA; DAmbrosia, Christine M., Inventor, NASA Langley Research Center, USA; Sep. 07, 1999; In English; Provisional US-Patent-Appl-SN-016669, filed 1 May 1996

Patent Info.: Filed 28 Apr. 1997; NASA-Case-LAR-15525-1-CU; US-Patent-5,948,965; US-Patent-Appl-SN-845899; US-Patent-Appl-SN-016669; No Copyright; Avail: US Patent and Trademark Office, Hardcopy

A means for detecting carbon monoxide which utilizes an un-heated catalytic material to oxidize carbon monoxide at ambient temperatures. Because this reaction is exothermic, a thermistor in contact with the catalytic material is used as a sensing element to detect the heat evolved as carbon monoxide is oxidized to carbon dioxide at the catalyst surface, without any heaters or external heating elements for the ambient air or catalytic element material. Upon comparison to a reference thermistor, relative increases in the temperature of the sensing thermistor correspond positively with an increased concentration of carbon monoxide in the ambient medium and are thus used as an indicator of the presence of carbon monoxide.

Author

Solid State; Carbon Monoxide; Gas Detectors; Thermistors

19990108744 Novosibirsk State Univ., USSR

The String Fluxmeter: How to Make and How to Use

Strumminsky, V. I., Novosibirsk State Univ., USSR; 11th International Conference on Atmospheric Electricity; June 1999, pp. 567-570; In English; See also 19990108601; No Copyright; Avail: CASI; A01, Hardcopy; A10, Microfiche

Undoubtedly, the electric field strength is the most often measured parameter of the atmospheric electricity. At the same time, many of researchers have limited possibilities to obtain industrially produced equipment for this purpose. This paper describes a simple easy-to-make string fluxmeter with sensitivity of 0.2 V/m and more, frequency range 0-50 Hz or wider. The main advantages of the string fluxmeter are: 1) relatively high frequency of electric field conversion; 2) extremely small area of the sensitive electrodes; 3) low power consumption. These features make the string fluxmeter especially useful for electric field

measurements in the medium with high level of conductive and convective electric currents, for instance, in the balloon and rocket experiments.
Author
Electric Field Strength; Electrical Measurement; Atmospheric Electricity; Measuring Instruments

19990109145 NASA Johnson Space Center, Houston, TX USA
Soft-Sided Air Displacement Volumometer
Siconolfi, Steven F., Inventor, NASA Johnson Space Center, USA; Sep. 07, 1999; In English
Patent Info.: Filed 31 Mar. 1998; NASA-Case-MSC-22653-1; US-Patent-5,948,977; US-Patent-Appl-SN-054311; No Copyright; Avail: US Patent and Trademark Office, Hardcopy

A soft-sided air displacement volumometer includes a soft-sided bag, an air injector, a pressure transducer, and a recording device. The soft-sided volumometer is used to measure the total body volume of a person or the volume of one limb of a person. After the person enters the soft-sided bag, the bag is sealed and pressurized to a predetermined level using the air injector. The pressure inside the soft-sided bag is continuously monitored using the pressure transducer and recording device while the volume of the soft-side bag is incrementally reduced. The elasticity of the soft-sided bag is eliminated from the volume calculations by operating the soft-sided air displacement volumometer over a relatively small range of volumes and pressures in which the elasticity is substantially constant. The volume of the person inside the soft-sided bag is calculated as the volume of the empty bag (i.e. without a person) minus the initial volume of the bag with the person pressurized to an initial pressure level.
Author
Volumetric Analysis; Body Volume (Biology); Human Beings; Air; Displacement; Level (Quantity)

19990109151 NASA Goddard Space Flight Center, Greenbelt, MD USA
A Rotating Space Interferometer with Variable Baselines and Low Power Consumption
Gezari, Daniel Y., NASA Goddard Space Flight Center, USA; [1999]; 3p; In English; Working on the Fringe: Optical and IR Interferometry from Ground and Space, May 1996, Dana Point, CA, USA; No Copyright; Avail: CASI; A01, Hardcopy; A01, Microfiche

A new concept is presented here for a large, rotating space interferometer which would achieve full u, v plane coverage with reasonably uniform integration times, yet once set in motion no additional energy would be required to change collector separations, maintain constant baseline rotation rates, or to counteract centrifugal forces on the collectors.
Author
Very Long Base Interferometry; Very Long Baseline Array (VLBA); Design Analysis; Spacecraft Configurations

19990110098 Jet Propulsion Lab., California Inst. of Tech., Pasadena, CA USA
Hydrazine Detection with a Tunable Diode Laser Spectrometer
Houseman, John, Jet Propulsion Lab., California Inst. of Tech., USA; Webster, C. R., Jet Propulsion Lab., California Inst. of Tech., USA; May, R. D., Jet Propulsion Lab., California Inst. of Tech., USA; Anderson, M. S., Jet Propulsion Lab., California Inst. of Tech., USA; Margolis, J. S., Jet Propulsion Lab., California Inst. of Tech., USA; Jackson, Julie R., Jet Propulsion Lab., California Inst. of Tech., USA; Brown, Pamela R., Jet Propulsion Lab., California Inst. of Tech., USA; JANNAF 28th Propellant Development and Characterization Subcommittee and 17th Safety and Environmental Protection Subcommitte Joint Meeting; April 1999; Volume 1, pp. 103-116; In English; See also 19990110087; No Copyright; Avail: CPIA, 10630 Little Patuxent Pkwy., Suite 202, Columbia, MD 21044-3200 HC, Hardcopy

Several instruments have been developed to measure low concentrations of hydrazine but none completely meet the sensitivity requirements while satisfying additional criteria such as quick response, stable calibration, interference free operation, online operation, reasonable cost, etc. A brief review is presented of the current technology including the electrochemical cell, the ion mobility spectrometer, the mass spectrometer, and the gas chromatograph. A review of the advantages and disadvantages of these instruments are presented here. The review also includes commercially unavailable technology such as the electronic nose and the Tunable Diode Laser (TDL) IR Spectrometer. It was found that the TDL could meet the majority of these criteria including fast response, minimum maintenance, portability, and reasonable cost. An experiment was conducted to demonstrate the feasibility of such a system using an existing (non-portable) instrument. A lead-salt tunable diode laser, cooled to 85 degrees Kelvin was used to record direct absorption and second-derivative spectra of Hydrazine at several pressures to study the sensitivity to low levels of Hydrazine. Spectra of NH3 and CO2 were used for wavelength identification of the scanned region. With a pathlength of 80 m, detection sensitivities of about 1 ppb were achieved for hydrazine in dry nitrogen at a cell pressure of 100 mbar. For spectroscopic detection of Hydrazine, spectral regions including strong Ammonia or Carbon Dioxide lines must be avoided. Strong Hydrazine absorption features were identified at 940/cm showing minimal contribution from Ammonia

interferences as suitable candidates for Hydrazine gas detection. For the studies reported here, the particular laser diode could only cover the narrow regions near 962/cm and 965/cm where strong Ammonia interferences were expected. However, the high resolution (0.001/cm) of the TDL spectrometer allowed individual lines of Hydrazine to be identified away from interferences from either Ammonia or Carbon Dioxide, especially at lower pressures. A Hydrazine line was identified at 961.75/cm which was free from Ammonia absorption and would be suitable to monitor hydrazine levels. This paper also shows data on the degradation of the detectivity of Hydrazine with increasing pressure. Several design options for a portable unit are presented, including designs with near IR and Quantum Cascade laser components which do not require liquid nitrogen cooling.
Author
Methylhydrazine; Dimethylhydrazines; Hypergolic Rocket Propellants; Tunable Lasers; Semiconductor Lasers; Laser Spectrometers

19990110099 Dynacs Engineering Co., Inc., Cocoa Beach, FL USA
A Review of Hydrazine Sensors: The State of the Art
Meneghelli, B. J., Dynacs Engineering Co., Inc., USA; JANNAF 28th Propellant Development and Characterization Subcommittee and 17th Safety and Environmental Protection Subcommitte Joint Meeting; April 1999; Volume 1, pp. 117-125; In English; See also 19990110087
Contract(s)/Grant(s): NAS10-98001; No Copyright; Avail: CPIA, 10630 Little Patuxent Pkwy., Suite 202, Columbia, MD 21044-3200 HC, Hardcopy

Several types of sensors have been developed over the past few years that quantify the vapor concentrations of the hydrazines. These sensors are able to detect concentrations as low as 10 parts per billion (ppb) up to several parts per million (ppm). The scope of this review will be focused on those sensors that are most current in the marketplace as either leak detectors or personnel monitors. Some technical information on the theory of operations of each hydrazine detector will also be included. The review will highlight current operations that utilize hydrazine sensors including the Kennedy Space Center (KSC), the USA Air Force (USAF) at Cape Canaveral Air Station (CCAS), USAF F-16 facilities. The orientation of the review will be towards giving users usable practical information on hydrazine sensors.
Author
Hydrazines; Liquid Rocket Propellants; Monitors

19990110100 NASA White Sands Test Facility, NM USA
Gas Sensor Evaluations in Polymer Combustion Product Atmospheres
Delgado, Rafael H., Allied-Signal Technical Services Corp., USA; Davis, Dennis D., Allied-Signal Technical Services Corp., USA; Beeson, Harold D., NASA White Sands Test Facility, USA; JANNAF 28th Propellant Development and Characterization Subcommittee and 17th Safety and Environmental Protection Subcommitte Joint Meeting; April 1999; Volume 1, pp. 127-136; In English; See also 19990110087; No Copyright; Avail: CPIA, 10630 Little Patuxent Pkwy., Suite 202, Columbia, MD 21044-3200 HC, Hardcopy

Toxic gases produced by the combustion or thermo-oxidative degradation of materials such as wire insulation, foam, plastics, or electronic circuit boards in space shuttle or space station crew cabins may pose a significant hazard to the flight crew. Toxic gas sensors are routinely evaluated in pure gas standard mixtures, but the possible interferences from polymer combustion products are not routinely evaluated. The NASA White Sands Test Facility (WSTF) has developed a test system that provides atmospheres containing predetermined quantities of target gases combined with the coincidental combustion products of common spacecraft materials. The target gases are quantitated in real time by infrared (IR) spectroscopy and verified by grab samples. The sensor responses are recorded in real time and are compared to the IR and validation analyses. Target gases such as carbon monoxide, hydrogen cyanide, hydrogen chloride, and hydrogen fluoride can be generated by the combustion of poly(vinyl chloride), polyimide-fluoropolymer wire insulation, polyurethane foam, or electronic circuit board materials. The kinetics and product identifications for the combustion of the various materials were determined by thermogravimetric-IR spectroscopic studies. These data were then scaled to provide the required levels of target gases in the sensor evaluation system. Multisensor toxic gas monitors from two manufacturers were evaluated using this system. In general, the sensor responses satisfactorily tracked the real-time concentrations of toxic gases in a dynamic mixture. Interferences from a number of organic combustion products including acetaldehyde and bisphenol-A were minimal. Hydrogen bromide in the products of circuit board combustion registered as hydrogen chloride. The use of actual polymer combustion atmospheres for the evaluation of sensors can provide additional confidence in the reliability of the sensor response.
Author
Gas Detectors; Gas Mixtures; Combustion Products; Gas Composition; Atmospheric Composition; Gas Analysis; Infrared Spectroscopy

19990110101 NASA White Sands Test Facility, NM USA

A Hydrazine Leak Sensor Based on Chemically Reactive Thermistors

Davis, Dennis D., Allied-Signal Technical Services Corp., USA; Mast, Dion J., Allied-Signal Technical Services Corp., USA; Baker, David L., NASA White Sands Test Facility, USA; JANNAF 28th Propellant Development and Characterization Subcommittee and 17th Safety and Environmental Protection Subcommitte Joint Meeting; April 1999; Volume 1, pp. 137-144; In English; See also 19990110087; No Copyright; Avail: CPIA, 10630 Little Patuxent Pkwy., Suite 202, Columbia, MD 21044-3200 HC, Hardcopy

Leaks in the hydrazine supply system of the Shuttle APU can result in hydrazine ignition and fire in the aft compartment of the Shuttle. Indication of the location of a leak could provide valuable information required for operational decisions. WSTF has developed a small, single use sensor for detection of hydrazine leaks. The sensor is composed of a thermistor bead coated with copper(II) oxide (CuO) dispersed in a clay or alumina binder. The CuO-coated thermistor is one of a pair of closely located thermistors, the other being a reference. On exposure to hydrazine the CuO reacts exothermically with the hydrazine and increases the temperature of the coated-thermistor by several degrees. The temperature rise is sensed by a resistive bridge circuit and an alarm registered by data acquisition software. Responses of this sensor to humidity changes, hydrazine concentration, binder characteristics, distance from a liquid leak, and ambient pressure levels as well as application of this sensor concept to other fluids are presented.

Author

Hydrazines; Ignition; Fires; Compartments; Leakage; Thermistors

19990110314 NASA Johnson Space Center, Houston, TX USA

Method of Manufacturing a Micromechanical Oscillating Mass Balance

Altemir, David A., Inventor, NASA Johnson Space Center, USA; Sep. 07, 1999; In English; Division of US-Patent-Appl-SN-587762, filed 12 Dec. 1995

Patent Info.: Filed 24 Jul. 1997; NASA-Case-MSC22569-2; US-Patent-5,946,795; US-Patent-Appl-SN-910537; US-Patent-Appl-SN-587762; No Copyright; Avail: US Patent and Trademark Office, Hardcopy

A micromechanical oscillating mass balance and method adapted for measuring minute quantities of material deposited at a selected location, such as during a vapor deposition process. The invention comprises a vibratory composite beam which includes a dielectric layer sandwiched between two conductive layers.The beam is positioned in a magnetic field. An alternating current passes through one conductive layers, the beam oscillates, inducing an output current in the second conductive layer, which is analyzed to determine the resonant frequency of the beam. As material is deposited on the beam, the mass of the beam increases and the resonant frequency of the beam shifts, and the mass added is determined.

Author

Manufacturing; Micromechanics; Oscillations; Mass Distribution; Balance

19990110317 NASA Marshall Space Flight Center, Huntsville, AL USA

Evaluation of the Use of Optical Fiber Thermometers for Thermal Control of the Quench Module Insert

Jones, Matthew R., Arizona Univ., USA; Farmer, Jeffrey T., NASA Marshall Space Flight Center, USA; Breeding, Shawn P., Tec-Masters, Inc., USA; [1999]; 7p; In English; 10th; Thermal and Fluids Analysis (TFAWS99) Workshop, 13-17 Sep. 1999, Huntsville, AL, USA; No Copyright; Avail: CASI; A02, Hardcopy; A01, Microfiche

Issues regarding the use of optical fiber thermometers to control heater settings in a microgravity vacuum furnace are addressed. It is desirable to use these probes in environments such as the International Space Station, because they can be operated without re-calibration for extended periods. However, the analysis presented in this paper shows that temperature readings obtained using optical fiber thermometers are corrupted due to emissions from the fiber when extended portions of the probe are exposed to elevated temperatures.

Author

Evaluation; Optical Fibers; Thermometers; Temperature Control; Calibrating

19990110318 Boeing Co., Rocketdyne Propulsion and Power, Canoga Park, CA USA

Rotor Re-Design for the SSME Fuel Flowmeter

Marcu, Bogdan, Boeing Co., USA; [1999]; 34p; In English; Thermal and Fluids Analysis Workshop, 13-17 Sep. 1999, Huntsville, AL, USA; Original contains color illustrations

Contract(s)/Grant(s): NAS8-45000; No Copyright; Avail: CASI; A03, Hardcopy; A01, Microfiche

The present report describes the process of redesigning a new rotor for the SSME Fuel Flowmeter. The new design addresses the specific requirement of a lower rotor speed which would allow the SSME operation at 1 15% rated power level without

reaching a blade excitation by the wakes behind the hexagonal flow straightener upstream at frequencies close to the blade natural frequency. A series of calculations combining fleet flowmeters test data, airfoil fluid dynamics and CFD simulations of flow patterns behind the flowmeter's hexagonal straightener has led to a blade twist design alpha = alpha (radius) targeting a kf constant of 0.8256. The kf constant relates the fuel volume flow to the flowmeter rotor speed, for this particular value 17685 GPM at 3650 RPM. Based on this angle distribution, two actual blade designs were developed. A first design using the same blade airfoil as the original design targeted the new kf value only. A second design using a variable blade chord length and airfoil relative thickness targeted simultaneously the new kf value and an optimum blade design destined to provide smooth and stable operation and a significant increase in the blade natural frequency associated with the first bending mode, such that a comfortable margin could be obtained at 115% RPL. The second design is a result of a concurrent engineering process, during which several iterations were made in order to achieve a targeted blade natural frequency associated with the first bending mode of 1300 Hz. Water flow tests preliminary results indicate a kf value of 0.8179 for the f-irst design, which is within 1% of the target value. The second design rotor shows a natural frequency associated with the first bending mode of 1308 Hz, and a water-flow calibration constant of kf 0.8169.
Author
Design Analysis; Rotors; Flowmeters; Computational Fluid Dynamics; Flow Distribution; Fluid Dynamics; Rotor Speed

19990110469 NASA Marshall Space Flight Center, Huntsville, AL USA
A Photometric Technique for Determining Fluid Concentration using Consumer-Grade Hardware
Leslie, F., NASA Marshall Space Flight Center, USA; Ramachandran, N., Universities Space Research Association, USA; February 1999; 28p; In English
Report No.(s): NASA/TM-1999-209091; M-910; NAS 1.15:209091; No Copyright; Avail: CASI; A03, Hardcopy; A01, Microfiche

In support of a separate study to produce an exponential concentration gradient in a magnetic fluid, a noninvasive technique for determining, species concentration from off-the-shelf hardware has been developed. The approach uses a backlighted fluid test cell photographed with a commercial digital camcorder. Because the light extinction coefficient is wavelength dependent, tests were conducted to determine the best filter color to use, although some guidance was also provided using an absorption spectrophotometer. With the appropriate filter in place, the provide attenuation of the light passing, through the test cell was captured by the camcorder. The digital image was analyzed for intensity using, software from Scion Image Corp. downloaded from the Internet. The analysis provides a two-dimensional array of concentration with an average error of 0.0095 ml/ml. This technique is superior to invasive techniques, which require extraction of a sample that disturbs the concentration distribution in the test cell. Refinements of this technique using a true monochromatic laser light Source are also discussed.
Author
Fluid Mechanics; Photometry; Attenuation Coefficients; Extraction; Gradients

19990110687 Japan Broadcasting Corp., Science and Technical Research Labs., Tokyo, Japan
A Precise VTR Tracking Method Using Buried Pilot Signals
Yanagisawa, Hitoshi, Japan Broadcasting Corp., Japan; June 1999; ISSN 0027-657X; 8p; In English; Copyright; Avail: Issuing Activity, Hardcopy

Any slight deviation of the VTR head on the track becomes a serious problem when narrower tracks are used to improve the surface and volume recording densities of VTR tape. Therefore, it is indispensable to improve the linearity of recording tracks and the precision of playback tracking. In this study, pilot signals are recorded on the tape at the initial recording time for use as a reference to find the scanning position of the head, and the positions of the recording/playback heads with actuators are controlled so as to align the head scanning trace with the standardized track pattern.
Author
Tracking (Position); Tracking Problem; Control Theory; Playbacks; Recording Heads

19990111587 Japan Broadcasting Corp., Recording Technology and Mechanical Engineering, Tokyo, Japan
Magneto-Optical Properties of Garnet Multi-Layered Film for Wavelength Multiplex Recording Media Prepared by Pulsed Laser Deposition
Ishii, Norihiko, Japan Broadcasting Corp., Japan; Tamaki, Takahiko, Japan Broadcasting Corp., Japan; Tanaka, Isao, Japan Broadcasting Corp., Japan; Sato, Ryuji, Japan Broadcasting Corp., Japan; May 1999; ISSN 0027-657X; 12p; In English; Copyright; Avail: Issuing Activity, Hardcopy

The wavelength multiplex recording method is one of the approaches for high-density recording on a rewritable optical disk. to develop the wavelength multiplex recording media, we prepared a multi-layered magnetic garnet film prepared by using the

pulsed laser deposition method. Wavelength and temperature dependence of the Faraday rotation angle has been measured for the Co, Ge, and Bi substituted dysprosium iron garnet film. The new composition was found to be suitable for wavelength multiplexing recording media. Our findings show that wavelength multiplexing is an effective way to significantly increase recording capacity.
Author
Magneto-Optics; Faraday Effect; Curie Temperature; Garnets; Metal Films; Magnetic Films; Multiplexing

19990111739 NASA Marshall Space Flight Center, Huntsville, AL USA
Construction of a Chemical Sensor/Instrumentation Package Using Fiber Optic and Miniaturization Technology ***Final Report***
Newton, R. L., NASA Marshall Space Flight Center, USA; October 1999; 28p; In English
Contract(s)/Grant(s): Proj. 97-12
Report No.(s): NASA/TM-1999-209732; M-943; NAS 1.15:209732; No Copyright; Avail: CASI; A03, Hardcopy; A01, Microfiche

The objective of this research was to construct a chemical sensor/instrumentation package that was smaller in weight and volume than conventional instrumentation. This reduction in weight and volume is needed to assist in further reducing the cost of launching payloads into space. To accomplish this, fiber optic sensors, miniaturized spectrometers, and wireless modems were employed. The system was evaluated using iodine as a calibration analyte.
Author
Miniaturization; Fiber Optics; Fabrication; Spectrometers; Chemical Analysis

36
LASERS AND MASERS

Includes parametric amplifiers. For related information see also 76 Solid-State Physics.

19990107356 Sandia National Labs., Albuquerque, NM USA
Exploring New Active Regions for Type 1 InasSb Strained-Layer Lasers
Biefeld, R. M.; Kurtz, S. R.; Phillips, J. D.; May 13, 1999; 11p; In English; 9th; Organometallic Vapor Phase Epitaxy, 23-27 May 1999, Ponte Vedra Beach, FL, USA; Sponsored by Department of Energy, USA
Report No.(s): DE00-007142; SAND99-0415C; No Copyright; Avail: Department of Energy Information Bridge, Hardcopy

We report on the metal-organic chemical vapor deposition (MOCVD) of mid- infrared InAsSb/InPSb optically pumped lasers grown using a high speed rotating disk reactor (RDR). The devices contain AlAsSb claddings and strained, type 1, InAsSb/InPSb active regions. by changing the layer thickness and composition of InAsSb/InPSb SLSs, we have prepared structures with low temperature (<20K) photoluminescence wavelengths ranging from 3.4 to 4.8 micro-m. We find a variation of bandgap from 0.272 to 0.324 eV for layer thicknesses of 9.0 to 18.2 nm. From these data we have estimated a valence band offset for the InAsSb/InPSb interface of about 400 meV. An InAsSb/InPSb SLS, optically pumped laser structure was grown on an InAs substrate with AlAs(0.l6)Sb(0.84) claddings. A lasing threshold and spectrally narrowed laser emission was seen from 80 K through 200 K, the maximum temperature where Iasing occurred. The temperature dependence of the SLS laser threshold is described by a characteristic temperature, T = 72 K, from 80 to 200 K.
NTIS
Semiconductor Lasers; Indium Arsenides; Indium Antimonides; Metalorganic Chemical Vapor Deposition; Infrared Radiation; Laser Outputs; Photoluminescence; Temperature Dependence

37
MECHANICAL ENGINEERING

Includes auxiliary systems (nonpower); machine elements and processes; and mechanical equipment.

19990108572 NASA Johnson Space Center, Houston, TX USA
Blood Pump Bearing System
Aber, Gregory S., Inventor, NASA Johnson Space Center, USA; Sep. 28, 1999; In English; Continuation-in-part of US-Patent-Appl-SN-153595, filed 10 Nov. 1993 and continuation-in-part of US-Patent-Appl-SN-451709, filed 26 May 1995
Patent Info.: Filed 17 Jun. 1996; NASA-Case-MSC-22721-1; US-Patent-5,957,672; US-Patent-Appl-SN-664579;

US-Patent-Appl-SN-153595; US-Patent-Appl-SN-451709; No Copyright; Avail: US Patent and Trademark Office, Hardcopy

Methods and apparatus are provided for a blood pump bearing system within a pump housing to support long-term high-speed rotation of a rotor with an impeller blade having a plurality of individual magnets disposed thereon to provide a small radial air gap between the magnets and a stator of less than 0.025 inches. The bearing system may be mounted within a flow straightener, diffuser, or other pump element to support the shaft of a pump rotor. The bearing system includes a zirconia shaft having a radiused end. The radiused end has a first radius selected to be about three times greater than the radius of the zirconia shaft. The radiused end of the zirconia shaft engages a flat sapphire endstone. Due to the relative hardness of these materials a flat is quickly produced during break-in on the zirconia radiused end of precisely the size necessary to support thrust loads whereupon wear substantially ceases. Due to the selection of the first radius, the change in shaft end-play during pump break-in is limited to a total desired end-play of less than about 0.010 inches. Radial loads are supported by an olive hole ring jewel that makes near line contact around the circumference of the shaft to support high speed rotation with little friction. The width of olive hole ring jewel is small to allow heat to conduct through to thereby prevent heat build-up in the bearing. A void defined by the bearing elements may fill with blood that then coagulates within the void. The coagulated blood is then conformed to the shape of the bearing surfaces.
Author

Blood; Blood Pumps; Bearings; Axial Flow; Radial Flow

19990111461 Howard Univ., Dept. of Electrical Engineering, Washington, DC USA

A Neuro-Fuzzy Approach for Load Forecasting and Fuel Minimization for the Hybrid Electric Vehicle

Momoh, James A., Howard Univ., USA; Elfayoumy, Mahmoud, Howard Univ., USA; HBCUs/OMUs Research Conference Agenda and Abstracts; August 1999, pp. 14; In English; See also 19990111455; No Copyright; Avail: Issuing Activity, Hardcopy; Abstract Only

The paper presents an Artificial Neural Network (ANN) based-load forecasting and Fuzzy Logic (FL) based-fuel minimization for the energy control of the Hybrid Electric Vehicle (HEV). A detailed design of the forecaster and fuzzy logic module including data collection scheme, training, developing of the fuzzy rules, testing and implementation is presented. The data needed for the training and testing processes is obtained using simulation results from analysis of the HEV simulation model program, HEVA, developed by NASA Glenn Research Center. The ANN based-Load Forecaster is trained using the Error Back Propagation (EBP) algorithm, which is implemented using a robust back propagation program. Also, Matlab-based fuzzy rules for fuel minimization are developed. The scheme is integrated around HEVA program and tested for different operating conditions. The proposed scheme is capable of guiding the HEV operator to the optimal operating performance parameters.
Author

Electric Motor Vehicles; Fuzzy Systems; Neural Nets; Optimization; Automatic Control; Cybernetics; Control Systems Design; Fuel Control

19990111533 Department of Energy, Washington, DC USA

Oxidation of automotive primary reference fuels in a high pressure flow reactor

Curran, H. J., Department of Energy, USA; Pitz, W. J., Department of Energy, USA; Westbrook, C. K., Department of Energy, USA; Callahan, C. V., Department of Energy, USA; Dryer, F. L., Department of Energy, USA; Jan. 01, 1998; 31p; In English
Report No.(s): DE98-057774; UCRL-JC-129298; CONF-9803101; No Copyright; Avail: Department of Energy Information Bridge, Microfiche

Automotive engine knock limits the maximum operating compression ratio and ultimate thermodynamic efficiency of spark-ignition (SI) engines. In compression-ignition (CI) or diesel cycle engines, the premixed burn phase, which occurs shortly after injection, determines the time it takes for autoignition to occur. In order to improve engine efficiency and to recommend more efficient, cleaner-burning alternative fuels, we must understand the chemical kinetic processes which lead to autoignition in both SI and CI engines. In this study, experiments were performed under engine-like conditions in a high pressure flow reactor using both the pure PRF fuels and their mixtures in the temperature range 550-880 K and at 12.5 atm pressure. These experiments not only provide information on the reactivity of each fuel but also identify the major intermediate products formed during the oxidation process. A detailed chemical kinetic mechanism is used to simulate these experiments and comparisons of experimentally measures and model predicted profiles for O2, CO, CO2, H2O and temperature rise are presented. Intermediates identified in the flow reactor are compared with those present in the computations, and the kinetic pathways leading to their formation are discussed. In addition, autoignition delay times measured in a shock tube over the temperature range 690-1220 K and at 40 atm pressure were simulated. Good agreement between experiment and simulation was obtained for both the pure fuels

and their mixtures. Finally, quantitative values of major intermediates measured in the exhaust gas of a cooperative fuels research engine operating under motored engine conditions are presented together with those predicted by the detailed method.
NTIS
Automobile Fuels; Spontaneous Combustion; Pressure Dependence; Oxidation; Diesel Engines; Internal Combustion Engines; Ignition

19990111609 NASA Marshall Space Flight Center, Huntsville, AL USA
Experimental Rotordynamic Characterization of Annular Seals: Facility and Methodology
Darden, J. Mark, NASA Marshall Space Flight Center, USA; Earhart, Eric M., NASA Marshall Space Flight Center, USA; Flowers, George T., Auburn Univ., USA; 1998; 1p; In English; 43rd; Gas Turbine and Aero Engine Congress, 2-9 Jun. 1998, Stockholm, Sweden; Sponsored by American Society of Mechanical Engineers, USA
Contract(s)/Grant(s): NASA Order H-28054-D; Copyright; Avail: Issuing Activity, Hardcopy; Abstract Only

Annular seals are employed in a variety of rotating machinery. They are known to enhance rotordynamic stability margins and help minimize vibration response levels. In many cases, the dynamic characteristics of a particular machine are strongly dependent upon its annular seals. This is particularly true in cryogenic rocket engine turbopumps. Efforts to experimentally characterize annular seals have been carried out but the need for additional data remains. This paper describes NASA's Marshall Space Flight Center (MSFC) annular seal test rig/facility. The rig provides a test vehicle for the experimental characterization of a variety of annular seals. The objective of the test rig is to yield rotordynamic coefficients (direct and cross-coupled stiffness, damping, and added mass) along with steady state parameters of a high Reynolds number annular seal. The MSFC test rig supports testing of seals with inlet pressures up to 2000 psi and flowrates of over 250 gallons per minute (gpm). The rig's shaft is powered by a 250 horsepower steam turbine capable of rotational speeds of over 20,000 rpm. The paper will also describe the identification process for obtaining rotordynamic coefficients as well as procedures for ensuring quality data.
Author
Rotor Dynamics; Dynamic Characteristics; Dynamic Stability; Structural Vibration

19990111611 Kinki Univ., Faculty of Engineering, Hiroshima, Japan
The Effect of Bleed Air Flow Rate on Transient Characteristics of Carburetor
Gakumasawa, Hidetaka, Kinki Univ., Japan; Hohsho, Yukio, Kinki Univ., Japan; Research Reports of the Faculty of Engineering, Kinki University; 1993; ISSN 0386-491X, No. 27, pp. 55-61; In Japanese; Copyright; Avail: Issuing Activity, Hardcopy, Microfiche

This paper describes the transient fuel supply characteristics in a carburetor with main metering system under accelerating condition. Numerical calculation has been made on the fuel delay time by a personal computer. Experimental work was also performed to verify the validity of the numerical results. A carburetor under throttle operation was suddenly accelerated and first appearance of fuel discharged from the outlet of main nozzle was detected by a timelapse video system. The results showed that the present analysis was successful in giving results consistent with experimental data. The main air bleed was found to be useful for improving the transient response of a carburetor. Delay time was mostly due to the period of time elapsed for bleed air to arrive at the top emulsion holes.
Derived from text
Carburetors; Flow Velocity; Transient Response; Air Flow

19990113099 Southwest Research Inst., San Antonio, TX USA
Three-Way Catalyst Technology for Off-Road Equipment Powered by Gasoline and LPG Engines ***Final Report***
White, J. J.; Ingalls, M. N.; Carroll, J. N.; Chan, L. M.; Apr. 1999; 286p; In English
Report No.(s): PB99-175507; No Copyright; Avail: CASI; A13, Hardcopy; A03, Microfiche

Research was done to demonstrate the feasibility of using closed-loop three-way catalyst (TWC) technology in off-road large spark-ignited (LSI) engine applications to meet California State Implementation Plan (SIP) emission reduction goals. Available technology was investigated for applicability to engines in this category. Appropriate test cycles were recommended, and five representative engines were selected and baseline emission tested. Total feasible emission reductions were calculated. The retail price equivalent (RPE) for the recommended emission control technology was determined, and cost-effectiveness was calculated. Emission standards necessary to meet SIP goals were recommended.
NTIS
Exhaust Emission; Exhaust Gases; Pollution Transport; Air Pollution; Pollution Control

19990113119 Florida Univ., Dept. of Aerospace Engineering, Mechanics and Engineering Science, Gainesville, FL USA
Thermal Analysis of Magnetically-Coupled Pump for Cryogenic Applications ***Final Report***
Senocak, Inanc, Florida Univ., USA; Udaykumar, H. S., Florida Univ., USA; Ndri, Narcisse, Florida Univ., USA; Francois, Marianne, Florida Univ., USA; Shyy, Wei, Florida Univ., USA; 1999; 1p; In English
Contract(s)/Grant(s): NAG10-0261; No Copyright; Avail: Issuing Activity, Hardcopy; Abstract Only

Magnetically-coupled pump is under evaluation at Kennedy Space Center for possible cryogenic applications. A major concern is the impact of low temperature fluid flows on the pump performance. As a first step toward addressing this and related issues, a computational fluid dynamics and heat transfer tool has been adopted in a pump geometry. The computational tool includes (i) a commercial grid generator to handle multiple grid blocks and complicated geometric definitions, and (ii) an in-house computational fluid dynamics and heat transfer software developed in the Principal Investigator's group at the University of Florida. Both pure-conduction and combined convection-conduction computations have been conducted. A pure-conduction analysis gives insufficient information about the overall thermal distribution. Combined convection-conduction analysis indicates the significant influence of the coolant over the entire flow path. Since 2-D simulation is of limited help, future work on full 3-D modeling of the pump using multi-materials is needed. A comprehensive and accurate model can be developed to take into account the effect of multi-phase flow in the cooling flow loop, and the magnetic interactions.
Author
Computational Fluid Dynamics; Cryogenics; Thermal Analysis; Fuel Pumps; Grid Generation (Mathematics); Applications Programs (Computers); Conductive Heat Transfer; Convective Heat Transfer; Computerized Simulation

19990113172 Allied-Signal Corp., Bendix, Elyria, OH USA
Simulation of a Hydraulic Pump Control Valve
Molen, G. Vander, Allied-Signal Corp., USA; Akers, A., Iowa State Univ. of Science and Technology, USA; 19870409; ISSN 01487191; In English; Earthmoving Industry, 7-9 Apr. 1987, Peoria, IL, USA; Sponsored by Society of Automotive Engineers, Inc., USA
Report No.(s): SAE-TP-870807; Copyright; Avail: Issuing Activity, Hardcopy, Microfiche

This paper describes the mode of operation of a control valve assembly that is used with a hydraulic pump. The operating system of the valve is modelled in a simplified form, and an analogy for hydraulic resonance of the pressure sensing system is presented. For the control valve investigated, air entrainment, length and diameter of the resonator neck, and valve mass produced the greatest shift in resonant frequency. Experimental work was conducted on the hydraulic system so that the resonance levels and frequencies could be measured and the accuracy of the theory verified. The results obtained make it possible to evaluate what changes to any of the variables considered would be most effective in driving the second harmonic frequency above the operating range.
Author
Hydraulic Equipment; Control Valves; Pumps; Simulation

38
QUALITY ASSURANCE AND RELIABILITY

Includes product sampling procedures and techniques; and quality control.

19990107411 National Inst. of Standards and Technology, Materials Reliability Div., Boulder, CO USA
IIW Commission 5: Quality Control and Quality Assurance of Welded Products ***Annual Report, 1998 - 1999***
Siewert, T. A., National Inst. of Standards and Technology, USA; Jan. 1999; 40p; In English
Report No.(s): PB99-123879; NISTIR-5081; No Copyright; Avail: CASI; A03, Hardcopy; A01, Microfiche

This Annual Report 1998/99 for Commission V, Quality Control and Quality Assurance of Welded Products, of the International Institute of Welding includes (a) minutes, resolutions, and the future program adopted at its Annual Assembly in September 1998, (b) the organization, officials, and delegates, (c) schedules of meetings, and (d) the status of documents published by Commission V. It reviews current research and work on standardization.
NTIS
Welded Joints; Inspection; Nondestructive Tests; Ultrasonic Tests; Standardization; Welding

19990108798 Jozef Stefan Inst., Odsek za Racunalnisko Avtomatizacijo in Regulacije, Ljubljana, Slovenia
Transferable Belief Model in Fault Diagnosis of Industrial Processes ***Uporaba Metode Prenosa Zaupanja pri Odkrivanju Napak v Industrijskih Procesih***
Rakar, Andrej, Jozef Stefan Inst., Slovenia; Juricic, Dani, Jozef Stefan Inst., Slovenia; Electrotechnical Review; 1999; Volume 66, No. 2, pp. 109-119; In Slovene; See also 19990108795
Contract(s)/Grant(s): J2-9064-0106-97; No Copyright; Avail: CASI; A03, Hardcopy; A01, Microfiche

The transferable belief model (TBM) is an approximate reasoning method which derives from the Dempster-Shafers mathematical theory of evidence. It is a means for representing quantified degrees of belief. Degrees of belief are obtained from agents providing evidence at a given time within a given frame of discernment. Tile method is capable of treating inconsistency in data by introducing the ”open world” assumption. In TBM, a set of all propositions consists of the three subsets: a set of propositions known as possible (PP), a set of propositions known as impossible (IP), and a set of unknown propositions (Up). The content of the subsets depends not only on the given problem, but also on the evidence, which is available at a given time. The paper concerns the applicability of TBM in process fault diagnosis where the residuals are used as basic agents providing evidence of faults.
Author
Mathematical Models; Diagnosis; Industrial Management

39
STRUCTURAL MECHANICS

Includes structural element design and weight analysis; fatigue; and thermal stress. For applications see 05 Aircraft Design, Testing and Performance and 18 Spacecraft Design, Testing and Performance.

19990106560 Norwegian Defence Research Establishment, Kjeller, Norway
Cavity Expansion and Penetration Mechanics ***Cavity Expandion og Penetrasjonsmekanikk: Materialmodeller og Numeriske Losningsmetoder***
Berthelsen, Petter Andreas, Norwegian Defence Research Establishment, Norway; Aug. 31, 1999; 54p; In Norwegian
Contract(s)/Grant(s): Proj. FFIBM/766/130
Report No.(s): FFI/RAPPORT-99/04260; ISBN 82-464-0366-4; No Copyright; Avail: CASI; A04, Hardcopy; A01, Microfiche

This report gives a short introduction to the cavity expansion theory and penetration mechanics. We derive and describe numerical methods to solve the cavity expansion problem for different strength models. Then we solve the penetration equations by numerical methods for spherical and ogival nose projectiles. The different strength models considered are the Tresca yield criterion, Mohr-Coulomb yield criterion, and a piecewise linear Mohr-Coulomb criterion. The script for the Matlab package developed is reproduced in Appendix A.
Author
Cavities; Numerical Analysis; Penetration

19990107327 NASA Marshall Space Flight Center, Huntsville, AL USA
Deflections of a Uniformly Loaded Circular Plate with Multiple Support Points, 1, Introduction
Craig, L. D., NASA Marshall Space Flight Center, USA; Boulet, J. A. M., Tennessee Univ., USA; September 1999; 22p; In English
Report No.(s): NASA/TM-1999-209631; NAS 1.15:209631; M-942; No Copyright; Avail: CASI; A03, Hardcopy; A01, Microfiche

This technical memorandum describes a method for determining the transverse deflections of a uniformly loaded, thin circular plate of constant thickness supported by single or multiple rings of equally spaced discreet points. The rotations are assumed free at each point. This could have application in the design of telescope mirror supports that must minimize structural gravitational deformations. It could also be of general use to the structural analyst.
Author
Deflection; Support Systems; Telescopes; Mirrors

19990109227 Institute of Space Medico, Space Medicine and Medical Engineering, Beijing, China
Strength analysis of metal spheroidal high pressure vessel
Jiabai, Rui, Institute of Space Medico, China; Chuanxian, Zheng, Institute of Space Medico, China; Fengwu, Zhang, Institute of Space Medico, China; Jun, Wang, Institute of Space Medico, China; Dekai, Sun, Institute of Space Medico, China; Xinjun, Liu, Institute of Space Medico, China; Space Medicine and Medical Engineering; Jun. 1997; Volume 10, No. 3, pp. 192-196; In

English; In Chinese; See also 19990109220; No Copyright; Avail: CASI; A01, Hardcopy; A01, Microfiche

The metal spheroidal high pressure vessel employed in the space and aviation industry was analyzed with the ADINA finite element program. Some practical methods enhancing the calculation efficiency and meeting special needs were discussed. The front end program for input of finite element information was arranged. It was a useful implement for accurate strength and reliability analysis. As an example, a special steel spheroidal high pressure vessel was calculated and analysed.

Author

Finite Element Method; High Pressure; Pressure Vessels; Reliability Analysis; Spherical Tanks; Algorithms

19990110580 NASA Langley Research Center, Hampton, VA USA

Signal Prediction with Input Identification

Juang, Jer–Nan, NASA Langley Research Center, USA; Chen, Ya–Chin, Institute for Computer Applications in Science and Engineering, USA; October 1999; 36p; In English

Contract(s)/Grant(s): NAS1-19480; RTOP 632-10-14-04

Report No.(s): NASA/TM-1999-209705; NAS 1.15:209705; L-17889; No Copyright; Avail: CASI; A03, Hardcopy; A01, Microfiche

A novel coding technique is presented for signal prediction with applications including speech coding, system identification, and estimation of input excitation. The approach is based on the blind equalization method for speech signal processing in conjunction with the geometric subspace projection theory to formulate the basic prediction equation. The speech-coding problem is often divided into two parts, a linear prediction model and excitation input. The parameter coefficients of the linear predictor and the input excitation are solved simultaneously and recursively by a conventional recursive least-squares algorithm. The excitation input is computed by coding all possible outcomes into a binary codebook. The coefficients of the linear predictor and excitation, and the index of the codebook can then be used to represent the signal. In addition, a variable-frame concept is proposed to block the same excitation signal in sequence in order to reduce the storage size and increase the transmission rate. The results of this work can be easily extended to the problem of disturbance identification. The basic principles are outlined in this report and differences from other existing methods are discussed. Simulations are included to demonstrate the proposed method.

Author

Voice Data Processing; System Identification; Coding; Speech Recognition

19990111479 Texas Univ., San Antonio, TX USA

Research and Education in Probabilistic Structural Analysis and Reliability

Godines, Cody, Texas Univ., USA; HBCUs/OMUs Research Conference Agenda and Abstracts; August 1999, pp. 33; In English; See also 19990111455; No Copyright; Avail: Issuing Activity, Hardcopy; Abstract Only

This paper deals with stress analysis of a cantilever beam. The analysis was performed three different ways. The first calculations of the stresses at different regions within the body were done using simple beam theory. This is an algebraic way of arriving at the stresses without having to do extensive calculations. Stress elements were calculated at the regions of highest stress. These high stress locations were estimated by the load type/placement, and experience. The second way that the stress was calculated was by modeling and analyzing the same beam using NESSUS, a probabilistic finite element code. The final way of calculating the stresses within the beam was done by using the theory of elasticity and plane stress assumptions. This resulted in two coupled partial differential equations existing over a two dimensional domain. These plane stress equations were then solved using the finite element method by way of weighted residuals. The Galerkin-Bubov approach was implemented on the weight and shape functions. The stresses obtained from all three of the analysis methods will be compared to each other and results will be discussed.

Author

Cantilever Beams; Finite Element Method; Galerkin Method; Partial Differential Equations; Plane Stress; Stress Analysis; Structural Analysis; Elastic Properties

19990111512 Department of Transportation, Washington, DC USA

Pressure reversal study through tensile tests

Swinson, W. F., Department of Transportation, USA; Battiste, R. L., Department of Transportation, USA; Wright, A. L., Department of Transportation, USA; Yahr, G. T., Department of Transportation, USA; Robertson, J. P., Department of Transportation, USA; Dec. 31, 1997; 10p; In English; Energy Sources Technology, 1998, USA; Sponsored by Department of Energy, USA

Report No.(s): DE98-000126; No Copyright; Avail: Department of Energy Information Bridge, Microfiche

This paper is a summary of the results from a study of the variables related to pressure reversal and was sponsored by the US Department of Transportation, Office of Pipeline Safety. The circumferential pipe stress, which is the most significant variable in pressure reversal, was examined by using tensile specimens and then relating the results to pressurized pipe. A model is proposed that gives some insight into how pressure reversal can be minimized when a section of pipe is being hydrotested. Twenty tensile specimens from X-42 electric resistance welded (ERW) pipe and twenty specimens from X-52 ERW pipe were tested. Each specimen had a machined flaw. The flaw regions were monitored using strain gages and photoelasticity. These tensile tests represent the first phase of a research effort to examine and understand the variables related to pressure reversal.
NTIS
Pipelines; High Strength Steels; Leakage; Stress Analysis; Tensile Tests

19990111597 NASA Langley Research Center, Hampton, VA USA
Buckling Behavior of Compression-Loaded Quasi-Isotropic Curved Panels with A Circular Cutout
Hilburger, Mark W., National Academy of Sciences - National Research Council, USA; Britt, Vicki O., Gulf Stream Aerospace Corp., USA; Nemeth, Michael P., NASA Langley Research Center, USA; Jan. 01, 1999; In English; Structures, Structural Dynamics, and Material, 12-15 Apr. 1999, Saint Louis, MO, USA; Sponsored by American Inst. of Aeronautics and Astronautics, USA
Contract(s)/Grant(s): NASw-8154
Report No.(s): AIAA Paper 99-1279; Copyright; Avail: Issuing Activity, Hardcopy, Microfiche

Results from a numerical and experimental study of the response of compression-loaded quasi-isotropic curved panels with a centrally located circular cutout are presented. The numerical results were obtained by using a geometrically nonlinear finite element analysis code. The effects of cutout size, panel curvature and initial geometric imperfections on the overall response of compression-loaded panels are described. In addition, results are presented from a numerical parametric study that indicate the effects of elastic circumferential edge restraints on the prebuckling and buckling response of a selected panel and these numerical results are compared to experimentally measured results. These restraints are used to identify the effects of circumferential edge restraints that are introduced by the test fixture that was used in the present study. It is shown that circumferential edge restraints can introduce substantial nonlinear prebuckling deformations into shallow compression-loaded curved panels that can results in a significant increase in buckling load.
Author
Buckling; Deformation; Structural Failure; Structural Strain; Compression Loads; Curved Panels

19990111737 Textron Bell Helicopter, Fort Worth, TX USA
Parametric Study of Three-Stringer-Panel Compression-After-Impact Strength
Rousseau, Carl Q., Textron Bell Helicopter, USA; Hethcock, J. Donn, Textron Bell Helicopter, USA; Baker, Donald J., Army Research Lab., USA; 1999; 58p; In English; Composite Structures: Theory and Practice, 17-18 May 1999, Seattle, WA, USA; Sponsored by American Society for Testing and Materials, USA
Contract(s)/Grant(s): NCCW-76; NAS1-19853; N00019-85-C-0145; F3361-C-5729; No Copyright; Avail: CASI; A04, Hardcopy; A01, Microfiche

Damage tolerance requirements for integrally-stiffened composite wing skins are typically met using design allowables generated by testing impact-damaged subcomponents, such as three-stringer stiffened panels. To improve these structures, it is necessary to evaluate the critical design parameters associated with three-stringer stiffened-panel compressive behavior. During recent research and development programs, four structural parameters were identified as sources for strength variation: (a) material system, (b) stringer configuration, (c) skin layup, and (d) form of axial reinforcement (tape versus pultruded carbon rods). Relative effects of these parameters on damage resistance and damage tolerance were evaluated numerically and experimentally. Material system and geometric configuration had the largest influence on damage resistance; location and extent of the damage zone influenced the sublaminate buckling behavior, failure initiation site, and compressive ultimate strength. A practical global-local modeling technique captured observed experimental behavior and has the potential to identify critical damage sites and estimate failure loads prior to testing. More careful consideration should be given to accurate simulation of boundary conditions in numerical and experimental studies.
Author
Boundary Conditions; Composite Materials; Composite Structures; Compressive Strength; Damage Assessment; Tolerances (Mechanics)

19990111740 NASA Marshall Space Flight Center, Huntsville, AL USA
Static Strength Characteristics of Mechanically Fastened Composite Joints ***Final Report***
Fox, D. E., NASA Marshall Space Flight Center, USA; Swaim, K. W., NASA Marshall Space Flight Center, USA; September 1999; 32p; In English
Contract(s)/Grant(s): Proj. 95-07
Report No.(s): NASA/TM-1999-209735; M-947; NAS 1.15:209735; No Copyright; Avail: CASI; A03, Hardcopy; A01, Microfiche

The analysis of mechanically fastened composite joints presents a great challenge to structural analysts because of the large number of parameters that influence strength. These parameters include edge distance, width, bolt diameter, laminate thickness, ply orientation, and bolt torque. The research presented in this report investigates the influence of some of these parameters through testing and analysis. A methodology is presented for estimating the strength of the bolt-hole based on classical lamination theory using the Tsai-Hill failure criteria and typical bolthole bearing analytical methods.
Author
Static Characteristics; Failure; Estimating; Joints (Junctions)

19990113142 SAQ Kontroll A.B., Stockholm, Sweden
Effect of Thermal and Weld-Induced Residual Stresses on the J-Integral and CTOD in Elastic-Plastic Fracture Analyses
Delfin, P.; Sattari–Far, I.; Brickstad, B.; 1999; ISSN 1401-5331; 54p; In English
Report No.(s): PB99-173981; SAQ/FOU-97/02; No Copyright; Avail: CASI; A01, Microfiche; A04, Hardcopy

An investigation of how the residual stress of a welded pipe contributes to the CTOD and the J-integral has been performed. Many experiments show that for ductile materials and high L(sub r) values the contribution from the residual stress to the risk of fracture is negligible. The objective of the present numerical analyses is to investigate how the weld residual stresses interact with other types of stresses and if possible give some recommendations on how to treat weld residual stresses in fracture assessments. The welding process has been simulated according to generally accepted methods in order to obtain a proper plastic strain field. The results imply that although the relative contribution of the residual stress to fracture decreases rapidly for high L(sub r), the residual stress still makes a contribution even for quite high loads.
NTIS
Welding; Residual Stress; Thermal Stresses; Structural Analysis; Elastic Properties; Plastic Properties; J Integral; Crack Opening Displacement

42
GEOSCIENCES (GENERAL)

19990107362 New Mexico State Univ., Water Resources Research Inst., Las Cruces, NM USA
Proceedings of the Annual New Mexico Water Conference
Mar. 1999; 166p; In English; 43rd; Water Challenges on the Lower Rio Grande, 22-23 Oct. 1998, Las Cruces, NM, USA
Report No.(s): PB99-169096; WRRI-310; No Copyright; Avail: CASI; A02, Microfiche; A08, Hardcopy

The 43rd Annual New Mexico Water Conference was held in Las Cruces, New Mexico on October 22-23, 1998. The Proceedings contain all papers delivered at the conference. Topics include: Transfer of irrigation water to municipal and industrial sue; a review of the Rio Grande Compact; regional water planning; evolution of the Rio Grande; New Mexico/Texas Water Commission update; hydrographic survey of the Lower Rio Grande; groundwater modeling in the Lower Rio Grande; removal of arsenic compounds from natural water sources; effects of fire on the distribution of mercury in sediments of a reservoir; aquifer sensitivity assessment for the Mesilla Valley; concentration of viral particles from water by ultrafiltration; an assay for toxic chemicals using microorganisms; New Mexico legislative agenda for 1999; and water quality on the Lower Rio Grande.
NTIS
Water Resources; Ground Water; Aquifers; Surface Water; Irrigation; Toxicity; Conferences; Water Management; Water Pollution

19990108601 NASA Marshall Space Flight Center, Huntsville, AL USA
11th International Conference on Atmospheric Electricity
Christian, H. J., Compiler, NASA Marshall Space Flight Center, USA; 11th International Conference on Atmospheric Electricity; June 1999; 797p; In English; Sponsored by NASA Marshall Space Flight Center, USA; See also 19990108602 through 19990108794

Report No.(s): NASA/CP-1999-209261; M-923; NAS 1.55:209261; No Copyright; Avail: CASI; A99, Hardcopy; A10, Microfiche

This document contains the proceedings from the 11th International Conference on Atmospheric Electricity (ICAE 99), held June 7-11, 1999. This conference was attended by scientists and researchers from around the world. The subjects covered included natural and artificially initiated lightning, lightning in the middle and upper atmosphere (sprites and jets), lightning protection and safety, lightning detection techniques (ground, airborne, and space-based), storm physics, electric fields near and within thunderstorms, storm electrification, atmospheric ions and chemistry, shumann resonances, satellite observations of lightning, global electrical processes, fair weather electricity, and instrumentation.

Author

Atmospheric Composition; Conferences; Electric Fields; Electrification; Lightning; Thunderstorms; Atmospheric Electricity; Cloud Physics; Atmospheric Chemistry

19990109669 NASA Goddard Space Flight Center, Greenbelt, MD USA

A Constellation of Microsatellites Promises to Help in a Range of Geoscience Research

Kuo, Y. H., University Corp. for Atmospheric Research, USA; Chao, B. F., NASA Goddard Space Flight Center, USA; Lee, L. C., National Space Program Office, Taiwan, Province of China; [1999]; 13p; In English; No Copyright; Avail: CASI; A03, Hardcopy; A01, Microfiche

An octet of microsatellites to be launched in 2003 promises to deliver a large amount of useful data for meteorological, climatic, ionospheric, and geodetic research as well as for operational weather forecasting and space weather monitoring. Known as the Constellation Observing System for Meteorology, Ionosphere, and Climate (COSMIC), the joint Taiwan-U.S. scientific satellite project makes use of Global Positioning System (GPS) occultation and tracking signals. COSMIC's final operational configuration is depicted in Figure 1. Each of the eight microsatellites in low-Earth-orbit (LEO, shown relative to the high-altitude GPS satellite orbits) will carry in particular an advanced limb-sounding GPS receiver, a Tiny Ionospheric Photometer, and a triband beacon transmitter.

Derived from text

Constellations; Meteorology; Climatology; Global Positioning System; Scientific Satellites; Space Weather; Weather Forecasting

19990110600 Meteorological Satellite Center, Kiyose, Japan

Meteorological Satellite Center Technical Note, No. 37

March 1999; ISSN 0388-9653; 82p; In Japanese; See also 19990110601 through 19990110604; Original contains color illustrations; No Copyright; Avail: CASI; A05, Hardcopy; A01, Microfiche

This note contains papers in the subject area of meteorology. Titles include: Image pre-processing algorithm for MTSAT; Improvement of the derivative method of sea surface temperature from GMS-5 Data; The features of the extratropical cyclones passing through around Japan; and Detection of fog and low level clouds in the nighttime using near-infrared imageries (3.7 micrometers).

CASI

Meteorological Satellites; Meteorology; Infrared Photography; Satellite Observation; Weather Stations

19990111490 NASA Goddard Space Flight Center, Greenbelt, MD USA

NASA/NOAA/AMS Earth Science Electronic Theater

Hasler, Fritz, NASA Goddard Space Flight Center, USA; 1999; 1p; In English; Satellites and Education, 10 Mar. 1999, West Chester, PA, USA; No Copyright; Avail: Issuing Activity, Hardcopy; Abstract Only

Selections from the following very large Earth science observed & simulated datasets shown from: Historical: GOES-10 & AVHRR, SeaWIFS, TRMM, Meteosat, GMS, FY2, and ADEOS. and Simulated: EOS-AM1, LANDSAT 7, Astrovision, and 3D numerical storm model. Also highlights of the 1998 Hurricane & Severe Storm Seasons will be reviewed. A spectacular animations of La Nina season hurricanes: Bonnie, Georges, etc. 5000 frame 5-min GOES 10 continuous 28 day animation of the'98 Spring tornadic thunderstorm season and other special GOES test datasets will be shown.

Derived from text

Earth Sciences; Hurricanes; Remote Sensing; Sea Surface Temperature; Three Dimensional Models; Thunderstorms; Tornadoes

19990113071 Forest Service, Pacific Northwest Research Station, Portland, OR USA

Forest Ecosystem Study: Background, Rationale, Implementation, Baseline Conditions and Silvicultural Assessment

Carey, A. B.; Thysell, D. R.; Brodie, A. W.; May 1999; 144p

Report No.(s): PB99-157299; FSGTR-PNW-457; No Copyright; Avail: CASI; A07, Hardcopy; A02, Microfiche

The Forest Ecosystem Study (FES) came about as an early response to the need for innovative silvicultural methods designed to stimulate development of late-successional attributes in managed forests-a need ensuing from the exceptional and long-standing controversies over old-growth forests and endangered species concerns in the Pacific Northwest. In 1991, scientists with the FES applied experimental, variable-density thinning to even-aged Douglass-fir (Pseudotsuga menziesii (Mirbel) (Franco) forests on the Fort Lewis Military Reservation in western Washington after having first accumulated extensive baseline data on arboreal rodents, small mammals, trees and other vascular plants, and fungi. Since thinning, further research elements have been incorporated into the FES, including top rot fungal inoculation and soil food web response to thinnings, in addition to the ongoing prey base, vegetation, fungal and silvicultural assessment investigations. The authors present study background, rationale, baseline conditions, and selected preliminary responses, as well as silvicultural assessment of the variable-density thinning.

NTIS

Ecosystems; Forest Management; Ecology

43
EARTH RESOURCES AND REMOTE SENSING

Includes remote sensing of earth resources by aircraft and spacecraft; photogrammetry; and aerial photography. For instrumentation see 35 Instrumentation and Photography.

19990106562 Instituto Nacional de Pesquisas Espacias, Sao Jose dos Campos, Brazil

Hyperspectral Remote Sensing for Mineral Characterization and Identification in Tropical Soils ***Sensoriamento Remoto Hiperespectral Para a Caracterizacao e Identificacao Mineral em Solos Tropicais***

Pizarro, Marco Antonio, Instituto Nacional de Pesquisas Espacias, Brazil; 1999; 200p; In Portuguese

Report No.(s): INPE-7249-TDI/693; No Copyright; Avail: CASI; A09, Hardcopy; A03, Microfiche

The objective of this work was to evaluate the use of the data generated by the imaging spectrometer Airborne Visible/InfraRed Imaging Spectrometer (AVIRIS) during the mission Smoke, Sulfate, Clouds, and Radiation - Brazil (SCAR-B), in the period of August to September of 1995, for the spectral characterization and mineral identification in soils. The study area was near Campo Grande (MS) city, Brazil. The AVIRIS data were converted from radiance values to surface reflectance through a method of atmospheric correction based on the MODTRAN radiative transfer model. In order to make the spectral analysis of the soil characteristics and to discriminate the main types of soils present in the area, Principal Components Analysis (PCA) was applied on the AVIRIS data. PCA reduced the high dimensionality of AVIRIS data. AVIRIS spectral data were compared to laboratory IRIS (InfraRed Intelligent Spectroradiometer) data of 18 soil samples. Correlation analysis, derivative analysis and the calculation of Normalized Difference Vegetation Index (NDVI), were applied for both laboratory and AVIRIS data. Finally, the Spectral Feature Fitting, (SFF) technique was used for the identification of some minerals in the AVIPIS scene. The main minerals studied were from the group of the iron oxides (hematite and goethite) and from the group of the clays (kaolinite, montmorillonite and gibbsite). The main results were: (a) the soil classes Podzolico Vermielho-Amarelo (PV, Arenica Abruptic Paleudult), Latossolo Vermelho-Escuro (LE, Typic Haplorthox) and Latossolo Roxo (LR, Typic Acrorthox) could be discriminated, mainly, in function of their albedo (first Principal Component - PC). The variation in the shape of the spectra, associated with PC2 and PC3, allowed the discrimination of PV in relation to LR and LE; (b) the relationships among the laboratory (IRIS) and field (AVFRIS) spectra reflected the inherent differences between both data sources mainly due to the influence of the atmosphere; c) the pixel contamination by residues of photosynthetic or non-photosynthetic vegetation affected the correlations between the two groups of data, especially in the 500-1,220 nm spectral region; and (d) the soils in the studied area are spectrally dominated by the presence of hematite and kaolinite, according to the results obtained from the use of the SFF technique. The results showed the potential of imaging spectroscopy in characterizing the albedo variations, shapes of the spectra and mineral absorption. Thus, by using this approach, it was possible to discriminate different tropical soil classes and to identify surface materials on a pixel basis.

Author

Characterization; Clays; Contamination; Emission Spectra; Imaging Techniques; Kaolinite; Remote Sensing; Soil Sampling; Minerals; Tropical Regions; Vegetation

19990106568 NASA Goddard Space Flight Center, Greenbelt, MD USA

An Overview of Future NASA Missions, Concepts, and Technologies Related to Imaging of the World's Land Areas

Salomonson, Vincent V., NASA Goddard Space Flight Center, USA; [1999]; 1p; In English; Pecora 14 Land Satellite Information

III Conference, 6-10 Dec. 1999, Denver, CO, USA; No Copyright; Avail: Issuing Activity, Hardcopy; Abstract Only

In the near term NASA is entering into the peak activity period of the Earth Observing System (EOS). The EOS AM-1 /"Terra" spacecraft is nearing launch and operation to be followed soon by the New Millennium Program (NMP) Earth Observing (EO-1) mission. Other missions related to land imaging and studies include EOS PM-1 mission, the Earth System Sciences Program (ESSP) Vegetation Canopy Lidar (VCL) mission, the EOS/IceSat mission. These missions involve clear advances in technologies and observational capability including improvements in multispectral imaging and other observing strategies, for example, "formation flying". Plans are underway to define the next era of EOS missions, commonly called "EOS Follow-on" or EOS II. The programmatic planning includes concepts that represent advances over the present LANDSAT-7 mission that concomitantly recognize the advances being made in land imaging within the private sector. The National Polar Orbiting Environmental Satellite Series (NPOESS) Preparatory Project (NPP) is an effort that will help to transition EOS medium resolution (herein meaning spatial resolutions near 500 meters), multispectral measurement capabilities such as represented by the EOS Moderate Resolution Imaging Spectroradiometer (MODIS) into the NPOESS operational series of satellites. Developments in Synthetic Aperture Radar (SAR) and passive microwave land observing capabilities are also proceeding. Beyond these efforts the Earth Science Enterprise Technology Strategy is embarking efforts to advance technologies in several basic areas: instruments, flight systems and operational capability, and information systems. In the case of instruments architectures will be examined that offer significant reductions in mass, volume, power and observational flexibility. For flight systems and operational capability, formation flying including calibration and data fusion, systems operation autonomy, and mechanical and electronic innovations that can reduce spacecraft and subsystem resource requirements. The efforts in information systems will include better approaches for linking multiple data sets, extracting and visualizing information, and improvements in collecting, compressing, transmitting, processing, distributing and archiving data from multiple platforms. Overall concepts such as sensor webs, constellations of observing systems, and rapid and tailored data availability and delivery to multiple users comprise and notions Earth Science Vision for the future.

Author

NASA Programs; Optical Radar; Earth Observing System (EOS); LANDSAT 7; Remote Sensing

19990106585 Instituto Nacional de Pesquisas Espacias, Sao Jose dos Campos, Brazil

Classification and Monitoring Vegetation Cover of Mato Grosso State Using NOAA-AVHRR Images ***Classificacao e Monitoramento da Cobertura da Cobertura Vegetal do Estado de Mato Grosso Atraves de Imagens NOAA-AVHRR***

Shimabukuro, Yosio Edemir, Instituto Nacional de Pesquisas Espacias, Brazil; Yi, Jose Luis Rodriques, Instituto Nacional de Pesquisas Espacias, Brazil; Duarte, Valdete, Instituto Nacional de Pesquisas Espacias, Brazil; 1999; 92p; In Portuguese

Report No.(s): INPE-7234-RPQ/698; No Copyright; Avail: CASI; A05, Hardcopy; A01, Microfiche

The objective of this report is to classify and monitor the vegetation cover of Mato Grosso state, using a series of multitemporal images from the Advanced Very High Resolution Radiometer (AVHRR) sensor on board of NOAA-11 (National Oceanographic and Atmospheric Administration) satellite. Initially, the period from August 1992 to August 1994 was defined to select the images to be analyzed in this study. This period corresponds to latest years of NOAA-11 satellite operation. Due to difficulties in acquiring images, during this period, from INPE's Cachoeira Paulista receiving station, images acquired during 1989 were also used and provided by NASA/Goddard Space Flight Center. These images were processed using the "GMS" software available at NASA, generating images corresponding to the original AVHRR spectral bands (I to 5) and the transformed vegetation index (NDVI) derived from bands I and 2. In addition, bands I and 2 were used in the spectral linear mixing model algorithm to generate 3 new bands named: vegetation, soil, and shade. The methodology presents the procedures to acquire, process and analyze AVHRR images. The results show the usefulness of this type of information to map vegetation cover on a regional level, and to study seasonal variation of vegetation cover classes.

Author

Annual Variations; Oceanography; Vegetation; Image Classification

19990106589 Instituto Nacional de Pesquisas Espacias, Sao Jose dos Campos, Brazil

Evaluation of the Conversion from Forest to Pasture Land in Amazon using Remote Sensing and the Soil Fertility ***Avaliacao da Conversao de Floresta para Pastagem na Amazonia Usando Sensoriamento Remoto e a Fertilidade do Solo***

Numata, Izaya, Instituto Nacional de Pesquisas Espacias, Brazil; 1999; 110p; In Portuguese; Original contains color illustrations

Report No.(s): INPE-7232-TDI/696; No Copyright; Avail: CASI; A06, Hardcopy; A02, Microfiche

The study deals with the variation of soil fertility on pasture land with time (four classes of age) in a region of the State of Rondonia. Adjacent areas were also surveyed for comparison A remote sensing method was developed for the identification of the classes of age (since conversion from forest into pasture) through the multitemporal analysis, using shade fraction images, generated by a linear mixture model techniques derived from TM images obtained during the period 1987 - 1997. Based on the

results of these methods, four sites were established for soil sampling. Three of these sites belong to the class ”Podz6lico Vennelho-Amarelo” (PVA - Ultissol), and the other to the ”Podz6lico Vermelho-Escuro” (PE - Alfissol). The soil samples were collected at the depth of 20 cm and fertility and granulometric analysis were carried out. From these analysis, pH, exchangeable bases, available phosphorus, aluminum and base saturation and organic matter were obtained. The results allowed to identify two principal phases of the dynamic behavior of soil fertility in pasture-. 1) the dramatic increase of the fertility level, as well as reduction in aluminum saturation in the five first years after the pasture installation, caused by the ash addition derived from the forest burning and vegetal residue; 2) the decline of fertility, after reaching to the peak. The trend of the stabilizing or the reducing of velocity of the decline on the fertility level also was noticed after the period of more than 10 years as pasture. Two different behaviors were observed on these two types of soil. For PVA soil class, with low natural fertility, the level kept higher in the pasture land even more than 10 years of use, than the one found in the forest land. On the other hand, for PE, soil of high fertility in natural conditions, the fertility level became lower then the original, after more than 10 years of land use with pasture. This is probably due to the leaching of nutrient and the erosion associated to the lower clay amount of this soil and the local topography. About the available phosphorous, however, the same trend was observed in both soil classes. The rapid decline was verified after the peak and its level became very close to the one found in the forest area, after more than 10 years of use with pasture.
Author
Evaluation; Amazon Region (South America); Ashes; Dynamic Characteristics; Erosion; Forests; Grasslands; Soil Sampling; Topography

19990106599 NASA Goddard Space Flight Center, Greenbelt, MD USA
Estimates of Long Term Surface Soil Moisture in the Midwestern U.S. Derived from Satellite Microwave Observations
Owe, M., NASA Goddard Space Flight Center, USA; deJeu, R., NASA Goddard Space Flight Center, USA; VandeGriend, A. A., NASA Goddard Space Flight Center, USA; Ag, R. J., Vrije Univ., Netherlands; [1999]; 1p; In English; Sponsored by Electro-Optical Systems, Inc., USA; No Copyright; Avail: Issuing Activity, Hardcopy; Abstract Only

Soil moisture is a key component of the water and energy balances of the Earth’s surface, and has been identified as a parameter of significant potential for improving the accuracy of large-scale land surface-atmosphere interaction models. However, soil moisture is often somewhat difficult to measure accurately in both space and time, especially at large spatial scales. Soil moisture is highly variable, and while point measurements are typically quite accurate, subsequent areal averaging of these measurements often leads to large errors. Since remotely sensed land surface observations are already a spatially averaged or areally integrated value, they are a logical input parameter to regional or larger scale land process models. A database of long-term soil moisture was compared to satellite microwave observations over test sites in the Midwestern USA. Ground measurements of average volumetric surface soil moisture in the top ten cm were made bimonthly at 19 locations throughout the state of Illinois. Nighttime microwave brightness temperatures were observed at a frequency of 6.6 GHz, by the Scanning Multichannel Microwave Radiometer (SMMR), onboard the Nimbus 7 satellite. The life of the SMMR instrument spanned from Nov. 1978 to Aug. 1987. At 6.6 GHz, the instrument provided a spatial resolution of approximately 150 km, and a temporal frequency over the test area of about 3 nighttime orbits per week. Vegetation radiative transfer characteristics, such as the canopy transmissivity, were estimated from vegetation indices such as the Normalized Difference Vegetation Index (NDVI) and the 37 GHz Microwave Polarization Difference Index (MPDI). Because the time of satellite coverage does not always coincide with the ground measurements of soil moisture, the existing ground data were used to calibrate a water balance for the top IO cm surface layer in order to interpolate daily surface moisture values. Such a climate-based approach is often more appropriate for estimating large-area average soil moisture because meteorological data are generally more spatially representative than isolated point measurements of soil moisture, Passive microwave remote sensing presents the greatest potential for providing regular spatially representative estimates of surface soil moisture at global scales. Real time estimates should improve weather and climate modelling efforts, while the development of historical data sets will provide necessary information for simulation and validation of long-term climate and global change studies.
Author
Atmospheric Models; Climate Change; Data Acquisition; Microwave Imagery; Microwave Radiometers; Remote Sensing; Soil Moisture; Surface Layers; Water Balance

19990106600 NASA Goddard Space Flight Center, Greenbelt, MD USA
Remote Sensing for Agriculture, Ecosystems and Hydrology III
Engman, Edwin T., NASA Goddard Space Flight Center, USA; [1999]; 2p; In English; Remote Sensing, 20-24 Sep. 1999, Florence, Italy; Sponsored by Electro-Optical Systems, Inc.; No Copyright; Avail: Issuing Activity, Hardcopy; Abstract Only

The science need for remotely sensed soil moisture has been well established in the hydrologic, climate change and weather forecasting communities. In spite of this well documented science need there are currently no satellite missions flying or funded

to make this very important geophysical measurement. There have been a number of experimental aircraft programs that have demonstrated the feasibility of using long wave microwave sensors for estimating soil moisture. Unfortunately, this science driver, soil moisture, imposes very difficult technical requirements for a satellite sensor system. Global soil moisture is driven by a spatial resolution on the order of 20 to 30 km and measurements need to be taken every two to three days to be useful to the science community. The principal sensor to accomplish the soil moisture measurements is an L- band passive microwave radiometer and achieving the spatial and temporal requirements requires a very large antenna. This paper describes the several alternatives to solve the very large antenna challenge and still meet the radiometer sensitivity requirement. The paper also discusses the alternatives considered to obtain the necessary ancillary data for characterizing the surface roughness, the surface temperature and the attenuation affects of vegetation needed to derive the geophysical parameter. Finally, the paper discusses proposed missions and how well they will meet the science requirements.
Author
Soil Moisture; Agriculture; Climate Change; Ecosystems; Hydrology; Microwave Sensors; Remote Sensing; Spatial Resolution

19990108576 NASA Goddard Space Flight Center, Greenbelt, MD USA
Physics Based Modeling and Rendering of Vegetation in the Thermal Infrared
Smith, J. A., NASA Goddard Space Flight Center, USA; Ballard, J. R., Jr., Corps of Engineers, USA; [1999]; 5p; In English; Computer Vision and Pattern Recognition, 20-25 Jun. 1999, Fort Collins, CO, USA; Sponsored by Institute of Electrical and Electronic Engineers, USA; No Copyright; Avail: CASI; A01, Hardcopy; A01, Microfiche

We outline a procedure for rendering physically-based thermal infrared images of simple vegetation scenes. Our approach incorporates the biophysical processes that affect the temperature distribution of the elements within a scene. Computer graphics plays a key role in two respects. First, in computing the distribution of scene shaded and sunlit facets and, second, in the final image rendering once the temperatures of all the elements in the scene have been computed. We illustrate our approach for a simple corn scene where the three-dimensional geometry is constructed based on measured morphological attributes of the row crop. Statistical methods are used to construct a representation of the scene in agreement with the measured characteristics. Our results are quite good. The rendered images exhibit realistic behavior in directional properties as a function of view and sun angle. The root-mean-square error in measured versus predicted brightness temperatures for the scene was 2.1 deg C.
Author
Models; Vegetation; Infrared Radiation; Infrared Imagery; Remote Sensing; Vegetative Index; Vegetation Growth; Corn

19990108599 NASA Goddard Space Flight Center, Greenbelt, MD USA
Radiometric Measurement Comparisons Using Transfer Radiometers in Support of the Calibration of NASA's Earth Observing System (EOS) Sensors
Butler, James J., NASA Goddard Space Flight Center, USA; Johnson, B. Carol, National Inst. of Science and Technology, USA; Brown, Steven W., National Inst. of Science and Technology, USA; Yoon, Howard W., National Inst. of Science and Technology, USA; Barnes, Robert A., Science Applications International Corp., USA; Markham, Brian L., NASA Goddard Space Flight Center, USA; Biggar, Stuart F., Arizona Univ., USA; Zalewski, Edward F., Arizona Univ., USA; Spyak, Paul R., Arizona Univ., USA; Cooper, John W., Raytheon STX Corp., USA; Sakuma, Fumihiro, National Research Lab. of Metrology, Japan; [1999]; 13p; In English; Proceedings of EUROPTO 1999, 22 Sep. 1999, Florence, Italy; Sponsored by International Society for Optical Engineering, USA; No Copyright; Avail: CASI; A03, Hardcopy; A01, Microfiche

EOS satellite instruments operating in the visible through the shortwave infrared wavelength regions (from 0.4 micrometers to 2.5 micrometers) are calibrated prior to flight for radiance response using integrating spheres at a number of instrument builder facilities. The traceability of the radiance produced by these spheres with respect to international standards is the responsibility of the instrument builder, and different calibration techniques are employed by those builders. The National Aeronautics and Space Administration's (NASA's) Earth Observing System (EOS) Project Science Office, realizing the importance of preflight calibration and cross-calibration, has sponsored a number of radiometric measurement comparisons, the main purpose of which is to validate the radiometric scale assigned to the integrating spheres by the instrument builders. This paper describes the radiometric measurement comparisons, the use of stable transfer radiometers to perform the measurements, and the measurement approaches and protocols used to validate integrating sphere radiances. Stable transfer radiometers from the National Institute of Standards and Technology, the University of Arizona Optical Sciences Center Remote Sensing Group, NASA's Goddard Space Flight Center, and the National Research Laboratory of Metrology in Japan, have participated in these comparisons. The approaches used in the comparisons include the measurement of multiple integrating sphere lamp levels, repeat measurements of select lamp levels, the use of the stable radiometers as external sphere monitors, and the rapid reporting of measurement results. Results from several comparisons are presented. The absolute radiometric calibration standard uncertainties required by the EOS satellite instruments are typically in the +/- 3% to +/- 5% range. Preliminary results reported during eleven radiometric

measurement comparisons held between February 1995 and May 1998 have shown the radiance of integrating spheres agreed to within +/- 2.5% from the average at blue wavelengths and to within +/- 1.7% from the average at red and near infrared wavelengths. This level of agreement lends confidence in the use of the transfer radiometers in validating the radiance scales assigned by EOS instrument calibration facilities to their integrating sphere sources.
Author
Calibrating; Cross Correlation; Radiance; Radiometers; Radiation Measurement

19990108841 Instituto Nacional de Pesquisas Espacias, Sao Jose dos Campos, Brazil
The Radiation Balance over Forest and Pasture in Amazonia ***Estudo do Balanco de Radiacao em Areas de Floresta e Pastagem na Amazonia***
daCostaGalvao, Jose Alexandre, Instituto Nacional de Pesquisas Espacias, Brazil; 1999; 130p; In Portuguese; Original contains color illustrations
Report No.(s): INPE-7236-TDI/689; No Copyright; Avail: CASI; A07, Hardcopy; A02, Microfiche

Micrometeorological observations of the Anglo-Brazilian Amazonian Climate Study (ABRACOS) have been used to study the surface balance radiation, to test the validity of several methods used for estimating of the long-wave atmospheric radiation flux and surface balance energy behaviour of paired forest and pasture sites at Ji-Parana (RO) during the end of the wet season and the start of the dry season of 1993. The performance of 5 methods for estimating the long-wave atmospheric radiation flux (L(sub d)) were tested for a pasture site in Amazon. However, the estimates of L(sub d) from these methods underestimate the L(sub d) values, when compared to the measurements. The root 2 mean square error ranges from 50.7 to 75.2 W/sq m. The values of the mean bias error are negative and range from -73.0 to -49.1 W/sq m. This can be associated to the coefficients used by empirical equations, since they are specific to the place in which they had been developed. A local adjustment of these coefficients were made. Thus, much better estimates of L(sub d) were obtained by methods in which the emissivity is only function of the temperature. The statistical tests of the adjusted equations show correlation coefficients near of unit, smaller values of root mean square error and mean bias error near to zero. The balance energy were considered and the results show that during the wet period, the transfer of energy to atmosphere is done mainly by the latent heat flux, which used 0.79 of the net radiation (LE/R(sub n)) at the forest site and 0.65 at the pasture site. The corresponding values to heat the atmosphere (H/R(sub n)) were 0,17 at the forest site and 0.20 at the pasture site. In the dry period, the forest continue to use most of the energy to evaporation and less energy to heat to the air. At the pasture the transfer of energy to atmosphere is made likely by latent heat flux and sensible heat flux, mainly between 11 e 14 Local Hour (LH). During a ”friagem” event, the transfer of energy to atmosphere is done mainly by latent heat flux (before the friagem crosses the region), which used 0.79 of the net radiation (LE/R(sub n)) at the forest and 0.71 at the pasture site. When the ”friagem” is crossing the sites, the ratio LE/R, is greater than 1 at the forest site and 0.88 at the pasture site. After the ”friagem” has crossed the area, the values of the ratio LE/R(sub n) and H/R(sub n) at the forest and pasture sites return to the characteristic pre-friagem values. In the case of the fog, the transfer of energy to atmosphere is also done mainly by latent heat flux, and the values of Bowen ratio were positives until 9 LH.
Author
Amazon Region (South America); Atmospheric Radiation; Energy Budgets; Flux Quantization; Forests; Statistical Tests; Long Wave Radiation

19990110589 Instituto Nacional de Pesquisas Espacias, Sao Jose dos Campos, Brazil
Tabu Search Application for Point Features Cartographic Label Placement Problem ***Uma Aplicacao da Busca Tabu ao Problema de Rotulacao Cartografica de Pontos***
Yamamoto, Missae, Instituto Nacional de Pesquisas Espacias, Brazil; 1999; 136p; In Portuguese
Report No.(s): INPE-7520-TDI/694; No Copyright; Avail: CASI; A07, Hardcopy; A02, Microfiche

The generation of better label placement configurations in maps is a problem that comes up in automated cartographic production. The objective of a good label placement is to show the geographic position of the features with their corresponding texts clearly, respecting the cartographic conventions, with an esthetic and a harmonious quality when presenting the information. We approached the label placement problem from a combinatorial optimization point of view. In this perspective, the cartographic label placement belongs to a problem area of difficult solution, leading us to the need of approximation algorithms as there is no exact algorithm that is able to solve this problem within an acceptable amount of time. Our research consisted in the evaluation of the tabu search optimization algorithm applied to cartographic label placement. The tabu search implemented in SCARTA, a cartographic production software, in development by the Image Processing Division of the National Institute of Aerospace Researches, proved to be an efficient algorithm, in real and random test cases. When compared with alternative techniques such as ”simulated annealing”, genetic algorithm with mask and others described in literature, the tabu search had the best performance in quality. We concluded that tabu search is a recommended method to solve cartographic label placement problem of point

features, due to its simplicity, practicality, efficiency and good performance along with its ability to generate quality solutions in acceptable computational time.
Author
Genetic Algorithms; Image Processing; Mapping; Computer Programming

19990110601 Meteorological Satellite Center, Kiyose, Japan
Image Pre-Processing Algorithm for MTSAT
Kigawa, Seiichiro, Meteorological Satellite Center, Japan; Meteorological Satellite Center Technical Note; March 1999, No. 37, pp. 1-18; In Japanese; See also 19990110600; No Copyright; Avail: CASI; A03, Hardcopy; A01, Microfiche

Image Pre-processing for MTSAT (Multi-functional Transport Satellite) is designed to process image navigation and calibration for Imager data. The Image Pre-processing introduces autonomous real-time navigation and calibration to improve the accuracy of the image navigation and calibration. Image Pre-processing system consists of two Image Pre-processing Equipment (IPPE), one Quality Analysis Unit (QA Unit), and two image analysis terminals. This note describes the algorithm of the image pre-processing system.
Author
Image Processing; Image Analysis; Imaging Techniques; Image Reconstruction; Algorithms

19990110602 Meteorological Satellite Center, Kiyose, Japan
Improvement of the Derivation Method of Sea Surface Temperature from GMS-5 Data
Yasuda, Hiroaki, Meteorological Satellite Center, Japan; Shirakawa, Yoshishige, Meteorological Satellite Center, Japan; Meteorological Satellite Center Technical Note; March 1999, No. 37, pp. 19-33; In Japanese; See also 19990110600; No Copyright; Avail: CASI; A03, Hardcopy; A01, Microfiche

In Meteorological Satellite Center, the sea surface temperature (SST) is derived for the area from 60 degrees North to 60 degrees South and from 80 degrees East to 160 degrees West with the spatial resolution of 0.25 degrees latitude by 0.25 degrees longitude for every 3 hours by using the observation data of GMS. Since the start of the operation of GMS-5 in June 1995, SST has been derived by using the Multi-Channel Sea Surface Temperature (MCSST) retrieval algorithm which was originally developed by NOAA/NESDIS and adapted for GMS-5 sensors. We made some modifications in the algorithm, and the new algorithm has been used for the SST derivation since August 1997. The points of modification are as follows. 1) The cloud screening in the new algorithm is carried out by using both the multi-channel method and the histogram method. 2) SST calculated from NLSST (Non-Linear SST) retrieval equation, which was developed by NOAA/NESDIS, is used in the quality check. 3) In addition to the climate SST data, the objective analysis data of the satellite derived SST and those of the daily SST [produced by Climate and Marine Department of JMA] are available for the quality check. The accuracy of the SST derived from the new algorithm has improved about 0.3K in RMS (root mean square difference from the in situ ocean buoy data), compared with that from the former algorithm.
Author
Meteorological Satellites; Meteorology; Satellite Observation; Climate; Sea Surface Temperature; Algorithms

19990111518 NASA Goddard Space Flight Center, Greenbelt, MD USA
Remote Sensing May Provide Unprecedented Hydrological Data
Koster, R., NASA Goddard Space Flight Center, USA; Houser, P., NASA Goddard Space Flight Center, USA; Engman, E., NASA Goddard Space Flight Center, USA; Kustas, W., NASA Goddard Space Flight Center, USA; [1999]; 1p; In English; No Copyright; Avail: Issuing Activity, Hardcopy; Abstract Only

Basic hydrological research and water resources management may reap tremendous benefits from remote sensing technology, studies are showing. Satellite coverage may allow unprecedented accuracy in the quantification of the global hydrological cycle, for example. Yet despite such benefits, few hydrologists currently use such data. This is partly because the needed tools and algorithms are not fully developed. Such development requires field experiments that combine remotely sensed data with detailed in situ observations. AGU's Remote Sensing in Hydrology Committee has constructed a Web site (http://land.gsfc.nasa.gov/RSHC.html) that gives an overview of many such experiments. Included on the site is information on each experiment's overall goal, the types of in situ and remotely sensed measurements taken, relevant climate and vegetation conditions, and so forth. Links to additional relevant Web sites are included. The site is designed to be a suitable starting point for those interested in learning more about remote sensing in hydrology. It lists members of the committee who can be contacted for further information. Hydrologists have recognized the potential of remote sensing technology since the 1970s. It offers a way to avoid the logistical and economic difficulties associated with obtaining continuous in situ measurements of various hydrological variables, difficulties that are particularly pronounced in remote regions. Microwave instruments in particular can

potentially provide all-weather, areally averaged estimates of certain variables (such as precipitation, soil moisture, and snow water content) that have been essentially unattainable in the past. In remote sensing, the conversion of emitted and reflected radiances into useful hydrological data is a complex problem. The measured radiances, for example, reflect the integrated character of a pixel area, a scale inconsistent with the point measurements of traditional hydrology. To develop the needed algorithms, field experiments must be designed that combine relevant satellite measurements with traditional in situ measurements in regions that are al- ready well understood hydrologically. Such field experiments can lead to the development of hydrological models that are driven with remotely sensed data. Once the performance of these models is deemed acceptable in the heavily monitored basins, they can be ”transported” for use in regions having little or no in situ measurement system. Author,5: Randal D. Koster, Paul R. Houser and Edwin T. Engman, Hydrological Sciences Branch, Laboratory for Hydrospheric Process, NASA Goddard Space Flight Center, Greenbelt, Maryland, USA; William P. Kustas, Hydrology Laboratory, Agricultural Research Service, U.S. Department of Agriculture, Beltsville, Maryland, USA.
Author
Remote Sensing; Hydrological Cycle; Water Resources; Management; Resources Management; In Situ Measurement

19990113113 Colorado Univ., Boulder, CO USA
Hyperspectral Imaging and Related Field Methods: Building the Science ***Final Report***
Goetz, Alexander F. H., Colorado Univ., USA; Steffen, Konrad, Colorado Univ., USA; Wessman, Carol, Colorado Univ., USA; [1999]; 17p; In English
Contract(s)/Grant(s): NAG5-6651; No Copyright; Avail: CASI; A03, Hardcopy; A01, Microfiche

The proposal requested funds for the computing power to bring hyperspectral image processing into undergraduate and graduate remote sensing courses. This upgrade made it possible to handle more students in these oversubscribed courses and to enhance CSES’ summer short course entitled ”Hyperspectral Imaging and Data Analysis” provided for government, industry, university and military. Funds were also requested to build field measurement capabilities through the purchase of spectroradiometers, canopy radiation sensors and a differential GPS system. These instruments provided systematic and complete sets of field data for the analysis of hyperspectral data with the appropriate radiometric and wavelength calibration as well as atmospheric data needed for application of radiative transfer models. The proposed field equipment made it possible to team-teach a new field methods course, unique in the country, that took advantage of the expertise of the investigators rostered in three different departments, Geology, Geography and Biology.
Author
Global Positioning System; Image Processing; Imaging Techniques; Radiative Transfer; Spectroradiometers

19990113193 NASA Marshall Space Flight Center, Huntsville, AL USA
Multi-Scale Fractal Analysis of Image Texture and Pattern
Emerson, Charles W., Southwest Missouri State Univ., USA; Quattrochi, Dale A., NASA Marshall Space Flight Center, USA; Luvall, Jeffrey C., NASA Marshall Space Flight Center, USA; [1997]; 1p; In English; 1998 Association of American Geographers, 25-29 Mar. 1998, Boston, MA, USA; Copyright; Avail: Issuing Activity; Abstract Only, Hardcopy, Microfiche

Fractals embody important ideas of self-similarity, in which the spatial behavior or appearance of a system is largely scale-independent. Self-similarity is a property of curves or surfaces where each part is indistinguishable from the whole. The fractal dimension D of remote sensing data yields quantitative insight on the spatial complexity and information content contained within these data. Analyses of Normalized Difference Vegetation Index (NDVI) images of homogeneous land covers near Huntsville, Alabama revealed that the fractal dimension of an image of an agricultural land cover indicates greater complexity as pixel size increases, a forested land cover gradually grows smoother, and an urban image remains roughly self-similar over the range of pixel sizes analyzed(l0 to 80 meters). The forested scene behaves as one would expect-larger pixel sizes decrease the complexity of the image as individual clumps of trees are averaged into larger blocks. The increased complexity of the agricultural image with increasing pixel size results from the loss of homogeneous groups of pixels in the large fields to mixed pixels composed of varying combinations of NDVI values that correspond to roads and vegetation. The same process occur’s in the urban image to some extent, but the lack of large, homogeneous areas in the high resolution NDVI image means the initially high D value is maintained as pixel size increases. The slope of the fractal dimension-resolution relationship provides indications of how image classification or feature identification will be affected by changes in sensor resolution.
Author
Fractals; Textures; Image Classification

19990113194 NASA Marshall Space Flight Center, Huntsville, AL USA

Multitemporal and Multiscaled Fractal Analysis of LANDSAT Satellite Data Using the Image Characterization and Modeling System (ICAMS)

Quattrochi, Dale A., NASA Marshall Space Flight Center, USA; Emerson, Charles W., Southwest Missouri State Univ., USA; Lam, Nina Siu–Ngan, Louisiana State Univ., USA; Laymon, Charles A., NASA Marshall Space Flight Center, USA; [1997]; 1p; In English; Association of American Geographers, 25-29 Mar. 1998, Boston, MA, USA; Copyright; Avail: Issuing Activity; Abstract Only, Hardcopy, Microfiche

The Image Characterization and Modeling System (ICAMS) is a public domain software package that is designed to provide scientists with innovative spatial analytical tools to visualize, measure, and characterize landscape patterns so that environmental conditions or processes can be assessed and monitored more effectively. In this study ICAMS has been used to evaluate how changes in fractal dimension, as a landscape characterization index, and resolution, are related to differences in LANDSAT images collected at different dates for the same area. LANDSAT Thematic Mapper (TM) data obtained in May and August 1993 over a portion of the Great Basin Desert in eastern Nevada were used for analysis. These data represent contrasting periods of peak ”green-up” and ”dry-down” for the study area. The TM data sets were converted into Normalized Difference Vegetation Index (NDVI) images to expedite analysis of differences in fractal dimension between the two dates. These NDVI images were also resampled to resolutions of 60, 120, 240, 480, and 960 meters from the original 30 meter pixel size, to permit an assessment of how fractal dimension varies with spatial resolution. Tests of fractal dimension for two dates at various pixel resolutions show that the D values in the August image become increasingly more complex as pixel size increases to 480 meters. The D values in the May image show an even more complex relationship to pixel size than that expressed in the August image. Fractal dimension for a difference image computed for the May and August dates increase with pixel size up to a resolution of 120 meters, and then decline with increasing pixel size. This means that the greatest complexity in the difference images occur around a resolution of 120 meters, which is analogous to the operational domain of changes in vegetation and snow cover that constitute differences between the two dates.

Author

Temporal Resolution; Fractals; LANDSAT Satellites; Characterization; Satellite Imagery; Topography; Image Analysis

44
ENERGY PRODUCTION AND CONVERSION

Includes specific energy conversion systems, e.g., fuel cells; global sources of energy; geophysical conversion; and windpower. For related information see also 07 Aircraft Propulsion and Power, 20 Spacecraft Propulsion and Power, and 28 Propellants and Fuels.

19990107353 Sandia National Labs., Albuquerque, NM USA

Low Temperature Electrical Performance Characteristics of Li-Ion Cells

Nagasubramanian, G.; Apr. 29, 1999; 4p; In English; 34th, 1-5 Aug. 1999, Vancouver, British Columbia, Canada; Sponsored by Intersociety Energy Conversion, USA

Report No.(s): DE00-007203; SAND99-1076C; No Copyright; Avail: Department of Energy Information Bridge, Hardcopy

Advanced rechargeable lithium-ion batteries are presently being developed and commercialized worldwide for use in consumer electronics, military and space applications. The motivation behind these efforts involves, among other things, a favorable combination of energy and power density. For some of the applications the power sources may need to perform at a reasonable rate at subambient temperatures. Given the nature of the lithium-ion cell chemistry the low temperature performance of the cells may not be very good. At Sandia National Laboratories, we have used different electrochemical techniques such as impedance and charge/discharge at ambient and subambient temperatures to probe the various electrochemical processes that are occurring in Li-ion cells. The purpose of this study is to identify the component that reduces the cell performance at subambient temperatures. We carried out 3-electrode impedance measurements on the cells which allowed us to measure the anode and cathode impedances separately. Our impedance data suggests that while the variation in the electrolyte resistance between room temperature and -20 C is negligible, the cathode electrolyte interracial resistance increases substantially in the same temperature span. We believe that the slow interracial charge transfer kinetics at the cathode electrolyte may be responsible for the increase in cell impedance and poor cell performance.

NTIS

Electric Batteries; Metal Ions; Lithium; Electrical Properties; Temperature Dependence; Performance Tests

19990110278 NASA Glenn Research Center, Cleveland, OH USA

Refractive Secondary Concentrators for Solar Thermal Applications

Wong, Wayne A., NASA Glenn Research Center, USA; Macosko, Robert P., Analex Corp., USA; July 1999; 12p; In English; 34th; Intersociety Energy Conversion Engineering, 1-5 Aug. 1999, Vancouver, British Columbia, Canada; Sponsored by Society of Automotive Engineers; Original contains color illustrations

Contract(s)/Grant(s): RTOP 632-81-OA

Report No.(s): NASA/TM-1999-209379; NAS 1.15:209379; IECEC-99-01-2678; E-11793; No Copyright; Avail: CASI; A03, Hardcopy; A01, Microfiche

The NASA Glenn Research Center is developing technologies that utilize solar energy for various space applications including electrical power conversion, thermal propulsion, and furnaces. Common to all of these applications is the need for highly efficient, solar concentration systems. An effort is underway to develop the innovative single crystal refractive secondary concentrator, which uses refraction and total internal reflection to efficiently concentrate and direct solar energy. The refractive secondary offers very high throughput efficiencies (greater than 90%), and when used in combination with advanced primary concentrators, enables very high concentration ratios (10,0(X) to 1) and very high temperatures (greater than 2000 K). Presented is an overview of the refractive secondary concentrator development effort at the NASA Glenn Research Center, including optical design and analysis techniques, thermal modeling capabilities, crystal materials characterization testing, optical coatings evaluation, and component testing. Also presented is a discussion of potential future activity and technical issues yet to be resolved. Much of the work performed to date has been in support of the NASA Marshall Space Flight Center's Solar Thermal Propulsion Program. The many benefits of a refractive secondary concentrator that enable efficient, high temperature thermal propulsion system designs, apply equally well to other solar applications including furnaces and power generation systems such as solar dynamics, concentrated thermal photovoltaics, and thermionics.

Author

Refractivity; Concentrators; Solar Thermal Propulsion; Technology Utilization; Single Crystals; Fabrication; Optical Equipment; Design Analysis

19990111457 Fisk Univ., Nashville, TN USA

Consortium for Advancing Renewable Energy Technology

Gordon, Edward M., Fisk Univ., USA; Henderson, D. O., Fisk Univ., USA; Buffinger, D. R., Fisk Univ., USA; Fuller, Clark W., Fisk Univ., USA; Uribe, R. M., Fisk Univ., USA; Vargas–Aburto, C., Fisk Univ., USA; Hepp, Al F., Fisk Univ., USA; HBCUs/OMUs Research Conference Agenda and Abstracts; August 1999, pp. 10; In English; See also 19990111455; No Copyright; Avail: Issuing Activity, Hardcopy; Abstract Only

The Consortium For Advancing Renewable Energy Technology (CARET) program is a research and education program involving four universities and NASA's John H. Glenn Research Center at Lewis Field. These four universities (Fisk, Wilberforce, Central State and Kent State Universities) are working together with NASA Glenn to use the theme of renewable energy to improve science education and research for minority students. CARET is pursuing this improvement by involving some students and postdoctoral mentors in research on materials, quantum dot phenomena and radiation effects. Other students are involved in more applied activities such as participating in the design and installation of renewable energy power and water pumping demonstration systems. Still others focus more on educational activities such as preparing and presenting PowerPoint presentations on renewable energy to secondary school students. The consortium is also developing a pipeline mechanism which actively works with students interested in these areas to manage their educational opportunities within the consortium and working with students to develop educational programs for secondary school students. This has resulted in students from member HBCUs attending summer internship programs at other member institutions and a graduate of Wilberforce enrolling in graduate school at Kent State University. And finally, CARET is addressing this objective by expanding the educational opportunities available to consortium students. This is being done by establishing a distance learning link between Wilberforce and Kent State Universities whereby presentations and resources of the School of Technology at Kent State are made available to Wilberforce and Central State students. This presentation will focus on the student involvement and achievements in the educational area, while a presentation of some of the research results will be provided in the accompanying poster.

Author

Education; Energy Technology; Renewable Energy; University Program; Minorities

45
ENVIRONMENT POLLUTION

Includes atmospheric, noise, thermal, and water pollution.

19990106569 NASA Goddard Space Flight Center, Greenbelt, MD USA
On the Nature of the Signal and Noise in Seasonal Forecasts
Schubert, Siegfried, NASA Goddard Space Flight Center, USA; Chang, Yehui, NASA Goddard Space Flight Center, USA; Suarez, Max, NASA Goddard Space Flight Center, USA; [1999]; 1p; In English; 24th; Climate Diagnostics and Prediction Workshop, 1-5 Nov. 1999, Tucson, AZ, USA; No Copyright; Avail: Issuing Activity, Hardcopy; Abstract Only

An ensemble of nine GEOS-2 GCM boreal winter seasonal forecasts for the period 1981-95 is examined to assess the nature of the signal and noise on seasonal time scales. The focus is on the spatial structure and year-to year differences in the (SST) forced and unforced variability. Two years (1983 and 1989) are examined in more detail with larger ensembles. The results show that the cold event is considerably less predictable than the warm event. A preliminary analysis of these two events suggests the increased noise for the cold event is due to differences in the stability of the east Asian jet. Comparisons are made with forecasts from several other GCMs to assess the degree to which these results are model-dependent.
Author
Weather Forecasting; Atmospheric Models; Climate Models; Climatology; Atmospheric Circulation; Atmospheric General Circulation Models

19990106583 NASA Goddard Space Flight Center, Greenbelt, MD USA
Vegetation Interaction Enhances Interdecadal Climate Variability in the Sahel
Zeng, Ning, California Univ., USA; Neelin, J. David, California Univ., USA; Lau, William K.–M., NASA Goddard Space Flight Center, USA; Jul. 13, 1999; 14p; In English; No Copyright; Avail: CASI; A03, Hardcopy; A01, Microfiche

The role of naturally varying vegetation in influencing the climate variability in the Sahel is explored in a coupled atmosphere-land-vegetation model. The Sahel rainfall variability is influenced by sea surface temperature (SST) variations in the oceans. Land-surface feedback is found to increase this variability both on interannual and interdecadal time scales. Interactive vegetation enhances the interdecadal variation significantly, but can reduce year to year variability due to a phase lag introduced by the relatively slow vegetation adjustment time. Variations in vegetation accompany the changes in rainfall, in particular, the multi-decadal drying trend from the 1950s to the 80s.
Author
Variability; Periodic Variations; Vegetation; Climate; Climate Change; Climatology; Deserts; Rain

19990107395 NASA Marshall Space Flight Center, Huntsville, AL USA
Nitrogen Oxides and Ozone from B-747 Measurements (NOXAR) During POLINAT-2 and SONEX: Overview and Case Studies on Continental and Marine Convection
Jeker, Dominique P., Institute for Atmospheric Science, Switzerland; Pfister, Lenny, NASA Ames Research Center, USA; Brunner, Dominik, Royal Netherlands Meteorological Inst., Netherlands; Boccippio, Dennis J., NASA Marshall Space Flight Center, USA; Pickering, Kenneth E., Maryland Univ., USA; Thompson, Anne M., NASA Goddard Space Flight Center, USA; Wernli, Heini, Institute for Atmospheric Science, Switzerland; Selkirk, Rennie B., NASA Ames Research Center, USA; Kondo, Yutaka, Nagoya Univ., Japan; Koike, Matoke, Nagoya Univ., Japan; [1997]; 2p; In English; No Copyright; Avail: Issuing Activity, Hardcopy; Abstract Only

In the framework of the project POLINAT 2 (Pollution in the North Atlantic Flight Corridor) we measured NO(x) (NO and NO2) and ozone on 85 flights through the North Atlantic Flight Corridor (NAFC) with a fully automated system permanently installed aboard an in-service Swissair B-747 airliner in the period of August to November 1997. The averaged NO(x) concentrations both in the NAFC and at the U.S. east coast were similar to that measured in autumn 1995 with the same system. The patchy occurrence of NO(x) enhancements up to 3000 pptv over several hundred kilometers (plumes), predominately found over the U.S. east coast lead to a log-normal NO(x) probability density function. In three case studies we examine the origins of such plumes by combining back-trajectories with brightness temperature enhanced (IR) satellite imagery, lightning observations from the U.S. National Lightning Detection Network (NLDN) and the Optical Transient Detector (OTD) satellite. We demonstrate that the location of NO(x) plumes can be well explained with maps of convective influence. We show that the number of lightning flashes in cluster of marine thunderstorms is proportional to the NO(x) concentrations observed several hundred kilometers downwind of the anvil outflows. From the fact that in autumn the NO(x) maximum was found several hundred kilometers off the

U.S. east coast, it can be inferred that thunderstorms triggered over the warm Gulf Stream current are major sources for the regional upper tropospheric NO(x) budget in autumn.
Author
Boeing 747 Aircraft; Transport Aircraft; Jet Exhaust; Exhaust Gases; Nitrogen Oxides; Ozone; Plumes

19990107412 Post, Buckley, Schuh and Jernigan, Inc., Bowie, MD USA
Review of EPRI Mercury Cycling Models ***Final Report***
Logan, D. T., Post, Buckley, Schuh and Jernigan, Inc., USA; Dec. 1998; 126p; In English
Report No.(s): PB99-123861; No Copyright; Avail: CASI; A07, Hardcopy; A02, Microfiche

The objective of this project was to assess the degree to which two mercury cycling models develooped by EPRI might be used to help understand the cycling and bioaccumulation of mercury in Maryland.
NTIS
Mercury (Metal); Accumulations; Ecosystems; Environment Effects; Maryland

19990107413 ENVIRON, Novato, CA USA
Uncertainties Associated with Application of Episodic Models to Prediction of Annual Average Particulate Matter Concentrations ***Final Report***
Stoeckenius, T. E., ENVIRON, USA; Taylor, A., ENVIRON, USA; Lee, K., ENVIRON, USA; Aug. 21, 1998; 46p; In English
Report No.(s): PB99-123598; No Copyright; Avail: CASI; A03, Hardcopy; A01, Microfiche

In this study, ENVIRON prepared some initial quantitative estimates of the uncertainties likely to arise from the use of episodic model results to calculate annual average PM10 and PM2.5 concentrations. Model results were assumed to be available for a certain number of days and ENVIRON calculated the resulting uncertainty in an annual mean concentration computed from these limited results. A key element in computing the uncertainty of the estimated annual mean is defining whether or not year-to-year variations in the true annual mean due to year-to-year variations in meteorology (but not emission) are to be included in the uncertainty estimate.
NTIS
Particulates; Air Pollution; Air Sampling; Meteorology

19990107428 Lembaga Penerbangan dan Antariksa Nasional, Peneliti Bidang Dinamika Atmosfer Puslitbang Pengetahuan Atmosfer, Jakarta, Indonesia
Variations in Surface Ozone Concentration Above Bandung in 1995 ***Variasi Konsentrasi Ozon Permukaan di Atas Bandung Pada Periode 1995***
R., Yeti Priyati, Lembaga Penerbangan dan Antariksa Nasional, Indonesia; Warta: Lembaran Tambahan Majalah LAPAN; October 1998; ISSN 0126-9754; Volume 22, No. 57, pp. 15-18; In Malay-Indonesian; No Copyright; Avail: CASI; A01, Hardcopy; A01, Microfiche

Surface Ozone Concentration was measured by LAPAN continuously at Bandung for a period of one year during 1995 by using Dasibi Ozone Monitor 1006-AHJ. From data analysis showed that diurnal variation in concentration of surface Ozone with clearly follows the diurnal variation of surface temperature. The monthly average of surface Ozone concentration was observed during period 1995 ranged from 8.09 to 14.64 ppb, while hourly average of surface Ozon concentration ranged from 1.56 to 29.96 ppb. It trend to increase in the day time (11.00 a.m - 1.00 p.m) and trend to decrease in the night (10.00 p.m - 7.00 a.m) . The result indicated that the surface Ozone concentration in Bandung was still under the limit of primary air quality standard for Ozone.
Author
Diurnal Variations; Ozone; Gas Composition

19990108762 National Observatory of Athens, Inst. of Meteorology and Physics of the Atmospheric Environment, Greece
A Study of the Atmospheric Electrical Parameters and the Meteorological Conditions During Some Intense Air Pollution Episodes in Athens
Retalis, D. A., National Observatory of Athens, Greece; Retalis, A. D., Integrated Information Systems S.A., Greece; 11th International Conference on Atmospheric Electricity; June 1999, pp. 638-641; In English; See also 19990108601; No Copyright; Avail: CASI; A01, Hardcopy; A10, Microfiche

In this study the variations of the air electrical parameters (large and small ions and conductivity) and the meteorological conditions during some intense air pollution episodes (smoke and SO2) in Athens, for the period 1971-1985, were examined. It was found out that, during intense air pollution episodes, the large ions concentration were increased from its normal value, while small ions concentration and air conductivity were decreased. Synoptic weather conditions prevailing during the occurrence of

episodes were investigated in detail for the period 1984-1985. It was noticed that the onset of these episodes was found to have been associated with a warm air advection from the southwest or with the withdrawal of a cold air mass that had been previously established over Greece.
Author
Atmospheric Electricity; Atmospheric Boundary Layer; Greece; Meteorological Parameters; Air Conductivity

19990108763 Airborne Research Associates, Weston, MA USA
Ionospheric Potential as a Measure of Global Temperature Variation
Markson, Ralph, Airborne Research Associates, USA; Vogel, Daniel, Carnegie-Mellon Univ., USA; 11th International Conference on Atmospheric Electricity; June 1999, pp. 642-645; In English; See also 19990108601
Contract(s)/Grant(s): NSF DMI-93-04487; No Copyright; Avail: CASI; A01, Hardcopy; A10, Microfiche

This report covers the final phase of an investigation of the relationship of ionospheric potential (Vi) to global temperature. Twenty reliable Vi balloon soundings were obtained at Orlando, Florida in March 1998. These were compared with hourly temperature measurements from South America and Africa, the major global thunderstorm regions. by using hourly time resolution METAR temperature data it is possible to do lag correlation analysis at hourly intervals. While data analysis is still being conducted (March 1999), some preliminary conclusions have emerged. A major complication in the analysis is that both temperature and Vi follow well established quasi-sinusoidal diurnal cycles that are out of phase. This can lead to apparent correlation between temperature and Vi depending on when the measurements are made and the lag. To minimize this effect, the Vi and temperature data were normalized. The tentative conclusion is that the inherent variation of Vi, caused by factors in addition to temperature, prevents this parameter from being used as a short term measure of continental scale temperature variation. However, equatorial temperatures before the time of the Vi measurements are positively correlated with Vi. It appears that Vi variation may be most useful for studying global change on seasonal and annual ”climatological” time scales rather than short period ”weather” time scales.
Author
Balloon Sounding; Earth Ionosphere; Temperature Dependence; Electric Potential; Atmospheric Electricity; Data Correlation

19990109084 NASA Goddard Space Flight Center, Greenbelt, MD USA
Late Pleistocene Interstadial Environment on Faddeyevskiy Island, East-Siberian Sea, Russia
Andreev, Andrei A., NASA Goddard Space Flight Center, USA; Peteet, Dorothy M., NASA Goddard Space Flight Center, USA; Romanenko, Fedor A., Moscow State Univ., Russia; Filimonova, Ludmila V., Russian Academy of Sciences, Russia; Sulerzhitsky, Leopold D., Russian Academy of Natural Sciences, Russia; Tarasov, Pavel E., Moscow State Univ., Russia; [1999]; 31p; In English
Report No.(s): GNC-99-57; No Copyright; Avail: CASI; A03, Hardcopy; A01, Microfiche

Pollen, plant macrofossil, LOI and radiocarbon analyses of a 1.4-m section from Faddeyevskiy Island, Novosibirskie Ostrova archipelago (75 deg 20 min N, 143 deg 50 min E, 30m elevation) provide new information on the Late Pleistocene interstadial environmental history of this high Arctic region. Bulk radiocarbon dates of 25,700 +/- 1000, 32,780 +/- 500, 35,200 +/- 650 and two AMS dates of 29,950 +/- 660 and 42,990 +/- 1280 indicate that the deposits accumulated during the Kargian (Boutellier) interval. Numerous mammoth (Mammuthus primigenius) remains collected in the vicinity of the site were radiocarbon dated to 36,700-18,500 yr. BP. Rare bison (Bison priscus) bones were dated to 32,200 +/- 600 and 33,100 +/- 320. Poaceae, Cyperaceae, and Artemisia pollen dominate the pollen spectra with some Ranunculaceae, Caryophyllaceae, Rosaceae, and Compositae. These pollen spectra reflect a tundra-steppe vegetation which probably was dominant on the exposed shelf of the Arctic Ocean. The presence of Carex macrofossils infer a summer climate two degrees warmer than today. The productivity of this local vegetation during the Kargian interstadial was apparently high enough to feed the grass-eater herds.
Author
Fossils; Pollen; Carbon 14; Radioactive Materials; Radiolysis

19990109085 NASA Goddard Inst. for Space Studies, New York, NY USA
Aerosol Retrievals over the Ocean using Channel 1 and 2 AVHRR Data: A Sensitivity Analysis and Preliminary Results
Mishchenko, Michael I., NASA Goddard Inst. for Space Studies, USA; Geogdzhayev, Igor V., NASA Goddard Inst. for Space Studies, USA; Cairns, Brian, NASA Goddard Inst. for Space Studies, USA; Rossow, William B., NASA Goddard Inst. for Space Studies, USA; Lacis, Andrew A., NASA Goddard Inst. for Space Studies, USA; [1999]; 49p; In English; Original contains color illustrations
Report No.(s): GCN-99-60; No Copyright; Avail: CASI; A03, Hardcopy; A01, Microfiche

This paper outlines the methodology of interpreting channel 1 and 2 AVHRR radiance data over the oceans and describes a detailed analysis of the sensitivity of monthly averages of retrieved aerosol parameters to the assumptions made in different retrieval algorithms. The analysis is based on using real AVHRR data and exploiting accurate numerical techniques for computing single and multiple scattering and spectral absorption of light in the vertically inhomogeneous atmosphere-ocean system. We show that two-channel algorithms can be expected to provide significantly more accurate and less biased retrievals of the aerosol optical thickness than one-channel algorithms and that imperfect cloud screening and calibration uncertainties are by far the largest sources of errors in the retrieved aerosol parameters. Both underestimating and overestimating aerosol absorption as well as the potentially strong variability of the real part of the aerosol refractive index may lead to regional and/or seasonal biases in optical thickness retrievals. The Angstrom exponent appears to be the most invariant aerosol size characteristic and should be retrieved along with optical thickness as the second aerosol parameter.
Author
Aerosols; Data Retrieval; Size Distribution; Air Water Interactions; Atmospheric Models; Radiative Transfer; Algorithms; Ocean Models; Ocean Surface

19990109157 NASA Goddard Space Flight Center, Greenbelt, MD USA
Seasonal Variability of Middle Latitude Ozone in the Lowermost Stratosphere Derived from Probability Distribution Functions
Rood, Richard B., NASA Goddard Space Flight Center, USA; Douglass, Anne R., NASA Goddard Space Flight Center, USA; Cerniglia, Mark C., Atmospheric and Environmental Research, Inc., USA; Sparling, Lynn C., NASA Goddard Space Flight Center, USA; Nielsen, J. Eric, NASA Goddard Space Flight Center, USA; [1999]; 36p; In English; Original contains color illustrations; No Copyright; Avail: CASI; A03, Hardcopy; A01, Microfiche

We present a study of the distribution of ozone in the lowermost stratosphere with the goal of characterizing the observed variability. The air in the lowermost stratosphere is divided into two population groups based on Ertel's potential vorticity at 300 hPa. High (low) potential vorticity at 300 hPa indicates that the tropopause is low (high), and the identification of these two groups is made to account for the dynamic variability. Conditional probability distribution functions are used to define the statistics of the ozone distribution from both observations and a three-dimensional model simulation using winds from the Goddard Earth Observing System Data Assimilation System for transport. Ozone data sets include ozonesonde observations from northern midlatitude stations (1991-96) and midlatitude observations made by the Halogen Occultation Experiment (HALOE) on the Upper Atmosphere Research Satellite (UARS) (1994- 1998). The conditional probability distribution functions are calculated at a series of potential temperature surfaces spanning the domain from the midlatitude tropopause to surfaces higher than the mean tropical tropopause (approximately 380K). The probability distribution functions are similar for the two data sources, despite differences in horizontal and vertical resolution and spatial and temporal sampling. Comparisons with the model demonstrate that the model maintains a mix of air in the lowermost stratosphere similar to the observations. The model also simulates a realistic annual cycle. Results show that during summer, much of the observed variability is explained by the height of the tropopause. During the winter and spring, when the tropopause fluctuations are larger, less of the variability is explained by tropopause height. This suggests that more mixing occurs during these seasons. During all seasons, there is a transition zone near the tropopause that contains air characteristic of both the troposphere and the stratosphere. The relevance of the results to the assessment of the environmental impact of aircraft effluence is also discussed.
Author
Annual Variations; Temperate Regions; Ozone; Stratosphere; Probability Distribution Functions

19990109166 NASA Goddard Inst. for Space Studies, New York, NY USA
Climate Change and a Global City: An Assessment of the Metropolitan East Coast Region
Rosenzweig, Cynthia, NASA Goddard Inst. for Space Studies, USA; Solecki, William, NASA Goddard Inst. for Space Studies, USA; [1999]; 1p; In English, 4 Jun. 1999, Boston, MA, USA; Sponsored by American Geophysical Union, USA; No Copyright; Avail: Issuing Activity, Hardcopy; Abstract Only

The objective of the research is to derive an assessment of the potential climate change impacts on a global city - in this case the 31 county region that comprises the New York City metropolitan area. This study comprises one of the regional components that contribute to the ongoing U.S. National Assessment: The Potential Consequences of Climate Variability and Change and is an application of state-of-the-art climate change science to a set of linked sectoral assessment analyses for the Metro East Coast (MEC) region. We illustrate how three interacting elements of global cities react and respond to climate variability and change with a broad conceptual model. These elements include: people (e.g., socio- demographic conditions), place (e.g., physical systems), and pulse (e.g., decision-making and economic activities). The model assumes that a comprehensive assessment of potential climate change can be derived from examining the impacts within each of these elements and at their intersections. Thus,

the assessment attempts to determine the within-element and the inter-element effects. Five interacting sector studies representing the three intersecting elements are evaluated. They include the Coastal Zone, Infrastructure, Water Supply, Public Health, and Institutional Decision-making. Each study assesses potential climate change impacts on the sector and on the intersecting elements, through the analysis of the following parts: 1. Current conditions of sector in the region; 2. Lessons and evidence derived from past climate variability; 3. Scenario predictions affecting sector; potential impacts of scenario predictions; 4. Knowledge/information gaps and critical issues including identification of additional research questions, effectiveness of modeling efforts, equity of impacts, potential non-local interactions, and policy recommendations; and 5. Identification of coping strategies - i.e., resilience building, mitigation strategies, new technologies, education that affects decision-making, and better preparedness for contingencies.
Author
Climate Change; Assessments; Contingency; Economics; Public Health; Atmospheric Models

19990109663 Michigan Univ., Dept. of Atmospheric, Oceanic, and Space Science, Ann Arbor, MI USA
Development of the Double Etalon Fabry-Perot Interferometer for Determining Total and Tropospheric Ozone Concentrations ***Final Report, 8 May 1995 - 31 Dec. 1998***
Cook, William, Michigan Univ., USA; Oct. 06, 1999; 14p; In English
Contract(s)/Grant(s): NAG1-1720; No Copyright; Avail: CASI; A03, Hardcopy; A01, Microfiche

Measuring and understanding the distribution of ozone through the lower levels of Earth's atmosphere are high priorities in global change and climate research. of particular interest now is the global distribution of ozone in the upper troposphere and lower stratosphere. Global coverage of the stratospheric ozone is feasible only via remote sensing instruments on a space-based platform. And though extensive monitoring tropospheric ozone is possible using instruments flown aboard conventional aircraft, a space-based system would be significantly less costly and provide information over a much broader area and produce more uniform coverage. Here we describe the prototype of an instrument being developed to monitor, from an orbiting spacecraft, the ozone found in Earth's upper troposphere and lower stratosphere. Our new spectrometer is an infrared Fabry-Perot interferometer which uses two synchrounously tuned etalons: a high resolution narrow band device and a lower resolution broader band filtering etalon. The prototype is a scanning device making use of nearly collimated input radiation and a single element detector. As presently configured, it is capable of providing a resolution better than 0.07/cm with a spectral band width approximately 5/cm wide and centered at 1054.7/cm. For the future space-based emission device a modification of the the prototype was to be made to employ innovative circle-to-line detector optics, those developed or in development at UM/SPRL, and a focal plane array detector. These enhancements would enable a simultaneous recording of the entire spectral range of interest, but with simple detection electronics and a significant gain in signal-to-noise over that of the scanning version.
Derived from text
Fabrication; Ozone; Troposphere; Atmospheric Composition; Remote Sensing; Fabry-Perot Interferometers

19990109667 NASA Goddard Space Flight Center, Greenbelt, MD USA
Climate Change and Greenhouse Gases
Ledley, Tamara S., NASA Goddard Space Flight Center, USA; Sundquist, Eric, NASA Goddard Space Flight Center, USA; Schwartz, Stephen, NASA Goddard Space Flight Center, USA; Hall, Dorothy K., NASA Goddard Space Flight Center, USA; Fellows, Jack, NASA Goddard Space Flight Center, USA; Killeen, Timothy, NASA Goddard Space Flight Center, USA; [1999]; 22p; In English; No Copyright; Avail: CASI; A03, Hardcopy; A01, Microfiche

The American Geophysical Union (AGU), as a scientific organization devoted to research on the Earth and space sciences, provides current scientific information to the public on issues pertinent to geophysics. The Council of the AGU approved a position statement on Climate Change and Greenhouse Gases in December 1998. The statement, together with a short summary of the procedures that were followed in its preparation, review, and adoption were published in the February 2, 1999 issue of EOS ([AGU, 1999]. The present article reviews scientific understanding of this issue as presented in peer-reviewed publications that serves as the underlying basis of the position statement.
Author
Climate Change; Greenhouse Effect; Data Acquisition

19990109964 SRI International Corp., Applied Physical Science Lab., Menlo Park, CA USA
Characterization of Atmospheric Aerosol Behavior and Climatic Effects by Analysis of SAGE 2 and Other Space, Air, and Ground Measurements ***Final Report, 1 Apr. 1997 - 31 Mar. 1999***
Livingston, John M., SRI International Corp., USA; Jun. 22, 1999; 9p; In English; Original contains color illustrations
Contract(s)/Grant(s): NCC2-991; SRI Proj. 1881; No Copyright; Avail: CASI; A02, Hardcopy; A01, Microfiche

This report documents the research performed under NASA Ames Cooperative Agreement NCC 2-991, which covered the period 1 April 1997 through 31 March 1999. Previously, an interim technical report (Technical Report No. 1, 20 March 1998) summarized the work completed during the period 1 April 1997 through 31 March 1998. The objective of the proposed research was to advance our understanding of atmospheric aerosol behavior, aerosol-induced climatic effects, and the remote measurement and retrieval capabilities of spaceborne sensors such as SAGE II by combining and comparing data from these instruments and from airborne and ground-based instruments.
Derived from text
Aerosols; Climatology; Remote Sensing; Sage Satellite

19990110095 Aerospace Corp., El Segundo, CA USA
Tracer Puff Dispersion at Launch Sites
Abernathy, R. N., Aerospace Corp., USA; Min, I. A., Aerospace Corp., USA; Lundblad, B. L., Aerospace Corp., USA; Kempf, W. S., Space and Missile Systems Organization, USA; JANNAF 28th Propellant Development and Characterization Subcommittee and 17th Safety and Environmental Protection Subcommitte Joint Meeting; April 1999; Volume 1, pp. 71-79; In English; See also 19990110087; No Copyright; Avail: CPIA, 10630 Little Patuxent Pkwy., Suite 202, Columbia, MD 21044-3200 HC, Hardcopy

As part of the USAF Atmospheric Dispersion Model Validation Program (MVP), puffs of tracer gas were released from a blimp over the rocket launch sites at Cape Canaveral AS and Vandenberg AFB. Multiple infrared cameras imaged the transport and diffusion of the puffs. The imagery is being analyzed to determine the position, movement, and growth of the puffs with time. The objective of the activity is to correlate atmospheric diffusion rates with measurements of atmospheric turbulence. Results of the activity will be used to evaluate and improve the models that are used at the launch ranges to predict the dispersion of toxic clouds generated by launch operations. This is the first time that tracer gases have been released from a free-flying blimp and imaged by infrared cameras at ground locations.
Author
Exhaust Clouds; Exhaust Gases; Rocket Exhaust; Rocket Launching; Launching Sites; Trace Elements

19990110103 Thiokol Propulsion, Brigham City, UT USA
Local Environmental and Toxicity Issues for Rocket Launching and Testing
Bennett, R. R., Thiokol Propulsion, USA; McDonald, A. J., Thiokol Propulsion, USA; JANNAF 28th Propellant Development and Characterization Subcommittee and 17th Safety and Environmental Protection Subcommitte Joint Meeting; April 1999; Volume 1, pp. 153-173; In English; See also 19990110087; No Copyright; Avail: CPIA, 10630 Little Patuxent Pkwy., Suite 202, Columbia, MD 21044-3200 HC, Hardcopy

There have been several recent efforts seeking to understand the effects of rocket launches and static testing on the local environment and human population. Work to further refine the Rocket Exhaust Effluent Diffusion Model (REEDM), the computer model used to calculate the downwind concentrations of exhaust species continues, as do field experiments to validate the model predictions. A report entitled 'Assessment of Exposure-Response Functions for Rocket-Emission Toxicants' was issued in August of 1998 by the Committee on Toxicology of the National Research Council that assessed the methodology of the Launch Area Toxic Risk Analysis (LATRA) program and the exposure response functions (ERFs) that it uses to help predict the potential health effects of exposure to rocket effluents. The committee investigated three species; HCl, NO2 and HNO3, discussed the existing toxicology data for each, and made recommendations for further studies. This paper will summarize the recent findings in these areas from the perspective of the various propellant formulations used in US rockets.
Author
Toxicity; Toxicology; Rocket Launching; Environmental Monitoring; Rocket Exhaust; Exhaust Emission

19990110104 Army Tank-Automative Research and Development Command, Picatinny Arsenal, NJ USA
Mathematical Modeling used in Risk Assessment Methodologies
Bixon, Eric R., Army Tank-Automative Research and Development Command, USA; JANNAF 28th Propellant Development and Characterization Subcommittee and 17th Safety and Environmental Protection Subcommitte Joint Meeting; April 1999; Volume 1, pp. 175-182; In English; See also 19990110087; No Copyright; Avail: CPIA, 10630 Little Patuxent Pkwy., Suite 202, Columbia, MD 21044-3200 HC, Hardcopy

When environmental clean-up or pollution prevention efforts are implemented at a plant, there are often many problems, which must be considered. These problems involve a number of different chemicals as well as a number of different areas within the plant site. This is especially true for older plants (plants, which were developed during the 40's,) which is the case for some army ammunition plants. Usually, there are separate environmental clean up efforts (remediation) and ongoing pollution

prevention efforts that are generally run by two different organizations. For each pollution prevention situation, which is encountered there, are often multiple solutions. These solutions must be weighed based on two factors: cost and risk. Many cost models exist.. One that was recently developed by TACOM-ARDEC in conjunction with the National Defense Center for Environmental Excellence is the ECAM (Environmental Cost Assessment Model). That model uses some traditional cost indicators including Net Present Value, Payback period, and Internal rate of return. These factors are calculated over the project lifetime, which for pollution prevention projects can be 5 10 or 15 years or less, depending on the decisions of management. The other factor, which must be considered in conjunction with the cost of each pollution prevention project, is risk. The ideal decision as to which project, area, or solution will be used for a particular threat would optimize the dollars spent so as to eliminate the largest risk for each dollar spent. This paper discusses some of the models and concepts currently in existence in the assessment of the risk for a particular environmental threat.
Derived from text
Mathematical Models; Environmental Cleanup; Environment Management; Environment Pollution; Pollution Control

19990110105 ACTA, Inc., Torrance, CA USA
Launch Area Toxic Risk Analysis (LATRA): Risk Management Computer Program
Hudson, J. M., ACTA, Inc., USA; See, A. M., ACTA, Inc., USA; Philipson, L. L., ACTA, Inc., USA; JANNAF 28th Propellant Development and Characterization Subcommittee and 17th Safety and Environmental Protection Subcommitte Joint Meeting; April 1999; Volume 1, pp. 183-191; In English; See also 19990110087
Contract(s)/Grant(s): F04684-97-C-0001; No Copyright; Avail: CPIA, 10630 Little Patuxent Pkwy., Suite 202, Columbia, MD 21044-3200 HC, Hardcopy

LATRA is used to assess the risk to people from toxic gas clouds from successful launches and catastrophic aborts of launch vehicles. It supplements the REEDM hazard analysis code, which is used in a launch support role at the 30th and 45th Space Wings (SWs). LATRA's results, computed during the last 5 hours of countdown, are used as part of the GO/NO-GO launch recommendation. LATRA uses REEDM to predict ground level toxic material concentrations at population centers to develop casualty expectations (E(sub c)) and risk profiles. It uses several databases, which include: Vehicle failure rates (STS, Titan, Delta, Atlas and MSLS); Weather parameters including covariance matrices that define their degree of correlation; Population data for different groups (children, aged, bronchitis and healthy adults); Shelter types including schools, hospitals, offices, and single family homes (by type of construction related to in-leakage of toxic gases); and Exposure-response functions (ERFs) that define the probability of a specified effect (mild, or significant) for each population group. LATRA conducts several thousands simulations (scenarios) to determine casualty expectations (E(sub c)) and a risk profile for each population group and a total across all groups. Each scenario is initiated by randomly computing the time at which an accident occurs, which determines scenario probability and launch altitude. Weather variables used in each simulation are selected from a rawinsonde data file and a weather statistical data file for the appropriate altitude, using a correlated random sampling scheme. These weather samples are entered to the REEDM module and dispersed concentrations at each population receptor location are computed. These concentrations are then entered into the relevant exposure-response functions to compute the probability of each specified effect for each population group. The mean and variance of the number of casualties, at each receptor location and across all receptors, are computed and this information stored while subsequent scenarios are simulated. On completion of all simulations, the model computes the expected number of casualties for each population group, for each severity classification, and the corresponding risk profiles. LATRA is intended to provide increased launch probability, and hence reduce the costs associated with launch holds, without compromising launch safety.
Author
Launching Sites; Toxicity; Risk; Computer Programs

19990110111 Naval Surface Warfare Center, Indian Head, MD USA
Investigating the Treatability of Ordnance Related Wastewater Using Cell Respirometry
Sims, B. L., Naval Surface Warfare Center, USA; JANNAF 28th Propellant Development and Characterization Subcommittee and 17th Safety and Environmental Protection Subcommitte Joint Meeting; April 1999; Volume 1, pp. 257-266; In English; See also 19990110087; No Copyright; Avail: CPIA, 10630 Little Patuxent Pkwy., Suite 202, Columbia, MD 21044-3200 HC, Hardcopy

The treatability or industrial ordnance material and wastewater containing these materials using activated sludge was analyzed by cell respirometry. The objective of this study is to develop and validate an approach to predict the joint toxic effects of multiple ordnance and industrial chemicals on the microbial population or the Indian Head Division, Naval Surface Warfare Center (IHDIV/NSWC) municipal waste treatment plant while biologically decomposing the chemicals. The treatability and toxicity are established as a function of oxygen uptake by the microbial cell population as the substrate containing the test pollutant

is converted to biomass water and CO2. The resulting oxygen consumption of activated sludge microorganisms was recorded for 24 hours. The respiration rate of microorganisms in the presence of test pollutants ranging from very low to high concentrations is recorded. IHDIV/NSWC proposes to connect its production facilities to the domestic sewer, however, before this can be done maximum treatability limits database will be established for each waste stream and each contaminant. Also, any adverse affects on the indigenous microorganisms must be determined. An eight-cell respirometer unit containing test compounds in various concentrations in a total volume of one liter of activated sludge was run. The specific test compounds and the dilution volumes are based on the theoretical composition of each production facility's expected load and the dilution ratios are based on the total load and volume to aeration basin volume. Analytical lab samples are collected at the beginning of each test and at the conclusion to determine the degree of decomposition of each test substances present. While the activated sludge decomposed surrogate organics such as Dextrose, the inorganic concentrations remained constant. Declining oxygen uptake was apparent with increasing concentration of contaminants indicating toxicity to the cell population. For example, ammonium perchlorate caused toxicity to the sludge organisms above 50 ppm.
Author
Waste Treatment; Waste Water; Water Treatment; Aeration; Activated Sludge; Respirometers

19990110113 AmDyne Corp., Huntsville, AL USA
The Impact of Aerospace NESHAPs on Missile System Maintainability
Morgan, R. E., AmDyne Corp., USA; Hagler, R. A., Army Aviation and Missile Command, USA; JANNAF 28th Propellant Development and Characterization Subcommittee and 17th Safety and Environmental Protection Subcommitte Joint Meeting; April 1999; Volume 1, pp. 277-282; In English; See also 19990110087
Contract(s)/Grant(s): DAAH01-96-C-R207; No Copyright; Avail: CPIA, 10630 Little Patuxent Pkwy., Suite 202, Columbia, MD 21044-3200 HC, Hardcopy

On September 1, 1998 the National Emissions Standards for Hazardous Air Pollutants (NE-SHAPs) for Aerospace Manufacturing and Rework Facilities took effect. This paper discusses the effect this piece of legislation has on U.S. Army depots that maintain missile systems. The targeted processes and chemicals are identified and the new pollution prevention initiatives are described in detail. The need for new technology to cover the areas of present concern where a shortfall exists is addressed. The result of this work is described in relation to the other Pollution Prevention activities the Army is conducting on missile systems.
Author
Aerospace Environments; Exhaust Gases; Exhaust Emission; Air Pollution; Pollution Monitoring; Pollution Control

19990110321 NASA Goddard Space Flight Center, Greenbelt, MD USA
Sensitivity of Climate to Changes in NDVI
Bounoua, L., NASA Goddard Space Flight Center, USA; Collatz, G. J., NASA Goddard Space Flight Center, USA; Los, S. O., Science Systems and Applications, Inc., USA; Sellers, P. J., NASA Johnson Space Center, USA; Dazlich, D. A., Colorado State Univ., USA; Tucker, C. J., NASA Goddard Space Flight Center, USA; Randall, D. A., Colorado State Univ., USA; [1999]; 61p; In English
Contract(s)/Grant(s): NAG5-3172; No Copyright; Avail: CASI; A04, Hardcopy; A01, Microfiche

The sensitivity of global and regional climate to changes in vegetation density is investigated using a coupled biosphere-atmosphere model. The magnitude of the vegetation changes and their spatial distribution are based on natural decadal variability of the normalized difference vegetation index (ndvi). Different scenarios using maximum and minimum vegetation cover were derived from satellite records spanning the period 1982-1990. Albedo decreased in the northern latitudes and increased in the tropics with increased ndvi. The increase in vegetation density revealed that the vegetation's physiological response was constrained by the limits of the available water resources. The difference between the maximum and minimum vegetation scenarios resulted in a 46% increase in absorbed visible solar radiation and a similar increase in gross photosynthetic C02 uptake on a global annual basis. This caused the canopy transpiration and interception fluxes to increase, and reduced those from the soil. The redistribution of the surface energy fluxes substantially reduced the Bowen ratio during the growing season, resulting in cooler and moister near-surface climate, except when soil moisture was limiting. Important effects of increased vegetation on climate are : (1) A cooling of about 1.8 K in the northern latitudes during the growing season and a slight warming during the winter, which is primarily due to the masking of high albedo of snow by a denser canopy. and (2) A year round cooling of 0.8 K in the tropics. These results suggest that increases in vegetation density could partially compensate for parallel increases in greenhouse warming . Increasing vegetation density globally caused both evapotranspiration and precipitation to increase. Evapotranspiration, however increased more than precipitation resulting in a global soil-water deficit of about 15 %. A spectral analysis on the

simulated results showed that changes in the state of vegetation could affect the low-frequency modes of the precipitation distribution and might reduce its low frequency variability in the tropics while increasing it in northern latitudes.
Author
Atmospheric Heating; Greenhouse Effect; Atmospheric Models; Vegetation; Climate Change

19990110478 Department of Energy, Washington, DC USA
Are revised models better models. a skill score assessment
Sperber, K. R., Department of Energy, USA; Dec. 01, 1997; 9p; In English; Dynamical Extended-Range Forecasting, USA
Report No.(s): DE98-057454; UCRL-JC-129367; CONF-9711186; No Copyright; Avail: Department of Energy Information Bridge, Microfiche

Standardized experimentation and sensitivity testing are prerequisites for ascertaining the fidelity of new physical and dynamical elements of model formulations. to this end, the climate-modeling community has adopted the Atmospheric Model Intercomparison Project (AMIP), a World Climate Research Program/Working Group on Numerical Experimentation initiative, as one of many vehicles for model validation. The benefit of this experimental design is that the models were integrated in a standardized fashion, all using the same SST boundary conditions, solar constant and CO2 concentration for the 10-year period 1979-1988. Thus, differences among the simulations are directly attributable to the wide variety of model formulations.
NTIS
Climate Models; Atmospheric Circulation; Climate; Tropical Regions; Precipitation (Meteorology)

19990110583 NASA Goddard Space Flight Center, Greenbelt, MD USA
The Seasonal and Interannual Variability of the Budgets of N2O and CCl3F
Wong, Sun, Columbia Univ., USA; Prather, Michael J., California Univ., USA; Rind, David H., NASA Goddard Space Flight Center, USA; [1999]; 33p; In English; Original contains color illustrations
Report No.(s): GCN-99-59; No Copyright; Avail: CASI; A03, Hardcopy; A01, Microfiche

The 6-year wind archives from the Goddard Institute for Space Studies/Global Climate-Middle Atmosphere Model (GISS/GCMAM) were in- put to the GISS/Harvard/Irvine Chemical Transport Model (G/H/I CTM) to study the seasonal and interannual variability of the budgets and distributions of nitrous oxide (N2O) and trichlorofluoromethane (CCl3F), with the corresponding chemical loss frequencies recycled and boundary conditions kept unchanged from year to year. The effects of ozone feedback and quasi-biennial oscillation (QBO) were not included. However, the role of circulation variation in driving the lifetime variability is investigated. It was found that the global loss rates of these tracers are related to the extratropical planetary wave activity, which drives the tropical upward mass flux. For N2O, a semiannual signal in the loss rate variation is associated with the interhemispheric asymmetry in the upper stratospheric wave activity. For CCl3F, the semiannual signal is weaker, associated with the comparatively uniform wave episodes in the lower stratosphere. The loss rates lag behind the wave activity by about 1-2 months. The interannual variation of the GCM generated winds drives the interannual variation of the annually averaged lifetime. The year-to-year variations of the annually averaged lifetimes can be about 3% for N2O and 4% for CCl3F.
Author
Annual Variations; Atmospheric Models; Boundary Conditions; Climate Models; Nitrogen Oxides; Carbon; Chlorine Fluorides

19990110661 Royal Netherlands Meteorological Inst., De Bilt, Netherlands
Model Calculations of the Impact of NO(x) from Air Traffic, Lightning and Surface Emissions, Compared with Measurements
Meijer, E. W., Royal Netherlands Meteorological Inst., Netherlands; vanVelthoven, P. F. J., Royal Netherlands Meteorological Inst., Netherlands; Thompson, A. M., NASA Goddard Space Flight Center, USA; Pfister, L., NASA Ames Research Center, USA; Schlager, H., Deutsche Forschungs- und Versuchsanstalt fuer Luft- und Raumfahrt, Germany; Schulte, P., Deutsche Forschungs- und Versuchsanstalt fuer Luft- und Raumfahrt, Germany; Kelder, H., Royal Netherlands Meteorological Inst., Netherlands; 1999; 22p; In English
Contract(s)/Grant(s): CEC-ENV4-CT-95-0043; No Copyright; Avail: Issuing Activity, Hardcopy

The impact of NO(x) from aircraft emissions, lightning and surface contributions on atmospheric nitrogen oxides and ozone has been investigated with the three-dimensional global chemistry transport model TM3 by partitioning the nitrogen oxides and ozone according to source category. The results have been compared with POLINAT II and SONEX airborne measurements in the North Atlantic flight corridor in 1997. Various cases have been investigated: measurements during a stagnant anti-cyclone and an almost cut-off low, both with expected high aircraft contributions, a southward bound flight with an expected strong flight corridor gradient and lightning contributions in the South, and a transatlantic flight with expected boundary layer pollution near the U.S. coast. The agreement between modeled results and measurements is reasonably good for NO and ozone. Also, the

calculated impact of the three defined sources were consistent with the estimated exposure of the sampled air to these sources, obtained by specialized back-trajectory model products.
Author
Nitrogen Oxides; Ozone; Air Pollution; Atmospheric Chemistry; Atmospheric Composition; Lightning; Air Traffic

19990110670 New York Academy of Sciences, New York, NY USA
First Forum on Science and Technology Goals: The Environment
Ahearne, John F., Duke Univ., USA; Science, Technology, and the Economic Future; [1998], pp. 41-48; In English; ISBN 1-57331-147-2; Copyright; Avail: Issuing Activity, Hardcopy

Finding a way to develop a national consensus on something as complex and potentially divisive as environmental priorities for the nation is a difficult, yet critically important problem. A concerted and unique effort to gather and combine a comprehensive set of views and opinions on future environmental priorities, National Forum on Science and Technology Goals, took place under the auspices of the National Academy of Sciences in 1995. It is important to understand the National Forum process to understand the importance of the findings.
Derived from text
Research and Development; Technologies; Environmental Monitoring; Environment Management; Environment Protection

19990111493 Department of Energy, Washington, DC USA
Development of a climate data analysis tool (CDAT)
Marlais, S. M., Department of Energy, USA; Sep. 01, 1997; 96p; In English
Report No.(s): DE98-057703; UCRL-LR-130150; No Copyright; Avail: Department of Energy Information Bridge, Microfiche

The Climate Data Analysis Tool (CDAT) is designed to provide the Program for Climate Model Diagnosis and Intercomparison (PCMDI) at Lawrence Livermore National Laboratory, California, with the capabilities needed to analyze model data with little effort on the part of the scientist, while performing complex mathematical calculations, and graphically displaying the results. This computer software will meet the demanding need of climate scientists by providing the necessary tools to diagnose, validate, and intercompare large observational and global climate model datasets.
NTIS
Climate Models; Climatology; Applications Programs (Computers)

19990111520 NASA Goddard Space Flight Center, Greenbelt, MD USA
The GEOS Ozone Data Assimilation System: Design and Validation
Stajner, I., NASA Goddard Space Flight Center, USA; Riishojgaard, L. P., NASA Goddard Space Flight Center, USA; 1999; 1p; In English; 24th, 19-23 Apr. 1999, Hague, USA; Sponsored by European Geophysical Union, Netherlands; No Copyright; Avail: Issuing Activity, Hardcopy; Abstract Only

An ozone data assimilation system has been developed at the Data Assimilation Office of the NASA/Goddard Space Flight Center to provide global three-dimensional analyzed ozone mixing ratio and total column ozone. The Total Ozone Mapping Spectrometer (TOMS) total column ozone and the Solar Backscatter Ultraviolet (SBUV) or SBUV/2 partial ozone profile data are assimilated. The analyzed winds from the Goddard Earth Observing System Data Assimilation System (GEOS-DAS) drive the ozone transport. Following every transport model timestep, the model prediction is combined with the observations using a global, physical-space based, statistical analysis scheme. Due to the smaller size of the ozone system than that of a global meteorological data assimilation system, new statistical analysis methodology, including anisotropic and flow-dependent forecast error correlation models, can be implemented and tested in the ozone system more easily. Sample results from the winter 1992 validation period are presented. There is a close agreement between the analyzed fields and the independent observations from ozone sondes and the Halogen Occultation Experiment (HALOE).
Author
Design Analysis; Data Systems; Ozone; Three Dimensional Models; Mixing Ratios; Chemical Analysis; Statistical Analysis; Meteorological Parameters; Proving

19990111534 Department of Energy, Office of Energy Research, Washington, DC USA
Plasma technology for tail pipe reduction of NO(x) in diesel exhaust
Penetrante, B. M., Department of Energy, USA; Vogtlin, G. E., Department of Energy, USA; Merritt, B. T., Department of Energy, USA; Brusasco, R. M., Department of Energy, USA; Mar. 01, 1998; 9p; In English; Air Pollution Health Impacts: Recent Findings, Implications, Dieselization and Policy Initiatives, USA

Report No.(s): DE98-057718; UCRL-JC-129948; CONF-9711189; No Copyright; Avail: Department of Energy Information Bridge, Microfiche

In the conventional application of plasmas to the treatment of power plant flue gases, the plasma is used to oxidize NO(x) to nitric acid; the final product us ammonium nitrate, which is obtained by addition of ammonia. A critical issue in the application of plasmas to cars and trucks is whether the plasma can remove the NO(x) by direct chemical reduction to N2. We have found that gas-phase reactions in the plasma alone cannot lead to true chemical reduction of NO(x). Any reduction of NO(x)to N2 can only be accomplished through heterogeneous reactions of NO2 with surfaces or particulates. This paper discusses how the plasma oxidation of NO to NO2 can be utilized to enhance the heterogeneous catalytic reduction of NO(x) to N2. Plasma-assisted heterogeneous catalysis can enhance the NO(x) reduction under conditions that normally make it difficult for either the plasma or the catalyst to function by itself. The combination of a plasmas with a catalyst opens the opportunity for a new class of catalysts that are potentially more durable, more active, more selective and more sulfur-tolerant compared to conventional lean-NO(x) catalysts.

NTIS

Flue Gases; Exhaust Gases; Exhaust Emission; Chemical Reactions; Catalysis; Plasmas (Physics); Nitrogen Oxides

19990111574 NASA Goddard Space Flight Center, Greenbelt, MD USA

Impact of Aircraft Emissions on NO(x) in the Lowermost Stratosphere at Northern Midlatitudes

Kondo, Y., Nagoya Univ., Japan; Koike, M., Nagoya Univ., Japan; Ikeda, H., Nagoya Univ., Japan; Anderson, B. E., NASA Langley Research Center, USA; Brunke, K. E., Christopher Newport Univ., USA; Zhao, Y., Nagoya Univ., Japan; Kita, K., Tokyo Univ. of Agriculture and Technology, Japan; Sugita, T., National Inst. for Environmental Studies, Japan; Singh, H. B., NASA Ames Research Center, USA; Liu, S. C., Georgia Inst. of Tech., USA; 1999; 18p; In English; No Copyright; Avail: CASI; A03, Hardcopy; A01, Microfiche

Airborne measurements of NO(x) total reactive nitrogen (NO(y)), O3 and condensation nuclei (CN) were made within air traffic corridors over the U.S. and North Atlantic regions (35-60 deg N) in the fall of 1997. NO(x) and NO(y) data obtained in the lowermost stratosphere (LS) were examined using the calculated increase in NO(y) ((delta)NO(y)) along five-day back trajectories as a parameter to identify possible effects of aircraft on reactive nitrogen. It is very likely that aircraft emissions had a significant impact on the NO(x) levels in the LS inasmuch as the NO(s), mixing ratios at 8.5-12 km were significantly correlated with the independent parameters of aircraft emissions, i.e., (delta)NO(y) levels and CN values. In order to estimate quantitatively the impact of aircraft emissions on NO(x), and CN, the background levels of CN and NO(x) at O3 = 100-200 ppbv were derived from the correlations of these quantities with (delta)NO(y)). On average, the aircraft emissions are estimated to have increased the NO(x) and CN values by 130 pptv and 400 STP,cc, respectively, which corresponds to 70 -/+ 30 % and 30 -/+ 20 % of the observed median values.

Author

Nitrogen Oxides; Stratosphere; Reactivity; Median (Statistics); Condensation Nuclei; Atlantic Ocean; Amount; Airborne Equipment

19990111576 NASA Langley Research Center, Hampton, VA USA

Horizontal Wavenumber Spectra of Winds, Temperature and Trace Gases During the Pacific Exploratory Missions, 2, Gravity Waves, Quasi-Two-Dimensional Turbulence, and Vortical Modes

Cho, John Y. N., Massachusetts Inst. of Tech., USA; Newell, Reginald E., Massachusetts Inst. of Tech., USA; Barrick, John D., NASA Langley Research Center, USA; Journal of Geophysical Research; Jul. 20, 1999; ISSN 0148-0227; Volume 104, No. D13, pp. 16,297-16,308; In English

Contract(s)/Grant(s): NAG1-1758; NAG1-1901; Copyright; Avail: Issuing Activity, Hardcopy

We examine the horizontal wavenumber spectra of horizontal velocity and potential temperature collected by aircraft above the Pacific Ocean to determine whether gravity waves, quasi-two-dimensional (Q-2-D) turbulence, or vortical modes dominate atmospheric fluctuations at scale sizes of 1-100 km and altitudes of 2-12 km. We conclude from the study of Doppler-shifting effects that Q-2-D turbulence and/or vortical modes are more prevalent than gravity waves over the ocean, except in the equatorial zone. The results are consistent with recent numerical simulations of Q-2-D turbulence, which show that the characteristic inverse cascade of energy is greatly facilitated by the presence of background rotation. Furthermore, a Stokes-parameter analysis reveals the general paucity of coherent wavelike motions, although specific cases of gravity-wave propagation are observed. Finally, a case study of a long flight segment displays a k(sup -3) horizontal velocity variance spectrum at scales longer than about 100 km.

A Stokes-parameter analysis indicates that these large-scale fluctuations were likely due to vortical modes rather than inertio-gravity waves.
Author
Wind (Meteorology); Gravity Waves; Gravitational Waves; Wave Propagation; Wind Velocity

19990111742 NASA Goddard Space Flight Center, Greenbelt, MD USA
Trends in the Vertical Distribution of Ozone
Randel, William J., National Center for Atmospheric Research, USA; Stolarski, Richard S., NASA Goddard Space Flight Center, USA; Cunnold, Derek M., Georgia Inst. of Tech., USA; Logan, Jennifer A., Harvard Univ., USA; Newchurch, M. J., Alabama Univ., USA; Zawodny, Joseph M., NASA Langley Research Center, USA; Science; Sep. 10, 1999; Volume 285, pp. 1689-1692; In English; Copyright; Avail: Issuing Activity, Hardcopy

Analyses of satellite, ground-based, and balloon measurements allow updated estimates of trends in the vertical profile of ozone since 1979. The results show overall consistency among several independent measurement systems, particularly for northern hemisphere midlatitudes where most balloon and ground-based measurements are made. Combined trend estimates over these latitudes for the period 1979-96 show statistically significant negative trends at ail attitudes between 10 and 45 km, with two local extremes: -7.4 +/- 2.0% per decade at 40 km and -7.3 +/- 4.6% per decade at 15 km attitude. There is a strong seasonal variation in trends over northern midlatitudes in the altitude range of 10 to 18 km, with the largest ozone loss during winter and spring. The profile trends are in quantitative agreement with independently measured trends in column ozone, the amount of ozone in a column above the surface. The vertical profiles of ozone trends provide a fingerprint for the mechanisms of ozone depletion over the last two decades.
Author
Annual Variations; Estimates; Ozone Depletion; Temperate Regions; Vertical Distribution

19990113065 Harvard Univ., Div, of Engineering and Applied Sciences, Cambridge, MA USA
Airborne Instruments for the In Situ Detection of ClONO2, NO2, ClO, and BrO in the Stratosphere ***Final Report, 1 Jan. 1996 - 30 Jun. 1997***
Anderson, James G., Harvard Univ., USA; Mar. 18, 1999; 4p; In English
Contract(s)/Grant(s): NCC2-892; No Copyright; Avail: CASI; A01, Hardcopy; A01, Microfiche

The objective of the research was the development of a new small, lightweight instrument for the detection of ClONO2, NO2, ClO, and BrO, carried aboard a robotic aircraft, specifically the NASA ER-2. The schematic of the instrument is shown. Some of the observations which this instrument is designed to make are discussed. The observations of the instrument during the Photochemistry of Ozone Loss in the Arctic Region in Summer (POLARIS) mission are also reviewed.
CASI
Airborne Equipment; Photochemical Reactions; Stratosphere; In Situ Measurement; Chlorine Oxides; Nitrogen Dioxide; Bromine Compounds; Measuring Instruments

19990113069 Office of Air Quality Planning and Standards, Research Triangle Park, NC USA
National Emission Standards for Hazardous Air Pollutants for Source Categories: Oil and Natural Gas Production and Natural Gas Transmission and Storage. Background Information for Final Standards. Summary of Public Comments and Responses
May 1999; 290p; In English
Report No.(s): PB99-155269; EPA/453/R-99/004B; No Copyright; Avail: CASI; A13, Hardcopy; A03, Microfiche

On February 6, 1998, the Environmental Protection Agency (EPA) proposed standards of performance for the oil and natural gas production source category (63 FR 6288) under authority of Section 111 of the Clean Air Act. There were 54 commenters composed mainly of industry and trade associations. Also commenting were State and local agencies, consultants and engineers, environmental groups, and other interested parties. The written comments were submitted, along with the responses to these comments, are summarized in this document.
NTIS
Crude Oil; Air Pollution; Natural Gas

19990113072 ARCADIS Geraghty and Miller, Inc., Research Triangle Park, NC USA
Characterization of Low-VOC Latex Paints: Volatile Organic Compound Content, VOC and Aldehyde Emissions, and Paint Performance ***Final Report, Jan. 1997 - Jan. 1999***
Fortmann, R.; Lao, H. C.; Ng, A.; Roache, N.; Apr. 1999; 92p; In English

Report No.(s): PB99-146920; No Copyright; Avail: CASI; A05, Hardcopy; A01, Microfiche

The report gives results of laboratory tests to evaluate commercially available latex paints advertised as 'low-odor,' 'low-VOC (volatile organic compound),' or 'no-VOC.' Measurements were performed to quantify the total content of VOCs in the paints and to identify the predominant VOCs and aldehydes in the emissions following application to test substrates. The performance of the paints was evaluated and compared to that of commonly used conventional latex paints by American Society for Testing and Materials (ASTM) standard methods that measured parameters such as scrubbability, cleanability, and hiding power. The report describes the paints that were tested, the test methods, and the experimental data. Results are presented that can be used to evaluate the low-odor/low-VOC paints as alternatives to conventional latex wall paints that contain and emit higher concentrations of VOCs.

NTIS

Latex; Aldehydes; Organic Compounds; Paints; Emission

19990113074 Office of Air Quality Planning and Standards, Research Triangle Park, NC USA

National Emission Standards for Hazardous Air Pollutants (NESHAP) Manufacturing Industry: Summary of Public Comments and Responses

Jul. 1998; 210p; In English

Report No.(s): PB99-158628; EPA/453/R-98/002; No Copyright; Avail: CASI; A10, Hardcopy; A03, Microfiche

Clean Air Act as amended in 1990. Public comments were received from 46 sources consisting mainly of States, pharmaceutical manufacturers, industry trade associations, environmental groups, and other interested parties. All of the comments that were submitted and the responses to these comments are summarized in this document. This summary is the basis for the revisions made to the standards between proposal and promulgation.

NTIS

Air Pollution; Industries; Manufacturing; Pharmacology

19990113122 Max-Planck-Inst. fuer Meteorologie, Hamburg, Germany

A Process-based, Climate-Sensitive Model to Derive Methane Emissions from Natural Wetlands: Application to 5 Wetland Sites, Sensitivity to Model Parameters and Climate

Walter, Bernadette P., Max-Planck-Inst. fuer Meteorologie, Germany; Heimann, Martin, Max-Planck-Inst., Jena, Germany; 1999; 48p; In English

Report No.(s): GCN-99-62; No Copyright; Avail: CASI; A03, Hardcopy; A01, Microfiche

Methane emissions from natural wetlands constitutes the largest methane source at present and depends highly on the climate. In order to investigate the response of methane emissions from natural wetlands to climate variations, a 1-dimensional process-based climate-sensitive model to derive methane emissions from natural wetlands is developed. In the model the processes leading to methane emission are simulated within a 1-dimensional soil column and the three different transport mechanisms diffusion, plant-mediated transport and ebullition are modeled explicitly. The model forcing consists of daily values of soil temperature, water table and Net Primary Productivity, and at permafrost sites the thaw depth is included. The methane model is tested using observational data obtained at 5 wetland sites located in North America, Europe and Central America, representing a large variety of environmental conditions. It can be shown that in most cases seasonal variations in methane emissions can be explained by the combined effect of changes in soil temperature and the position of the water table. Our results also show that a process-based approach is needed, because there is no simple relationship between these controlling factors and methane emissions that applies to a variety of wetland sites. The sensitivity of the model to the choice of key model parameters is tested and further sensitivity tests are performed to demonstrate how methane emissions from wetlands respond to climate variations.

Author

Methane; Wetlands; Climate Models; Sensitivity; Atmospheric Composition; Gaseous Diffusion; Atmospheric Diffusion

19990113138 ORTECH International, Mississauga, Ontario Canada

Documentation for the Gridded Hourly Atrazine Emissions Data Set for the Lake Michigan Mass Balance Study *Final Report*

Scholtz, M. T.; Van Heyst, B. J.; Ivanhoff, A.; Aug. 1999; 66p; In English

Report No.(s): PB99-175416; EPA/600/R-99/067; No Copyright; Avail: National Technical Information Service (NTIS), Hardcopy

In order to develop effective strategies for toxics management, the Great Lakes National Program Office (GLNPO) of the USA Environmental Protection Agency (US EPA), in 1994, launched an ambitious five year program to conduct a mass balance

study of selected toxic pollutants in Lake Michigan for the target year of 1995 (US EPA, 1998). Three persistent organic pollutants (POPs) and one heavy metal have been selected for the focus of the Lake Michigan Mass Balance (LMMB) study; polychlorinated biphenyls (PCBs), trans-nonachlor, atrazine and mercury. Atrazine is a broadleaf herbicide typically applied to corn, sorghum, sugarcane, pastures, sweet corn, seed crops and sod (Gianessi and Puffer, 1991). In 1991, applications to corn and sorghum accounted for approximately 95% of the total atrazine useage in the United State (Gianessi and Puffer, 1991). Atrazine is typically applied as a pre-emergent spray and/or a post-emergent spray although it can also be incorporated into the soil prior to planting (USDA, 1995a). Peer reviewed literature suggests that atmospheric sources of atrazine may be an important input of herbicide to the Lake Michigan system (Schottler and Eisenreich, 1997). The National Oceanic and Atmospheric Administration (NOAA) is collaborating with the LMMB study in its estimation of the atmospheric deposition of atrazine to Lake Michigan.
NTIS
Environment Protection; Mass Distribution; Balance; Emission

19990113145 ARCADIS Geraghty and Miller, Inc., Research Triangle Park, NC USA
Status of SO2 Scrubbing Technologies
Jozewicz, W.; Singer, C.; Srivastava, R. K.; Tsirigotis, P. E.; 1999; 24p; In English; Presented at Mega Symposium, Atlanta, GA., August 16-20, 1999
Report No.(s): PB99-171563; No Copyright; Avail: CASI; A03, Hardcopy; A01, Microfiche

The paper presents the extent of current sulfur dioxide (SO2) scrubber applications on electricity generating units in the U.S. and abroad. The technical performance of recent SO2 scrubber installations is discussed. Recently reported technical innovations to SO2 scrubbing technologies are also reviewed. Data on mercury removal achieved with scrubbers are presented and discussed. Current advances in scrubbing technologies to improve mercury capture are also presented.
NTIS
Sulfur Dioxides; Scrubbers; Washing; Acid Rain; Air Pollution; Pollution Control

19990113146 ARCADIS Geraghty and Miller, Inc., Research Triangle Park, NC USA
Preparation and Evaluation of Modified Lime and Silica-Lime Sorbents for Mercury Vapor Emissions Control
Ghorishi, S. B.; Singer, C. F.; Sedman, C. B.; 1999; 24p; In English; Presented at Mega Symposium, Atlanta, GA., August 16-20, 1999
Report No.(s): PB99-171555; No Copyright; Avail: CASI; A03, Hardcopy; A01, Microfiche

The paper discusses current efforts to improve the uptake of mercury species by increasing active sites and adding oxiditive species to the sorbent. (NOTE: Previous work showed that mercury chloride vapor is readily absorbed by calcium-based sorbents as an acid gas in environments typical of coal-fired boiler flue gas, white elemental mercury vapor is absorbed by calcium-based sorbents only when sulfur oxides are also present.) Preparation of modified lime and silica-lime sorbents and their behavior toward mercury species are compared to those of commercially available lime on a fixed-bed bench reactor. The implications of findings toward development of mutipollutant control technologies and planned field toward development of multipollutant control technologies and planned field pilot evaluations of more multipollutant control concepts are discussed.
NTIS
Mercury Compounds; Mercury Vapor; Sorbents; Silicon Dioxide; Calcium Oxides

19990113147 ARCADIS Geraghty and Miller, Inc., Research Triangle Park, NC USA
Role of HC1 in Adsorption of Elemental Mercury Vapor by Calcium-Based Sorbents
Ghorishi, B.; Gullett, B. K.; Jozewicz, W.; Kozlowski, W.; 1999; 22p; In English; Presented at EPRI/DOE/EPA Combined Utility Air Pollutant Control Symposium, Atlanta, GA., August 16-20, 1999
Report No.(s): PB99-171548; No Copyright; Avail: CASI; A03, Hardcopy; A01, Microfiche

The paper gives results of a study to identify active sites and surface functional groups that may contribute to the absorption of elemental mercury (Hg) by relatively inexpensive calcium (CA)-based sorbents. The study investigated the formation of chlorine (C1) sites in CA-based sorbents as well as their role and reactivity in the absorption of Hg. HC1-exposed calcium sulfate dihydrate (gypsum) exhibited a superior Hg sorption capability. Crystalline water molecules on the surface of the gypsum were confirmed to contribute indirectly to Hg uptake. These surface molecules may have absorbed HC1 through hydrogen bond formation between an oxygen atom of a crystalline water molecule and a hydrogen atom of an HC1 molecule, Two adjacent, physically absorbed HC1 molecules could then trap an Hg molecule through formation of a mercuric-chloride-like molecule. Significant correlations between C1 and Hg uptake by gypsum were noted.
NTIS
Mercury Compounds; Mercury Vapor; Sorbents; Air Pollution

19990113148 Research Triangle Inst., Research Triangle Park, NC USA
Investigating the Influence of Relative Humidity, Air Velocity and Amplification on the Emission Rates of Fungal Spores
Foarde, K. K.; VanOsdell, D. W.; Menetrez, M. Y.; Chang, J. C. S.; 1999; 10p; In English
Report No.(s): PB99-171530; No Copyright; Avail: CASI; A02, Hardcopy; A01, Microfiche

The paper discusses the impact of relative humidity (RH), air velocity, and surface growth on the emission rates of fungal spores from the surface of contaminated material. Although the results show a complex interaction of factors, the authors have determined, for this limited data set, that emission rates are inversely proportional to RH, but directly related to air flow rate and surface loading. (NOTE: Although a significant amount of work has been done to elucidate the conditions under which fungi will grow on the surfaces of materials, little information is available that quantitatively relates surface concentrations to airborne concentration and, ultimately, exposure.)
NTIS
Fungi; Spores

19990113150 ARCADIS Geraghty and Miller, Inc., Research Triangle Park, NC USA
Gas-Phase and Particulate Emissions during Application of a Water-Based Cleaner with a Hand-Pump Sprayer
Fortmann, R.; Ng, A.; Roache, N.; Howard, E.; 1999; 10p; In English
Report No.(s): PB99-171514; No Copyright; Avail: CASI; A02, Hardcopy; A01, Microfiche

The paper gives results of tests in a controlled environment test room to measure concentrations of 2-butoxyethanol and particles during application of a cleaner to realistic surfaces (counter tops, glass, walls). 2-Butoxyethanol was collected on Tenax and analyzed by gas chromatography. Concentrations of droplets were measured continuously with an aerodynamic particle sizer. During two sets with the cleaner diluted 1 part with 9 parts water, the average concentrations of 2-butoxy-ethanol during the 20-minute cleaning period were 13.5 and 10.3 mg/cu m, about half the NIOSH recommended exposure limit of 24 mg/cu m. After 2 hours, the concentrations dropped below 4 mg/cu m in the room exhausted at a rate of 1 air change per hour.
NTIS
Particulates; Vapor Phases; Emission; Gases; Cleaners; Sprayers

46
GEOPHYSICS

Includes aeronomy; upper and lower atmosphere studies; ionospheric and magnetospheric physics; and geomagnetism. For space radiation see 93 Space Radiation.

19990106563 Instituto Nacional de Pesquisas Espacias, Sao Jose dos Campos, Brazil
Retrieval of Vertical Temperature Profiles in the Atmosphere Using an Iterative Implicit Inversion Technique *Inferencia de Perfis Verticais de Temperatura Utilizando uma Tecnica Iterativa Implicita de Inversao*
Carvalho, Joao Carlos, Instituto Nacional de Pesquisas Espacias, Brazil; 1999; 114p; In Portuguese
Report No.(s): INPE-7228-TDI/682; No Copyright; Avail: CASI; A06, Hardcopy; A02, Microfiche

In this work, we present an iterative implicit inversion method (MIII) to retrieve vertical temperature profiles based on the mathematical inversion of the radiative transfer equation (RTE). The inverse problem is formulated as a nonlinear constrained optimization problem. A regularization term is added to the objective function with the help of a Lagrange multiplier. The regularization function considered is the Tikhonov regularization, and regularization based on the maximum entropy principle. As a first step, it is presented a set of simulations using synthetically data obtained directly from the RTE, then, the method is applied in a real situation with radiance data given by the HIRS/2 (High Resolution Infrared Radiation Sounder) sensors. Finally, a comparison with profiles obtained by radiosonde is presented. In general, the proposed algorithm converges to excellent temperature profiles mainly in the tropopause inversion region.
Author
Atmospheric Temperature; Temperature Profiles; Satellite Sounding; Remote Sensing; Radiative Transfer

19990106570 NASA Goddard Space Flight Center, Greenbelt, MD USA
Dynamics of Quasi-biennial Oscillations in Tropical Ocean-Atmosphere Coupled System
Kim, K.–M., Universities Space Research Association, USA; Lau, K.–M., NASA Goddard Space Flight Center, USA; [1999]; 1p; In English; 24th; Annual Climate Diagnostic Workshop, 1-5 Nov. 1999, Tucson, AZ, USA; No Copyright; Avail: Issuing Activity, Hardcopy; Abstract Only

In this study, quasi-biennial oscillation (QBO) in atmosphere-ocean coupled system is investigated using intermediate coupled model. Observation studies show that the easterly zonal winds anomalies prevail over the equatorial western Pacific during the warm phase of El Nino/Southern Oscillation (ENSO). At the time scale of QBO, SST variations and east Asia Summer monsoon rainfall are closely linked to the eastward propagating zonal winds anomalies originated from Indian ocean. to investigate the effect of zonal wind anomalies over western Pacific on the evolution of ENSO, simple anomalous winds are added to the western part of model domain as external forcing. Wind forcing is parameterized as a function of SST anomalies in the eastern Pacific with time lag. Time lag is adopted to mimic the relation between east Asian monsoon and ENSO. The results shows that the winds anomalies make coupled system oscillate through generating forced Kelvin waves even without the western boundary reflection of Rossby waves. Kelvin waves generated by external forcing are also crucial for the model to oscillate as well as Rossby wave reflections at the western boundary. When the monsoon forced Kelvin wave is strong during the northern winter, the coupled system damped out very quickly. In certain range of external winds amplitude and time lag, the model El Nino shows QBO features. It is suggested that the external wind forcing which is related to summer monsoon flow over western Pacific intensify the negative feedback process of off-equatorial Rossby waves and modify the ENSO periodicity.
Author
Air Water Interactions; Anomalies; El Nino; Southern Oscillation; Monsoons; Rain

19990106572 NASA Goddard Space Flight Center, Greenbelt, MD USA
Momentum Transport Obtained from 2D and 3D Cloud System Models
Tao, Wei–Kuo, NASA Goddard Space Flight Center, USA; Wang, Y., NASA Goddard Space Flight Center, USA; Johnson, D., NASA Goddard Space Flight Center, USA; [1999]; 1p; In English; GCSS Workshop, 4-8 Oct. 1999, Princeton, NJ, USA; No Copyright; Avail: Issuing Activity, Hardcopy; Abstract Only

The use of cloud resolving models (CRMs) in the study of tropical convection and its relation to the large-scale environment can generally be categorized into two groups. The first approach is called ”cloud ensemble modeling”. In this approach, many clouds of different sizes in various stages of their lifecycles can be present at any model simulation time. The observed large-scale effects (advective tendencies of potential temperature, water vapor mixing ratio, and horizontal momentum) are always applied to the model continuously (called semi-prognostic approach by Soong and Tao, 1980). In addition, the cloud ensemble models use cyclic lateral boundary conditions (to avoid reflection of gravity waves) and require a large horizontal domain (to allow for the existence of an ensemble of clouds). The model can be integrated for several days and its results are still in very good agreement with observation. The clouds simulated from this approach could be termed ”continuous large-scale forced convection”. On the other hand, the second type of CRM simulations do not require large-scale effects to initialize and maintain cloud development. This type of CRM usually requires initial temperature and water vapor profiles which have a medium to large CAPE, and an open lateral boundary condition is used. The modeled clouds, then, are initialized with either a cool pool, warm bubble or surface processes (i.e., land/ocean). These modeled clouds could be termed ”self-forced convection”; they are mainly for case study (i.e., for 8-16 h time integration). A two- and three-dimensional Goddard Cumulus Ensemble (GCE) Model are used to study the momentum transport by convective system associated with Westerly Wind Burst (WWB) event and a squall line occurred in West Pacific warm pool region. We will examine the difference in momentum between two and three dimensional modeling as well as the ”continuous large-scale forced convection” and ”continuous large-scale forced convection” approaches. The convective and stratiform region contribution to momentum transport will also be investigated.
Author
Momentum Transfer; Energy Transfer; Atmospheric Models; Cloud Physics; Atmospheric Circulation; Advection; Convection; Atmospheric Moisture

19990106573 NASA Goddard Space Flight Center, Greenbelt, MD USA
The Performance of GEOS II GCM in ARM SCM Evaluations: Tests with Case III Forcing Data
Sud, Yogesh C., NASA Goddard Space Flight Center, USA; Sep. 24, 1999; 1p; In English; GCSS Workshop, 4-8 Oct. 1999, Princeton, NJ, USA; No Copyright; Avail: Issuing Activity, Hardcopy; Abstract Only

Our simulations with ARM CART SCM evaluations have revealed that the Goddard cloud complex called Microphysics of clouds with Relaxed Arakawa-Schubert Scheme (McRAS) has been evaluating well in the past three cases produced with two ARM in situ datasets. Some of the deficiencies seen in these tests were related to inconsistencies in the forcing datasets. When those were removed, with a better reanalysis, the model performed much better in rainfall simulation but still had discernible errors in simulating the lapse rate. There was nothing systematic about these errors; particularly, the lapse rates in the observations were unattainable because they were not contained within the moist and dry lapse rates. This again suggested that a part of the model error may be related to the analysis being too warm perhaps due to imbeded inversions which the model is unable to simulate. We are currently running the third case with all its scenarios and options as required by the SCM validation group. In the workshop

we will have an opportunity to compare results from several models; this will enable us to determine as to how we can address the remaining model deficiencies of McRAS.
Author
Cloud Physics; Earth Observing System (EOS); In Situ Measurement; Remote Sensing; Atmospheric Models

19990106578 NASA Marshall Space Flight Center, Huntsville, AL USA
Low Energy Plasma in the Outer Magnetosphere as Observed by Interball Tail Probe
Coffey, Victoria N., NASA Marshall Space Flight Center, USA; Vaisberg, Oleg L., NASA Marshall Space Flight Center, USA; Gallagher, Dennis L., NASA Marshall Space Flight Center, USA; Chandler, Michael O., NASA Marshall Space Flight Center, USA; [1999]; 1p; In English, 13 Dec. 1999, San Francisco, CA, USA; Sponsored by American Geophysical Union, USA; No Copyright; Avail: Issuing Activity, Hardcopy; Abstract Only

The Interball Tail Probe crosses the dayside magnetopause at low latitudes where it frequently measures low energy ion plasma (is less than 100 eV) in the outer magnetosphere. We present the plasma characteristics of this cold component, including it's dependence on solar wind parameters and interaction with PC-5 type waves.
Author
Plasmas (Physics); Solar Wind; Magnetopause; Planetary Magnetotails

19990106581 NASA Marshall Space Flight Center, Huntsville, AL USA
PC-5 Waves and Low Energy Plasma in the Outer Magnetosphere
Gallanger, Dennis L., NASA Marshall Space Flight Center, USA; Vaisberg, Oleg L., NASA Marshall Space Flight Center, USA; Coffey, Victoria N., NASA Marshall Space Flight Center, USA; [1999]; 1p; In English, 13 Dec. 1999, San Francisco, CA, USA; Sponsored by American Geophysical Union, USA; No Copyright; Avail: Issuing Activity, Hardcopy; Abstract Only

The Interball Tail Probe crosses the dayside magnetopause at low latitudes where it frequently measures low energy ion plasma (is less than 100 eV) in the outer magnetosphere. We present the wave characteristics associated with this cold component.
Author
Plasmas (Physics); Gravitational Waves

19990106588 NASA Goddard Space Flight Center, Greenbelt, MD USA
Mesospheric Odd Nitrogen Enhancements During Relativistic Electron Precipitation Events
Aikin, A. C., NASA Goddard Space Flight Center, USA; Smith, H. J. P., TPE Associates, USA; [1999]; 21p; In English; No Copyright; Avail: CASI; A03, Hardcopy; A01, Microfiche

The behavior of mesospheric odd nitrogen species during and following relativistic and diffuse auroral precipitation events is simulated, Below 75 km nitric oxide is enhanced in proportion to the ion pair production function associated with the electron precipitation and the length of the event. Nitrogen dioxide and nitric acid are also enhanced. At 65 km the percentage of odd nitrogen for N is 0.1%, HNO3 is 1.6%, NO2 is 15%, and NO is 83.3%. Between 75 and 85 km NO is depleted during particle events due to the faster destruction of NO by N relative to the production of NO by N reacting with O2. Recovery of NO depends on transport from the lower thermosphere, where NO is produced in abundant amounts during particle events.
Author
Mesosphere; Nitrogen; Augmentation; Electron Precipitation

19990107329 NASA Marshall Space Flight Center, Huntsville, AL USA
The NASA/MSFC Global Reference Atmospheric Model: 1999 Version (GRAM-99)
Justus, C. G., Computer Sciences Corp., USA; Johnson, D. L., NASA Marshall Space Flight Center, USA; May 1999; 94p; In English
Report No.(s): NASA/TM-1999-209630; NAS 1.15:209630; M-941; No Copyright; Avail: CASI; A05, Hardcopy; A01, Microfiche

The latest version of Global Reference Atmospheric Model (GRAM-99) is presented and discussed. GRAM-99 uses either (binary) Global Upper Air Climatic Atlas (GUACA) or (ASCII) Global Gridded Upper Air Statistics (GGUAS) CD-ROM data sets, for 0-27 km altitudes. As with earlier versions, GRAM-99 provides complete geographical and altitude coverage for each month of the year. GRAM-99 uses a specially-developed data set, based on Middle Atmosphere Program (MAP) data, for 20-120 km altitudes, and NASA's 1999 version Marshall Engineering Thermosphere (MET-99) model for heights above 90 km. Fairing techniques assure smooth transition in overlap height ranges (20-27 km and 90-120 km). GRAM-99 includes water vapor and 11 other atmospheric constituents (O3, N2O, CO, CH4, CO2, N2, O2, O, A, He and H). A variable-scale perturbation model provides both large-scale (wave) and small-scale (stochastic) deviations from mean values for thermodynamic variables and

horizontal and vertical wind components. The small-scale perturbation model includes improvements in representing intermittency (”patchiness”). A major new feature is an option to substitute Range Reference Atmosphere (RRA) data for conventional GRAM climatology when a trajectory passes sufficiently near any RRA site. A complete user’s guide for running the program, plus sample input and output, is provided. An example is provided for how to incorporate GRAM-99 as subroutines in other programs (e.g., trajectory codes).
Author
Reference Atmospheres; Climatology; Atmospheric Temperature; Atmospheric Density; Middle Atmosphere; Atmospheric Circulation

19990107373 Lembaga Penerbangan dan Antariksa Nasional, Peneliti Bidang Komunidasi HF, Puslitbang PI, Jakarta, Indonesia
Ionosphere Slab Thickness Above Sumedang ***Slab Thickness Ionosfer di Atas Sumedang***
Rusnadi, Iyus Edi, Lembaga Penerbangan dan Antariksa Nasional, Indonesia; Warta: Lembaran Tambahan Majalah LAPAN; October 1998; ISSN 0126-9754; Volume 22, No. 57, pp. 38-43; In Malay-Indonesian; No Copyright; Avail: CASI; A02, Hardcopy; A01, Microfiche

Development of satellite excites scientist to progress the research of ionosphere. In application good quality receiver is needed to receive satellite signal, so that development of science can be used effectively. Using Sumedang Total Electron Content (TEC) data by Global Positioning System (GPS) satellite support the progress of the ionosphere’s research compared the research using the previous instrument. Slab thickness is important for deciding slab thickness model on one place. Calculated of slab thickness that use ionosphere data at Sumedang, Indonesia (equator) is greater than Salisbury, Australia (mid latitude) results, where as slab thickness at Sumedang must be less than Salisbury. Based on observation caused by: 1) allocated of time not fixed, so that no synchronized between TEC and ionosphere data. 2) Registered TEC data is manually. 3) Calculation of the slab thickness that is not suitable with the equator condition.
Author
Thickness; Slabs; Earth Ionosphere

19990107380 NASA Marshall Space Flight Center, Huntsville, AL USA
Polar Observations of Properties of H+ and O+ Conics in the Cusp Near ~5300 km Altitude
Hirahara, M., Alabama Univ., USA; Horwitz, J. L., Alabama Univ., USA; Moore, T. E., NASA Marshall Space Flight Center, USA; Chandler, M. O., NASA Marshall Space Flight Center, USA; Giles, B. L., NASA Marshall Space Flight Center, USA; Craven, P. D., NASA Marshall Space Flight Center, USA; Pollock, C. L., Southwest Research Inst., USA; [1996]; 1p; In English, Sep. 1996, Guntersville, AL, USA; No Copyright; Avail: CASI; A01, Hardcopy; A01, Microfiche; Abstract Only; Abstract Only

Observations by the thermal ion dynamics experiment (TIDE) on POLAR are used to explore features of low-energy ionospheric ion conical distributions at approximately 5300 km altitude over the southern cusp under different interplanetary magnetic field (IMF) conditions with negative and positive B(sub z) components. The properties are summarized as follows: (1) At the edge upstream of the convection in the cusp, the energy of outflowing ion distributions abruptly increased from a few eV to approximately 100 eV; (2) The angular distributions also abruptly changed from rammed is less than approximately 5 eV polar wind distributions to approximately 10-100 eV conics; (3) These conic signatures gradually gave way again to polar wind components further downstream of the cusp; (4) The uppermost energy of the detected O+ was larger than that of H+, while the density and flux of O+ were lower than those of H+; (5) The cone angles for both light and heavy ion conics were largest for the upstream region of the convection; (6) Cone angles are wider for O+ than H+; (7) The cone angles as well as the conic energies gradually decreased in the convection direction; (8) The UFI beams and conics were sometimes observed alternately, particularly for H+, and (9) In some cases, the distinct ion conic bursts occurred multiple times during a single cusp crossing.
Author
Interplanetary Magnetic Fields; Earth Ionosphere; Ion Concentration; Ion Distribution

19990107392 NASA Marshall Space Flight Center, Huntsville, AL USA
Global Dynamics of Dayside Auroral Precipitation in Conjunction with Solar Wind Pressure Pulses
Brittnacher, M., Washington Univ., USA; Chua, D., Washington Univ., USA; Fillingim, M., Washington Univ., USA; Parks, G. K., Washington Univ., USA; Spann, James F., Jr., NASA Marshall Space Flight Center, USA; Germany, G. A., Alabama Univ., USA; Carlson, C. W., California Univ., USA; Greenwald, R. A., Johns Hopkins Univ., USA; [1999]; 1p; In English, 31 May - 4 Jun. 1999, Boston, MA, USA; Sponsored by American Geophysical Union, USA; No Copyright; Avail: Issuing Activity, Hardcopy; Abstract Only

Global observation of the dayside auroral region by the Ultraviolet Imager (UVI) during transient solar wind pressure pulse events on October 1, 1997 has revealed unusual features in the auroral precipitation. The auroral arc structure on the dayside,

possibly connected with the LLBL, split into 2 arc structures; one moving poleward and fading over a 5 min period, and the other stationary or slightly shifted equatorward (by changes in the x component). The y component was large and positive, and the z component was small and negative. The splitting of the arc structure extended from 9 to 15 MLT and was concurrent with an enhancement of the convection in the cusp region identified by SuperDARN observations. The convection reversal on the morningside was adjacent to and poleward of the weak lower latitude band of precipitation. The sensitivity of the UVI instrument enabled observation of arc structures down to about 0.2 erg electron energy flux, as confirmed by comparison with particle measurements from the FAST satellite for other dayside events. Removal of the spacecraft wobble by PIXON image reconstruction restored the original resolution of the UVI of about 40 km from apogee. This event is being analyzed in connection with a larger study of global dynamics of dayside energy and momentum transfer related to changes in IMF conditions using UVI images in conjunction with observations from FAST and SuperDARN.
Author
Auroral Arcs; Auroral Zones; Polar Regions; Pressure Pulses; Solar Wind; Transient Pressures; Wind Pressure

19990107396 Swedish Inst. of Space Physics, MRI Atmospheric Research Programme, Kiruna, Sweden
Planetary-Wave Modulation of PMSE
Kirkwood, S., Swedish Inst. of Space Physics, Sweden; Rechou, A., Swedish Inst. of Space Physics, Sweden; Geophysical Research Letters; Dec. 15, 1998; ISSN 0094-8276; Volume 25, No. 24, pp. 4509-4512; In English; Original contains color illustrations
Report No.(s): Paper-1998GL900198; Copyright; Avail: Issuing Activity, Hardcopy

Variation in Polar Mesosphere Summer Echo (PMSE) occurrence with 4-6 day periods were observed by ESRAD radar during the summer of 1997. These are compared with temperature fluctuations in 5-day planetary waves extracted from the UKMO assimilated global data analyses. At the beginning and close to the end of the PMSE season, the PMSE variations are closely anti correlated with temperature variations associated with 5-day planetary waves at the 1mb level. The planetary wave amplitudes expected at the mesopause are 1-2 K. This is fo8und, by comparison with the seasonal decay of PMSE as the temperature rises at the end of summer, to be sufficient to explain the observed 5-10% amplitude fluctuations in PMSE daily occurrence.
Author
Atmospheric Temperature; Modulation; Planetary Waves; Summer; Polar Meteorology; Polar Regions; Mesopause

19990107398 Swedish Inst. of Space Physics, MRI Atmospheric Research Programme, Kiruna, Sweden
The 1997 PMSE Season: Its Relation to Wind, Temperature and Water Vapour
Kirkwood, S., Swedish Inst. of Space Physics, Sweden; Barabash, V., Swedish Inst. of Space Physics, Sweden; Chilson, P., Swedish Inst. of Space Physics, Sweden; Rechou, A., Swedish Inst. of Space Physics, Sweden; Stebel, K., Swedish Inst. of Space Physics, Sweden; Geophysical Research Letters; Jun. 01, 1998; ISSN 0094-8534; Volume 25, No. 11, pp. 1867-1870; In English; Sponsored in part by NFR
Report No.(s): Paper-98GL01243; Copyright; Avail: Issuing Activity, Hardcopy

Factors determining the onset and decay of the Polar Mesosphere Summer Echo (PMSE) season in 1997 are examined. PMSE from the ESRAD radar at 68N, 20E are compared with simultaneous observations of stratospheric winds, upper-mesosphere temperature, upper mesosphere water vapour and noctilucent clouds. There was a 3-week delay from the start of summer, defined by temperature or stratospheric winds, to the start of PMSE. At the end of the summer, the return to winter conditions was simultaneous in all three parameters. Noctilucent clouds at 55-60N were confined to the period of lowest temperatures, when PMSE were also present throughout the day. Water vapour observations show an increase during the summer, possibly taking place in late May, at about the time PMSE first appeared. It seems likely that the start of the PMSE season is determined by water vapour availability, while the end of the season is determined by temperature.
Author
Mesosphere; Noctilucent Clouds; Summer; Water Vapor; Winds Aloft; Polar Meteorology; Polar Regions

19990107399 Swedish Natural Science Research Council, Stockholm, Sweden
Incoherent Scatter Radar Observations of the Cusp Acceleration Region and Cusp Field-Aligned Currents
Nilsson, H., Swedish Natural Science Research Council, Sweden; Moretto, T., Danish Meteorological Inst., Denmark; Journal of Geophysical Research; Nov. 01, 1998; ISSN 0148-0227; Volume 103, No. A11, pp. 26,721-26,730; Original contains color illustrations
Report No.(s): Paper-98JA02269; Copyright; Avail: Issuing Activity, Hardcopy

Incoherent scatter radar measurements are used to study the E region and lower F region in the cusp proper. At the equatorward edge of the cusp a region of enhanced ionization is found, indicating precipitation of either electrons of about 1 keV energy or protons of about 3 keV. The signature is found at the same altitude, around 150 km, as the maximum of the solar EUV produced ionization., but is clearly recognizable. The position and likely proton energies indicate that this is probably the ionospheric signature of the cusp acceleration region. Regions of low electron densities are also found in the same altitude region, which may be explained by downward field-aligned currents causing depletions in the E and lower F region. First order estimates show that dense field aligned currents are needed to cause the observed depletions, possibly as dense as 30 micro A/square M. The ionization in the cusp acceleration region, and the depletion caused by downward field-aligned currents both influence the Pedersen conductivity of the ionosphere, and the resulting conductivity gradients strongly influence the small scale field aligned currents flowing in the cusp region.
Author
E Region; Extreme Ultraviolet Radiation; F Region; Ionization; Polar Cusps; Field Aligned Currents; Atmospheric Electricity; Earth Ionosphere; Ionospheric Conductivity; Particle Acceleration

19990108630 Novosibirsk State Univ., USSR
On the Nature of Mesospheric Electric Fields
Zadorozhny, A. M., Novosibirsk State Univ., USSR; 11th International Conference on Atmospheric Electricity; June 1999, pp. 76-79; In English; See also 19990108601
Contract(s)/Grant(s): RFBR-97-05-65242; No Copyright; Avail: CASI; A01, Hardcopy; A10, Microfiche

A possible mechanism for the generation of large vertical electric fields observed in the mesosphere is discussed. Simultaneous existence in the mesosphere both of negative and positive multiply charged aerosol particles of different sizes is assumed for explanation of the fields. More massive charged particles falling with larger velocities initiate a charge separation. Smaller particles carrying charges of the other sign are needed to reduce the effective conductivity of the mesospheric dusty plasma. The proposed model can explain the existence of the V/m electric fields observed both in the lower mesosphere and in the vicinity of noctilucent clouds and polar mesosphere summer echoes (PMSE).
Author
Aerosols; Electric Fields; Mesosphere; Mathematical Models

19990108651 Saint Petersburg Univ., Research Inst. of Physics, Saint Petersburg, Russia
Magnetic Field of a Branching Discharge
Borisov, V. V., Saint Petersburg Univ., Russia; Utkin, A. B., Vavilov State Optical Inst., USSR; 11th International Conference on Atmospheric Electricity; June 1999, pp. 127-130; In English; See also 19990108601; No Copyright; Avail: CASI; A01, Hardcopy; A10, Microfiche

We consider space-time representation to the magnetic field produced by a right-angle branching discharge. Current pulse starts and propagates to the T-branching point. Then one discharge segment carries a part of the initial current in the original direction to the first (cloud) terminal point. The rest of the current pulse propagates in the vertical direction to the other (ground) terminal point. This scheme can serve as a rough model of complicated cloud-to-cloud discharge that partially branches to the ground. The report was stimulated by observation of corresponding natural phenomenon in July 1996 at the Ladoga Lake.
Author
Cloud-to-Cloud Discharges; Magnetic Fields; Electromagnetic Wave Transmission; Wave Propagation

19990108703 NASA Marshall Space Flight Center, Huntsville, AL USA
The Relationship Between the Background and Transient Signals in Schumann Resonances
Williams, E., Massachusetts Inst. of Tech., USA; Castro, D., Massachusetts Inst. of Tech., USA; Boldi, R., Massachusetts Inst. of Tech., USA; Chang, T., Massachusetts Inst. of Tech., USA; Huang, E., Massachusetts Inst. of Tech., USA; Mushtak, V., Massachusetts Inst. of Tech., USA; Lyons, W., FMA Research, Inc., USA; Nelson, T., FMA Research, Inc., USA; Heckman, S., NASA Marshall Space Flight Center, USA; Boccippio, D., NASA Marshall Space Flight Center, USA; 11th International Conference on Atmospheric Electricity; June 1999, pp. 758-761; In English; See also 19990108601
Contract(s)/Grant(s): NSF ATM-96-33766; No Copyright; Avail: CASI; A01, Hardcopy; A10, Microfiche

Two distinct measures of the Earth's Schumann resonances-the background and the transients--are studied through comparisons at the mesoscale and at the continental scale. A rough proportionality is shown between the far more abundant

afternoon lightning activity and the larger positive mesoscale discharges that make sprites and simultaneously ring the Earth-ionosphere cavity to levels higher than the integration of all other lightnings.
Author
Earth Ionosphere; Surges; Atmospheric Electricity; Lightning; Cloud-to-Ground Discharges

19990108724 Indian Inst. of Tropical Meteorology, Poona, India
Effect of Coagulation on the Particle Charge Distribution and Air Conductivity
Dhanorkar, Savita, Indian Inst. of Tropical Meteorology, India; Kamra, A. K., Indian Inst. of Tropical Meteorology, India; 11th International Conference on Atmospheric Electricity; June 1999, pp. 539-542; In English; See also 19990108601; No Copyright; Avail: CASI; A01, Hardcopy; A10, Microfiche

The ion-aerosol balance equations including the effect of the coagulation of charged aerosols are solved. The effect of coagulation on the steady state charge distribution of the singly and multiply charged aerosol particles is examined for different ionization rates and aerosol concentrations. When the aerosol concentration is large, the coagulation results in an increase in the fraction of charged aerosols and the increase continues up to a critical value of aerosol concentration. The polar conductivity computed from this charge distribution first decreases and then increases with the increase in aerosol concentration. The critical value of aerosol concentration at which the minimum in conductivity occurs shifts to the higher values of aerosol concentration for larger ionization rates.
Author
Aerosols; Air Conductivity; Charge Distribution; Charged Particles; Electrical Resistivity; Atmospheric Conductivity

19990108725 Main Geophysical Observatory, Research Center for Atmospheric Remote Sounding, Saint Petersburg, Russia
Natural Atmospheric Ions as Electrostatic Systems
Klingo, V. V., Main Geophysical Observatory, Russia; 11th International Conference on Atmospheric Electricity; June 1999, pp. 543-546; In English; See also 19990108601; No Copyright; Avail: CASI; A01, Hardcopy; A10, Microfiche

Electrostatic parameters of atomic and molecular natural atmospheric ions have been calculated on a basis of the simplest quantum-mechanical approach. Electron wave functions of atomic orbitals are taken in the Slater-Zemer form. Necessary parameters have been determined for ions: H(-). H(+), O(+), O(-). Classical analogues of diatomic molecules Ions are found by a method of covalent bonds. The diatomic molecules ions H(sub 2)(+), N(sub 2)(+), O(sub 2)(+), O(sub 2)(-), are three centers of charges with an experimental value of the distance between atomic nuclei.
Author
Atmospheric Ionization; Molecular Ions; Quantum Mechanics; Cloud Physics

19990108726 Rostov State Univ., Dept. of Physics and Mathematics, Rostov-on-Don, USSR
On Factors Determining the Variations of the Electric Characteristics of a Surface Layer
Petrov, A. I., Rostov State Univ., USSR; Petrova, G. G., Rostov State Univ., USSR; Panchishkina, I. N., Rostov State Univ., USSR; 11th International Conference on Atmospheric Electricity; June 1999, pp. 547-550; In English; See also 19990108601; No Copyright; Avail: CASI; A01, Hardcopy; A10, Microfiche

During the study of electrode layer atmospheric-electrical characteristics were being studied within the other physical characteristics of atmosphere surface layer and upper layer of soil. Vertical profiles of polar conductivities in conditions of different atmosphere stratification for four points of observations with different contents of radon-222 in the soil and with different outcome of it into the atmosphere are presented in this study. Participation of convection and diffusion components of mechanical transfer current from atmosphere to earth in different conditions of thermal and dynamical instability of surface layer was analyzed. The values of Dolezalek criteria for different conditions were estimated.
Author
Atmospheric Boundary Layer; Electrical Properties; Atmospheric Electricity; Radon Isotopes; Vertical Distribution

19990108740 Academy of Sciences (Russia), Inst. of Applied Physics, Nizhny Novgorod, Russia
On the Description of Atmospheric Electric Field and Current Under Inhomogeneous Conductivity
Davydenko, S. S., Academy of Sciences (Russia), Russia; Bespalov, P. A., Academy of Sciences (Russia), Russia; 11th International Conference on Atmospheric Electricity; June 1999, pp. 551-554; In English; See also 19990108601
Contract(s)/Grant(s): RFBR-98-02-16236; No Copyright; Avail: CASI; A01, Hardcopy; A10, Microfiche

An approach to description of global electric processes under inhomogeneous distribution of atmospheric electric conductivity is elaborated. The conductivity is assumed to be varying arbitrary with latitude and increasing exponentially with altitude. Due to separation of variables established in a general equation describing an atmospheric electric potential, a set of the

ordinary differential equations is obtained and solved by expansion into a generalized power series. A method of the eigenvalue spectrum evaluation and properties of the appropriate eigenfunctions are considered. to estimate responses of global atmospheric electric field and air-earth current to variations of latitude conductivity profile, a model of global electric circuit is constructed taking into account both the spatial conductivity distribution and electric sources connected with large-scale magnetospheric convection. Using the approach elaborated, an exact general solution of the problem is obtained. It is shown that latitude variation of terrestrial atmospheric conductivity leads to appearance of additional latitude homogeneous electric potential in the lower atmosphere with the magnitude of about 15% of the global ground-ionosphere voltage.
Author
Atmospheric Electricity; Atmospheric Conductivity; Electric Fields; Electric Current; Lower Atmosphere; Electric Potential; Mathematical Models

19990108741 Taganrog Inst. of Radio Engineering, Dept. of Physics, USSR
Global Variations of Ionospheric Potential in Surface Layer
Kupovykh, G. V., Taganrog Inst. of Radio Engineering, USSR; 11th International Conference on Atmospheric Electricity; June 1999, pp. 555-558; In English; See also 19990108601; No Copyright; Avail: CASI; A01, Hardcopy; A10, Microfiche

Special features of the global variations of ionospheric potential in the surface layer have been studied by the models of the electrode effect. The changing of the eddy diffusion coefficient in twenty-four hours can explain the additional summer maximum in the diurnal variations of the electric field near the surface where the turbulent electrode effect takes place. Really it means that the variations caused by the turbulence diffusion are similar to the unitary ones.
Author
Atmospheric Boundary Layer; Electric Potential; Atmospheric Electricity; Electric Fields; Turbulent Diffusion

19990108742 Novosibirsk State Univ., USSR
A Sensor for Balloon Measurements of the Air Conductivity
Struminsky, V. I., Novosibirsk State Univ., USSR; 11th International Conference on Atmospheric Electricity; June 1999, pp. 559-562; In English; See also 19990108601; No Copyright; Avail: CASI; A01, Hardcopy; A10, Microfiche

Small constant - altitude balloons are one of the best facilities of direct, long-duration experimental investigation of the stratospheric electricity. Because of the weight and power consumption limitations scientific equipment mounted on the payload that carried by the balloon should be as simple, light, economical as possible. A sensor for automatic conversion of the negative and positive components of the total electrical conductivity was especially designed for small balloon payload.
Author
Balloon-Borne Instruments; Balloon Sounding; Data Acquisition; Electrical Measurement; Air Conductivity; Atmospheric Electricity

19990108743 Tartu State Univ., Inst. of Environmental Physics, USSR
Seasonal Dependence of Electrical Mobility Spectra of Small Air Ions
Parts, Tiia–Ene, Tartu State Univ., USSR; 11th International Conference on Atmospheric Electricity; June 1999, pp. 563-566; In English; See also 19990108601; Sponsored in part by the Estonian Science Foundation
Contract(s)/Grant(s): ESF-1879; No Copyright; Avail: CASI; A01, Hardcopy; A10, Microfiche

Experimental results of the measurements of electrical mobility spectra of small air ions of one second of age during a period of 1986 to 1996 are presented. Temperature approx. = 293 (+/-5) K, atmospheric pressure approx. = 101.3 (+/-) 1.5 kPa, relative humidity 30 to 80% and chemical composition of the air were the most important variable circumstances in a fresh ventilated laboratory room at different seasons. It has been concluded that chemical composition of dominant small air ions does not particularly depend on the changes in air constituent due to several volatile, semivolatile organics and/or other air pollutants during the different seasons. The increase of water concentration in spring, summer and autumn should influence the electrical mobility of ions and consequently the chemical composition of later. The chemical reactions of water with most abundant gases and small ions in the air are discussed.
Author
Atmospheric Ionization; Charged Particles; Mobility; Seasons

19990108745 Academy of Sciences (Russia), Geoelectromagnetic Monitoring Lab., Borok, Russia
Structures and Spectra of Aeroelectric Field Pulsations
Anisimov, S. V., Academy of Sciences (Russia), Russia; Bakastov, S. S., Academy of Sciences (Russia), Russia; Dmitrev, E. M., Academy of Sciences (Russia), Russia; Mareev, E. A., Academy of Sciences (Russia), Russia; 11th International Conference on

Atmospheric Electricity; June 1999, pp. 571-574; In English; See also 19990108601; No Copyright; Avail: CASI; A01, Hardcopy; A10, Microfiche

ULF pulsations of the atmospheric electric field are studied in terms of Kolmogorov-Obukhov turbulence description. The structural function method and fast Fourier Transformation have been used for fair weather aeroelectric field data. It's shown that frequency spectra of aeroelectric field in the presence of large scale structures have decay slopes from -1.75 to -2.50, while the structural function index changes from 0.32 to 0.98. In the absence of large scale structures the slopes of aeroelectric field spectra were found to be steeper (approximately -3). Theoretical estimates for ULF pulsation spectra are presented taking into account turbulent mixing of the atmospheric space charge.

Author

Extremely Low Frequencies; Electric Fields; Atmospheric Electricity; Electrodynamics; Mathematical Models; Spectrum Analysis

19990108746 Reading Univ., Dept. of Meteorology, UK

Turbulent Transfer of Space Charge in the Atmospheric Surface Layer

Barlow, Janet F., Reading Univ., UK; Harrison, R. Giles, Reading Univ., UK; 11th International Conference on Atmospheric Electricity; June 1999, pp. 575-578; In English; See also 19990108601; No Copyright; Avail: CASI; A01, Hardcopy; A10, Microfiche

Simultaneous measurements of electrical parameters and micrometeorological parameters were made near Reading, U.K. during July and August 1998. The diurnal cycle in the potential profile in the surface layer was observed to coincide with the daily cycle in atmospheric stability. Measurements of vertical wind speed w and electric field E were correlated. The covariance <w'E' gives the direct effect of turbulence on the electric field and showed a large positive peak during the daytime. Correlation with momentum flux (-<u'w') was observed during stable nocturnal periods. Spectral analysis of electric field data showed a dependence of spectral slope on aerosol mass concentration in the size range 0.1 to 15 im. For the frequency band 0.016 to 0.3 Hz, the spectral density S(n) was proportional to n(exp -1.1) in the high aerosol case and n(exp -2.3) in the low aerosol case, showing qualitative similarity to the results of Anderson (1977) for space charge.

Author

Space Charge; Atmospheric Boundary Layer; Spectrum Analysis; Meteorological Parameters; Micrometeorology; Diurnal Variations; Electric Fields; Turbulence Effects; Aerosols

19990108747 Science Univ. of Tokyo, Dept. of Physics, Japan

Properties of Ion-Induced Nucleation Obtained from Mobility Measurements

Hara, K., Science Univ. of Tokyo, Japan; Nakae, S., Science Univ. of Tokyo, Japan; Miura, K., Science Univ. of Tokyo, Japan; 11th International Conference on Atmospheric Electricity; June 1999, pp. 579-582; In English; See also 19990108601; No Copyright; Avail: CASI; A01, Hardcopy; A10, Microfiche

The ion-induced nucleation occurred at lower saturation ratio than that of homogeneous nucleation. The saturation ratios initiating growth of droplets differed in ion polarities. Electrical mobility of ions was examined relating to an ion-induced nucleation. It was measured with ion electrical mobility spectrometer of time-of-flight type. Measurements were made at various temperature and relative humidity. As a result, mobility of ions differed with different polarities under various conditions of atmosphere.

Author

Ion Mobility Spectroscopy; Nucleation; Stratosphere; Ionic Mobility

19990108748 Mississippi Univ., Dept. of Physics and Astronomy, University, MS USA

Enhanced Fair-Weather Electric Fields Soon After Sunrise

Marshall, T. C., Mississippi Univ., USA; Rust, W. D., National Severe Storms Lab., USA; Stolzenburg, M., Mississippi Univ., USA; Roeder, W., Weather Squadron (45th), USA; Krehbiel, P. R., New Mexico Inst. of Mining and Technology, USA; 11th International Conference on Atmospheric Electricity; June 1999, pp. 583-586; In English; See also 19990108601; No Copyright; Avail: CASI; A01, Hardcopy; A10, Microfiche

The typical fair weather electric field at the ground is between -100 and -300 V/m. At the NASA Kennedy Space Center and US Air Force Cape Canaveral Air Station (KSC) the electric field at the ground sometimes reaches -400 to -1200 V/m within an hour or two after sunrise on days that otherwise seem to be fair weather. We refer to the enhanced negative electric fields as the "sunrise enhancement." to investigate the sunrise enhancement at KSC we measured the electric field (E) in the first few hundred

meters above the ground before and during several sunrise enhancements. From these E soundings we can infer the presence of charge layers and determine their thickness and charge density.
Derived from text
Electric Fields; Electric Field Strength; Atmospheric Electricity; Sunrise; Florida; Lower Atmosphere

19990108750 Roorkee Univ., Dept. of Physics, Roorkee, India
Measurement of Atmospheric Electrical Conductivity During Monsoon Period
Rai, Jagdish, Roorkee Univ., India; Kumar, Adarsh, Roorkee Univ., India; Singh, A. K., Roorkee Univ., India; 11th International Conference on Atmospheric Electricity; June 1999, pp. 591-594; In English; See also 19990108601; No Copyright; Avail: CASI; A01, Hardcopy; A10, Microfiche

A Gerdian condenser was employed to study the positive conductivity during the monsoon period of 1996. Some meteorological parameters like temperature, wind speed, relative humidity, rainfall and atmospheric pressure were also measured simultaneously. The average value of conductivity for the months of June, July and August 1996 were found to be 26.71 x 10(exp -16), 37.55 x 10(exp -16) and 40.62 x 10(exp -16) mhos/m respectively. The average rainfall for the above three months was 6.5 mm, 170.8 mm and 715.0 mm respectively. The increase of conductivity with the increase in monthly rainfall has been attributed to the fact that the rain contains charged particles, which increases conductivity near ground surface. The conductivity increases with temperature and relative humidity for the entire monsoon period. It may be attributed to the condensation of droplets on aerosols. which influences the magnitude of ionization and ionic mobility near ground surface. Our results have been discussed in light of the existing theoretical and experimental studies.
Author
Atmospheric Electricity; Electrical Resistivity; Monsoons; Electrical Measurement; Charged Particles

19990108752 Reading Univ., Dept. of Meteorology, UK
Ion-Aerosol Interactions in Atmospheric Air
Aplin, K. L., Reading Univ., UK; Harrison, R. G., Reading Univ., UK; 11th International Conference on Atmospheric Electricity; June 1999, pp. 598-601; In English; See also 19990108601; No Copyright; Avail: CASI; A01, Hardcopy; A10, Microfiche

Charged particles are continually generated in atmospheric air, and the interaction between natural ionisation and atmospheric particles is complicated. It is of some climatic importance to establish if ions are implicated in particle formation. Atmospheric ion concentrations have been investigated here at high temporal resolution, using Gerdien ion analysers at a site where synchronous meteorological measurements were also made. The background ionisation rate was also monitored with a Geiger counter, enabling ion production from natural radioactivity to be distinguished from other effects. Measurements at lHz offer some promise in establishing the atmospheric electrical influences in ionic nucleation bursts, although combinations of other meteorological factors are also known to be significant. High time resolution meteorological and ion measurements are therefore clearly necessary in advancing basic understanding in the behaviour of atmospheric aerosol.
Author
Atmospheric Ionization; Aerosols; Charged Particles; Ion Density (Concentration)

19990108753 Texas Univ., W. B. Hanson Center for Space Science, Dallas, TX USA
South Pole Electric Field Responses to Changes in Overhead Ionospheric Potential
Tinsley, Brian A., Texas Univ., USA; 11th International Conference on Atmospheric Electricity; June 1999, pp. 602-605; In English; See also 19990108601
Contract(s)/Grant(s): NSF DPP-92-08937; NSF ATM-95-04828; No Copyright; Avail: CASI; A01, Hardcopy; A10, Microfiche

Measurements of the vertical atmospheric electrical field Ez at the South Pole made between 1982 and 1986 have been analyzed, and the results reveal an important component due to extraterrestrial influences. The measurements are consistent with the theoretical expectation that the potential patterns in the polar caps that are measured by satellites, and that change with changes in solar wind parameters, are superimposed on the otherwise nearly uniform (but varying in time) global ionospheric potential due to low-latitude thunderstorm sources. The analysis technique was to calculate the overhead ionospheric convection potential from a satellite empirical model, using as inputs measured solar wind parameters, except that when the solar wind data were not available we used as inputs measured ground based magnetic disturbance parameters. We fitted the average low latitude E variation (the Carnegie curve) to the individually measured South Pole diurnal curves during the time intervals when the superimposed polar cap potential was near zero. We then subtracted the fitted Carnegie curves from the measured curves and performed a regression analysis of the residuals on the calculated superimposed polar cap potential values, averaging the data in three hour intervals. Positive correlations with correlation coefficients of about 0.5 were found. Most of the remaining variability

in Ez can be attributed to local meteorologically induced noise and the day-to-day variability of the low latitude thunderstorm generators.
Author
Electric Fields; Polar Caps; Earth Ionosphere; Magnetic Disturbances; Electric Potential; Electrical Measurement; Atmospheric Electricity

19990108754 Instituto Nacional de Pesquisas Espacias, Sao Jose dos Campos, Brazil
Stratospheric Balloon Measurements of Conductivity and Electric Fields Associated with Sferics in Brazil
Saba, M. M. F., Instituto Nacional de Pesquisas Espacias, Brazil; Pinto, O., Jr., Instituto Nacional de Pesquisas Espacias, Brazil; Pinto, I. R. C. A., Instituto Nacional de Pesquisas Espacias, Brazil; Mendes, O., Jr., Instituto Nacional de Pesquisas Espacias, Brazil; 11th International Conference on Atmospheric Electricity; June 1999, pp. 606-609; In English; See also 19990108601
Contract(s)/Grant(s): FAPESP-92/4774-2; FAPESP-93/0907-0; No Copyright; Avail: CASI; A01, Hardcopy; A10, Microfiche

Measurements of stratospheric conductivity and of electric fields associated with sferics, were obtained during two balloon flights carrying double-probe electric field detectors launched from Cachoeira Paulista, Brazil (geographic coordinates 22 deg 44'S, 44 deg 56'W) on 26 January 1994 and 23 March 1995. From data obtained in 1994, a linear relationship between the vertical quasi-DC electric field peak amplitude and the decay time constant of sferics was found for negative flashes. The results are compared to similar data for intracloud flashes. The data were supported by radar and METEOSAT satellite images. For the first time, positive and negative conductivity vertical profiles were obtained in Brazil. During the flight, at an average altitude of 27.5 km, the balloon passed over two thunderclouds as identified, by on-board video images and photographs. The simultaneous conductivity measurements and thundercloud on-board observations allowed to determine that the presence of clouds affects the stratospheric negative conductivity, producing a extended and cumulative drop after the balloon passed over each cloud. Based on data obtained in 1995 and on the present knowledge about the differences between positive cloud-to-ground and intracloud flashes, two methods to distinguish between them in balloon electric field data are presented: the first is based on an estimation of the charge destroyed in the event; the second is based on the ratio between the vertical quasi-DC and the VLF electric field. The behavior of the vertical quasi-DC electric field before and after large cloud-to-ground lightning flashes is discussed and attributed to the existence a shielding layer around the thunderstorm caused by a factor decrease of three or more in the conductivity inside the cloud.
Author
Balloon Sounding; Electrical Measurement; Electric Fields; Atmospherics; Atmospheric Electricity; Stratosphere; Electrical Resistivity

19990108755 Colombo Univ., Dept. of Physics, Colombo, SRi Lanka
Effect of Wind on Horizontal Wire Antenna Collecting Atmospheric Air-Earth Current
Lelwala, R., Colombo Univ., SRi Lanka; Tuomi, T. J., Finnish Meteorological Inst., Finland; Israelsson, S., Uppsala Univ., Sweden; Jayaratne, K. P. S. C., Colombo Univ., SRi Lanka; 11th International Conference on Atmospheric Electricity; June 1999, pp. 610-613; In English; See also 19990108601; No Copyright; Avail: CASI; A01, Hardcopy; A10, Microfiche

The electromagnetic hydrodynamic structure of a horizontal long-wire antenna collecting fair weather atmospheric air-earth current is investigated. The model consists of a set of equations for the motions of air ions and the solution is found by shooting analytical techniques. The solution shows that the resultant effect of wind on the current collected by the antenna is zero. From our solution, the current collecting area, which is called the effective area of the wire antenna, is inversely proportional to the speed of air ions. On the other hand, the current is directly proportional to the speed of air ions. These two effects compensate each other to nullify the resultant effect. In this case, the wire antenna should be kept at a considerably high level to avoid the electrode layer and the electrostatic mirror effect of the earth. The horizontal variation of wind is considered as constant and the logarithmic vertical wind profile was assumed. The solution was found numerically.
Author
Atmospheric Electricity; Ions; Wind Effects; Electric Current; Mathematical Models

19990108756 Academy of Sciences (Russia), Inst. of Applied Physics, Nizhny Novgorod, Russia
Synergetic Models of Space Charge Structures in the Atmosphere
Mareeva, O. V., State Pedagogical Univ., Russia; Mareev, E. A., Academy of Sciences (Russia), Russia; Israelsson, S., Uppsala Univ., Sweden; Anisimov, S. V., Academy of Sciences (Russia), Russia; 11th International Conference on Atmospheric Electricity; June 1999, pp. 614-617; In English; See also 19990108601; No Copyright; Avail: CASI; A01, Hardcopy; A10, Microfiche

A dynamical nonlinear model of the formation of space charge structures has been developed, taking into account recombination and drift of small ions in the electric field. Quasi-stationary solutions in the form of the running wave of the space charge density are found. It is shown that non-stationary inhomogeneous distributions of space charge density are described under definite conditions by the Burgers equation. Estimations show that the found self-consistent solutions can be displayed in the boundary layer both under fair weather conditions and below thunderclouds. Theoretical results are confirmed by examples of the vertical electric field recording, which exhibit nonlinear behavior of the field.
Author
Space Charge; Atmospheric Electricity; Dynamical Systems; Dynamic Models; Nonlinear Systems

19990108757 Tartu Univ., Inst. of Environmental Physics, Tartu, Estonia
Classification of Natural Air Ions Near The Ground
Horrak, U., Tartu Univ., Estonia; Salm, J., Tartu Univ., Estonia; Tammet, H., Tartu Univ., Estonia; 11th International Conference on Atmospheric Electricity; June 1999, pp. 618-621; In English; See also 19990108601
Contract(s)/Grant(s): ESF-1879; ESF-3326; ESF-3050; No Copyright; Avail: CASI; A01, Hardcopy; A10, Microfiche

The structure of air ion mobility spectrum recorded at Tahkuse Observatory, Estonia, during 14 months, is studied using factor analysis. The air ions in a mobility range of 0.00041-3.2 sq cm/V s (diameters 0.36-80 nm) are divided into five classes: small and big cluster ions, intermediate ions, light and heavy large ions. The boundaries between the classes are 1.3 sq cm/V s, 0.5 sq cm/V s, 0.034 sq cm/V s, 0.0042 sq cm/V s. Five factors correlated with respective ion classes explain 92% of total variance. According to their physical nature, the intermediate and large ions are called aerosol ions. The classification of air ions according to their mobility leads to a correlated classification of atmospheric aerosol particles according to size. The 1.6 nm boundary diameter between clusters and aerosol particles is confirmed, and the boundary diameters between the nanometer particles, the ultrafine particles and the Aitken particles as classes of tropospheric aerosol are estimated to be 7.4 nm and 22 nm.
Author
Atmospheric Ionization; Ion Mobility Spectroscopy; Aerosols; Heavy Ions; Light Ions

19990108758 Tartu Univ., Inst. of Environmental Physics, Tartu, Estonia
Atmospheric Electricity as a Factor of Dry Deposition of Particulate Pollution
Tammet, H., Tartu Univ., Estonia; Israelsson, S., Tartu Univ., Estonia; 11th International Conference on Atmospheric Electricity; June 1999, pp. 622-625; In English; See also 19990108601; Sponsored in part by the Swedish Inst. Visby Programme.
Contract(s)/Grant(s): ESF-3050; No Copyright; Avail: CASI; A01, Hardcopy; A10, Microfiche

The electrical deposition is known in case of unattached radon daughter clusters which are unipolarily charged and of high mobility. The role of the electrical forces in deposition of aerosol particles is estimated comparing the fluxes of particles carried by different deposition mechanisms in a model situation. The ratio of electrical and diffusion deposition fluxes decreases about ten times only when the mobility decreases thousand times from the values characteristic for small ions to the values characteristic for large ions. The electrical flux of fine particles can dominate on the tips of leaves and needles even in a moderate atmospheric electric field of few hundreds V/m as measured over the plain ground surface. Unlike the diffusion deposition, the electrical deposition is essentially non-uniform: the plate out on the tips of leaves and especially on needles of top branches of conifer trees is more intensive than on the ground surface and electrically shielded surfaces of plants. The knowledge of deposition geometry could improve our understanding of air pollution damages of plants.
Author
Atmospheric Electricity; Deposition; Air Pollution; Particulates

19990108759 Tartu Univ., Inst. of Environment Physics, Tartu, Estonia
The Limits of Air Ion Mobility Resolution
Tammet, H., Tartu Univ., Estonia; 11th International Conference on Atmospheric Electricity; June 1999, pp. 626-629; In English; See also 19990108601; Sponsored in part by the Swedish Inst. Visby Programme.; No Copyright; Avail: CASI; A01, Hardcopy; A10, Microfiche

An innovation by Loscertales [1998] forced the revision of the theory of the diffusion-limited mobility resolution. Traditionally, the limit of resolution has been estimated according to the ratio of the thermal energy kT to the work of the electric field expressed as qV, where q is the ion charge and V is the voltage between electrodes. This is correct when the electric field is transverse to the air flow. Otherwise, the term qV should be replaced by the term qEL, where L is the Lagrangian length of the passage of an ion through the air in the mobility separation zone. The work qEL exceeds q V in the longitudinal or inclined field analyzers which promise further improvement of the mobility resolution when compared with traditional transverse field

instruments. The inclined field method can be accomplished as proposed by Loscertales [1998] or by using inclined grids as suggested in the present paper.
Author
Ionic Mobility; Electric Fields; Ion Charge; Air; Atmospheric Electricity

19990108760 Academy of Sciences (Russia), Geoelectromagnetic Monitoring Lab., Borok, Russia
Aeroelectrical Measurements in Geoelectromagnetic Complete Set of Geophysical Observatory "BOROK"
Anisimov, S. V., Academy of Sciences (Russia), Russia; Bakastov, S. S., Academy of Sciences (Russia), Russia; Dmitriev, E. M., Academy of Sciences (Russia), Russia; Anisimova, E. B., Academy of Sciences (Russia), Russia; 11th International Conference on Atmospheric Electricity; June 1999, pp. 630-633; In English; See also 19990108601; No Copyright; Avail: CASI; A01, Hardcopy; A10, Microfiche

Atmospheric electricity is an integral part of the Earth's electromagnetic environment. An extensive database, which obtained on long-term ground aeroelectrical measurement, is a background for experimental research of the solar-terrestrial relationship. Mid-latitude Geophysical Observatory "Borok" (58.03 deg N, 38.97 deg E) is equipped with the installation for geoelectromagnetic monitoring including aeroelectric, geomagnetic and radiophysics measurements. The basic data logging system is an 16-th channel analog to digital converter with sampling rate 10Hz and final storage data on CD. Local data bank is created as result of continuous observations.
Author
Measuring Instruments; Analog to Digital Converters; Atmospheric Electricity; Electrical Measurement; Solar Terrestrial Interactions; Geomagnetism

19990108761 NASA Marshall Space Flight Center, Huntsville, AL USA
Simulation of the Universal-Time Diurnal Variation of the Global Electric Circuit Charging Rate
Mackerras, D., Queensland Univ. of Technology, Australia; Darvenzia, M., Queensland Univ. of Technology, Australia; Orville, R. E., Texas A&M Univ., USA; Williams, E. R., Massachusetts Inst. of Tech., USA; Goodman, S. J., NASA Marshall Space Flight Center, USA; 11th International Conference on Atmospheric Electricity; June 1999, pp. 634-637; In English; See also 19990108601; Sponsored in part by the Australian Electrical Research Board, the Australian Research Grants Scheme, and University of Queensland grants.; No Copyright; Avail: CASI; A01, Hardcopy; A10, Microfiche

A global lightning model that includes diurnal and annual lightning variation, and total flash density versus latitude for each major land and ocean, has been used as the basis for simulating the global electric circuit charging rate. A particular objective has been to reconcile the difference in amplitude ratios [AR=(max-min)/mean] between global lightning diurnal variation (AR approx. = 0.8) and the diurnal variation of typical atmospheric potential gradient curves (AR approx. = 0.35). A constraint on the simulation is that the annual mean charging current should be about 1000 A. The global lightning model shows that negative ground flashes can contribute, at most, about 10-15% of the required current. For the purpose of the charging rate simulation, it was assumed that each ground flash contributes 5 C to the charging process. It was necessary to assume that all electrified clouds contribute to charging by means other than lightning, that the total flash rate can serve as an indirect indicator of the rate of charge transfer, and that oceanic electrified clouds contribute to charging even though they are relatively inefficient in producing lightning. It was also found necessary to add a diurnally invariant charging current component. by trial and error it was found that charging rate diurnal variation curves in Universal time (UT) could be produced with amplitude ratios and general shapes similar to those of the potential gradient diurnal variation curves measured over ocean and arctic regions during voyages of the Carnegie Institute research vessels.
Author
Universal Time; Diurnal Variations; Electric Charge; Mathematical Models; Charge Transfer; Atmospheric Electricity

19990108766 Academy of Sciences (USSR), Inst. for Geosphere Dynamics, Moscow, USSR
Impact of Lightning Discharge on Stratospheric Ozone
Klumov, B., Academy of Sciences (USSR), USSR; 11th International Conference on Atmospheric Electricity; June 1999, pp. 660-663; In English; See also 19990108601; No Copyright; Avail: CASI; A01, Hardcopy; A10, Microfiche

We have investigated the dynamics and chemical composition of the hot lightning channel at lower stratospheric altitudes. Two-dimensional gas dynamical code ZEUS-2D was used to calculate the expansion of the hot air channel. As the hot air channel expands, quenching occurs: the chemical composition of the gas stops changing and corresponds to the equilibrium composition at the moment of quenching. We focused our attention mainly on nitrogen oxides NO and N02 production by lightning as these minor constituents strongly affect ozone. The temperature of NO quenching in lightning channel was found to be about 2300-2500 K. At these temperatures NO mixing ratio in the channel is about 0.03 and weakly depends on the ambient air pressure. Later, such

lightning-produced column of NO spreads by turbulent diffusion processes with a typical timescale of the order of 100 s, forming the region with radial space scale of the order of 100 m, where NO mixing ratio far above then the ambient one. We calculated the photochemistry of the ozone in the region. It has been shown that strong ozone transient (on the order of a few minutes) depletion is formed in the region.
Author
Lightning; Ozone; Stratosphere; Photochemical Reactions; Nitrogen Oxides

19990108767 Bulgarian Academy of Sciences, National Inst. of Meteorology and Hydrology, Sofia, Bulgaria
An Estimation of Nitric Oxide Variation Caused by Lightning over a Bulgarian Area Based on Experimental and Model Data
Kolev, Staytcho I., Bulgarian Academy of Sciences, Bulgaria; 11th International Conference on Atmospheric Electricity; June 1999, pp. 664-667; In English; See also 19990108601
Contract(s)/Grant(s): NZ-624/1996; No Copyright; Avail: CASI; A01, Hardcopy; A10, Microfiche

Recently, it has been qualitatively confirmed by direct observation of enhanced levels of nitric oxides (NOx) in and around active thunder clouds, that lightning can alter radically the chemical composition of the air. On the basis of both experimentally obtained data of lightning activity over Sofia area for a ten year period and modelled accepted magnitudes of energy and frequency of strokes, the variation of nitric oxides production due to lightning has been estimated. Annual and mean monthly runs of nitric oxides at the ground measured contents and the parallel lightning frequencies have been presented, as well and their calculated trends for the studied period, 1982-1995. The obtained values have been partly compared with the published ones. Specially attention has been paid to some discrepancies and the possible explanation connected with the limitations associated with measuring procedures has been discussed.
Author
Lightning; Nitrogen Oxides; Atmospheric Composition

19990108777 Hungarian Academy of Sciences, Geodetic and Geophysical Research Inst., Sopron, Hungary
Periodic Variations of Solar and Tropospheric Origins in Schumann Resonances
Zieger, B., Hungarian Academy of Sciences, Hungary; Satori, G., Hungarian Academy of Sciences, Hungary; 11th International Conference on Atmospheric Electricity; June 1999, pp. 701-704; In English; See also 19990108601; Sponsored in part by the U.S.-Hungarian Joint Fund, the Danish Research Council, and the Hungarian Ministry of Culture and Education under the State Eoetvoes Fellowship
Contract(s)/Grant(s): T023111; JF554; No Copyright; Avail: CASI; A01, Hardcopy; A10, Microfiche

Long-term periodic variations in Schumann resonance parameters were studied in the period range from 5 days to half a year. Dynamic spectra of daily Schumann resonance amplitudes and frequencies were computed for the first three modes and were compared with dynamic spectra of solar wind speed and geomagnetic indices such as KP and DST. Several periodicities were identified including 108 days, 73 days, 47 days, 27 days, 20 days, 13.5 days and 9-10 days. The most significant correlation between Schumann resonance parameters and solar wind speed (or geomagnetic activity) was found at the period of 13.5 days (half a solar rotation period). This implies a solar influence on the upper boundary of the Earth-ionosphere waveguide most probably through energetic particles (MeV protons and electrons).
Author
Periodic Variations; Solar Activity; Solar Wind; Resonant Frequencies; Troposphere

19990108778 NASA Marshall Space Flight Center, Huntsville, AL USA
Comparisons of Long-Term Schumann Resonance Records in Europe and North America
Satori, G., Hungarian Academy of Sciences, Hungary; Williams, E. R., Massachusetts Inst. of Tech., USA; Zieger, B., Hungarian Academy of Sciences, Hungary; Boldi, R., Massachusetts Inst. of Tech., USA; Heckman, S., NASA Marshall Space Flight Center, USA; Rothkin, K., Massachusetts Inst. of Tech., USA; 11th International Conference on Atmospheric Electricity; June 1999, pp. 705-708; In English; See also 19990108601; Sponsored in part by the U.S.-Hungarian Joint Research Foundation
Contract(s)/Grant(s): T023111; JF554; No Copyright; Avail: CASI; A01, Hardcopy; A10, Microfiche

Two stations at a distance comparable with the wavelength in the Schumann resonance (SR) frequency range, one in Europe (Nagycenk, Hungary) and one in North America (West Greenwich, Rhode Island) have simultaneously monitored the natural vertical electric and horizontal magnetic field components in the frequency range of 3-25 Hz. This is a unique opportunity, as Schumann resonance stations are scarce and even fewer station have records with 5-6 year durations. The main purpose of this paper is to make comparisons in the SR time series measured simultaneously at the two field site, thereby providing access to global behavior on the seasonal and interannual time scales. The comparative measurements described here point out distinct

differences in the nature of convection in South America and in Africa and reveal new aspects about the behavior of tropical continental convection on the ENSO time scale.
Author
Schumann-Runge Bands; Resonant Frequencies; Europe; North America; Periodic Variations; Frequency Ranges

19990108793 University of Electro-Communications, Chofu, Japan
Long-Term SR and ELF Transients Observed in a Japanese Site
Hayakawa, M., University of Electro-Communications, Japan; Nickolaenko, A. P., University of Electro-Communications, Japan; Hobara, Y., University of Electro-Communications, Japan; Williams, E. R., Massachusetts Inst. of Tech., USA; 11th International Conference on Atmospheric Electricity; June 1999, pp. 762-765; In English; See also 19990108601; No Copyright; Avail: CASI; A01, Hardcopy; A10, Microfiche

We deduce temporal variations of the level of the global lightning activity from the long-term Schumann resonance (SR) monitoring. We analyze the continuous analog records of the horizontal magnetic field component covering period from August 1967 to November 1970. The amplitudes of the first, second, and third SR modes were monitored at the Tottori observatory (35.5 deg N, 134.33 deg E). The experimental records show that the temporal changes of the SR amplitudes considerably vary from day to day. Meanwhile, the regular diurnal and longer scale variations appear in the data after applying the statistical processing. We found annual, biennial, and semi-annual components in variations of the global thunderstorm activity between 1967 and 1970. In addition, the initial results from our new ELF station established in Moshiri, Hokkaido will be presented, in which we observe the SR and ELF transients associated with Sprite events during the winter lightning activity in Japan sea. These results will be compared with the long-term Tottori data.
Author
Schumann-Runge Bands; Lightning; Thunderstorms; Temporal Distribution; Japan; Periodic Variations

19990109105 Naval Facilities Engineering Service Center, Port Hueneme, CA USA
Effective Stress Drydock Analysis ***Final Report, Jul. - Sep. 1998***
Ferritto, J. M.; Sep. 1998; 105p; In English
Report No.(s): AD-A364716; NFESC-TR-2093-SHR; No Copyright; Avail: CASI; A06, Hardcopy; A02, Microfiche

Recent earthquakes have emphasized the high damage threat the soil liquefaction phenomenon poses to water-front structures. These experiences have shown that both the nature of waterfront facilities, such as earth-retaining structures, and the depositional environment of the coastal marine soil contribute to major liquefaction damage. Drydocks are critical structures containing high value ships and as such represent a class of structure which can not fail during an earthquake. Consequently, drydock certification studies have been conducted to evaluate the safety of drydocks under all possible load conditions. The recent development of effective stress finite difference technology now permits a more accurate assessment of these structures. The newly developed FATIGUE OF LAMINATED COMPOSITES (FLAC) computer program was evaluated as part of this study and a demonstration case performed on the drydock located at Naval Station, San Diego. The results of this study show that the drydock has adequate factors of safety for the static load considered. This is in agreement with the drydock certification study. This analysis shows the drydock to be at yield levels during dynamic earthquake loading. The levels of liquefaction are limited and controlled. The FLAC analysis is better able to represent the actual loading conditions on the drydock than the traditional hand calculations performed in the drydock certification studies. As a result the more accurate FLAC analysis shows a lower level of loading both under static and dynamic conditions and higher factors of safety. The conclusion of this study is that for the conditions established in the drydock certification report, the drydock is safer than indicated in the report under dynamic loading.
DTIC
Drydocks; Loads (Forces); Liquefaction

19990109126 NASA Marshall Space Flight Center, Huntsville, AL USA
New NOAA-15 Advanced Microwave Sounding Unit (AMSU) Datasets for Stratospheric Research
Spencer, Roy W., NASA Marshall Space Flight Center, USA; Braswell, William D., Nichols Research Corp., USA; [1999]; 1p; In English, 4 Jun. 1999, Boston, MA, USA; Sponsored by American Geophysical Union, USA; Copyright; Avail: Issuing Activity, Hardcopy; Abstract Only

The NOAA-15 spacecraft launched in May 1998 carried the first Advanced Microwave Sounding Unit (AMSU). The AMSU has eleven oxygen absorption channels with weighting functions peaking from near the surface to 2 mb. Twice-daily, limb-corrected I degree gridded datasets of layer temperatures have been constructed since the AMSU went operational in early August 1998. Examples of AMSU imagery will be shown, as will preliminary analyses of daily fluctuations in tropical

stratospheric temperatures and their relationship to daily variations in tropical-average rainfall measured by the Special Sensor Microwave Imager (SSM/I). The AMSU datasets are now available for other researchers to utilize.
Author
NOAA Satellites; Microwave Imagery; Remote Sensing; Advanced Microwave Sounding Unit

19990109128 NASA Marshall Space Flight Center, Huntsville, AL USA
Empirical Modeling of the Plasmasphere
Gallagher, Dennis L., NASA Marshall Space Flight Center, USA; Craven, Paul D., NASA Marshall Space Flight Center, USA; Comfort, Richard H., Alabama Univ., USA; [1999]; 1p; In English; Ionosphere Workshop, 12 Aug. 1999, Lowell, mA, USA; Sponsored by Committee on Space Research, France; Copyright; Avail: Issuing Activity, Hardcopy; Abstract Only

Over 40 years of ground and spacecraft plasmaspheric measurements have resulted in many statistical descriptions of plasmaspheric properties. In some cases, these properties have been represented as analytical descriptions that are valid for specific regions or conditions. For the most part, what has not been done is to extend regional empirical descriptions or models to the plasmasphere as a whole. In contrast, many related investigations depend on the use of representative plasmaspheric conditions throughout the inner magnetosphere. Wave propagation, involving the transport of energy through the magnetosphere, is strongly affected by thermal plasma density and its composition. Ring current collisional and wave particle losses also strongly depend on these quantities, Plasmaspheric also plays a secondary role in influencing radio signals from the Global Positioning System satellites. The Global Core Plasma Model (GCPM) is an attempt to assimilate previous empirical evidence and regional models for plasmaspheric density into a continuous, smooth model of then-nal plasma density in the inner magnetosphere. In that spirit, the International Reference Ionosphere is currently used to complete the low altitude description of density and composition in the model. The models and measurements on which the GCPM is currently based and its relationship to IRI will be discussed.
Author
Numerical Analysis; Plasmasphere; Energy Transfer; Plasma Density; Statistical Distributions; Thermal Plasmas

19990109130 NASA Marshall Space Flight Center, Huntsville, AL USA
GEOTAIL and POLAR Observations of Auroral Kilometric Radiation and Terrestrial Low Frequency Bursts and their Relationship to Energetic Particles, Auroras, and Other Substorm Phenomena
Anderson, R . R., NASA Marshall Space Flight Center, USA; Gurnett, D. A., NASA Marshall Space Flight Center, USA; Frank, L. A., NASA Marshall Space Flight Center, USA; Thomsen, Michelle F., NASA Marshall Space Flight Center, USA; Parks, G. K., NASA Marshall Space Flight Center, USA; Brittnacher, M. J., NASA Marshall Space Flight Center, USA; Spann, James F., Jr., NASA Marshall Space Flight Center, USA; Imhoff, W. L., NASA Marshall Space Flight Center, USA; Mobilia, J. H., NASA Marshall Space Flight Center, USA; [1999]; 2p; In English, 31 May - 4 Jun. 1999, Boston, MA, USA; Sponsored by American Geophysical Union, USA; Copyright; Avail: Issuing Activity, Hardcopy; Abstract Only

Terrestrial low frequency (LF) bursts are plasma wave phenomena that appear to be a part of the low frequency end of the auroral kilometric radiation (AKR) spectrum and are observed during strong substorms, GEOTAIL and POLAR plasma wave observations from within the magnetosphere show that the AKR increases in intensity and its lower frequency limits decrease when LF bursts are observed. The first is expected as it is shows substorm onset and the latter indicates that the AKR source region is expanding to higher altitudes. Images from the POLAR VIS Earth Camera operating in the far-UV range and the POLAR UVI experiment usually feature an auroral brightening and an expansion of the aurora to higher latitudes at the time of the LF bursts. Enhanced fluxes of X-rays from precipitating electrons have also been observed by POLAR PIXIE. High resolution ground Abstract: magnetometer data from the CANOPUS and IMAGE networks show that the LF bursts occur when the expansive phase onset signatures are most intense. The ground magnetometer data and the CANOPUS meridian scanning photometer data sometimes show that during the LF burst events the expansive phase onset starts at unusually low latitudes and moves poleward. Large injections of energetic protons and electrons have also been detected by the GOES and LANL geosynchronous satellites during LF burst events. While most of the auroral brightenings and energetic particle injections associated with the LF bursts occur near local midnight, several have been observed as early as mid-afternoon. From these various measurements, we are achieving a better understanding of the plasma and particle motions during substorms that are associated with the generation and propagation of terrestrial LF bursts
Author
Auroras; Cameras; Data Acquisition; Energetic Particles; Geomagnetic Tail; Magnetic Storms; Particle Motion

19990109139 Lunar and Planetary Inst., Houston, TX USA
Geoid Anomalies and Dynamic Topography from Time Dependent, Spherical Axisymmetric Mantle Convection
Kiefer, Walter S., Lunar and Planetary Inst., USA; Kellogg, Louise H., California Univ., USA; Physics of the Earth and Planetary

Interiors; 1998; ISSN 0031-9201; Volume 106, pp. 237-256; In English
Contract(s)/Grant(s): NASw-4574; NAGw-3814
Report No.(s): LPI-Contrib-939; Copyright; Avail: Issuing Activity, Hardcopy

Geoid anomalies and dynamic topography are two important diagnostics of mantle convection. We present geoid and topography results for several time-dependent convection models in spherical axisymmetric geometry for Rayleigh numbers between 10(exp 6) and 10(exp 7) with depth-dependent viscosity and mixtures of bottom and internal heating. The models are strongly chaotic, with boundary layer instabilities erupting out of both thermal boundary layers. In some instances, instabilities from one boundary layer influence the development of instabilities in the other boundary layer. Such coupling between events at the top and bottom of the mantle has been suggested to play a role in a mid-Cretaceous episode of enhanced volcanism in the Pacific. These boundary layer instabilities produce large temporal variations in the geoid anomalies and dynamic nd to the topography associated with the convection. The amplitudes of these fluctuations depend on the detailed model parameter,.% it of this but fluctuations of 30-50% relative to the time-averaged geoid and topography are common. The convective planform is strongly sensitive to the specific initial conditions. Convection cells with larger aspect ratio tend to have larger fractional fluctuations in their geoid and topography amplitudes, because boundary layer instabilities have more time to develop in long cells. In some instances, we observe low-amplitude topographic highs adjacent to the topographic lows produced by cold downwellings. We discuss applications of these results to several situations, including the temporal variability of m basis. hotspots such as Hawaii, the topography of subduction zone outer rises, and the topography of coronae on Venus.
Author
Geoids; Anomalies; Topography; Dynamic Characteristics; Time Dependence; Convection; Earth Mantle

19990109147 NASA Goddard Space Flight Center, Greenbelt, MD USA
Influence of Transport on Two-Dimensional Model Simulation. Tracer Sensitivity to 2-D Model Transport, 1, Long Lived Tracers
Fleming, Eric L., NASA Goddard Space Flight Center, USA; Jackman, Charles H., NASA Goddard Space Flight Center, USA; Considine, David B., NASA Goddard Space Flight Center, USA; Stolarski, Richard S., NASA Goddard Space Flight Center, USA; 1999; 85p; In English; Sponsored in part by Upper Atmosphere Research Satellite Science Investigation Program; No Copyright; Avail: CASI; A05, Hardcopy; A01, Microfiche

In this study, we examine the sensitivity of long lived tracers to changes in the base transport components in our 2-D model. Changes to the strength of the residual circulation in the upper troposphere and stratosphere and changes to the lower stratospheric K(sub zz) had similar effects in that increasing the transport rates decreased the overall stratospheric mean age, and increased the rate of removal of material from the stratosphere. Increasing the stratospheric K(sub yy) increased the mean age due to the greater recycling of air parcels through the middle atmosphere, via the residual circulation, before returning to the troposphere. However, increasing K(sub yy) along with self-consistent increases in the corresponding planetary wave drive, which leads to a stronger residual circulation, more than compensates for the K(sub yy)-effect, and produces significantly younger ages throughout the stratosphere. Simulations with very small tropical stratospheric K(sub yy) decreased the globally averaged age of air by as much as 25% in the middle and upper stratosphere, and resulted in substantially weaker vertical age gradients above 20 km in the extratropics. We found only very small stratospheric tracer sensitivity to the magnitude of the horizontal mixing across the tropopause, and to the strength of the mesospheric gravity wave drag and diffusion used in the model. We also investigated the transport influence on chemically active tracers and found a strong age-tracer correlation, both in concentration and calculated lifetimes. The base model transport gives the most favorable overall comparison with a variety of inert tracer observations, and provides a significant improvement over our previous 1995 model transport. Moderate changes to the base transport were found to provide modest agreement with some of the measurements. Transport scenarios with residence times ranging from moderately shorter to slightly longer relative to the base case simulated N2O lifetimes that were within the observational estimates of Volk et al. [1997]. However, only scenarios with rather fast transport rates were comparable with the Volk et al. estimates of CFCl3 lifetimes. This is inconsistent with model-measurement comparisons of mean age in which the base model or slightly slower transport rates compared the most favorably with balloon SF6 data. For all comparisons shown, large transport changes away from the base case resulted in simulations that were outside the range of measurements, and in many cases, far outside this range.
Author
Transport Theory; Diffusion Theory; Two Dimensional Models; Simulation; Gravity Waves; Planetary Waves; Wave Drag

19990110084 Finnish Geodetic Inst., Kirkkonummi, Finland
The Vaisala Baselines in Finland
Jokela, Jorma, Finnish Geodetic Inst., Finland; Poutanen, Markku, Finnish Geodetic Inst., Finland; 1998; ISSN 0085-6932; 104p; In English; See also 19990110085 through 19990110086
Report No.(s): FGI-127; ISBN 951-711-220-3; No Copyright; Avail: CASI; A06, Hardcopy; A02, Microfiche

Contents include the following: 50 years of interference observations at the Nummela standard baseline and the HUT Vaisala baseline.

CASI
Procedures; Geodesy

19990110085 Finnish Geodetic Inst., Kirkkonummi, Finland
50 Years of Interference Observations at the Nummela Standard Baseline, Pt. 1
Jokela, Jorma, Finnish Geodetic Inst., Finland; Poutanen, Markku, Finnish Geodetic Inst., Finland; The Vaisala Baselines in Finland; 1998, pp. 7-43; In English; See also 19990110084; No Copyright; Avail: CASI; A03, Hardcopy; A02, Microfiche

We review the interference observation method for measuring geodetic length standards known as the Vaisala baseline method. The Nummela Standard Baseline is a part of the Finnish National Standards Laboratory of geodetic length. In 1996 the baseline was measured for the 13th time using the Vaisala comparator; we describe the processing of the observations and present the results. The standard error has always been less than 0. 1 mm for the entire 864-m distance, and the variation in length has remained below 0.6 mm since 1947. With this 0.09-ppm accuracy the baseline still presents an outstanding base for geodetic and geophysical operations making use of distance measurements.

Author
Geodesy; Geophysics; Length

19990110086 Finnish Geodetic Inst., Kirkkonummi, Finland
The HUT Vaisala Baseline, Pt. 2
Jokela, Jorma, Finnish Geodetic Inst., Finland; Poutanen, Markku, Finnish Geodetic Inst., Finland; The Vaisala Baselines in Finland; 1998, pp. 45-61; In English; See also 19990110084; No Copyright; Avail: CASI; A03, Hardcopy; A02, Microfiche

A 75-m-long calibration baseline was measured with the Vaisala interference comparator as a joint project between the Finnish Geodetic Institute (FGI) and the Laboratory of Geodesy and Cartography of the Helsinki University of Technology (HUT). In addition to the length determination the purpose was to examine the usability of the Vaisala baseline measurement method indoors and to improve comparability between this method and other high-precision geodetic distance measurement methods. Here we present the results and experience gained in the project.

Author
Geodesy; Mapping; Dimensional Measurement

19990110306 NASA Goddard Space Flight Center, Greenbelt, MD USA
The Geomagnetic Field and Radiation in Near-Earth Orbits
Heirtzler, J. R., NASA Goddard Space Flight Center, USA; October 1999; 50p; In English
Report No.(s): NASA/TM-1999-209481; NAS 1.15:209481; Rept-99B00083; No Copyright; Avail: CASI; A03, Hardcopy; A01, Microfiche

This report shows, in detail, how the geomagnetic field interacts with the particle flux of the radiation belts to create a hazard to spacecraft and humans in near-Earth orbit. It illustrates the geometry of the geomagnetic field lines, especially around the area where the field strength is anomalously low in the South Atlantic Ocean. It discusses how the field will probably change in the future and the consequences that may have on hazards in near space.

Author
Geomagnetism; Field Strength; Flux (Rate)

19990110323 SRI International Corp., Menlo Park, CA USA
High-Latitude Incoherent-Scatter Radar Measurements for the ISTP Program ***Final Report, 1 Sep. 1997 - 31 Aug. 1998***
Kelly, John D., SRI International Corp., USA; Sep. 09, 1999; 11p; In English
Contract(s)/Grant(s): NAS5-31185; SRI Proj. 1431; No Copyright; Avail: CASI; A03, Hardcopy; A01, Microfiche

Over the course of this contract, the ISTP mission became a reality and proved to be one of NASA's success stories. SRI and the NSF-sponsored Sondrestrom radar contributed significantly to the success. We provided dedicated radar experiment time with operation modes specifically designed to complement the ISTP spacecraft. Data collected during coronal mass ejection events

indicated that at times significant energy is fed from the ionosphere to the magnetosphere. A model of global conductance is emerging from combined POLAR and Sondrestrom data sets. We initiated a study to investigate the behavior of the global energy budget during the evolution of magnetospheric storms and substorms using a number of ground-based and satellite data sets.
Author
Radar Measurement; Latitude; Magnetic Storms; Incoherent Scatter Radar

19990110479 Department of Energy, Washington, DC USA
Modeling anomalous surface: wave propagation across the Southern Caspian basin
Priestly, K. F., Department of Energy, USA; Patton, H. J., Department of Energy, USA; Schultz, C. A., Department of Energy, USA; Jan. 09, 1998; 29p; In English
Report No.(s): DE98-057455; UCRL-ID-129556; No Copyright; Avail: Department of Energy Information Bridge, Microfiche

The crust of the south Caspian basin consists of 15-25 km of low velocity, highly attenuating sediment overlying high velocity crystalline crust. The Moho depth beneath the basin is about 30 km as compared to about 50 km in the surrounding region. Preliminary modeling of the phase velocity curves shows that this thick sediments of the south Caspian basin are also under-lain by a 30-35 km thick crystalline crust and not by typical oceanic crust. This analysis also suggest that if the effect of the over-pressuring of the sediments is to reduce Poissons' ratio, the over-pressured sediments observed to approximately 5 km do not persist to great depths. It has been shown since 1960's that the south Caspian basin blocks the regional phase Lg. Intermediate frequency (0.02-0.04 Hz) fundamental mode Raleigh waves propagating across the basin are also severely attenuated, but the low frequency surface waves are largely unaffected. This attenuation is observed along the both east-to-west and west-to-east great circle paths across the basin, and therefore it cannot be related to a seismograph site effect. We have modeled the response of surface waves in an idealized rendition of the south Caspian basin model using a hybrid normal mode / 2-D finite difference approach. to gain insight into the features of the basin which cause the anomalous surface wave propagation, we have varied parameters of the basin model and computed synthetic record sections to compare with the observed seismograms. We varied the amount of mantel up-warp, the shape of the boundaries, the thickness and shear wave Q of the sediments and mantle, and the depth of the water layer. of these parameters, the intermediate frequency surface waves are most severely affected by the sediments thickness and shear wave attenuation. fundamental mode Raleigh wave phase velocities measure for paths crossing the basin are extremely low.
NTIS
Seismic Waves; Finite Difference Theory; Wave Propagation; Ocean Bottom; Wave Attenuation

19990110480 Department of Energy, Washington, DC USA
Strong ground motion synthesis for a M=7.2 earthquake in the Gulf of Corinth, Greece using Empirical Green's functions
Hutchings, L., Department of Energy, USA; Stavrakakis, G. N., Department of Energy, USA; Ioannidou, E., Department of Energy, USA; Wu, F. T., Department of Energy, USA; Jarpe, S., Department of Energy, USA; Jan. 01, 1998; 17p; In English; 29th; Seismology and Physics on the Earth's Interior General Assembly, USA
Report No.(s): DE98-057456; UCRL-JC-129394; CONF-9708179; No Copyright; Avail: Department of Energy Information Bridge, Microfiche

We synthesize strong ground motion at three sites from a M=7.2 earthquake along the MW-trending Gulf of Cornith seismic zone. We model rupture along an 80 segment of the zone. The entire length of the fault, if activated at one time, can lead to an event comparable to that of the 1995 Kobe earthquake. With the improved digital data now routinely available, it becomes possible to use recordings of small earthquakes as empirical Green's functions to synthesize potential ground motion for future large earthquakes. We developed a suite of 100 rupture scenarios for the earthquake and computed the commensurate strong ground motion time histories. We synthesized strong ground motion with physics- based solutions of earthquake rupture and applied physical bounds on rupture parameters. The synthesized ground motions obtained are source and site specific. by having a suite of rupture scenarios of hazardous earthquakes for a fixed magnitude and identifying the hazard to a site from the statistical distribution of engineering parameters, we have introduced a probabilistic component to the deterministic hazard calculation. The time histories suggested for engineering design are the ones that most closely match either the average or one standard deviation absolute accelerations response values.
NTIS
Greece; Earthquakes; Earth Movements; Green'S Functions; Seismology

19990111497 Department of Energy, Washington, DC USA
Validation of a ground motion synthesis and prediction methodology for the 1988, M=6.0, Saguenay Earthquake
Hutchings, L., Department of Energy, USA; Jarpe, S., Department of Energy, USA; Kasameyer, P., Department of Energy, USA;

Foxall, W., Department of Energy, USA; Jan. 01, 1998; 25p; In English; Ground Motion Methodologies for the Eastern USA, USA Report No.(s): DE98-057457; UCRL-JC-129395; CONF-9710252; No Copyright; Avail: Department of Energy Information Bridge, Microfiche

We model the 1988, M=6.0, Saguenay earthquake. We utilize an approach that has been developed to predict strong ground motion. This approach involves developing a set of rupture scenarios based upon bounds on rupture parameters. Rupture parameters include rupture geometry, hypocenter, rupture roughness, rupture velocity, healing velocity (rise times), slip distribution, asperity size and location, and slip vector. Scenario here refers to specific values of these parameters for an hypothesized earthquake. Synthetic strong ground motion are then generated for each rupture scenario. A sufficient number of scenarios are run to span the variability in strong ground motion due to the source uncertainties. by having a suite of rupture scenarios of hazardous earthquakes for a fixed magnitude and identifying the hazard to the site from the one standard deviation value of engineering parameters we have introduced a probabilistic component to the deterministic hazard calculation, For this study we developed bounds on rupture scenarios from previous research on this earthquake. The time history closest to the observed ground motion was selected as a model for the Saguenay earthquake.

NTIS

Earthquakes; Seismology; Earth Movements; Prediction Analysis Techniques

19990111594 NASA Marshall Space Flight Center, Huntsville, AL USA

A Study of Ion Velocities Observed by TIDE and How It Relates to Magnetospheric Circulation

Elliott, H. A., Alabama Univ., USA; Comfort, R. H., Alabama Univ., USA; Craven, P. D., NASA Marshall Space Flight Center, USA; Chandler, M. O., NASA Marshall Space Flight Center, USA; Moore, T. E., NASA Goddard Space Flight Center, USA; 1998; In English; American Geophysical Union Meeting, 26-29 May 1998, Boston, MA, USA; Copyright; Avail: Issuing Activity, Hardcopy, Microfiche

The high-latitude ion velocities measured by the Thermal Ion Dynamics Experiment (TIDE) instrument on the Polar spacecraft will be examined in relation to magnetospheric circulation. TIDE derives ion velocities from moments of measured distribution functions. Hydrogen and oxygen ions are E X B drifting in the polar cap and cleft regions with a speed of about 5-20 km/s at apogee (approximately 9 Re) and a speed of 1-2 km/s at perigee (approximately 1.8 Re). At perigee 0+ is typically seen flowing down in the polar cap and outflowing from the cleft. At the transition from downflowing to upflowing there is also seen a reversal in the ion convection. The convection at perigee is consistent with standard ionospheric convection models for given Interplanetary Magnetic Field (IMF) conditions. Convection at high altitude (approximately 8.9 Re) polar regions has not been studied very much since there have not been many satellites in this region. Unlike previous missions to this region TIDE in conjunction the Plasma Source Instrument (PSI) can measure ions with as low an energy as several electron Volts. The outflowing ions observed by TIDE at apogee are believed to be important to the overall circulation of the magnetosphere. The convection of these outflowing ions at apogee will be related to the IMF. This study tries to answer the question of how the IMF response of the convection influences the overall circulation of the magnetosphere.

Author

Velocity; Circulation; Earth Ionosphere; Earth Magnetosphere

19990111595 NASA Marshall Space Flight Center, Huntsville, AL USA

A Close Look at the Plasmasphere

Craven, Paul D., NASA Marshall Space Flight Center, USA; 1998; In English; American Geophysical Union Meeting, 1998, Boston, MA, USA; Sponsored by American Geophysical Union, USA; Copyright; Avail: Issuing Activity, Hardcopy, Microfiche

The plasmasphere is a toroidal region around the Earth and is filled with cold dense plasma in which the magnetic field lines are mainly closed. The plasmasphere has been studied since the discovery of the plasmaspause by Carpenter in 19xx. Since that time an impressive array of satellites and rockets have been brought to bear on studies of the region. It is a region in which the science seems to be considered as mature. We will explore the known aspects of the plasmasphere, those things that appear to be known well enough to be modeled with some degree of confidence. The areas that are not as confidently modeled, mostly on the outer boundary, aspects of refilling, convection around to the dayside, and duskside phenomenon, will be examined with the object of showing the areas of research in the plasmasphere that need further investment of resources.

Author

Plasmasphere; Toroidal Plasmas

19990111608 NASA Goddard Space Flight Center, Greenbelt, MD USA

The Spatial-Temporal Structure of US Southern Great Plains Soil Moisture: An Analysis of In-Situ SGP97 Profile Observations

Houser, Paul R., NASA Goddard Space Flight Center, USA; Mohanty, B. P.; 1998; 1p; In English; 14th; 79th; Hydrology, Dallas, TX, USA, USA; Sponsored by American Meteorological Society, USA

Report No.(s): P1.24; Copyright; Avail: Issuing Activity, Hardcopy; Abstract Only

Soil moisture links the hydrologic cycle and the energy budget of land surfaces by regulating the partitioning of surface radiative energy between latent and sensible heat fluxes. Therefore, accurate assessment of the spatial and temporal variation of soil moisture is important for the study, understanding, and management of surface biogeophysical processes. However, soil moisture exhibits a high degree of variability whose cause has been elusive, but is thought to be determined by heterogeneity in soil properties, vegetation, topography, water table depth, precipitation, and other meteorological factors. Understanding and assessment of these variations across a range of scales will enable the definition of the vertical and horizontal soil moisture error correlation structures which are essential in soil moisture data assimilation studies and for understanding the processes that drive soil moisture variability. During the Southern Great Plains 1997 Experiment (SGP97), soil moisture, soil properties, vegetation characteristics, and meteorological information was measured for 30 days at a wide range of scales ranging from 1 meter to 250 km. A preliminary analysis of these observations will be presented here. This analysis is focused on the assessment of the spatial and temporal structure of profile (0-1 m below the soil surface) soil moisture at a scales ranging from one square meter to 10 thousand square meters over the 30 days of the experiment. Specific issues include: 1) the relation of point measurements to area averages, 2) the examination of in-field soil moisture structure with implications for soil and/or topographic controlled variability, 3) the cross-field soil moisture structure with implications on vegetation controlled variability, 4) the regional soil moisture structures with implications for meteorological controlled variability, and 5) the change of the dominant control on variability with moisture content.

Author

Soil Moisture; Moisture Content; Variability; Energy Budgets; Atmospheric Energy Sources; Hydrological Cycle

19990111658 NASA Marshall Space Flight Center, Huntsville, AL USA

Auroral Boundaries: Comparison Between UV Images, In Situ Precipitation, and Groundbased Optical Observations

Germany, G. A., Alabama Univ., USA; Swift, W. R., Alabama Univ., USA; Creutzberg, F., National Research Council of Canada, Canada; Eastes, R., Air Force Research Lab., USA; Rich, F., Air Force Research Lab., USA; Spann, James F., Jr., NASA Marshall Space Flight Center, USA; Brittnacher, M., Washington Univ., USA; Parks, G. K., Washington Univ., USA; [1998]; 1p; In English, Dec. 1998, San Francisco, CA, USA; Sponsored by American Geophysical Union, USA; Copyright; Avail: Issuing Activity, Hardcopy; Abstract Only

The location of poleward and equatorward boundaries are used as diagnostics of substorm phase and energy storage in the magnetosphere. Boundaries are estimated from groundbased observations (all sky imagers, meridian scanning photometers, and magnetometers), from in situ particle observations, and from spacebased global auroral observations. Each observational technique has relative advantages. However, recent studies suggest caution when comparing boundaries derived from different methods. in the study, FUV auroral images from the POLAR Ultraviolet Imager are used to estimate auroral boundaries. These boundaries are then compared with similar boundaries derived from DMSP in situ particle precipitation observations and from groundbased meridian scanning photometers. The goal is to see how well the boundaries from these three dissimilar observations correlate, to estimate dependencies on instrumental capabilities, i.e. imager resolution, and to serve as a potential first step to derive an algorithm for finding oval boundaries from groundbased optical data.

Author

Auroras; Auroral Zones; Energy Storage; Magnetic Storms; Earth Magnetosphere

19990111700 NASA Marshall Space Flight Center, Huntsville, AL USA

Initial Comparison of POLAR UVI and Sondrestrom IS Radar Estimates for Auroral Electron Energy Flux

Doe, R. A., NASA Marshall Space Flight Center, USA; Kelly, J. D., NASA Marshall Space Flight Center, USA; Lummerzheim, D., NASA Marshall Space Flight Center, USA; Parks, G. K., NASA Marshall Space Flight Center, USA; Brittnacher, M. J., NASA Marshall Space Flight Center, USA; Germany, G. A., NASA Marshall Space Flight Center, USA; Spann, J. F., Jr., NASA Marshall Space Flight Center, USA; Geophysical Research Letters; [1997]; 1p; In English; Copyright; Avail: Issuing Activity, Hardcopy; Abstract Only

Calibrated images from the POLAR satellite untraviolet imager (UVI) in the 165.5 to 174.5 nm portion of the N2 Lyman-Birge-Hopfield band (LBH-long) can be used to estimate the energy flux (Fe) of auroral electrons precipitating into the high-latitude ionosphere. Similarly, electron density profiles, as measured by ground-based incoherent-scatter radar, can be used

to estimate Fe and mean energy (Eo) by solving a system of linear equations relating the E-region ionization rate profile to a family of monoenergetic ion production profiles. A coordinated POLAR/Sondrestrom radar experiment, designed as an initial comparison of POLAR UVI and ground-based estimates of Fe for a stable auroral arc, was executed during a POLAR apogee on May 20, 1996 at the Sondrestrom radar facility (lat. 66.99 deg N, long. 50.95 deg W). Reconstructed energy distributions, based on radar-measured Ne profiles, indicate an approximately 2keV Maxwellian source with an energy flux of from 6.4 to 14 mW m-2. LBH-long images, binned over 0.5 degrees of latitude and 1.0 degrees of longitude, were used to derive energy flux as well. The UVI-derived Fe time history agrees favorably with radar estimates both in absolute magnituyde and in the trend for this period. This experiment suggests that reliable estimates for the precipitating electron source energy and its ionospheric resonse can be derived from either ground-based radar or POLAR UVI images during summertime conditions.
Author
Ultraviolet Imagery; Incoherent Scatter Radar; Incoherent Scattering; Radar Scattering

19990113190 NASA Marshall Space Flight Center, Huntsville, AL USA
Global Auroral Remote Sensing Using GGS UVI Images
Germany, G. A., NASA Marshall Space Flight Center, USA; Parks, G. K., NASA Marshall Space Flight Center, USA; Brittnacher, M. J., NASA Marshall Space Flight Center, USA; Spann, J. F., Jr., NASA Marshall Space Flight Center, USA; Cumnock, J., NASA Marshall Space Flight Center, USA; Lummerzheim, D., NASA Marshall Space Flight Center, USA; Encounter Between Global Observations and Models in the ISTP Era; [1997]; 1p; In English; Copyright; Avail: Issuing Activity; Abstract Only, Hardcopy, Microfiche

The GGS POLAR satellite, with an apogee distance of 9 Earth radii, provides an excellent platform for extended viewing of the northern auroral zone. Global FUV auroral images from the Ultraviolet Imager onboard the POLAR satellite can be used as quantitative remote diagnostics of the auroral regions, yielding estimates of incident energy characteristics, compositional changes, and other higher order data products. In particular, images of long and short wavelength Earth Far Ultraviolet (FUV) Lyman-Birge-Hopfield (LBH) emissions can be modeled to obtain functions of energy flux and average energy that are basically insensitive to changes in seasonal and solar activity changes. The determination of maps of incident auroral energy characteristics is demonstrated here and compared with in situ measurements.
Author
Remote Sensing; Ultraviolet Imagery; Satellite Imagery; Geophysics

19990113191 NASA Marshall Space Flight Center, Huntsville, AL USA
Remote Determination of Auroral Energy Characteristics During Substorm Activity
Germany, G. A., NASA Marshall Space Flight Center, USA; Parks, G. K., NASA Marshall Space Flight Center, USA; Brittnacher, M. J., NASA Marshall Space Flight Center, USA; Cumnock, J., NASA Marshall Space Flight Center, USA; Lummerzheim, D., NASA Marshall Space Flight Center, USA; Spann, J. F., Jr., NASA Marshall Space Flight Center, USA; Geophysical Research Letters; [1997]; 1p; In English; Copyright; Avail: Issuing Activity; Abstract Only, Hardcopy, Microfiche

Ultraviolet auroral images from the Ultraviolet Imager onboard the POLAR satellite can be used as quantitative remote diagnostics of the auroral regions, yielding estimates of incident energy characteristics, compositional changes, and other higher order data products. In particular, images of long and short wavelength N2 Lyman-Birge-Hopfield (LBH) emissions can be modeled to obtain functions of energy flux and average energy that are basically insensitive to changes in seasonal and solar activity changes. This technique is used in this study to estimate incident electron energy flux and average energy during substorm activity occurring on May 19, 1996. This event was simultaneously observed by WIND, GEOTAIL, INTERBALL, DMSP and NOAA spacecraft as well as by POLAR. Here incident energy estimates derived from Ultraviolet Imager (UVI) are compared with in situ measurements of the same parameters from an overflight by the DMSP F12 satellite coincident with the UVI image times.
Author
Geophysics; Auroras; Magnetic Storms; Remote Sensing

47
METEOROLOGY AND CLIMATOLOGY

Includes weather forecasting and modification.

19990106571 NASA Goddard Space Flight Center, Greenbelt, MD USA
Global Precipitation Patterns Associated with ENSO and Tropical Circulations
Curtis, Scott, NASA Goddard Space Flight Center, USA; Adler, Robert, NASA Goddard Space Flight Center, USA; Huffman, George, NASA Goddard Space Flight Center, USA; Bolvin, David, NASA Goddard Space Flight Center, USA; Nelkin, Eric, NASA Goddard Space Flight Center, USA; [1999]; 2p; In English; 24th; Climate Diagnostics Prediction, 1-5 Nov. 1999, Tucson, AZ, USA; No Copyright; Avail: Issuing Activity, Hardcopy; Abstract Only

Tropical precipitation and the accompanying latent heat release is the engine that drives the global circulation. An increase or decrease in rainfall in the tropics not only leads to the local effects of flooding or drought, but contributes to changes in the large scale circulation and global climate system. Rainfall in the tropics is highly variable, both seasonally (monsoons) and interannually (ENSO). Two experimental observational data sets, developed under the auspices of the Global Precipitation Climatology Project (GPCP), are used in this study to examine the relationships between global precipitation and ENSO and extreme monsoon events over the past 20 years. The V2x79 monthly product is a globally complete, 2.5 deg x 2.5 deg, satellite-gauge merged data set that covers the period 1979 to the present. Indices based on patterns of satellite-derived rainfall anomalies in the Pacific are used to analyze the teleconnections between ENSO and global precipitation, with emphasis on the monsoon systems. It has been well documented that dry (wet) Asian monsoons accompany warm (cold) ENSO events. However, during the summer seasons of the 1997/98 ENSO the precipitation anomalies were mostly positive over India and the Bay of Bengal, which may be related to an epoch-scale variability in the Asian monsoon circulation. The North American monsoon may be less well linked to ENSO, but a positive precipitation anomaly was observed over Mexico around the September following the 1997/98 event. For the twenty-year record, precipitation and SST patterns in the tropics are analyzed during wet and dry monsoons. For the Asian summer monsoon, positive rainfall anomalies accompany two distinct patterns of tropical precipitation and a warm Indian Ocean. Negative anomalies coincide with a wet Maritime Continent.
Author
Precipitation (Meteorology); Climatology; El Nino; Southern Oscillation; Rain; Monsoons; Teleconnections (Meteorology); Atmospheric Circulation

19990106601 NASA Goddard Space Flight Center, Greenbelt, MD USA
Earth Sciences Electronic Theater ”999
Hasler, Fritz, NASA Goddard Space Flight Center, USA; Manyin, Mike, NASA Goddard Space Flight Center, USA; [1999]; 2p; In English, 26 Sep. - 1 Oct. 1999, Santa Clara, CA, USA; Sponsored by Optical Society of America, USA; No Copyright; Avail: Issuing Activity, Hardcopy; Abstract Only

The Etheater presents visualizations which span the period from the original Suomi/Hasler animations of the first ATS-1 GEO weather satellite images in 1966 ..... to the latest 1999 NASA Earth Science Vision for the next 25 years. Hot off the SGI-Onyx Graphics-Supercomputer are NASA’s visualizations of Hurricanes Mitch, Georges, Fran and Linda. These storms have been recently featured on the covers of National Geographic, Time, Newsweek and Popular Science. Highlights will be shown from the NASA hurricane visualization resource video tape that has been used repeatedly this season on National and International network TV. Results will be presented from a new paper on automatic wind measurements in Hurricane Luis from 1-min GOES images that appeared in the November BAMS.
Author
Earth Sciences; Satellite Imagery; Hurricanes; Television Systems; Wind Measurement

19990107341 Los Alamos National Lab., NM USA
Observations and Inferred Physical Characteristics of Compact Intracloud Discharges
Argo, P. E.; Eack, K. B.; Holden, D. N.; Massey, R. S.; Shao, X.; Feb. 01, 1999; 5p; In English; 11th; 11th International Conference on Atmospheric Electricity, 7-11 Jun. 1999, Guntersville, AL, USA
Report No.(s): DE00-007591; LA-UR-99-942; No Copyright; Avail: Department of Energy Information Bridge, Hardcopy

Compact intracloud discharges (CIDS) represent a distinct class of electrical discharges that occur within intense regions of thunderstorms. They are singular discharges that produce brief (typically 3 in duration) broadband RF emissions that are 20 to 30 dB more powerful than radiation from all other recorded lightning processes in the HF and VHF radio spectrum. Far field electric field change recordings of CIDS consist of a single, large-amplitude bipolar pulse that begins to rise during the RF-producing phase of the CID and typically lasts for 20 During the summer of 1998 we operated a 4-station array of electric field

change meters in New Mexico to support FORTE satellite observations of transient RF and optical sources and to learn more about the phenomenology and physical characteristics of CIDS. Over 800 CIDS were detected and located during the campaign. The events were identified on the basis of their unique field change waveforms. CID source heights determined using the relative delays of ionospherically reflected source emissions were typically between 4 and 11 km above ground level. Events of both positive and negative polarity were observed with events' of initially-negative polarity (indicative of discharges occurring between underlying positive and overlying negative charge) occurring at slightly higher altitudes. Within CID field change waveforms the CID pulse was often followed within a few ms by one or more smaller-amplitude pulses. We associate these subsequent pulses with the initial activity of a 'normal' intracloud flash, the inference being that some fraction of the time, a CID initiates an intracloud lightning flash.
NTIS
Atmospheric Electricity; Charge Injection Devices; Thunderstorms; Phenomenology; Intracloud Discharges; Electric Fields; Clouds (Meteorology)

19990107345 Los Alamos National Lab., NM USA
Thunderstorm and Lightning Studies using the FORTE Optical Lightning System (FORTE/OLS)
Argo, P.; Franz, R.; Green, J.; Guillen, J. L.; Jacobson, A. R.; Feb. 01, 1999; 11p; In English; 11th; 11th International Conference on Atmospheric Electricity, 7-11 Jun. 1999, Guntersville, AL, USA
Report No.(s): DE00-007428; LA-UR-99-869; No Copyright; Avail: Department of Energy Information Bridge, Hardcopy

Preliminary observations of simultaneous RF and optical emissions from lightning as seen by the FORTE spacecraft are presented. RF/optical pairs of waveforms are routinely collected both as individual lightning events and as sequences of events associated with cloud-to-ground (CG) and intra-cloud (IC) flashes. CG pulses can be distinguished from IC pulses based on the properties of the RF and optical waveforms, but mostly based on the associated RF spectrograms. The RF spectrograms are very similar to previous ground-based VHF observations of lightning and show signatures associated with return strokes, stepped and dart leaders, and attachment processes. RF emissions are observed to precede the arrival of optical emissions at the satellite by a mean value of 280 microseconds. The dual phenomenology nature of these observations are discussed in terms of their ability to contribute to a satellite-based lightning monitoring mission.
NTIS
Lightning; Storms; Thunderstorms; Research; Radio Frequencies; Cloud-to-Ground Discharges

19990107372 Lembaga Penerbangan dan Antariksa Nasional, Peneliti Bidang Dinamika Atmosfer, Puslitbang Atmosfer, Jakarta, Indonesia
Statistical Test of Temperature Changes in Jakarta 1971-1989 ***Uji Statistik Perubahan Suhu DKI Jakarta Periode 1971-1989***
Sjamsuar, Suharnis, Lembaga Penerbangan dan Antariksa Nasional, Indonesia; Warta: Lembaran Tambahan Majalah LAPAN; October 1998; ISSN 0126-9754; Volume 22, No. 57, pp. 44-48; In Malay-Indonesian; No Copyright; Avail: CASI; A01, Hardcopy; A01, Microfiche

A research about temperature change in DKI Jakarta between 1971-1979 and 1980-1989 periods has been done. In this case was used equality test two means two side, that is H(sub 0) : mu(sub 1) = mu(sub 2) and contrariwise H(sub 1) : mu(sub 1) does not equal mu(sub 2), and equality test two variances two side, that is H(sub 0) : variance(sub 1) = variance(sub 2) and contrariwise H(sub 1) : variance(sub 1) does not equal variance(sub 2). For means at level of significant alpha = 0.10 and statistic test t, obtained -t(sub 0.95) = -1.645 is less than t = -1.00615 is less than t(sub 0.95) = 1.645 . It means that there are not difference in between the two means. Similarly for equality test the two variances at level of significant alpha = 0,10 and statistic test F obtained F = 1.0839 is less than F((sub 0,05)(119,107)) = 1,28 , it means that there are not difference in between the two variances. Therefore there were no temperature change in DKI Jakarta in between 1971-1979 and 1980-1989 periods.
Author
Statistical Tests; Temperature

19990107374 Lembaga Penerbangan dan Antariksa Nasional, Peneliti Bidang Standard Atmosfer, Puslitbang Pengetahuan Atmosfer, Jakarta, Indonesia
Relationship Between Temperature and Rainfall on Java in the Enso Period ***Hubungan Temperatur dan Curah Hujan di Pulau Jawa Pada Periode Enso***
Kurniaty, Tatty, Lembaga Penerbangan dan Antariksa Nasional, Indonesia; Prabowo, Anondo, Lembaga Penerbangan dan Antariksa Nasional, Indonesia; Wirasasmita, Mulyana, Lembaga Penerbangan dan Antariksa Nasional, Indonesia; Rosida, Lembaga Penerbangan dan Antariksa Nasional, Indonesia; Rangkuti, Alzah S., Lembaga Penerbangan dan Antariksa Nasional,

Indonesia; Syarifudin, M., Lembaga Penerbangan dan Antariksa Nasional, Indonesia; Warta: Lembaran Tambahan Majalah LAPAN; October 1998; ISSN 0126-9754; Volume 22, No. 57, pp. 32-37; In Malay-Indonesian; No Copyright; Avail: CASI; A02, Hardcopy; A01, Microfiche

Once of nature phenomena that always been discuss is climate change. From many elements of climate such as air temperature, Humidity, rain rate, wind, etc., just temperature and rain rate as a main element of climate change. This research will be find how for the before ENSO, the ENSO and after the ENSO relation to the change in temperature and rain rate above will be using Spectral analysis, and form the result could find that in ENSO period correlation between temperature and rain rate is weak with value 0.001, 0.006 and 0.002. Than in before and after ENSO period is between 0.05 - 0.18.
Author

Climate Change; Rain; Atmospheric Temperature

19990107388 NASA Goddard Space Flight Center, Greenbelt, MD USA

Rainfall Estimates from the TMI and the SSM/I

Hong, Ye, Caelum Research Corp.; Kummerow, Christian D., NASA Goddard Space Flight Center, USA; Olson, William S., Maryland Univ. Baltimore County, USA; Viltard, Nicolas, Universities Space Research Association, USA; 1999; 1p; In English; Progress in Electromagnetics Research, 22-26 Mar. 1999, Taipei, Taiwan, Province of China; Copyright; Avail: Issuing Activity, Hardcopy; Abstract Only

The Tropical Rainfall Measuring Mission (TRMM), which is a joint Japan-U.S. Earth observing satellite, has been successfully launched from Japan on November 27, 1997. The main purpose of the TRMM is to measure quantitatively rainfall over the tropics for the research of climate and weather. One of three rainfall measuring instruments abroad the TRMM is the high resolution TRMM Microwave Imager (TMI). The TMI instrument is essentially the copy of the SSM/I with a dual-polarized pair of 10.7 GHz channels added to increase the dynamic range of rainfall estimates. In addition, the 21.3 GHz water vapor absorption channel is designed in the TMI as opposed to the 22.235 GHz in the SSM/I to avoid saturation in the tropics. This paper will present instantaneous rain rates estimated from the coincident TMI and SSM/I observations. The algorithm for estimating instantaneous rainfall rates from both sensors is the Goddard Profiling algorithm (Gprof). The Gprof algorithm is a physically based, multichannel rainfall retrieval algorithm, The algorithm is very portable and can be used for various sensors with different channels and resolutions. The comparison of rain rates estimated from TMI and SSM/I on the same rain regions will be performed. The results from the comparison and the insight of tile retrieval algorithm will be given.
Author

Estimates; Rain; Remote Sensing; Tropical Regions; Comparison

19990107393 NASA Marshall Space Flight Center, Huntsville, AL USA

Optical Observations of Lightning in Northern India Himalayan Mountain Countries and Tibet

Boeck, William L., Niagara Univ., USA; Mach, D. M., NASA Marshall Space Flight Center, USA; Goodman, S. J., NASA Marshall Space Flight Center, USA; Christian, Hugh J., Jr., NASA Marshall Space Flight Center, USA; [1999]; 1p; In English; 11th; Atmospheric Electricity, 7-11 Jun. 1999, Guntersville,AL, USA; No Copyright; Avail: Issuing Activity, Hardcopy; Abstract Only

This study summarizes the results of an analysis of data from the LIS instrument on the TRMM platform. The data for the Indian summer monsoon season is examined to study the seasonal patterns of the geographic and diurnal distribution of lightning storms. The storms on the Tibetan plateau show a single large diurnal peak at about 1400 local solar time. A region of Northern Pakistan has two storm peaks at 0200 and 1400 local solar time. The morning peak is half the magnitude of the afternoon peak. The region south of the Himalayan Mountains has a combined diurnal cycle in location and time of storm occurrence.
Author

Visual Observation; Lightning; Diurnal Variations; Geographic Distribution

19990108483 NASA Goddard Space Flight Center, Greenbelt, MD USA

On Orbit Measurement of Response vs. Scan Angle for the Infrared Bands on TRMM/VIRS

Barnes, William L., NASA Goddard Space Flight Center, USA; Lyu, Cheng–Hsuan, Caelum Research Corp., USA; Barnes, Robert A., Science Applications International Corp., USA; [1999]; 9p; In English, 20-24 Sep. 1999, Florence, Italy; Sponsored by Electro-Optical Systems, Inc., USA; No Copyright; Avail: CASI; A02, Hardcopy; A01, Microfiche

The Visible and Infrared Scanner on the Tropical Rainfall Measuring Mission (TRMM/VIRS) is a whiskbroom imaging radiometer with two reflected solar bands and three emissive infrared bands. All five detectors are on a single cooled focal plane. This configuration necessitated the use of a paddlewheel scan mirror to avoid the effects of focal plane rotation that arise when using a scan mirror that is inclined to its axis of rotation. System radiometric requirements led to the need for protected silver as

the mirror surface. Unfortunately, the SiO(x) coatings currently used to protect silver from oxidation introduce a change in reflectance with angle of incidence (AOI). This AOI dependence results in a modulation of system level response with scan angle. Measurement of system response vs. scan angle (RVS) was not difficult for the VIRS reflected solar bands, but attaining the required accuracy for the IR bands in the laboratory was not possible without a large vacuum chamber and a considerable amount of custom designed testing apparatus. Therefore, the decision was made to conduct the measurement on-orbit. On three separate occasions, the TRMM spacecraft was rotated about its pitch axis and, after the nadir view passed over the Earth's limb, the VIRS performed several thousand scans while viewing deep space. The resulting data has been analyzed and the RVS curves generated for the three IR bands are being used in the VIRS radiometric calibration algorithm. This, to our knowledge, the first time this measurement has been made on-orbit. Similar measurements are planned for the EOS-AM and EOS-PM MODIS sensors and are being considered for several systems under development. The VIRS on-orbit results will be compared to VIRS and MODIS system level laboratory measurements, MODIS scan mirror witness sample measurements and modeled data.
Author
Infrared Radiation; Infrared Scanners; Visible Infrared Spin Scan Radiometer; Spacecraft Maneuvers; Maneuverability

19990108602 Osaka Univ., Osaka, Japan
Broadband Interferometer and 3D Observations
Mardiana, R., Osaka Univ., Japan; Ota, Y., Osaka Univ., Japan; Kawasaki, Z. I., Osaka Univ., Japan; Murakami, M., Osaka Univ., Japan; Matsuura, K., Osaka Univ., Japan; 11th International Conference on Atmospheric Electricity; June 1999, pp. 2-5; In English; See also 19990108601; No Copyright; Avail: CASI; A01, Hardcopy; A10, Microfiche

Lightning observations to image lightning channel progression in 3D by means of broadband radio interferometer is performed. Using two sets of broadband systems at two different sites, we observed many lightning discharges during a field campaign in Darwin, Australia in 1998. We carried out the data processing to investigate the development of lightning discharges. The system shows that for several tens of kilometers, lightning discharges can be detected, their progression can be reconstructed and their positions can be mapped into three-dimensionally spatial formats and time sequences.
Author
Lightning; Australia; Interferometry; Imaging Techniques

19990108603 Los Alamos National Lab., Space and Atmospheric Sciences, NM USA
Observations and Inferred Physical Characteristics of Compact Intracloud Discharges
Smith, D. A., Los Alamos National Lab., USA; Massey, R. S., Los Alamos National Lab., USA; Wiens, K. C., New Mexico Inst. of Mining and Technology, USA; Eack, K. B., Los Alamos National Lab., USA; Shao, X. M., Los Alamos National Lab., USA; Holden, D. N., Los Alamos National Lab., USA; Argo, P. E., Los Alamos National Lab., USA; 11th International Conference on Atmospheric Electricity; June 1999, pp. 6-9; In English; See also 19990108601; No Copyright; Avail: CASI; A01, Hardcopy; A10, Microfiche

Compact intracloud discharges (CIDS) represent a distinct class of electrical discharges that occur within intense regions of thunderstorms. They are singular discharges that produce brief (typically 3 microseconds in duration) broadband RF emissions that are 20 to 30 dB more powerful than radiation from all other recorded lightning processes in the HF and VHF radio spectrum. Far field electric field change recordings of CIDs consist of a single, large-amplitude, narrow bipolar pulse (NBP) that begins to rise during the RF-producing phase of the CID and typically lasts for 20 microseconds. During the summer of 1998 we operated a 4-station array of electric field change meters in New Mexico to support FORTE satellite observations of transient RF and optical sources and to learn more about the phenomenology and physical characteristics of CIDs. Over 800 CIDs were detected and located during the campaign. The events were identified on the basis of their unique field change waveforms. CID source heights determined using the relative delays of ionospherically reflected source emissions were typically between 4 and 11 km above ground level. Events of both positive and negative polarity were observed with events of initially-negative polarity (indicative of discharges occurring between underlying positive and overlying negative charge) occurring at slightly higher altitudes. Within CID field change waveforms the CID pulse was often followed within a few ms by one or more smaller-amplitude pulses. We associate these subsequent pulses with the initial activity of a "normal" intracloud flash, the inference being that some fraction of the time, a CID initiates an intracloud lightning flash.
Author
Lightning; Satellite Observation; Thunderstorms; Radio Frequency Discharge

19990108604 Tokyo Univ., Japan
Height of Radiation Sources Associated with Lightning Discharges
Ishii, M., Tokyo Univ., Japan; Hojo, J., Tokyo Univ., Japan; Shimizu, K., Tokyo Univ., Japan; Sato, K., Tokyo Univ., Japan; Shinjo,

K., Hokuriku Electric Power Co., Japan; 11th International Conference on Atmospheric Electricity; June 1999, pp. 10-13; In English; See also 19990108601; No Copyright; Avail: CASI; A01, Hardcopy; A10, Microfiche

Radiation sources of in-cloud discharges are located three-dimensionally by the TOA technique using data from a network of fast antennas and VHF receivers. The location accuracy of most of the analyzed radiation sources was within 0.5 km in the z-direction. The sources of VHF pulses, radiated within 50 microseconds of a bipolar pulse observed by a fast antenna, were located mostly within 0.5 km from the source of the bipolar pulse. The distributions of the height of the origins of bipolar pulses are clearly separated depending on the initial polarity of a bipolar pulse, regardless of the seasons or the kinds of flashes. The polarity of the bipolar pulses is consistent with the hypothesis that there is a negative charge center at the temperature height of about -5 to -10 C. The peaks of the two distributions correspond to the peaks of the reported bimodal distribution of VHF sources in the beginning of flashes.

Author

Bipolarity; Lightning; Radiation Sources; Very High Frequencies; Electromagnetic Pulses

19990108605 Office National d'Etudes et de Recherches Aerospatiales, Paris, France

VHF Observations During a Spider Lightning Flash

Defer, E., Office National d'Etudes et de Recherches Aerospatiales, France; Thery, C., Office National d'Etudes et de Recherches Aerospatiales, France; Blanchet, P., Office National d'Etudes et de Recherches Aerospatiales, France; Laroche, P., Office National d'Etudes et de Recherches Aerospatiales, France; 11th International Conference on Atmospheric Electricity; June 1999, pp. 14-17; In English; See also 19990108601; No Copyright; Avail: CASI; A01, Hardcopy; A10, Microfiche

We have analyzed VHF radiations detected during a spider lightning flash with the ONERA three-dimensional interferometric mapper. Two states have been identified during this horizontal extended flash. First, a 40 km long horizontally extended event that lasted 130 ms was recorded. Then, few tens of milliseconds later, some short duration events were recorded. The first event exhibited the same characteristics as observed during a negative downward stepped leader occurring during a negative cloud-to-ground lightning flash, i.e. a 4 x 10(exp 5) m/s global velocity and a continuous radiation recorded on our narrow band interferometer.

Author

Interferometry; Lightning; Very High Frequencies; Radiation Sources

19990108606 Osaka Univ., Dept. of Electrical Engineering, Osaka, Japan

Broad Band Interferometric Measurement of Intra-Cloud Lightning In Chinese Inland Plateau Area

Ushio, Tomo, Osaka Univ., Japan; Kawasaki, Z. –I., Osaka Univ., Japan; Chen, M., Gifu Univ., Japan; Wang, D., Gifu Univ., Japan; Takagi, N., Gifu Univ., Japan; Watanabe, T., Gifu Univ., Japan; Liu, X., Lanzhou Inst. of Plateau Atmospheric Physics, China; Xiushu, Q., Lanzhou Inst. of Plateau Atmospheric Physics, China; Guo, C., Shanghai Meteorological Inst., China; 11th International Conference on Atmospheric Electricity; June 1999, pp. 18-21; In English; See also 19990108601; No Copyright; Avail: CASI; A01, Hardcopy; A10, Microfiche

We have measured the characteristics of intra-cloud lightning at Pingliang, a plateau area in north-western China, using a broad band interferometer system developed by Ushio et al. (1997). This system, using a 500 MHz digitizer with 8 Megabyte memory and operating at the frequencies from 30 to 250 MHz, measures the two dimensional direction of arrival of the radiation from lightning discharges. A detailed study of two instances of intra-cloud lightning has shown that the intra-cloud lightning usually begins with an activity which lasts a few hundred milliseconds and involves the development of several horizontal streamers at the lower part inside the cloud. Since the similar initial activity to this has not been observed from the summer storms either in Florida or in New Mexico by Shao et al.(1996), our results appear to support the unique charge structure of the thunderstorms around Pingliang area as suggested by Liu et al. (1989). Followed this initial activity, the most active stage was observed to occur simultaneously in two directions, one tracing the previously-produced horizontal channel and the other connecting to the upper part of the cloud. From our electric field data which have been simultaneously recorded with the broad band interferometer data, the latter is inferred to transfer negative charge upward. As a whole, the intra-cloud lightning studied here exhibits a two-level structure in which the two levels were connected by a single upward channel as reported by Shao et al. (1996). In addition, in a comparison to the narrow band interferometer and the time of arrival system, the advantage and the disadvantage of our system are also discussed.

Author

Interferometry; Lightning; Plateaus; Thunderstorms

19990108607 Office National d'Etudes et de Recherches Aerospatiales, Paris, France

The Inception Phase of Positive Leaders in Triggered Lightning: Comparison of Modeling with Experimental Data

Bondiou–Clergerie, A., Office National d'Etudes et de Recherches Aerospatiales, France; Lalande, P., Office National d'Etudes et de Recherches Aerospatiales, France; Laroche, P., Office National d'Etudes et de Recherches Aerospatiales, France; Willett, J. C., Air Force Research Lab., USA; Davis, D., State Univ. of New York, USA; Gallimberti, I., Padua Univ., Italy; 11th International Conference on Atmospheric Electricity; June 1999, pp. 22-25; In English; See also 19990108601; No Copyright; Avail: CASI; A01, Hardcopy; A10, Microfiche

A self consistent model simulating inception and development of positive leaders has been previously derived from theoretical studies of laboratory long sparks. The model was successfully tested in the case of positive leaders in long laboratory gaps and has been extended to the positive leaders in triggered lightning flashes by including channel thermalization processes. In this last case, full testing and validation of the model requires measurement of the vertical profile of ambient electric field prior to the triggering of the flash. A recent experiment has provided ambient field profiles a few seconds before nine lightning flashes triggered by the rocket-and-wire technique. This paper presents a comparison between calculated and measured features of the positive leader during its inception and first few milliseconds of propagation in one of these cases. Relationships between average ambient field and wire length at inception are analyzed over the whole set of data and the concept of a is much less than leader stabilization field is greater than > is presented.

Author

Lightning; Electric Discharges; Stabilization; Simulation

19990108608 National Severe Storms Lab., Norman, OK USA

Computer Simulation of a Downward Negative Stepped Leader

Mazur, V., National Severe Storms Lab., USA; Bondiou–Clergerie, A., Office National d'Etudes et de Recherches Aerospatiales, France; Lalande, P., Office National d'Etudes et de Recherches Aerospatiales, France; Ruhnke, L. H.; 11th International Conference on Atmospheric Electricity; June 1999, pp. 26-29; In English; See also 19990108601; No Copyright; Avail: CASI; A01, Hardcopy; A10, Microfiche

In a realistic computer simulation (model) of interaction between a downward negative stepped leader and a ground structure, the results will depend heavily upon the assumptions made about the manner process of propagation of both the downward and upward and induced leaders. It is important to base these assumptions on descriptions that are physically sound and which have emerged from theoretical modeling of negative and positive leaders, as well as laboratory experiments on long sparks. The objective of this study is twofold: (1) to develop a scheme of computer simulation for negative lightning leader interaction with a ground structure that reflects known physical concepts, and which is reasonably simple to model; and (2) to determine the dominant factors affecting interception of the downward negative leader with a ground structure.

Author

Lightning; Computerized Simulation; Mathematical Models; Electric Potential; Stepped Leaders

19990108609 Lanzhou Inst. of Plateau Atmospheric Physics, China

1997 Triggered Lightning Experiment in the Inland Plateau of China

Liu, X., Lanzhou Inst. of Plateau Atmospheric Physics, China; Wang, C., Lanzhou Inst. of Plateau Atmospheric Physics, China; Qie, X., Lanzhou Inst. of Plateau Atmospheric Physics, China; Zhang, Y., Lanzhou Inst. of Plateau Atmospheric Physics, China; Dong, W., Lanzhou Inst. of Plateau Atmospheric Physics, China; Xiao, Q., Lanzhou Inst. of Plateau Atmospheric Physics, China; Zhang, G., Lanzhou Inst. of Plateau Atmospheric Physics, China; Guo, C., Shanghai Meteorological Inst., China; Chen, M., Lanzhou Inst. of Plateau Atmospheric Physics, China; Watanabe, T., Gifu Univ., Japan; Wang, D., Gifu Univ., Japan; Takagi, N., Gifu Univ., Japan; Nakano, M., Toyota Coll. of Technology, Japan; Nakamura, K., Nagoya Inst. of Tech., Japan; Kawazaki, Z., Osaka Univ., Japan; Sumi, S., Chubu Univ., Japan; 11th International Conference on Atmospheric Electricity; June 1999, pp. 30-33; In English; Sponsored by National Science Foundation of China, China; See also 19990108601; No Copyright; Avail: CASI; A01, Hardcopy; A10, Microfiche

This paper presents main results of triggered lightning experiment conducted in 1997 in the inland plateau of China, with the emphasis on the characteristics of an altitude triggered lightning. The bi-directional leader propagation was identified by simultaneous electrical and photographic observation. After initiation the downward moving positive leader, which produced at the lower end of aloft steel wire under the action of dominated lower positive charge of thundercloud, connected in the period of 0.7 ms to the upward moving attachment negative leader and occurred a junction process, similar to in some respects but actually different from in the strict sense return stroke of natural lightning discharges.

Author

Lightning; Leaders (Meteorology); Propagation (Extension); Thunderstorms

19990108610 National Defence Academy, Yokosuka, Japan

Characteristics of "Superbolt" Related Winter Thunderclouds over the Japan Sea

Shimura, T., National Defence Academy, Japan; Kobayashi, F., National Defence Academy, Japan; Shindo, Takatoshi, Central Research Inst. of Electric Power Industry, Japan; Wada, A., Central Research Inst. of Electric Power Industry, Japan; Sakai, T., Hokuriku Electric Power Co., Japan; 11th International Conference on Atmospheric Electricity; June 1999, pp. 380-383; In English; See also 19990108601; No Copyright; Avail: CASI; A01, Hardcopy; A10, Microfiche

One of the typical features of winter thunderclouds in the Hokuriku district of Japan is positive lightning strikes with large lightning currents or huge charges neutralized by lightning. "Superbolt" thunderclouds which generated large current lightning strikes twice in succession to the 200m-high stack were observed using a Doppler radar on December 21, 1995. Both of the peak currents observed by shunt register were over 25OkA. On that day, meso- alpha -scale low pressure system formed over the Japan sea and a band-shaped radar echo about 100 km long, developed near the coastline within only about 1 hour. The results of the Doppler radar observation show that the first lightning strike occurred at the leading edge of the echo band whose intensity was weak (less than 16dBZ or no echo), and the second one occurred at the core of those whose intensity was strong (greater than 3OdBZ). "Superbolt" occurred after a long time charge accumulation in the southern part of the band echo system.

Author

Cumulonimbus Clouds; Thunderstorms; Radar Tracking; Radar Echoes; Lightning

19990108611 Toulouse Univ., Lab. d'Aerologie, France

Some Aspects of Correlation Between Lightning Activity and Rainfall in Thunderstorms

Soula, S., Toulouse Univ., France; Molinie, G., Toulouse Univ., France; Defoy, S., Toulouse Univ., France; Chauzy, S., Toulouse Univ., France; Simond, N., Toulouse Univ., France; 11th International Conference on Atmospheric Electricity; June 1999, pp. 384-387; In English; See also 19990108601; No Copyright; Avail: CASI; A01, Hardcopy; A10, Microfiche

The correlations between cloud-to-ground (CG) lightning flashes and rain activities have been widely studied during the past ten years. They are usually estimated in terms of location, of rates evolution and of water volume per flash. This work presents some results obtained from this kind of study with data issued from French networks. The CG lightning flash activity is detected by the Meteorage network and the rain is estimated from the radar observations. We studied 21 thundercells or systems from 4 days most of them occurring over the French territory. The water volume per flash ranges from 6.2 x 10(exp 3)cu m to 75 x 10(exp 3)cu m with an average value of 26 x 10(exp 3)cu m. The time lag between the peaks of both activities depends on the detection height of the rain by the radar and the flash maximum precedes by a few minutes the rain detection at low altitude. The flash density maximum is tightly related to the location of the heavy rainfall, especially in the case of a flash flood caused by a thunderstorm in Northern Spain.

Author

Cloud-to-Ground Discharges; Data Correlation; Lightning; Radar Tracking; Rain; Thunderstorms

19990108612 Osaka Univ., Dept. of Electrical Engineering, Suita, Japan

Verification of Bi-Directional Leader Concept Using Interferometric Measurement

Yoshihashi, Sachi, Osaka Univ., Japan; Kawasaki, Zen, Osaka Univ., Japan; 11th International Conference on Atmospheric Electricity; June 1999, pp. 34-37; In English; See also 19990108601; No Copyright; Avail: CASI; A01, Hardcopy; A10, Microfiche

Bi-directional leader concept is discussed from the aspects of field observations. For this purpose field observations are conducted during winter and summer thunderstorm seasons at Hokuriku in Japan and Darwin in Australia respectively. The main instrument presented in this paper is UHF interferometers, and 2D and 3D lighting channel images are shown in terms of UHF radiation sources. Currents of lightning discharges triggered from a tip of a high artificial construction are measured to confirm the polarity of upward initiating leaders, and features of UHF radiation depending on the polarity are given. Three-dimensional UHF radiation source images during leader progression for "negative" and "positive" cloud to ground flashes are shown, and the correctness of the bi-directional leader concept is shown.

Author

Thunderstorms; Leaders (Meteorology); Cloud-to-Ground Discharges; Interferometry; Ultrahigh Frequencies

19990108613 Mississippi Univ., Dept. of Physics and Astronomy, University, MS USA

An Investigation of the Horizontal Extent of Charge Regions in One Thunderstorm

Marshall, T. C., Mississippi Univ., USA; Stolzenburg, M., Mississippi Univ., USA; Bartels, D. L., National Severe Storms Lab., USA; Rust, W. D., National Severe Storms Lab., USA; 11th International Conference on Atmospheric Electricity; June 1999, pp. 388-391; In English; See also 19990108601

Contract(s)/Grant(s): NSF ATM-96-26542; No Copyright; Avail: CASI; A01, Hardcopy; A10, Microfiche

On June 10, 1998, we flew two balloons, each carrying an electric field meter and a radiosonde, into a small thunderstorm in central Oklahoma. The balloons were launched about six minutes apart from the same location (near Tupelo, OK) as the storm passed overhead; both were launched ahead of the main convective precipitation region of the storm. In this presentation we compare electric fields and lightning field changes observed with the two balloons to get an idea of the horizontal extent of the main charge structure and of the localization of charge affected by the lightning flashes.

Derived from text

Thunderstorms; Electric Charge; Balloon Sounding; Atmospheric Sounding; Atmospheric Electricity; Electrical Measurement; Horizontal Distribution

19990108614 Instituto Nacional de Pesquisas Espacias, Div. de Geofisica Espacial, Sao Jose dos Campos, Brazil

On Lightning Current Probability Distribution from Southeastern Brazilian Measurements

Mendes, O., Jr., Instituto Nacional de Pesquisas Espacias, Brazil; Domingues, M. O., Instituto Nacional de Pesquisas Espacias, Brazil; Pinto, I. R. C. A., Instituto Nacional de Pesquisas Espacias, Brazil; Pinto, O., Jr., Instituto Nacional de Pesquisas Espacias, Brazil; Diniz, J. H., Companhia Energetica de Minas Gerais, Brazil; Carvalho, A. M., Companhia Energetica de Minas Gerais, Brazil; Cazetta, A. M., Companhia Energetica de Minas Gerais, Brazil; 11th International Conference on Atmospheric Electricity; June 1999, pp. 38-41; In English; See also 19990108601

Contract(s)/Grant(s): FAPESP-1998-3860-9; No Copyright; Avail: CASI; A01, Hardcopy; A10, Microfiche

The estimated peak-current amplitude of Brazilian southeastern lightning occurrences measured by the Lightning Positioning and Tracking System (LPATS), from 1988 to 1995, is analysed here. The Log-Normal and the three parameter Weibull Probability Density Functions are used to investigate this data set. This work identified approx. 62% of negative, approx. 37% of positive and approx. 1% of bipolar lightning flashes. The mode of negative flashes is higher than the mode of positive ones. All lightning current distributions are leptokurtic distributions. The Log Normal PDF fits better this current data set than the three parameter Weibull PDF. However, in consequence of its representative behaviour, the last one could be very useful as an index for classification of thunderstorm events.

Author

Lightning; Weibull Density Functions; Probability Density Functions; Distribution Functions; Current Distribution

19990108615 Instituto Nacional de Pesquisas Espacias, Sao Jose dos Campos, Brazil

Analysis of Negative Downward Lightning Current Curves From 1985 to 1994 at Morro Do Cachimbo Research Station (Brazil)

Lacerda, Moacir, Instituto Nacional de Pesquisas Espacias, Brazil; Pinto, Osmar, Jr., Instituto Nacional de Pesquisas Espacias, Brazil; Pinto, Iara R. C. A., Instituto Nacional de Pesquisas Espacias, Brazil; Diniz, Jose H., Companhia Energetica de Minas Gerais, Brazil; Carvalho, Andre M., Companhia Energetica de Minas Gerais, Brazil; 11th International Conference on Atmospheric Electricity; June 1999, pp. 42-45; In English; See also 19990108601

Contract(s)/Grant(s): FAPESP Proj. 98/11958-9; No Copyright; Avail: CASI; A01, Hardcopy; A10, Microfiche

This paper presents an analysis of negative descendent cloud to ground lightning captured by a 60 m metallic tower between 1985 and 1994 in the ”Morro do Cachimbo” research station (43 deg 58 min 26 sec W, 20 deg 00 min 39 sec S) of the Companhia Energetica de Minas Gerais (CEMIG), Brazil. From the comparison of return strokes with those of another station in Switzerland it was noted that electric current wave forms are similar in both countries, although the mean peak current in Brazil (41 kA) is greater than that in Switzerland (30 kA) and the time to peak is greater in Brazil (22 microsec) than in Switzerland (13 microsec). Differences in subsequent strokes were observed too. It was found that the time to peak current is correlated to the time to peak of derivative current with a linear correlation coefficient of about 94%. The mean third return stroke current was found to be stronger than the second and an explanation for that was suggested. M-components recorded at about 200 microsec (geometric mean peak current of 2.37 kA) had time to peak lower than those obtained after 1 ms in Florida and Alabama.

Author

Cloud-to-Ground Discharges; Electric Current; Waveforms

19990108616 Universidad del Pais Vasco, Dpto. Fisica Aplicada, San Sebastian, Spain

Lightning Characteristics in the 1992-1996 Period in the Basque Country Area: Lightning-Precipitation Relationships

Areitio, J., Universidad del Pais Vasco, Spain; Herrero, I., Universidad del Pais Vasco, Spain; Ezcurra, A., Universidad del Pais Vasco, Spain; 11th International Conference on Atmospheric Electricity; June 1999, pp. 392-395; In English; See also 19990108601; No Copyright; Avail: CASI; A01, Hardcopy; A10, Microfiche

This study is focused in the Spanish Basque Country in the north of the Iberian Peninsula. Lightning data bases has been provided by the INM (Instituto Nacional de Meteorologia) direction finder network (DF) and the Time of Arrival (TOA) network of the Iberdola power supply company. The number of lightning flashes recorded in the 1992-1996 period was 92212. Positive lightning fraction ranges between 4% in July and 39% in January. Mean intensity for negative and positive lightning is 27 kA and 55 kA respectively. Negative lightning single strokes vary between 80% in winter and 40% in summer while positive lightning single strokes are approximately 90% throughout the year. The annual flash density maximum (3 lightning/sq km) was observed over Bilbao, the largest city in the area. Relationships between lightning density and precipitation are unclear. Three storm events present different correlation coefficients between lightning density and several precipitation parameters. In this way, two flash floods with few lightning occurrences were observed.
Author
Lightning; Thunderstorms; Data Correlation; Phenomenology; Electric Charge; Rain

19990108617 Florida Univ., Gainesville, FL USA
Lightning Subsequent Strokes Producing New Terminations to Ground
Davis, Stepehen M., Florida Univ., USA; Thomson, Ewen M., Florida Univ., USA; 11th International Conference on Atmospheric Electricity; June 1999, pp. 46-49; In English; See also 19990108601; No Copyright; Avail: CASI; A01, Hardcopy; A10, Microfiche

We analyze results from 16 flashes to ground containing dE/dt pulse trains prior to subsequent strokes in new terminations. Strokes in new terminations were preceded by leaders that were dart-stepped in nature, producing the observed pulse trains, prior to adopting a new path to ground via a stepped leader. Locations of individual sources in the trains were obtained using the time of arrival method from dE/dt measured at five ground stations. Point-to-point source velocities in trains ranged from 1.0 x 10(exp 6) m/s to 1.2 x 10(exp 7) m/s. All dE/dt waveforms from strokes creating a new termination to ground contained fine structure after the return stroke peak, similar to that seen in first strokes. However, fine structure accompanying new terminations to ground was shorter, with a median duration of 37 microsec, than that of first strokes, median value 141 microsec. Sources of fine structure were located in the channel apparently formed by the stepped leader portion of the leader.
Author
Cloud-to-Ground Discharges; Leaders (Meteorology); Stepped Leaders

19990108618 Universidad del Pais Vasco, Dpto. Fisica Aplicada, San Sebastian, Spain
First Measurements of the Atmospheric Electric Field in the Spanish Basque Country
Herrero, I., Universidad del Pais Vasco, Spain; Areitio, J., Universidad del Pais Vasco, Spain; Ezcurra, A., Universidad del Pais Vasco, Spain; 11th International Conference on Atmospheric Electricity; June 1999, pp. 396-399; In English; See also 19990108601; No Copyright; Avail: CASI; A01, Hardcopy; A10, Microfiche

First measurements of atmospheric electricity field in the Spanish Basque Country were made during the summer of 1997 with an electric field mill located inside of an automatic meteorological closure. Data from the field mill was afterwards compared with those of the meteorological station. Data from the INM lightning detection system in order to compare the lightning stroke and the field signal were also considered. The aim of this paper is to determine characteristic behaviors of the electric field under different meteorological conditions and to focus on those situations that originate severe thunderstorms, and severe precipitation. Under thunderstorm conditions, the behavior described by many authors is observed in our study: sign inversion, strong oscillations and high values. When considering the lightning stroke, the value of the intensity and the distance to the measuring point appears to play an important roll affecting the signal structure. Finally, an FFT analysis of signal shows waves with a day and half a day of periodicity, probably connected to the diurnal and semidiurnal variation of the global fair weather electric field. Nevertheless, some shorter periodicities are also detected, that could correspond with precipitation-related phenomena.
Author
Atmospheric Electricity; Electric Fields; Electrical Measurement; Signal Measurement; Meteorological Parameters

19990108619 State Univ. of New York, Dept. of Earth and Atmospheric Sciences, Albany, NY USA
Photographic Documentation of Two Return Strokes Along the Same Channel Separated by About a Millisecond
Idone, Vincent P., State Univ. of New York, USA; Davis, Daniel A., State Univ. of New York, USA; 11th International Conference on Atmospheric Electricity; June 1999, pp. 50-53; In English; See also 19990108601
Contract(s)/Grant(s): NSF ATM-90-21909; NSF ATM-96-27276; No Copyright; Avail: CASI; A01, Hardcopy; A10, Microfiche

Two strokes in a triggered lightning flash initiated in 1996 at Camp Blanding, Florida, were recorded with a time-resolved photographic system that unequivocally documents the occurrence of these strokes along the same channel with an interstroke interval of only 1.09 ms. Each stroke has a distinct downward leader phase. This observation appears to confirm effectively the

hypothesis of Rakov and Uman [1994] that such stroke couplets, consisting of a primary and secondary stroke, can occur with an interval of a millisecond or less. We reproduce these records and provide analyses of the leader propagation speeds of the primary and secondary stroke: 0.96 x 10(exp 7) m/s and 1.4 x 10(exp 7) m/s, respectively. We also present qualitative analyses of the difference in optical characteristics of the two strokes, which may be typical of such short interstroke interval events.
Author
Lightning; Optical Properties; Cloud-to-Ground Discharges

19990108620 Osaka Univ., Dept. of Electrical Engineering, Suita, Japan
3D Imaging of Lightning Channel and Leader Progression Velocity
Kawasaki, Zen, Osaka Univ., Japan; Isoda, Hitoshi, Osaka Univ., Japan; Yoshihashi, Sachi, Osaka Univ., Japan; 11th International Conference on Atmospheric Electricity; June 1999, pp. 54-57; In English; See also 19990108601; No Copyright; Avail: CASI; A01, Hardcopy; A10, Microfiche

Three dimensional imaging of lightning channels, especially for leader progression, by means of UHF interferometers has been achieved. A field campaign with two observation sites is conducted at Darwin Australia for further study. The distance between two sites is 14.2 km, and the triangulation scheme is applied to locate UHF radiation sources in three dimensions. Since the UHF radiation during the leader progression is more expected than the return stroke, images of lightning channels are given mainly for downward leaders. Velocities of downward leaders are calculated, and statistics are derived for the first, and subsequent strokes. The comparison of the mean velocity of the early phase of leaders inside thundercloud with the final phase of leaders below a thurdercloud is conducted. Since the optical measurement of invisible leader progression velocity inside thundercloud is impossible, the presented results are concluded to be unique and significant.
Author
Lightning; Leaders (Meteorology); Optical Measurement; Interferometry

19990108621 State Univ. of New York, Dept. of Earth and Atmospheric Sciences, Albany, NY USA
Lightning in the Hurricane Core: Distribution and Significance
Molinari, John E., State Univ. of New York, USA; Black, Michael, National Oceanic and Atmospheric Administration, USA; Black, Peter, National Oceanic and Atmospheric Administration, USA; Idone, Vincent, State Univ. of New York, USA; 11th International Conference on Atmospheric Electricity; June 1999, pp. 400-403; In English; See also 19990108601
Contract(s)/Grant(s): NSF ATM-94-23229; No Copyright; Avail: CASI; A01, Hardcopy; A10, Microfiche

Observations of lightning in hurricanes have been made using the National Lightning Detection Network (NLDN). This paper will focus on the ground flashes detected in the vicinity of the eyewall of Hurricane Elena (1985). NILDN-based lightning locations are combined with high-frequency ground-based PPI radar images, infrared satellite images, airborne vertically pointing Doppler radar, and airborne flight-level wind data. The evidence shows that on-and-off periods of lightning in the hurricane core are related to whether or not elevated reflectivity occurs in the mixed-phase region, as has been found by many others. It is proposed that increases in vertical velocity and presumably buoyancy associated with elevated high reflectivity occur simultaneously with a shear instability in the eyewall. The results suggest that inner core lightning can serve as an early warning signal for significant impending changes in eyewall structure and hurricane intensity.
Author
Hurricanes; Lightning; Cloud-to-Ground Discharges; Vertical Air Currents

19990108622 Air Force Research Lab., Hanscom AFB, MA USA
Positive Leaders in Rocket-Triggered Lightning: Propagation Velocity from Measured Current and Ambient-Field Profile
Willett, J. C., Air Force Research Lab., USA; Davis, D. A., State Univ. of New York, USA; Laroche, P., Office National d'Etudes et de Recherches Aerospatiales, France; 11th International Conference on Atmospheric Electricity; June 1999, pp. 58-61; In English; See also 19990108601; No Copyright; Avail: CASI; A01, Hardcopy; A10, Microfiche

A recent field experiment has provided ambient-field profiles a few seconds before nine rocket-triggered lightning flashes. Currents flowing in the grounded triggering wires were recorded during most of the positive leaders that initiated these flashes. We present deductions of leader velocity from the measured data for one of these events, based on three simple electrostatic models. Deduced velocities range from 1-5 x 10(exp 4) m/s.
Author
Lightning; Leaders (Meteorology); Propagation Velocity; Mathematical Models

19990108623 Maryland Univ. Baltimore County, Joint Center for Earth Systems Technology, Catonsville, MD USA

A Multi-Platform Study of the February 10, 1998 Squall Line Event and TRMM Overpass of Southeast Texas

Wolff, David B., Maryland Univ. Baltimore County, USA; Orville, Richard E., Texas A&M Univ., USA; Zipser, Edward L., Texas A&M Univ., USA; 11th International Conference on Atmospheric Electricity; June 1999, pp. 404-407; In English; See also 19990108601; No Copyright; Avail: CASI; A01, Hardcopy; A10, Microfiche

A vigorous Mesoscale Convective System (MCS) propagated over southeast Texas in the morning and early afternoon hours of February 10, 1998. This was one of the first significant precipitation events that coincided with a Tropical Rainfall Measuring Mission (TRMM) overpass of the Houston WSR-88D radar/TRMM Ground Validation site. The first part of this study investigates the relation between vertical structure of reflectivity and National Lightning Detection Network (NLDN) cloud-to-ground lightning data for this event. Using standard TRMM products, including three-dimensional reflectivity (2A-55) and stratiform-convective rain type maps (2A-54), vertical profiles of reflectivity were constructed in areas where lightning occurred. The profiles were classified as either ”convective” or ”stratiform”, and as being associated with either ”positive” or ”negative” flashes. The resultant profiles are consistent with previous studies showing a well-defined bright band in the stratiform region, and significantly more intense and deeper echoes in the convective region. This study also investigates the relation between the TRMM Microwave Imager (TMI) measurements and lightning peak current and polarity. The TMI 85.5 GHz brightness temperatures show that approximately 42% of negative flashes occur in regions of depressed 85.5 GHz Polarization Corrected Temperature (PCT) is less than 200 K, while only half as many (21%) of the positive flashes were associated with PCT is less than 200 K.

Author

Cloud-to-Ground Discharges; Mesoscale Phenomena; Reflectance; Vertical Distribution; Data Correlation; Electric Charge

19990108624 Instituto Nacional de Pesquisas Espacias, Sao Jose dos Campos, Brazil

Cloud-to -Ground Lightning Flash Characteristics Obtained in the Southeastern Brazil Using the LPATS Technique and the New hybrid Lightning Location Methodology

Pinto, Osmar Jr., Instituto Nacional de Pesquisas Espacias, Brazil; Pinto, Iara R. C. A., Instituto Nacional de Pesquisas Espacias, Brazil; Diniz, Jose H., Companhia Energetica de Minas Gerais, Brazil; Carvalho, Andre M., Companhia Energetica de Minas Gerais, Brazil; Filho, Armando Cazetta, Companhia Energetica de Minas Gerais, Brazil; 11th International Conference on Atmospheric Electricity; June 1999, pp. 62-64; In English; See also 19990108601; No Copyright; Avail: CASI; A01, Hardcopy; A10, Microfiche

Cloud-to-ground lightning flash characteristics in the southeastern Brazil were determined during two months based on data obtained by two different lightning location systems. In December 1995, the data were obtained by a lightning positioning and tracking system (LPATS), version III, and in December 1997, by a new hybrid lightning location methodology combining time-of-arrival (LPATS) and direction-finding techniques (Impact sensors). The results indicate that the flash characteristics are quite different from 1995 to 1997, mainly for positive flashes. Although limited to the small data sample, we believe that the most differences are mainly due to differences in the systems. We suggest that other independent techniques should be used in order to evaluate the performance of such systems.

Author

Cloud-to-Cloud Discharges; Direction Finding; Tracking (Position)

19990108625 Central Research Inst. of Electric Power Industry, Tokyo, Japan

Conditions of Plasma Channels Required for Triggered Lightning

Miki, Megumu, Central Research Inst. of Electric Power Industry, Japan; Wada, Atsushi, Central Research Inst. of Electric Power Industry, Japan; Goshima, Hisashi, Central Research Inst. of Electric Power Industry, Japan; Shindo, Takatoshi, Central Research Inst. of Electric Power Industry, Japan; 11th International Conference on Atmospheric Electricity; June 1999, pp. 65-68; In English; See also 19990108601; No Copyright; Avail: CASI; A01, Hardcopy; A10, Microfiche

The conditions of a plasma channel required for the triggering of lightning have been estimated by comparison of observations of the actual lightning phenomenon and experiments on laser-produced plasma. The decay of the parameters of the plasma channel produced by the CO2 laser was measured with microwave interferometry. From our observations on multi stroke flashes, we estimated the state of the discharge channel required to guide upward lightning discharges. Our results show that the electrical conductivity of more than 2 S/m is required for the triggering of lightning.

Author

Laser Plasmas; Lightning; Channels; Interferometry; Electrical Resistivity

19990108626 Voeikov Main Geophysical Observatory, Leningrad, USSR

Calculation of Electric Field Strength Necessary for Altitude Discharge Above Thunderstorms

Morosov, V. N., Voeikov Main Geophysical Observatory, USSR; 11th International Conference on Atmospheric Electricity; June 1999, pp. 69-71; In English; See also 19990108601; No Copyright; Avail: CASI; A01, Hardcopy; A10, Microfiche

Electrical field produced by thunderstorm lightning at high altitude atmosphere is calculated by solutions of the non-stationary equation of continuity of the electrical charge and Poisson's equation. Magnitudes and electric field strength of the electrical cloud charge necessary for high altitude atmosphere breakdown and discharges via the run away electron process are estimated.

Author

Electric Charge; Electric Field Strength; Lightning; Mathematical Models

19990108627 Instituto Nacional de Pesquisas Espacias, Sao Jose dos Campos, Brazil

Cloud-to-Ground Lightning Activity in Mesoscale Convective Complexes in Southeastern Brazil in 1993-94

Pinto, lara R. C. A., Instituto Nacional de Pesquisas Espacias, Brazil; Pinto, Osmar, Jr., Instituto Nacional de Pesquisas Espacias, Brazil; Conforte, Jorge C., Instituto Nacional de Pesquisas Espacias, Brazil; Diniz, Jose H., Companhia Energetica de Minas Gerais, Brazil; Carvalho, Andre M., Companhia Energetica de Minas Gerais, Brazil; Filho, Armando Cazetta, Companhia Energetica de Minas Gerais, Brazil; 11th International Conference on Atmospheric Electricity; June 1999, pp. 408-411; In English; See also 19990108601

Contract(s)/Grant(s): FAPESP Proj. 1995/5266-9; FAPESP Proj. 1996/2239-3; No Copyright; Avail: CASI; A01, Hardcopy; A10, Microfiche

The characteristics of cloud-to-ground lightning flashes in association with Mesoscale Convective Complexes (MCC) which occurred in southeastern Brazil in the years of 1993 and 1994 were investigated. During this period 4 MCCs were identified. However, only 1 of 4 MCCs occurring in 1993-94 spent their entire life cycle within the 50% detection efficiency region. It had a duration of 15 hours and at time of maximum extent its area was approximately 110,000 sq km. The characteristics of cloud-to-ground flashes during their major life-cycle phases were studied in terms of the hourly flash rate, polarity, multiplicity and average peak current intensity.

Author

Cloud-to-Ground Discharges; Mesoscale Phenomena; Polarity; Electric Charge

19990108628 Texas A&M Univ., Dept. of Meteorology, College Station, TX USA

Lightning Ground Flash Measurements Over the Contiguous USA: A Ten-Year Summary 1989-1998

Orville, Richard E., Texas A&M Univ., USA; Huffines, Gary R., Texas A&M Univ., USA; 11th International Conference on Atmospheric Electricity; June 1999, pp. 412-415; In English; See also 19990108601

Contract(s)/Grant(s): NA87WA0063; NSF ATM-98-06189; No Copyright; Avail: CASI; A01, Hardcopy; A10, Microfiche

The National Lightning Detection Network (NLDN) has recorded cloud-to-ground lightning characteristics for ten years over the contiguous USA producing a database of 216 million flashes. What have we learned? Results are a combination of natural observations free of instrumentation effects and biased observations affected by the characteristics of the network. The valid natural observations appear to be 1) maximum cloud-to-ground negative flash densities in central Florida in most years, but moving to the upper Midwest during high precipitation years, 2) maximum cloud-to-ground positive flash densities in the Midwest, 3) maximum percentage positive lightning in the upper Midwest and along the West Coast, 4) highest median negative currents in the Southeast, 5) highest median positive currents in the upper Midwest and the lowest in Louisiana and Florida. The biased observations include, apparently, 1) low median negative and positive peak currents in the western Carolinas resulting from close (is less than 100 km) spacing of the sensors and 2) high flash negative multiplicity in the same region for the same reason.

Author

USA; Cloud-to-Ground Discharges; Detection; Data Correlation; Direction Finding

19990108629 Los Alamos National Lab., Atmospheric and Climate Sciences Group, NM USA

On the Temporal Evolution of Red Sprites, Runaway Theory Versus Data

Yukhimuk, V., Los Alamos National Lab., USA; Roussel–Dupre, R. A., Los Alamos National Lab., USA; Symbalisty, E. M. D., Los Alamos National Lab., USA; 11th International Conference on Atmospheric Electricity; June 1999, pp. 72-75; In English; See also 19990108601

Contract(s)/Grant(s): NRA-95-11-ITM-029; No Copyright; Avail: CASI; A01, Hardcopy; A10, Microfiche

The results of numerical simulations of red sprite discharges, namely the temporal evolutions of optical emissions, are presented and compared with observations. The simulations are done using the recently recalculated runaway avalanche rates.

The temporal evolution of these simulations is in good agreement with ground-based photometer and CCD TV camera observations of red sprites. Our model naturally explains the ”hairline” of red sprites as a boundary between the region where the intensity of optical emissions associated with runaway breakdown has a maximum and the region where the intensity of optical emissions caused by conventional breakdown and ambient electron heating has a maximum. We also present for the first time simulations of red sprites with a daytime conductivity profile.
Author
Electric Discharges; Upper Atmosphere; Computerized Simulation; Light Emission; Plasma Heating; Electric Fields

19990108631 York Univ., Center for Research in Earth and Space Science, Toronto, Ontario Canada
Satellite Detection of Sprites and Other Middle Atmosphere Storm Effects
Clodman, Stephen, York Univ., Canada; 11th International Conference on Atmospheric Electricity; June 1999, pp. 80-83; In English; See also 19990108601; No Copyright; Avail: CASI; A01, Hardcopy; A10, Microfiche

Satellite measurements of sprites, jets, and elves, and other middle atmosphere storm effects, would be of great scientific value. These phenomena could be found anywhere in the world that they occur. It would be possible to obtain data not available any other way. One might even be able to detect some of these phenomena in daytime. There are significant problems to overcome: signal to noise ratio limitations, false indications such as from lightning, the need to detect a sufficient number of targets, and the task of obtaining and analyzing a large quantity of data. Still, it can be done, and in several ways, each having advantages. The instrument may point straight down, or obliquely, or toward the earth’s limb. The wavelengths sensed might range from ultraviolet to far infrared. Also, there are possible preliminary studies which could help prepare for a satellite mission.
Author
Middle Atmosphere; Satellite Observation; Electric Discharges; Atmospheric Effects

19990108632 Miyagi Polytechnic Coll., Tsukidate, Japan
Vertical Profile of Space Charge Near Ground Surface Estimated with Corona Current
Narita, K., Miyagi Polytechnic Coll., Japan; Goto, Y., Tohoku Gakuin Univ., Japan; Takeuchi, N., Tohoku Univ., Japan; Honma, N., Tohoku Electric Power Co., Inc., Japan; Suzuki, N., Tohoku Electric Power Co., Inc., Japan; 11th International Conference on Atmospheric Electricity; June 1999, pp. 416-419; In English; See also 19990108601; No Copyright; Avail: CASI; A01, Hardcopy; A10, Microfiche

To investigate a winter thunderstorm, we have been acquiring data on the corona currents through the needle point electrodes from the 1972 winter season at the west coast of Japan. We prepare three needle electrodes, and they are installed at the different altitudes of 4.5m, 8.5m and 21m. The corona current signals are terminated at the pen-recorder which is controlled by the personal computer, and collected in the Hard Disk Unit. The corona currents at lower altitude are changed mainly within the same minus polarity, on the other hand, that current at 21m height are oscillated to both polarities. That’s reason will be contributed by the space charge near the ground surface.
Author
Winter; Thunderstorms; Japan; Space Charge; Electric Corona; Vertical Distribution

19990108633 FMA Research, Inc., Fort Collins, CO USA
Characteristics of Thunderstorms and Lightning Flashes Which Produce Mesospheric Transient Luminous Events
Lyons, W. A., FMA Research, Inc., USA; Nelson, T. E., FMA Research, Inc., USA; Armstrong, R. A., Mission Research Corp., USA; Williams, E. R., Massachusetts Inst. of Tech., USA; Suszcynsky, D. M., Los Alamos National Lab., USA; Strabley, R., Los Alamos National Lab., USA; Taylor, M., Utah State Univ., USA; Gardner, L., Utah State Univ., USA; 11th International Conference on Atmospheric Electricity; June 1999, pp. 84-87; In English; See also 19990108601; No Copyright; Avail: CASI; A01, Hardcopy; A10, Microfiche

A six year record of optical observations of lightning-induced mesospheric transient luminous events (TLEs) is available from the Yucca Ridge Field Station (YRFS) near Ft. Collins, CO. Climatological analyses reveal sprites and elves occur in a variety of convective storm types, but principally mesoscale convective systems (MCSs) and squall lines. Severe supercell storms rarely produce TLEs, except during their dissipating stage. Few TLEs are observed during storms with radar echo areas is less than 7,500 sq km. Above this size there is a modest correlation with radar areal coverage. A typical High Plains storm produces 45 TLEs over a 143 interval. Sprites and most elves are associated with +CGs. The probability of a TLE increases with peak current. In six storms, 5.1% of +CGs produced TLEs, the number increasing to 32% of +CGs with is greater than 75 kA and 52% of +CGs with is greater than 100 kA peak current.
Author
Thunderstorms; Mesosphere; Electric Discharges; Lightning; Visual Observation

19990108634 Niagara Univ., New York, NY USA

Optical Observations of Lightning in Northern India, Himalayan Mountain Countries and Tibet

Boeck, W. L., Niagara Univ., USA; Mach, D., Global Hydrology and Climate Center, USA; Goodman, S. J., Global Hydrology and Climate Center, USA; Christian, H. J., Jr., Global Hydrology and Climate Center, USA; 11th International Conference on Atmospheric Electricity; June 1999, pp. 420-423; In English; See also 19990108601; No Copyright; Avail: CASI; A01, Hardcopy; A10, Microfiche

This study summarizes the results of an analysis of data from the LIS instrument on the TRMM platform. The data for the Indian summer monsoon season is examined to study the seasonal patterns of the geographic and diurnal distribution of lightning storms. The storms on the Tibetan plateau show a single large diurnal peak at about 1400 local solar time. A region of Northern Pakistan has two storm peaks at 0200 and 1400 local solar time. The morning peak is half the magnitude of the afternoon peak. The region south of the Himalayan Mountains has a combined diurnal cycle in location and time of storm occurrence.
Author

Diurnal Variations; Himalayas; Lightning; Visual Observation

19990108635 New Mexico Inst. of Mining and Technology, Socorro, NM USA

Parameterization of Sprites and their Parent Discharges

Stanley, M., New Mexico Inst. of Mining and Technology, USA; Krehbiel, P., New Mexico Inst. of Mining and Technology, USA; Brook, M., New Mexico Inst. of Mining and Technology, USA; Rison, W., New Mexico Inst. of Mining and Technology, USA; Moore, C. B., New Mexico Inst. of Mining and Technology, USA; Thomas, R., New Mexico Inst. of Mining and Technology, USA; 11th International Conference on Atmospheric Electricity; June 1999, pp. 88-91; In English; See also 19990108601; No Copyright; Avail: CASI; A01, Hardcopy; A10, Microfiche

Analysis of a close sprite-producing positive cloud-to-ground discharge (CG) indicated that it had a total charge moment change of 460-740 C.km. Analysis of high speed video observations have determined that the initiation altitude of sprites is within the altitude range of 70-85 km with a mean of approx. 75 km. These results are consistent with a conventional breakdown mechanism for sprite initiation. Once initiated, corona streamer characteristics are clearly visible in developing sprites.
Author

Cloud-to-Ground Discharges; Parameterization; Electric Fields; Electric Corona

19990108636 Mission Research Corp., Nashua, NH USA

Ionization in the Middle Atmosphere Associated with Thunderstorms-Multi-Color Photometric Analysis of Sprite Emissions

Armstrong, R. A., Mission Research Corp., USA; Suszcynsky, D. M., Los Alamos National Lab., USA; Strabley, R., Los Alamos National Lab., USA; Lyons, W. A., FMA Research, Inc., USA; Nelson, T. E., FMA Research, Inc., USA; 11th International Conference on Atmospheric Electricity; June 1999, pp. 92-95; In English; See also 19990108601; No Copyright; Avail: CASI; A01, Hardcopy; A10, Microfiche

Observations of transient luminous events (TLEs) above mesoscale convective systems (MCSs) have been a topic of much research in the last several years. Early VLF and photometric data on these events suggested the presence of substantial ionization associated with their initiation. Recent time-resolved multi-color photometric data obtained on one class of TLEs called sprites, has confirmed an impulsive ionization at the sprite initiation. Although more data is required to quantify the ionization levels and initiation mechanisms, analysis of this data suggests that for some events, ionization rates are sufficient to achieve electron densities approaching 10(exp 5)/cu cm at approx. 65 km. Data has also been obtained which suggests that some events exhibit little, if any, ionization, indicating that more than one operative mechanism is responsible for the phenomena. We present the recent data along with the analysis supporting the level of ionization. Plans for future measurements to quantify the spatial behavior of the ionization are also presented.
Author

Atmospheric Ionization; Thunderstorms; Middle Atmosphere; Electric Discharges

19990108637 University of Electro-Communications, Dept. of Electronic Engineering, Tokyo, Japan

EM Radiation Associated with Sprites?

Otsuyama, T., University of Electro-Communications, Japan; Hobara, Y., University of Electro-Communications, Japan; Hayakawa, M., University of Electro-Communications, Japan; 11th International Conference on Atmospheric Electricity; June 1999, pp. 96-98; In English; See also 19990108601; No Copyright; Avail: CASI; A01, Hardcopy; A10, Microfiche

The mesospheric optical flashes (sprites) are associated mostly with large positive cloud-to-ground discharges (+CG). In addition, transient events in ELF range are observed often in association with sprites. Several theoretical studies including the

numerical computations have been performed to explain the optical emission, but the EM (electromagnetic) radiation during the sprites emission has not been studied intensively. In this paper we try to derive the generation mechanism of the EM radiation during the process of the sprites in VLF/ELF range using numerical computations simulating the sprite triggering discharges. As a result, considerably large amplitude of the EM fields from the triggering discharge is obtained particularly in the ELF range, which is possibly connected with the source of the ELF transient observed for distances away from the sprites.
Author
Electromagnetic Radiation; Light Emission; Mesosphere; Cloud-to-Ground Discharges; Mathematical Models

19990108638 Gifu Univ., Dept. of Electrical and Electronic Engineering, Japan
Propagation Characteristics of Return Strokes and M-Components in Florida Rocket-Triggered Lightning
Wang, D., Gifu Univ., Japan; Ito, T., Gifu Univ., Japan; Takagi, N., Gifu Univ., Japan; Watanabe, T., Gifu Univ., Japan; Rakov, V. A., Florida Univ., USA; Uman, M. A., Florida Univ., USA; 11th International Conference on Atmospheric Electricity; June 1999, pp. 99-102; In English; See also 19990108601; No Copyright; Avail: CASI; A01, Hardcopy; A10, Microfiche

To study the propagation characteristics of return strokes and M-components, a Fourier Transform analysis has been performed on the light signals of two return strokes and two M-components recorded using a high speed digital imaging system from flashes triggered at Camp Blanding, Florida in the summer of 1997. For the two return strokes, the light signals from the higher channel sections exhibit larger phase differences relative to the signal from the channel bottom over all frequencies investigated, from below 1 kHz to more than 500 kHz. This observation suggests that all frequency waves are moving upward. The waves of different frequencies propagate at different phase velocities with higher frequency waves usually having larger phase velocities. No apparent relation has been noted between the phase velocities and the channel heights although the signals from different heights indeed show different phase velocities. The group velocities show a tendency to decrease at the higher channel sections. For the two M-components, one shows an upward propagation above 38 m, but a seemingly downward propagation at the channel bottom. The other, with a better spatial resolution, shows much more complicated phase differences at the channel bottom, so that we can not determine even the direction of its propagation.
Author
Lightning; Phase Velocity; Propagation Velocity; Wave Propagation; Light Transmission; Optical Measurement

19990108639 High Mountain Geophysical Inst., Nalchik, USSR
Thunderstorm Development in Convective Clouds
Adzhiev, A. Kh, High Mountain Geophysical Inst., USSR; Kalov, R. Kh., High Mountain Geophysical Inst., USSR; Sizhahev, S. M., High Mountain Geophysical Inst., USSR; Agzagova, M. B., High Mountain Geophysical Inst., USSR; Kumykov, Kh. K., High Mountain Geophysical Inst., USSR; 11th International Conference on Atmospheric Electricity; June 1999, pp. 424-427; In English; See also 19990108601; No Copyright; Avail: CASI; A01, Hardcopy; A10, Microfiche

ABSTRACT: The thunderstorm development in convective clouds is the important part in the thunder cloud theory. That's why it is necessary to make the complex investigation of the development of all electrical and non-electrical parameters of convective cloud. In this work we used the active-passive radiolocation of thunderstorms in cm(exp -1), dm-bands of wavelengths allowing us to receive the qualitatively new information on electrical state of cloud during its development. The received data allow to follow the change character of pulse-time characteristics of thunder activity in convective clouds at the natural development and seeding. It is shown that the reception of the non-thermal radio-emission from convective clouds in USW- bands of wavelengths allows to warn of the thunderstorm approaching long before the appearance of thunder discharges. Our studies showed that at the certain stage of development of convective cloud, when its upper boundary reaches the level of natural crystallization of cloud droplets, the pre-thunder electromagnetic radio-emission (EME) appears in it spontaneously. When the convective cloud approaches to the upper boundary of radar echo at the -18...-35 C level and radar reflectivity of 6- 10-8 cm-' at 3,2 cm wavelength the transition of the cloud from pre-thunder state into the state of thunder activity occurs. The detailed investigation of change tendency of amplitude-frequency characteristics of ERE in the intervals between the lightning discharges was made. This investigation showed that the pulse duration of radio-emission increases with the approaching of the next lightning discharge. It was shown that the thunderstorm development in convective clouds has the gradual character. The increase of EME packets of lightning discharges, the frequency of appearance and time of existence of signals reflected from the ionized channels at the lightning discharge are the evidence of it.
Author
Convection Clouds; Thunderstorms; Cumulonimbus Clouds; Electrical Measurement; Electrification

19990108640 Lanzhou Inst. of Plateau Atmospheric Physics, China

An Analysis of Natural Lightning Discharge to the Ground in Chinese Inland Plateau

Qie, X., Lanzhou Inst. of Plateau Atmospheric Physics, China; Liu, X., Lanzhou Inst. of Plateau Atmospheric Physics, China; Zhang, G., Lanzhou Inst. of Plateau Atmospheric Physics, China; Yu, Y., Lanzhou Inst. of Plateau Atmospheric Physics, China; Guo, C., Shanghai Meteorological Inst., China; Wang, D., Gifu Univ., Japan; Watanabe, T., Gifu Univ., Japan; Takagi, N., Gifu Univ., Japan; Kawasaki, Z., Osaka Univ., Japan; Ushio, T., Osaka Univ., Japan; Nakano, M., Toyota Coll. of Technology, Japan; Nakamura, K., Nagoya Inst. of Tech., Japan; 11th International Conference on Atmospheric Electricity; June 1999, pp. 103-106; In English; See also 19990108601; No Copyright; Avail: CASI; A01, Hardcopy; A10, Microfiche

In this paper, we present some general features of natural ground lightning discharges in the Chinese inland plateau by using the data from 5-station slow antenna system synchronized by GPS with 1 microsecond time resolution. The result is shown that the altitude of the neutralized negative charge is between 2.7 - 5.4 km above the ground, while that of neutralized positive charge is at about 2.0 km above the ground. The K-changes were initiated from the negative charge region in the middle part of the cloud and propagated downward to the positive charge region at the bottom of the cloud with an average speed of 1.5 x 10(exp 7) m/s. Author

Cloud-to-Ground Discharges; Thunderstorms; Intracloud Discharges

19990108641 Ibadan Univ., Physics Dept., Nigeria

The Characteristics of Positive Ground Discharges of Tropical Thunderstorms at Ibadan, Nigeria

Oladiran, E. O., Ibadan Univ., Nigeria; Akpan, U. E., Uyo Univ., Nigeria; Numphas, E. F., Federal Univ. of Agriculture, Nigeria; Israelsson, S., Uppsala Univ., Sweden; 11th International Conference on Atmospheric Electricity; June 1999, pp. 428-431; In English; See also 19990108601; No Copyright; Avail: CASI; A01, Hardcopy; A10, Microfiche

Positive ground lightning discharges were continuously recorded over a period of three years at Ibadan to supplement earlier composite records from 1987 by adapting the earlier design of Oladiran, et al. (1988a) using the shape of the radiation field signatures and the frequency components of positive discharges (Oladiran and Israelsson, 1990). We recorded a 92% discrimination between negative and positive ground flashes. The positive ground flashes were recorded at vlf and 17.3 kHz, 3dB attenuation and yielded an average 13 and 11.6% ratios for (+CG)/(-CG) respectively. Compared to our results of 1988, the flash-rate characteristics for positive ground flashes is not significantly different from those of negative ground flashes and it does not show any seasonal preference. This leads to the conclusion that the occurrence of positive and negative ground flashes depends only on the cloud charge structure, its dynamics and the ground conditions.
Author

Tropical Regions; Thunderstorms; Cloud-to-Ground Discharges; Nigeria; Electric Charge

19990108642 Lanzhou Inst. of Plateau Atmospheric Physics, China

Broad Band Interferometric Measurement of Rocket Triggered Lightning

Dong, Wansheng, Lanzhou Inst. of Plateau Atmospheric Physics, China; Liu, Xinsheng, Lanzhou Inst. of Plateau Atmospheric Physics, China; Qie, Xiushu, Lanzhou Inst. of Plateau Atmospheric Physics, China; 11th International Conference on Atmospheric Electricity; June 1999, pp. 107-110; In English; See also 19990108601; No Copyright; Avail: CASI; A01, Hardcopy; A10, Microfiche

A broad band interferometer for locating lightning radiation in two dimensions has been manufactured and evaluated during the rocket triggered lightning experiment in China in 1997. We have obtained several data sets of upward leaders for both negative and positive polarity during experiments. Results showed that the altitude triggered lightning were initiated by bi-directional leaders. The onset of downward moving positive leader was prior to upward moving negative leader in an altitude triggered lightning under positive charged cloud base. A number of branches occurred during negative leader propagation. The waveforms of broad band electromagnetic pulses can be divided into two categories: isolated pulses and serial pulses. Isolated pulses refer to radiation whose duration were less than 35ns, serial pulses refer to radiation with longer duration. For triggered lightning, the numbers of serial pulses were dominant to isolated ones. Spectral analyses of all these pulses showed that the average energy spectral densities(ESDs) of the serial pulses were wider, in entire frequency range, the average ESDs of the isolated pulses were at lower frequencies. The time intervals between successive electromagnetic pulses were from 65us to 677us, with a mean of 106.4us. The results of broad band interferometric observations agreed well with the video observation.
Author

Interferometry; Lightning; Electromagnetic Pulses; Wave Propagation

19990108643 Russian Federal Nuclear Center, Russia

About the Positive Leader Propagation Mechanism

Ivanovsky, A. V., Russian Federal Nuclear Center, Russia; 11th International Conference on Atmospheric Electricity; June 1999, pp. 111-114; In English; See also 19990108601; No Copyright; Avail: CASI; A01, Hardcopy; A10, Microfiche

The model of the leader breakdown of air in which the channel is formed by warming-up of the streamer track in the streamer zone field is discussed. The previous streamer models is expanded for the description of the charged particle recombination. The mathematical model of the streamer track heating is created. It is obtained that only the streamers with specific charge and corresponding propagation velocity create the channel. The velocity of these streamers determines the velocity of the leader discharge in steady-state conditions. The cloud potential dependence of the leader velocity is determined.

Author

Leaders (Meteorology); Wave Propagation; Electromagnetic Wave Transmission; Mathematical Models; Gas Dissociation; Propagation Velocity

19990108644 New Mexico Inst. of Mining and Technology, Socorro, NM USA

3-Dimensional Lightning and Dual-Polarization Observations of Thunderstorms in Central New Mexico

Rison, W., New Mexico Inst. of Mining and Technology, USA; Scott, R., New Mexico Inst. of Mining and Technology, USA; Thomas, R. J., New Mexico Inst. of Mining and Technology, USA; Krehbiel, P. R., New Mexico Inst. of Mining and Technology, USA; Hamlin, T., New Mexico Inst. of Mining and Technology, USA; Harlin, J., New Mexico Inst. of Mining and Technology, USA; 11th International Conference on Atmospheric Electricity; June 1999, pp. 432-435; In English; See also 19990108601; No Copyright; Avail: CASI; A01, Hardcopy; A10, Microfiche

Following its initial operation in Oklahoma, Tech's 3-dimensional Lightning Mapping System (LMS) was set up in August of 1998 over a 60-km diameter area around Langmuir Laboratory and the New Mexico Tech campus in central New Mexico. Preliminary results show that lightning activity in New Mexico storms has a simpler structure and smaller extent than in the larger Great Plains storms. Lightning discharges are also much less frequent in a storm, compared to the nearly continuous activity observed in Oklahoma. Intracloud (IC) lightning often has only a vertical channel but in more developed storms shows a clear bilevel structure, undoubtedly associated with the main negative and upper positive charge regions of the storm. These results agree with previous observations both in New Mexico and Florida. Cloud-to-ground (CG) discharges often show considerable activity in a third region below the negative charge level, presumably associated with lower positive charge. The overall lightning activity exhibits a clear trilevel structure, consistent with the tripole model of storm electrification, and appears to map out the basic charge structure of the storm. Similar structures have been observed in the more complex Oklahoma storms. A few negative CG discharges originate in the main negative charge region, propagate up through the upper positive charge region, and then horizontally out of the upper positive region before going to ground. Narrow positive bipolar (+BP) events, located by a Los Alamos sferics network (Smith et al., this conference) were also detected by the LMS. All the +BP events detected were the first RF events in an otherwise ordinary IC discharge. The RF power of the +BP events were 20 to 30 dB stronger than the RF power from any other part of a lightning discharge. A few isolated events (RF radiation lasting less than 100 microseconds) were observed.

Author

Lightning; Polarization (Charge Separation); Bipolarity; Atmospherics; New Mexico; Thunderstorms

19990108645 Gifu Univ., Dept. of Electrical and Electronic Engineering, Japan

Properties of Leader Development in Altitude-Triggered Lightning

Chen, M., Gifu Univ., Japan; Watanabe, T., Gifu Univ., Japan; Takagi, N., Gifu Univ., Japan; Wang, D., Gifu Univ., Japan; Liu, X., Lanzhou Inst. of Plateau Atmospheric Physics, China; Zhang, Y., Lanzhou Inst. of Plateau Atmospheric Physics, China; Zhou, L., Guangzhou Inst. of Electrical Power Test, China; Zhong, D., Guangzhou Inst. of Electrical Power Test, China; 11th International Conference on Atmospheric Electricity; June 1999, pp. 115-118; In English; See also 19990108601; No Copyright; Avail: CASI; A01, Hardcopy; A10, Microfiche

Simultaneous measurements of two-station electric fields and space- and time-resolved light signals (sampling time 0.1 u s) made for 5 negative altitude-triggered lightning flashes, in Guangzhou, China, during the summer of 1998, are analyzed. Results show that these 5 flashes have similar main chronological sequence of events, including a bidirectional leader initiated from extremities of the floating wire with the onset of the upper positive leader prior to that of the lower negative stepped leader by just 20-30 u s, followed by a mini-return stroke occurring several milliseconds later. The mini-return stroke (speed 1-2 x 10 (exp 8) m/s) rapidly weakens down when it reaches the lower end of the wire, and a few microseconds later a bright discharge process (speed 1.5-5.4 x 10 (exp 7)m/s) appears from the upper end of the wire which becomes optically undetectable after extending forward

(upward) several hundred meters. Just after the upper bright discharge process weakens down, another bidirectional leader starts from the lower end of the wire with the upward speed being 3-10 x 10(exp 5)m/s and downward one 2-2.6 x 10(exp 5)m/s.
Author
Lightning; Leaders (Meteorology); Propagation Velocity

19990108646 Colorado State Univ., Dept. of Atmospheric Science, Fort Collins, CO USA
Characteristics of Cloud-to-Ground Lightning in the Contiguous U.S. from 1995-1997
Zajac, Bard A., Colorado State Univ., USA; Rutledge, Steven A., Colorado State Univ., USA; Carey, Lawrence A., Colorado State Univ., USA; 11th International Conference on Atmospheric Electricity; June 1999, pp. 436-439; In English; See also 19990108601; No Copyright; Avail: CASI; A01, Hardcopy; A10, Microfiche

Convective storms play an important role in our society. In addition to producing beneficial rainfall, convective storms can also produce flooding, severe weather (e.g., tornadoes, hail, strong winds), and deadly lightning. Knowledge of the distribution of these weather phenomena in space and time can be used to 1) plan for the beneficial and destructive effects of convective storms, 2) understand what physical processes control the frequency of occurrence of convective storms, 3) forecast for convective storms, and 4) verify output from numerical models which resolve the effects of convective storms. For these reasons, climatologies of precipitation, flash floods, tornadoes, hail and strong winds, cloud-to-ground lightning, and thunder have been developed. These climatologies have documented significant spatial, annual, and diurnal variations in convective activity over the contiguous U.S. Interestingly, the diurnal variations in cloud-to-ground (CG) lightning activity have not been documented over the contiguous U.S. For this reason, the first goal of this study is to extend the national climatology of cloud-to-ground lightning and document the spatial, annual, and diurnal variations in CG lightning activity over the contiguous U.S. This study of CG lightning activity in the contiguous U.S. from 1995-97 compliments climatologies of convective activity in the contiguous U.S. and helps refine our knowledge of convective storms. The second goal of this study is to document the spatial, annual, and diurnal variations of positive cloud-to-ground lightning activity in the contiguous U.S. The documentation of these variations from 1995-97 provides a large-scale context for storm-scale studies of positive CG lightning. Case studies of convective storms have shown that positive CG lightning tends to be produced by: 1) dissipating non-severe thunderstorms, 2) dissipating severe storms, 3) convective and stratiform regions of mesoscale convective systems, and 4) positive strike dominated storms. The production of positive cloud-to-ground lightning is examined in greater detail over two case study areas located in the north-central U.S. (Sioux Falls, SD; KFSD) and along the Gulf Coast (Ft. Rucker, AL; KEOX). These two case study areas were chosen for specific reasons. The KFSD area was chosen because it is located within a region characterized by a high percentage of positive polarity lightning and by high positive peak current values. The KEOX area was chosen because it is located within a region where diurnally-forced convection tends to occur during the warm season and synoptically-forced convection tends to occur during the cold season. Positive CG lightning activity over the KEOX area is compared between the warm and cold seasons. In both case studies, annual and diurnal variations in positive CG lightning activity are documented from 1995-97. Morphological and electrical characteristics of convective events which produce positive lightning over the two case study areas during 1996 are identified by comparing maps of low-level radar reflectivity with maps of CG strike locations.
Author
Cloud-to-Ground Discharges; Forced Convection; Diurnal Variations; Annual Variations; Thunderstorms; USA

19990108647 Uppsala Univ., Inst. of High Voltage Research, Sweden
Peak Radiation Fields of Lightning Return Strokes over Finitely Conducting Ground
Cooray, Vernon, Uppsala Univ., Sweden; 11th International Conference on Atmospheric Electricity; June 1999, pp. 119-122; In English; See also 19990108601; No Copyright; Avail: CASI; A01, Hardcopy; A10, Microfiche

This paper elucidates the propagation effects on the lightning generated electric fields. A simple procedure that can be used to predict the propagation effects is outlined together with its experimental confirmation. This procedure is used to analyze the propagation effects on the radiation fields of negative first return strokes, positive first return strokes and subsequent return strokes in triggered lightning flashes. From the results empirical equations that can be used to correct for the propagation effects are extracted. The results show that the propagation effects may differ in negative and positive return strokes and that the data from triggered lightning flashes should be applied with caution in correcting for the propagation effects of natural lightning flashes.
Author
Radiation Distribution; Lightning; Wave Propagation; Electric Fields

19990108648 Texas A&M Univ., Dept. of Meteorology, College Station, TX USA
Lightning and 85-GHz MCSs in the Global Tropics
Toracinta, E. Richard, Texas A&M Univ., USA; Zipser, E. J., Utah Univ., USA; 11th International Conference on Atmospheric

Electricity; June 1999, pp. 440-443; In English; See also 19990108601
Contract(s)/Grant(s): NAG5-4699; No Copyright; Avail: CASI; A01, Hardcopy; A10, Microfiche

Numerous observations of tropical convection show that tropical continental mesoscale convective systems (MCSs) are much more prolific lightning producers than their oceanic counterparts. Satellite-based climatologies using 85-GHz passive microwave ice-scattering signatures from the Special Sensor Microwave/Imager (SSM/I) indicate that MCSs of various size and intensity are found throughout the global tropics. In contrast, global lightning distributions show a strong land bias with an order of magnitude difference between land and ocean lightning. This is somewhat puzzling, since 85-GHz ice-scattering and the charge separation processes that lead to lightning are both thought to depend upon the existence of large graupel particles. The fact that low 85-GHz brightness temperatures are observed in tropical oceanic MCSs containing virtually no lightning leads to the postulate that tropical oceanic and tropical continental MCSs have fundamentally different hydrometeor profiles through the mixed phase region of the cloud (0 C is less than or equal to T is less than or equal to 20 C). Until recently, validation of this postulate has not been practicable on a global scale. Recent deployment of the Tropical Rainfall Measuring Mission (TRMM) satellite presents a unique opportunity for MCS studies. The multi-sensor instrument ensemble aboard TRMM, including a multi-channel microwave radiometer, the Lightning Imaging Sensor (LIS), and the first space-borne radar, facilitates high-resolution case studies of MCS structure throughout the global tropics. An important precursor, however, is to better understand the distribution of MCSs and lightning in the tropics. With that objective in mind, this research undertakes a systematic comparison of 85-GHz-defined MCSs and lightning over the global tropics for a full year, as an initial step toward quantifying differences between land and ocean convective systems.

Derived from text

Lightning; Tropical Regions; Mesoscale Phenomena; Multisensor Applications; Convection Cells; Polarization (Charge Separation)

19990108649 Kiev Polytechnic, Dept. of High Voltage Engineering and Electrophysics, USSR

Return-Stroke Current Modeling of Lightning Striking a Tall Tower Accounting for Reflections Within the Growing Channel and for Upward-Connecting Discharges

Shostak, V., Kiev Polytechnic, USSR; Janischewskyj, W., Toronto Univ., Canada; Hussein, A. M., Toronto Univ., Canada; Chang, J. –S., McMaster Univ., Canada; Kordi, B., Toronto Univ., Canada; 11th International Conference on Atmospheric Electricity; June 1999, pp. 123-126; In English; See also 19990108601; No Copyright; Avail: CASI; A01, Hardcopy; A10, Microfiche

Results of return stroke (RS) current simulation in case of lightning strikes to a tall tower are presented. Calculations are performed on the basis of the new extended version of the modified transmission line (MTL) model which takes into account: (1) reflections that occur within the continuously growing RS channel, and (2) the situation of RS channel initiation above the top of the tower (when an upward-connecting discharge is present). The results of modeling are compared to those obtained using the previously developed MTL model for strikes to elevated objects, and to experimental observations made at the 553-m tall CN Tower in Toronto.

Author

Electric Current; Mathematical Models; Lightning; Computerized Simulation

19990108650 National Severe Storms Lab., Norman, OK USA

Electric Field Profiles and Lightning in Storms with Frequent Positive Cloud-to-Ground Lightning

MacGorman, D. R., National Severe Storms Lab., USA; Rust, W. D., National Severe Storms Lab., USA; Krehbiel, P., New Mexico Inst. of Mining and Technology, USA; Thomas, R., New Mexico Inst. of Mining and Technology, USA; Rison, W., New Mexico Inst. of Mining and Technology, USA; Lockwood, M., Oklahoma Univ., USA; Beasley, W., Oklahoma Univ., USA; Eack, K., Los Alamos National Lab., USA; 11th International Conference on Atmospheric Electricity; June 1999, pp. 444-447; In English; See also 19990108601

Contract(s)/Grant(s): NSF ATM-98-07179; No Copyright; Avail: CASI; A01, Hardcopy; A10, Microfiche

Eight balloon soundings of the electric field have been obtained in severe storms in which the majority of ground flashes lowered positive charge to ground, instead of the more usual negative charge. The majority of the soundings have data gaps. These storms occurred in Oklahoma, Texas, and Kansas on four days. Cloud-to-ground lightning data from the U.S. National Lightning Detection Network indicate that, in each of two severe storms on one day, the dominant polarity of ground flashes switched multiple times during the storm. On all other days, the majority of ground flashes were positive continually throughout most of the lifetime of the storm. Preliminary analyses of the soundings are compared with published soundings from storms that produced primarily negative ground flashes. Though some features of several of the electric field profiles appear different from those obtained from storms dominated by negative ground flashes, the electric field profiles in storms dominated by positive ground flashes did not have a single, clear consistent pattern. Lightning also was mapped in three dimensions for one of the isolated storms

in which a sounding was obtained and for several other severe storms that occurred in central Oklahoma during field operations. Cloud flash rates often were more than an order of magnitude larger than ground flash rates, particularly during periods when the storms produced severe weather.
Author
Lightning; Cloud-to-Ground Discharges; Balloon Sounding; Electric Fields; Thunderstorms; Electric Charge; Charge Distribution

19990108652 Institute of Tropical Meteorology, Poona, India
Thunderstorm Activity over Land and Sea Regions of India and the Sensitivity of Wet-Bulb and Sea Surface Temperatures to their Occurrence
Manohar, G. K., Institute of Tropical Meteorology, India; Kandalgaonkar, S. S., Institute of Tropical Meteorology, India; Tinmaker, M. I. R., Institute of Tropical Meteorology, India; 11th International Conference on Atmospheric Electricity; June 1999, pp. 448-451; In English; See also 19990108601; No Copyright; Avail: CASI; A01, Hardcopy; A10, Microfiche

Thunderstorms over the tropical land and sea regions of the Indian sub-continent are characterized by their seasonal occurrence during the premonsoon (M-A-M) and monsoon (J-A-S) seasons. Monthly data on the number of thunderstorm days (THN), surface mean maximum wet-bulb temperatures (T(sub w)) and mean sea surface temperatures (SST) for a period of 11 years (1970-1980), over several land stations across the latitude range 8-30 deg N and at one island station, Port Blair (PBL) and Minicoy (MNC) each in the Bay of Bengal and Arabian Sea, have been used for this study. For the two data sets (THN and T(sub w)/SST), at these two categories of locations, we present the results of their monthly (January-December) mean latitudinal (8-30 deg N) and latitude-belts averaged seasonal variation. The seasonal variation of the T(sub w), SST and THN at these two locations has shown clear signal of its semiannual oscillation over land and sea areas. The central focus, therefore, of this study was the issue of the sensitivity of the occurrence of THN to T(sub w)/SST. This issue is similar to the numerous sensitivity studies of lightning and the occurrence of the thunderstorms with that of the T(sub w) on the land regions in the tropics. This information is an exceedingly important result towards documenting the response of tropical convection to modest changes in surface thermodynamics over land and oceans. The results of the sensitivity analysis of THN to T(sub w)/SST are presented. The month to month SST variation showed that the peak SST heating occurs usually in the month of April. The SST then systematically cools down from the month of May until about July-August. It is worthwhile to note that the period of significant SST heating precedes the onset of normal monsoon (1 June) by about 30-45 days. It is proposed that the use of SSTs may well be made as a proxy for wet-bulb temperatures over the oceans for oceanic convection and monsoon studies where they are usually not available.
Author
Thunderstorms; India; Sea Surface Temperature; Moisture Content; Atmospheric Moisture; Tropical Regions; Atmospheric Temperature; Annual Variations

19990108653 Riga Aviation Univ., Riga, Latvia
Thin Structure of Atmospherics
Krasnitsky, Y. A., Riga Aviation Univ., Latvia; 11th International Conference on Atmospheric Electricity; June 1999, pp. 131-134; In English; See also 19990108601; No Copyright; Avail: CASI; A01, Hardcopy; A10, Microfiche

A convolutional model has been developed for spherics waveform radiated from a lightning channel. Any spherics is supposed to be a result of convolution of the channel base current with channel radiation pulse function (CRPF) mapping channel structural inhomogeneities into the spherics. The relations of the CRPF with essential types of channel inhomogeneities are considered. Estimation of CRPF from real spherics data by digital processing methods are briefly described.
Author
Atmospherics; Waveforms; Lightning

19990108654 NASA Marshall Space Flight Center, Huntsville, AL USA
Investigation of a Frequency Spectrum of Discharges Generated by a Charged Aerosol Cloud
Christian, H. J., NASA Marshall Space Flight Center, USA; 11th International Conference on Atmospheric Electricity; June 1999, pp. 135-137; In English; See also 19990108601; No Copyright; Avail: CASI; A01, Hardcopy; A10, Microfiche

Charged aerosol clouds allow to create strong electric fields which generate discharges. A character of appearance and development of the discharges is similar to thundercloud processes. That is why the charged aerosol clouds are used for experiments on studying of discharges in air. Experimental data on electromagnetic fields investigation produced by discharges between charged cloud and ground are considered.
Author
Aerosols; Cloud-to-Ground Discharges; Charged Particles

19990108655 Moscow Inst. of Power Engineering, USSR

Formation of Plasma Space Stems in Charged Aerosol Clouds: Experimental Results and Theoretical Explanation

Temnikov, A. G., Moscow Inst. of Power Engineering, USSR; Orlov, A. V., Moscow Inst. of Power Engineering, USSR; Syssoev, V. S., Moscow Inst. of Power Engineering, USSR; 11th International Conference on Atmospheric Electricity; June 1999, pp. 138-141; In English; See also 19990108601; No Copyright; Avail: CASI; A01, Hardcopy; A10, Microfiche

Experimental investigations of plasma space stem formation in the charged water aerosol clouds allowed to describe the phenomenology and suggest the possible mechanism of their appearance. These space stems can appear on the charged flow boundary where the external electric field strength becomes enough for intensive ionization when the weak streamer arrives there. Rarity and accidental nature of the space stem appearance are explained.

Author

Plasmas (Physics); Aerosols; Charged Particles; Electric Discharges; Ionization

19990108656 Institute for High Temperatures, Moscow, USSR

Statistical Analysis and Polymer-Composite Structure of Ball Lightning

Amirov, A. K., Institute for High Temperatures, USSR; Bychkov, Vladimir L., Institute for High Temperatures, USSR; 11th International Conference on Atmospheric Electricity; June 1999, pp. 142-145; In English; See also 19990108601; No Copyright; Avail: CASI; A01, Hardcopy; A10, Microfiche

The work is devoted to the statistical analysis of events of observation Ball Lightning (BL) collected in the Stakhanov-Keul-Bychkov (SKB) computer data bank on BL. This data bank provided data for analysis of BL properties using a personal computer and modern statistical software such as analysis of variance, ANOVA, for revelation of significant factors and methods of non-parametric regression. The properties of BL as a high energy storing and an object with the framework are analyzed. The model of BL as a highly charged polymer-composite dielectric structure is described. All obtained results show that BL can be heterogeneous (polymer or composite) formation, with movable framework and glowing surface. At least one type of BL can be the object with the material structure or the framework.

Author

Ball Lightning; Statistical Analysis; Analysis of Variance; Composite Structures

19990108657 Toyota Coll. of Technology, Japan

Current Measurements of Upward Negative Leaders in Rocket Triggered Lightning

Nakano, M., Toyota Coll. of Technology, Japan; Sumi, S., Chubu Univ., Japan; Nakamura, K., Nagoya Inst. of Tech., Japan; 11th International Conference on Atmospheric Electricity; June 1999, pp. 146-149; In English; See also 19990108601; No Copyright; Avail: CASI; A01, Hardcopy; A10, Microfiche

Negative upward leader currents in rocket triggered lightning are measured with high and low sensitive measuring systems. The upward developing leader from the ground show different two stages, that is, the initial stage in which the mean current amplitude of the leader pulses is 129 A, and the following developing stage of large current pulses. The mean current amplitude is 9kA. The current amplitude of the initial stage is similar to a leader current which is reported in natural negative ground flash. The mean time interval between leader pulses are 30us in the initial stage and 77us in the following developing stage, which are in the same range as those of a negative leader in natural lightning and lightning to a tower. The transition from the initial stage to the developing stage is very clear, and this suggests that two different discharge processes exist when the leader develops upward to cloud charge center.

Author

Lightning; Leaders (Meteorology); Electrical Measurement

19990108658 Pennsylvania State Univ., Communications and Space Sciences Lab., University Park, PA USA

Lightning, the Global Circuit, and the Middle Atmosphere

Hale, Leslie C., Pennsylvania State Univ., USA; 11th International Conference on Atmospheric Electricity; June 1999, pp. 150-153; In English; See also 19990108601; No Copyright; Avail: CASI; A01, Hardcopy; A10, Microfiche

A capacitive discharge model of a thundercloud can be used to explain AC (ELF(extremely low frequency) and below) and DC current and energy coupling to the middle atmosphere and global circuit (GC). It is found that the DC GC current can approach the basic ”meteorological” charge separation generator for thunderclouds with only CE lightning but is reduced by IC lightning. Point discharge and precipitation currents reduce the cloud and cloud-to-earth capacitance charging and hence the lightning rate. The waveshape and hence frequency spectrum of the current pulses to the GC are controlled by the middle atmosphere conductivity profile, which is extremely variable. The low conductivity of the nighttime mesosphere is probably due to ”invisible”

aerosol. The acceleration by the ELF pulse of free electrons photo-detached from the aerosol particles by lightning may explain the VBF pulses observed in connection with ”red sprites” and other lightning.
Author
Atmospheric Models; Capacitance; Extremely Low Frequencies; Lightning; Middle Atmosphere; Polarization (Charge Separation); Current Density

19990108659 Florida Univ., Gainesville, FL USA
Multiple-Station Measurements of Triggered-Lightning Electric and Magnetic Fields
Crawford, D. E., Florida Univ., USA; Rakov, V. A., Florida Univ., USA; Uman, M. A., Florida Univ., USA; Schnetzer, G. H., Florida Univ., USA; Rambo, K. J., Florida Univ., USA; Stapleton, M. V., Florida Univ., USA; 11th International Conference on Atmospheric Electricity; June 1999, pp. 155-158; In English; See also 19990108601; No Copyright; Avail: CASI; A01, Hardcopy; A10, Microfiche

We have measured electric and magnetic fields produced by 12 strokes in five lightning flashes triggered using the rocket-and-wire technique in 1997 at Camp Blanding, Florida. The measurements have been made at seven distances from the triggered-lightning channel ranging from 5 to 500 m although not every measuring station acquired valid data for every event. Additionally, for each lightning stroke we measured channel-base current and obtained photographic and video images of the channel. In this paper, we present selected results of the ongoing analysis of the acquired data including: (1) electric field waveforms due to leader/return-stroke sequences as a function of distance, (2) the magnitude of leader electric field change as a function of distance, and (3) the magnitude of M-component electric field change as a function of distance. We compare these results with our previous findings and, for the case of M-components, with the predictions of the two-wave mechanism of this lightning process.
Author
Electric Fields; Lightning; Waveforms; Magnetic Fields; Field Strength

19990108660 Albany Univ., Albany, NY USA
Positive Leaders in Rocket Triggered Lightning: Propagation Velocity from Measured Current and Electric Field Derivative at Ground
Davis, D. A., Albany Univ., USA; Laroche, P., Office National d’Etudes et de Recherches Aerospatiales, France; 11th International Conference on Atmospheric Electricity; June 1999, pp. 158-161; In English; See also 19990108601; No Copyright; Avail: CASI; A01, Hardcopy; A10, Microfiche

In 1996, current and surface electric field change recordings were obtained coincident with the inception of positive leaders initiating rocket-and-wire triggered lightning flashes. The current records show initially isolated (approx. 10 ms separation), and later occasionally grouped (approx. 20-30 ms separation), intermittent current pulses (approx. 10’s of Amperes). The onset of the main positive leader follows with a sequence of approx. 10- 15 similar grouped pulses, whose amplitudes decline into a continuous current of a fraction to a few amperes. The assertion that pulses prior to the main leader onset are associated with positive leader development arrested after a few meters of propagation is investigated by comparison, between the main leader and prior grouped multiple-pulsed events, of crude velocity and line charge density estimates. These estimates, deduced from the current and surface field change records, range from 1.6-2.5 x 10(exp 5) m/s and 0-150 uC/m for the main leader velocity and line charge density, respectively, whereas the same parameters deduced for prior grouped multiple-pulsed events range from 0.13-2.8 x 10(exp 5) m/s and 4-92 uC/m.
Author
Leaders (Meteorology); Lightning; Propagation Velocity; Electric Fields; Electric Charge; Current Density; Electric Pulses

19990108661 Uppsala Univ., Inst. of High Voltage Research, Sweden
Signal Strength of Return Strokes Occurring Over the Sea and Over Land: A Sensitivity Analysis
Galvan, Arturo, Uppsala Univ., Sweden; Cooray, Vernon, Uppsala Univ., Sweden; Goetschl, Thomas, Uppsala Univ., Sweden; Scuka, Viktor, Uppsala Univ., Sweden; 11th International Conference on Atmospheric Electricity; June 1999, pp. 162-165; In English; See also 19990108601; No Copyright; Avail: CASI; A01, Hardcopy; A10, Microfiche

This paper attempts to answer the following question: Is the initial peak of radiation fields generated by lightning return strokes striking the sea higher than that of return strokes occurring over the land? to answer this question, a sensitivity analysis was conducted using the information collected by the Swedish Lightning Location System from 1990 to 1997. After correcting

for the propagation effects and the limited bandwidth of the direction finding system, the results show that there is no significant difference in the peak radiation fields of the two categories of lightning flashes.
Author
Lightning; Radiation Distribution; Direction Finding; Signal Measurement; Land; Seas

19990108662 NASA Marshall Space Flight Center, Huntsville, AL USA
An Intercomparison of Ground, Airborne, and Space Instrumentation Definitions of the Lightning Element
Mach, Douglas, Alabama Univ., USA; Boeck, William, Niagara Univ., USA; Christian, Hugh, NASA Marshall Space Flight Center, USA; 11th International Conference on Atmospheric Electricity; June 1999, pp. 166-169; In English; See also 19990108601; No Copyright; Avail: CASI; A01, Hardcopy; A10, Microfiche

For the past century, scientists have made quantitative measurements of lightning discharges. In the process, they refined the definition of a lightning unit, or basic quantum of lightning, in order to base it on observable parameters. In this paper, we will use cluster analysis to derive a basic spatial and temporal definition or scale length for the unit of lightning. We will use data from three different systems that detected pulses from the same storm complex over Central Oklahoma during June, 1998. Since the different instruments detect lightning in different ways with different resolutions, there may not be a single definition of the unit of lightning that can be applied to all three systems. However, common components can be found since all instrumentation are detecting aspects of the same phenomenon.
Author
Cluster Analysis; Lightning; Electromagnetic Measurement; Characterization

19990108663 New Mexico Inst. of Mining and Technology, Socorro, NM USA
Comparison of Ground-Based 3-Dimensional Lightning Mapping Observations with Satellite-Based LIS Observations in Oklahoma
Thomas, Ronald J., New Mexico Inst. of Mining and Technology, USA; Krehbiel, Paul R., New Mexico Inst. of Mining and Technology, USA; Rison, William, New Mexico Inst. of Mining and Technology, USA; Hamlin, Timothy, New Mexico Inst. of Mining and Technology, USA; Boccipio, Dennis, Global Hydrology and Climate Center, USA; Goodman, Steve, Global Hydrology and Climate Center, USA; Christian, Hugh, Global Hydrology and Climate Center, USA; 11th International Conference on Atmospheric Electricity; June 1999, pp. 172-175; In English; See also 19990108601; No Copyright; Avail: CASI; A01, Hardcopy; A10, Microfiche

Three-dimensional lightning mapping observations obtained during the MEaPRS program in central Oklahoma during June, 1998 have been compared with observations of the discharges from space, obtained by NASA's Lightning Imaging Sensor (LIS) on the TRMM satellite. Excellent spatial and temporal correlations are observed between the two sets of observations. Most of the detected optical events were associated with intracloud discharges that developed into the upper part of the storm. Cloud-to-ground discharges that were confined to mid- and lower-altitudes tended not to be detected by LIS. Extensive illumination tended to occur in impulsive bursts toward the end or part way through intracloud flashes and appeared to be produced by energetic K-changes that typically occur at these times.
Author
Intracloud Discharges; Cloud-to-Ground Discharges; Thunderstorms; Satellite Imagery; Satellite Observation; Thematic Mapping

19990108664 Osaka Univ., Dept. of Electrical Engineering, Suita, Japan
TRMM/LIS Observations of Lightning Activity
Kawasaki, Zen, Osaka Univ., Japan; Yoshihashi, Sachi, Osaka Univ., Japan; 11th International Conference on Atmospheric Electricity; June 1999, pp. 176-179; In English; See also 19990108601; No Copyright; Avail: CASI; A01, Hardcopy; A10, Microfiche

Lightning Imaging Sensor (LIS) which is equipped on Tropical Rainfall Measuring Mission satellite (TRMM) is introduced in the report. It is noticed that LIS consists of an optical detection system with telescope lens and CCD matrix, and a data processing unit. The specification of LIS is given from the aspects of both hardware and software. The preliminary observation results are presented and discussions from meteorological aspects are shown. The comparison with ground based measurement for the evaluation of LIS function is also shown.
Author
Trmm Satellite; Lightning; Imaging Techniques; Satellite Instruments; Satellite Observation

19990108665 Lightning Protection Technology, Inc., Tucson, AZ USA

Towers, Lightning and Human Affairs

Byerley, L. G., III, Lightning Protection Technology, Inc., USA; Brooks, W. A., Global Atmospherics, Inc., USA; Noggle, R. C., Global Atmospherics, Inc., USA; Cummins, K. L., Global Atmospherics, Inc., USA; 11th International Conference on Atmospheric Electricity; June 1999, pp. 180-183; In English; See also 19990108601; No Copyright; Avail: CASI; A01, Hardcopy; A10, Microfiche

The number of tower structures to support cellular-telephone and wireless communications in North America has grown dramatically in the last ten years. In addition to cell-phone antenna towers, there are hundreds of thousands of towers with heights between thirty and two hundred meters. These towers include ham radio towers, water towers, microwave repeater and VHF communication towers. Tall towers are in some cases erected in residential and industrial areas. Some municipalities now lease public spaces for tower sites. Measurements of lightning strikes to towers between 30 and 200 m in height have shown that such towers increase the incidence of lightning at the tower location and that the probability of lightning to a tower increases roughly as the square of the tower height. Recent work has characterized the multiple ground attachments of natural, negative discharges and the electromagnetic environment near the ground strike point. We review the tower/lightning problem in light of these findings and relate a recent case of multiple lightning incidents at a water tower in which it appears that the tall structure is a land-use-nuisance to people nearby. We use lightning ground flash density data to show the skew of lightning incidence near towers of 300 m or more in height. We review mitigation measures for some lightning effects at towers.
Author

Lightning; Towers

19990108666 Office National d'Etudes et de Recherches Aerospatiales, Chatillon, France

A Project for Space-Borne Detection of Lightning Flashes Using Interferometry in the VHF-UHF Band

Bondiou–Clergerie, A., Office National d'Etudes et de Recherches Aerospatiales, France; Blanchet, P., Office National d'Etudes et de Recherches Aerospatiales, France; Thery, C., Office National d'Etudes et de Recherches Aerospatiales, France; Delannoy, A., Office National d'Etudes et de Recherches Aerospatiales, France; Lojou, J. Y., DIMENSIONS, France; Soulage, A., DIMENSIONS, France; Richard, P., DIMENSIONS, France; Roux, F., Laboratoire d'Aerologie, France; Chauzy, S., Laboratoire d'Aerologie, France; 11th International Conference on Atmospheric Electricity; June 1999, pp. 184-187; In English; See also 19990108601; No Copyright; Avail: CASI; A01, Hardcopy; A10, Microfiche

Recent successful experiments have demonstrated the high scientific interest for the detection of lightning from space. The main objectives of these projects are the analysis, at large geographic and temporal scales, of the relationships between electrical activity and other thundercloud parameters. Within the frame of increasing the knowledge of the behavior of convective systems, the objectives of the "ORAGES" project is to locate the lightning flashes within the inter-tropical region from a low orbit microsatellite. The "ORAGES" instrument will determine the location of lightning discharges at the Earth's surface through interferometric analysis of VHF-UHF sources associated with intracloud and cloud-to-ground flashes. This project has been selected by the French Space Agency (CNES) with an expected launch date around the year 2004.
Author

Satellite Observation; Cloud-to-Cloud Discharges; Cloud-to-Ground Discharges; Thunderstorms; Interferometry

19990108667 Airborne Research Associates, Weston, MA USA

Lightning First Pulses Used in the "Last" (Time-of-Arrival) and "Atlas" (Single Station) Total Lightning Mapping Systems

Markson, Ralph, Airborne Research Associates, USA; Ruhnke, Lothar, Airborne Research Associates, USA; 11th International Conference on Atmospheric Electricity; June 1999, pp. 188-191; In English; See also 19990108601
Contract(s)/Grant(s): NAS1-20594; NAS1-97039; No Copyright; Avail: CASI; A01, Hardcopy; A10, Microfiche

The first RF pulse from "total lightning' discharges (cloud and ground flashes) has been used in different ways to locate the origin of flashes in two new types of lightning detection systems. The multisensor LASI time-of-arrival (TOA) system uses GPS timing of the first pulse. The ATLAS single sensor system uses the amplitude of the first pulse, which is invariant in magnitude and polarization for all lightning discharges, to determine distance from the sensor. It is significantly more accurate than past single sensor lightning mapping systems. The polarity of the first pulse generally identifies lightning type (IC or CG). Both systems utilize only the first pulse which makes signal processing much simpler than with previous lightning locating systems. Knowing the position where lightning begins (maximum electric fields, mixed phase hydrometeors and updrafts) is valuable for identifying

convective cells producing the hazardous meteorological conditions caused by thunderstorms. It is also important for research studying thunderstorm electrification and associated microphysical problems.
Author
Lightning; Electric Fields; Signal Detection; Electromagnetic Pulses; Mapping

19990108668 NASA Marshall Space Flight Center, Huntsville, AL USA
A Spherical Earth Solution for TOA Lightning Location Retrieval
Koshak, W. J., NASA Marshall Space Flight Center, USA; Solakiewicz, R. J., Chicago State Univ., USA; 11th International Conference on Atmospheric Electricity; June 1999, pp. 192-195; In English; See also 19990108601; No Copyright; Avail: CASI; A01, Hardcopy; A10, Microfiche

The problem of retrieving lightning, ground-strike location on a spherical Earth surface using a network of 4 or more time-of-arrival (TOA) sensors is considered, It is shown that this problem has an analytic solution and therefore does not require the use of nonlinear estimation theory (e.g., minimization). The mathematical robustness of the analytic solution is tested using computer-generated lightning sources and simulated TOA measurement errors. A summary of a quasi-analytic extension of the spherical Earth solution to an oblate spheroid Earth geometry is also provided.
Author
Lightning; Position (Location); Earth Surface; Analysis (Mathematics); Robustness (Mathematics); Optimization; Mathematical Models

19990108669 Finnish Meteorological Inst., Helsinki, Finland
Performance of the New LLP-Impact System in Finland
Tuomi, Tapio J., Finnish Meteorological Inst., Finland; 11th International Conference on Atmospheric Electricity; June 1999, pp. 196-199; In English; See also 19990108601; No Copyright; Avail: CASI; A01, Hardcopy; A10, Microfiche

In 1984-1997, the southern half of Finland was covered by an LLP lightning location system based on four model DF-80-02 direction finders. In August 1997, it was replaced by a system consisting of five IMPACT sensors, with coverage extended further to the north. Parallel operation of the two systems in August and September 1997 showed a substantial increase in both the location accuracy and the detection efficiency, although the declining thunderstorm season provided only limited data. The improvements are due to better-chosen sites and the inclusion of time-of-arrival techniques, and to the higher sensitivity to detect weak strokes. The full season in 1998 provided enough data for intrinsic analysis of the new system (the old system was closed down in October 1997). The angular errors, given automatically by the system, show typical double-period sine curves with +/- 5 deg maximum errors. The initial typical error of 2-3 km was improved to the 1-km level. The improving accuracy has remedied some bad locations and even some non-intersecting cases, hence also improving the detection efficiency. A case study suggests that a maximum flash detection efficiency is greater than 80% estimated by the manufacturer is reached in the central region of the network.
Author
Lightning; Position (Location); Radio Direction Finders

19990108670 National Severe Storms Lab., Norman, OK USA
Demographics of U.S. Lightning Casualties and Damages from 1959-1994
Holle, Ronald L., National Severe Storms Lab., USA; Lopez, Raul E., National Severe Storms Lab., USA; Curran, E. Brian, National Weather Service, USA; 11th International Conference on Atmospheric Electricity; June 1999, pp. 200-203; In English; See also 19990108601; No Copyright; Avail: CASI; A01, Hardcopy; A10, Microfiche

The NOAA Publication Storm Data has 3,239 deaths, 9,818 injuries, and 19,814 property-damage reports due to lightning from 1959-1994 in the U.S. Spatial and temporal variations that are identifiable with this dataset will be described by state, region, year, month, and hour of the day. The number of lightning casualty and damage events is less variable from year to year than nearly all other weather causes. Therefore, lightning is a constant and widespread threat to people and property during the thunderstorm season. Florida leads the nation in deaths and injuries, while the largest number of damage reports comes from Pennsylvania. When population is taken into account, New Mexico and Wyoming lead the nation in death, injury, and casualty rates per million people. Highest rates of damage reports weighted by population are on the plains. All types of lightning reports in Storm Data reach maxima during July. Damage reports are spread more evenly through the year than casualties. In northern states, casualties and damages have narrower distributions centered on summer than southern regions. There are more damage reports during the night in the plains and midwest states than elsewhere. Most incidents involve one person. Locations of casualties in Storm Data

are not well identified. Comparison with other datasets shows that Storm Data entries tend to include more expensive widely-known events and to exclude most of the small losses.
Author
Lightning; Casualties; Damage; Spatial Distribution; Temporal Distribution; USA

19990108671 National Lightning Safety Inst., Louisville, CO USA
Results of Investigations into Annual USA Lightning Costs and Losses
Kithil, R., National Lightning Safety Inst., USA; 11th International Conference on Atmospheric Electricity; June 1999, pp. 204-206; In English; See also 19990108601; No Copyright; Avail: CASI; A01, Hardcopy; A10, Microfiche

Researchers who attempt to describe the economic impact of lightning in the USA are confronted with contradictory data. National Weather Service (NWS) figures place the most recent yearly losses at some $35 million. Such a severe understatement of costs from an official source tends to inhibit attentions focused at lightning problems. In general, lightning safety issues are not taken seriously by individuals, by business, or by government. If actual dollar losses were understood more fully, then awareness and mitigation measures might be raised to a higher priority.
Author
Lightning; Economic Impact; Meteorological Services; Damage Assessment

19990108672 Central Lightning Protection, Inc., Urawa, Japan
The Two Important Characteristics of Ground Flashes for the Human Safety
Kitagawa, N., Central Lightning Protection, Inc., Japan; Sugita, A., Franklin Japan, Japan; Takahashi, S., Franklin Japan, Japan; 11th International Conference on Atmospheric Electricity; June 1999, pp. 207-210; In English; See also 19990108601; No Copyright; Avail: CASI; A01, Hardcopy; A10, Microfiche

For the safety of human beings against lightning, it is essential to keep away from direct strikes. A person in the outdoors has to move into the safe space against the lightning incidence. to provide proper guides to avoid lightning strikes, the following two factors have to be disclosed: (1) Time intervals between subsequent flashes that strike the ground within a small area; and (2) The distances between struck points of subsequent ground flashes. The authors analyzed the data obtained by the lightning location system, covering Kanto District, Japan for two years and obtained the statistical distributions of the above two factors.
Author
Lightning; Statistical Distributions; Position (Location)

19990108673 Shanghai Meteorological Inst., China
Comments on the E.S.E. Air Terminals
Guo, C., Shanghai Meteorological Inst., China; 11th International Conference on Atmospheric Electricity; June 1999, pp. 211-213; In English; See also 19990108601; No Copyright; Avail: CASI; A01, Hardcopy; A10, Microfiche

Based on analyzing the ”E.S.E. lightning conductor assessment procedure” provided by the French Standard NF C 17-102, it is inferred that if the product is manufactured following this assessment procedure, the declared improvement or performance could not be ensured, mainly due to imperfect simulation of natural condition. In turn, the products manufactured under such a Standard cannot be considered with enough experimental evidence as having declared performance. Some suggestions are provided to improve such a situation.
Author
Lightning; Electric Conductors; Standards; Computerized Simulation

19990108674 Electricite de France, Service des Etudes Medicales, Paris, France
Lightning Injuries to Humans in France
Gourbiere, Elisabeth, Electricite de France, France; 11th International Conference on Atmospheric Electricity; June 1999, pp. 214-217; In English; See also 19990108601; No Copyright; Avail: CASI; A01, Hardcopy; A10, Microfiche

The pathology of lightning, or keraunopathology is known only to a few specialists. In an average year in France, lightning kills ten people and injuries another 60, often with serious sequelae. Because of the seriousness of the lightning accidents, increased promotion of awareness among the entire population is essential and not necessarily expensive.
Author
France; Lightning; Injuries; Accident Prevention

19990108675 Global Atmospherics, Inc., Tucson, AZ USA

An Integrated North American Lightning Detection Network

Cummins, K. L., Global Atmospherics, Inc., USA; Pyle, R. B., Global Atmospherics, Inc., USA; Fournier, G., Environment Canada, Canada; 11th International Conference on Atmospheric Electricity; June 1999, pp. 218-221; In English; See also 19990108601; No Copyright; Avail: CASI; A01, Hardcopy; A10, Microfiche

The U.S. National Lightning Detection Network (NLDN) and the recently-completed Canadian Lightning Detection Network (CLDN) are operated as an integrated North American Lightning Detection Network (NALDN), employing 187 sensors covering nearly 20 Million square kilometers. This large network provides a unique opportunity to study lightning characteristics over a wide range of climate and terrain. In this paper we briefly discuss the NLDN and CLDN and their performance characteristics. The first measured continental-scale (U.S./Canada) annual ground flash density is presented. Taking advantage of the vast range in latitude covered by the NALDN, we also provide evidence for a latitude and regional dependence for cloud-to-ground flash parameters. An example ”storm day” with over 200,000 cloud-to-ground flashes is shown to cover large portions of the U.S., Canada, and Mexico.

Author

Lightning; Detection; Tracking Networks; Cloud-to-Ground Discharges

19990108676 Oklahoma Univ., School of Meteorology, Norman, OK USA

Electric-Field Changes of Lightning Observed with Balloon-Borne Slow Antennas

Beasley, William H., Oklahoma Univ., USA; Eack, Kenneth B., Los Alamos National Lab., USA; Morris, Heidi E., Los Alamos National Lab., USA; Rust, W. David, National Severe Storms Lab., USA; MacGorman, Donald R., National Severe Storms Lab., USA; 11th International Conference on Atmospheric Electricity; June 1999, pp. 222-225; In English; See also 19990108601

Contract(s)/Grant(s): F49620-96-1-0430; NSF ATM-98-07179; No Copyright; Avail: CASI; A01, Hardcopy; A10, Microfiche

During the Summer and Fall of 1998 we launched five balloon-borne slow antennas into thunderstorms to observe the changes in electric field caused by lightning. Four of these were for measurement of field change only. The fifth was part of a larger package that included an x-ray detector and a GPS receiver on board. We have processed electric-field-change data from two of these flights. Interpretation of the field-change waveforms has not been as straight-forward as we had hoped. Several appear to be coincident in time with cloud-to-ground lightning flashes that were recorded by the National Lightning Detection Network (NLDN). We discuss examples of field changes observed at altitude and compare them with data from the NLDN. Limits on time resolution and timing accuracy prevent us from making unambiguous identification of the lightning processes that caused the field changes. It appears that the field changes we have observed may have been caused by charge movements relatively near the instruments as compared with the ground-strike location of coincident flashes, but nonetheless possibly related in some way to the ground flashes.

Author

Lightning; Electric Field Strength; Waveforms; Balloon-Borne Instruments; Antennas

19990108677 ERICO Lightning Technologies, Hobart, Australia

A New, High Voltage, Arbitrary Waveform Generator for Simulating Pre-Return Stroke C-G Lightning Electric Fields

DAlessandro, F., ERICO Lightning Technologies, Australia; Gumley, J. R., ERICO Lightning Technologies, Australia; 11th International Conference on Atmospheric Electricity; June 1999, pp. 226-229; In English; See also 19990108601; No Copyright; Avail: CASI; A01, Hardcopy; A10, Microfiche

In this paper we describe the main features of a new prototype high voltage impulse generator designed to produce a variable, programmable wavefront up to a 150 kV peak voltage. This generator is capable of precisely simulating the range of rapidly escalating electric fields due to a lightning downward leader as it approaches an attachment point near or on the ground. It utilises a computer-controlled interface that drives a unique set of series-stacked flyback transformers. The resulting output is any desired, monotonically increasing waveform or ”wavefront”, downloaded from the computer.

Author

Voltage Generators; Electric Potential; Electric Fields; Waveforms

19990108678 Hokuriku Electric Power Co., Research and Development Center, Toyama, Japan

Lightning Activities of Winter Thundercloud Observe by Dual-Polarization Doppler Radar on the Hokuriku Coast of Japan

Kami, Kouichirou, Hokuriku Electric Power Co., Japan; Shinjo, Kazuo, Hokuriku Electric Power Co., Japan; Sakai, Tsutomu, Hokuriku Electric Power Co., Japan; Wakai, Takeo, Hokuriku Electric Power Co., Japan; 11th International Conference on

Atmospheric Electricity; June 1999, pp. 452-455; In English; See also 19990108601; No Copyright; Avail: CASI; A01, Hardcopy; A10, Microfiche

Lightning often occurs not only in summer but also in winter on the Hokuriku coast of Japan. Many damages of equipments and interruptions of power supply are caused by winter lightning. We have installed a dual-polarization Doppler radar (C-band) at Noto Peninsula in Hokuriku district to clear the relation between atmospheric activities and electrical activities of thunderclouds, and to establish a method of lightning forecast for winter season. In this paper, we describe an example of observation.

Author

Thunderstorms; Lightning; Radar Detection; Graupel; Winter; Japan

19990108679 ERICO Lightning Technologies, Hobart, Australia

A Preliminary Assessment of the Long-Term Performance in the Field of an Enhanced Air Terminal and the Lightning Protection Design Method

DAlessandro, F., ERICO Lightning Technologies, Australia; 11th International Conference on Atmospheric Electricity; June 1999, pp. 230-233; In English; See also 19990108601; No Copyright; Avail: CASI; A01, Hardcopy; A10, Microfiche

The aim of this study was to assess the performance of an enhanced air terminal installed on a wide range of structures in Hong Kong using a design method based on an improved electrogeometric model. Lightning strike statistics for 161 suitable installations over the period 1988-1996 have been collated. Analysis of these data shows that there is a highly significant positive correlation between the actual and expected annual strike frequency to the air terminals. The result provides strong evidence that the air terminal, and the lightning protection design principle, is performing according to its specifications.

Author

Lightning; Protection; Safety Devices; Statistical Analysis

19990108680 Bureau of Meteorology, Melbourne, Australia

Operational LPATS Network in Australia

Sharp, A. J., Bureau of Meteorology, Australia; 11th International Conference on Atmospheric Electricity; June 1999, pp. 234-237; In English; See also 19990108601; No Copyright; Avail: CASI; A01, Hardcopy; A10, Microfiche

In a collaborative agreement, the Bureau of Meteorology has arranged for the company Global Position and Tracking Systems Pty Ltd (GPATS) to install a lightning detection network in Australia based on Lightning Position and Tracking System (LPATS) technology. This involved the use of Bureau of Meteorology observing sites and communications networks. An initial network of five sensors existed covering parts of New South Wales and Queensland. A network expansion was commenced in 1997 with the first phase covering the Eastern half of Australia and a second phase to cover the remainder of the country. Lightning stroke rates of over 20,000 per hour have been observed over Australia and adjacent waters. Demand for this new data is already high. Within the Bureau of Meteorology, forecasters are already finding the data invaluable, particularly over large areas of the country that are not adequately covered by weather watch radar. The availability of data within seconds of the event means that developing storms can be detected well before satellite imagery is available. Significant uses include forecasting for aviation, fire weather and severe thunderstorms. After a small number of years of operation, it is anticipated that a high quality climatological database on lightning frequencies will be available for the whole of Australia.

Author

Lightning; Detection; Communication Networks; Position (Location); Tracking (Position)

19990108681 National Defense Academy, Dept. of Geoscience, Japan

Development of Heat Thunderstorms and Distribution of Lightning Strokes Around the Northern Part of the Kanto Plain Japan

Suzuki, Tomoyuki, National Defense Academy, Japan; Kobayashi, Fumiaki, National Defense Academy, Japan; Shimura, Takatsuga, National Defense Academy, Japan; Miyazaki, Tadaomi, Maebashi Inst. of Technology, Japan; Hirai, Takeo, Tokyo Electric Power Co., Inc., Japan; 11th International Conference on Atmospheric Electricity; June 1999, pp. 456-459; In English; See also 19990108601; No Copyright; Avail: CASI; A01, Hardcopy; A10, Microfiche

Doppler radar observation was carried out to investigate the generation and evolution processes of initial convective clouds of heat thunderstorms in the Kanto region of Japan in summer. The results of analysis in late August 1997 shows heat thunderstorms: (1) Initial convective echoes (hereafter referred to as ”first echo”) were generated at the base of mountains in the

evening. Most of the first echoes were generated at an altitude of 4-5 km AGL. (2) The first echoes which developed into meso-Beta -scale thunderstorms were generated above the specific mountain areas. (3) CG strokes occurred after the mature stage cells. Author

Thunderstorms; Radar Tracking; Lightning; Doppler Radar; Radar Echoes; Japan

19990108682 Open Univ., Dept. of Natural and Life Sciences, Tel-Aviv, Israel

Two Types of PGF-Producing Clouds in Winter Thunderstorms in Israel

Yair, Yoav, Open Univ., Israel; Altaratz, Orit, Tel-Aviv Univ., Ramat-Aviv, Israel; Levin, Zev, Tel-Aviv Univ., Ramat-Aviv, Israel; 11th International Conference on Atmospheric Electricity; June 1999, pp. 460-463; In English; See also 19990108601; No Copyright; Avail: CASI; A01, Hardcopy; A10, Microfiche

A study of the occurrence of positive ground flashes (PGF) in winter thunderstorms in Israel was conducted for the 1995/6-1997/8 seasons. We used data from 2 CGR lightning counters, an operational LPATS network and the Tel-Aviv University (TAU) weather radar. The study shows that PGFs occur primarily in events when the reflectivity pattern in a vertical cross-section of the cloud parallel to the prevailing winds, has a distinct tilted echo, with the PGFs located downwind of the main core of reflectivity. A relation between wind shear and PGF fraction was established. Other events show that very strong PGFs also occurred even though the wind shear was weak. In these events, the PGFs were located in regions of weaker reflectivity, typical of stratiform precipitation. RHI profiles of the active cells showed a bell structure with distinct bright bands. A time series showed that strong PGFs (with currents exceeding 100kA) occurred after successive CFs and NGFs. As the regions above the melting layer contain both supercooled water drops, graupel and ice crystals, we can assume that appropriate conditions for charge generation prevail, that possibly lead to the creation of an inverted dipole.

Author

Thunderstorms; Cumulonimbus Clouds; Israel; Winter; Radar Tracking; Electric Charge

19990108683 National Defence Academy, Dept. of Geoscience, Tokyo, Japan

Relation Between Lightning Activity of Summer and Winter Thunderclouds and Surface Electric Field Variation, Japan

Michimoto, K., Air Weather Service, H.Q., Defense Agency, Japan; Shimura, T., National Defence Academy, Japan; Suzuki, T., National Defence Academy, Japan; 11th International Conference on Atmospheric Electricity; June 1999, pp. 464-467; In English; See also 19990108601; No Copyright; Avail: CASI; A01, Hardcopy; A10, Microfiche

In winter, active convective clouds frequently form along the coastline of the Hokuriku district, in association with strong advection of Siberian air masses over the Sea of Japan. On the other hand, in summer, many thunderclouds form in the Kanto region in the afternoon every day. Summer and winter thunderclouds were investigated by field works, operation of the C- and X-band weather radars and a car-borne fieldmill. The investigation found a very close relation between the temporal variation of 3-dimensional radar echo and surface electric field magnitude detected by a car-borne fieldmill in the case of summer thunderclouds and winter convective clouds or thunderclouds. The study probed the close relation among radar echoes, quantity of thunderclouds and surface electric field magnitude in the summer and winter seasons. We think that summer thundercloud activity can basically be equated with winter thundercloud lightning activity, except that the magnitude of surface electric field under summer thunderclouds in the case of the Kanto region cannot be equated with that under winter thunderclouds in the case of the Hokuriku district in winter.

Author

Thunderstorms; Lightning; Radar Tracking; Electric Fields; Radar Echoes; Japan; Winter; Summer; Data Correlation

19990108684 Tel-Aviv Univ., Ramat-Aviv, Dept. of Geophysics and Planetary Sciences, Tel-Aviv, Israel

Electrical and Radar Observations of Thunderstorms in the Eastern Mediterranean

Altaratz, Orit, Tel-Aviv Univ., Ramat-Aviv, Israel; Levin, Zev, Open Univ., Israel; Yair, Yoav, Open Univ., Israel; 11th International Conference on Atmospheric Electricity; June 1999, pp. 468-471; In English; See also 19990108601; No Copyright; Avail: CASI; A01, Hardcopy; A10, Microfiche

The meteorological conditions for thunderstorm development in Israel have been reviewed by Levin et al. (1996). Most thunderstorms in our region occur between October and April and are usually associated with the passage of ”Cyprus Lows”, cyclones that originate in southern Europe, and travel over the northern part of the eastern Mediterranean Sea. A different, less prevalent, synoptic situation for the occurrence of thunderstorms is the Red Sea Trough, a tropical low pressure wave from the Red Sea that intrudes toward the Mediterranean Sea, bringing moist air from the tropics. Thunderclouds that form over the sea and the coastal area are typically with cloud base temperatures of about 5 C, and vertical dimensions of 6-8 km. Cloud top temperatures are found in the range of -30 C to -40 C and rarely below - 50 C. The resemblance between the winter thunderstorms in the eastern Mediterranean and those that occur in the western coast of Japan have been pointed out by Yair et al. (1998). The

synoptic conditions in both areas are similar: cold, dry, continental air masses passing over relatively warm sea water, changing and becoming unstable as they approach the coast, generating convective clouds and thunderstorms. Levin et al. (1996) also showed that the tilted dipole mechanism, suggested by Brook et al. (1982) to account for the occurrence of positive ground flashes is probably active in storms producing a high fraction of PGFs in the Tel-Aviv area.
Author
Radar Tracking; Israel; Thunderstorms; Lightning; Radar Echoes; Cumulonimbus Clouds; Free Convection

19990108685 NASA Kennedy Space Center, Cocoa Beach, FL USA
Lightning Launch Commit Criteria for America's Space Program
Roeder, W. P., Weather Squadron (45th), USA; Sardonia, J. E., Weather Squadron (45th), USA; Jacobs, S. C., Weather Squadron (45th), USA; Hinson, M. S., Weather Squadron (45th), USA; Harms, D. E., Weather Squadron (45th), USA; Madura, J. T., NASA Kennedy Space Center, USA; DeSordi, S. P., Weather Squadron (30th), USA; 11th International Conference on Atmospheric Electricity; June 1999, pp. 238-241; In English; See also 19990108601; No Copyright; Avail: CASI; A01, Hardcopy; A10, Microfiche

The danger of natural and triggered lightning significantly impacts space launch operations supported by the USAF. The lightning Launch Commit Criteria (LCC) are used by the USAF to avoid these lightning threats to space launches. This paper presents a brief overview of the LCC.
Author
Lightning; Spacecraft Launching; Criteria; Flight Hazards

19990108686 State Univ. of New York, Dept. of Earth and Atmospheric Sciences, Albany, NY USA
Cloud-to-Ground Lightning at Low Surface Temperatures
Moore, Paul K., State Univ. of New York, USA; Idone, Vincent P., State Univ. of New York, USA; 11th International Conference on Atmospheric Electricity; June 1999, pp. 472-475; In English; See also 19990108601; No Copyright; Avail: CASI; A01, Hardcopy; A10, Microfiche

A simple study was carried out to assess the absolute amount of cloud-to-ground (CG) lightning occurring at low surface temperatures in the continental U.S. The impetus for this study was the practical need to determine a lower operational temperature limit for certain lightning protection devices used in the telecommunication industry. These devices use a temperature dependent medium; a new lower limit of -4 F had been proposed for design of these devices. Meteorological experience suggested that there was a negligible amount of lightning activity at this temperature and that this could be confirmed with CG lightning data from the National Lightning Detection Network (NLDN). Consequently, we examined the occurrence of CG lightning over the U.S. during the winter months of December-February for a total of six winters: 1988-89 through 1993-94. Three-hourly surface temperatures recorded at the nearest National Weather Service (NWS) reporting stations were correlated with all CG lightning events occurring below 32 F. Both the number of storm events and number of flashes were binned by temperature interval. We identified spurious flashes in clear air regions by examining radar maps and satellite imagery; such flashes were eliminated from the analysis. We found hundreds of CG lightning storm events that occurred below 32 F over the six-winter period. Each storm typically consisted of just a few flashes though some occasionally contained hundreds of flashes. As anticipated, both the number of storm events and flashes fell dramatically with lower surface temperature. Out of 1,410,272 flashes recorded by the NLDN for the six winters studied, only 7,701 (0.55%) occurred below 32 F, 633 (0.045%) occurred at or below 13 F, and just 11 (0.00079%) occurred below 0 F. No CG strikes were observed at surface temperatures below -4 F. A simple regression analysis yields (via 95% prediction bounds) an expected maximum number of flashes for T is less than 9 F of only 1046 nationwide for the entire six-winter period. This confirmed our expectation that such a low temperature limit was an extreme design constraint. As anticipated, CG lightning at low surface temperatures was most often associated with strong warm advection over a shallow, very cold surface layer. Most of this lightning occurred in the southeastern Great Plains, with the remainder extending northeastward into New England.
Author
Cloud-to-Ground Discharges; Low Temperature; Temperature Dependence; Land Surface Temperature

19990108687 Central Aerological Observatory, Dolgoprudnyi, USSR
New Mechanism of Thundercloud Electricity and Lightning Production
Ermakov, V. I., Central Aerological Observatory, USSR; Stozhkov, Y. I., Lebedev Physical Inst., Russia; 11th International Conference on Atmospheric Electricity; June 1999, pp. 242-245; In English; See also 19990108601; No Copyright; Avail: CASI; A01, Hardcopy; A10, Microfiche

A new mechanism of thundercloud electricity and lightning production is given. The essential role in this mechanism belongs to cosmic rays. Cosmic rays ionize atoms of air. When in the low atmosphere there are powerful ascending wet air masses thunderclouds are produced. Near the Earth's surface in the low atmosphere positive and negative heavy ions are present. When air masses are rising to the altitude of several km they are cooled and the process of the condensation of water vapor on nucleation centers begins. On negative charged nuclei the condensation is going on faster than on positive ones. Upward air fluxes produce the large-scaled spatial separation of negative and positive charges and in turn it gives an electric field within a cloud. As soon as the electric field goes up to about 3 kV/cm the cloud becomes electric active and begins to work as a generator of new electric charges. Intracloud and cloud-to-ground discharges arise when extensive air showers of charged particles in the cloud are produced by high energy cosmic particles. These discharges propagate along the ionized tracks of particles of these showers. The mechanism proposed allows to estimate electric characteristics of thundercloud and describes lightning parameters known from the observations.
Author
Lightning; Charged Particles; Cosmic Ray Showers; Electric Fields; Cumulonimbus Clouds

19990108688 Federal Aviation Administration, Washington, DC USA
Preliminary FAA Investigations Into Using Total Lightning to Improve Convective Forecasting for Aviation
Nierow, A., Federal Aviation Administration, USA; Showalter, R. C., CTA, Inc., USA; Souders, C. G., Science Applications International Corp., USA; 11th International Conference on Atmospheric Electricity; June 1999, pp. 246-249; In English; See also 19990108601; No Copyright; Avail: CASI; A01, Hardcopy; A10, Microfiche

The Federal Aviation Administration (FAA) is investigating the use of total lightning (Cloud-to-Ground (CG), Intra-Cloud (IC), and Cloud-to-Cloud (CC) strokes) to supplement existing weather data sets in order to meet current requirements for convective forecasting, enhance aviation safety, and increase capacity. Total lightning could significantly enhance the ability to provide information on rapidly developing hazardous weather to both en route and terminal air traffic control personnel. The FAA is also evaluating the use of lightning data over oceanic regions.
Author
Lightning; Detection; Aircraft Safety; Weather Forecasting; Computer Networks

19990108689 Global Atmospherics, Inc., Tucson, AZ USA
Long-Range and Trans-Oceanic Lightning Detection
Cramer, J. A., Global Atmospherics, Inc., USA; Cummins, K. L., Global Atmospherics, Inc., USA; 11th International Conference on Atmospheric Electricity; June 1999, pp. 250-253; In English; See also 19990108601; No Copyright; Avail: CASI; A01, Hardcopy; A10, Microfiche

Lightning observations over the oceans provide valuable information for identifying regions of severe weather and the related threat of turbulence. Global Atmospherics, Inc. has provided real-time lightning observations over the oceans for use by the U.S. National Weather Service Aviation Weather Center since 1996. This paper discusses the features and limitations of this information, and summarizes recent experiments that quantify the performance of an integrated system composed of widely-separated networks of sensors.
Author
Lightning; Signal Detection; Computer Networks; Ocean Data Acquisitions Systems

19990108690 Alberta Univ., Edmonton, Alberta Canada
Lightning in Supercell Storms
Reuter, Gerhard, Alberta Univ., Canada; Kozak, Steven, Alberta Univ., Canada; 11th International Conference on Atmospheric Electricity; June 1999, pp. 476-479; In English; See also 19990108601; No Copyright; Avail: CASI; A01, Hardcopy; A10, Microfiche

Severe convective storms are often associated with lightning strike activity. How are cloud-to-ground (CG) lightning strikes related to the storm structure? CG lightning occur mostly downshear of the main radar reflectivity core in supercell storms, while in multicell storms the lighting strikes near the radar reflectivity core. In developing supercells, CG lightning was found mostly on the storm's left side with respect to its track. Holle et al. found that there were more lightning strikes per precipitation core area, when compared with the remainder of the storm area. Rust et al. found that increases in radar reflectivity magnitudes were correlated with increases in CG lightning strikes. Rutledge and MacGorman observed that maximum CG activity is approximately correlated with the period of most intense rainfall with a delay on the time scale of hours. In this conference paper the spatial and temporal patterns of lightning and precipitation are investigated for four Alberta hailstorms. Storm 1 and storm 2 occurred on 19 August 1992, while storm 3 and storm 4 formed on 30 July 1993. All four cases were long-lived hailstorms of quasi-supercell

structure that moved across central Alberta. The Alberta Forestry Lightning Network had direction finders that synthesized the position and timing of the CG lightning strikes. All four storms were monitored by operational weather radar located at Carvel (53.34 deg N, 114.09 deg W). This C-band radar takes volume scans at intervals of 10 minutes by scanning at 24 different elevation angles from 0.4 to 24.6 deg.
Author
Lightning; Cloud-to-Ground Discharges; Alberta; Hailstorms; Thunderstorms; Direction Finding; Radar Tracking; Rain

19990108691 Global Hydrology and Climate Center, Huntsville, AL USA
A Diagnostic Analysis of the Kennedy Space Center LDAR Network
Boccippio, D. J., Global Hydrology and Climate Center, USA; Heckman, S., Global Hydrology and Climate Center, USA; Goodman, S. J., Global Hydrology and Climate Center, USA; 11th International Conference on Atmospheric Electricity; June 1999, pp. 254-257; In English; See also 19990108601; No Copyright; Avail: CASI; A01, Hardcopy; A10, Microfiche

The performance characteristics of the Kennedy Space Center Lightning Detection and Ranging (LDAR) network are investigated at medium-far range (50-300 km). A 19 month noise-filtered sample of LDAR observations is examined, from which it is determined that the ”climatological” VHF source density as observed by LDAR falls off approximately 10 dB every 71 km of ground range from the network centroid. The underlying vertical distribution of LDAR sources is approximately normally distributed with a mean of 9 km and a standard deviation of 2.7 km, implying that loss of below-horizon sources has a negligible effect on column-integrated source densities within 200 km ground range. At medium to far ranges, location errors are primarily radial and have a slightly asymmetric distribution whose first moment increases as r squared . A range calibration derived from these results is used to normalize source density maps on monthly, daily and hourly time scales and yields significant improvements in correlation with NLDN ground strike densities.
Author
Lightning; Rangefinding; Signal Detection; Networks; Position (Location)

19990108692 Colorado State Univ., Dept. of Atmospheric Science, Fort Collins, CO USA
Polarimetric Radar Observations and Cloud Modeling Studies of Low Lightning Producing Convection in the Fort Collins Flash Flood
Petersen, Walter A., Colorado State Univ., USA; Carey, Lawrence D., Colorado State Univ., USA; Rutledge, Steven D., Colorado State Univ., USA; 11th International Conference on Atmospheric Electricity; June 1999, pp. 480-483; In English; See also 19990108601; No Copyright; Avail: CASI; A01, Hardcopy; A10, Microfiche

Several recent studies have noted the presence of frequent lightning in flash flood-producing convection. However, heavy convective precipitation ultimately responsible for the Fort Collins flash flood of 28 July 1997 occurred with relatively little concomitant lightning activity. Analysis of CSU-CHILL multiparameter radar observations combined with cloud modeling simulations suggests that warm rain microphysics coupled with accretional growth of ice near the freezing level led to efficient precipitation production in the flood convection. However, the precipitation process may have suppressed electrification processes by rapidly removing precipitation ice mass and cloud water from the mixed phase region of the convection.
Author
Lightning; Ice Clouds; Electrification; Radar Tracking; Computerized Simulation; Radar Scattering; Polarimetry; Cloud Physics

19990108693 New Mexico Inst. of Mining and Technology, Langmuir Lab., Socorro, NM USA
Aircraft Measurements of Particle Image and Charge Inside a New Mexico Thundercloud
Murray, W. Clifton, New Mexico Inst. of Mining and Technology, USA; Winn, W. P., New Mexico Inst. of Mining and Technology, USA; Thomas, Ronald J., New Mexico Inst. of Mining and Technology, USA; Ebneter, Arnold E., New Mexico Inst. of Mining and Technology, USA; Fleischhacker, Peter R., New Mexico Inst. of Mining and Technology, USA; Lawson, R. Paul, SPEC, Inc., USA; Weaver, Kim A., SPEC, Inc., USA; Stewart, Roy, Tesseract Design and Instrument, Colorado; Wieland, Chris, Della Enterprises, Inc., USA; 11th International Conference on Atmospheric Electricity; June 1999, pp. 260-263; In English; See also 19990108601
Contract(s)/Grant(s): NSF ATM-93-18887; No Copyright; Avail: CASI; A01, Hardcopy; A10, Microfiche

The popular hypothesis for how thunderclouds become electrified invokes collisions between graupel (or hail) and small ice crystals. While there has been considerable laboratory investigation of this ice-ice mechanism, in-situ testing of it by particle observations consists only of a few instrumented balloon and aircraft flights into actual thunderclouds. Some of the results of these in-cloud measurements are puzzling because the larger charges are not especially associated with the larger particles. to better understand this puzzling result, Langmuir Laboratory’s airplane SPTVAR (Special Purpose Test Vehicle for Atmospheric

Research) was equipped with an instrument for imaging particles and measuring their charge. On August 19, 1998, the airplane was able to fly into a growing cloud a few minutes before its first lightning flash. In this case the particle data are limited to the edge of the region of strong electric field, possibly because icing obscured the laser beam used to image the particles. Analysis of the data reveals that many of the larger charges were carried by the smaller particles.
Author
Cumulonimbus Clouds; Graupel; Charged Particles; Electric Fields; Cloud Physics

19990108694 Kansai Electric Power Co., Inc., Technical Research Center, Osaka, Japan
Observations of Thunderclouds and Lightning Activity in Winter by Dual Polarization Radar and SAFIR
Sonoi, Y., Kansai Electric Power Co., Inc., Japan; Uyeda, H., Hokkaido Univ., Japan; Kawasaki, Z. I., Osaka Univ., Japan; Maekawa, Y., Osaka Electro-Communication Univ., Japan; Fukao, S., Kyoto Univ., Japan; Takahashi, T., Obirin Univ., Japan; 11th International Conference on Atmospheric Electricity; June 1999, pp. 484-487; In English; See also 19990108601; No Copyright; Avail: CASI; A01, Hardcopy; A10, Microfiche

It is very important for the protection of electric power systems to comprehend the productive mechanism and the characteristics of lightning discharges in winter season. From these points of view, the authors have been investigating the thunderclouds in winter using a dual polarization Doppler radar, SAFIR (System de Surveillance et d' Alerte Fudre par Radioelectrique, in French) and other observational instruments. In this paper, we denote the relationship between electrical polarities of cloud to ground lightning discharges (from here on abbreviated as CG lightning) and the internal structure of thunderclouds, and the statistically analyzed lightning characteristics observed by SAFIR and other equipment around the coast of Wakasa Bay located in the Northern Kin-ki District, and also the relationship between lightning occurrence and the meteorological upper atmospheric temperature.
Author
Winter; Japan; Thunderstorms; Cumulonimbus Clouds; Cloud-to-Ground Discharges; Atmospheric Temperature; Upper Atmosphere; Radar Tracking; Polarity

19990108695 Nehru Coll., Dept. of Physics, Chhibramau, India
A Possible Mechanism of Gushes of Rain or Hail After Lightning
Singh, N., Nehru Coll., India; Mohan, Avinash, Nehru Coll., India; 11th International Conference on Atmospheric Electricity; June 1999, pp. 488-491; In English; See also 19990108601; No Copyright; Avail: CASI; A01, Hardcopy; A10, Microfiche

Radar observations inferred that the lightning often followed by a rapidly intensifying echo and then a gush of rain or hail at the ground. This has been explained by several theoretical explanations. The present work explains that developed break even electric field gives rise to the lightning, which ionizes the gases in clouds. The ions get attached to the nuclei of water or ice, so that Gibb's free energy for formation of critical nuclei is reduced. Hence the nucleation rate and equilibrium concentration of critical water nuclei are increased. Also, the increased electric field enhances the nucleation rate of water droplets and at the same time reduces the relaxation time. The growth of electric field is provided due to non-inductive charging mechanism. Thus, the phenomenon of rain gush after lightning is explained.
Author
Radar Tracking; Lightning; Electric Fields; Atmospheric Ionization; Nucleation; Condensation Nuclei; Ice Nuclei

19990108696 North Carolina State Univ., Raleigh, NC USA
An Experimental Study of Charge and Mass Transfer During Ice Contact Interactions
Mason, B. L., North Carolina State Univ., USA; Dash, J. G., Washington Univ., USA; 11th International Conference on Atmospheric Electricity; June 1999, pp. 264-267; In English; See also 19990108601; Sponsored in part by the Leonard X. Bosack and Bette M. Kruger Foundation and the Seattle Chapter of the ARCS Foundation; No Copyright; Avail: CASI; A01, Hardcopy; A10, Microfiche

An experiment to test the prediction of Baker and Dash (1989, 1994) that charge transfer in ice contact interactions is associated with the transfer of microscopic quantities of surface melted liquid has been performed. The results, while presenting a new challenge to the model, have clearly illustrated one important phenomenon. Earlier researchers have indicated that charge transfer may be related to the growth state of the ice particles involved, rather than temperature effects. The present work, by presenting charge and mass contact transfer data with respect to the measured growth rate of the ice surfaces, confirms this observation.
Author
Charge Transfer; Mass Transfer; Ice Formation; Cloud Physics

19990108697 Voeikov Main Geophysical Observatory, Leningrad, USSR

Results of Electrical Field Strength Investigations in Convective Clouds

Sinkevich, A. A., Voeikov Main Geophysical Observatory, USSR; Dovgaluk, Ju. A., Voeikov Main Geophysical Observatory, USSR; Ponomarev, Yu. Ph., Voeikov Main Geophysical Observatory, USSR; Stepananeko, V. D., Voeikov Main Geophysical Observatory, USSR; 11th International Conference on Atmospheric Electricity; June 1999, pp. 492-495; In English; See also 19990108601; No Copyright; Avail: CASI; A01, Hardcopy; A10, Microfiche

Relatively small number of electrical field strength investigations in convective clouds were carried out due to danger of aircraft traverses through them and great cost of investigations. Measurements of electric field strength, made by the flying laboratory 11-14 in Russia are analyzed. The electric field strength within the Cu med clouds was found not usually to exceed 600 V/m, mounting to 75 kV/m within the Cu cong-Cb clouds.The impact of crystallizing agent yields an average double electric field strength compared with the natural cycle of cloud development.

Author

Electric Field Strength; Convection Clouds; Cloud Seeding; Cloud Physics

19990108698 Manchester Univ., Physics Dept., UK

Vapor and Heat Supply to Riming Graupel Effect on Charging

Saunders, C. P. R., Manchester Univ., UK; Avila, E. E., Universidad Nacional de Cordoba, Argentina; Peck, S. L., Manchester Univ., UK; Castellano, N. E., Universidad Nacional de Cordoba, Argentina; Varela, G. G. Aguirre, Universidad Nacional de Cordoba, Argentina; 11th International Conference on Atmospheric Electricity; June 1999, pp. 268-271; In English; See also 19990108601; No Copyright; Avail: CASI; A01, Hardcopy; A10, Microfiche

Graupel charging in thunderstorms may involve collisions with ice crystals. Laboratory studies of this process have shown that the charge transfer depends on many variables including the surface states of the interacting particles. This work shows the importance of the supply of heat and vapor to the riming graupel in influencing the sign of the charge transferred. The effects of rimer heating and cloud droplet size are considered.

Author

Charge Transfer; Graupel; Thunderstorms; Particle Collisions

19990108699 Pennsylvania State Univ., Dept. of Meteorology, University Park, PA USA

Studies of Florida Thunderstorms Using LDAR, LLP, and Single Doppler Radar Data

Forbes, Gregory S., Pennsylvania State Univ., USA; Hoffert, Steven G., Template Software, Inc., USA; 11th International Conference on Atmospheric Electricity; June 1999, pp. 496-499; In English; See also 19990108601

Contract(s)/Grant(s): NAG10-0187; NAG10-1054; NAG10-0137; NGT-60002; No Copyright; Avail: CASI; A01, Hardcopy; A10, Microfiche

The paper summarizes results from research conducted on thunderstorms in the vicinity of the Kennedy Space Center (KSC) Florida, between 1993 and 1998. The focus of the research was to identify procedures that would assist weather forecasters at the Cape Canaveral Air Station (CCAS) in real-time detection and forecasting of the lightning threat to launches and daily ground operations at KSC/CCAS sites. The research was divided into three topics: (1) studies aimed at improving the forecasting of the initial cloud-ground (CG) lightning threat, (2) studies aimed at improving the forecasting of the end-of-storm termination of the CG lightning threat, and (3) studies of the location of CG strikes relative to the thunderstorm radar echo and to lightning discharges aloft. Only the first two topics are covered in this preprint.

Author

Lightning; Florida; Thunderstorms; Weather Forecasting; Radar Data; Radar Echoes; Radar Tracking; Cloud-to-Ground Discharges

19990108700 Colorado State Univ., Dept. of Atmospheric Science, Fort Collins, CO USA

Combined Dual-Doppler, Multiparameter Radar, and Lightning Observations of a Severe Convective Storm

Lang, Timothy J., Colorado State Univ., USA; Rutledge, Steven A., Colorado State Univ., USA; Kennedy, Patrick C., CSU-CHILL National Radar Facility, USA; 11th International Conference on Atmospheric Electricity; June 1999, pp. 500-502; In English; See also 19990108601; No Copyright; Avail: CASI; A01, Hardcopy; A10, Microfiche

During the evening of 1 July 1998, a powerful severe convective storm passed through the plains of northeastern Colorado. The storm featured large hail and a possible tornado. Throughout a significant portion of its lifetime, the storm produced large amounts of intracloud (IC) lightning, as measured by a network of electric field change meters, but little cloud-to-ground (CG) lightning, as measured by the National Lightning Detection Network. The CG lightning that did occur during this time was predominantly positive in polarity. This storm passed through the dual-Doppler network formed by the CSU-CHILL

multiparameter radar and the newly installed HOT radar, providing approximately two hours of combined dual-Doppler, multiparameter radar, and lightning observations during significant portions of the storm's mature and decay phases. This level of radar and lightning observations for a severe storm is largely unprecedented, and it provides a wealth of data with which to explore the relationships between the microphysical and kinematic structures of a severe storm and the lightning it produces. Key topics to be examined include relating the microphysical structure, as inferred from multiparameter radar, to the kinematic structure, as inferred from dual-Doppler analysis, for the two hours that these data are available. These radar analyses then will be compared to the amount, type, and predominant polarity of lightning produced, and the results will be discussed in light of previous, less-detailed observational studies of similar storms.
Author
Cloud-to-Ground Discharges; Intracloud Discharges; Radar Tracking; Convection Clouds; Thunderstorms; Radar Data

19990108701 Academy of Sciences (Russia), Inst. of Applied Physics, Nizhny Novgorod, Russia
Turbulent Electric Dynamo in Thunderstorm Clouds
Mareev, E. A., Academy of Sciences (Russia), Russia; 11th International Conference on Atmospheric Electricity; June 1999, pp. 272-275; In English; See also 19990108601; No Copyright; Avail: CASI; A01, Hardcopy; A10, Microfiche

Electric dynamo due to random motion of a medium is of particular interest with respect to numerous applications especially to thunderstorm clouds. In the present paper we focus on the theory of turbulent, electric dynamo in a multi-component multi-flow system and its applications to the thunderstorm electrification problem. The mean field formation in weakly ionized aerosol medium has been investigated, taking into account charging of aerosols due to their collisions during turbulent mixing. The effect of the mean field growth has been found, caused by induction charging of aerosol particles. This phenomenon takes place when the turbulence is intensive enough while the air conductivity is sufficiently small.
Author
Dynamo Theory; Aerosols; Turbulent Mixing; Thunderstorms; Electrification; Charged Particles

19990108702 Washington Univ., Geophysics Program, Seattle, WA USA
Inferring Selected Cloud Properties from Satellite Lightning Data
Schroeder, Vicki, Washington Univ., USA; Baker, M. B., Washington Univ., USA; 11th International Conference on Atmospheric Electricity; June 1999, pp. 276-279; In English; See also 19990108601
Contract(s)/Grant(s): NAG8-1150; NAG8-1512; No Copyright; Avail: CASI; A01, Hardcopy; A10, Microfiche

The recent advent of satellite lightning detection programs has introduced a new potential for obtaining global information about other (hard to measure) cloud properties. We have made use of observations together with numerical model studies to show that positive correlations exist between: (1) lightning flashrate (F) and vertical velocity (w); and (2) flashrate (F) and the amount of condensate (water and ice) lofted through the -10 C isotherm (C(sub u)). The lightning flashrate appears to be very sensitive to the magnitude of the updraft velocity, with F increasing rapidly with w above a threshold of w approx. = 5-10 m/s. by contrast, we have found that the flashrate/condensate relationship appears to be approximately linear. We are currently refining the F-updraft and F-condensate relationships with further model studies before applying them to lightning data from the Optical Transient Detector (OTD) and the Lightning Imaging Sensor (LIS). We hope, with this method, to provide estimates of the large scale vertical water transport by continental convective systems over seasonal timescales.
Author
Vertical Air Currents; Mathematical Models; Cloud Physics; Lightning; Data Correlation; Atmospheric Moisture; Convection Cells

19990108704 Universidad Nacional de Cordoba, FaMAF, Argentina
Contact Time in Ice-Ice Collisions
Caranti, Giorgio M., Universidad Nacional de Cordoba, Argentina; Varela, Guillermo G. Aguirre, Universidad Nacional de Cordoba, Argentina; Pereyra, Rodolfo G., Universidad Nacional de Cordoba, Argentina; 11th International Conference on Atmospheric Electricity; June 1999, pp. 280-283; In English; See also 19990108601; Sponsored in part by CONICOR.; No Copyright; Avail: CASI; A01, Hardcopy; A10, Microfiche

There is strong indication that the interactions among ice particles in clouds are the main cause for their electrification. Therefore a characterization of the collisions themselves is of great importance. In this work we present measurements of contact time in metal-metal, ice-metal and ice-ice collisions by a simple electrical method. The method assumes that the ice is conductive enough to allow a measurable current to flow during contact. The experiments were carried out in a cold room under controlled ambient conditions. Temperatures between -3 to -25 C and impact velocities 0.5 to 2.5 m/s were used for particles formed from tri-distilled water. Preliminary measurements suggest times much longer than theory predicts for ice and for elastic collisions. One

cm spheres at the above velocities give times between 200 and 600 microseconds when they collide with a plane ice surface. These times are more compatible to plastic deformation than to elastic interactions. Variability is also very large, successive collisions of the same sphere can give very different contact times. It was possible to observe that on some occasions fracture developed after the first impact which affected the following one resulting in larger contact times, some times, by a factor greater than 2. The yield for the beginning of cracking or plastic flow whichever come first could be estimated as about 7 bars assuming constant stress during the deformation at - 10 C. Implications for the mechanisms of charge separation in ice-ice collision are discussed.
Author
Impact Velocity; Particle Collisions; Solid-Solid Interfaces; Electrification; Ice Clouds; Charged Particles

19990108705 Missouri Univ., Dept. of Physics and Astronomy, Saint Louis, MO USA
Electrical Structure of Clouds and Thundercloud Electrification
Handel, Peter H., Missouri Univ., USA; 11th International Conference on Atmospheric Electricity; June 1999, pp. 284-287; In English; See also 19990108601; No Copyright; Avail: CASI; A01, Hardcopy; A10, Microfiche

The electrification processes in clouds and thunderclouds determine to a large extent their electrical structure. Therefore, the observed electrical structure can be compared with the structure calculated on the basis of various electrification models. The models used include charge transfer between ice crystals and riming graupel pellets, the inductive mechanism, a combination of these two models, and also the polarization catastrophe model. Both the electric field profile and the charge density profile are calculated. For the polarization catastrophe model, the free energy of the cloud is calculated as a function of the order parameter and is minimized in two stages. First, the free energy is minimized for a homogeneous cloud, and then large-scale inhomogeneities are considered. The free energy is finally minimized in the presence of arbitrary inhomogeneities. This later step leads in certain conditions to the generation of a structure which is characterized by thick horizontal sheets of alternating polarization direction and by thin horizontal space charge regions of polarization charges and masking charges separating them. Finally, both the characteristic times governing the transition from an arbitrary non-equilibrium state to the polarized state, and the stratification times during which a stratified structure is obtained, are estimated theoretically. Considering these four electrification models, the theoretical field and charge distributions are compared with the experimental field and charge distributions in nimbostratus, cumulonimbus, in stratus clouds and in mesoscale convective system (MCS) stratus formations. In particular, the observed altitude dependence of the length scale of the field-reversals in the upper regions of MCS stratus formations is compared with the altitude dependence of the theoretical field-reversal length scales obtained from the four models considered. Furthermore, the measured charge densities are compared with the theoretical charge densities in the corresponding horizontal layers. The observed and calculated characteristic times are also compared. Finally, the position and timing of the expected flashes is roughly estimated for the four models and compared with the airborne observations of Christian et al. These observations included thunder reconstruction which located the sources of the first flash of a thunderstorm cell and of the subsequent flashes from progressively lower levels in the cloud. The acoustic sources were correlated with regions of high radar reflectivity. The coincident timing and localization of the reflectivity maxima and earliest sound sources provides a particularly sensitive discrimination of the four models considered.
Author
Cumulonimbus Clouds; Electric Fields; Electrification; Mesoscale Phenomena; Nimbostratus Clouds; Thunderstorms; Charge Distribution; Polarization (Charge Separation)

19990108706 National Severe Storms Lab., Norman, OK USA
Electric Field Profiles in a Mesoscale Convective System with Multiple Bow Echoes 25 May 1998 During the MCS Electrification and Polarization Radar Study (MEaPRS)
Rust, W. D., National Severe Storms Lab., USA; Marshall, T. C., Mississippi Univ., USA; Stolzenburg, M., Mississippi Univ., USA; Jorgensen, D. P., National Severe Storms Lab., USA; Shepherd, T. R., Oklahoma Univ., USA; MacGorman, D. R., National Severe Storms Lab., USA; 11th International Conference on Atmospheric Electricity; June 1999, pp. 507-510; In English; See also 19990108601
Contract(s)/Grant(s): NSF ATM-98-07179; No Copyright; Avail: CASI; A01, Hardcopy; A10, Microfiche

Two mobile laboratories for mobile ballooning and a NOAA P-3 instrumented aircraft equipped with airborne Doppler radar were used to probe a mesoscale convective system (MCS) on 25 May 1998. The main convection region was aligned east to west (along the Kansas border) with storm motion from 287 deg at 15 m/s. The overall structure of the MCS was deep convection on the south side with a transition zone and large stratiform region on the north side. The MCS produced a series of eight bow-shaped radar echoes that moved rapidly during the night from 0000 UTC to 1200 UTC. Two electric field profiles were accomplished in the convective regions of two successive convective bow echoes. The magnitude of the maximum measured electric field, E, was about 100 kV/m. The majority of the ground flashes in the convective region were positive. A third sounding was made in

the transition zone about 100 km north-northeast of the soundings in the convective region. Very few transition-zone soundings are in the literature: This one shows a peak E = 100 kV/m and an inferred five regions of charge, with positive lowermost. Another profile was made into the rearmost part of the stratiform precipitation region about 55 km north-northeast and downwind of the transition zone launch site. The peak E magnitude was about 25 kV/m; there were three alternating charge regions, with negative lowest. The final sounding was just at the back edge of the stratiform region. The E was less than 5 kV/m along the flight path. Maximum reflectivity in the stratiform rain region was 35-40 dBZ, about typical for mid-latitude MCSs. The electric field and inferred charge regions from the soundings are combined with Doppler derived horizontal winds and reflectivities.
Author
Thunderstorms; Mesoscale Phenomena; Radar Echoes; Electric Fields; Electrification; Radar Tracking; Atmospheric Sounding

19990108707 South Dakota School of Mines and Technology, Inst. of Atmospheric Sciences, Rapid City, SD USA
An Examination of the Convective Charging Hypothesis
Helsdon, J. H., South Dakota School of Mines and Technology, USA; Gattaleeradapan, S., South Dakota School of Mines and Technology, USA; Farley, R. D., South Dakota School of Mines and Technology, USA; 11th International Conference on Atmospheric Electricity; June 1999, pp. 288-291; In English; See also 19990108601
Contract(s)/Grant(s): NSF ATM-92-00698; NSF ATM-96-13679; No Copyright; Avail: CASI; A01, Hardcopy; A10, Microfiche

An examination of the convective charging hypothesis is undertaken using the 3D Storm Electrification Model (SEM). Elements of the model relevant to the convective hypothesis are the full treatment of polar small ions including attachment to hydrometeors, the inclusion of point discharge from the surface depending on the electric field strength, the 3D motion field associated with storm development, and the components of the Maxwell current. Simulations for both a small storm and a large storm were run to test the efficacy of convective charging in two very different dynamic frameworks. Each storm was also simulated using anoninductive charging mechanism to compare the magnitude and development of the attendant electrification. The simulations show that, while the Maxwell current distributions for conduction and convection are as envisaged by Vonnegut, the magnitude is not great enough to provide any significant electrification to these storms during their life cycles. Use of a noninductive charging mechanism leads to significant electrification for both storms.
Author
Electrification; Electric Charge; Particle Charging; Mathematical Models; Computerized Simulation; Convective Flow; Charge Distribution

19990108708 NASA Marshall Space Flight Center, Huntsville, AL USA
Cloud-to-Ground Lightning Characteristics of a Major Tropical Cyclone Tornado Outbreak
McCaul, Eugene W., Jr., Universities Space Research Association, USA; Buechler, Dennis, Alabama Univ., USA; Goodman, Steven J., NASA Marshall Space Flight Center, USA; 11th International Conference on Atmospheric Electricity; June 1999, pp. 511-514; In English; See also 19990108601; No Copyright; Avail: CASI; A01, Hardcopy; A10, Microfiche

It is well known that most tropical cyclones (TCs) that make landfall along the Gulf coast of the USA spawn at least a few tornadoes. Although most landfalling TCs generate fewer than a dozen such tornadoes, a small proportion produce large swarm outbreaks, with as many as 25 or more tornadoes. Usually, these major outbreaks occur in large, intense hurricane-strength TCs, but on 15-17 August 1994 Tropical Storm Beryl spun off 37 tornadoes along its path from the Florida panhandle through the mid-Atlantic states. Some 32 of these tornadoes occurred on 16 August 1994 from eastern Georgia to southern Virginia, with most of these taking place in South Carolina. Beryl's 37 tornadoes moved it into what was at that time fifth place historically in terms of TC tornado productivity. The Beryl outbreak is especially noteworthy in that at least three of the tornadoes achieved peak intensity of F3 on the Fujita damage intensity scale. Although no fatalities resulted from the Beryl outbreak, at least 50 persons suffered injuries, and property damages totalled more than $50 million . The Beryl outbreak is a good example of a TC whose greatest danger to the public is its post-landfall severe weather. In this respect, and in the character of its swarm outbreak of tornadoes, it resembles another large tornado outbreak spawned by a relatively weak TC, Hurricane Danny of 1985). In the Danny outbreak, numerous shallow mini-supercell storms were found to have occurred, and it was noted that, because of the storms' relatively shallow depth, cloud-to-ground (CG) lightning was negligible. Better observations of future TC tornado outbreaks, especially with modern surveillance tools such as Doppler radars and the National Lightning Detection Network (NLDN), were recommended. Although the Beryl tornado outbreak is not the first set of TC-spawned tornado storms to be observed with the NLDN, it is one of the largest and likely the most intense such outbreak. The purpose of this paper is to document the NLDN-derived CG lightning characteristics of Beryl's tornadic storms, and to see how they compare with observations of CG lightning activity in other types of severe storms. In particular, we attempt to quantify the CG flash rates of TC tornadic cells, and

to discover if there are any characteristics of their CG activity that may be useful to operational forecasters seeking to distinguish which cells are most likely to produce severe weather.
Derived from text
Hurricanes; Tornadoes; Cloud-to-Ground Discharges; Radar Tracking; USA

19990108709 Universidad Nacional de Cordoba, Faculty of Mathematics and Physics, Argentina
The Effect of the Cloud Droplet Spectrum on Electrical Charge Transfer During Individual Ice-Ice Collisions
Pereyra, Rodolfo, Universidad Nacional de Cordoba, Argentina; Avila, Eldo E., Universidad Nacional de Cordoba, Argentina; Caranti, Giorgio M., Universidad Nacional de Cordoba, Argentina; Varela, Guillermo G. Aguirre, Universidad Nacional de Cordoba, Argentina; 11th International Conference on Atmospheric Electricity; June 1999, pp. 292-295; In English; See also 19990108601; No Copyright; Avail: CASI; A01, Hardcopy; A10, Microfiche

New experiments were performed with a wind tunnel in a cold room in order to investigate the influence of the cloud droplet spectrum on the charges transferred during ice-ice collisions. A fixed artificial graupel growing by riming, placed inside a wind tunnel, is collided by ice spheres. The experiments were performed using two different cloud droplet spectra; the ice spheres used were of about 100 microns in diameter; the impact velocity around 4 m/s. The ambient temperature (T(sub a)) was varied in the range -10 to -30 C. The effective water content EW, was between 0.2 and 1.1 g/cu m. The results show that the predominant sign of the charge transfer for a set of given conditions is dependent on the cloud droplet spectrum which means that the charge sign reversal temperature is also a function of the spectrum. In particular, using smaller droplets, the reversal sign occurs below -25 C, while for larger droplets the reversal sign is produced at -18 C. These results show that the droplet spectrum is an important parameter to keep under control when natural cloud conditions are being simulated.
Author
Charge Transfer; Particle Collisions; Drops (Liquids); Electric Charge; Ice Clouds; Polarization (Charge Separation); Spectrum Analysis

19990108710 NASA Marshall Space Flight Center, Huntsville, AL USA
Total Lightning Activity Associated with Tornadic Storms
Goodman, Steven J., NASA Marshall Space Flight Center, USA; Buechler, Dennis, Alabama Univ., USA; Hodanish, Stephen, National Weather Service, USA; Sharp, David, National Weather Service, USA; Williams, Earle, Massachusetts Inst. of Tech., USA; Boldi, Bob, Massachusetts Inst. of Tech., USA; Matlin, Anne, Massachusetts Inst. of Tech., USA; Weber, Mark, Massachusetts Inst. of Tech., USA; 11th International Conference on Atmospheric Electricity; June 1999, pp. 515-518; In English; See also 19990108601; No Copyright; Avail: CASI; A01, Hardcopy; A10, Microfiche

Severe storms often have high flash rates (in excess of one flash per second) and are dominated by intracloud lightning activity. In addition to the extraordinary flash rates, there is a second distinguishing lightning characteristic of severe storms that seems to be important. When the total lightning history is examined, one finds sudden increases in the lightning rate, which we refer to as lightning ”jumps,” that precede the occurrence of severe weather by ten or more minutes. These jumps are typically 30-60 flashes/min, and are easily identified as anomalously large derivatives in the flash rate. This relationship is associated with updraft intensification and updraft strength is an important factor in storm severity (through the accumulation of condensate aloft and the stretching of vorticity). In several cases, evidence for diminishment of midlevel rotation and the descent of angular momentum from aloft is present prior to the appearance of the surface tornado. Based on our experience with severe and tornadic storms in Central Florida, we believe the total lightning may augment the more traditional use of NEXRAD radars and storm spotters. However, a more rigorous relation of these jumps to storm kinematics is needed if we are to apply total lightning in a decision tree that leads to improved warning lead times and decreased false alarm rates.
Author
Tornadoes; Lightning; Radar Tracking; Florida; Direction Finding

19990108711 University of Central Florida, Dept. of Electrical and Computer Engineering, Orlando, FL USA
Charge Transfer Process During Collision of Riming Graupel Pellet with Small Ice Crystals within a Thundercloud
Datta, Saswati, University of Central Florida, USA; De, Utpal K., Jadavpur Univ., India; Goswami, K., Jadavpur Univ., India; Jones, Linwood, University of Central Florida, USA; 11th International Conference on Atmospheric Electricity; June 1999, pp. 296-299; In English; See also 19990108601; No Copyright; Avail: CASI; A01, Hardcopy; A10, Microfiche

A charge transfer process during the collision of a riming graupel pellet and an ice-crystal at low temperature is proposed. During riming, the surface structure of graupel deviates from perfect crystalline structure. A concept of quasi-solid layer (QSL) formation on the surface is introduced. This QSL contains defects formed during riming. In absence of impurities, positively charged X-defect abundance is considered in the outer layer. These defects are assumed to be the charge carriers during the charge

transfer process. Some part of the QSL is stripped off by the colliding ice crystals, which thereby gain some positive charge, leaving the graupel pellet negatively charged. With the proposed model, fC to pC of charge transfer is observed per collision. A transition temperature between -10 C to -15 C is also noted beyond which the QSL concept does not hold. This transition temperature is dependent on the bulk liquid water content of the cloud.
Author
Charge Transfer; Particle Collisions; Graupel; Ice; Mathematical Models; Cumulonimbus Clouds

19990108712 Polish Academy of Sciences, Inst. of Geophysics, Warsaw, Poland
Electric Charge on Raindrops During Thunderstorm Precipitations
Baranski, P., Polish Academy of Sciences, Poland; 11th International Conference on Atmospheric Electricity; June 1999, pp. 300-303; In English; See also 19990108601; No Copyright; Avail: CASI; A01, Hardcopy; A10, Microfiche

The ground-based measurements of electric charge on the raindrops (or other precipitation particles) that was brought to the earth surface during thunderstorm were carried out in Warsaw thunderstorms throughout summer seasons of 1996, 1997 and 1998. The examination of the obtained data, together with the data from simultaneous measurements of the electric field and the Maxwell current (total and convective component), allowed us to distinguish different types of observed storms. The electrical parameters used to characterize the charge transport during the period of the considered rainfall are as follows: numbers of positive (N+) and negative (N-) drops counted in the given time interval (delta t); total positive (I(sub p))+ and negative (I(sub p))- precipitation current for At; total positive (Q+) and negative (Q-) electric charge of drops for delta t; average positive charge <q+ of a single drop for delta t; average negative charge <q– of a single drop for delta t; and precipitation charge density D=(Q+ + Q-)/S, where S is the entrance area of the measuring device. In spite of various difficulties discussed, ground based measurements of the electrical properties of thundercloud precipitation seem to be able to bring some valuable information concerning electrical structure and electrification processes acting in the observed cloud and below it.
Author
Raindrops; Electrical Properties; Thunderstorms; Charge Transfer

19990108713 Obirin Univ., School of International Studies, Machida, Japan
Reversal of the Sign of the Charge on Graupel During Riming Electrification: Measurements in Hokuriku Winter Clouds and in a Wind Tunnel
Takahashi, Tsutomu, Obirin Univ., Japan; 11th International Conference on Atmospheric Electricity; June 1999, pp. 304-307; In English; See also 19990108601; No Copyright; Avail: CASI; A01, Hardcopy; A10, Microfiche

Riming electrification was examined in a wind tunnel in which semi-hemispherical ice particles were floated in updrafts of either 3 or 9 m/s. Cloud drops and ice crystals were then introduced into the tunnel and the ice particles were subsequently forced to fall through an induction ring. The experiments were conducted in three different critical regimes: water content at 1 gm/cu m at -15 C; water content at 0.2 gm/cu m at -15 C; and water content at 1 gm/cu m at -5 C. The results of the experiments showed the ice particles to be highly charged when both cloud drops and ice crystals were supplied and the charge sign reversal to occur at the temperature and cloud water content previously reported by Takahashi (1978).
Author
Graupel; Ice Clouds; Moisture Content; Charge Transfer; Electrification; Electric Charge

19990108714 NASA Marshall Space Flight Center, Huntsville, AL USA
The 1997-98 El-Nino Event and Related Lightning Variations in the Southeastern USA
Buechler, D. E., Alabama Univ., USA; Goodman, S. J., NASA Marshall Space Flight Center, USA; McCaul, E. W., Universities Space Research Association, USA; Knupp, K., Alabama Univ., USA; 11th International Conference on Atmospheric Electricity; June 1999, pp. 519-522; In English; See also 19990108601; No Copyright; Avail: CASI; A01, Hardcopy; A10, Microfiche

The El Nino Southern Oscillation (ENSO) is a climate anomaly responsible for world-wide weather impacts ranging from droughts to floods. In the United States, warm episode years are known to produce above normal rainfall along the Southeast US Gulf Coast and into the Gulf of Mexico, with the greatest response observed in the October-March period of the current warm-episode year. The 1997-98 warm episode, notable for being the strongest event since 1982-83, presents our first opportunity to examine the response to a major ENSO event and determine the variation of wintertime thunderstorm activity in this part of the world. Due to the recent launch of a lightning sensor on NASA's Tropical Rainfall Measuring Mission (TRMM) in November 1997 and the expanded coverage of the National Lightning Detection Network (NLDN), we are able to examine such year-to-year changes in lightning activity with far greater detail than ever before.
Author
El Nino; Lightning; USA; Thunderstorms

19990108715 Botswana Univ., Dept. of Physics, Gaborone, Botswana

Separation of Charge During Rebounding Collisions Between Graupel as a Possible Mechanism of Thunderstorm Electrification

Jayaratne, E. Rohan, Botswana Univ., Botswana; 11th International Conference on Atmospheric Electricity; June 1999, pp. 308-311; In English; See also 19990108601; No Copyright; Avail: CASI; A01, Hardcopy; A10, Microfiche

A laboratory study was conducted in a large chest freezer to determine the sign and magnitude of the electric charge separated during rebounding collisions between graupel. A cloud of supercooled droplets was drawn through a tube to form a deposit of soft rime on a wire mesh. A rimed metal rod simulating a graupel pellet was mounted downwind of the mesh. The rod could be heated or cooled by means of a Peltier element. With the air flow on, the fragments of rime were gently dislodged from the mesh and allowed to impact on the graupel target. The charge separated on impact was measured at an air temperature of -15 C. The graupel charged negatively when it was warmer than the fragments of rime and positive when its temperature was more than about 2 C colder. The introduction of droplets into the airstream shifted the charge reversal temperature to warmer values. In nature, owing to the latent heat released by the accretion of supercooled droplets, larger graupel pellets are generally warmer and fall faster than the smaller pellets. Resulting interactions between these particles followed bv subsequent gravitational separation may thus lead to a dipolar charge structure with the smaller positively charged graupel above the larger negatively charged pellets. It is suggested that this process may form the basis of a viable charge generation mechanism in thunderstorms which may explain the reported existence of graupel pellets carrying charges larger than that can be expected by interactions with vapor grown ice crystals alone.

Author

Electric Charge; Thunderstorms; Polarization (Charge Separation); Graupel; Electrification

19990108716 Global Hydrology and Climate Center, Huntsville, AL USA

A Comparison Between Lightning Activity and Passive Microwave Measurements

Driscoll, Kevin, Global Hydrology and Climate Center, USA; 11th International Conference on Atmospheric Electricity; June 1999, pp. 523-526; In English; See also 19990108601; No Copyright; Avail: CASI; A01, Hardcopy; A10, Microfiche

For more than a decade, space-based passive microwave radiometers have been used to infer a variety of climatological information, including precipitation, cloud water content, and cloud ice content. The microwave frequencies at 37 and 85 GHz are particularly useful in identifying storm systems with high ice content, due to the properties of ice which cause the scattering of upwelling radiation from the surface of the Earth. An examination of data from the Lightning Imaging Sensor and the TRMM Microwave Imager suggests that storms with the highest frequency of total lightning also possess the most pronounced microwave scattering signatures at 37 and 85 GHz. A total of 292 individual thunderstorms were examined, and a log-linear relationship was shown to exist between the number of optical lightning pulses produced by each storm and the corresponding microwave brightness temperatures. This relationship is consistent throughout the seasons in a variety of regimes, suggesting that there is a global dependence between lightning activity and cloud ice content.

Author

Lightning; Thunderstorms; Ice Clouds; Microwave Imagery; Microwave Scattering; Brightness Temperature

19990108717 NASA Marshall Space Flight Center, Huntsville, AL USA

High-Altitude Aircraft-Based Electric-Field Measurements Above Thunderstorms

Bateman, M. G., Universities Space Research Association, USA; Blakeslee, R. J., NASA Marshall Space Flight Center, USA; Bailey, J. C., Raytheon ITSS, USA; Stewart, M. F., Alabama Univ., USA; Blair, A. K., Alabama Univ., USA; 11th International Conference on Atmospheric Electricity; June 1999, pp. 527-529; In English; See also 19990108601; No Copyright; Avail: CASI; A01, Hardcopy; A10, Microfiche

We have developed a new set of eight electric field mills that were flown on a NASA ER-2 high-altitude aircraft. During the Third Convection and Moisture EXperiment (CAMEX-3; Fall, 1998), measurements of electric field, storm dynamics, and ice microphysics were made over several hurricanes. Concurrently, the TExas-FLorida UNderflights (TEFLUN) program was being conducted to make the same measurements over Gulf Coast thunderstorms. Sample measurements are shown: typical flight altitude is 20km. Our new mills have an internal 16-bit A/D, with a resolution of 0.25V/m per bit at high gain, with a noise level less than the least significant bit. A second, lower gain channel gives us the ability to measure fields as high as 150 kV/m.

Author

Electric Field Strength; Electrical Measurement; Thunderstorms; Airborne Equipment; Hurricanes

19990108718 National Center for Atmospheric Research, Boulder, CO USA

Lightning Discharge Locations Relative to Reflectivity and Updraft/Downdraft Structures in a Colorado Thunderstorm

Dye, J. E., National Center for Atmospheric Research, USA; Matejka, T., National Severe Storms Lab., USA; Laroche, P., Office National d'Etudes et de Recherches Aerospatiales, France; Defer, E., Office National d'Etudes et de Recherches Aerospatiales, France; Hubler, G., National Oceanic and Atmospheric Administration, USA; Rutledge, S. A., Colorado State Univ., USA; 11th International Conference on Atmospheric Electricity; June 1999, pp. 530-533; In English; See also 19990108601; No Copyright; Avail: CASI; A01, Hardcopy; A10, Microfiche

The Stratospheric-Tropospheric Experiment: Radiation, Aerosols and Ozone (STERAO) Deep Convection project was conducted in NE Colorado in June/July 1996 to investigate the production of NOx (= NO + NO2) by lightning and vertical transport of chemical species by thunderstorms. Herein we report on the location of VHF sources along lightning channels detected by the ONERA lightning interferometer within the 10 July thunderstorm. The location of these sources is examined relative to the reflectivity determined from the Colorado State University CHILL multi-parameter radar and airflow structure derived from multiple Doppler radar analyses using NOAA WP3D tail Doppler radar and CHILL measurements. During the intense multicell stage of the storm most of the VHF lightning sources were in moderate updrafts with many sources also in the core updraft. Interestingly there were only a few VHF lightning sources in the main downdraft, although the paucity of sources in the downdrafts was not true during the entire storm lifetime. Results from this and other periods during the 5 hour storm history are presented.

Author

Lightning; Reflectance; Thunderstorms; Radar Measurement; Vertical Air Currents

19990108719 Botswana Univ., Dept. of Physics, Gaborone, Botswana

Thunderstorm Electrification: The Effect of Chemical Impurities in Cloud Water

Jayaratne, E. Rohan, Botswana Univ., Botswana; 11th International Conference on Atmospheric Electricity; June 1999, pp. 312-315; In English; See also 19990108601; No Copyright; Avail: CASI; A01, Hardcopy; A10, Microfiche

It is known that trace chemical impurities in cloud water may control the sign and magnitude of the electric charge separated when vapor-grown ice crystals rebound off riming graupel - a mechanism thought to be responsible for the electrification of thunderstorms. In a series of laboratory experiments, ice crystals interacting with a simulated graupel pellet charged the graupel negatively, when the riming cloud droplets contained traces of sodium chloride. Ammonium salts in the droplets had the opposite effect of charging the graupel positively. A very similar result was observed when particles of sand were made to rebound off a steel target coated with slightly contaminated ice. In all cases. the magnitude of the charge separated increased sharply as the temperature decreased. The results of the two sets of experiments are compared in an attempt to understand the physical mechanism controlling the charge transfer. The results also have important bearing on the location of charge centers in thunderstorms forming over different geographical regimes such as deep continental interiors and in maritime environments.

Author

Thunderstorms; Electrification; Impurities; Electric Charge; Charge Transfer; Drops (Liquids); Trace Contaminants; Cloud Physics

19990108720 Toulouse Univ., Lab. d'Aerologie, France

Estimation of the Total Corona Charge Transfer From the Surface to the Thundercloud

Chauzy, Serge, Toulouse Univ., France; Soula, Serge, Toulouse Univ., France; 11th International Conference on Atmospheric Electricity; June 1999, pp. 316-319; In English; See also 19990108601; No Copyright; Avail: CASI; A01, Hardcopy; A10, Microfiche

The present work estimates the efficiency of the convective charging mechanism, by computing the amount of ground corona charge which is expected to reach cloud base by conduction and convection processes during the lifetime of a thunderstorm. This estimate is made using the numerical model PICASSO, previously designed to characterize the evolution of the ground corona space charge, and initiated by the surface electric field evolution measured during six events. The overall charge amount roughly estimated for the considered events suggests that the convective charging mechanism is unlikely to account for one of the major electrification processes of the thundercloud. However, it could be considered as a relevant mechanism contributing to the lower positive charge center of the thundercloud.

Author

Thunderstorms; Cumulonimbus Clouds; Charge Transfer; Mathematical Models; Electrification; Electric Corona

19990108721 Centre National de la Recherche Scientifique, Laboratoire d'Aerologie, Toulouse, France

Discharge Initiation by Uncharged Raindrops Falling at Terminal Velocity in a Horizontal Electric Field

Coquillat, S., Centre National de la Recherche Scientifique, France; Chauzy, S., Centre National de la Recherche Scientifique, France; Georgis, J. F., Centre National de la Recherche Scientifique, France; Combal, B., Centre National de la Recherche Scientifique, France; Silvani, X., Centre National de la Recherche Scientifique, France; 11th International Conference on Atmospheric Electricity; June 1999, pp. 320-323; In English; See also 19990108601; No Copyright; Avail: CASI; A01, Hardcopy; A10, Microfiche

The behavior of uncharged raindrops falling at terminal velocity in still air and submitted to a horizontal electric field is analyzed by means of a laboratory experiment and by modeling. In the former, the disruption field is measured and compared to previous results. Moreover, the electrical circuit is designed to detect the bi-directional discharge using a 2-channel digital oscilloscope. The amount of charge involved in the discharge process is therefore evaluated. In the latter, the previous model by Coquillat and Chauzy [1993] is adapted to the horizontal field configuration and the disruption field, the change in fall speed, and the corona occurrence altitude are computed. As expected, the corona emission from raindrops is more easily triggered in a horizontal than in a vertical ambient field.

Author

Raindrops; Electric Fields; Electrification; Electric Discharges

19990108722 Main Geophysical Observatory, Research Center for Atmospheric Remote Sounding, Saint Petersburg, Russia

Data Processing at Special Data Center on the Surface Layer Atmospheric Electricity: A. I. Voeikov MGO RC ARS

Shvarts, Ya. M., Main Geophysical Observatory, Russia; Petrenko, I. A., Main Geophysical Observatory, Russia; Shchukin, G. G., Main Geophysical Observatory, Russia; 11th International Conference on Atmospheric Electricity; June 1999, pp. 536-538; In English; See also 19990108601; No Copyright; Avail: CASI; A01, Hardcopy; A10, Microfiche

Measurements of atmospheric electric field potential gradient and polar air electric conductivity's are being continued at several meteorological stations of the Russia Hydrometeorological Service. Special data center on the surface layer atmospheric electricity (SDC/AE) collects, processes and archives data of these measurements. SDC/AE provides a safety of the archive and an access to it, including the archive of the WDC/AE. The operation of the SDC/AE are described. The need is underlined for a resumption of the information exchange between the SDC/AE and the AE stations, which are placed beyond the Russia frontiers.

Author

Atmospheric Electricity; Electric Fields; Data Processing

19990108723 Sofia Univ., Faculty of Physics, Bulgaria

Effect of Droplet Size on Graupel Surface Properties in Connection with Noninductive Charge Transfer

Mitzeva, Rumjana, Sofia Univ., Bulgaria; Kassabova, Tzveta, Sofia Univ., Bulgaria; Saunders, Clive, Manchester Univ., UK; 11th International Conference on Atmospheric Electricity; June 1999, pp. 324-327; In English; See also 19990108601

Contract(s)/Grant(s): NZ-624/96; 330/98; No Copyright; Avail: CASI; A01, Hardcopy; A10, Microfiche

Results from a numerical study concerning the effect of droplet size on graupel surface properties (surface temperature, growth rate of graupel size, sublimation/deposition) are presented. The calculations are based on the published equations for graupel surface temperature and growth rate by vapor diffusion. to account for the fact that graupel surface temperature depends on droplet size the results from laboratory experiments in UMIST concerning the beat balance and ventilation coefficient of riming graupel as a function of the droplet spectrum were used. The results demonstrate the significant effect of cloud droplet size on graupel surface properties, hence on the sign of the noninductive charge transferred.

Author

Drop Size; Raindrops; Graupel; Surface Properties; Charge Transfer

19990108727 Hokkaido Univ. of Education, Dept. of Physics, Iwamizawa, Japan

On Charging Phenomena in Snowstorm

Shio, Hisashi, Hokkaido Univ. of Education, Japan; 11th International Conference on Atmospheric Electricity; June 1999, pp. 328-331; In English; See also 19990108601; No Copyright; Avail: CASI; A01, Hardcopy; A10, Microfiche

Charging phenomenon of snowstorms were investigated at ASAHI-Hill (Height: 1970 m). Results were obtained as rollows: 1) In a case of snowstorm with precipitation, snowflakes drifting in lower layer (height 2 m) were positively charged, while those drifting in higher layer (height 2 m) were negatively charged. During all periods in the snowstorms, total of charge of snowflakes collected in Faraday Cage is electrically neutral, namely to be near zero mV. These results bring us to the conclusion that a snow crystal is separated into two kinds of snowflakes charged positively and negatively by the destroying of the snow crystal; 2) In a case of snowstorms consisting irregularly formed ice particles generated by peeling of hardened snowfield hardened by powerful

wind pressures, a charge polarity was controlled by crystallographic characteristics of particularly windward area of hardened snow field where the ice particles were generated by peeling off and the ice particles became to be charged by saltating of them.
Author
Snowstorms; Electrification; Electric Charge; Ice; Polarity

19990108728 Odessa State Univ., Laboratory of Physics and Aerodisperse Systems, USSR
The Electric Charge's Separation During Break-Up of the Electrolyte Solutions
Kolpakov, A. V., Odessa State Univ., USSR; Maliarova, L. V., Odessa State Univ., USSR; Titova, E. I., Odessa State Univ., USSR; 11th International Conference on Atmospheric Electricity; June 1999, pp. 332-334; In English; See also 19990108601; No Copyright; Avail: CASI; A01, Hardcopy; A10, Microfiche

The electric charges of cloud drops containing NaCl solutions of different low concentrations were measured. The drops were created during break-up of the liquid in the generator of monodisperse drops of vibrating needle type. Such a characteristic as monodispersion doesn't determine unambiguously the physical and chemical properties of the drop's arising during break-up of the liquid of the same composition. The identity of mechanical process of formation for separate drops is of much importance. Only in such a case the properties of the drops of the same dimensions (d(sub k)) will be the same. Such drops may be called monoparametric. For monoparametric drops of different dimensions we have obtained the dependencies of the value of electric charges (q) with the concentration of the solution (c). The charge (q) arises during the process of break-up by the separating of the double electric layer. The curves of the function q=f(c) for solution of NaCl (d=const) have typical minimum at the same concentration of the NaCl solution for drops of different dimensions. It shows the complex character of the process of separation of electric charges.
Author
Sodium Chlorides; Drops (Liquids); Electrolytes; Electric Charge; Polarization (Charge Separation)

19990108729 Office National d'Etudes et de Recherches Aerospatiales, Chatillon, France
Thunderstorm and Lightning Development: Modeling and Observations
Solomon, Robert, Office National d'Etudes et de Recherches Aerospatiales, France; Thery, Claire, Office National d'Etudes et de Recherches Aerospatiales, France; Defer, Eric, Office National d'Etudes et de Recherches Aerospatiales, France; Bondiou–Clergerie, Anne, Office National d'Etudes et de Recherches Aerospatiales, France; 11th International Conference on Atmospheric Electricity; June 1999, pp. 335-338; In English; See also 19990108601
Contract(s)/Grant(s): NCC8-142; No Copyright; Avail: CASI; A01, Hardcopy; A10, Microfiche

We use results of a numerical model of convective clouds with a lightning parameterization to examine thunderstorm development and the location of lightning initiation in a Florida storm. These results are compared with radar observations and interferometric measurements of VHF emissions from both intra-cloud (IC) and cloud-to-ground (CG) lightning flashes. Observed rate and mean duration of flashes are analyzed through model results, and we comment altitudes of VHF sources given by the ONERA 3D interferometric system.
Author
Thunderstorms; Mathematical Models; Cloud-to-Cloud Discharges; Cloud-to-Ground Discharges; Convection Cells

19990108730 Lanzhou Inst. of Plateau Atmospheric Physics, China
Simulation Study of Non-Inductive Charging and Discharge Processes in the Thunderstorm
Zhang, Yijun, Lanzhou Inst. of Plateau Atmospheric Physics, China; Yan, Muhong, Lanzhou Inst. of Plateau Atmospheric Physics, China; Liu, Xinsheng, Lanzhou Inst. of Plateau Atmospheric Physics, China; 11th International Conference on Atmospheric Electricity; June 1999, pp. 339-342; In English; See also 19990108601
Contract(s)/Grant(s): KZ951-B1-405; NNSFC-49775254; No Copyright; Avail: CASI; A01, Hardcopy; A10, Microfiche

An axisymmetric, time-dependent numerical cloud model has been applied to study non-inductive charging and discharge characteristics in thunderstorms. The affect of environmental stratification factors, convection, rainfall and ice crystal size distribution on charging process and the relationships among convection, precipitation and lightning are discussed.
Author
Mathematical Models; Thunderstorms; Computerized Simulation; Electric Discharges; Electrification; Cloud Physics

19990108731 Indian Inst. of Tropical Meteorology, Poona, India
Rate of Evaporation of the Charged and Uncharged Water Drops Suspended in the Air Stream of a Wind Tunnel
Kamra, A. K., Indian Inst. of Tropical Meteorology, India; Bhalwankar, Rohini V., Indian Inst. of Tropical Meteorology, India; Sathe, A. B., Indian Inst. of Tropical Meteorology, India; 11th International Conference on Atmospheric Electricity; June 1999,

pp. 343-346; In English; See also 19990108601; No Copyright; Avail: CASI; A01, Hardcopy; A10, Microfiche

A laboratory simulation experiment has been performed to study the effect of ventilation on the rate of evaporation of millimeter-sized charged and uncharged water drops falling at terminal velocity in air. Water drops range in size from 1.91 is greater than D is greater than 4.10 mm and carry a charge of 10(exp -10)C. The mean ventilation coefficients computed for each size of the drop have been plotted against (N(sub Sc)exp 1/3)(N(sub Re)exp 1/2) where N(sub Sc) is the Schmidt number and N(sub Re) is the Reynold's number. Our results for the uncharged drops are in conformity with those of Pruppacher and Rasmussen (1979). However, these results show that charged drops evaporate at a rate slower than that of uncharged drops. Moreover, the effect of ventilation is stronger on the evaporation of uncharged drops than that of charged drops. The results are interpreted in terms of the changes in terminal velocity, distortion and oscillation of the water drops when these are charged. The distance which is required for a water drop to fall from cloud base through a NACA Standard Atmosphere of various relative humidites in order to reach the earth's surface with a given size has been computed. The calculations show that at the cloud base, a charged water drop is required to be smaller in size as compared to an uncharged drop in order to reach the earth's surface with the same size. Author

Raindrops; Evaporation; Air Flow; Charged Particles; Ventilation

19990108732 Universidad Nacional de Cordoba, FaMAF, Argentina

A Study of the Ion Attachment by Droplets in Cloud Conditions: Implication for Pollutant Transport

Caranti, G. M., Universidad Nacional de Cordoba, Argentina; Masuelli, S., Universidad Nacional de Cordoba, Argentina; 11th International Conference on Atmospheric Electricity; June 1999, pp. 347-350; In English; See also 19990108601; No Copyright; Avail: CASI; A01, Hardcopy; A10, Microfiche

In this work, we study the ion attachment by droplets for a wide range of ambient conditions. by means of a numerical model we simulate the ion trajectories in the fields (air flow and electrical) determined by a spherical charged conductor immersed in uniform ambient electric and air velocity field. From these trajectories we calculated the capture cross section and the ion current. This cross section depends on many variables: droplet radius, ambient electric field, droplet charge, droplet terminal velocity, ion mobility, air viscosity, etc. It is important to note that, when the electric field is not vertically oriented, this problem becomes a three dimensional and a much more complex one. We studied various different situations depending on what force was predominant, the electrical (due to droplet charge or due to ambient electric field) or the aerodynamical. Both ion mobilities and ambient parameters varied over the range encountered in storms with the former including small and large ions.

Author

Atmospheric Ionization; Drops (Liquids); Electric Fields; Mathematical Models; Absorption Cross Sections; Ion Currents; Particle Trajectories

19990108733 Academy of Sciences (Russia), Inst. of Applied Physics, Nizhny Novgorod, Russia

To Selective Ion Charging of Water Drops in Thunderstorms

Sorokin, Andrew E., Academy of Sciences (Russia), Russia; 11th International Conference on Atmospheric Electricity; June 1999, pp. 351-354; In English; See also 19990108601; No Copyright; Avail: CASI; A01, Hardcopy; A10, Microfiche

The interaction between cloud droplet and moving ionized air has been investigated in the uniform Electric Field (EF). The attachment coefficients of air ions were obtained , taking into consideration the track assumption. It has been shown that droplet charging regimes are strongly connected with the parameter Xi(sub +/-) - ratio of drift ions velocity to air flow velocity far away from droplet. The classical Wilson effect, that was shown, lies in the limit |Xi(sub l)| is less than |Xi(sub d)| is less than Xi(sub up) approx. = 1. The upper limit Xi(sub up) is determined by the diffusive and volume ionization current influence to space charge distribution around the droplet. The lower limit Xi(sub l) depends on Ions diffusivity coefficient D(sub i). On the basis of attachment coefficient obtained, the electrohydrodynamic 1D model for the collective of charging drops has been designed. The homogeneous stationary state for certain cloud conditions is examined. It is shown that high EF, like 1 kV/cm, can change ions concentration through droplets-ions interactions. Also, it is obtained that the system can be unstable to the wide spectra fluctuations of space charge and EF.

Author

Drops (Liquids); Ions; Diffusivity; Ion Charge; Charge Distribution; Electric Fields; Thunderstorms; Atmospheric Ionization

19990108734 Desert Research Inst., Reno, NV USA

Charge Generation with and without Secondary Ice Production

Hallett, John, Desert Research Inst., USA; 11th International Conference on Atmospheric Electricity; June 1999, pp. 355-358; In English; See also 19990108601

Contract(s)/Grant(s): NSF ATM-94-13437; No Copyright; Avail: CASI; A01, Hardcopy; A10, Microfiche

Aircraft observations and laboratory experiments demonstrate that separation of electric charge is associated with the simultaneous presence of graupel growing from supercooled cloud droplets, together with vapor grown ice crystals. Laboratory measurements suggest that charge is separated during collision and bounce of the vapor grown crystals, with magnitude and sign of the separated charge depending on temperature, liquid water content and the droplet size distribution. The conditions necessary for the optimum mix of particles in the atmosphere relates to the shear of horizontal wind with height in the environment of the convective cloud. This determines not only the input of graupel from aloft to the developing water cloud below but also the turbulent transport of ice/water at the sloping interface between the ascending upshear supercooled water cloud and the descending downshear ice cloud. Conditions for the occurrence of secondary ice are present for a deep, warm base temperature cloud (>20 C) and are necessary for beginning electrification; inhibition of secondary ice for a cool cloud base temperature (is less than 0 C) leads to efficient transport of supercooled cloud to low temperatures aloft and ultimately a much higher separation rate of charge, with positive charge aloft.

Author

Drops (Liquids); Electric Charge; Electrification; Graupel; Ice Clouds; Cloud Physics; Polarization (Charge Separation)

19990108735 National Severe Storms Lab., Norman, OK USA

Simulation of Early Electrification in a Three-Dimensional Dynamic Cloud Model

Ziegler, C. L., National Severe Storms Lab., USA; Straka, J. M., Oklahoma Univ., USA; MacGorman, D. R., National Severe Storms Lab., USA; 11th International Conference on Atmospheric Electricity; June 1999, pp. 359-362; In English; See also 19990108601

Contract(s)/Grant(s): NSF ATM-93-11911; NSF ATM-91-20009; NSF ATM-96-17318; NSF EAR-95-12145; No Copyright; Avail: CASI; A01, Hardcopy; A10, Microfiche

This paper highlights the results of our efforts to incorporate parameterized expressions for non-inductive and inductive charging, lightning discharges, and formation of screening layers into a three-dimensional dynamic cloud model (ie. ”cloud model”). The cloud model is time dependent and involves simultaneous solution of the equations of atmospheric motion with equations for mass, heat, and water substance continuity. Electrification is modeled by solving additional continuity equations for liquid and ice hydrometeor space charge densities and a Poisson equation for scalar electric potential. The present dynamical cloud simulation approach extends earlier kinematic modeling studies of tornadic supercell and New Mexico mountain thunderstorms. At present we are engaged in efforts to validate the preliminary simulations versus observations of morphologically similar storms and also to investigate the impact of the storm environment on the simulated electrical and lightning morphology.

Author

Atmospheric Models; Electric Charge; Electrification; Equations of Motion; Computerized Simulation; Three Dimensional Models; Cloud Physics

19990108736 NASA Marshall Space Flight Center, Huntsville, AL USA

Determination of Thunderstorm Anvil Ice Contents and Other Cloud Properties from Satellite Observations of Lightning

Blyth, Alan M., New Mexico Inst. of Mining and Technology, USA; Christian, Hugh J., Jr., NASA Marshall Space Flight Center, USA; Latham, John, National Center for Atmospheric Research, USA; 11th International Conference on Atmospheric Electricity; June 1999, pp. 363-366; In English; See also 19990108601; No Copyright; Avail: CASI; A01, Hardcopy; A10, Microfiche

The lightning frequency model developed by Baker, Christian and Latham (1995) has been refined and extended, in an effort to provide a more realistic framework from which to examine computationally the relationships that might exist between lightning frequency f (which is now being routinely measured from satellites, using NASA/MSFC devices) and a variety of cloud physical parameters, including precipitation rate, updraught speed and non-precipitating ice content. Model results indicate the existence of a simple relationship between lightning frequency f and the upward flux of ice crystals into the thunderstorm anvil. It follows that, for a particular situation, one can assign a specific mass of non-precipitating ice to an individual lightning stroke. Therefore it may prove possible - using satellite measurements of global lightning - to estimate the atmospheric loading of ice crystals in thunderstorm anvils: a parameter of climatological importance. Early results from this work are presented, together with further studies of the relationships between f and other thundercloud parameters.

Author

Cloud Physics; Cumulonimbus Clouds; Lightning; Thunderstorms; Ice Clouds

19990108737 Texas A&M Univ., Dept. of Meteorology, College Station, TX USA

Lightning and Radar Characteristics of the Bow Echo Event of May 24-25, 1998

Murray, Natalie, Texas A&M Univ., USA; Orville, Richard E., Texas A&M Univ., USA; 11th International Conference on

Atmospheric Electricity; June 1999, pp. 368-371; In English; See also 19990108601
Contract(s)/Grant(s): NSF ATM-98-06189; NA87WA0063; No Copyright; Avail: CASI; A01, Hardcopy; A10, Microfiche

The mesoscale convective system of May 24-25, 1998 in Kansas and northern Oklahoma produced numerous regions of intense convection associated with bow echoes. Data collected by the National Lightning Detection Network (NLDN) have been analyzed for this storm which had a duration of twenty-six hours. Overall, 42% of the 50,000 cloud-to-ground flashes lowered positive charge. The maximum percent positive reached 75% per half-hour interval and occurred during the first quarter of the storm's lifetime. Our analysis has been narrowed to small time intervals of twenty minutes, which complement the available NOWRAD MOSAIC images for this date. Percent positives range between 60 and 70%. Locations of cloud-to-ground lightning flashes occurring in each interval are overlaid on the corresponding radar image. Further analysis provides information about the electrical structure of the intense convection.
Author
Radar Echoes; Thunderstorms; Cloud-to-Ground Discharges; Free Convection; Radar Imagery

19990108738 NASA Goddard Space Flight Center, Greenbelt, MD USA
Combined Microwave and Sferics Measurements as a Continuous Proxy for Latent Heating in Mesoscale Model Predictions
Chang, D. –E., Universities Space Research Association, USA; Morales, C. A., Maryland Univ., USA; Weinman, J. A., NASA Goddard Space Flight Center, USA; Olson, W. S., Maryland Univ. Baltimore County, USA; 11th International Conference on Atmospheric Electricity; June 1999, pp. 372-375; In English; See also 19990108601
Contract(s)/Grant(s): NAS5-32484; No Copyright; Avail: CASI; A01, Hardcopy; A10, Microfiche

Planar rainfall distributions were retrieved from data provided by the Tropical Rainfall Measuring Mission (TRMM) Microwave Imager (TMI) and Special Sensor Microwave Imager (SSM/I) radiometers. Lightning generates Very Low Frequency (VLF) radio noise pulses called sferics. Those pulses propagate over large distances so that they can be continuously monitored with a network of ground based radio receivers. An empirical relationship between the sferics rate and the convective rainfall permitted maps of convective latent heating profiles to be derived continuously from the sferics distributions. Those inferred latent heating rates were assimilated into the Penn State/NCAR Mesoscale Model (MM5) that depicted an intense winter cyclone that passed over Florida on 2 February 1998. When compared to a 14 hour MM5 rainfall forecast using conventional data, the use of lightning data improved the forecast.
Author
Atmospherics; Lightning; Mesoscale Phenomena; Microwave Imagery; Remote Sensing; Atmospheric Models; Weather Forecasting; Rain; Cyclones

19990108739 New Mexico Inst. of Mining and Technology, Socorro, NM USA
Three-Dimensional Lightning Mapping Observations During MEaPRS in Central Oklahoma
Krehbiel, P. R., New Mexico Inst. of Mining and Technology, USA; Thomas, R. J., New Mexico Inst. of Mining and Technology, USA; Rison, W., New Mexico Inst. of Mining and Technology, USA; Hamlin, T., New Mexico Inst. of Mining and Technology, USA; Harlin, J., New Mexico Inst. of Mining and Technology, USA; Davis, M., New Mexico Inst. of Mining and Technology, USA; 11th International Conference on Atmospheric Electricity; June 1999, pp. 376-379; In English; See also 19990108601; No Copyright; Avail: CASI; A01, Hardcopy; A10, Microfiche

Three-dimensional observations of lightning have been obtained for different kinds of storms in central Oklahoma, including several supercell storms, a tornadic storm, and storms having a large fraction of positive cloud-to-ground (+CG) lightning. A number of interesting results continue to emerge from the observations. Among these are: a) the occurrence of inverted polarity intracloud discharges in storms; b) the observation of a new regime of lightning at very high altitudes in storms (15-20 km MSL), apparently in overshooting convective tops; and c) the result that lightning in supercell storms is essentially continuous and volume-filling, and sometimes contains 'holes' that appear to be associated with strong updraft regions.
Author
Lightning; Signal Detection; Signal Measurement; Thunderstorms; Mapping

19990108749 Uppsala Univ., Dept. of Earth Sciences, Uppsala, Sweden
On Electric Properties of Radiation Fog
Israelsson, S., Uppsala Univ., Sweden; 11th International Conference on Atmospheric Electricity; June 1999, pp. 587-590; In English; See also 19990108601; No Copyright; Avail: CASI; A01, Hardcopy; A10, Microfiche

The results from 9 field studies of the electrical and meteorological properties of radiation fog are presented. The radiation cooling and turbulence is controlling radiation fog. About 1 hour before sunset the negative radiation balance leads to a cooling

of the surface layer, which leads to a reduction in the turbulent diffusion and an increasing concentration of radioactivity in the lowest layer. The shallow layer of enhanced ionization can cause a reversed electrode effect with a stratum of negative space charges. Periods of significant fog development appeared to occur when wind speeds dropped below 0.5 - 1 m/s below 10 m. There is also in radiation fog a distinct tendency of quasi-periodic oscillations of the meteorological and electrical parameters on a time scale longer than 10 min. Fog formation starting also above the ground and an attachment of ions to the fog droplets occurs, which leads to negative space charge density in the radiation fog, 30 - 100 pC/cu m, and a sedimentation current on average -1.4 pA/sq m. Both the conductivity and electric potential gradient in radiation fog are on the average reduced to one-third of their values in fog-free air. For conductivity by reason of the attachment of small ions to the fog particles. That leads to that the conduction current will be reduced to one-tenth of the the value in fog-free air. The effect of radiation fog on the potential gradient is normally a consequence of the change of the conductivity. But in the present study the potential gradient decreases in the radiation fog.
Author

Fog; Atmospheric Radiation; Meteorological Parameters; Electrical Properties; Turbulent Diffusion; Turbulence Effects

19990108751 Utrecht Univ., Inst. for Marine and Atmospheric Research Utrecht, Utrecht, Netherlands

The Atmospheric Electric Fog Effect

vanderHage, J. C. H., Utrecht Univ., Netherlands; deBruin, T. F., Netherlands Inst. for Sea Research, Netherlands; 11th International Conference on Atmospheric Electricity; June 1999, pp. 595-597; In English; See also 19990108601; No Copyright; Avail: CASI; A01, Hardcopy; A10, Microfiche

The onset and the dissipation of fog is always accompanied by variations of the electric conductivity of the air. Fog forecasts by various authors, made on the basis of this effect are discussed. In the urban environment of Utrecht these forecasts prove to be unreliable. Forecasting may perhaps be applied with more success in marine environments. One case study of the atmospheric electric fog effect on the North Sea is presented.
Author

Atmospheric Electricity; Fog; Air Conductivity; Electrical Measurement

19990108764 NASA Marshall Space Flight Center, Huntsville, AL USA

Evidence for the Absence of Conductivity Variations Above Thunderstorms

Bailey, Jeff C., Raytheon Co., USA; Blakeslee, Richard J., NASA Marshall Space Flight Center, USA; Driscoll, Kevin T., Alabama Univ., USA; 11th International Conference on Atmospheric Electricity; June 1999, pp. 646-649; In English; See also 19990108601; No Copyright; Avail: CASI; A01, Hardcopy; A10, Microfiche

In recent years, atmospheric conductivity and electric field measurements over thunderstorms have been made at 20 km with a high altitude aircraft. After compensating for the effects of aircraft charging induced by external electric fields no significant variations in ambient conductivity above thunderstorms have been found. These Gerdien results contrast strongly with the large (and frequent) conductivity variations reported in studies using relaxation probe techniques.
Author

Atmospheric Conductivity; Electric Fields; Electrical Measurement; Thunderstorms

19990108765 Texas A&M Univ., Dept. of Meteorology, College Station, TX USA

Enhanced NOx by Lightning in the Upper Troposphere and Lower Stratosphere Inferred from the Global NO2 Measurements of the Upper Atmosphere Research Satellite (UARS)

Sanger, N. T., Texas A&M Univ., USA; Zhang, R., Texas A&M Univ., USA; Orville, R. E., Texas A&M Univ., USA; Tie, X., National Center for Atmospheric Research, USA; Randel, W., National Center for Atmospheric Research, USA; Williams, E. R., Massachusetts Inst. of Tech., USA; 11th International Conference on Atmospheric Electricity; June 1999, pp. 652-655; In English; See also 19990108601; No Copyright; Avail: CASI; A01, Hardcopy; A10, Microfiche

This paper focuses on a possible link between lightning activity and the UARS NO2 data on a global scale. The NO2 data from the Upper Atmosphere Research Satellite (UARS) are analyzed for the entire year of 1993 and compared to the seasonal and global lightning distribution inferred from the Optical Transient Detector (OTD). The comparison of the two data sets reveals that there is a strong correlation between increased lightning activity and higher observed levels of NO2 in the upper troposphere and lower stratosphere. Enhanced NO2 mixing ratios above the background level are consistently found in areas of elevated lightning activities. This correlation is strongest during the summer months in the Northern and Southern Hemispheres and in the tropics regions. Moreover, the results indicate that expected background levels of NO2 mixing ratios generally correspond to areas of little or no lightning activity.
Author

Nitrogen Oxides; Lightning; Mixing Ratios; Troposphere; Stratosphere; Data Correlation

19990108768 Los Alamos National Lab., NM USA

Recent Results from the FORTE rf Payload

Jacobson, Abram R., Los Alamos National Lab., USA; 11th International Conference on Atmospheric Electricity; June 1999, pp. 668-671; In English; See also 19990108601; No Copyright; Avail: CASI; A01, Hardcopy; A10, Microfiche

This work compares contemporaneous observations of lightning from two complementary systems. FORTE is a low-Earth-orbit satellite carrying radio-wave and optical instruments for the study of lightning. The radio receivers aboard FORTE observed very-high-frequency (VHF) emissions from the air-breakdown process preceding and (sometimes) accompanying large-scale current flow. Only VHF (and higher) emissions from lightning can reliably penetrate the ionosphere to a satellite, especially along grazing-incidence paths. The National Lightning Detection Network (NLDN) is a ground-based array of sensors in the continental USA (CONUS) observing the low-frequency (LF) and very-low-frequency (VLF) radiation from large-scale vertical currents. Prior to the launch of FORTE in 1997, essentially no work had been done on the statistical correlations between (a) ground-based LF/VLF and (b) spaced-based VHF remote sensing of lightning. During April-September 1998, FORTE was tasked with taking maximum triggered VHF data over and near the CONUS, and NLDN data was specially post-processed in a loosened-criterion mode providing enhanced detection range beyond the CONUS. We found during this campaign - 15,000 correlated NLDN/FORTE detections.

Author

Lightning; Very High Frequencies; Detection; Satellite Observation

19990108769 Los Alamos National Lab., Space and Atmospherics Group, NM USA

Thunderstorm and Lightning Studies Using the Forte Optical Lightning System (FORTE/OLS)

Suszcynsky, D., Los Alamos National Lab., USA; Kirkland, M., Los Alamos National Lab., USA; Argo, P., Los Alamos National Lab., USA; Franz, R., Los Alamos National Lab., USA; Jacobson, A., Los Alamos National Lab., USA; Knox, S., Los Alamos National Lab., USA; Guillen, J., Sandia National Labs., USA; Green, J., Sandia National Labs., USA; Spalding, R., Sandia National Labs., USA; 11th International Conference on Atmospheric Electricity; June 1999, pp. 672-675; In English; See also 19990108601; No Copyright; Avail: CASI; A01, Hardcopy; A10, Microfiche

A summary of FORTE/OLS satellite observations and analysis is presented with emphasis on correlating the OLS data with the FORTE/VHF and National Lightning Detection Network (NLDN) data sets. General statistics for the photo-diode (PDD) data are presented. Optical signals are detected both as individual events and as sequences of events associated with cloud-to-ground (CG) and intra-cloud (IC) flashes. The optical signals in concert with the associated VHF signals can be used to discriminate between CG and IC strokes and can also be used to deduce values for the mean cloud scattering delay of the emitted light. The benefits of a dual phenomenology approach to the detection and identification of lightning from space are discussed. PDD/NLDN correlation statistics are analyzed and used to estimate the sensitivity of the PDD to different types of lightning.

Author

Cloud-to-Ground Discharges; Intracloud Discharges; Satellite Observation; Data Correlation; Signal Detection

19990108770 California Univ., Inst. of Geophysics and Planetary Physics, Los Angeles, CA USA

Detection Rates of Lightning Generated Radio Emissions by FORTE

Zuelsdorf, R. S., California Univ., USA; Jacobson, A. R., Los Alamos National Lab., USA; Kirkland, M., Los Alamos National Lab., USA; Strangeway, R. J., California Univ., USA; Russell, C. T., California Univ., USA; 11th International Conference on Atmospheric Electricity; June 1999, pp. 676-679; In English; See also 19990108601; No Copyright; Avail: CASI; A01, Hardcopy; A10, Microfiche

Near-continuous observation at 38 and 130 MHz by the FORTE satellite has enabled a global investigation of the radio processes associated with lightning. Using FORTE data acquired between 1 November 1997 and 31 August 1998 we are able to determine the rates of RF detection for the entire globe during the months sampled. Here we present rate maps of all detected RF signals, signals with the characteristic 2nd pulse of a TIPP, and hard TIPPs of the kind previously detected by the ALEXIS spacecraft - those in which the peak power as detected in the 130 MHz centered band is at least 30% of the peak power detected in the 38 MHz centered band. Areas of greatest detection are the continental equatorial regions and from Indonesia up into India, but moderate levels of detection persist even over the oceans. Whereas the rate of detection of lightning with the characteristic second pulse of a TIPP is about half the rate of all detected RF pulses, the rate of hard TIPP detection is a small fraction of total RF detection. Analysis of the data three months at a time reveals the migration of lightning occurrence northwards from November throughout August. We also monitor the background noise in the eight 1-MHz sub-bands of both 20 MHz bands. By comparing

the levels of background noise with the peak amplitude of the natural pulses detected, we determine what portion of the lightning generated signals is lost in the background noise.
Author
Satellite Observation; Radio Frequencies; Lightning; Detection

19990108771 Los Alamos National Lab., Space and Atmospheric Sciences Group, NM USA
Satellite Observations of Transient Radio Impulses form Thunderstorms
Argo, P. E., Los Alamos National Lab., USA; Kirkland, M., Los Alamos National Lab., USA; Jacobson, A., Los Alamos National Lab., USA; Massey, R., Los Alamos National Lab., USA; Suszynsky, D., Los Alamos National Lab., USA; Eack, K., Los Alamos National Lab., USA; Fitzgerald, T. J., Los Alamos National Lab., USA; Smith, D., Los Alamos National Lab., USA; 11th International Conference on Atmospheric Electricity; June 1999, pp. 680-683; In English; See also 19990108601; No Copyright; Avail: CASI; A01, Hardcopy; A10, Microfiche

Transient radio frequency emissions from thunderstorms detected by satellites were first reported in 1995. The nature and source of these emissions remained a mystery until the launch of the FORTE satellite in 1997. FORTE, with its more sophisticated triggering and larger memory capacity showed that these emissions were connected to major thunderstorm systems. The analysis reported here, connecting FORTE RF events with ground based lightning location data from the National Lightning Detection Network (NLDN), shows that localized regions within thunderstorms are responsible for the creation of the satellite detected RF signals. These regions are connected with the areas of strong radar returns from the NEXRAD Doppler radar system, indicating that they are from regions of intense convection. We will also show data from several storms detected in the extended Caribbean, in which the height profile of the source regions can be determined. Although as a single low earth orbit satellite FORTE cannot provide global coverage of thunderstorm lightning events or locate single lightning flashes, follow-on satellite constellations should be able to provide detailed information on global lightning in near real-time.
Author
Satellite Observation; Radio Frequencies; Lightning; Thunderstorms; Detection; Data Correlation

19990108772 Los Alamos National Lab., Space and Atmospheric Sciences Group, NM USA
Operation of an Array of Field-Change Detectors to Provide Ground Truth for Forte Data
Massey, Robert S., Los Alamos National Lab., USA; Eack, Kenneth B., Los Alamos National Lab., USA; Eberle, Marc H., Los Alamos National Lab., USA; Shao, Xuan–Min, Los Alamos National Lab., USA; Smith, David A., Los Alamos National Lab., USA; Wiens, Kyle C., New Mexico Inst. of Mining and Technology, USA; 11th International Conference on Atmospheric Electricity; June 1999, pp. 684-687; In English; See also 19990108601; No Copyright; Avail: CASI; A01, Hardcopy; A10, Microfiche

We have deployed an array of fast electric-field-change sensors around the state of New Mexico to help identify the lightning processes responsible for the VHF RF signals detected by the FORTE satellite's wide-band transient radio emission receivers. The array operates continuously, and provides us with locations and electric-field waveforms for events within New Mexico and into surrounding states. We are particularly interested in events for which there are coincident FORTE observations. For these events, we can correct both the array and FORTE waveforms for time of flight, and can plot the two waveforms on a common time axis. Most of the coincident events are from cloud-to-ground discharges, but the most powerful RF emitters are a little-studied class of events variously called "narrow bipolar events" and "compact intra-cloud discharges". We have therefore focussed our attention on these events whether or not FORTE was in position to observe them,
Author
Ground Truth; Signal Detectors; Radio Emission; Radio Frequencies; Antenna Arrays

19990108773 Main Geophysical Observatory, Saint Petersburg, Russia
Investigation of Possibilities to Obtain the Information on Thunderstorm Clouds by Satellite Radar TRMM
Stepanenko, V. D., Main Geophysical Observatory, Russia; 11th International Conference on Atmospheric Electricity; June 1999, pp. 688-690; In English; See also 19990108601; No Copyright; Avail: CASI; A01, Hardcopy; A10, Microfiche

Results of theoretical estimations indicates the possibility to obtain the information on thunderstorm clouds using the satellite radar TRMM at the global scale and the advisablilty of joint application of its data and lightning imaging sensor (LIS) data.
Author
Trmm Satellite; Satellite-Borne Radar; Remote Sensing; Cumulonimbus Clouds

19990108774 Hungarian Academy of Sciences, Geodetic and Geophysical Research Inst., Sopron, Hungary

El-Nino Related Meridional Shifts in the Global Position of the Worldwide Thunderstorm Activity

Satroi, G., Hungarian Academy of Sciences, Hungary; Zieger, B., Hungarian Academy of Sciences, Hungary; 11th International Conference on Atmospheric Electricity; June 1999, pp. 691-694; In English; See also 19990108601; Sponsored in part by the U.S-Hungarian Joint Research Foundation

Contract(s)/Grant(s): T023111; JF554; No Copyright; Avail: CASI; A01, Hardcopy; A10, Microfiche

The self-consistent behaviour of the frequency level and semiannual intensity variations of the first three Schumann resonance (SR) modes observed at Nagycenk (47.6 deg N, 16.7 deg E) indicates a southward shift in the global position of the lightning activity in warm El Nino years (1994, from March 1997 to April 1998) and a northward shift in cool La Nina years (1996, (1998)). The third SR mode has a crucial role in recognizing these meridional shifts due to the special angular distance of Nagycenk with respect to the African thunderstorm region. The diurnal zonal redistribution of the worldwide thunderstorm activity manifests in characteristic daily zonal frequency patterns. The preserved daily frequency patterns with changing frequency levels in the same months of the different years imply that the meridional shifts of the lightning activity exist in worldwide sense on the ENSO time scale. The estimated shifts are about 4-8 deg in latitude. The authors suggest that there are two temperature dependent and quasi-synchronous global oscillations in the atmosphere-ocean-land system. One of them is the El Nino Southern Oscillation (ENSO) known already, which is basically a zonal oscillation, the other is a meridional oscillation manifested in the average position of the land related global lightning activity which can be monitored by Schumann resonances. Author

Thunderstorms; El Nino; Southern Oscillation; Schumann-Runge Bands

19990108775 Tel-Aviv Univ., Ramat-Aviv, Dept. of Geophysics and Planetary Sciences, Tel-Aviv, Israel

A New Schumann Resonance Station in the Negev Desert for Monitoring Global Lightning Activity

Price, C., Tel-Aviv Univ., Ramat-Aviv, Israel; Finkelstein, M., Tel-Aviv Univ., Ramat-Aviv, Israel; Starobinets, B., Tel-Aviv Univ., Ramat-Aviv, Israel; Williams, E., Massachusetts Inst. of Tech., USA; 11th International Conference on Atmospheric Electricity; June 1999, pp. 695-697; In English; See also 19990108601

Contract(s)/Grant(s): BSF-95-00441; No Copyright; Avail: CASI; A01, Hardcopy; A10, Microfiche

Due to increasing interest in global lightning activity, and its connection to the global climate system, a new field site has been established in the Negev Desert, Israel, to monitor the Schumann resonances on a continuous basis. As the result of a joint Israel-USA project, we are now monitoring the three components (horizontal N-S and E-W magnetic field; and vertical electric field) of the extremely low frequency (ELF) electromagnetic waves (1-50 Hz) produced by lightning. Data has been archived since February 1998, and the initial analysis indicates that the monitoring site is very ”clean” with low anthropogenic noise levels. We observe all 7 modes of the Schumann resonance between 1-50 Hz on a regular basis. In addition, due to the location of our station (30N, 34E), we are north of Africa. and equi-distant between Asia and South America, the three main source regions of thunderstorm activity around the globe. Due to this geometry the individual magnetic detectors can easily be used to distinguish between the different source regions during the day, to study the dynamics and variability of each source region separately. We have noticed an interesting periodicity of approximately 5-days in global lightning activity. On a global scale, our Schumann resonance signals have been compared with simultaneous observations in California, and a daily correlation of 0.92 indicates that our measurements are truly global in nature.

Author

Israel; Lightning; Detection; Schumann-Runge Bands; Ground Stations; Periodic Variations

19990108776 Massachusetts Inst. of Tech., Dept. of Civil and Environmental Engineering, Boston, MA USA

Schumann Resonances and the Temporal-Spatial Dynamics of Global Thunderstorm Activity

Mushtak, V., Massachusetts Inst. of Tech., USA; Boldi, R., Massachusetts Inst. of Tech., USA; Williams, E., Massachusetts Inst. of Tech., USA; 11th International Conference on Atmospheric Electricity; June 1999, pp. 698-700; In English; See also 19990108601; No Copyright; Avail: CASI; A01, Hardcopy; A10, Microfiche

A two-dimensional computational ELF technique has been applied to interpret variations of peak frequencies of Schumann resonances (SR) observed at the MIT experimental site (West Greenwich, Rhode Island). The spatial-temporal dynamics of global thunderstorm activity has been simulated on the basis of general meteorological data. It is shown that the proposed models provide a reasonable qualitative agreement between computed and observed variations for SR I to I-V. Some inverse task diagrams have been constructed as an instrument for distinguishing between day-to-day thunderstorm scenarios.

Author

Thunderstorms; Schumann-Runge Bands; Atmospheric Models; Computerized Simulation; Resonant Frequencies

19990108779 Johann-Wolfgang-Goethe-Univ., Inst. for Meteorology and Geophysics, Frankfurt am Main, Germany

Global Lightning Triangulation

Fuellekrug, Martin, Johann-Wolfgang-Goethe-Univ., Germany; 11th International Conference on Atmospheric Electricity; June 1999, pp. 709-711; In English; See also 19990108601; No Copyright; Avail: CASI; A01, Hardcopy; A10, Microfiche

Three GPS synchronized measurement stations recorded horizontal magnetic field variations in the ULF/ELF transition range from 4-200 Hz at Silberborn, Germany (51.8 deg N, 9.5 deg E), and 4-19 Hz at Hollister, California (36.8 deg N, 121.4 deg W), and at Lameroo, Australia (35.5 deg E, 140.6 deg E), during April 1998. The three station records exhibit simultaneous discrete excitations of Earth-ionosphere cavity (or Schumann) resonances which result from the constructive interference of electromagnetic waves which propagate with little attenuation in the spherical Earth-ionosphere waveguide (Schumann, 1952; Sentman, 1995). These Earth-ionosphere cavity resonances are mainly excited by particularly strong lightning flashes which can be triangulated by use of the orientation of the Poynting vector along the great circle path of propagation.

Derived from text

Lightning; Triangulation; Earth Ionosphere; Resonant Frequencies

19990108780 Technische Univ., Inst. for Meteorology and Climatology, Hanover, Germany

The European Lightning NOx Project: First Results of the Field Experiment 1998

Finke, U., Technische Univ., Germany; Laroche, P., Office National d'Etudes et de Recherches Aerospatiales, France; Hoeller, H., Deutsche Forschungsanstalt fuer Luft- und Raumfahrt, Germany; Huntrieser, H., Deutsche Forschungsanstalt fuer Luft- und Raumfahrt, Germany; Fehr, T., Deutsche Forschungsanstalt fuer Luft- und Raumfahrt, Germany; 11th International Conference on Atmospheric Electricity; June 1999, pp. 712-714; In English; See also 19990108601

Contract(s)/Grant(s): ENV4-CT97-0409; No Copyright; Avail: CASI; A01, Hardcopy; A10, Microfiche

The European lightning NOx project investigates the production and transport of NOx in thunderstorms. In summer 1998 a 3-month field experiment was organized in Central Europe. A unique set of instruments were used including two aircraft for in-situ chemical measurements, 3-dimensional high-resolution lightning mapper, and polarimetric radar for cloud observation. During the various anvil crossings extraordinary high concentrations of nitrogen oxide (exceeding 20ppbV) have been observed. The spiky nature of the signal and the observation of lightning in the near vicinity of the flight path are strong indicators for the NOx being produced by lightning.

Author

Nitrogen Oxides; Lightning; Central Europe; Thunderstorms

19990108781 NASA Marshall Space Flight Center, Huntsville, AL USA

Optical Detection of Lightning from Space

Christian, H. J., NASA Marshall Space Flight Center, USA; 11th International Conference on Atmospheric Electricity; June 1999, pp. 715-718; In English; See also 19990108601; No Copyright; Avail: CASI; A01, Hardcopy; A10, Microfiche

Two primary detection techniques (optical and RF) have a proven capability for detecting lightning from low earth orbit. However, the lightning processes that generate the optical and RF signals are vastly different providing significantly different information content from each sensor type. Because of the intervening ionosphere, low frequency RF components do not reach satellite altitudes. As a consequence, many of the processes associated with the major energy release of a lightning event (i.e. return strokes, k-changes, recoil streamers, etc), in all likelihood contribute little to the RF signal arriving at the satellite. The optical output from lighting, on the other hand, has been shown to be highly correlated with the energetic, charge-transferring processes mentioned above. On the down side, the optical energy, while essentially unaffected by the atmosphere once it emerges from the cloud, is heavily scattered within the cloud. While there is little absorption by the cloud, the great optical depth makes the total light energy emerging from the cloud to be dependent on where in the cloud the lightning occurred. Analyses suggest that when lightning is confined to the lowest regions of the cloud, the light is strongly attenuated and detection becomes problematic. Fortunately, the vast majority of lightning flashes are comprised of channels that propagate through the middle of the cloud and higher. These flashes produce bright signals at the top of a cloud and are readily detectable. Presently, we have two optical instruments in orbit. The Optical Transient Detector (OTD) has been orbiting the earth since April, 1995, while the Lightning Imaging Sensor (LIS) was launched on the Tropical Rainfall Measuring Mission (TRMM) in November of 1997. Both instruments are relatively small, solid state optical imagers, designed specifically to detect and locate lightning activity from low earth orbit with high detection efficiency and location accuracy.

Derived from text

Lightning; Imaging Techniques; Optical Equipment; Optical Measurement; Trmm Satellite

19990108782 NASA Marshall Space Flight Center, Huntsville, AL USA

An Optimal Relation of Radar Reflectivity to Lightning Rate

Heckman, S., NASA Marshall Space Flight Center, USA; 11th International Conference on Atmospheric Electricity; June 1999, pp. 719-721; In English; See also 19990108601; No Copyright; Avail: CASI; A01, Hardcopy; A10, Microfiche

Thunderstorms separate charge. Most places they lift positive charge or lower negative, a few places they lift negative or lower positive. The electrical generator is stronger in some parts of the cloud than in others. Our long term goal is to map this generator. Cloud physicists tell us that uncharged ice and water particles become charged by collision, and that the charge transferred depends on size, temperature and humidity. There is still some disagreement about exactly how the charge transferred depends on size, temperature, and humidity. In principle, if we knew this ice physics, and also knew the distribution of particles everywhere in the storm, and the winds everywhere and the temperature and humidity everywhere, then we could compute everywhere the electrical power of the thunderstorm generator. In practice it is difficult to know all these things, particularly the distribution of particles, so it is difficult to use real thunderstorms to falsify cloud electrification theories. We here take one small step towards computing that map of electrical generator power, by relating radar reflectivity profiles of 2000 storms to lightning flash rates of those storms. This small step by itself doesn't falsify any existing electrification theories; it merely places weak constraints on the relation of electric generator power to cloud ice.

Derived from text

Lightning; Radar Echoes; Reflectance; Meteorological Parameters; Cloud Physics; Atmospheric Models

19990108783 NASA Marshall Space Flight Center, Huntsville, AL USA

Optical Transient Detector (OTD) Observations of a Tornadic Thunderstorm

Buechler, D. E., Alabama Univ., USA; Goodman, S. J., NASA Marshall Space Flight Center, USA; Christian, H. J., NASA Marshall Space Flight Center, USA; Driscoll, K., Alabama Univ., USA; 11th International Conference on Atmospheric Electricity; June 1999, pp. 722-725; In English; See also 19990108601; No Copyright; Avail: CASI; A01, Hardcopy; A10, Microfiche

Total lightning observations made by the Optical Transient Detector (OTD) of a tornadic thunderstorm that occurred over Oklahoma on 17 April 1995 are presented. The average flash rate of the tornadic storm during the 3.2 min observation period was 45 flashes/min, with a flash rate density of 1.16 x 10(exp -4)/s sq km. The total flash rate was almost 18 times higher than the cloud-to-ground rate measured by the National Lightning Detection Network (NLDN). In addition, total lightning rates were observed to decrease prior to tornadic development.

Author

Lightning; Detection; Thunderstorms; Tornadoes; Satellite Observation

19990108784 NASA Marshall Space Flight Center, Huntsville, AL USA

Global Frequency and Distribution of Lightning as Observed by the Optical Transient Detector (OTD)

Christian, Hugh J., NASA Marshall Space Flight Center, USA; Blakeslee, Richard J., NASA Marshall Space Flight Center, USA; Boccippio, Dennis J., NASA Marshall Space Flight Center, USA; Boeck, William L., Niagara Univ., USA; Buechler, Dennis E., Alabama Univ., USA; Driscoll, Kevin T., Alabama Univ., USA; Goodman, Steven J., NASA Marshall Space Flight Center, USA; Hall, John M., CSC Huntsville, USA; Koshak, William J., NASA Marshall Space Flight Center, USA; Mach, Douglas M., Alabama Univ., USA; Stewart, Michael F., Alabama Univ., USA; 11th International Conference on Atmospheric Electricity; June 1999, pp. 726-729; In English; See also 19990108601; No Copyright; Avail: CASI; A01, Hardcopy; A10, Microfiche

The Optical Transient Detector (OTD) is a space-based instrument specifically designed to detect and locate lightning discharges (intracloud and cloud-to-ground) as it orbits the Earth. A statistical examination of OTD lightning data reveals that nearly 1.2 billion flashes occurred over the entire earth during the one year period from September 1995 through August 1996. This translates to an average of 37 lightning flashes occurring around the globe every second, which is well below the traditional estimate of 100 flashes per second. An average of 75% of the global lightning activity during the year occurs between 30' S and 30' N. An analysis of the annual lightning distribution reveals that an average of 82% of the lightning flashes occur over the continents and 18% over the oceans, which translates to an average land-ocean flash density ratio of nearly 11.

Author

Satellite Observation; Cloud-to-Ground Discharges; Lightning; Intracloud Discharges; Detection

19990108785 South Dakota School of Mines and Technology, Inst. of Atmospheric Science, Rapid City, SD USA

Lightning Production of NO(x) in a 3D Storm Model

Helsdon, J. H., South Dakota School of Mines and Technology, USA; Zhang, X., South Dakota School of Mines and Technology, USA; Farley, R. D., South Dakota School of Mines and Technology, USA; 11th International Conference on Atmospheric

Electricity; June 1999, pp. 730-733; In English; See also 19990108601
Contract(s)/Grant(s): NSF ATM-93-22588; NSF ATM-98-03762; No Copyright; Avail: CASI; A01, Hardcopy; A10, Microfiche

The 3D Storm Electrification Model (SEM) has been configured to account for the production of nitric oxide (NO) during a lightning flash, based on the energy dissipated. Following Borucki and Chameides (1984) we adopt a production rate of p(NO) = 9.2 x 10(exp 16) Molecules/J. The lightning-produced NO (LNO) is distributed along the simulated channel and then transported with the storm flow. Chemistry involving 9 species and 18 reactions is included. The model simulations are being used to address a number of questions concerning the fate of LNO and other species within a storm, including their distribution within the storm structure. Results with a simpler set of chemical reactions within a 2D version of the model have indicated that the majority of the LNO and other species ends up in the upwind portion of the anvil. This 3D simulation, using the same storm as a basis, shows that there are significant concentrations of LNO both within the anvil and in the lower portion of the storm as it dissipates. Comparison between model concentrations of LNO and data from the recent STERAO project show reasonable agreement.
Author

Lightning; Three Dimensional Models; Atmospheric Models; Computerized Simulation; Nitric Oxide

19990108786 NASA Marshall Space Flight Center, Huntsville, AL USA

Land-Ocean Differences in LIS and OTD Tropical Lightning Observations

Boccippio, D. J., NASA Marshall Space Flight Center, USA; Koshak, W. J., NASA Marshall Space Flight Center, USA; Christian, H. J., NASA Marshall Space Flight Center, USA; Goodman, S. J., NASA Marshall Space Flight Center, USA; 11th International Conference on Atmospheric Electricity; June 1999, pp. 734-737; In English; See also 19990108601; No Copyright; Avail: CASI; A01, Hardcopy; A10, Microfiche

Significant differences are known to exist on a global scale between continental and oceanic total lightning regional flash rates, suggesting differences in the properties of convective storms in these regimes. Lightning properties observed by the Optical Transient Detector (OTD) and Lightning Imaging Sensor (LIS) over land and ocean are compared, limited to analysis over the tropics in order to simplify physical interpretation. We find that the mean flash rates of individual storms over tropical land only exceed those over ocean by a factor of 2 (far less than the observed differences in regional flash rates). However, the average nearest neighbor distance of continental thunderstorms is half that over oceans. Cloud-top lightning optical radiance in oceanic storms is also twice as large as over land, suggesting either more energetic flashes over the oceans or less intervening cloud particles.
Author

Tropical Regions; Thunderstorms; Lightning; Oceans; Land; Satellite Observation

19990108787 NASA Marshall Space Flight Center, Huntsville, AL USA

Initial Comparison of the Lightning Imaging Sensor (LIS) with Lightning Detection and Ranging (LDAR)

Ushio, Tomoo, NASA Marshall Space Flight Center, USA; Driscoll, Kevin, NASA Marshall Space Flight Center, USA; Heckman, Stan, NASA Marshall Space Flight Center, USA; Boccippio, Dennis, NASA Marshall Space Flight Center, USA; Koshak, William, NASA Marshall Space Flight Center, USA; Christian, Hugh, NASA Marshall Space Flight Center, USA; 11th International Conference on Atmospheric Electricity; June 1999, pp. 738-741; In English; See also 19990108601; No Copyright; Avail: CASI; A01, Hardcopy; A10, Microfiche

The mapping of the lightning optical pulses detected by the Lightning Imaging Sensor (LIS) is compared with the radiation sources by Lightning Detection and Ranging (LDAR) and the National Lightning Detection Network (NLDN) for three thunderstorms observed during and overpasses on 15 August 1998. The comparison involves 122 flashes including 42 ground and 80 cloud flashes. For ground flash, the LIS recorded the subsequent strokes and changes inside the cloud. For cloud flashes, LIS recorded those with higher sources in altitude and larger number of sources. The discrepancies between the LIS and LDAR flash locations are about 4.3 km for cloud flashes and 12.2 km for ground flashes. The reason for these differences remain a mystery.
Author

Satellite Observation; Detection; Lightning; Thunderstorms; Cloud-to-Ground Discharges; Intracloud Discharges

19990108788 NASA Marshall Space Flight Center, Huntsville, AL USA

Diurnal Lightning Distribution as Observed by the Optical Transient Detector (OTD)

Blakeslee, Richard J., NASA Marshall Space Flight Center, USA; Driscoll, Kevin T., Alabama Univ., USA; Buechler, Dennis E., Alabama Univ., USA; Boccippio, Dennis J., NASA Marshall Space Flight Center, USA; Boeck, William L., Niagara Univ., USA; Christian, Hugh J., NASA Marshall Space Flight Center, USA; Goodman, Steven J., NASA Marshall Space Flight Center, USA; Hall, John M., CSC Huntsville, USA; Koshak, William J., NASA Marshall Space Flight Center, USA; Mach, Douglas M.,

Alabama Univ., USA; Stewart, Michael F., Alabama Univ., USA; 11th International Conference on Atmospheric Electricity; June 1999, pp. 742-745; In English; See also 19990108601; No Copyright; Avail: CASI; A01, Hardcopy; A10, Microfiche

Since April 1995, lightning activity around the globe has been monitored with the Optical Transient Detector (OTD). The OTD observations acquired during the one year period from September 1995 through August 1996 have been used to statistically determine the number of flashes that occur over the Earth during each hour of the diurnal cycle, expressed both as a function of local time and universal time. The globally averaged local [il,htnina activity displays a peak in late afternoon (1500-1800 local time) and a minimum in the morning hours (0600- 1000 local time) consistent with convection associated with diurnal heating. No diurnal variation is found for oceanic storms. The diurnal lightning distribution (universal time) for the globe displays a variation of about 35% about its mean as compared to the Carnegie curve which has a variation of only 15% above and below the mean.

Author

Lightning; Diurnal Variations; Display Devices; Time Dependence

19990108789 NASA Marshall Space Flight Center, Huntsville, AL USA

The Lightning Imaging Sensor

Christian, Hugh J., NASA Marshall Space Flight Center, USA; Blakeslee, Richard J., NASA Marshall Space Flight Center, USA; Goodman, Steven J., NASA Marshall Space Flight Center, USA; Mach, Douglas A., Alabama Univ., USA; Stewart, Michael F., Alabama Univ., USA; Buechler, Dennis E., Alabama Univ., USA; Koshak, William J., NASA Marshall Space Flight Center, USA; Hall, John M., CSC Huntsville, USA; Boeck, William, Niagara Univ., USA; Driscoll, Kevin T., Alabama Univ., USA; Boccippio, Dennis J., NASA Marshall Space Flight Center, USA; 11th International Conference on Atmospheric Electricity; June 1999, pp. 746-749; In English; See also 19990108601; No Copyright; Avail: CASI; A01, Hardcopy; A10, Microfiche

The Lightning Imaging Sensor (LIS) is a NASA Earth Observing System (EOS) instrument on the Tropical Rainfall Measuring Mission (TRMM) platform designed to acquire and investigate the distribution and variability of total lightning (i.e., cloud-to-ground and intracloud) between q35' in latitude. Since lightning is one of the responses of the atmosphere to thermodynamic and dynamic forcing, the LIS data is being used to detect deep convection without land-ocean bias, estimate the precipitation mass in the mixed phased region of thunderclouds, and differentiate storms with strong updrafts from those with weak vertical motion.

Author

Imaging Techniques; Lightning; Thunderstorms

19990108790 NASA Marshall Space Flight Center, Huntsville, AL USA

Global Lightning Variations Caused by Changes in Flash Rate and by Changes in Number of Thunderstorms

Williams, E., Massachusetts Inst. of Tech., USA; Rothkin, K., Massachusetts Inst. of Tech., USA; Stevenson, D., Massachusetts Inst. of Tech., USA; Boccippio, D., NASA Marshall Space Flight Center, USA; 11th International Conference on Atmospheric Electricity; June 1999, pp. 750-753; In English; See also 19990108601

Contract(s)/Grant(s): NAG8-935; No Copyright; Avail: CASI; A01, Hardcopy; A10, Microfiche

Observations from the Optical Transient Detector in space are used to examine the response of the number of storms and the total flash rate to thermodynamic forcing of deep convection on the diurnal and annual time scales. On the diurnal time scale, the flash rate appears to track with cloud buoyancy, and storm numbers dominate later in the cycle. On the annual time scale, almost all of the total lightning response is due to changes in the number of storms, with a negligible contribution from flash rate.

Author

Diurnal Variations; Lightning; Thunderstorms

19990108791 NASA Marshall Space Flight Center, Huntsville, AL USA

The Role of Boundary Layer Aerosol in the Vertical Development of Precipitation and Electrification: Another Look at the Contrast Between Lightning over Land and Over Ocean

Williams, E., Massachusetts Inst. of Tech., USA; Rosenfeld, D., Hebrew Univ., Israel; Madden, N., Massachusetts Inst. of Tech., USA; Labrada, C., Massachusetts Inst. of Tech., USA; Gerlach, J., NASA Wallops Flight Facility, USA; Atkinson, L., NASA Wallops Flight Facility, USA; 11th International Conference on Atmospheric Electricity; June 1999, pp. 754-757; In English; See also 19990108601

Contract(s)/Grant(s): NAG5-4778; No Copyright; Avail: CASI; A01, Hardcopy; A10, Microfiche

Comparisons are made between the cloud condensation nuclei (CCN) concentration in the boundary layer and radar/electrical observations of the vertical development of precipitation and lightning in both the 'break period' and 'monsoon' regimes in tropical Brazil. The initial radar echoes and the maximum flash rates are found to be higher when the CCN concentration is higher,

characteristic of the 'break period' conditions. One possible explanation for both observations is the survival of cloud droplets against coalescence and their attainment of the mixed phase region aloft.
Author
Condensation Nuclei; Aerosols; Boundary Layers; Lightning; Radar Tracking

19990108792 Indian Inst. of Tropical Meteorology, Poona, India
Relationship Between Initial Development of Precipitation and Onset of Cloud Electrification and the Observed Behaviour of Point Discharge Current During "Rain" and "No-Rain" Situations in the Thunderstorms at Pune
Kandalgaonkar, S. S., Indian Inst. of Tropical Meteorology, India; Tinmaker, M. I. R., Indian Inst. of Tropical Meteorology, India; Manohar, G. K., Indian Inst. of Tropical Meteorology, India; 11th International Conference on Atmospheric Electricity; June 1999, pp. 503-506; In English; See also 19990108601; No Copyright; Avail: CASI; A01, Hardcopy; A10, Microfiche

Thunderstorms are known to be more severe in the tropics and subtropics than elsewhere. The observations of lightning and precipitation show that the thunder clouds are the seat of intense cloud electrification and precipitation development. As the storm forms and dissipates several complex cloud physical and electrical processes such as charge separation, precipitation formation, occurrence of lightning and point discharge current are taking place. The understanding of the time sequence between these processes (i.e. initial development of precipitation and onset of cloud electrification) is important as the convection, electrification and precipitation are the remarkable aspects of thunder clouds. In addition to this, in thunderstorm activity the reports of occurrence of precipitation associated with point discharge current (PDC) are quite common. Measurements have shown that these precipitation elements are electrically charged bodies and normally deposit positive charge to the Earth's surface. A pertinent question that surrounds this situation is the interaction (scavenging and attachment) between the PD ions and precipitation elements near the ground surface and its likely effect on PDC. It appears that very little information on this intuitively appealing problem is available in literature. This short communication describes the results of the above two studies by using one-minute interval data of electric field, rainfall and PDC during the evolution of 14 and 21 thunderstorms which occurred at Pune (18 deg 32'N, 73 deg 51'E, 559 m asl). The results of the first part of the study are presented in the form of one table and figure. The combined result of this study indicated in-cloud development of precipitation at least 3-7 minutes in advance of electric field intensification. Our result suggests that in most cases precipitation development in thunderstorms is initiated well before the electric field begins to intensify. This results appears to be in good agreement with the results of earlier studies. The results of the second part of the study are presented in one table giving average PDC for every half a kilo width of electric field in the range -7.0 to +6.5 kV/m. We also present scatter diagrams of one-minute interval values of PDC vs. electric field drawn over the "two" situations. Our results strongly suggest that PDC of both polarities in "rain" is reduced more than that in "no-rain". The reduction for negative current was more obvious.
Author
Cloud Physics; Electric Fields; Electrification; Lightning; Thunderstorms; Rain

19990108794 Office National d'Etudes et de Recherches Aerospatiales, Chatillon, France
Evaluation of NOx Produced by Storms Based on 3D VHF Lightning Mapping
Laroche, P., Office National d'Etudes et de Recherches Aerospatiales, France; Defer, E., Office National d'Etudes et de Recherches Aerospatiales, France; Blanchet, P., Office National d'Etudes et de Recherches Aerospatiales, France; Thery, C., Office National d'Etudes et de Recherches Aerospatiales, France; 11th International Conference on Atmospheric Electricity; June 1999, pp. 656-659; In English; See also 19990108601
Contract(s)/Grant(s): DGAC-C94.03; No Copyright; Avail: CASI; A01, Hardcopy; A10, Microfiche

The evaluations of NOx production by lightning within storms are commonly based on modeling, laboratory and field experiments. to apply laboratory experiment and physical modeling to observed storms or at global scales, the authors use schematic representation of a lightning flash. We describe the actual observed 3D structure of a lightning flash derived from VHF lightning mapping and we comment on a method for the evaluation of NOx production.
Author
Thunderstorms; Lightning; Nitrogen Oxides; Electric Discharges

19990109079 NASA Goddard Space Flight Center, Greenbelt, MD USA
Sensitivity of High-Resolution Simulations of Hurricane Bob (1991) to Planetary Boundary Layer Parameterizations
Braun, Scott A., NASA Goddard Space Flight Center, USA; Tao, Wei–Kuo, NASA Goddard Space Flight Center, USA; 1999; 57p; In English; No Copyright; Avail: CASI; A04, Hardcopy; A01, Microfiche

The MM5 mesoscale model is used to simulate Hurricane Bob (1991) using grids nested to high resolution (4 km). Tests are conducted to determine the sensitivity of the simulation to the available planetary boundary layer parameterizations, including

the bulk-aerodynamic, Blackadar, Medium-RanGe Forecast (MRF) model, and Burk-Thompson boundary-layer schemes. Significant sensitivity is seen, with minimum central pressures varying by up to 17 mb. The Burk-Thompson and bulk-aerodynamic boundary-layer schemes produced the strongest storms while the MRF scheme produced the weakest storm. Precipitation structure of the simulated hurricanes also varied substantially with the boundary layer parameterizations. Diagnostics of boundary-layer variables indicated that the intensity of the simulated hurricanes generally increased as the ratio of the surface exchange coefficients for heat and momentum, C(sub h)/C(sub M), although the manner in which the vertical mixing takes place was also important. Findings specific to the boundary-layer schemes include: 1) the MRF scheme produces mixing that is too deep and causes drying of the lower boundary layer in the inner-core region of the hurricane; 2) the bulk-aerodynamic scheme produces mixing that is probably too shallow, but results in a strong hurricane because of a large value of C(sub h)/C(sub M) (approximately 1.3); 3) the MRF and Blackadar schemes are weak partly because of smaller surface moisture fluxes that result in a reduced value of C(sub h)/C(sub M) (approximately 0.7); 4) the Burk-Thompson scheme produces a strong storm with C(sub h)/C(sub M) approximately 1; and 5) the formulation of the wind-speed dependence of the surface roughness parameter, z(sub 0), is important for getting appropriate values of the surface exchange coefficients in hurricanes based upon current estimates of these parameters.

Author

Mesoscale Phenomena; Planetary Boundary Layer; Atmospheric Boundary Layer; Atmospheric Circulation; Wind (Meteorology); Parameterization; Hurricanes

19990109080 NASA Goddard Space Flight Center, Greenbelt, MD USA

Tropical Rainfall Distributions Determined Using TRMM Combined with other Satellite and Raingauge Information

Adler, Robert F., NASA Goddard Space Flight Center, USA; Huffman, George J., NASA Goddard Space Flight Center, USA; Bolvin, David T., NASA Goddard Space Flight Center, USA; Curtis, Scott, NASA Goddard Space Flight Center, USA; Nelkin, Eric J., NASA Goddard Space Flight Center, USA; 1999; 34p; In English; Original contains color illustrations; No Copyright; Avail: CASI; A03, Hardcopy; A01, Microfiche

Abstract A technique is described to use Tropical Rain Measuring Mission (TRMM) combined radar/radiometer information to adjust geosynchronous infrared satellite data (the TRMM Adjusted GOES Precipitation Index, or TRMM AGPI). The AGPI is then merged with rain gauge information (mostly over land; the TRMM merged product) to provide fine- scale (1 deg latitude/longitude) pentad and monthly analyses, respectively. The TRMM merged estimates are 10% higher than those from the Global Precipitation Climatology Project (GPCP) when integrated over the tropical oceans (37 deg N-S) for 1998, with 20% differences noted in the most heavily raining areas. In the dry subtropics the TRMM values are smaller than the GPCP estimates. The TRMM merged-product tropical-mean estimates for 1998 are 3.3 mm/ day over ocean and 3.1 mm/ day over land and ocean combined. Regional differences are noted between the western and eastern Pacific Ocean maxima when TRMM and GPCP are compared. In the eastern Pacific rain maximum the TRMM and GPCP mean values are nearly equal, very different from the other tropical rainy areas where TRMM merged-product estimates are higher. This regional difference may indicate that TRMM is better at taking in to account the vertical structure of the rain systems and the difference in structure between the western and eastern (shallower) Pacific convection. Comparisons of these TRMM merged analysis estimates with surface data sets shows varied results; the bias is near zero when compared to western Pacific Ocean atoll raingauge data, but significantly positive compared to Kwajalein radar estimates (adjusted by rain gauges). Over land the TRMM estimates also show a significant positive bias. The inclusion of gauge information in the final merged product significantly reduces the bias over land, as expected. The monthly precipitation patterns produced by the TRMM merged data process clearly show the evolution of the ENSO tropical precipitation pattern from early 1998 (El Nino) through early 1999 (La Nina) and beyond. The El Nino minus La Nina difference map shows the eastern Pacific maximum, the maritime continent minima and other tropical and mid-latitude features. The differences in the Pacific are very similar to those detected by the GPCP analyses. However, summing the El Nino minus La Nina differences over the global tropical oceans yields divergent answers from TRMM, GPCP and other estimates. This emphasizes the need for additional validation and analysis before it is feasible to understand the relations between global precipitation anomalies and Pacific Ocean ENSO temperature changes.

Author

Rain; Tropical Regions; Procedures; Measuring Instruments; Meteorological Radar; Rain Gages; Precipitation (Meteorology)

19990109082 NASA Goddard Space Flight Center, Greenbelt, MD USA

Interaction Between Tropical Convection and its Embedding Environment: An Energetics Analysis of a 2-D Cloud Resolving Simulation

Li, Xiaofan, SM and A Corp., USA; Sui, C.–H., NASA Goddard Space Flight Center, USA; Lau, K.–M., NASA Goddard Space Flight Center, USA; 1999; 26p; In English; No Copyright; Avail: CASI; A03, Hardcopy; A01, Microfiche

The phase relation between the perturbation kinetic energy (K') associated with the tropical convection and the horizontal-mean moist available potential energy (bar-P) associated with environmental conditions is investigated by an energetics analysis of a numerical experiment. This experiment is performed using a 2-D cloud resolving model forced by the TOGA-COARE derived vertical velocity. The imposed upward motion leads to a decrease of bar-P directly through the associated vertical advective cooling, and to an increase of K' directly through cloud related processes, feeding the convection. The maximum K' and its maximum growth rate lags and leads, respectively, the maximum imposed large-scale upward motion by about 1-2 hours, indicating that convection is phase locked with large-scale forcing. The dominant life cycle of the simulated convection is about 9 hours, whereas the time scales of the imposed large-scale forcing are longer than the diurnal cycle. In the convective events, maximum growth of K' leads maximum decay of the perturbation moist available potential energy (P') by about 3 hours through vertical heat transport by perturbation circulation, and perturbation cloud heating. Maximum decay of P' leads maximum decay of bar-P by about one hour through the perturbation radiative, processes, the horizontal-mean cloud heating, and the large-scale vertical advective cooling. Therefore, maximum gain of K' occurs about 4-5 hours before maximum decay of bar-P.

Author

Perturbation; Kinetic Energy; Potential Energy; Convection; Advection

19990109086 NASA Goddard Space Flight Center, Greenbelt, MD USA

The Status of the Tropical Rainfall Measuring Mission (TRMM) after 2 Years in Orbit

Kummerow, C., NASA Goddard Space Flight Center, USA; Simpson, J., NASA Goddard Space Flight Center, USA; Thiele, O., NASA Goddard Space Flight Center, USA; Barnes, W., NASA Goddard Space Flight Center, USA; Chang, A. T. C., NASA Goddard Space Flight Center, USA; Stocker, E., NASA Goddard Space Flight Center, USA; Adler, R. F., NASA Goddard Space Flight Center, USA; Hou, A., NASA Goddard Space Flight Center, USA; Kakar, R., NASA, USA; Wentz, F., Remote Sensing Systems, Inc., USA; 19990929; 54p; In English; Original contains color illustrations; No Copyright; Avail: CASI; A04, Hardcopy; A01, Microfiche

The Tropical Rainfall Measuring Mission (TRMM) satellite was launched on November 27, 1997, and data from all the instruments first became available approximately 30 days after launch. Since then, much progress has been made in the calibration of the sensors, the improvement of the rainfall algorithms, in related modeling applications and in new datasets tailored specifically for these applications. This paper reports the latest results regarding the calibration of the TRMM Microwave Imager, (TMI), Precipitation Radar (PR) and Visible and Infrared Sensor (VIRS). For the TMI, a new product is in place that corrects for a still unknown source of radiation leaking in to the TMI receiver. The PR calibration has been adjusted upward slightly (by 0.6 dBZ) to better match ground reference targets, while the VIRS calibration remains largely unchanged. In addition to the instrument calibration, great strides have been made with the rainfall algorithms as well, with the new rainfall products agreeing with each other to within less than 20% over monthly zonally averaged statistics. The TRMM Science Data and Information System (TSDIS) has responded equally well by making a number of new products, including real-time and fine resolution gridded rainfall fields available to the modeling community. The TRMM Ground Validation (GV) program is also responding with improved radar calibration techniques and rainfall algorithms to provide more accurate GV products which will be further enhanced with the new multiparameter 10 cm radar being developed for TRMM validation and precipitation studies. Progress in these various areas has, in turn, led to exciting new developments in the modeling area where Data Assimilation, and Weather Forecast models are showing dramatic improvements after the assimilation of observed rainfall fields.

Author

Trmm Satellite; Rain; Climatology; Tropical Meteorology; Zonal Flow (Meteorology); Hurricanes

19990109092 Los Alamos National Lab., Atmospheric and Space Sciences Group, NM USA

Satellite observations of transient radio impulses from thunderstorms

Argo, P. E.; Kirkland, M.; Jacobson, A.; Massey, R.; Suszynsky, D.; Dec. 31, 1999; 5p; In English; 11th; Atmospheric electricity (ICAE 1999)

Report No.(s): DE99-002734; LA-UR-99-977; No Copyright; Avail: Department of Energy Information Bridge, Hardcopy

Transient radio emissions from thunderstorms detected by satellites were first reported in 1995. The nature and source of these emissions remained a mystery until the launch of the FORTE satellite in 1997. FORTE, with its more sophisticated triggering and larger memory capacity showed that these emissions were connected to major thunderstorm systems. The analysis reported here, connecting FORTE RF events with ground based lightning location data from the National Lightning Detection Network (NLDN), shows that localized regions within thunderstorms are responsible for the creation of the satellite detected rf signals. These regions are connected with the areas of strong radar returns from the NEXRAD Doppler radar system, indicating that they are from regions of intense convection. The authors will also show data from several storms detected in the extended Caribbean, in which the height

profile of the source regions can be determined. Although as a single low earth orbit satellite FORTE cannot provide global coverage of thunderstorm/lightning events, follow-on satellite constellations should be able to provide detailed information on global lightning in near real-time.
NTIS
Satellite Observation; Radio Frequencies; Thunderstorms; Impulses

19990109106 Desert Research Inst., Desert Research Inst., Reno, NV USA
Forecast Model Applications of Satellite-Derived Cloud Parameters ***Annual Report, 1 May 1998 - 30 Apr. 1999***
Wetzel, Melanie; Chai, Steven; Apr. 30, 1999; 14p; In English
Contract(s)/Grant(s): N00014-98-1-0556
Report No.(s): AD-A364726; No Copyright; Avail: CASI; A03, Hardcopy; A01, Microfiche

Microphysical characteristics in maritime cloud have significant control on cloud layer evolution, electromagnetic propagation, cloud aerosol interactions, visibility, and aircraft flight hazards. While the Coupled Ocean/Atmosphere Mesoscale Prediction System (COAMPS) model may not in the immediate future explicitly represent cloud microphysical parameters, the relationship of cloud structure to the predicted variables must be assessed, particularly when considering physical or radiative parameterizations. Electromagnetic signal propagation through the atmosphere is directly influenced by the size and composition of atmospheric particles. Cloud droplet size, particularly at cloud top in the marine atmospheric boundary layer (MABL), plays a role in the rate at which turbulent entrainment produces aerosol via evaporation or removes aerosol via collection by droplets. The droplet size distribution also controls the effectiveness of the stochastic collision coalescence process in producing drizzle or rain, thereby also impacting the evaporative source (or collection loss) of aerosol during drop sedimentation below cloud. These processes can be incorporated into combined aerosol cloud simulation models by explicit or parameterized treatments.
DTIC
Weather Forecasting; Raindrops; Cloud Physics

19990109129 NASA Marshall Space Flight Center, Huntsville, AL USA
A Comparison between Lightning Activity and Passive Microwave Measurements
Kevin, Driscoll T., NASA Marshall Space Flight Center, USA; Hugh, Christian J., NASA Marshall Space Flight Center, USA; Goodman, Steven J., NASA Marshall Space Flight Center, USA; [1999]; 1p; In English; 11th; Atmospheric Electricity, 7-11 Jun. 1999, Guntersville, AL, USA; Copyright; Avail: Issuing Activity, Hardcopy; Abstract Only

A recent examination of data from the Lightning Imaging Sensor (LIS) and the TRMM Microwave Imager (TMI) suggests that storm with the highest frequency of lightning also possess the most pronounced microwave scattering signatures at 37 and 85 GHz. This study demonstrates a clear dependence between lightning and the passive microwave measurements, and accentuates how direct the relationship really is between cloud ice and lightning activity. In addition, the relationship between the quantity of ice content and the frequency of lightning (not just the presence of lightning) , is consistent throughout the seasons in a variety of regimes. Scatter plots will be presented which show the storm-averaged brightness temperatures as a function of the lightning density of the storms (L/Area) . In the 85 GHz and 37 GHz scatter plots, the brightness temperature is presented in the form Tb = k1 x log10(L/Area) + k2, where the slope of the regression, k1, is 58 for the 85 GHz relationship and 30.7 for the 37 GHz relationship. The regression for both these fits showed a correlation of 0.76 (r2 = 0.58), which is quite promising considering the simple procedure used to make the comparisons, which have not yet even been corrected for the view angle differences between the instruments, or the polarization corrections in the microwave imager.
Author
Lightning; Data Processing; Imaging Techniques; Microwave Imagery; Brightness Temperature

19990109159 NASA Goddard Space Flight Center, Greenbelt, MD USA
Rain Fallspeeds and Rates Derived from Airborne Nadir-Pointing Doppler Radar Measurements
Heymsfield, Gerald M., NASA Goddard Space Flight Center, USA; Tian, L., NASA Goddard Space Flight Center, USA; Geerts, Bart, NASA Goddard Space Flight Center, USA; [1999]; 3p; In English; 29th; Radar Meteorology, Jul. 1999, Montreal, Canada; Sponsored by American Meteorology Society, USA; No Copyright; Avail: CASI; A01, Hardcopy; A01, Microfiche

The use of vertical-incidence Doppler velocity in addition to radar reflectivity may yield information on drop size distribution and therefore result in better rainrate estimates. Doppler velocity can provide useful information on the raindrop size distribution. Doppler velocities from a zenith-pointing radar represent the sum of the mean reflectivity-weighted hydrometeor fallspeed and the vertical air motion. Dual-parameter rain estimation methods using the Doppler velocity, require that the latter can be removed, or is negligible. Atlas et al. (1972) derived relations between Doppler velocity, reflectivity, and rain rate assuming an exponential size distribution for rain. Ulbrich (1994) expanded on this work by deriving the relation between the Doppler velocity and the

reflectivity assuming a Gamma size distribution. This distribution provides a more realistic representation of the small rain drops. to get accurate information on raindrop size distributions with the above method, the air motions must be removed from the observed Doppler velocities
Author
Drop Size; Rain; Raindrops; Size Distribution; Estimates

19990109160 NASA Goddard Space Flight Center, Greenbelt, MD USA
High Resolution Reflectivity Profiles in Various Convectively Generated Precipitation Systems
Greet, Bart, NASA Goddard Space Flight Center, USA; Heymsfield, G., NASA Goddard Space Flight Center, USA; Tian, L., NASA Goddard Space Flight Center, USA; [1999]; 3p; In English; 29th; Radar Meteorology, Jul. 1999, Montreal, Canada; Sponsored by American Meteorology Society, USA; No Copyright; Avail: CASI; A01, Hardcopy; A01, Microfiche

This brief paper illustrates some profiles of radar reflectivity in various precipitation systems observed during the 1998-99 Tropical Rainfall Measuring Mission (TRMM) field campaigns. the profiles were collected by a nadir-viewing radar on the NASA ER-2 flying around 20 km altitude. The paper focuses on hurricane environments.
Author
High Resolution; Reflectance; Rain; Data Acquisition

19990109670 NASA Goddard Space Flight Center, Greenbelt, MD USA
Contribution of Tropical Cyclones to the North Pacific Climatological Rainfall as Observed from Satellites
Rodgers, Edward B., NASA Goddard Space Flight Center, USA; Adler, Robert F., NASA Goddard Space Flight Center, USA; Pierce, Harold F., Science Systems and Applications, Inc., USA; [1997]; 54p; In English; Original contains color illustrations
Contract(s)/Grant(s): RTOP 912-622-28-06-25; No Copyright; Avail: CASI; A04, Hardcopy; A01, Microfiche

Tropical cyclone monthly rainfall amounts are estimated from passive microwave satellite observations for an eleven year period. These satellite-derived rainfall amounts are used to assess the impact of tropical cyclone rainfall in altering the geographical, seasonal, and inter-annual distribution of the North Pacific Ocean total rainfall during June-November when tropical cyclones are most important. to estimate these tropical cyclone rainfall amounts, mean monthly rain rates are derived from passive microwave satellite observations within 444 km radius of the center of those North Pacific tropical cyclones that reached storm stage and greater. These rain rate observations are converted to monthly rainfall amounts and then compared to those for non-tropical cyclone systems. The main results of this study indicate that: 1) tropical cyclones contribute 7% of the rainfall to the entire domain of the North Pacific during the tropical cyclone season and 12%, 3%, and 4% when the study area is limited to, respectively, the western, central, and eastern third of the ocean; 2) the maxima in tropical cyclone rainfall are poleward (5 deg to 10 deg latitude depending on longitude) of the maxima in non-tropical cyclone rainfall; 3) tropical cyclones contribute a maximum of 30% northeast of the Philippine Islands and 40% of the lower Baja California coast; 4) in the western North Pacific, the tropical cyclone rainfall lags the total rainfall by approximately two months and shows seasonal latitudinal variation following the ITCZ; and 5) in general, tropical cyclone rainfall is enhanced during the El Nino years by warm SSTs in the eastern North Pacific and by the monsoon trough in the western and central North Pacific.
Author
Annual Variations; Climatology; Cyclones; Microwaves; Monsoons; Tropical Storms

19990109990 Oregon Univ., Coll. of Arts and Sciences, Eugene, OR USA
Atmospheric and Spectroscopic Research in the Far Infrared ***Final Report, 22 Feb. 1995 - 21 Feb. 1998***
Park, Kwangjai, Oregon Univ., USA; 1998; 4p; In English
Contract(s)/Grant(s): NAG1-1650; No Copyright; Avail: CASI; A01, Hardcopy; A01, Microfiche

The spectroscopic measurements of molecular parameters constitute one of the major areas of our research program. This part of our program has been conducted in close collaboration with Smithsonian Astrophysical Observatory (SAO) and National Institute of Standards and Technology (NIST). The references on HO2, OH, and O2 that appear on the publication list are examples of this type of work completed during the grant period. These pressure-broadening studies have provided the kind of improvements needed in the database for retrieving atmospheric profiles from far infrared limb sensing data. Authors summarized the laboratory spectroscopic studies conducted during the grant period. We attempted to measure the pressure broadening coefficients of the O2 lines in the 50 and 117/ cm regions. An accurate characterization of these lines using the IBEX detector system was needed to analyze the flight data. These are difficult lines to measure because they arise from weak magnetic dipole transitions. We used a 4-meter absorption cell to obtain the pressure broadening coefficients for the 50 and 83 /cm lines. We also completed the pressure broadening studies including the temperature dependence of two lines of OH at 83 and 118 /cm. These

two lines are important not only for the balloon data retrieval work but also for the future project proposals.Another area of focus in our program is the far infrared detector research. The third area of focus deals with data distribution and dissemination.
Derived from text
Far Infrared Radiation; Molecular Dynamics; Temperature Dependence; Pressure Broadening; Data Retrieval

19990110094 Weather Squadron (45th), Patrick AFB, FL USA
Weather Support to Range Safety
Boyd, B. F., Weather Squadron (45th), USA; Harms, D. E., Weather Squadron (45th), USA; Fitzpatrick, M. E., Weather Squadron (45th), USA; Stout, R. P., Space Wing (45th), USA; Rosati, P. N., Space Wing (45th), USA; Berlinrut, D. D., Space Wing (45th), USA; Parks, C. R., ACTA, Inc., USA; Overbeck, K. B., ACTA, Inc., USA; JANNAF 28th Propellant Development and Characterization Subcommittee and 17th Safety and Environmental Protection Subcommitte Joint Meeting; April 1999; Volume 1, pp. 59-69; In English; See also 19990110087; No Copyright; Avail: CPIA, 10630 Little Patuxent Pkwy., Suite 202, Columbia, MD 21044-3200 HC, Hardcopy

The Air Force's 45th Weather Squadron (45 WS) provides comprehensive operational meteorological services to the Eastern Range (ER) and the Kennedy Space Center (KSC). These services include weather support for resource protection, pre-launch ground processing and day-of-launch operations for up to 40 launches per year by the Department of Defense (DOD), National Aeronautics and Space Administration (NASA), and commercial launch customers. to ensure safety of government personnel and the civilian population, the Safety Office of the Eastern Range must ingest weather data into physical models which, in turn, assess the risk to safety of each operation. Most weather support, in essence, is to assure safety of resources -- people and material. This support includes: evaluating and issuing weather advisories/warnings, determining and assessing the specialized lightning Launch Commit Criteria (LCC) for avoidance of triggered lightning strikes during launch, and providing upper-air data to users for vehicle stress analysis prior to launch. However, Range Safety has additional special weather requirements in the following areas: (1) weather data input for the Range Safety model to forecast blast overpressure in case of an accident; (2) weather data input to models, which in turn determine potential toxic hazard corridors for ground processing operations, nominal launch operations, and catastrophic launch failures; (3) weather data input to Range Safety Flight Analysis prior to launch to determine flight trajectories, launch impact limit lines, and potential debris fallout; and (4) operational weather evaluation to ensure Range Safety can visually observe that the vehicle and payload remains intact during launch (stack integrity).
Author
Meteorological Parameters; Meteorological Services; Weather Forecasting; Range Safety

19990110603 Meteorological Satellite Center, Kiyose, Japan
The Features of the Extratropical Cyclones Passing Through Around Japan
Suzuki, Kazufumi, Meteorological Satellite Center, Japan; Meteorological Satellite Center Technical Note; March 1999, No. 37, pp. 35-62; In Japanese; See also 19990110600; Original contains color illustrations; No Copyright; Avail: CASI; A03, Hardcopy; A01, Microfiche

The features of the extratropical cyclones passing through around Japan are investigated using satellite images. "South Coast Cyclones"(cyclones passing through south of Japan Islands) conform to the typical cloud pattern of the developing cyclone. For these cyclones, it is easy to identify cold fronts and warm fronts by the satellite images. "Japan Sea Cyclones"(cyclones passing through north of Japan Islands) are classified into two types. One is the cyclones having active rainbands in the warm sector. For these cyclones, identifying warm fronts are easy but deciding the positions of cold fronts have the alternative of the rainband or the cold advection maximum far away from the rainband. The other is the cyclones having ana-cold fronts. For these cyclones, identifying cold fronts is easier than warm fronts. For "Coupled Cyclones"(cyclones passing through south and north of Japan Islands simultaneously), the cyclone passing through south is similar to the South Coast Cyclone and the cyclone passing through north is similar to the Japan Sea Cyclone with ana-cold front. It seems that these features are influenced by the orographic effect of Japan Islands and by the warm temperature of the sea south of Japan.
Author
Cyclones; Meteorology; Wind (Meteorology); Cold Fronts; Warm Fronts

19990110604 Meteorological Satellite Center, Kiyose, Japan
Detection of Fog and Low Level Clouds in the Nighttime Using Near-Infrared Imageries (3.7 Microns)
Yamazaki, Shin–Ichi, Meteorological Satellite Center, Japan; Kanda, Kazufumi, Meteorological Satellite Center, Japan; Yamagiwa, Ryutaro, Meteorological Satellite Center, Japan; Meteorological Satellite Center Technical Note; March 1999, No. 37, pp. 63-77; In Japanese; See also 19990110600; No Copyright; Avail: CASI; A03, Hardcopy; A01, Microfiche

In summer of 1999, a Multi-functional Transport Satellite (MTSAT) will be launched as a successor of the GMS-5. The meteorological mission of MTSAT fundamentally succeeds major specification of GMS-5 and a 'near-infrared' sensor with wavelength of 3.7 microns will be added. to examine an efficiency of 3.7 microns sensor, a 'MTSAT IR Simulation Image (MISI)' was made from NOAA/AVHRR IR image by reducing its spatial resolution from about 1 km to 5 km at sub satellite point. by using the MISI, it is confirmed that the image of the TBB difference between 3.7 microns and 11 microns channel from MTSAT will be useful for detecting 1) a fog or low-level stratus area and 2) system center of a typhoon in the stage of 'Shear-pattern' which is characterized that the location of dense cloud shears from the cloud system center determined by the low level cloud lines.
Author
Fog; Clouds (Meteorology); Night; Infrared Imagery; Meteorological Satellites; Satellite Observation; Meteorology

19990110690 NASA Goddard Space Flight Center, Greenbelt, MD USA
The Variation of Tropical Cyclone Rainfall within the North Atlantic and Pacific as Observed from Satellites
Rodgers, Edward, NASA Goddard Space Flight Center, USA; Pierce, Harold, Science Systems and Applications, Inc., USA; Adler, Robert, NASA Goddard Space Flight Center, USA; [1999]; 2p; In English; 8th; Climate, 13-17 Sep. 1999, Boulder, CO, USA; No Copyright; Avail: CASI; A01, Hardcopy; A01, Microfiche

Tropical cyclone monthly rainfall amounts are estimated from passive microwave satellite observations in the North Atlantic and in three equal geographical regions of the North Pacific (i.e., Western, Central, and Eastern North Pacific). These satellite-derived rainfall amounts are used to assess the impact of tropical cyclone rainfall in altering the geographical, seasonal, and inter-annual distribution of the 1987-1989, 1991-1998 North Atlantic and Pacific rainfall during June-November when tropical cyclones are most abundant. To estimate these tropical cyclone rainfall amounts, mean monthly rain rates are derived from the Defence Meteorological Satellite Program (DMSP) Special Sensor Microwave/ Radiometer (SSM/I) observations within 444 km radius of the center of those North Atlantic and Pacific tropical cyclones that reached storm stage and greater. These rain rate observations are then multiplied by the number of hours in a given month. Mean monthly rainfall amounts are also constructed for all the other North Atlantic and Pacific raining systems during this eleven year period for the purpose of estimating the geographical distribution and intensity of rainfall contributed by non-tropical cyclone systems. Further, the combination of the non-tropical cyclone and tropical cyclone (i.e., total) rainfall is constructed to delineate the fractional amount that tropical cyclones contributed to the total North Pacific rainfall.
Author
Cyclones; Estimating; Microwave Radiometers; Rain; Remote Sensing; Satellite Observation; Tropical Storms

19990110694 NASA Goddard Space Flight Center, Greenbelt, MD USA
Longwave Radiative Flux Calculations in the TOVS Pathfinder Path A Data Set
Mehta, Amita, General Sciences Corp., USA; Susskind, Joel, NASA Goddard Space Flight Center, USA; September 1999; 46p; In English; Original contains color illustrations
Report No.(s): NASA/CR-1999-208643; NAS 1.26:208643; Rept-99B00065; No Copyright; Avail: CASI; A03, Hardcopy; A01, Microfiche

A radiative transfer model developed to calculate outgoing longwave radiation (OLR) and downwelling longwave, surface flux (DSF) from the Television and Infrared Operational Satellite (TIROS) Operational Vertical Sounder (TOVS) Pathfinder Path A retrieval products is described. The model covers the spectral range of 2 to 2800 cm in 14 medium medium spectral bands. For each band, transmittances are parameterized as a function of temperature, water vapor, and ozone profiles. The form of the band transmittance parameterization is a modified version of the approach we use to model channel transmittances for the High Resolution Infrared Sounder 2 (HIRS2) instrument. We separately derive effective zenith angle for each spectral band such that band-averaged radiance calculated at that angle best approximates directionally integrated radiance for that band. We develop the transmittance parameterization at these band-dependent effective zenith angles to incorporate directional integration of radiances required in the calculations of OLR and DSF. The model calculations of OLR and DSF are accurate and differ by less than 1% from our line-by-line calculations. Also, the model results are within 1% range of other line-by-line calculations provided by the Intercomparison of Radiation Codes in Climate Models (ICRCCM) project for clear-sky and cloudy conditions. The model is currently used to calculate global, multiyear (1985-1998) OLR and DSF from the TOVS Pathfinder Path A Retrievals.
Author
Atmospheric Sounding; Long Wave Radiation; Radiative Transfer; Satellite Sounding; Transmittance

19990111491 NASA Goddard Space Flight Center, Greenbelt, MD USA
Application of Lidar Winds to Data Assimilation
Atlas, Robert, NASA Goddard Space Flight Center, USA; 1999; 1p; In English; 13th, 5-9 Apr. 1999, Orlando, FL, USA;

Sponsored by International Society for Optical Engineering; No Copyright; Avail: Issuing Activity, Hardcopy; Abstract Only

One of the major applications of space-based doppler wind lidar is to improve atmospheric analyses and numerical weather prediction (NWP). Since the mid 198,0's, Observing System Simulation Experiments (OSSE's) have been conducted in order to evaluate the potential impact of lidar winds on NWP. These experiments have shown tremendous potential for satellite lidar observations to improve atmospheric analyses and forecasts. In addition, the OSSE's are providing an evaluation of trade-offs in lidar design, and are currently being used to define the specific requirements for lidar winds in terms of horizontal and vertical coverage and accuracy. At the meeting the methodology for these experiments and the main results relating to proposed lidars will be presented.

Author

Optical Radar; Wind (Meteorology); Data Processing; Atmospheric Chemistry; Numerical Weather Forecasting

19990111535 Department of Energy, Assistant Secretary for Environment, Safety, and Health, Washington, DC USA

Diagnostic study on retrieving bulk microphysical properties of low-level stratiform clouds and its implication on climate research

Chin, H. N. S., Department of Energy, USA; Rodriguez, D. J., Department of Energy, USA; Cederwall, R. T., Department of Energy, USA; Chuang, C. C., Department of Energy, USA; Grossman, A. S., Department of Energy, USA; Mar. 01, 1998; 8p; In English; 8th; Atmospheric Radiation Measurements (ARM, USA

Report No.(s): DE98-057701; UCRL-JC-130364; CONF-9703164; No Copyright; Avail: Department of Energy Information Bridge, Microfiche

The importance of low-level stratiform clouds to the planetary radiation balance is due to their persistence and coverage, and their effect on the planetary albedo. The vertical distribution of liquid water in these clouds is pertinent to many applications in atmospheric research. As a result, some cloud retrieval techniques have been developed with the assumptions, such as an adiabatic condition, no loss of liquid water via drizzle and/or a large liquid water path.

NTIS

Stratus Clouds; Atmospheric Radiation; Climate; Planetary Radiation

19990111537 NASA Goddard Space Flight Center, Greenbelt, MD USA

TRMM Realtime Data Production, Transfer, and Future Plans

Stocker, Erich Franz, NASA Goddard Space Flight Center, USA; 1999; 1p; In English, 18-20 Feb. 1999, Osaka, Japan; Sponsored by Asia-Pacific Advanced Network, Japan; No Copyright; Avail: Issuing Activity, Hardcopy; Abstract Only

The Tropical Rainfall Measuring Mission, a joint US NASA and Japan NASDA mission, was launched on November 27, 1997 from Tanegashima Island, Japan on a NASDA provided H-II launch vehicle. The TRMM objectives are: to obtain and study multi-year science data sets of tropical and sub- tropical rainfall measurement; to understand how interactions between the sea, air, and land masses produce changes in global rainfall and climate; to help improve modeling of tropical rainfall processes; to test, evaluate, and improve the performance of satellite rainfall estimates measurements and techniques. The routine production and quick distribution of standard products provides an important underpinning to these objectives. The determination of standard TRMM algorithms and the requirements for routine production and distribution fall within the authority of the joint US-Japan Science Team. In April of 1998, the Joint TRMM Science team requested that TRMM data be made available in near real-time to approved international agencies and modelers. This request was an addition to the routine production of the standard TRMM data products. The science team requested that near-realtime products be as small as possible to facilitate their transfer via networks. Indeed, it was determined that only network transfer would be available. This presentation provides an overview of the type of products available from the realtime system and how the TRMM system was developed at the lowest cost in the shortest amount of time. It then describes the real-time data flow. The presentation also summarizes how the science quality of real-time data is maintained. It describes how interested groups can get access to this data and the importance of networks for the future of real-time data expansion. The presentation concludes real-time possibilities and improvements possible as part of the proposed Global Precipitation Mission. High speed network access availability is an important catalyst to real-time data flow during the proposed mission.

Author

Algorithms; Climatology; Communication Networks; Precipitation (Meteorology); Rain; Trmm Satellite; Tropical Regions

19990111727 NASA Langley Research Center, Hampton, VA USA

Absorption of Solar Radiation by Clouds: Observations Versus Models

Cess, R. D., State Univ. of New York, USA; Zhang, M. H., State Univ. of New York, USA; Minnis, P., NASA Langley Research Center, USA; Corsetti, L., Lawrence Livermore National Lab., USA; Dutton, E. G., National Oceanic and Atmospheric

Administration, USA; Forgan, B. W., Bureau of Meteorology, Australia; Garber, D. P., Lockheed Engineering and Sciences Co., USA; Gates, W. L., Lawrence Livermore National Lab., USA; Hack, J. J., National Center for Atmospheric Research, USA; Harrison, E. F., NASA Langley Research Center, USA; Jing, X., State Univ. of New York, USA; Kiehl, J. T., National Center for Atmospheric Research, USA; Long, C. N., Pennsylvania State Univ., USA; Morcrette, J.–J., European Centre for Medium-Range Weather Forecasts, UK; Potter, G. L., Lawrence Livermore National Lab., USA; Ramanathan, V., Scripps Institution of Oceanography, USA; Subasilar, B., Scripps Institution of Oceanography, USA; Whitlock, C. H., NASA Langley Research Center, USA; Young, D. F., Lockheed Engineering and Sciences Co., USA; Zhou, Y., State Univ. of New York, USA; Science; Jan. 27, 1995; Volume 267, pp. 496-499; In English; Copyright; Avail: Issuing Activity, Hardcopy, Microfiche

There has been a long history of unexplained anomalous absorption of solar radiation by clouds. Collocated satellite and surface measurements of solar radiation at five geographically diverse locations showed significant solar absorption by clouds, resulting in about 25 watts per square meter more global-mean absorption by the cloudy atmosphere than predicted by theoretical models. It has often been suggested that tropospheric aerosols could increase cloud absorption. But these aerosols are temporally and spatially heterogeneous, whereas the observed cloud absorption is remarkably invariant with respect to season and location. Although its physical cause is unknown, enhanced cloud absorption substantially alters our understanding of the atmosphere's energy budget.

Author

Radiation Absorption; Solar Radiation; Albedo; Cloud Physics; Earth Radiation Budget; Atmospheric Heat Budget; Atmospheric Radiation

19990113137 Environmental Protection Agency, National Exposure Research Lab., Research Triangle Park, NC USA

Using MM5 Version 2 with Models-3/CMAQ: A User's Guide and Tutorial

Otte, T. L.; Jul. 1999; 62p

Report No.(s): PB99-175424; EPA/600/R-99/065; No Copyright; Avail: CASI; A04, Hardcopy; A01, Microfiche

Meteorological data are important in many of the processes simulated in the Community Multi-Scale Air Quality (CMAQ) and the Models-3 framework. The first meteorology model that has been selected and evaluated with CMAQ is the Fifth-Generation Pennsylvania State University/National Center for Atmospheric Research (NCAR) Mesoscale Model (MM5). All software in the Penn State/NCAR mesoscale modeling system has been dedicated to the public domain and is presently used for both research and operational purposes at many organizations worldwide. Other meteorological models are being considered for compatibility with CMAQ but are not available at this time. This document is a basic overview of MM5 and its relationship with CMAQ and Models-3. Some general information is provided to help the user get started with aMM5 in preparation for Models-3 and CMAQ, and it is meant to supplement NCARS's official documentation of MM5.

NTIS

Mesoscale Phenomena; Micrometeorology; Mesometeorology; Atmospheric Models; Weather Forecasting; Meteorological Parameters

19990113144 Environmental Protection Agency, National Exposure Research Lab., Research Triangle Park, NC USA

Analysis of Carbonaceous Aerosols Using the Thermal Optical Transmittance and Thermal Optical Reflectance Methods

Norris, G. A.; Birch, M. E.; Tolocka, M. P.; Lewis, C. W.; Solomon, P. A.; 1999; 16p; In English

Report No.(s): PB99-171597; EPA/600/R-99/059; No Copyright; Avail: CASI; A03, Hardcopy; A01, Microfiche

Carbonaceous particulate typically represents a large fraction of PN25 (20-40%). Two primary techniques presently used for the analysis of particulate carbon are Thermal Optical Transmission (TOT-NIOSH Method 5040) and Thermal Optical Reflectance (TOR). These two methods both quantify carbon by heating filters and volatilizing the carbon that is oxidized in a granular bed of MnO2 reduced to CH4 in a Ni methanator, and quantified as CH4 with a flame ionization detector. However, the methods use different techniques to correct for the formation of pyrolysis products and the temperature programs for defining organic and elemental carbon. The TOT and TOR measurement techniques are being compared using samples from the Chemical Speciation Monitor Evaluation Field Study. All of the samples will be measured with TOR and a subset of samples representing a range of mass concentrations will be measured with TOT. This comparison will provide insight into the effect of the measurement technique parameters on organic and elemental carbon concentrations.

NTIS

Aerosols; Carbon; Carbonaceous Materials; Carbon Compounds; Particulates

19990113186 Washington Univ., Dept. of Earth and Planetary Sciences, Saint Louis, MO USA

Remote Sensing of Aircraft Contrails Using a Field Portable Digital Array Scanned Interferometer ***Final Report***

Smith, William Hayden, Washington Univ., USA; 1997; 4p; In English

Contract(s)/Grant(s): NCC2-5159; No Copyright; Avail: CASI; A01, Hardcopy; A01, Microfiche

With a Digital Array Scanned Interferometer (DASI), we have obtained proof-of-concept observations with which we demonstrate DASI capabilities for the determination of contrail properties. These include the measurement of the cloud and soot microphysical parameters, as well, the abundances of specific pollutant species such as SO(sub x) or NO(sub x). From high quality hyperspectral data and using radiative transfer methods and atmospheric chemistry analysis in the data reduction and interpretation, powerful inferences concerning cloud formation, evolution and dissipation can be made. Under this sub-topic, we will integrate DASI with computer controlled scanning of the field-of-view to direct the sensor towards contrails and exhaust plumes for tracking the emitting vehicles. The optimum DASI wavelength sensitivity range for sensing contrails is 0.35 - 2.5 micron. DASI deploys on the ground or from aircraft to observe contrails in the vicinity. This enables rapid, accurate measurement of the temporal, spatial, and chemical evolution of contrails (or other plumes or exhaust sources) with a low cost, efficient sensor. Author

Atmospheric Chemistry; Contrails; Exhaust Gases; Interferometers; Plumes; Remote Sensing; Condensates

19990113192 NASA Marshall Space Flight Center, Huntsville, AL USA

The Characteristics of Total Lightning Activity in Severe Florida Thunderstorms

Williams, E., Massachusetts Inst. of Tech., USA; Goodman, S. J., NASA Marshall Space Flight Center, USA; Raghavan, R., NASA Marshall Space Flight Center, USA; Boldi, R., Massachusetts Inst. of Tech., USA; Matlin, A., Massachusetts Inst. of Tech., USA; Weber, M., Massachusetts Inst. of Tech., USA; Hodanish, S., National Weather Service, USA; Sharp, D., National Weather Service, USA; [1997]; 1p; In English, 8-12 Dec. 1997, San Francisco, CA, USA; Sponsored by American Geophysical Union, USA; Copyright; Avail: Issuing Activity; Abstract Only, Hardcopy, Microfiche

Severe thunderstorms are defined by specific exceedance criteria regarding either wind speed (greater than or equal to 50 kts), hailstone diameter (greater than or equal to 3/4 inch), the occurrence of a tornado, or any combination thereof. Although traditional radar signatures of severe thunderstorms have been well documented, the characteristics of associated total lightning activity (both intracloud and cloud-to-ground) of severe thunderstorms remain poorly established. The reason for this are (1) less than 1% of all storms are actually severe, (2) intracloud lightning, which is typically the dominant form of electrical discharge within thunderstorms, is not routinely measured or recorded, (3) direct visual observations of intracloud lightning are obscured during the daytime, and (4) the migratory nature of many severe thunderstorms can make the accurate detection and mapping of intracloud lightning difficult when using fixed-location sensors. The recent establishment of LISDAD (Lightning Imaging Sensor Data Acquisition and Display - discussed in Goodman et al, this Meeting) has substantially addressed these limitations in east central Florida (ECFL). Analysis of total lightning flash Count histories using the LDAR (Lightning Detection and Ranging) system for known severe thunderstorms (currently irrespective of seasonal aspects and severe storm-type) has revealed flash rates exceeding 1 per second. This appears to be a necessary, but not sufficient,condition for most ECFL severe storm cases. The differences in radar-observed storm structure for high flash rate storms (to include both severe and non-severe categories) will be described together with the timing of peak flash rate vs. the timing of the severe weather manifestation. Comparisons with the satellite-bases OTD (Optical Transient Detector) overhead passes will also be presented when possible.
Author

Lightning; Thunderstorms

48
OCEANOGRAPHY

Includes biological, dynamic, and physical oceanography; and marine resources. For related information see also 43 Earth Resources and Remote Sensing.

19990109664 NASA Goddard Space Flight Center, Greenbelt, MD USA

Ocean Turbulence V: Mesoscale Modeling in Level Coordinates. The Effect of Random Nature of Density

Canuto, V. M., NASA Goddard Space Flight Center, USA; Dubovikov, M. S., NASA Goddard Space Flight Center, USA; [1998]; 22p; In English; No Copyright; Avail: CASI; A03, Hardcopy; A01, Microfiche

The main result of this paper is the derivation of a new expression for the tracer subgrid term in level coordinates S(l) to be employed in O-GCM. The novel feature is the proper account of the random nature of the density field which strongly affects the transformation from isopycnal to level coordinates of the variables of interest, velocity and tracer fields, their correlation functions and ultimately the subgrid terms. In deriving our result we made use of measured properties of vertical ocean turbulence. The major new results are: 1) the new subgrid expression is different from that of the heuristic GM model, 2) u++(tracer)=1/2u+(thickness), where u++ and u+ are the tracer and thickness bolus velocities. In previous models, u++ = u+, 2)

the subgrid for a tracer tau is not the same as that for the density rho even when one accounts for the obvious absence of a diffusion term in the latter. The difference stems from a new treatment of the stochastic nature of the density, 3) the mesoscale diffusivity enters both locally and non-locally, as the integral over all z's from the bottom of the ocean to the level z.
Author
Oceans; Turbulence; Mesoscale Phenomena; Turbulence Models; Statistical Distributions; Oceanography

19990109665 NASA Goddard Space Flight Center, Greenbelt, MD USA
Ocean Turbulence, Part 4, Mesoscale Modeling in Isopycnal Coordinates the role of the Spectrum of Vertical Shear
Canuto, V. M., NASA Goddard Space Flight Center, USA; Dubovikov, M. S., NASA Goddard Space Flight Center, USA; [1999]; 18p; In English; No Copyright; Avail: CASI; A03, Hardcopy; A01, Microfiche

We study the tracer subgrid term in isopycnal coordinates, S(sub I). We employ two ingredients: the experimental data on vertical spectra of ocean turbulence measured by Gargett et al.(1981) and the stochastic approach recently developed by Dukowicz and Smith (1997). Our result confirms that S(sub I) is made of two parts: an advection and a diffusion term. However, the tracer bolus velocity u** consists of two terms u** = u(sub 1) + u(sub 2) while in the GM model there is only a term related to u(sub 1) which is shown to be: u(sub 1) = k(bar-q)(sup -1)(delta)(sub rho) where bar-q is the thickness weighted average potential vorticity, a result in agreement with the recent suggestions by Treguier et al. (1997), Lee et al. (1997) and Greatbatch (1998). The second component u(sub 2) IS new. We compute it in the geostrophic approximation using the Gargett et al. data (1981) on ocean vertical turbulence. We find that u(sub 2) much greater than u(sub 1) and that u(sub 2) is orthogonal to u(sub 1).
Author
Oceans; Turbulence; Research

19990109666 NASA Goddard Space Flight Center, Greenbelt, MD USA
The Formation each Winter of the Circumpolar Wave in the Sea Ice around Antarctica
Gloersen, Per, NASA Goddard Space Flight Center, USA; White, Warren B., Scripps Institution of Oceanography, USA; [1999]; 5p; In English; Original contains color illustrations; No Copyright; Avail: CASI; A01, Hardcopy; A01, Microfiche

Seeking to improve upon the visualization of the Antarctic Circumpolar Wave (ACW) , we compare a 16-year sequence of 6-month winter averages of Antarctic sea ice extents and concentrations with those of adjacent sea surface temperatures (SSTs). Here we follow SSTs around the globe along the maximum sea ice edge rather than in a zonal band equatorward of it. The results are similar to the earlier ones, but the ACWs do not propagate with equal amplitude or speed. Additionally in a sequence of 4 polar stereographic plots of these SSTs and sea ice concentrations, we find a remarkable correlation between SST minima and sea ice concentration maxima, even to the extent of matching contours across the ice-sea boundary, in the sector between 900E and the Palmer Peninsula. Based on these observations, we suggest that the memory of the ACW in the sea ice is carried from one Austral winter to the next by the neighboring SSTS, since the sea ice is nearly absent in the Austral summer.
Author
Antarctic Regions; Sea Ice; Sea Surface Temperature; Wave Excitation

19990111519 NASA Goddard Space Flight Center, Greenbelt, MD USA
Massively Parallel Assimilation of TOGA/TAO and TOPEX/Poseidon Measurements into a Quasi Isopycnal Ocean General Circulation Model Using an Ensemble Kalman Filter
Keppenne, Christian L., NASA Goddard Space Flight Center, USA; Rienecker, Michele, NASA Goddard Space Flight Center, USA; Borovikov, Anna Y., NASA Goddard Space Flight Center, USA; Suarez, Max, NASA Goddard Space Flight Center, USA; 1999; 1p; In English; 24th, 19-23 Apr. 1999, Hague, Netherlands; Sponsored by European Geophysical Union, Netherlands; No Copyright; Avail: Issuing Activity, Hardcopy; Abstract Only

A massively parallel ensemble Kalman filter (EnKF)is used to assimilate temperature data from the TOGA/TAO array and altimetry from TOPEX/POSEIDON into a Pacific basin version of the NASA Seasonal to Interannual Prediction Project (NSIPP)ls quasi-isopycnal ocean general circulation model. The EnKF is an approximate Kalman filter in which the error-covariance propagation step is modeled by the integration of multiple instances of a numerical model. An estimate of the true error covariances is then inferred from the distribution of the ensemble of model state vectors. This inplementation of the filter takes advantage of the inherent parallelism in the EnKF algorithm by running all the model instances concurrently. The Kalman filter update step also occurs in parallel by having each processor process the observations that occur in the region of physical space for which it is responsible. The massively parallel data assimilation system is validated by withholding some of the data

and then quantifying the extent to which the withheld information can be inferred from the assimilation of the remaining data. The distributions of the forecast and analysis error covariances predicted by the ENKF are also examined.
Author
Kalman Filters; Massively Parallel Processors; Ocean Models; Ocean Currents; Data Systems; Temperature Measurement

19990111590 NASA Goddard Inst. for Space Studies, New York, NY USA
Ocean Turbulence, Paper 3, Two-Point Closure Model Momentum, Heat and Salt Vertical Diffusivities in the Presence of Shear
Canuto, V. M., NASA Goddard Inst. for Space Studies, USA; Dubovikov, M. S., NASA Goddard Inst. for Space Studies, USA; Howard, A., NASA Goddard Inst. for Space Studies, USA; Cheng, Y., NASA Goddard Inst. for Space Studies, USA; 1999; 74p; In English
Report No.(s): GCN-99-54Paper-3; No Copyright; Avail: CASI; A04, Hardcopy; A01, Microfiche

In papers 1 and 2 we have presented the results of the most updated 1-point closure model for the turbulent vertical diffusivities of momentum, heat and salt, K(sub m,h,s). In this paper, we derive the analytic expressions for K(sub m,h,s) using a new 2-point closure model that has recently been developed and successfully tested against some approx. 80 turbulence statistics for different flows. The new model has no free parameters. The expressions for K(sub m, h. s) are analytical functions of two stability parameters: the Turner number R(sub rho) (salinity gradient/temperature gradient) and the Richardson number R(sub i) (temperature gradient/shear). The turbulent kinetic energy K and its rate of dissipation may be taken local or non-local (K-epsilon model). Contrary to all previous models that to describe turbulent mixing below the mixed layer (ML) have adopted three adjustable "background diffusivities" for momentum. heat and salt, we propose a model that avoids such adjustable diffusivities. We assume that below the ML, K(sub m,h,s) have the same functional dependence on R(sub i) and R(sub rho) derived from the turbulence model. However, in order to compute R(sub i) below the ML, we use data of vertical shear due to wave-breaking measured by Gargett et al. (1981). The procedure frees the model from adjustable background diffusivities and indeed we use the same model throughout the entire vertical extent of the ocean. Using the new K(sub m,h, s), we run an O-GCM and present a variety of results that we compare with Levitus and the KPP model. Since the traditional 1-point (used in papers 1 and 2) and the new 2-point closure models used here represent different modeling philosophies and procedures, testing them in an O-GCM is indispensable. The basic motivation is to show that the new 2-point closure model gives results that are overall superior to the 1-point closure in spite of the fact that the latter rely on several adjustable parameters while the new 2-point closure has none. After the extensive comparisons presented in papers 1 and 2, we conclude that the new model presented here is overall superior for it not only is parameter free but also 2 because is part of a more general turbulence model that has been previously successfully tested on a wide variety of other types of turbulent flows.
Author
Oceans; Turbulent Flow; Turbulence Models; Numerical Analysis; K-Epsilon Turbulence Model; Temperature Gradients

51
LIFE SCIENCES (GENERAL)

19990108575 NASA Johnson Space Center, Houston, TX USA
Three Dimensional Optic Tissue Culture and Process
OConnor, Kim C., Inventor, NASA Johnson Space Center, USA; Spaulding, Glenn F., Inventor, NASA Johnson Space Center, USA; Goodwin, Thomas J., Inventor, NASA Johnson Space Center, USA; Aten, Laurie A., Inventor, NASA Johnson Space Center, USA; Francis, Karen M., Inventor, NASA Johnson Space Center, USA; Caldwell, Delmar R., Inventor, NASA Johnson Space Center, USA; Prewett, Tacey L., Inventor, NASA Johnson Space Center, USA; Fitzgerald, Wendy S., Inventor, NASA Johnson Space Center, USA; Oct. 05, 1999; In English; Continuation-in-part of US-Patent-Appl-SN-066292, filed 25 May 1993, US-Patent-Appl-SN-939791, filed 3 Sep. 1992, US-Patent-Appl-SN-317931, US-Patent-Appl-SN-317776, US-Patent-Appl-SN-213588, US-Patent-Appl-SN-213559, US-Patent-Appl-SN-625345
Patent Info.: Filed 13 May 1994; NASA-Case-MSC-223684; US-Patent-5,962,324; US-Patent-Appl-SN-242546; US-Patent-Appl-SN-066292; US-Patent-Appl-SN-939791; US-Patent-Appl-SN-317931; US-Patent-Appl-SN-153132; US-Patent-Appl-SN-317776; US-Patent-Appl-SN-213588; US-Patent-Appl-SN-213559; US-Patent-Appl-SN-625345; No Copyright; Avail: US Patent and Trademark Office, Hardcopy

A process for artificially producing three-dimensional optic tissue has been developed. The optic cells are cultured in a bioireactor at low shear conditions. The tissue forms as normal, functional tissue grows with tissue organization and extracellular matrix formation.
Official Gazette of the U.S. Patent and Trademark Office
Three Dimensional Models; Tissues (Biology); Cells

19990108842 Japan Society of Aerospace and Environmental Medicine, Tokyo, Japan
Morphological and Histochemical Changes in Leydig Cells After Endurance Training During Hypobaric Hypoxia in Rats
Japanese Journal of Aerospace and Environmental Medicine; December 1998; ISSN 0387-0723; Volume 35, No. 4, pp. 180; In English; No Copyright; Avail: CASI; A01, Hardcopy; A01, Microfiche

The purpose of present study was to investigate the morphological and histochemical changes in Leydig cells after endurance training during hypobaric hypoxia. The rats swam at a water temperature of 32-36 C with a load of 2.63% body weight for 90 min in the continuous training groups, 15 min swimming separated by 7 min pause x 6 times, with 90 min total exercise duration in the intermittent training groups, 6 days per week for 5 weeks at simulated altitude of 4,000 m. Hypoxia training induced a smaller size of cytoblast and cytosome, an increased activity of SDH and LDH, and an attenuation in activity of G6PDH in Leydig cells, which were similar to those of hypoxia sedentary group. The activity of beta-HBDH in the training groups did not decrease as compared to normoxia sedentary group, which was contrary to that of hypoxia sedentary group.
Author
Morphology; Histochemical Analysis; Cells (Biology); Education; Hypoxia; Hypobaric Atmospheres

19990109223 Institute of Space Medico, Beijing, China
Effect of simulated weightlessness on TNF-Alpha production and the response of bone marrow cells to GM-CSF in rats
Tao, Wang, Institute of Space Medico, China; Cuanghua, Yang, Institute of Space Medico, China; Ping, Hu, Institute of Space Medico, China; Xiulan, Wen, Institute of Space Medico, China; Space Medicine and Medical Engineering; Jun. 1997; Volume 10, No. 3, pp. 168-171; In English; In Chinese; See also 19990109220; No Copyright; Avail: CASI; A01, Hardcopy; A01, Microfiche

The purpose of this experiment was to investigate the effect of 15 and 30 d simulated weightlessness (SWL) on tumor necrosis factor - a (TNF-alpha) production secreted by macrophage stimulated with lipopolysaccharide(LPS) and the ability of bone marrow cells to respond to granulocyte/monocyte colony-stimulating factor(GM - CSF) in tail-suspension rats. The TNF-alpha production was assessed by radioimmunoassay. The ability of bone marrow cells to respond to GM-CSF was measured by 3H-TdR incorporation method. The results showed that after 15 d SWL, TNF-alpha production showed a tendency to decrease;and that after 30 d of SWL, the decrease became significant (P is less than O.05) . The results also demonstrated that the ability of bone marrow cells to respond to GM-CSF decreased significantly after 15 d SWL(P is less than O.01); and there was no significant change after 30 d SWL. It suggested that SWL could depress immune function, and that reduction of TNF-alpha production might be related to bone marrow cell proliferation function.
Author
Bone Marrow; Rats; Tumors; Weightlessness Simulation; Aerospace Medicine; Gravitational Physiology; Biological Effects; Physiological Effects; Immune Systems

19990110082 Bio-Rad Microscience Div., Hemel Hempstead, UK
New Developments in Optical Microscopy for Biological Applications
Dixon, Andrew, Bio-Rad Microscience Div., UK; Australian Journal of Physics; 1998; Volume 51, No. 4, pp. 729-750; In English; See also 19990110071; Copyright; Avail: Issuing Activity (Australian Journal of Physics, P.O. Box 1139, 150 Oxford St., Collingwood, Victoria 3066, Australia), Hardcopy, Microfiche

In the past ten years a quiet revolution has been taking place in optical microscopy. So quiet indeed that if one has not been working in life sciences research one may have seen little or no evidence of it. Yet what has been going on is an excellent example of how developments in physical instrumentation drive research and research in turn drives further developments in instrumentation. In this paper I will briefly review these developments in optical microscopy and, in particular, show how processes originally proposed 65 years ago as esoteric theoretical solutions to Dirac's equation are now used in practice for some of the most adventurous biological microscopy yet attempted.
Author
Optical Equipment; Microscopy

19990111572 Texas Univ. Health Science Center, Dept. of Otolaryngology, San Antonio, TX USA

The Structure of the Statocyst of the Freshwater Snail Biomphalaria Glabrata (Pulmonata, Basommatophora)

Gao, Wenyuan, Texas Univ. Health Science Center, USA; Wiederhold, Michael L., Texas Univ. Health Science Center, USA; Hearing Research; 1997; ISSN 0378-5955; Volume 109, pp. 109-124; In English

Contract(s)/Grant(s): NAG2-952; NSF IBN-95-29136; Copyright; Avail: Issuing Activity, Hardcopy

The structure of the statocyst of the freshwater snail Biomphalaria glabrata has been examined by light and electron microscopy. The two statocysts are located on the dorsal-lateral side of the left and right pedal ganglion. The statocysts are spherical, fluid-filled capsules with a diameter of approximately 60 microns for young and 110 microns for adult snails. The wall of the cyst is composed of large receptor cells and many smaller supporting cells. The receptor cells bear cilia which are evenly distributed on the apical surface. The cilia have the typical 9+2 internal tubule configuration. Striate rootlets originate from the base of the basal body and run downward into the cytoplasm. Side-roots arise from one side of the basal body and a basal foot from the other. For each receptor cell, the basal foot always points to the periphery of the surface, indicating that the receptor cell is non-polarized. The receptor cells contain cytoplasmic organelles such as mitochondria, ribosomes, rough and smooth endoplasmic reticulum, compact Golgi bodies and multivesicular bodies. Supporting cells bearing microvilli are interposed between the receptor cells. The junction complex between the supporting cells and the receptor cells is composed of adherens and septate junctions, while between supporting cells only the adherens junctions are present. The static nerve arises from the lateral side of the cyst and contains axons in which parallel neurotubules and mitochondria are found. The axons arise directly from the base of the receptor cells without synapse. In the cyst lumen there are unattached statoconia. The statoconia have a plate-like or concentric membranous ring structure. Based on the morphology, the function of the statocyst in Biomphalaria is discussed. Author

Ring Structures; Fresh Water; Snails

52
AEROSPACE MEDICINE

Includes physiological factors; biological effects of radiation; and effects of weightlessness on man and animals.

19990108485 Los Alamos National Lab., NM USA

Bayesian Inference for Neural Electromagnetic Source Localization: Analysis of MEG Visual Evoked Activity

George, J. S.; Schmidt, D. M.; Wood, C. C.; Feb. 01, 1999; 12p; In English; Medical Imaging Conference, 20-26 Feb. 1999, Sam Diego, CA, USA; Sponsored by International Society for Optical Engineering, USA

Report No.(s): DE00-007429; LA-UR-99-554; No Copyright; Avail: Department of Energy Information Bridge, Hardcopy

We have developed a Bayesian approach to the analysis of neural electromagnetic (MEG/EEG) data that can incorporate or fuse information from other imaging modalities and addresses the ill-posed inverse problem by sampling the many different solutions which could have produced the given data. From these samples one can draw probabilistic inferences about regions of activation. Our source model assumes a variable number of variable size cortical regions of stimulus-correlated activity. An active region consists of locations on the cortical surf ace, within a sphere centered on some location in cortex. The number and radii of active regions can vary to defined maximum values. The goal of the analysis is to determine the posterior probability distribution for the set of parameters that govern the number, location, and extent of active regions. Markov Chain Monte Carlo is used to generate a large sample of sets of parameters distributed according to the posterior distribution. This sample is representative of the many different source distributions that could account for given data, and allows identification of probable (i.e. consistent) features across solutions. Examples of the use of this analysis technique with both simulated and empirical MEG data are presented.

NTIS

Brain; Imaging Techniques; Numerical Analysis; Mathematical Models; Bayes Theorem; Electromagnetism

19990108844 Japan Society of Aerospace and Environmental Medicine, Tokyo, Japan

A Comparison of the Effects of Lower Body Positive Pressure and Head-Down Tilt on Cardiovascular Responses in Humans

Fu, Qi, Nagoya Univ., Japan; Sugiyama, Yoshiki, Aichi Medical Univ., Japan; Kamiya, Atsunori, Nagoya Univ., Japan; Mano, Tadaaki, Nagoya Univ., Japan; Japanese Journal of Aerospace and Environmental Medicine; December 1998; ISSN 0387-0723; Volume 35, No. 4, pp. 162; In English; No Copyright; Avail: CASI; A02, Hardcopy; A01, Microfiche

To compare the different effects of lower body positive pressure (LBPP) and head-down tilt (HDT) on cardiovascular responses in humans, 10 healthy male aged 21-42 yr were selected to the graded LBPP at 10, 20 and 30 mmHg as well as the short

term 6 degree HDT muscle sympathetic nerve activity (MSNA) was microneurographically recorded from the tibial nerve along with hemodynamic variables during the procedures. We found that MSNA declined boty at low levels of LBPP (such as 10 and 20 mmHg) and HDT; However, at high level LBPP (30 mmHg), MSNA tended to increase. Mean arterial pressure was elevated significantly only at 30 mmHg LBPP while kept unchanged at low levels of LBPP and HDT. Heart rate remained unchanged during LBPP and HDT. Total peripheral resistance markedly increased at 30 mmHg LBPP but decreased at HDT. Both stroke volume and cardiac output tended to decrease at 30 mmHg LBPP while increased at HDT. The results suggested that although both LBPP and HDT can induce simulated weightlessness by fluid shift, the cardiovascular responses are quite different. Since LBPP can not only activate the cardiopulmonary and arterial baroreceptors but also the intramuscular pressure sensitive receptors while short term 6-degree HDT may just stimulate the cardiopulmonary baroreceptors.
Author
Aerospace Medicine; Head Down Tilt; Hypokinesia; Arteries; Physiological Responses

19990109049 California Univ., Computer Science Dept., Los Angeles, CA USA
The Van Capelle and Durrer Model of Cardiac Action Potential Generation and 2D Propagation: Modifications and Application to Spiral Wave Propagation
Kogan, Boris, Y., California Univ., USA; Karplus, Walter J., California Univ., USA; Karpoukhin, Mikhail G., California Univ., USA; 1996; 8p; In English; Simulation in the Medical Sciences Conference, 14-17 Jan. 1996, San Diego, CA, USA
Contract(s)/Grant(s): NCC2-374; NSF BBS-87-14206; Copyright; Avail: Issuing Activity, Hardcopy, Microfiche

The properties of the Van Capelle and Durrer (VC-D) simplified model are studied to estimate how adequately it reproduces the physiological properties of cardiac cells and tissue. It is shown that the transition from a membrane capacitance of 10 micro F/sq cm, used 2 in previous studies, to 1 micro F/sq cm , the introduction of adjustable action potential duration restitution, and the appropriate adjustment of action potential duration (APD) bring the simulation result closer to reality. In particular, it is shown that in the 2D model of anisotropic tissue, nonstationary propagation of spiral waves in response to premature beat is possible when the cells of the tissue have specific APD restitution properties. The continuous pacemaker activity in this case leads to the creation of multiple spiral waves.
Author
Two Dimensional Models; Wave Propagation; Research; Cardiology; Heart

19990109141 California Univ., Computer Science Dept., Los Angeles, CA USA
Heart Fibrillation and Parallel Supercomputers
Kogan, B. Y., California Univ., USA; Karplus, W. J., California Univ., USA; Chudin, E. E., California Univ., USA; [1997]; In English; International Conference on Informatics and Control (ICI&C'97), 1997, Saint Petersburg, Russia
Contract(s)/Grant(s): NCC2-374; Copyright; Avail: Issuing Activity, Hardcopy

The Luo and Rudy 3 cardiac cell mathematical model is implemented on the parallel supercomputer CRAY - T3D. The splitting algorithm combined with variable time step and an explicit method of integration provide reasonable solution times and almost perfect scaling for rectilinear wave propagation. The computer simulation makes it possible to observe new phenomena: the break-up of spiral waves caused by intracellular calcium and dynamics and the non-uniformity of the calcium distribution in space during the onset of the spiral wave.
Author
Mathematical Models; Computerized Simulation; Fibrillation; Heart

19990109220 Institute of Space Medico, Space Medicine and Medical Engineering, Beijing, China
Space Medicine and Medical Engineering, Volume 10 ***Hangtian Yixue Yu Yixue Gongcheng, dai 10 kan***
Jinhe, Wei, Editor, Institute of Space Medico, China; Jun. 1997; ISSN 1002-0837; 83p; In English; In Japanese; See also 19990109221 through 19990109234
Report No.(s): CN 11-2774/R; No Copyright; Avail: CASI; A05, Hardcopy; A01, Microfiche

Contents include the following: (1) comparison of effect of 5 and 20 Hz magnetic field of brain responses; (2) experimental study on biodynamic response to vibration in human and animal; (3) effect of simulated weightlessness on TNF-alpha production and the response of bone marrow; (4) physiological effects of cabin temperature decrease in human;(5) legibility of chinese character of different height and stroke on liquid crystal display (LCD) under vibration; (6) comparison of evaluation methods on changes of facial microcirculation during induction of motion sickness;(7) human dynamic equations and analysis of opening the hatch door under weightlessness; (8) strength analysis of metal spheroidal high pressure vessel; (9) dynamic analysis of 24 h blood pressure in pilots and hypertensive patient; (10) observation of changes of cardiovascular function during 2.5 h HDT (-15

C) with sphygmogram method; (11) adaption of myocardial function to simulated weightlessness; and (12) thermoregulation under simulated weightlessness.
CASI
Aerospace Medicine; Biodynamics; Body Temperature; Cardiovascular System; High Pressure; Motion Sickness; Myocardium; Physiological Effects; Thermoregulation; Weightlessness Simulation

19990109221 Institute of Space Medico, Beijing, China
Comparison of effects of 5 and 20Hz magnetic field on brain responses
Jinhe, Wei, Institute of Space Medico, China; Gongdong, Yan, Institute of Space Medico, China; Lun, Zhao, Institute of Space Medico, China; Ran, Duan, Institute of Space Medico, China; Space Medicine and Medical Engineering; Jun. 1997; Volume 10, nO. 3, pp. 157-162; In English; In Chinese; See also 19990109220; No Copyright; Avail: CASI; A02, Hardcopy; A01, Microfiche

Effects of 5 and 20 Hz magnetic field(MF) on brain response were compared in 22 normal subjects during selective response(SRP) and selective mental arithmetic(SMA). It was found that significant changes in event - related potentials and EEG power spectra were induced by 5 Hz MF, but changes induced by 20 Hz MF were only in EEG coherence during SMA. The features of brain response changes suggest that the brain is in a more well being state after 5 Hz MF stimulation.
Author
Magnetic Fields; Brain; Neurology

19990109222 Institute of Space Medico, Beijing, China
Experimental study on biodynamic response to vibration in human and animals
Fangzi, Wang, Institute of Space Medico, China; Shiliang, Dai, Tsinghua Univ., China; Chi, Xu, International Conference Centre for Science and Technology, China; Chengwu, Shen, Wuhan Jiao Tong Science and Technology Univ., China; Space Medicine and Medical Engineering; Jun. 1997; Volume 10, No. 3, pp. 163-167; In English; In Chinese; See also 19990109220; No Copyright; Avail: CASI; A01, Hardcopy; A01, Microfiche

In order to study the characteristics of human dynamic response to vibration, 56 subjects were exposed to vibration on X, Y and Z axes. It showed that there were two resonance peaks of most local parts of the human body. The curves of transmissibility are essentially the same in all the subjects. It was found that resonance frequencies of the human body decreased with increase of G levels of vibration. These characteristics were also proved in animals. Using three- level artificial neural network, common reflective relation of the resonance frequency with height and weight of the human body and exciting acceleration were obtained. The above findings might be applicable to studies of vibration ergonomics.
Author
Animals; Biodynamics; Dynamic Response; Human Reactions; Resonant Frequencies; Vibration

19990109224 Institute of Space Medico, Space Medicine and Medical Engineering, Beijing, China
Physiological effects of cabin temperature decrease on human
Shaoyong, Chang, Institute of Space Medico, China; Daixiu, Cui, Institute of Space Medico, China; Jianmin, Wu, Institute of Space Medico, China; Man, Qiu, Institute of Space Medico, China; Xuejun, Yu, Institute of Space Medico, China; Space Medicine and Medical Engineering; Jun. 1997; Volume 10, No. 3, pp. 177-181; In English; In Chinese; See also 19990109220; No Copyright; Avail: CASI; A01, Hardcopy; A01, Microfiche

To study effects of cabin temperature on human body, changes in rectal temperature, local skin temperature, local skin heat fluxes and skin infrared thermogram were observed in 5 male subjects dressed in different thermal insulation clothing under 20 C, 15 C and 10 C cabin temperatures. The results showed that, average skin temperature and tip temperature obviously dropped, and skin heat fluxes increased with falling of cabin temperature, and the changes of the local skin infrared thermogram were significant. Subjective feelings were that of comfort and coolness at cabin temperature of 20 C and 15 C, respectively. While the subjective feeling was of cold; also there was a thermal debt of body 144 kJ/sq m at 10 C which indicated that it was slightly cold but tolerable. The results may be valuable in determining the lowest tolerable limit of cabin temperature.
Author
Body Temperature; Human Body; Physiological Effects; Skin Temperature (Biology); Temperature Effects; Spacecraft Cabins; Spacecraft Environments; Thermal Environments

19990109225 Institute of Space Medico, Space Medicine and Medical Engineering, Beijing, China
Comparison of evaluation methods on changes of facial microcirculation during induction of motion sickness
Xinying, Zhang, Institute of Space Medico, China; Bolun, Tong, Institute of Space Medico, China; Huaguang, Gu, Institute of Space Medico, China; Linjie, Wang, Institute of Space Medico, China; Jianmin, Wu, Institute of Space Medico, China; Xuejun,

Yu, Institute of Space Medico, China; Space Medicine and Medical Engineering; Jun. 1997; Volume 10, No. 3, pp. 182-186; In English; In Chinese; See also 19990109220; No Copyright; Avail: CASI; A01, Hardcopy; A01, Microfiche

In order to increase the accuracy of motion sickness grading criteria, infrared thermography and a Laser Doppler microcirculation blood-flow detector were used in 60 healthy male individuals: before, immediately, and 20 min after paralleled-swing stimulation. Facial skin temperature and microvessel blood-flow were recorded. The results showed that facial skin temperature and blood flow in facial microvessels fell together with the appearance of pallor. However, the degree of pallor observed with the naked eye was inconsistent with that found by thermography or facial blood flow. It suggests that the accuracy of grading might be improved with the use of thermography or measurement of facial microvessel blood flow.

Author

Blood Flow; Motion Sickness; Stimulation; Capillary Flow; Face (Anatomy)

19990109226 Institute of Space Medico, Space Medicine and Medical Engineering, Beijing, China

Human dynamic equations and analysis of opening the hatch door under weightlessness

Xianmin, Wang, Institute of Space Medico, China; Yongjun, Zhao, Institute of Space Medico, China; Tiancheng, Sun, Institute of Space Medico, China; Yong, Huang, Institute of Space Medico, China; Space Medicine and Medical Engineering; Jun. 1997; Volume 10, No. 3, pp. 187-191; In English; In Chinese; See also 19990109220; No Copyright; Avail: CASI; A01, Hardcopy; A01, Microfiche

The general human dynamic equations under weightlessness were derived using Kane-Huston' s Method. According to manned spaceflight circumstances, specific equations for models of floating in space and having a single point support were derived from the above general equations. The action with which the astronaut opens the hatch door was analyzed, the "float" evolution was calculated, and the evolutionary curves were drawn.

Author

Astronauts; Hatches; Weightlessness; Extravehicular Activity; Spacecraft Environments; Human Performance; Biodynamics; Equations

19990109228 Institute of Space Medico, Space Medicine and Medical Engineering, Beijing, China

Dynamic analysis of 24 h blood pressure in pilots and hypertensive patients

Yuanhuai, Zhao, Institute of Space Medico, China; Bo, Liang, Institute of Space Medico, China; Yuqing, Gai, Institute of Space Medico, China; Yafu, Xu, Institute of Space Medico, China; Jingtai, Sun, Institute of Space Medico, China; Yaorong, Yu, Institute of Space Medico, China; Space Medicine and Medical Engineering; Jun. 1997; Volume 10, No. 3, pp. 197-200; In English; In Chinese; See also 19990109220; No Copyright; Avail: CASI; A01, Hardcopy; A01, Microfiche

Blood pressure of 63 healthy male pilots and 20 primary hypertensive patients was measured with the "Smart LINK Ambulatory Monitoring System". The BP readings were taken every 30 min in daytime and 60 min at night for 24 h. The results showed that two peaks appeared at 7:00 to about 9:00 A.M.and 16:00 to about 19:00 P.M. and two valleys at 12:00 to about 14:00 P. M . and 24:00 to about 5:00 A. M. in healthy pilots, but the hypertensive subjects showed higher systolic or/and diastolic blood pressure continuously.

Author

Blood Pressure; Hypertension; Diurnal Variations; Pilots (Personnel)

19990109229 Institute of Space Medico, Space Medicine and Medical Engineering, Beijing, China

Observation of Changes of Cardiovascular function during 2.5h HDT (1.5 deg) with sphygmogram method

Xianyun, Shen, Institute of Space Medico, China; Jianhe, Chen, Institute of Space Medico, China; Jingrui, Meng, Institute of Space Medico, China; Qiulu, Xiang, Institute of Space Medico, China; Xianmin, Wang, Institute of Space Medico, China; Bolun, Tong, Institute of Space Medico, China; Space Medicine and Medical Engineering; Jun. 1997; Volume 10, No. 3, pp. 201-205; In English; In Chinese; See also 19990109220; No Copyright; Avail: CASI; A01, Hardcopy; A01, Microfiche

To understand the changes of cardiovascular functions in the initial stage of space flight, the changes in 19 healthy young men during 2. 5h head down tilt(HDT) (15 degrees) were observed with a CF - II cardiovascular function detecting and diagnosing equipment. The blood pressure and sphygmogram of the left radial artery were recorded in sedentary condition and at 10 th, 30 th, 60 th, 90 th, 120 th and 140 th minute of HDT. The results showed that changes of cardiovascular indices during HDT can be divided into acute regulation stage (is less than 1 hour) and the regulation stage (1 to about 2.5 hours); circulatory blood volume, stroke volume and cardiac output were increased, while heart rate, pre and after load on the heart, CVP, coronary circulatory function, blood pressure and systemic vascular resistance were decreased; the vagus feedback index increased and the regulation function of the vascule decreased. Most of the changes of cardiovascular indices as reflected in the sphygmogram are in consistent

with the reported result in space flight or simulated micro-gravity, so the sphygmogram method might be applied to space medical research.
Author
Cardiovascular System; Head Down Tilt; Heart Function; Microgravity; Stroke Volume; Arteries; Blood Pressure; Hemodynamic Responses; Physiological Effects; Weightlessness Simulation; Bioastronautics

19990109230 Institute of Space Medico, Space Medicine and Medical Engineering, Beijing, China
Adaptation of myocardial function to simulated weightlessness
Zhibin, Yu, Institute of Space Medico, China; Lifan, Zhang, Institute of Space Medico, China; Space Medicine and Medical Engineering; Jun. 1997; Volume 10, No. 3, pp. 206-209; In English; In Chinese; See also 19990109220; No Copyright; Avail: CASI; A01, Hardcopy; A01, Microfiche

To observe the changes in myocardial function and calcium ion release of sarcoplasmic reticulum in rats under simulated weightlessness, 24 Sprague - Dawley male rats were divided into control (CON), 8 week tail-suspension (SUS) and recovery for 2 weeks (RE) groups. The results showed that there was no change in resting tension of myocardial twitch in SUS. While the developed tension (DT) of myocardial twitch significantly decreased in SUS as compared with CON. The time to peak tension (TPT) and time to half relaxation (T1/2R) of myocardial twitch were prolonged in SUS. DT, TPT and T1/2R recovered to their corresponding control values after 2 w of recovery from tail-suspension. The early recovery curve of force-interval relation in SUS was in a higher position over that of CON, but the rest potentiation and rest depression curve was positioned under that of CON. These results suggested that there might be an adaptative change in myocardial function in medium- or long-term tail-suspended rats while 8 week tail-suspension reduces calcium ion release from cardiac sarcoplasmic reticulum in rats.
Author
Myocardium; Rats; Sarcoplasmic Reticulum; Weightlessness Simulation

19990109231 Institute of Space Medico, Space Medicine and Medical Engineering, Beijing, China
Thermoregulation under simulated weightlessness
Man, Qiu, Institute of Space Medico, China; Wu, Liu, Institute of Space Medico, China; Gang, Liu, Institute of Space Medico, China; Jifu, Wen, Institute of Space Medico, China; Guoyin, Liu, Institute of Space Medico, China; Shaoyong, Chang, Institute of Space Medico, China; Space Medicine and Medical Engineering; Jun. 1997; Volume 10, No. 3, pp. 210-213; In English; In Chinese; See also 19990109220; No Copyright; Avail: CASI; A01, Hardcopy; A01, Microfiche

The effect of simulated weightlessness on thermoregulation was studied in 5 subjects. The experiment consisted of 3 day baseline measurements, 7 day head-down bed rest and 2 day recovery. Circadian rhythm was assessed by continuous measurements of rectal temperature and skin temperature with 2 hour intervals. Heat Stress Protein 70(HSP70) was measured by Western-blot Dot method and the facial surface temperature distribution was measured by HR-2 infrared thermography. The results showed that rectal temperature keeps the wake sleep variation, but the circadian rhythm changed during bed rest, and the change of rectal temperature rhythm appeared mainly in the early-days of bed rest; HSP70 and facial surface temperature increased during bed rest.
Author
Body Temperature; Circadian Rhythms; Thermoregulation; Weightlessness Simulation; Head Down Tilt; Physiological Effects; Bioastronautics

19990109232 Institute of Space Medico, Space Medicine and Medical Engineering, Beijing, China
Effect of noise in submarine compartment on signal discrimination and arithmetic performance
Zhengyuan, Hu, Institute of Space Medico, China; Zhenfu, Liang, Institute of Space Medico, China; Xiufeng, Shi, Institute of Space Medico, China; Zhiwen, Tang, Institute of Space Medico, China; Space Medicine and Medical Engineering; Jun. 1997; Volume 10, No. 3, pp. 214-216; In English; In Chinese; See also 19990109220; No Copyright; Avail: CASI; A01, Hardcopy; A01, Microfiche

To study the effects of noise level in submarine compartment on signal discrimination and arithmetic performance, experiments were carried out on 13 subjects. The results showed that as noise level raised from moderate (73 dBA)to higher levels (85 to about 92 dBA), work efficiency showed a progressive decrease, but when noise level reached 96 dBA the decrease in efficiency reached a steady state. The results indicated that impairment of efficiency apparently occurred at a level of 85 dBA and that the interference effect of noise was more pronounced on task performance with mental strain.
Author
Human Performance; Noise Intensity; Stress (Psychology)

19990109233 Institute of Space Medico, Space Medicine and Medical Engineering, Beijing, China

Effect of wind tunnel noise on left ventricular function of heart

Tiancheng, Zhang, Institute of Space Medico, China; Ju, Liu, Institute of Space Medico, China; Space Medicine and Medical Engineering; Jun. 1997; Volume 10, No. 3, pp. 217-219; In English; In Chinese; See also 19990109220; No Copyright; Avail: CASI; A01, Hardcopy; A01, Microfiche

A two-dimensional color doppler ultrasonic imaging instrument was used to detect the left ventricular function in 36 wind tunnel technicians before and after their work in the wind tunnel. The results showed that under the noise between 91.5 and 101. 5 dB(A)inside the wind tunnel SV, EF, Fs, MVCF, PE, SE and EAC decreased while SA, PA/PE increased. It indicates that high level wind tunnel noise has certain harmful effect on the left ventricular function of wind tunnel technicians.

Author

Aerodynamic Noise; Heart; Wind Effects; Wind Tunnels; Physiological Effects

19990109234 Institute of Space Medico, Space Medicine and Medical Engineering, Beijing, China

Application of graphical technology in medrians diagnosis

Yun, Yang, Institute of Space Medico, China; Xingye, Fang, Institute of Space Medico, China; Space Medicine and Medical Engineering; Jun. 1997; Volume 10, No. 3, pp. 220-222; In English; In Chinese; See also 19990109220; No Copyright; Avail: CASI; A01, Hardcopy; A01, Microfiche

After analyzing the difficulties in the research and application of medrians diagnosis, a two-dimensional graphical pattern of the distribution in the channels of the whole human body and collaterals was produced using graphical technology. A special algorithm was used to solve the problems of medrians diagnosis. Some examples of the application of the graphical model were given.

Author

Diagnosis; Human Body; Graphs (Charts); Computer Graphics

19990109668 Hebrew Univ., Jerusalem Israel

Fifth IBRO World Congress of Neuroscience, Jerusalem, Israel, July 11-15, 1999 ***Final Report***

Soreq, Hermona; Jul. 15, 1999; 238p; In English

Contract(s)/Grant(s): DAMD17-99-1-9554

Report No.(s): AD-A367295; No Copyright; Avail: CASI; A11, Hardcopy; A03, Microfiche

The final proceedings of the Fifth IBRO World Congress of Neuroscience, Jerusalem, Israel, July 11-15, 1999.

DTIC

Abstracts; Central Nervous System; Neurology; Europe

19990111612 Kinki Univ., Faculty of Engineering, Hiroshima, Japan

The Energy Absorbing Properties and Mechanisms of Human Articular Cartilage and Subchondral Bone: Dependence on Interstitial Fluid and a Role of Subchondral Bone Plate

Hayami, Takashi, Kinki Univ., Japan; Oka, Masanori, Kyoto Univ., Japan; Ikeuchi, Ken, Kyoto Univ., Japan; Research Reports of the Faculty of Engineering, Kinki University; 1993; ISSN 0386-491X, No. 27, pp. 21-28; In English; Copyright; Avail: Issuing Activity, Hardcopy, Microfiche

It is well known that the cause of Osteoarthritis is deeply related to mechanical environment for joint tissues, or energy absorbing ability of articular cartilage and cancellous bone. However, the investigation of energy absorbing ability and mechanisms of cartilage and/or cancellous bone is not thoroughgoing enough. A few published reports concerning energy absorbing properties of them have not referred to the effect of interstitial fluid or composite structure of cartilage and cancellous bone on the same ability of them. In the orthopaedic clinical fields, the complications of total joint replacement surgery, or ”loosening” have frequently occurred and that revision cases have been increasing in number year by year. Also it is considerable that a cause of loosening is to resect large quantities of subchondral cancellous bones. Therefore, investigation of the energy absorbing ability and mechanisms of this joint tissue is very important, to understand mechanisms of the cancellous bones remodeling. In this article, we examine the effect of interstitial fluid of cartilage and cancellous bone on energy absorbing ability, and consider relation between fluid flow resistance and mechanical energy dissipation. Second, the role of subchondral bone plate

within composite structure that is composed of three layers, cartilage, subchondral plate and cancellous bone is discussed from a viewpoint of energy absorption of that structure.
Derived from text
Cartilage; Bones; Energy Absorption; Bone Mineral Content; Energy Dissipation; Absorbers (Materials)

53
BEHAVIORAL SCIENCES

Includes psychological factors; individual and group behavior; crew training and evaluation; and psychiatric research.

19990108843 Japan Society of Aerospace and Environmental Medicine, Tokyo, Japan
Importance of Somatosensory Input for Spatial Orientation in Supine Subjects: Evaluated by Target Arm Pointing Response During Positive and Negative Acceleration
Chen, Yani, Nagoya Univ., Japan; Mori, Shigeo, Nagoya Univ., Japan; Japanese Journal of Aerospace and Environmental Medicine; December 1998; ISSN 0387-0723; Volume 35, No. 4, pp. 168; In English; No Copyright; Avail: CASI; A03, Hardcopy; A01, Microfiche

In the present study, we examined whether pointing arm movements would follow the direction of resultant G-force factor or not, when subjects were supine and were exposed to horizontal acceleration along their body axes. Arm pointing movements were measured goniometrically around the shoulder joint and eye movements were recorded by a conventional Electrooculograph (EOG) method. Subjects were exposed to a step-mode linear acceleration up to 0.5 G in 0.1 G step, with and without a small LED target in darkness, also with and without a weight in hand. No significant pointing deviation was observed when pointing to a memorized target during acceleration up to 0.5 G. A slight but consistent downward shift of several degrees was observed when pointing to a visible target instead of a memorized one in positive accelerations above 0.2 G. We concluded that rich somatosensory inputs might suppress the otolith inputs for spatial orientation, when arm-pointing to a target was made without visual feedback in supine position.
Author
Sensory Perception; Supine Position; Targets; Arm (Anatomy); Acceleration (Physics); Attitude (Inclination); Aerospace Medicine

19990113153 Civil Aeromedical Inst., Oklahoma City, OK USA
Air Traffic Control Specialist Age and Cognitive Test Performance ***Final Report***
Heil, Michael C., Civil Aeromedical Inst., USA; August 1998; 22p; In English
Report No.(s): DOT/FAA/AM-98/23; No Copyright; Avail: CASI; A03, Hardcopy; A01, Microfiche

Researchers have explored the issue of air traffic control specialist (ATCS) age and performance many times over the past few decades. These researchers have consistently found a negative relationship between the age of ATCSs and both training success and ratings of job performance. A recent study found a curvilinear relationship between ATCS age and performance on a computerized simulation of air traffic situations, with performance decreasing for people in their mid 40s. Some researchers have speculated that these relationships may be due to a decline in cognitive ability with age. The purpose of the current study is to investigate the relationship between age and performance on tests of cognitive ability for incumbent ATCSS. As part of a concurrent validation study, 1083 incumbent ATCSs from 12 enroute centers took a newly developed air traffic control selection test. The tests included in the 6 hour battery were developed to measure the knowledge, skills, abilities, and other characteristics (KSAOS) relevant to the ATCS job. Some of the KSAOs measured by the battery include: ability to prioritize, situational awareness, planning, execution, thinking ahead, short-term memory, reasoning, decisiveness, concentration, perceptual speed and accuracy, mathematical reasoning, and ability to deal with dynamic visual movement. The relationship between current age and performance on these cognitive tests was compared using regression analysis and analysis of variance procedures. The results of these analyses suggest some age-related decline in those cognitive abilities that are most important to successful job performance.
Author
Age Factor; Human Performance; Mental Performance; Performance Prediction; Performance Tests; Personnel Selection; Air Traffic Controllers (Personnel)

54
MAN/SYSTEM TECHNOLOGY AND LIFE SUPPORT

Includes human engineering; biotechnology; and space suits and protective clothing. For related information see also 16 Space Transportation.

19990107371 Institute for Human Factors TNO, Soesterberg, Netherlands
Interfaces in Future Ship Control Centres: Evaluation of Shared Workspaces ***Interim Report Interfaces in Toekomstige Technische Centrales: Evaluatie Shared Workspaces***
Passenier, P. O., Institute for Human Factors TNO, Netherlands; Houttuin, K., Institute for Human Factors TNO, Netherlands; Sep. 06, 1999; 32p; In Dutch; Original contains color illustrations
Contract(s)/Grant(s): A97/KM/333; TNO Proj. 787.2
Report No.(s): TD99-0338; TNO-TM-99-A060; Copyright; Avail: Issuing Activity, Hardcopy

Under contract to the Royal Netherlands Navy (A97/KM/333), in the experimental Command and Control laboratory (C2-Lab) of TNO-HFRI an evaluation study was conducted regarding the use of shared workspaces for overview and conferencing purposes in the Ship Control Centre (SCC) on-board future frigates, like the Air Defence and Command frigate (ADCF). The results of the study show that for the SCC-team an added value is offered by the (automatically) updated overview presentation according to the 'General Arrangement Plan' (GAP) concept, presenting damage and system-related information at different levels of detail. At the highest level, presenting mainly damage-related information for the whole ship, an additional need was identified for information regarding the ship's operational status and system availability. On the other hand, especially at the lower levels of GAP presentation, care has to be taken that the amount of available information does not make the presentation unclear. Also, the possibility of using the GAP presentation for supporting the communication between team members (e.g. command huddles) is regarded to have a positive effect on the efficiency and unambiguity of the internal information transfer. However, for this purpose, additional facilities are required for a temporary copy of more detailed, mimic-like information from the individual workstations. Regarding the use of a Large Screen Display (LSD), this device is foreseen to be useful for the presentation of a common overview, with direct availability for the visual support of communication between team members (e.g. 'pointing function' during command huddles). Important for this setup is to have a Clear protocol for display management, calling for a minimal overhead for the different team members. Further, for communication support within the different domains (damage and technical), in many cases other means of information exchange will be used, for instance based on mimics from individual operator positions. The use of a central overview screen for this purpose might cause unnecessary "crosstalk' with the other team members. On the other hand, regarding conferencing based on individual workstations, a possible danger is recognized of 'discommunication', because of ambiguities in the layer settings on the individual screens. Regarding future research it is proposed to, based on the current findings, further develop the GAP information specification for application on board the ADCF. This follow-up study has to take into account the ADCF specific constraints regarding the implementation of a shared workspace (for instance, the limited possibilities for a large screen presentation for all team members, given the planned dimensions of the SCC).
Author
Evaluation; Command and Control; Information Transfer; Navy; Ships; Workstations

19990109091 New Hampshire Univ., Inst. for the Study of Earth, Oceans and Space, Durham, NH USA
Measurements of Nitric Acid and Aerosol Species Aboard the NASA DC-8 Aircraft During the SASS OZone and Nitrogen Oxide Experiment (SONEX) ***Final Report***
Talbot, Robert W., New Hampshire Univ., USA; Dibb, Jack E., New Hampshire Univ., USA; June 1999; 48p; In English
Contract(s)/Grant(s): NAG2-1101; No Copyright; Avail: CASI; A03, Hardcopy; A01, Microfiche

The SASS Ozone and Nitrogen Oxides Experiment (SONEX) over the north Atlantic during October/November 1997 offered an excellent opportunity to examine the budget of total reactive nitrogen (NO(y)) in the upper troposphere (8 - 12 km altitude). The median measured NO(y) mixing ratio was 425 parts per trillion by volume (pptv). Two different methods were used to measure HNO3: (1) the mist chamber technique and, (2) chemical ionization mass spectrometry. Two merged data sets using these HNO3 measurements were used to calculate NO(y) by summing the reactive nitrogen species (a combination of measured plus modeled results) and comparing the resultant values to measured NO(y) (gold catalytic reduction method). Both comparisons showed good agreement in the two quantities (slope greater than 0.9 and r(sup 2) greater than 0.9). Thus, the total reactive nitrogen budget in the upper troposphere over the North Atlantic can be explained in a general manner as a simple mixture of NO(x). (NO + NO2), HNO3, and PAN. Median values of NO(x)/NO(y) were approx. = 0.25, HNO3/NO(y) approx. = 0.35 and PAN/NO(y)

approx. = 0.17. Particulate NO3 and alkyl nitrates together composed less than 10% of NO(y), while model estimated HNO4 averaged 12%.
Author
Nitric Acid; Experimentation; Ozone; North Sea; Atlantic Ocean; Estimating; Nitrogen; Chemical Analysis

19990109652 Institute for Human Factors TNO, Soesterberg, Netherlands
Acoustical Leakage Test for Pilot Helmets ***Final Report Akoestische Lektest voor Vliegerhelmen***
Steeneken, H. J. M., Institute for Human Factors TNO, Netherlands; May 25, 1999; 20p; In Dutch; Original contains color illustrations
Contract(s)/Grant(s): A98/KLu/309; TNO Proj. 786.4
Report No.(s): TD-99-0044; TNO-TM-99-A038; Copyright; Avail: Issuing Activity, Hardcopy

A simple sound attenuation test was developed for the determination of the correct fit of a pilot helmet. This test is based on using the telephone cartridges of a pilot helmet as a microphone, hence no specific sensors are required and the helmet can be tested in situ, The performance of the telephone cartridge is also determined. Under laboratory conditions the results of the present ”screening” test and the more elaborate standard MIRE-method were compared and it was shown that the correlation between both method is high r = 0.95). However the absolute results differ, an overestimation of the attenuation by the screening test is observed. This is not relevant for the purpose of the test. In a field experiment the method was used by 41 subjects. A good reproducibility was obtained. Also five helmets were detected with an inadequate performance. The use of the method is not restricted to pilot helmets and can also be applied to tank helmets and headsets.
Author
Leakage; Helmets; Acoustic Attenuation; Performance Tests

19990111513 Department of Energy, Washington, DC USA
Effect of compositional variation in plutonium on process shielding design
Brown, T. H., Department of Energy, USA; Nov. 30, 1997; 8p; In English
Report No.(s): DE97-009138; LA-UR-97-2546; No Copyright; Avail: Department of Energy Information Bridge, Microfiche

Radiation dose rate from plutonium with high Pu-239 content varies with initial nuclidic content, radioactive decay time, and impurity elemental content. The two idealized states of old plutonium and clean plutonium, whose initial compositions are given, provide approximate upper and lower bounds on dose rate variation. Whole-body dose rates were calculated for the two composition states, using unshielded and shielded plutonium spheres of varying density. The dose rates from these variable density spheres are similar to those from expanded plutonium configurations encountered during processing. The results have shielding implications for glove boxes with only structurally inherent shielding, especially for processing of old plutonium in an expanded configuration. Further reduction in total dose rate by using lead to reduce photon dose rate is shown for two density cases representing compact and expanded plutonium configurations.
NTIS
Plutonium 239; Radiation Shielding; Radioactive Decay; Radiation Protection

59
MATHEMATICAL AND COMPUTER SCIENCES (GENERAL

19990109096 Royal Inst. of Tech., Dept. of Mathematics, Stockholm, Sweden
Weighted Inequalities for Two-Dimensional Discrete Hardy Operators
Kamaly, A.; Rakotondrasimba, Y.; Apr. 1998; 28p; In English
Report No.(s): PB99-161705; TRITA-MAT-1998-21; No Copyright; Avail: CASI; A03, Hardcopy; A01, Microfiche

For certain classes of nonnegative double sequences V(n) and U(n), a necessary and sufficient condition for the boundedness of the two-dimensional discrete Hardy operator H from l(sup p, sub V) into l(sup q, sub U) is found whenever p is less than or equal to q or p is greater than q with 1 is less than p is less than infinity and 0 is less than q is less than infinity.
NTIS
Sequencing; Two Dimensional Models; Operators (Mathematics)

19990109097 Royal Inst. of Tech., Dept. of Mathematics, Stockholm, Sweden
Recent Results on Sidon Sequences: A Survey
Lindstroem, B.; May 1998; 14p

Report No.(s): PB99-161648; TRITA-MAT-98-MA-29; No Copyright; Avail: CASI; A03, Hardcopy; A01, Microfiche

A sequence of positive integers a(sub 1) is less than a(sub 2) is less than ... is less than a(sub r) is less than or equal to n is called a B(sub 2)-sequence (or Sidon sequence) if the sums a(sub i) + a(sub j), 1 is less than or equal to i is less than or equal to j is less than or equal to r, are different.

NTIS

Sequential Analysis; Quadratic Equations; Polynomials

19990109098 Institut des Hautes Etudes Scientifiques, Bures-sur-Yvette France

Non-Abelian Cohomology and Rational Points

Harari, D.; Skorobogatov, A. N.; Jun. 1999; 40p; In English

Report No.(s): PB99-159337; IHES/M/99/42; No Copyright; Avail: CASI; A03, Hardcopy; A01, Microfiche

The purpose of this paper is to discuss non-abelian cohomology and rational points. Sections of this paper includes: Preliminaries, Obstruction given by a class in H(sup 2), Applications, Descent obstructions, and Examples.

CASI

Algebra; Group Theory; Homology

19990109099 Institut des Hautes Etudes Scientifiques, Bures-sur-Yvette France

Functional-Differential Equation Related to Golomb's Self-Described Sequence

Petermann, Y. F. S.; Remy, J. L.; Vardi, I.; Apr. 1999; 24p; In English

Report No.(s): PB99-159220; IHES/M/99/25; No Copyright; Avail: CASI; A03, Hardcopy; A01, Microfiche

The functional-differential equation f'(t) = 1/f(f(t)) is closely related to Golomb's self-described sequence F. We describe the increasing solutions of this equation. We show that such a solution must have a nonnegative fixed point, and that for every number p is greater than = 0 there is exactly one increasing solution with p as a fixed point. We also show that in general an initial condition doesn't determine a unique solution: indeed the graphs of two distinct increasing solutions cross each other infinitely many times. In fact we conjecture that the difference of two increasing solutions behaves very similarly as the error term E(n) in the asymptotic expression F(n) = phi(sup 2 - o).n(sup phi - 1) + E(n) (where o is the golden number).

NTIS

Functional Analysis; Series (Mathematics); Asymptotic Series; Series Expansion

19990109101 Institut des Hautes Etudes Scientifiques, Bures-sur-Yvette France

Zeroes of Automorphic L-Functions

Soule, C.; Jun. 1999; 12p

Report No.(s): PB99-159402; IHES/M/99/47; No Copyright; Avail: CASI; A03, Hardcopy; A01, Microfiche

This paper discusses the zeros of automorphic L-functions. It explains how to solve these functions by using various theorems.

NTIS

Functions (Mathematics); Hilbert Space

19990109102 Institut des Hautes Etudes Scientifiques, Bures-sur-Yvette France

Cyclic Formality Conjecture

Shoikhet, B.; Apr. 1999; 32p

Report No.(s): PB99-159378; IHES/M/99/34; No Copyright; Avail: CASI; A03, Hardcopy; A01, Microfiche

We conjecture an explicit formula for a cyclic analog of the formality L(sub infinity)-morphism. We prove that its first Taylor component, the cyclic Hochschild-Kostant-Rosenberg map, is in fact a morphism (and a quasiisomorphism) of the complexes. to prove it we construct a cohomological version of the Connes-Tsygan bicomplex in cyclic homology. As an application of the cyclic Formality conjecture, we obtained an explicit formula for cyclically invariant deformation quantization. We show that (a more precise version of) the Connes-Flato-Sternheimer conjecture [CFS] on the existence of closed star-products on a symplectic manifold also follows from our conjecture.

NTIS

Isomorphism; Homomorphisms; Field Theory (Algebra)

19990109637 Institut des Hautes Etudes Scientifiques, Bures-sur-Yvette France
Cramer Functions and Guinand Equations
Illies, G.; Apr. 1999; 24p
Report No.(s): PB99-159204; IHES/M/99/35; No Copyright; Avail: CASI; A03, Hardcopy; A01, Microfiche
No abstract available.
NTIS
Meromorphic Functions; Dirichlet Problem; Functions (Mathematics)

19990113075 Institut des Hautes Etudes Scientifiques, Bures-sur-Yvette France
Diophantine Analysis of Conformal Iterated Function Systems
Urbanski, M.; May 1999; 22p; In English
Report No.(s): PB99-159352; IHES/M/99/40; No Copyright; Avail: CASI; A03, Hardcopy; A01, Microfiche
A formula for the Hausdorff dimension of a Besicovic-Jarnik subset of the limit set of a conformal infinite iterated function system is derived and expressed as a unique zero of the topoligical pressure of the corresponding strongly Holder family of functions.
NTIS
Diophantine Equation; Functions (Mathematics); Iteration; Mathematical Models

19990113076 Institut des Hautes Etudes Scientifiques, Bures-sur-Yvette France
Infinite Dimensional Manifold Structures on Principal Bundles
Dupre, M. J.; Glazebrook, J. F.; Apr. 1999; 18p
Report No.(s): PB99-159428; IHES/M/99/27; No Copyright; Avail: CASI; A03, Hardcopy; A01, Microfiche
Having introduced the notion of D-space and a D-group action, the authors develop a general framework for studying the mainfold structure of the resulting orbit spaces and their related theory of principal bundles.
NTIS
Manifolds (Mathematics); Topology; Mathematical Models

19990113077 Institut des Hautes Etudes Scientifiques, Bures-sur-Yvette France
Contact Reductions, Mechanics and Duality
Severa, P.; May 1999; 14p
Report No.(s): PB99-159436; IHES/M/99/38; No Copyright; Avail: CASI; A03, Hardcopy; A01, Microfiche
Contact reduction is very closely related to symplectic reduction, but it allows symmetries that are not manifest in Hamiltonian mechanics and moreover, solution of the reduced problems yields solution of the original problem without further integration.
NTIS
Quantum Mechanics; Duality Theorem

19990113139 Royal Inst. of Tech., Dept. of Mathematics, Stockholm, Sweden
Periodicity Versus Chaos in One Dimensional Dynamics
Thunberg, H.; Feb. 1999; ISSN 1401-2278; 40p; In English
Report No.(s): PB99-174211; TRITA-MAT-1999-02; No Copyright; Avail: CASI; A01, Microfiche; A03, Hardcopy
The authors survey recent results on the asymptotics of families of one-dimensional mappings, with the focus on generic behavior seen for many parameters and many initial conditions. There is an almost dichotomy between maps with stable cycles and strongly chaotic maps. The authors use the model case of the quadratic family, which is nowadays more or less completely understood, for an exposition. Most results hold in more general settings. After presenting the precise results, applications are given to the Hassell models and the Ricker models of population dynamics. The following generic results are applicable: (1) Each map has a unique metric attractor; (2) Maps with stable cycles are dense in parameter space; (3) Strongly chaotic maps appear with positive frequency in parameter space; (4) Asymptotic dynamics is almost independent of initial conditions, and can in most cases be described by an invariant probability measure; (5) Various (in)stability properties of these asymptotic distributions.
NTIS
Chaos; Periodic Variations

60
COMPUTER OPERATIONS AND HARDWARE

Includes hardware for computer graphics, firmware, and data processing. For components see 33 Electronics and Electrical Engineering.

19990107382 NASA Goddard Space Flight Center, Greenbelt, MD USA
The SGI/Cray T3E: Experiences and Insights
Bernard, Lisa Hamet, NASA Goddard Space Flight Center, USA; 1998; 1p; In English; High Performance Computing and Communications Computational Aerosciences, 25-27 Aug. 1998, Mountain View, CA, USA; Sponsored by NASA Ames Research Center, USA; Copyright; Avail: Issuing Activity, Hardcopy; Abstract Only

The NASA Goddard Space Flight Center is home to the fifth most powerful supercomputer in the world, a 1024 processor SGI/Cray T3E-600. The original 512 processor system was placed at Goddard in March, 1997 as part of a cooperative agreement between the High Performance Computing and Communications Program's Earth and Space Sciences Project (ESS) and SGI/Cray Research. The goal of this system is to facilitate achievement of the Project milestones of 10, 50 and 100 GFLOPS sustained performance on selected Earth and space science application codes. The additional 512 processors were purchased in March, 1998 by the NASA Earth Science Enterprise for the NASA Seasonal to Interannual Prediction Project (NSIPP). These two "halves" still operate as a single system, and must satisfy the unique requirements of both aforementioned groups, as well as guest researchers from the Earth, space, microgravity, manned space flight and aeronautics communities. Few large scalable parallel systems are configured for capability computing, so models are hard to find. This unique environment has created a challenging system administration task, and has yielded some insights into the supercomputing needs of the various NASA Enterprises, as well as insights into the strengths and weaknesses of the T3E architecture and software. The T3E is a distributed memory system in which the processing elements (PE's) are connected by a low latency, high bandwidth bidirectional 3-D torus. Due to the focus on high speed communication between PE's, the T3E requires PE's to be allocated contiguously per job. Further, jobs will only execute on the user specified number of PE's and PE timesharing is possible but impractical. With a highly varied job mix in both size and runtime of jobs, the resulting scenario is PE fragmentation and an inability to achieve near 100% utilization. SGI/Cray has provided several scheduling and configuration tools to minimize the impact of fragmentation. These tools include PScheD (the political scheduler), GRM (the global resource manager) and NQE (the Network Queuing Environment). Features and impact of these tools will be discussed, as will resulting performance and utilization data. As a distributed memory system, the T3E is designed to be programmed through explicit message passing. Consequently, certain assumptions related to code design are made by the operating system (UNICOS/mk) and its scheduling tools. With the exception of HPF, which does run on the T3E, however poorly, alternative programming styles have the potential to impact the T3E in unexpected and undesirable ways. Several examples will be presented (preceeded with the disclaimer, "Don't try this at home! Violators will be prosecuted!")
Author
Architecture (Computers); Cray Computers; Distributed Memory; Memory (Computers); Parallel Processing (Computers); Computer Design; Computer Components

19990113024 University of Electro-Communications, Tokyo, Japan
Bulletin of the University of Electro-Communications, Volume 10
December 1997; ISSN 0915-0935; 66p; In Japanese; See also 19990113025 through 19990113027; No Copyright; Avail: CASI; A04, Hardcopy; A01, Microfiche

This report contains the following: design and simulation of a superscalar processor, design and implementation of a 32 bit RISC processor MinIPS, and database construction of dipole moments of metal coordination complexes and related substances.
Derived from text
Computer Aided Design; Design Analysis; Computerized Simulation; Data Bases

19990113025 University of Electro-Communications, Dept. of Computer Science and Information Mathematics, Tokyo, Japan
Design and Simulation of a Superscalar Processor
Ando, Yutaka, University of Electro-Communications, Japan; Abe, Koki, University of Electro-Communications, Japan; Bulletin of the University of Electro-Communications; December 1997; Volume 10, No. 2, pp. 63-69; In Japanese; See also 19990113024; No Copyright; Avail: CASI; A02, Hardcopy; A01, Microfiche

In this paper we describe the design and simulation of a 32 bit superscalar processor. The design is based on a hardware model whose performance was already evaluated in various aspects by means of trace simulations. The model, however, is neither so concrete nor fully described that we are ready to build a processor. We fix a set of design alternatives, elaborate the design details,

and derive a concrete description using Verilog-HDL, a hardware description language. The design choice includes employing a reorder buffer and reservation stations. These hardware mechanisms increase the performance of superscalar processors by removing constraints due to dependences between instructions that force them to be executed in order. The description is at a functional level and functional simulations are performed to confirm the design correctness.
Author
Computerized Simulation; Design Analysis; Computer Aided Design; Central Processing Units

19990113026 University of Electro-Communications, Dept. of Computer Science and Information Mathematics, Tokyo, Japan
Design and Implementation of a 32 bit RISC Processor MinIPS
Katsu, Takeshi, University of Electro-Communications, Japan; Osuga, Daikichi, University of Electro-Communications, Japan; Tsuruta, Mitsutoshi, University of Electro-Communications, Japan; Abe, Koki, University of Electro-Communications, Japan; Bulletin of the University of Electro-Communications; December 1997; Volume 10, No. 2, pp. 71-78; In Japanese; See also 19990113024; No Copyright; Avail: CASI; A02, Hardcopy; A01, Microfiche

In this paper we describe the design and implementation of a 32 bit pipelined RISC processor MinIPS, The architecture of MinIPS is a subset of MIPS R3000. The processor is implemented on multiple Field Programmable Gate Arrays (FPGAs) of moderate capacity. Thus we need to partition the design considering the size of the FPGAs and the limited number of their available pins. We partitioned the design into four blocks, mapped each block to a Xilinx FPGA, and made some of the pins time shared among variables so that the wires connecting the FPGAs be minimized. The details of the partitioning and implementation results are also presented.
Author
RISC Processors; Design Analysis; Computer Aided Design; Pipelining (Computers)

19990113027 University of Electro-Communications, Dept. of Applied Physics and Chemistry, Tokyo, Japan
Database Construction of Dipole Moments of Metal Coordination Complexes and Related Substances
Yamasaki, Akira, University of Electro-Communications, Japan; Furuhashi, Akiko, Aoyamagakuin Univ., Japan; Bulletin of the University of Electro-Communications; December 1997; Volume 10, No. 2, pp. 79-82; In Japanese; See also 19990113024; No Copyright; Avail: CASI; A01, Hardcopy; A01, Microfiche

Personal-computer based dipole moment databases was constructed for coordination chemistry and organometallic chemistry. The magnitude of dipole moments of various metal complexes are much sensitive in the solutional state of these species, which are frequently interesting and important for various area such as Quantitative Structure Activity Relationships (QSAR) or non-linear optics material. The number of compiled records are currently exceeding 3000.
Author
Data Bases; Dipole Moments; Complex Compounds; Metals

61
COMPUTER PROGRAMMING AND SOFTWARE

Includes computer programs, routines, algorithms, and specific applications, e.g., CAD/CAM.

19990106590 Instituto Nacional de Pesquisas Espacias, Sao Jose dos Campos, Brazil
Dynamic Aspects Specification of the Systems *Especificacao dos Aspectos Dinamicos dos Sistemas*
Alves, Miriam Celia Bergue, Instituto Nacional de Pesquisas Espacias, Brazil; 1999; 284p; In Portuguese
Report No.(s): INPE-7229-TDI/683; No Copyright; Avail: CASI; A13, Hardcopy; A03, Microfiche

A consequence of the continuous growing of the systems size and complexity is the highlighting of the importance of the software requirements specification. Dynamic aspects must be early and carefully considered in this phase. This work suggests a set of key elements that would be considered in the dynamic modeling of the systems in order to improve their specification. The practical importance of these key elements are verified and analyzed based on some case studies. Considering the limitations of the existing models and techniques for these elements representation, a new approach using animation models is proposed to create the initial model of the systems. These models are graphically created and animated by using discrete simulation techniques. An user friendly environment is proposed to support the process of animation model creation and to allow interactivity during the model animation. This approach improves both the comprehension and dynamic aspects specification of the systems by

providing one more complete view of the system's dynamic. With successive model refinements, it is also possible to identify some of the software objects to be implemented.
Author
Computer Programming; Dynamic Characteristics; Dynamic Models

19990107384 NASA Goddard Space Flight Center, Greenbelt, MD USA
Spacecraft Software Maintenance: An Effective Approach to Reducing Costs and Increasing Science Return
Shell, Elaine M., NASA Goddard Space Flight Center, USA; Lue, Yvonne, Computer Sciences Corp., USA; Chu, Martha I., Johns Hopkins Univ., USA; 19990322; 2p; In English; 3rd; Reducing the Cost of Spacecraft Ground Systems and Operations, 22-24 Mar. 1999, USA; Copyright; Avail: Issuing Activity, Hardcopy; Abstract Only

Flight software is a mission critical element of spacecraft functionality and performance. When ground operations personnel interface to a spacecraft, they are typically dealing almost entirely with the capabilities of onboard software. This software, even more than critical ground/flight communications systems, is expected to perform perfectly during all phases of spacecraft life. Due to the fact that it can be reprogrammed on-orbit to accommodate degradations or failures in flight hardware, new insights into spacecraft characteristics, new control options which permit enhanced science options, etc., the on- orbit flight software maintenance team is usually significantly responsible for the long term success of a science mission. Failure of flight software to perform as needed can result in very expensive operations work-around costs and lost science opportunities. There are three basic approaches to maintaining spacecraft software--namely using the original developers, using the mission operations personnel, or assembling a center of excellence for multi-spacecraft software maintenance. Not planning properly for flight software maintenance can lead to unnecessarily high on-orbit costs and/or unacceptably long delays, or errors, in patch installations. A common approach for flight software maintenance is to access the original development staff. The argument for utilizing the development staff is that the people who developed the software will be the best people to modify the software on-orbit. However, it can quickly becomes a challenge to obtain the services of these key people. They may no longer be available to the organization. They may have a more urgent job to perform, quite likely on another project under different project management. If they havn't worked on the software for a long time, they may need precious time for refamiliarization to the software, testbeds and tools. Further, a lack of insight into issues related to flight software in its on-orbit environment, may find the developer unprepared for the challenges. The second approach is to train a member of the flight operations team to maintain the spacecraft software. This can prove to be a costly and inflexible solution. The person assigned to this duty may not have enough work to do during a problem free period and may have too much to do when a problem arises. If the person is a talented software engineer, he/she may not enjoy the limited software opportunities available in this position; and may eventually leave for newer technology computer science opportunities. Training replacement flight software personnel can be a difficult and lengthy process. The third approach is to assemble a center of excellence for on-orbit spacecraft software maintenance. Personnel in this specialty center can be managed to support flight software of multiple missions at once. The variety of challenges among a set of on-orbit missions, can result in a dedicated, talented staff which is fully trained and available to support each mission's needs. Such staff are not software developers but are rather spacecraft software systems engineers. The cost to any one mission is extremely low because the software staff works and charges, minimally on missions with no current operations issues; and their professional insight into on-orbit software troubleshooting and maintenance methods ensures low risk, effective and minimal-cost solutions to on-orbit issues.
Author
Applications Programs (Computers); Cost Reduction; Ground Operational Support System; Personnel; Project Management; Software Engineering; Retraining; Management Methods; Programming Environments

19990108581 NASA Goddard Space Flight Center, Greenbelt, MD USA
The Effects of Architecture and Process on the Hardness of Programmable Technologies
Katz, Richard, NASA Goddard Space Flight Center, USA; Wang, J. J., Actel Corp., USA; Reed, R., NASA Goddard Space Flight Center, USA; Kleyner, I., Orbital Sciences Corp., USA; DOrdine, M., Ball Aerospace and Technologies Corp., USA; McCollum, J,, Actel Corp., USA; Cronquist, B., Actel Corp., USA; Howard, J., Jackson and Tull, Inc., USA; [1999]; 8p; In English; No Copyright; Avail: CASI; A02, Hardcopy; A01, Microfiche

Architecture and process, combined, significantly affect the hardness of programmable technologies. The effects of high energy ions, ferroelectric memory architectures, and shallow trench isolation are investigated. A detailed single event latchup (SEL) study has been performed.
Author
Ferroelectricity; Memory (Computers); Architecture (Computers); Heavy Ions; Latch-Up; Electrical Impedance; Isolation

19990108600 NASA Goddard Space Flight Center, Greenbelt, MD USA

SRAM Based Re-programmable FPGA for Space Applications

Wang, J. J., Actel Corp., USA; Sun, J. S., Actel Corp., USA; Cronquist, B. E., Actel Corp., USA; McCollum, J. L., Actel Corp., USA; Speers, T. M., Actel Corp., USA; Plants, W. C., Actel Corp., USA; Katz, R. B., NASA Goddard Space Flight Center, USA; [1999]; 8p; In English; No Copyright; Avail: CASI; A02, Hardcopy; A01, Microfiche

An SRAM (static random access memory)-based reprogrammable FPGA (field programmable gate array) is investigated for space applications. A new commercial prototype, named the RS family, was used as an example for the investigation. The device is fabricated in a 0.25 micrometers CMOS technology. Its architecture is reviewed to provide a better understanding of the impact of single event upset (SEU) on the device during operation. The SEU effect of different memories available on the device is evaluated. Heavy ion test data and SPICE simulations are used integrally to extract the threshold LET (linear energy transfer). Together with the saturation cross-section measurement from the layout, a rate prediction is done on each memory type. The SEU in the configuration SRAM is identified as the dominant failure mode and is discussed in detail. The single event transient error in combinational logic is also investigated and simulated by SPICE. SEU mitigation by hardening the memories and employing EDAC (error detection and correction) at the device level are presented. For the configuration SRAM (CSRAM) cell, the trade-off between resistor de-coupling and redundancy hardening techniques are investigated with interesting results. Preliminary heavy ion test data show no sign of SEL (single event latch-up). With regard to ionizing radiation effects, the increase in static leakage current (static I(sub CC)) measured indicates a device tolerance of approximately 50krad(Si).

Author

Random Access; Random Access Memory; Single Event Upsets; Ionizing Radiation; Linear Energy Transfer (LET); Technology Utilization

19990108796 Ljubljana Univ., Faculty of Electrical Engineering, Yugoslavia

A Reconfigurable System for Prototyping Implementation of Image Processing Algorithms ***Rekonfiguracijski Sistem za Prototipno Implementacijo Algoritmov za Obdelavo Slik***

Trost, Andrej, Ljubljana Univ., Yugoslavia; Zemva, Andrej, Ljubljana Univ., Yugoslavia; Zajc, Baldomir, Ljubljana Univ., Yugoslavia; Electrotechnical Review; 1999; Volume 66, No. 2, pp. 77-83; In English; See also 19990108795; No Copyright; Avail: CASI; A02, Hardcopy; A01, Microfiche

In this paper, we present a reconfigurable system for prototyping hardware implementation of image processing algorithms. The system is composed of a PC, reconfigurable card with 2 FPGA circuits, microcontroller and memory circuit board. Programmable devices are used for implementing tile designed algorithm and the interface circuit for communication between the implemented design and tile PC. The software for an automatic interface circuit synthesis allows user to design and implement digital circuits without any specific knowledge of the structural details of the system. The implementation of the image segmentation circuit is described to demonstrate the operation of the reconfigurable system.

Author

Algorithms; Image Processing; Prototypes; Circuit Boards; Hardware

19990109048 California Univ., Computer Science Dept., Los Angeles, CA USA

Simulation and Visualization of the Fluid Flow Field in Aneurysms: A Virtual Environments Methodology

Karplus, Walter J., California Univ., USA; Harreld, Michael R., California Univ., USA; Valentino, Daniel J., California Univ., USA; 1996; 8p; In English; 7th; Micro Machine and Human Science, 2-4 Oct. 1996, Nagoya, Japan

Contract(s)/Grant(s): FSC2-374; NIH-1P01-CA-51198; Copyright; Avail: Issuing Activity, Hardcopy, Microfiche

Virtual environments, of the type described in this paper, employ hardware and software similar to that used for virtual reality displays. However, the viewer is presented with the outputs of computer simulations, involving the solution of systems of nonlinear partial differential equations in three dimensions, superimposed on a real-world physical model. In the present application, the objective is to aid physicians in the performance of a novel and challenging clinical procedure the noninvasive treatment of aneurysms located deep within the brain. to this end, the physician is given the opportunity of ”taking a walk” inside the aneurysm and to observe the transient pressure and stress fields in the blood flowing in the aneurysm, as the heart pulses and as therapeutic procedures are implemented.

Author

Computerized Simulation; Flow Visualization; Display Devices; Differential Equations

19990109143 Naval Academy, Computer Science Dept., Annapolis, MD USA

Weighted MinMax Algorithm for Color Image Quantization

Reitan, Paula J., Naval Academy, USA; 1999; 6p; In English; Computer Graphics and Imaging, 25-27 Oct. 1999, Palm Springs,

CA, USA; Original contains color illustrations; No Copyright; Avail: CASI; A02, Hardcopy; A01, Microfiche

The maximum intercluster distance and the maximum quantization error that are minimized by the MinMax algorithm are shown to be inappropriate error measures for color image quantization. A fast and effective (improves image quality) method for generalizing activity weighting to any histogram-based color quantization algorithm is presented. A new non-hierarchical color quantization technique called weighted MinMax that is a hybrid between the MinMax and Linde-Buzo-Gray (LBG) algorithms is also described. The weighted MinMax algorithm incorporates activity weighting and seeks to minimize WRMSE, whereby obtaining high quality quantized images with significantly less visual distortion than the MinMax algorithm.

Author

Minimax Technique; Algorithms; Computer Programming; Computer Graphics; Error Analysis

19990109155 NASA Goddard Space Flight Center, Greenbelt, MD USA

Programmable Logic Application Notes

Katz, Richard, NASA Goddard Space Flight Center, USA; [1999]; 8p; In English; No Copyright; Avail: CASI; A02, Hardcopy; A01, Microfiche

This column will be provided each quarter as a source for reliability, radiation results, NASA capabilities, and other information on programmable logic devices and related applications. This quarter the focus is on some experimental data on low voltage drop out regulators to support mixed 5 and 3.3 volt systems. A discussion of the Small Explorer WIRE spacecraft will also be given. Lastly, we show take a first look at robust state machines in Hardware Description Languages (VHDL) and their use in critical systems. If you have information that you would like to submit or an area you would like discussed or researched, please give me a call or e-mail.

Author

Programmable Logic Devices; Hardware Description Languages; Logic Programming

19990109158 NASA Goddard Space Flight Center, Greenbelt, MD USA

Implementation of Multispectral Image Classification on a Remote Adaptive Computer

Figueiredo, Marco A., SGT, Inc., USA; Gloster, Clay S., North Carolina State Univ., USA; Stephens, Mark, NASA Goddard Space Flight Center, USA; Graves, Corey A., North Carolina State Univ., USA; Nakkar, Mouna, North Carolina State Univ., USA; [1999]; 20p; In English; No Copyright; Avail: CASI; A03, Hardcopy; A01, Microfiche

As the demand for higher performance computers for the processing of remote sensing science algorithms increases, the need to investigate new computing paradigms its justified. Field Programmable Gate Arrays enable the implementation of algorithms at the hardware gate level, leading to orders of m a,gnitude performance increase over microprocessor based systems. The automatic classification of spaceborne multispectral images is an example of a computation intensive application, that, can benefit from implementation on an FPGA - based custom computing machine (adaptive or reconfigurable computer). A probabilistic neural network is used here to classify pixels of of a multispectral LANDSAT-2 image. The implementation described utilizes Java client/server application programs to access the adaptive computer from a remote site. Results verify that a remote hardware version of the algorithm (implemented on an adaptive computer) is significantly faster than a local software version of the same algorithm implemented on a typical general - purpose computer).

Author

Remote Sensing; Image Classification; Client Server Systems; Computers

19990110308 Hampton Univ., Dept. of Computer Science, VA USA

Parallelization of Rocket Engine Simulator Software (P.R.E.S.S.) ***Final Report, 19 Oct. 1995 - 18 Oct. 1999***

Cezzar, Ruknet, Hampton Univ., USA; Oct. 31, 1999; 14p; In English

Contract(s)/Grant(s): NAS3-1792; No Copyright; Avail: CASI; A03, Hardcopy; A01, Microfiche

Parallelization of Rocket Engine System Software (PRESS) project is part of a collaborative effort with Southern University at Baton Rouge (SUBR), University of West Florida (UWF), and Jackson State University (JSU). The project has started on October 19, 1995, and after a three-year period corresponding to project phases and fiscal-year funding by NASA Lewis Research Center (now Glenn Research Center), has ended on October 18, 1998. The one-year no-cost extension period was granted on June 7, 1998, until October 19, 1999. The aim of this one year no-cost extension period was to carry out further research to complete the work and lay the groundwork for subsequent research in the area of aerospace engine design optimization software tools. The previous progress for the research has been reported in great detail in respective interim and final research progress reports, seven

of them, in all. While the purpose of this report is to be a final summary and an valuative view of the entire work since the first year funding, the following is a quick recap of the most important sections of the interim report dated April 30, 1999.
Author
Rocket Engines; Simulators; Computer Programs

19990110489 Central Lab. of the Research Councils, Daresbury Lab., Warrington, UK
Daresbury Laboratory. Information Newsletter for Computer Simulation of Condensed Phases, No. 46
Leslie, M., Editor, Central Lab. of the Research Councils, UK; October 1998; 66p; In English; See also 19990110490 through 19990110492; No Copyright; Avail: CASI; A04, Hardcopy; A01, Microfiche

Contents include the following: RATTLE Recipe For General Holonomic Constraints: Angle and Torsion Constraints. Point Multipoles in the Ewald Summation (Revisited). Molecular Modelling and Neutron Scattering Workshop: Techniques for 30 Large-scale Systems.
CASI
Computerized Simulation; Neutron Scattering; Liquid Phases

19990110490 Queen Mary and Westfield Coll., Dept. of Physics, London, UK
RATTLE Recipe for General Holonomic Constraints: Angle and Torsion Constraints
Kutteh, Ramzi, Queen Mary and Westfield Coll., UK; Daresbury Laboratory Information Newsletter for Computer Simulation of Condensed Phases; October 1998, pp. 8-14; In English; See also 19990110489; No Copyright; Avail: CASI; A02, Hardcopy; A01, Microfiche

The popular RATTLE algorithm for imposing bond-stretch constraints in molecular dynamics simulations is generalized here to handle arbitrary holonomic constraints. In particular, RATTLE expressions are given for the important angle-bend and torsional internal-coordinate constraints. This general formulation of RATTLE combines the computational advantages of the velocity Verlet integration algorithm with the flexibility and computational advantages of using general holonomic constraints.
Author
Algorithms; Molecular Dynamics; Simulation

19990110491 Central Lab. of the Research Councils, Daresbury Lab., Warrington, UK
Point Multipoles in the Ewald Summation (Revisited)
Smith, W., Central Lab. of the Research Councils, UK; Daresbury Laboratory Information Newsletter for Computer Simulation of Condensed Phases; October 1998, pp. 15-25; In English; See also 19990110489; No Copyright; Avail: CASI; A03, Hardcopy; A01, Microfiche

This article describes how to incorporate point charges, dipoles and quadrupoles (or combinations of them i.e. point multipoles) into the Ewald summation method. A full description of the multipole potential, forces and torques in a periodic system is provided.
Author
Multipoles; Loads (Forces)

19990110710 NASA Goddard Space Flight Center, Greenbelt, MD USA
PARAMESH: A Parallel Adaptive Mesh Refinement Community Toolkit
MacNeice, Peter, Drexel Univ., USA; Olson, Kevin M., Chicago Univ., USA; Mobarry, Clark, NASA Goddard Space Flight Center, USA; deFainchtein, Rosalinda, Raytheon STX Corp., USA; Packer, Charles, Raytheon STX Corp., USA; October 1999; 40p; In English
Contract(s)/Grant(s): NAG5-6029
Report No.(s): NASA/CR-1999-209483; NAS 1.26:209483; Rept-2000-00298-0; No Copyright; Avail: CASI; A03, Hardcopy; A01, Microfiche

In this paper, we describe a community toolkit which is designed to provide parallel support with adaptive mesh capability for a large and important class of computational models, those using structured, logically cartesian meshes. The package of FORTRAN 90 subroutines, called PARAMESH, is designed to provide an application developer with an easy route to extend an existing serial code which uses a logically cartesian structured mesh into a parallel code with adaptive mesh refinement. Alternatively, in its simplest use, and with minimal effort, it can operate as a domain decomposition tool for users who want to parallelize their serial codes, but who do not wish to use adaptivity. The package can provide them with an incremental

evolutionary path for their code, converting it first to uniformly refined parallel code, and then later if they so desire, adding adaptivity.
Author
Grid Generation (Mathematics); Parallel Programming; Structured Grids (Mathematics)

19990111465 Jackson State Univ., Dept. of Computer Science, Jackson, MS USA
A Software Architecture for Intelligent Interface to a Rocket Engine Numerical Simulation Package
Mitra, Debasis, Jackson State Univ., USA; HBCUs/OMUs Research Conference Agenda and Abstracts; August 1999, pp. 18; In English; See also 19990111455; No Copyright; Avail: Issuing Activity, Hardcopy; Abstract Only

A rocket engine simulation system, like many other numerical packages, is primarily a library of routines. Each of these routines simulates the behavior of a component and/or a physical process. Using a package-specific scripting language the user develops a model, which primarily seeks to assemble some of those routines. A preprocessing program belonging to the package reads the user's script code and develops an executable program to be run on some input values provided by the user, possibly in another file. In our current project (ESA-RENS) we have developed software architecture of an intelligent interface to the package in order to relieve the burden of the user from knowing some details about the package itself. This would reduce the training cost, as well as improve the model development and debugging time to a great extent. It will also help the software developer's attempt in introducing new routines to the package. In this paper we present the architecture and its significance in the process of simulation. We will also discuss some problems related to our goal, and indicate the future direction that the research is likely to take.
Author
Computerized Simulation; Program Verification (Computers); Rocket Engines; Simulation; Systems Engineering; Software Engineering; Models

19990111502 Kinki Univ., Faculty of Engineering, Hiroshima, Japan
A Study of Systematic Formation for the Computer-Aided Design/Computer-Aided Manufacturing
Satonobu, Toshiyuki, Kinki Univ., Japan; Satonobu, Jun, Mazda Technical Research Center, Japan; Research Reports of the Faculty of Engineering, Kinki University; 1993; ISSN 0386-491X, No. 27, pp. 51-54; In Japanese; Copyright; Avail: Issuing Activity, Hardcopy, Microfiche

The present author have already reported that he accomplished a consistent study through "Machine Design" and "Drawing", which was carried out according to "Change of Figures" resulted by "Change of Design" by means of parametric change of SYNTHESIS-"Auto CAD" as an application software. In the present study, he presented that the present new system made possible for students to study CAD/CAM (Computer-Aided Design/Computer-Aided Manufacturing), in which the NC programmer system was newly added on the upper system-consistent study through "Machine Design" and "Drawing". This system was developed by application of Cam as a subject matter.
Derived from text
Applications Programs (Computers); Computer Aided Design; Computer Aided Manufacturing

19990111708 Research Inst. for Advanced Computer Science, Moffett Field, CA USA
Software for Data Analysis with Graphical Models
Buntine, Wray L., Research Inst. for Advanced Computer Science, USA; Roy, H. Scott, Heuristicrats Research, Inc., USA; November 1994; In English; Artificial Intelligence and Statistics, Jan. 1995, Fort Lauderdale, FL, USA
Report No.(s): TR-IC-94-01; Copyright; Avail: Issuing Activity, Hardcopy, Microfiche

Probabilistic graphical models are being used widely in artificial intelligence and statistics, for instance, in diagnosis and expert systems, as a framework for representing and reasoning with probabilities and independencies. They come with corresponding algorithms for performing statistical inference. This offers a unifying framework for prototyping and/or generating data analysis algorithms from graphical specifications. This paper illustrates the framework with an example and then presents some basic techniques for the task: problem decomposition and the calculation of exact Bayes factors. Other tools already developed, such as automatic differentiation, Gibbs sampling, and use of the EM algorithm, make this a broad basis for the generation of data analysis software.
Author
Algorithms; Computer Graphics; Computer Programs; Data Processing; Artificial Intelligence; Statistical Analysis

19990113095 National Inst. of Standards and Technology, Gaithersburg, MD USA

OOMMF User's Guide, Version 1.0

Sep. 14, 1999; 96p

Report No.(s): PB99-163214; NISTIR-6376; No Copyright; Avail: CASI; A05, Hardcopy; A01, Microfiche

This manual describes OOMMF (Object Oriented Micromagnetic Framework), a public domain micromagnetics program developed at the National Institute of Standards and Technology. The program is designed to be portable, flexible, and extensible, with a user-friendly graphical interface. The code is written in C++ and Tcl/Tk. Target systems include a wide range of UNIX platforms, Windows NT, and Windows 95/98.

NTIS

Object-Oriented Programming; C++ (Programming Language); Software Development Tools; Software Engineering; Computer Programming; Applications Programs (Computers); UNIX (Operating System)

19990113106 Technische Hogeschool Twente, Centre for Telematics and Information Technology, Enschede, Netherlands

Engineering an Implementation of the OSI CCR Protocol Using the Information Systems Techniques of Formal Specification and Program Transformation

Jones, V. M.; 1999; 174p; In English

Report No.(s): PB99-175986; CTIT-TR-97-19; Copyright; Avail: National Technical Information Service (NTIS), Hardcopy

The overall objective of the project was to engineer a C implementation of an Open Systems Interconnection (OSI) protocol on a UNIX platform. This document describes the authors' experience of engineering the implementation of the CCR (Commitment, Concurrency and Recovery) protocol using formal methods. The target language was C, and the formal specification language used was LOTOS. The method used was te Lotosphere method and the outputs from the process were: a C implementation of the CCR protocol, and a set of generalized transformation rules for generating C code from LOTOS specifications. The aim of the project was to apply sound information systems engineering principles to the problem using the techniques of formal specification, prototyping and program transformation to ensure that the implementation met professional standards of quality in terms of correctness, efficiency, portability and maintainability.

NTIS

Protocol (Computers); Systems Engineering; Information Systems; Software Development Tools

19990113108 Technische Hogeschool Twente, Enschede, Netherlands

Optimized Self-Synchronizing Byzantine Agreement Protocols

Postma, A.; Krol, T.; Molenkamp, E.; 1999; 26p; In English

Report No.(s): PB99-175879; CTIT-TR-97-20; Copyright; Avail: National Technical Information Service (NTIS), Hardcopy

In order to make a dependable distributed computer system resilient to arbitrary failures of its processors, deterministic Byzantine agreement protocols (BAPs) can be applied. Many BAPs found in literature require that communication takes place in synchronized rounds of information exchange and require that all correct processors know the start of the BAP and start the protocol simultaneously. It is hard to satisfy either or both requirements in a distributed system. As a consequence, it is hard to implement the above BAPs in a distributed system. Authenticated self-synchronizing BAPs evade this problem by guaranteeing Byzantine Agreement while allowing arbitrary clock skew between the clocks of the processors and not requiring correct processors to know the start of the BAP. However, authenticated self-synchronizing BAPs require much communication overhead. Therefore, in this paper, the authors introduce so-called optimized authenticated self-synchronizing BAPs, that require fewer message than the existing authenticated self-synchronizing BAPs.

NTIS

Protocol (Computers); Software Engineering; Synchronism

19990113110 Technische Hogeschool Twente, Centre for Telematics and Information Technology, Enschede, Netherlands

Testing Timed Automata

Springintveld, J.; Vaandrager, F.; D'Argenio, P. R.; 1999; 34p; In English

Report No.(s): PB99-175853; CTIT-TR-97-17; Copyright; Avail: National Technical Information Service (NTIS), Hardcopy

The authors present a generalization of the classical theory of testing for Mealy machines to a setting of dense real-time systems. A model of times I/O automata is introduced, inspired by the timed automation model of Alur and Dill, together with a notion of test sequence for this model. The authors' main contribution is a test generation algorithm for black-box conformance

testing of timed I/O automata. Although it is highly exponential and cannot be claimed to be of practical value, it is the first algorithm that yields a finite and complete set of tests for dense real-time systems.
NTIS
Automata Theory; Testing Time

19990113124 Technische Univ., Faculty of Aerospace Engineering, Delft, Netherlands
Lagrange-Like Contact in ETA Plus User's Manual
Volgers, P. T. G.; Mar. 1999; 132p; In English
Report No.(s): PB99-176760; Copyright; Avail: National Technical Information Service (NTIS), Hardcopy

This report describes the theory and implementation of a contact algorithm in the explicit finite element code ETA. First a motivation of the choice of the method is given. Theory of this method is described. The new input definition and the new data sets are described. Implementation is given, following the different subroutines. Tests and demos are shown to validate the algorithm. Finally results are discussed and recommendations made concerning future developments.
NTIS
User Manuals (Computer Programs); Lagrange Multipliers

19990113133 Technische Univ., Dept. of Mathematics and Computing Science, Eindhoven, Netherlands
Bounded Stacks, Bags and Queues
Baeten, J. C. M.; Bergstra, J. A.; Apr. 1999; 34p; In English
Report No.(s): PB99-176190; COMPUTING SCIENCE REPT-97/07; Copyright; Avail: National Technical Information Service (NTIS), Hardcopy

We prove that a bounded stack can be specified in process algebra with just the operators alternative and sequential composition and iteration. The bounded bag cannot be specified with these operators, but can be specified if we add the parallel composition operator without communication (free merge). The bounded queue cannot even be specified in this signature; we need a form of variable binding such as given by general communication and encapsulation, the state operator, or abstraction.
NTIS
Stacks; Bags; Queueing Theory

62
COMPUTER SYSTEMS

Includes computer networks and special application computer systems.

19990109125 NASA Goddard Space Flight Center, Greenbelt, MD USA
Secure Web-based Ground System User Interfaces over the Open Internet
Langston, James H., Computer Sciences Corp.; Murray, Henry L., NASA Goddard Space Flight Center, USA; Hunt, Gary R., Computer Sciences Corp.; 1998; 1p; In English; Ground System Architecture Workshop (GSAW) 1998, 25-27 Feb. 1998, El Segundo, CA, USA; Copyright; Avail: Issuing Activity, Hardcopy; Abstract Only

A prototype has been developed which makes use of commercially available products in conjunction with the Java programming language to provide a secure user interface for command and control over the open Internet. This paper reports successful demonstration of: (1) Security over the Internet, including encryption and certification; (2) Integration of Java applets with a COTS command and control product; (3) Remote spacecraft commanding using the Internet. The Java-based Spacecraft Web Interface to Telemetry and Command Handling (Jswitch) ground system prototype provides these capabilities. This activity demonstrates the use and integration of current technologies to enable a spacecraft engineer or flight operator to monitor and control a spacecraft from a user interface communicating over the open Internet using standard World Wide Web (WWW) protocols and commercial off-the-shelf (COTS) products. The core command and control functions are provided by the COTS Epoch 2000 product. The standard WWW tools and browsers are used in conjunction with the Java programming technology. Security is provided with the current encryption and certification technology. This system prototype is a step in the direction of giving scientist and flight operators Web-based access to instrument, payload, and spacecraft data.
Author
Applications Programs (Computers); Computer Programming; Java (Programming Language); Prototypes; World Wide Web; Computer Information Security

19990109133 Office of Personnel Management, Washington, DC USA

Automated Competency Assessment: Potentials and Pitfalls

Paskey, Ernest M.; Jan. 1998; 8p; In English

Report No.(s): AD-A362136; No Copyright; Avail: CASI; A02, Hardcopy; A01, Microfiche

This paper has discussed a few of the emerging technologies that have potential for implementation in the area of assessment. Other technologies such as artificial intelligence, computer adaptive testing, and neural network analysis also have potential for contributing to better practices in human resource management. While many of the technologies are still far from full development, and many limitations exist, organizations can recognize great gains utilizing these tools as they stand today. Voice Recognition Systems and Natural Language Processing provide new approaches to data collection. Implementation of text analysis tools can decrease the number of human raters needed and increase the efficiency of the rating process. Development of computer simulations can expand the number of predictive factors measured in an assessment. Delivering assessments via the Internet can increase the applicant pool and efficiency of the process. Incorporating new technology provides for great opportunity in both research and application of novel, efficient, and effective approaches to assessment.

Author (DTIC)

Computerized Simulation; Internets; Speech Recognition; Artificial Intelligence; Automata Theory; Neural Nets

19990110488 Department of Energy, Office of Energy Research, Washington, DC USA

Virtual queueing techniques for UBR+ service in ATM with fair access and minimum bandwidth guarantee

Siu, K. Y., Department of Energy, USA; Wu, Y., Department of Energy, USA; Ren, W., Department of Energy, USA; Dec. 31, 1998; 5p; In English

Report No.(s): DE99-000022; DOE/ER/25273-T1-PT.2; No Copyright; Avail: Department of Energy Information Bridge, Microfiche

The ATM Forum is currently discussing the need for a new best-effort service called UBR+, which is an enhancement to the existing UBR service, to support data traffic. The objective of the UBR+ service is to provide each user with a minimum service rate guarantee and a fair access to any excess available bandwidth. In this paper, the authors present a new efficient scheme for supporting this service. The key advantage of the scheme is that it employs only FIFO queueing (instead of per-VC queueing) and admits simple implementation in ATM switches. The ideas involve a simple scheduling mechanism that is based on per-VC queueing and incorporate the virtual queueing technique that can efficiently emulate per-VC queueing on a shared FIFO queue. Simulation results are presented to show that the schemes can deliver almost ideal performance for supporting the new service requirements of UBR+.

NTIS

Data Transmission; Computer Networks; Asynchronous Transfer Mode; Queueing Theory

63
CYBERNETICS

Includes feedback and control theory, artificial intelligence, robotics and expert systems. For related information see also 54 Man/System Technology and Life Support.

19990109046 California Univ., Electrical Engineering Dept., Los Angeles, CA USA

Robust Stabilizing Compensators for Flexible Structures with Collocated Controls

Balakrishman, A. V., California Univ., USA; Applied Mathematics Optimization; 1996; Volume 33, pp. 35-60; In English

Contract(s)/Grant(s): NCC2-374; Copyright; Avail: Issuing Activity, Hardcopy, Microfiche

For flexible structures with collocated rate and attitude sensors/actuators, we characterize compensator transfer functions which guarantee modal stability even when stiffness/inertia parameters are uncertain. While the compensators are finite-dimensional, the structure models are allowed to be infinite-dimensional (continuum models), with attendant complexity of the notion of stability; thus exponential stability is not possible and the best we can obtain is strong stability. Robustness is interpreted essentially as maintaining stability in the worst case. The conditions require that the compensator transfer functions be positive real and use is made of the Kalman-Yakubovic lemma to characterize them further. The concept of positive realness is shown to be equivalent to dissipativity in infinite dimensions. In particular we show that for a subclass of compensators it is possible to make the system strongly stable as well as dissipative in an appropriate energy norm.

Author

Actuators; Attitude Control; Attitude Indicators; Robustness (Mathematics); Stabilization

19990111464 Howard Univ., Electrical Engineering Dept., Washington, DC USA

Experimental Implementation of High Performance AC Drives using Neural Designs

Rubaai, Ahmed, Howard Univ., USA; Kotaru, Raj, Howard Univ., USA; HBCUs/OMUs Research Conference Agenda and Abstracts; August 1999, pp. 17; In English; See also 19990111455; No Copyright; Avail: Issuing Activity, Hardcopy; Abstract Only

This study presents an adaptive nonlinear-model-based observer, using an artificial neural network (ANN) which is trained while the observer is operating on-line. The adaptation mechanism uses continual on-line training (with no off-line training) to learn the unknown nonlinear dynamics and estimate the unmeasurable states of an induction machine. The proposed architecture incorporates five-multilayer perception ANNs that are on-line trained, using the Levenburg-Marquadt learning algorithm. The objective is to track the time-varying stator currents of the induction motor using only input/output observations. This is done by using the neural observer to emulate the motor dynamics and generate estimates of the unmeasurable states. Subsequently, the estimated states are fed into the neural controller to track the stator current trajectories. The actual controller is not constructed as the output of an independent system, but rather as a feedback signal, depending on the state variables of the motor supplied by the neural observer and the reference trajectories to be tracked by the outputs. An adaptive learning mechanism, which attempts to keep the learning, rate as large as possible, while maintaining the stability of the learning process, is proposed. This mechanism simplifies the learning algorithm in terms of computation time, which is important in real-time implementation. The control of the direct and quadrature components of the stator current successfully tracked a wide variety of trajectories after relatively short, on-line training periods.

Author

Feedback; Neural Nets; On-Line Systems; Real Time Operation; Stators; Control Systems Design

19990111577 NASA Langley Research Center, Hampton, VA USA

Multidisciplinary Optimization Branch Experience Using iSIGHT Software

Padula, S. L., NASA Langley Research Center, USA; Korte, J. J., NASA Langley Research Center, USA; Dunn, H. J., NASA Langley Research Center, USA; Salas, A. O., NASA Langley Research Center, USA; 1999; 16p; In English; iSIGHT Users, 4-6 Oct. 1999, Chapel Hill, NC, USA; No Copyright; Avail: CASI; A03, Hardcopy; A01, Microfiche

The Multidisciplinary Optimization (MDO) Branch at NASA Langley Research Center is investigating frameworks for supporting multidisciplinary analysis and optimization research. An optimization framework call improve the design process while reducing time and costs. A framework provides software and system services to integrate computational tasks and allows the researcher to concentrate more on the application and less on the programming details. A framework also provides a common working environment and a full range of optimization tools, and so increases the productivity of multidisciplinary research teams. Finally, a framework enables staff members to develop applications for use by disciplinary experts in other organizations. Since the release of version 4.0, the MDO Branch has gained experience with the iSIGHT framework developed by Engineous Software, Inc. This paper describes experiences with four aerospace applications: (1) reusable launch vehicle sizing, (2) aerospike nozzle design, (3) low-noise rotorcraft trajectories, and (4) acoustic liner design. All applications have been successfully tested using the iSIGHT framework, except for the aerospike nozzle problem, which is in progress. Brief overviews of each problem are provided. The problem descriptions include the number and type of disciplinary codes, as well as all estimate of the multidisciplinary analysis execution time. In addition, the optimization methods, objective functions, design variables, and design constraints are described for each problem. Discussions on the experience gained and lessons learned are provided for each problem. These discussions include the advantages and disadvantages of using the iSIGHT framework for each case as well as the ease of use of various advanced features. Potential areas of improvement are identified.

Author

Multidisciplinary Research; Research Management; Multidisciplinary Design Optimization; Aircraft Design; Design Analysis

19990111657 NASA Marshall Space Flight Center, Huntsville, AL USA

Probabilistic and Other Neural Nets in Multi-Hole Probe Calibration and Flow Angularity Pattern Recognition

Baskaran, Subbiah, Raytheon STX, USA; Ramachandran, Narayanan, Universities Space Research Association, USA; Noever, David, NASA Marshall Space Flight Center, USA; [1998]; 1p; In English; International Confernce on Advances in Patter Recognition, 23 Nov. 1998, Plymouth, UK; Copyright; Avail: Issuing Activity, Hardcopy; Abstract Only

The use of probabilistic (PNN) and multilayer feed forward (MLFNN) neural networks are investigated for calibration of multi-hole pressure probes and the prediction of associated flow angularity patterns in test flow fields. Both types of networks

are studied in detail for their calibration and prediction characteristics. The current formalism can be applied to any multi-hole probe, however the test results for the most commonly used five-hole Cone and Prism probe types alone are reported in this article. Author

Neural Nets; Probability Theory; Probe Method (Forecasting); Pattern Method (Forecasting)

19990111716 Naval Research Lab., Chemistry Div., Washington, DC USA

A Feasibility Study on Using Physics-Based Modeler Outputs to Train Probabilistic Neural Networks for UXO Classification ***Final Report***

Shaffer, R. E.; Rose–Pehrsson, S. L.; McDonald, J. R.; Hart, S. J.; Apr. 29, 1999; 46p; In English

Report No.(s): AD-A364744; No Copyright; Avail: CASI; A03, Hardcopy; A01, Microfiche

A probabilistic neural network (PNN) has been applied to the detection and classification of unexploded ordnance (UXO) measured using magnetometry data collected using the Multi-sensor Towed Array Detection System (MTADS). Physical parameters obtained from a physics based modeler were used to describe the UXO and scrap targets found at three sites: Badlands Bombing Range (BBR) Target 1 and 2 and the Former Buckley Field. The PNN was trained and tested using cross validation (CV) software developed at NRL. The PNN was able to correctly identify between 84% to 94% of the targets. by adjusting the probability threshold, further improvements in the discrimination of UXO were possible: 96% of the UXO were correctly identified for BBR Target 1, 100% for BBR Target 2, and 94% for the former Buckley Field. The ability to train using one site (BBR target 2) and predict another (BBR Target 1) was successful with 95% of the UXO correctly identified and a false alarm rate of 35%.

DTIC

Neural Nets; Ammunition; Explosives Detection; Multisensor Applications; Magnetic Measurement

64
NUMERICAL ANALYSIS

Includes iteration, difference equations, and numerical approximation.

19990108797 Ljubljana Univ., Fakulteta za Elektrotehniko, Yugoslavia

Lyapunov Exponents for a Harmonically Forced Van der Pol Oscillator with a Nonlinear Restoring Force ***Ljapunovi Eksponenti Van Der Polovega Oscilatorja s Harmonicno Zunanjo in Nelinerano Povratno Silo***

Gyergyek, Tomaza, Ljubljana Univ., Yugoslavia; Cercek, Milan, Jozef Stefan Inst., Slovenia; Stanojevic, Mladen, Jozef Stefan Inst., Slovenia; Electrotechnical Review; 1999; Volume 66, No. 2, pp. 84-91; In English; See also 19990108795; No Copyright; Avail: CASI; A02, Hardcopy; A01, Microfiche

A systematic calculation of the largest Lyapunov exponents versus several different parameters is presented for a harmonically forced Van der Pol oscillator with a nonlinear restoring force d(sup 2)y/dt(sup 2)-((alpha)-(beta)y(sup 2))dy/dt+(A(omega(sub 0, sup 2)cos(omega(sub t)). Some numerical details for the calculation of the largest Lyapunov exponent are described. The largest Lyapunov exponent is calculated directly from the variational equations. The largest Lyaptinov exponents are calculated for a strongly driven oscillator with a large alpha/omega(sub 0) ratio and for a moderate nonlinear restoring force. When the nonlinear restoring force is gradually increased, tile system undergoes transitions from periodic oscillations into chaos via period doubling bifurcations.

Author

Harmonic Oscillation; Liapunov Functions; Attractors (Mathematics)

19990111467 New Mexico Univ., Dept. of Mathematics and Statistics, Albuquerque, NM USA

Development of a High-Order Time-Accurate Simulator for Complex Combustion Models

Hagstrom, Thomas, New Mexico Univ., USA; Zhou, Ruhai, New Mexico Univ., USA; Radhakrishnan, Krishnan, New Mexico Univ., USA; HBCUs/OMUs Research Conference Agenda and Abstracts; August 1999, pp. 20; In English; See also 19990111455; No Copyright; Avail: Issuing Activity, Hardcopy; Abstract Only

We discuss our work on the design, implementation, and testing of high-order numerical methods for solving complex physical models of time-dependent, low Mach number, combustion phenomena. Features of the code include: (1). Fourth to sixth order, explicit and implicit, elliptic spatial differencing; (2). Linearly implicit time-stepping using simplified diffusion models as preconditioners. High order accuracy is achieved using spectral deferred correction; (3). Capability to directly compute steady

flames using convergence acceleration techniques; (4). Adaptive mesh refinement based on coordinate maps. Numerical examples in one space dimension will be given, along with a discussion of issues related to multidimensional implementations. Author
Combustion Physics; Numerical Analysis; Simulators; Computational Grids; Combustion; Combustion Control

19990111499 Kinki Univ., Faculty of Engineering, Hiroshima, Japan
Studies of Relations Between Many-Body Problems and Green Functions, 3, Elements of Quantum Theory for Bosons
Hashizume, Kunio, Kinki Univ., Japan; Research Reports of the Faculty of Engineering, Kinki University; 1993; ISSN 0386-491X, No. 27, pp. 111-126; In Japanese; Copyright; Avail: Issuing Activity, Hardcopy, Microfiche

In this paper the next subjects are discussed:(5) The solid as a continuous medium and the field operators u(r), p(r); (6) Classical field theory; and (7) Field operators and second quantization.
Derived from text
Field Theory (Physics); Many Body Problem; Solids; Functions (Mathematics)

19990111500 Kinki Univ., Faculty of Engineering, Hiroshima, Japan
Studies of Relations Between Many-Body Problems and Green Functions, 2, Elements of Perturbation Theory in Advanced Quantum Theory
Hashizume, Kunio, Kinki Univ., Japan; Research Reports of the Faculty of Engineering, Kinki University; 1993; ISSN 0386-491X, No. 27, pp. 93-109; In Japanese; Copyright; Avail: Issuing Activity, Hardcopy, Microfiche

In this paper the next subjects are discussed: (5) The expression by the integral equation of the time evolution operator U(t, t(sub 1)) and time-integral expansion series; (6) Calculations of the time-evolution operator U(t, t(sub 1)); (7) Some properties of the time-evolution operator U(t, t(sub 1)); (8) The time-evolution operator U(t, t(sub 1)) and transition probability W(sub a approaches b); and (9) The scattering theory and the S-matrix.
Derived from text
Time Series Analysis; Integral Equations; Transition Probabilities

65
STATISTICS AND PROBABILITY

Includes data sampling and smoothing: Monte Carlo method; and stochastic processes.

19990111589 Instituto Nacional de Pesquisas Espacias, Sao Jose dos Campos, Brazil
Decentralized Supervision in Systems Performance Models: An Approach for Decision Markovian Processes ***Supervisao Descentralizada em Modelos de Desempenho de Sistemas: Uma Abordagem por Processos Markovianos de Decisao***
Monteiro, Marcia Aparecida, Instituto Nacional de Pesquisas Espacias, Brazil; 1999; 134p; In Portuguese; Original contains color illustrations
Report No.(s): INPE-7231-TDI/685; No Copyright; Avail: CASI; A07, Hardcopy; A02, Microfiche

Most of the procedures to analyze and to control the behavior of a system is based on centralized supervision. However, in some complex systems, the centralized supervision is not the most adequate. In certain systems, a better alternative would be to adopt a decentralized supervision, that consists of several supervisors, each one observing a part of the system. In this work we present a strategy that allows the modeling of systems with decentralized supervision. A methodology using the theory of Markov Decision Process with Partial Information is proposed. Numerical results are shown where the proposed methodology is applied to optimize a production system.
Author
Personnel Management; Models; Complex Systems

66
SYSTEMS ANALYSIS

Includes mathematical modeling; network analysis; and operations research.

19990113203 Naval Air Systems Command, Washington, DC USA
The KHE SANH Airlift
Guay, Robert, Naval Air Systems Command, USA; 1969; In English; VTOL Research, Design, and Operations, 17-19 Feb. 1969, Atlanta, GA, USA; Sponsored by American Inst. of Aeronautics and Astronautics, USA
Report No.(s): AIAA Paper 69-191; Copyright; Avail: Issuing Activity, Hardcopy

This presentation is an analysis of the air logistical requirements that were created by the 11-week siege of Khe Sanh in South Viet Nam during the early Spring of 1968. The threat and the needs of the besieged U.S. forces and the manner in which the resulting requirements for equipment, supplies and personnel were met are examined in an attempt to suggest the lessons learned from this experience. Technological developments in recent years have enhanced the capability of U.S. forces to support isolated units by means of an Air Line of Communication (ALOC). In the past, only rare occasions demanded use of this capability, the most conspicuous cases since World War II being the blockade of West Berlin in 1948-49 and the siege of Dien Bien Phu in 1954. However, in recent years both technology advances and trends in warfare have pointed the way for the development of doctrine and the transport of supplies required to satisfy the need for the logistical support of isolated units often far removed from the main body of friendly forces. In the absence of actual field data, computerized war games and exercises have provided us with approximations as to what we may face in such situations and how to cope with the indicated problems. It was somewhat accidental that we encountered this very situation in South Viet Nam during the siege of Khe Sanh.
Derived from text
Supplying; Technology Assessment; Warfare; Vietnam; Logistics

67
THEORETICAL MATHEMATICS

Includes topology and number theory.

19990109675 National Inst. for Fusion Science, Toki, Japan
Multiresolution Approximation of the Vector Fields on T3
Araki, Keisuke, Okayama Univ. of Science, Japan; Suzuki, Katsuhiro, Tokyo Univ. of Agriculture and Technology, Japan; Kishida, Keiji, Hiroshima Univ., Japan; Kishiba, Seigo, Hiroshima Univ., Japan; March 1999; ISSN 0915-633X; 20p; In English
Report No.(s): NIFS-590; No Copyright; Avail: CASI; A03, Hardcopy; A01, Microfiche

Multiresolution approximation (MRA) of the vector fields on T(sup 3) is studied. We introduced in the Fourier space a triad of vector fields called helical vectors which derived from the spherical coordinate system basis. Utilizing the helical vectors, we proved the orthogonal decomposition of L(sup 2)(T(sup 3)) which is a synthesis of the Hodge decomposition of the differential 1- or 2-form on T(sup 3) and the Beltrami decomposition that decompose the space of solenoidal vector fields into the eigenspaces of curl operator. In the course of proof, a general construction procedure of the divergence-free orthonormal complete basis from the basis of scalar function space is presented. Applying this procedure to MRA of L(sup 2)(T(sup 3)), we discussed the MRA of vector fields on T(sup 3) and the analyticity and regularity of vector waveless. It is conjectured that the orthonormal solenoidal wavelet basis must break r-regular condition, i.e. some wavelet functions cannot be rapidly decreasing function because of the inevitable singularities of helical vectors. The localization property and spatial structure of solenoidal waveless derived from the Littlewood-Paley type MRA (Meyer's wavelet) are also investigated numerically.
Author
Wavelet Analysis; Singularity (Mathematics); Image Resolution; Approximation

19990110709 NASA Glenn Research Center, Cleveland, OH USA
Generalized Functions for the Fractional Calculus
Lorenzo, Carl F., NASA Glenn Research Center, USA; Hartley, Tom T., Akron Univ., USA; October 1999; 22p; In English
Contract(s)/Grant(s): RTOP 523-22-13
Report No.(s): NASA/TP-1999-209424; NAS 1.60:209424; E-11944; No Copyright; Avail: CASI; A03, Hardcopy; A01, Microfiche

Previous papers have used two important functions for the solution of fractional order differential equations, the Mittag-Leffler functionE(sub q)[at(exp q)](1903a, 1903b, 1905), and the F-function F(sub q)[a,t] of Hartley & Lorenzo (1998). These functions provided direct solution and important understanding for the fundamental linear fractional order differential equation and for the related initial value problem (Hartley and Lorenzo, 1999). This paper examines related functions and their Laplace transforms. Presented for consideration are two generalized functions, the R-function and the G-function, useful in analysis and as a basis for computation in the fractional calculus. The R-function is unique in that it contains all of the derivatives and integrals of the F-function. The R-function also returns itself on qth order differ-integration. An example application of the R-function is provided. A further generalization of the R-function, called the G-function brings in the effects of repeated and partially repeated fractional poles.
Author
Calculus; Laplace Transformation

70
PHYSICS (GENERAL)

For precision time and time interval (PTTI) see 35 Instrumentation and Photography; for geophysics, astrophysics or solar physics see 46 Geophysics, 90 Astrophysics, or 92 Solar Physics.

19990107337 Swedish Defence Research Establishment, Div. of Systems and Underwater Technology, Stockholm, Sweden
Extraction of Traveling-Wave Field Components by Green's Function Expansion ***Topical Report***
Ivansson, Sven, Swedish Defence Research Establishment, Sweden; Bishop, Judith, Swedish Defence Research Establishment, Sweden; Nov. 1998; 58p; In English
Report No.(s): PB99-172504; FOA-R-98-00914-409-SE; No Copyright; Avail: CASI; A01, Microfiche; A04, Hardcopy

The wave-field in a range-independent acoustic medium can be mathematically decomposed by a series expansion of the Green's function in terms of traveling waves. A useful ray interpretation of the component fields emerges by ignoring the evanescent regime of wavenumbers and applying the WKBJ approximation. However, these approximations can lead to servere modeling errors for important shallow-water applications. to prepare for an 'exact' implementation of the decomposition, a number of issues are clarified: (1) Being based on particular choices of solutions to the depth-dependent wave equation, the decomposition is inherently nonunique. 'Specification depths' are introduced where directionality is assigned; (2) Each component field appears as a generalized integral with respect to horizontal wavenumber. In order for these integrals to converge (at infinity) and in order to avoid certain anomalous growth, it is in general necessary to let the specification depths enclose the source and receiver depths. (3) With turning points for significant ray-like energy appearing between the specification depths, it appears, however, that the physical order of a multiple will not be respected by the decomposition. The corresponding energy tends to be distributed among terms with different cycle numbers, and unidesired 'multipath couping' appears.
NTIS
Evanescent Waves; Traveling Waves; Wave Equations; Shallow Water; Green'S Functions; Series Expansion; Evanescence

19990108482 NASA Marshall Space Flight Center, Huntsville, AL USA
A Laboratory Study of the Charging/Discharging Mechanisms of a Dust Particle Exposed to an Electron Beam
Venturini, C. C., Alabama Univ., USA; Spann, J. F., NASA Marshall Space Flight Center, USA; Comfort, R. H., Alabama Univ., USA; [1999]; 1p; In English; Plasma Science, 16 Nov. 1999, Seattle, WA, USA; Sponsored by American Physical Society, USA; No Copyright; Avail: Issuing Activity, Hardcopy; Abstract Only

The interaction of micron sized particles or "dust particles" with different space and planetary environments has become an important area of research. One particular area of interest is how dust particles interact with plasmas. Studies have shown that charged dust particles immersed in plasmas can alter plasma characteristics, while ions and electrons in plasmas can affect a particle's potential and thereby, its interaction with other particles. The basis for understanding these phenomena is the charging mechanisms of the dust particle, specifically, how the particle's charge and characteristics are affected when exposed to ions and electrons. At NASA Marshall Space Flight Center, a laboratory experiment has been developed to study the interaction of dust particles with electrons. Using a unique laboratory technique known as electrodynamic suspension, a single charged particle is suspended in a modified quadrupole trap. Once suspended, the particle is then exposed to an electron beam to study the charging/discharging mechanisms due to collisions of energetic electrons. The change in the particle's charge, approximations of the charging/discharging currents, and the charging/discharging yield are calculated.
Author
Laboratories; Research; Charged Particles; Dust; Particle Interactions; Electron Beams

71
ACOUSTICS

Includes sound generation, transmission and attenuation. For noise pollution see 45 Environmental Pollution.

19990107338 Swedish Defence Research Establishment, Div. of Systems and Underwater Technology, Stockholm, Sweden
Low-Frequency Wavenumber Limits for P-SV Modes ***Modvagtal vid lae Frekvens***
Ivansson, Sven, Swedish Defence Research Establishment, Sweden; Dec. 1998; 34p; In English
Report No.(s): PB99-172488; FOA-R-98-00918-409-SE; No Copyright; Avail: CASI; A01, Microfiche; A03, Hardcopy

For laterally homogeneous fluid-solid media, it has previously been shown that all low-frequency P-SV modes such that the horizontal wavenumber tends to zero with the frequency can be determined explicitly. Interface waves and different types of bending waves are particular examples of such modes. They continue to exist as propagating modes down to arbitrarily low frequencies. Propagating modes in general, however, typically have lower cutoff frequencies, below which the horizontal wavenumber leaves the real axis. In the present paper, it is shown how all low-frequency P-SV modes can be determined for which the horizontal wavenumber does not tend to infinity as the frequency tends to zero. It turns out that a low-frequency wavenumber limit will indeed exist for such a mode. For each fluid-solid medium, the low-frequency modal wavenumber limits can be determined as the zeros of a particular entire analytic function. The evaluation of this analytic function involves solution of ordinary differential equation (ODE) systems.
NTIS
Underwater Acoustics; Seismology; Media; Liquid-Solid Interfaces

19990110626 Sverdrup Technology, Inc., Lewis Research Center Group, Brook Park, OH USA
Numerical Simulation of Free Shear Flows Towards a Predictive Computational Aeroacoustics
Soh, W. Y., Sverdrup Technology, Inc., USA; First NASA/Industry High Speed Research Program Nozzle Symposium; September 1999, pp. 21-1 - 21-19; In English; See also 19990110605; No Copyright; Avail: CASI; A03, Hardcopy; A10, Microfiche

Implicit spatial differencing technique with fourth order accuracy has been developed based on the Pade compact scheme. A Dispersion Relation Preserving concept has been incorporated into the numerical scheme. Two dimensional Euler computation of a spatially-developing free shear flow, with and without external excitation, has been performed to demonstrate the capability of numerical scheme developed. Results are in good agreement with theory and experimental observation regarding the growth rate of fluctuating velocity, the convective velocity, and the vortex-pairing process. Far-field sound p generated by the unsteady shear flow solution using Lighthill's acoustic analogy shows a strong directivity with a zone of silence at the flow angle.
Author
Numerical Analysis; Aeroacoustics; Two Dimensional Models; Simulation; Predictions; Observation; Sound Pressure; Far Fields

19990110627 AeroChem Research Labs., Inc., Princeton, NJ USA
Recent Progress in 3D Noise Computations
Berman, C., AeroChem Research Labs., Inc., USA; Gordon, G., AeroChem Research Labs., Inc., USA; Karniadakis, G., Cambridge Hydrodynamics, Inc., USA; Jackson, E., Cambridge Hydrodynamics, Inc., USA; Orszag, S., Cambridge Hydrodynamics, Inc., USA; First NASA/Industry High Speed Research Program Nozzle Symposium; September 1999, pp. 22-1 - 22-27; In English; See also 19990110605; No Copyright; Avail: CASI; A03, Hardcopy; A10, Microfiche

Contents include the following: (1) Flow/Acoustics Overview. (2) LES Computations. (3) Sound Wave Propagation. (4) Noise Source Theory. (5) Quadrupole Source Tests. (6) VLES (K - epsilon). and (7) Frequency Domain Analysis. The paper briefly covers many aspects of flow and acoustics computations needed to develop methods for computing the sound of three-dimensional noise suppressors. Special emphasis is given to recent developments that can lead to more accurate and reliable results requiring less computer resources.
Author
Computational Fluid Dynamics; Acoustics; Noise Reduction; Computation; Wave Propagation

19990110628 NASA Lewis Research Center, Cleveland, OH USA
Computation of Supersonic Jet Mixing Noise Using PARC Code With a kappa-epsilon Turbulence Model
Khavaran, A., Sverdrup Technology, Inc., USA; Kim, C. M., NASA Lewis Research Center, USA; First NASA/Industry High Speed Research Program Nozzle Symposium; September 1999, pp. 23-1 - 23-19; In English; See also 19990110605; No Copyright; Avail: CASI; A03, Hardcopy; A10, Microfiche

A number of modifications have been proposed in order to improve the jet noise prediction capabilities of the MGB code. This code which was developed at General Electric, employees the concept of acoustic analogy for the prediction of turbulent mixing noise. The source convection and also refraction of sound due to the shrouding effect of the mean flow are accounted for by incorporating the high frequency solution to Lilley's equation for cylindrical jets (Balsa and Mani). The broadband shock-associated noise is estimated using Harper-Bourne and Fisher's shock noise theory. The proposed modifications are aimed at improving the aerodynamic predictions (source/spectrum computations) and allowing for the non- axisymmetric effects in the jet plume and nozzle geometry (sound/flow interaction). In addition, recent advances in shock noise prediction as proposed by Tam can be employed to predict the shock-associated noise as an addition to the jet mixing noise when the flow is not perfectly expanded. Here we concentrate on the aerodynamic predictions using the PARC code with a k-E turbulence model and the ensuing turbulent mixing noise. The geometry under consideration is an axisymmetric convergent-divergent nozzle at its design operating conditions. Aerodynamic and acoustic computations are compared with data as well as predictions due to the original MGB model using Reichardt's aerodynamic theory.
Author

Supersonic Jet Flow; Aerodynamic Noise; Computation; Jet Aircraft Noise; K-Epsilon Turbulence Model; Noise Prediction; Turbulence Models

19990110629 Pennsylvania State Univ., University Park, PA USA

Noise from Supersonic Non-Circular Jets

Morris, Philip J., Pennsylvania State Univ., USA; McLaughlin, Dennis K., Pennsylvania State Univ., USA; First NASA/Industry High Speed Research Program Nozzle Symposium; September 1999, pp. 24-1 - 24-24; In English; See also 19990110605; No Copyright; Avail: CASI; A03, Hardcopy; A10, Microfiche

The three main sources of noise in supersonic jets are jet mixing noise, broadband shock-associated noise, and screech. Each of these noise sources may be associated with the large-scale structures in the jet mixing layer. These large-scale structures are also responsible for the gross mixing of the jet. As is discussed below, these structures have a high axial coherence and are both temporally and spatially nearly periodic. In circular jets they may be axisymmetric or helical in nature with the latter form dominating at high jet exit Mach numbers. When the structures convect downstream supersonically with respect to the ambient speed of sound they radiate intense noise, predominantly in the downstream arc. This noise mechanism is called jet mixing or eddy Mach wave noise. If the jet is operating off-design a quasi-periodic shock-cell structure is formed in the jet plume. The interaction between the downstream-travelling large-scale turbulent structures in the jet shear layer and the shock-cell structure results in broadband shock-associated noise. This noise source radiates predominantly in the upstream arc with a peak frequency that depends on the shock cell spacing, the convection velocity of the large-scale turbulent structures, and the angle to the jet downstream axis. When this interaction noise radiates directly upstream it can trigger the phase-locked shedding of large-scale vortex structures from the jet lip. This results in jet screech. This is an intense, tonal noise radiation with a frequency that also depends on the shock cell spacing and the convection velocity of the large structures.
Author

Aerodynamic Noise; Air Jets; Jet Mixing Flow; Noise (Sound); Noise Generators; Screech Tones; Shock Waves; Sound Waves

19990110630 NASA Lewis Research Center, Cleveland, OH USA

Large Eddy Simulation in the Computation of Jet Noise

Mankbadi, R. R., NASA Lewis Research Center, USA; Goldstein, M. E., NASA Lewis Research Center, USA; Povinelli, L. A., NASA Lewis Research Center, USA; Hayder, M. E., NASA Lewis Research Center, USA; Turkel, E., NASA Lewis Research Center, USA; First NASA/Industry High Speed Research Program Nozzle Symposium; September 1999, pp. 25-1 - 25-7; In English; See also 19990110605; No Copyright; Avail: CASI; A02, Hardcopy; A10, Microfiche

Noise can be predicted by solving Full (time-dependent) Compressible Navier-Stokes Equation (FCNSE) with computational domain. The fluctuating near field of the jet produces propagating pressure waves that produce far-field sound. The fluctuating flow field as a function of time is needed in order to calculate sound from first principles. Noise can be predicted by solving the full, time-dependent, compressible Navier-Stokes equations with the computational domain extended to far field - but this is not feasible as indicated above. At high Reynolds number of technological interest turbulence has large range of scales. Direct numerical simulations (DNS) can not capture the small scales of turbulence. The large scales are more efficient than the small scales in radiating sound. The emphasize is thus on calculating sound radiated by large scales.
Author

Noise Prediction; Time Dependence; Navier-Stokes Equation; Jet Aircraft Noise

19990110631 Florida State Univ., Tallahassee, FL USA

Direct Numerical Simulation of Supersonic Jet Flow and Noise Radiation

Tam, Christopher K. W., Florida State Univ., USA; Webb, Jay C., Florida State Univ., USA; First NASA/Industry High Speed Research Program Nozzle Symposium; September 1999, pp. 26-1 - 26-14; In English; See also 19990110605; No Copyright; Avail: CASI; A03, Hardcopy; A10, Microfiche

We use an algebraic mapping to put a large number of mesh points in the mixing layer of the jet were there is a large velocity gradient. As can be seen the mapping does concentrate points in the shear layers. This map covers the initial region of the jet downstream of the nozzle exit. It seems that it is feasible to perform direct numerical simulations of noise generation and radiation from supersonic jets.

Derived from text

Numerical Analysis; Supersonic Jet Flow; Direct Numerical Simulation; Computerized Simulation

19990110632 NASA Langley Research Center, Hampton, VA USA

Prediction, Measurement, and Suppression of High Temperature Supersonic Jet Noise

Seiner, John M., NASA Langley Research Center, USA; Bhat, T. R. S., NASA Langley Research Center, USA; Jansen, Bernard J., Lockheed Engineering and Sciences Co., USA; First NASA/Industry High Speed Research Program Nozzle Symposium; September 1999, pp. 27-1 - 27-34; In English; See also 19990110605; No Copyright; Avail: CASI; A03, Hardcopy; A10, Microfiche

The photograph in figure 1 displays a water cooled round convergent-divergent supersonic nozzle operating slightly overexpanded near 2460 F. The nozzle is designed to produce shock free flow near this temperature at Mach 2. The exit diameter of this nozzle is 3.5 inches. This nozzle is used in the present study to establish properties of the sound field associated with high temperature supersonic jets operating fully pressure balanced (i.e. shock free) and to evaluate capability of the compressible Rayleigh model to account for principle physical features of the observed sound emission. The experiment is conducted statically (i.e. M(sub f) = 0.) in the NASA/LaRC Jet Noise Laboratory. Both aerodynamic and acoustic measurements are obtained in this study along with numerical plume simulation and theoretical prediction of jet noise. Detailed results from this study are reported previously by Seiner, Ponton, Jansen, and Lagen.

Author

Acoustic Measurement; Temperature Measurement; Supersonic Jet Flow; Jet Aircraft Noise; Noise Prediction (Aircraft); Acoustic Emission

19990110633 Lockheed Aeronautical Systems Co., Marietta, GA USA

Prediction of Broadband Shock Noise from Rectangular Nozzles

Reddy, N.N., Lockheed Aeronautical Systems Co., USA; Tam, Christopher K. W., Florida State Univ., USA; First NASA/Industry High Speed Research Program Nozzle Symposium; September 1999, pp. 28-1 - 28-16; In English; See also 19990110605; No Copyright; Avail: CASI; A03, Hardcopy; A10, Microfiche

The author describes the development of a semi-empirical broadband shock associated noise prediction program, for supersonic rectangular jets and broadband shock associated noise generation mechanism. by using the broadband, shock associated noise prediction formula, for circular jets, as a starting point, the author can make necessary changes to incorporate new physics of the shock cells and flow turbulence pertinent to supersonic rectangular jets.

Derived from text

Aerodynamic Noise; Noise Prediction; Shock Waves; Broadband

19990110634 NASA Langley Research Center, Hampton, VA USA

Climb to Cruise Noise Test Results

Joshi, M. C., McDonnell-Douglas Aerospace, USA; Yamamoto, K. J., McDonnell-Douglas Aerospace, USA; Donelson, M. J., McDonnell-Douglas Aerospace, USA; Golub, R. A., NASA Langley Research Center, USA; Rawls, J. W., NASA Langley Research Center, USA; First NASA/Industry High Speed Research Program Nozzle Symposium; September 1999, pp. 29-1 - 29-19; In English; See also 19990110605; No Copyright; Avail: CASI; A03, Hardcopy; A10, Microfiche

A semi-empirical formula for the prediction of the broadband shock associated noise from rectangular supersonic jets in the fly-over plane has been developed. The predicted noise spectra compared very favorable with the measurement of Ponton, Manning and Seiner. Extension to side-line directions will be carried out.

Author

Broadband; Shock Waves; Noise Spectra; Prediction Analysis Techniques

19990110635 NASA Langley Research Center, Hampton, VA USA

Comparisons of Shock Noise Predictions with Flight Data

Norum, T. D., NASA Langley Research Center, USA; Golub, R. A., NASA Langley Research Center, USA; Willshire, W. L., NASA Langley Research Center, USA; First NASA/Industry High Speed Research Program Nozzle Symposium; September 1999, pp. 30-1 - 30-13; In English; See also 19990110605; No Copyright; Avail: CASI; A03, Hardcopy; A10, Microfiche

A flight test was performed at NASA Dryden Research Center in November 1991 utilizing both F18 and Fl6 aircraft. These flights were designed to provide (1) acoustic data that could be extrapolated to that of an HSCT at various points of its climb-to-cruise operation and (2) a data base for noise from a supersonic jet exhausting from an aircraft moving at high subsonic speeds. This presentation utilizes data obtained from these flyovers to evaluate predictions of broadband shock noise from supersonic jets in flight. The Fl8 is particularly suitable for flyovers of shock noise since it can be flown with one engine at flight idle. The second engine can then be operated at a pressure high enough to produce a supersonic nozzle exhaust and still maintain an unaccelerated, level flyover.

Author

Shock Waves; Noise Prediction; Flight Tests; Data Bases; Supersonic Nozzles; Aerodynamic Noise

19990110636 NASA Lewis Research Center, Cleveland, OH USA

HSR Propulsion System Studies: A Status Report on the Down-Select Process

Strack, W. C., NASA Lewis Research Center, USA; First NASA/Industry High Speed Research Program Nozzle Symposium; September 1999, pp. 31-1 - 31-17; In English; See also 19990110605; No Copyright; Avail: CASI; A03, Hardcopy; A10, Microfiche

When the HSR program began there was widespread belief that a simple and familiar turbojet-like engine coupled to an advanced technology mixer-ejector nozzle was the propulsion system of choice for achieving FAR 36-Stage 3 noise requirements. Our ability to quickly demonstrate a practical 20(+) dB suppression nozzle was confidently presumed by many. Our rate of progress towards that objective, however, has been somewhat humbling. At the moment we are reasonably confident of achieving about 15 dB suppression with a mixer-ejector nozzle designed for a high specific thrust turbojet-like cycle. Therefore, if we make no further suppression progress and conservatively assume no new operational procedures such as programmed lapse rate (PLR), then meeting the Stage 3 goal requires a large amount of engine and/or wing oversizing which is economically prohibitive. The scenario is further aggravated by the possibility of eventually needing to comply with even more stringent regulations (Stage 4). While this status may be somewhat disappointing to some, it must be remembered that the HSR program plan involves two generations of mixer-ejector nozzles beyond the current generation I nozzle designs. It is premature to conclude that we cannot design a practical 20(+) dB mixer-ejector nozzle. On the other hand, it is prudent to consider alternative solutions to the noise problem. Thus, we are investigating four other propulsion system concepts.

Author (revised)

Engine Design; High Thrust; Nozzle Design; Project Planning; Propulsion System Configurations; Noise Reduction

19990110642 NASA Ames Research Center, Moffett Field, CA USA

Determination of Jet Noise Radiation Patterns and Source Locations using 2-Dimensional Intensity Measurements

Jaeger, S. M., NASA Ames Research Center, USA; Allen, C. S., NASA Ames Research Center, USA; First NASA/Industry High Speed Research Program Nozzle Symposium; September 1999, pp. 37-1 - 37-23; In English; See also 19990110605; No Copyright; Avail: CASI; A03, Hardcopy; A10, Microfiche

Contents include the following: (1) Outline Jet Noise extrapolation to far field. (2) Two dimensional sound intensity. (3) Anechoic chamber cold jet test. (4) Results: Intensity levels. Vector maps. Source location centroids. Directivity. and (5) Conclusions.

Derived from text

Antenna Radiation Patterns; Jet Aircraft Noise; Sound Intensity; Sound Waves; Two Dimensional Models

19990110643 NASA Ames Research Center, Moffett Field, CA USA

Determination of Jet Noise Radiation Source Locations using a Dual Sideline Cross-Correlation/Spectrum Technique

Allen, C. S., NASA Ames Research Center, USA; Jaeger, S. M., NASA Ames Research Center, USA; First NASA/Industry High Speed Research Program Nozzle Symposium; September 1999, pp. 38-1 - 38-26; In English; See also 19990110605; No Copyright; Avail: CASI; A03, Hardcopy; A10, Microfiche

The goal of our efforts is to extrapolate nearfield jet noise measurements to the geometric far field where the jet noise sources appear to radiate from a single point. to accomplish this, information about the location of noise sources in the jet plume, the radiation patterns of the noise sources and the sound pressure level distribution of the radiated field must be obtained. Since source

locations and radiation patterns can not be found with simple single microphone measurements, a more complicated method must be used.
Author
Noise Measurement; Extrapolation; Radiation Sources; Jet Aircraft Noise; Antenna Radiation Patterns

19990111539 Virginia Polytechnic Inst. and State Univ., Mechanical Engineering Dept., Blacksburg, VA USA
Active Control of Inlet Noise on the JT15D Turbofan Engine ***Final Report, Nov. 1997 - Dec. 1998***
Smith, Jerome P., Virginia Polytechnic Inst. and State Univ., USA; Hutcheson, Florence V., Virginia Polytechnic Inst. and State Univ., USA; Burdisso, Ricardo A., Virginia Polytechnic Inst. and State Univ., USA; Fuller, Chris R., Virginia Polytechnic Inst. and State Univ., USA; January 1999; 58p; In English; Original contains color illustrations
Contract(s)/Grant(s): NAG1-2001; VPI-ENGR.98.166; No Copyright; Avail: CASI; A04, Hardcopy; A01, Microfiche

This report presents the key results obtained by the Vibration and Acoustics Laboratories at Virginia Tech over the year from November 1997 to December 1998 on the Active Noise Control of Turbofan Engines research project funded by NASA Langley Research Center. The concept of implementing active noise control techniques with fuselage-mounted error sensors is investigated both analytically and experimentally. The analytical part of the project involves the continued development of an advanced modeling technique to provide prediction and design guidelines for application of active noise control techniques to large, realistic high bypass engines of the type on which active control methods are expected to be applied. Results from the advanced analytical model are presented that show the effectiveness of the control strategies, and the analytical results presented for fuselage error sensors show good agreement with the experimentally observed results and provide additional insight into the control phenomena. Additional analytical results are presented for active noise control used in conjunction with a wavenumber sensing technique. The experimental work is carried out on a running JT15D turbofan jet engine in a test stand at Virginia Tech. The control strategy used in these tests was the feedforward Filtered-X LMS algorithm. The control inputs were supplied by single and multiple circumferential arrays of acoustic sources equipped with neodymium iron cobalt magnets mounted upstream of the fan. The reference signal was obtained from an inlet mounted eddy current probe. The error signals were obtained from a number of pressure transducers flush-mounted in a simulated fuselage section mounted in the engine test cell. The active control methods are investigated when implemented with the control sources embedded within the acoustically absorptive material on a passively-lined inlet. The experimental results show that the combination of active control techniques with fuselage-mounted error sensors and passive control techniques is an effective means of reducing radiated noise from turbofan engines. Strategic selection of the location of the error transducers is shown to be effective for reducing the radiation towards particular directions in the farfield. An analytical model is used to predict the behavior of the control system and to guide the experimental design configurations, and the analytical results presented show good agreement with the experimentally observed results.
Author
Absorbers (Materials); Acoustics; Active Control; Engine Design; Noise Reduction; Turbofan Engines; Aerodynamic Noise; Intake Systems

19990111571 Norwegian Defence Research Establishment, Kjeller, Norway
Bias Error in Acoustic Direction, Bearing Finding, Due to Reflections From Parallel Crest Sea Surface Waves, and Bias Error Compensation
Heimdal, Per, Norwegian Defence Research Establishment, Norway; Jun. 21, 1999; 200p; In English
Report No.(s): FFI/PUBLICATION-99/03099; FFIE/771/116; No Copyright; Avail: CASI; A09, Hardcopy; A03, Microfiche

In passive acoustic direction, bearing measurements, errors due to reflections from the sea surface, can occur, both in terms of fluctuations and bias error, the latter for parallel crest sea surface waves. The task is to relate bias error to parameters for the sea surface waves, to frequency, and to position parameters for the target and own vessel, the latter a submarine. By such a relation, bearing bias error compensation can be obtained. A 3-dimensional treatment is needed for this. As preparation for this treatment, and for judgements on error variations, a large amount of 2-dimensional treatment is needed. Types of, and effects of water particle movements on rays and Doppler shift and spread, of regular and random sea surface wave ripple on strength of reflections, and for low grazing angles, of acoustic shadow zones and air bubbles, are treated. Bearing bias error compensation, with acceptable belief, is within a fraction of 1deg. Implementation of bearing bias error compensation, can be made simple.
Author
Acoustic Measurement; Error Analysis; Direction Finding; Ocean Surface; Surface Waves

19990111705 Southampton Univ., Fluid Dynamics and Acoustics Group, UK
Robustness of the Performance of the " Stereo Dipole" to Head Misalignment
Takeuchi, T., Southampton Univ., UK; Nelson, P. A., Southampton Univ., UK; October 1999; 40p; In English

Report No.(s): ISVR-TR-285; Copyright; Avail: Issuing Activity, Hardcopy

When binaural sound signals are presented with two loudspeakers, the listener's ears are required to be in the relatively small region which is under control of the system. Misalignment of the head results in inaccurate synthesis of the binaural signals. Consequently, directional information associated with the acoustic signals is inaccurately reproduced. When the two loudspeakers are placed close together, the spatial rate of change of the generated sound field is much smaller than that generated by two loudspeakers spaced apart. Therefore, the performance of such a system is expected to be more robust to misalignment of the listener's head. Robustness of performance is investigated here with respect to head displacement in three translational and three rotational directions. A comparison is given between systems consisting of two loudspeakers either placed close together or spaced apart. The extent of effective control with head displacement and the resulting deterioration in directional information is investigated by analysing temporal and spectral localisation cues estimated from synthesised binaural signals. Subjective localisation experiments are per- formed for cases in which notable differences in performance are expected from the previous analysis. It is shown that the system comprising two loudspeakers that are close together is very robust to misalignment of the listener's head.

Author

Robustness (Mathematics); Stereophonics; Deterioration; Loudspeakers; Misalignment; Sound Waves

72
ATOMIC AND MOLECULAR PHYSICS

Includes atomic structure, electron properties, and molecular spectra.

19990107331 National Inst. for Fusion Science, Toki, Japan

(delta)f Simulation of Ion Neoclassical Transport

Wang, W., National Inst. for Fusion Science, Japan; Nakajima, N., National Inst. for Fusion Science, Japan; Okamoto, M., National Inst. for Fusion Science, Japan; Murakami, S., National Inst. for Fusion Science, Japan; July 1999; ISSN 0915-633X; 14p; In English

Report No.(s): NIFS-604; No Copyright; Avail: CASI; A03, Hardcopy; A01, Microfiche

Ion neoclassical transport with finite orbit width dynamics is calculated over whole poloidal cross section by using accurate (delta)f method which employs an improved like-particle collision operator and an accurate weighting scheme to solve drift kinetic equation. Ion thermal transport near magnetic axis shows a great reduction from its conventional neoclassical level due to non-standard orbit topology, like that of previous (delta)f simulation. On other hand, the direct particle loss from confinement region may strongly increase]on energy transport near the edge. It is found that]on parallel flow near the axis is also largely reduced due to non-standard orbit topology. In the presence of steep density gradient, ion thermal conductivity is significantly reduced, a[id an ion particle flux is driven by self-collision alone.

Author

Ion Motion; Computation; Simulation; Parallel Flow; Kinetic Equations; Energy Transfer

19990107346 Los Alamos National Lab., NM USA

Recursive Estimation for the Tracking of Radioactive Sources

Howse, J. W.; Muske, K. R.; Ticknor, L. O.; Feb. 01, 1999; 6p; In English; 1999 American Control Conference, 2-4 Jun. 1999, San Diego, CA, USA

Report No.(s): DE00-007414; LA-UR-99-909; No Copyright; Avail: Department of Energy Information Bridge, Hardcopy

This paper describes a recursive estimation algorithm used for tracking the physical location of radioactive sources in real-time as they are moved around in a facility. The algorithm is a nonlinear least squares estimation that minimizes the change in, the source location and the deviation between measurements and model predictions simultaneously. The measurements used to estimate position consist of four count rates reported by four different gamma ray de tectors. There is an uncertainty in the source location due to the variance of the detected count rate. This work represents part of a suite of tools which will partially automate security and safety assessments, allow some assessments to be done remotely, and provide additional sensor modalities with which to make assessments.

NTIS

Radiation Sources; Management; Algorithms; Real Time Operation; Nuclear Scattering

19990108580 NASA Goddard Space Flight Center, Greenbelt, MD USA

Static Properties and Stark Effect of the Ground State of the HD Molecular Ion

Bhatia, A. K., NASA Goddard Space Flight Center, USA; Drachman, Richard J., NASA Goddard Space Flight Center, USA; [1999]; 26p; In English

Contract(s)/Grant(s): RTOP 344-12-53-14; No Copyright; Avail: CASI; A03, Hardcopy; A01, Microfiche

We have calculated static properties of the ground state of the HD(+) ion and its lowest-lying P-state without making use of the Born-Oppenheimer approximation, as was done in the case of H2(+) and D2(+) [Phys. Rev. A 58, 2787 (1998)]. The ion is treated as a three-body system whose ground state is spherically symmetric. The wavefunction is of generalized Hylleraas type, but it is necessary to include high powers of the internuclear distance to localize the nuclear motion. We obtain good values of the energies of the ground S-state and lowest P-state and compare them with earlier calculations. Expectation values are obtained for various operators, the Fermi contact parameters, and the permanent quadrupole moment. The cusp conditions are also calculated. The polarizability was then calculated using second-order perturbation theory with intermediate P pseudostates. Since the nuclei in HD(+) are not of equal mass there is dipole coupling between the lowest two rotational states, which are almost degenerate. This situation is carefully analyzed, and the Stark shift is calculated variationally as a function of the applied electric field.

Author

Stark Effect; Electric Fields; Ground State; Rotational States; Molecular Excitation; Molecular Ions; Internuclear Properties

19990109121 Academy of Sciences (USSR), Moscow, USSR

Collective Enchancement and Shell Effects in the Level Density of Spherical Nuclei

Junghans, A. R., Technische Hochschule, Germany; DeJong, M., Technische Hochschule, Germany; Clerc, H.–G., Technische Hochschule, Germany; Ignatyuk, A. V., Institute of Physics and Power Engineering, USSR; Kudyaev, G. A., Institute of Physics and Power Engineering, USSR; Schmidt, K.–H., Gesellschaft fuer Schwerionenforschung m.b.H., Germany; Academy of Science News: Physics Series; 1997; ISSN 0367-6765; Volume 61, No. 12, pp. 2467-2473; In English

Contract(s)/Grant(s): BMBF-06-DA-473; No Copyright; Avail: Issuing Activity, Hardcopy

Production cross sections of thorium, actinium, and radium fragments from U-238 projectiles are analyzed on the basis of the abrasion-ablation model taking into account the fission of heavy nuclei. It is found that the survival probability of highly excited compound nuclei against fission is a sensitive probe for the shell and collective effects in the nuclear level density of neutron-deficient actinides near the magic number N = 126. With the inclusion of collective enhancement in the level density the calculated survival probability is able to describe the experimental data. The lack of shell-stabilization against fission observed for the N = 126 shell is expected to have consequences for the production cross sections of spherical superheavy nuclei around N = 184.

Author

Heavy Nuclei; Uranium 238; Nuclear Fission; Radioactive Decay; Particle Interactions; High Energy Interactions

19990109122 Academy of Sciences (USSR), Moscow, USSR

Bulk Properties of Light Deformed Nuclei Derived from a Medium-Modified Meson-Exchange Interaction

Gruemmer, F., Forschungszentrum Juelich G.m.b.H., Germany; Chen, B. Q., Forschungszentrum Juelich G.m.b.H., Germany; Ma, Z. Y., Forschungszentrum Juelich G.m.b.H., Germany; Krewald, S., Forschungszentrum Juelich G.m.b.H., Germany; Academy of Science News: Physics Series; 1997; ISSN 0367-6765; Volume 61, No. 12, pp. 2488-2452; In English; Copyright; Avail: Issuing Activity, Hardcopy

Deformed Hartree-Fock-Bogoliubov calculations for finite nuclei are carried out. As residual interaction a Brueckner G-matrix derived from a meson-exchange potential is taken. Phenomenological medium modifications of the meson masses are introduced. The binding energies, radii, and deformation parameters of the Carbon, Oxygen, Neon, and Magnesium isotope chains are found to be in good agreement with the experimental data.

Author

Deformation; Hartree Approximation; Mesons; Nucleons; Charged Particles; Particle Interactions

19990109123 Academy of Sciences (USSR), Moscow, USSR

Decay of Neutron-Deficient Excited Heavy, Nuclei

Giardina, G., Istituto Nazionale di Fisica Nucleare, Italy; Academy of Science News: Physics Series; 1997; ISSN 0367-6765; Volume 61, No. 12, pp. 2458-2466; In English; No Copyright; Avail: Issuing Activity, Hardcopy

By studying the evaporation residue cross-sections of heavy nuclei formed by heavy ion induced reactions, it is possible to have information on the fission-evaporation competition along the de-excitation cascade of the compound nucleus leading to

neutron deficient residue nuclei. A refined statistical model code [1-5] is used, which accounts for dissipation effects and angular momentum dependence of the shell correction in the fission dynamics. A comparison between calculations and available experimental data is made for the Th-224 and Fm-(252,254) compound nuclei. An evaluation of the (sup 292)114 superheavy nucleus production by the Ca-48 + Pu-244 reaction is obtained.
Author
Excitation; Heavy Nuclei; Neutron Decay; Particle Decay; Radioactive Decay; Nuclear Interactions; High Energy Interactions; Nuclear Fission; Nuclear Fusion

19990109124 Academy of Sciences (USSR), Moscow, USSR
Self-Consistent Landau-Migdal Theory for Nuclear-Structure Calculations Around Semi-Magic Nuclei
Klemt, V., Forschungszentrum Juelich G.m.b.H., Germany; Academy of Science News: Physics Series; 1997; ISSN 0367-6765; Volume 61, No. 12, pp. 2453-2457; In English; Copyright; Avail: Issuing Activity, Hardcopy

The long known number-operator method of nuclear-structure theory has been supplemented by an additional energy-operator method. In this way a set of equations is obtained that describes consistently the low-energy spectra of closed-shell nuclei and their neighbors.
Author
Nuclear Structure; Ground State; Odd-Even Nuclei; Even-Even Nuclei

19990109154 NASA Goddard Space Flight Center, Greenbelt, MD USA
Measurements of Radiation Exposure on Commercial Aircraft with the LIULIN-3M Instrument
Stassinopoulos, E. G., NASA Goddard Space Flight Center, USA; Stauffer, C. A., Stinger Gaffarian Technologies, USA; Dachev, T. P., Bulgarian Academy of Sciences, Bulgaria; Brucker, G. J., Radiation Effects Consultants, USA; Tomov, B. T., Bulgarian Academy of Sciences, Bulgaria; Dimitrov, P. G., Bulgarian Academy of Sciences, Bulgaria; [1998]; 22p; In English; No Copyright; Avail: CASI; A03, Hardcopy; A01, Microfiche

This paper reports on the development of a compact radiation monitor/dosimeter, the LIULIN-3M, and on extended measurements conducted on the ground and on commercial aircraft on domestic and international flights.
Author
Fabrication; Dosimeters; Radiation Measurement

19990109165 NASA Goddard Space Flight Center, Greenbelt, MD USA
Re-examination of a Classic Experiment to Measure the Positronium-Helium Cross Section
Drachman, Richard J., NASA Goddard Space Flight Center, USA; DiRienzi, Joseph, College of Notre Dame of Maryland, USA; [1998]; 1p; In English; Low-Energy Positron and Positronium Physics, USA; No Copyright; Avail: Issuing Activity, Hardcopy; Abstract Only

In 1975, before the advent of positronium beams, a clever experiment was carried out in an attempt to measure low-energy Ps-atom scattering cross-sections, especially that of Ps-He. A series of parallel thin plates was placed in the vessel containing the sample of gas, and positrons were allowed to enter the chamber from a radioactive source. The time spectrum of annihilation radiation was observed in the traditional way, and the pickoff annihilation due to thermalized Ps striking one of the plates was to be the special feature of the experiment. Using a diffusion analysis the authors derived cross- sections for several gases, and for helium the value obtained was sigma = 0.0166 pi(alpha)(sub o, sup 2). Even then this value was thought to be very much too small, while recent measurements and some calculations suggest a more reasonable value would be sigma = 3 to 13 pi(alpha)(sub o,sup 2). It has always been puzzling that an apparently well-designed experiment should give such an unsatisfactory result. We have now re-examined the analysis of the data with some interesting consequences which may explain the discrepancy. Two main observations support our re-analysis. First, we note that the mean free path for Ps-He scattering would be quite long if the cross-section were as small as that quoted above; the diffusion method itself would seem to be questionable. For the larger values, however, there would be no such problem. Second, it was assumed that when the annihilation rate had settled down and was following an exponential decay curve the asymptotic solution of the diffusion equation had been reached. We find, instead, that a superposition of exponentials can accurately represent the decay curve, consistent with the higher cross-section value.
Author
Experimentation; Helium; Positronium; Scattering Cross Sections

19990110071 Commonwealth Scientific and Industrial Research Organization, Victoria, Australia
Australian Journal of Physics, Volume 51
Robertson, R. P., Editor, Commonwealth Scientific and Industrial Research Organization, Australia; 1998; ISSN 0004-9506; In

English; See also 19990110072 through 19990110083; Copyright; Avail: Issuing Activity (Australian Journal of Physics, P.O. Box 1139, 150 Oxford St., Collingwood, Victoria 3066, Australia), Hardcopy, Microfiche

Contents include following: the development of electron momentum spectroscopy; recent developments in electron momentum spectroscopy of solids; progress of electron momentum spectroscopy in China; new and old measurements of electron scattering in atomic hydrogen; electron dichroism; interaction of spin-polarized electrons with chiral molecules; helium double photoionisation: an accurate solution of a three body Coulomb problem; studies of the electron-impact double-ionisation process in magnesium using coincidence techniques; investigating inner shell ionisation via the (e, 2e) technique; a procedure to determine Dyson orbitals from electron momentum spectroscopy: application to 1,2-propadiene , 1,3-butadiene, cyclopropane and [1.1.1] propylene; application of DFT and EMS to the study of strained organic molecules; new development in optical microscopy for biological applications; and future directions in electron momentum spectroscopy of matter.

CASI

Electron Spectroscopy; Electron Scattering; Butadiene; Dichroism; Hydrogen; Ionization; Molecules

19990110075 University of Western Australia, Centre for Atomic, Molecular and Surface Physics, Nedlands, Australia

New and Old Measurements of Electron Scattering in Atomic Hydrogen

Williams, J. F., University of Western Australia, Australia; Australian Journal of Physics; 1998; Volume 51, No. 4, pp. 633-643; In English; See also 19990110071; Copyright; Avail: Issuing Activity (Australian Journal of Physics, P.O. Box 1139, 150 Oxford St., Collingwood, Victoria 3066, Australia), Hardcopy, Microfiche

A critical look is made of discrepancies and agreements between new and old measurements and theories for elastic and n = 2 excitation of atomic hydrogen by electron impact, mainly at 16.5, 54 and 100 eV. A discussion of earlier work indicates the contributions of Weigold and colleagues. The difficulties of observing and modelling small scattered fluxes at backward scattering angles and of making absolute cross section calibrations are noted. New measurements of elastic scattering at 16.5 eV confirm earlier measured angular distributions. An absolute calibration of the differential cross section at 16.5 eV gives agreement within one standard deviation with intermediate energy R-matrix and multi-pseudostate close coupling values. At 16.5 eV, measurements of the separate 2s and 2p differential cross sections and the lambda, R and I correlation parameters again support the values from those theories.

Author

Scattering Cross Sections; Atoms; Hydrogen; Measuring Instruments; Electron Scattering; Calibrating

19990110076 Technische Univ., Physikalisches Inst., Munich, Germany

Electron Dichroism: Interaction of Spin-Polarized Electrons with Chiral Molecules

Kessler, Joachim, Technische Univ., Germany; Australian Journal of Physics; 1998; Volume 51, No. 4, pp. 645-654; In English; See also 19990110071; Copyright; Avail: Issuing Activity (Australian Journal of Physics, P.O. Box 1139, 150 Oxford St., Collingwood, Victoria 3066, Australia), Hardcopy, Microfiche

This paper discusses a problem which would be worth studying with (e,2e) experiments, a technique which has been so successfully used by Erich Wigold Can spin-polarized electrons distinguish between left- and right-handed molecules? This has been a matter of long-standing discussion and speculation and of controversial experiments The results presented here show that the attenuation of electron beams passing through chiral molecules is clearly spin-dependent This is analogous to the circular dichroism of light and is therefore called electron dichroism The size of the effect agrees with what has been predicted by theoretical estimates

Author

Electron Beams; Polarization Characteristics; Spin Dynamics; Dichroism

19990110077 Australian National Univ., Research School of Physical Sciences, Canberra, Australia

Helium Double Photoionisation: An Accurate Solution of a Three-Body Coulomb Problem

Kheifets, Anatoli S., Australian National Univ., Australia; Bray, Igor, Flinders Univ., Australia; Australian Journal of Physics; 1998; Volume 51, No. 4, pp. 655-664; In English; See also 19990110071; Copyright; Avail: Issuing Activity (Australian Journal of Physics, P.O. Box 1139, 150 Oxford St., Collingwood, Victoria 3066, Australia), Hardcopy, Microfiche

We present here the solution of the helium double photoionisation problem by the convergent close-coupling (CCC) method. This method allows us to obtain the most detailed description of the double photoionisation process in the form of the fully resolved triply differential cross section (TDCS). The accuracy of our model is tested by calculating the TDCS in the three different

forms of the electromagnetic operator which produces essentially identical results. We compare our calculation with the most accurate experimental and theoretical data available to date.
Author
Scattering Cross Sections; Helium; Photoionization; Three Body Problem

19990110078 Maryland Univ., Dept. of Chemistry and Biochemistry, College Park, MD USA
Studies of the Electron-Impact Double-Ionisation Process in Magnesium Using Coincidence Techniques
Ford, M. J., Maryland Univ., USA; Australian Journal of Physics; 1998; Volume 51, No. 4, pp. 665-678; In English; See also 19990110071
Contract(s)/Grant(s): NATO-CRG-920101; NSF PHY-91-07337; NSF PHY-95-15516; Copyright; Avail: Abstract Only (Australian Journal of Physics, P.O. Box 1139, 150 Oxford St., Collingwood, Victoria 3066, Australia), Hardcopy, Microfiche

This article will review recent measurements of the electron-impact double-ionisation of atomic magnesium. Results for the resonant Auger double-ionisation process with coincident detection of all three outgoing electrons, the (e, 3e) experiment, and for the direct double-ionisation process where only two outgoing electrons are detected, the (e, (3 - l)e) experiment, will be discussed. The results are analysed with reference to ionisation mechanisms and comparisons are made with calculated double-ionisation cross sections.
Author
Research; Electron Impact; Ionization Cross Sections; Magnesium

19990110079 Griffith Univ., School of Science, Nathan, Australia
Investigating Inner Shell Ionisation via the (e, 2e) Technique
Lohmann, Birgit, Griffith Univ., Australia; Cavanagh, S. J., Griffith Univ., Australia; Haynes, M. A., Griffith Univ., Australia; Taouil, I., Paris XI Univ., France; Duguet, A., Paris XI Univ., France; Lahmam–Bennani, A., Paris XI Univ., France; Australian Journal of Physics; 1998; Volume 51, No. 4, pp. 679-689; In English; See also 19990110071; Copyright; Avail: Issuing Activity (Australian Journal of Physics, P.O. Box 1139, 150 Oxford St., Collingwood, Victoria 3066, Australia), Hardcopy, Microfiche

The (e, 2e) technique has been applied successfully to valence shell ionisation of many targets, but studies of inner shell ionisation by this technique have been limited. The triple differential cross section for the latter process exhibits behaviour which is very different to that observed for valence shell ionisation, particularly when the energy of the slow ejected electron is decreased below the binding energy of the inner shell orbital. Our recent results for inner shell ionisation of argon and krypton will be discussed, and comparisons made with distorted wave calculations.
Author
Research; Scattering Cross Sections; Ionization; Binding Energy

19990110080 Flinders Univ., Dept. of Physics, Adelaide, Australia
A Procedure to Determine Dyson Orbitals from Electron Momentum Spectroscopy: Application to 1,2-Propadiene, 1,3-Butadiene, Cyclopropane and [1.1.1]Propellane
Nicolson, R. J. F., Flinders Univ., Australia; McCarthy, I. E., Flinders Univ., Australia; Brunger, M. J., Flinders Univ., Australia; Australian Journal of Physics; 1998; Volume 51, No. 4, pp. 691-706; In English; See also 19990110071; Copyright; Avail: Issuing Activity (Australian Journal of Physics, P.O. Box 1139, 150 Oxford St., Collingwood, Victoria 3066, Australia), Hardcopy, Microfiche

We employ a numerical inverse method of extracting the target-ion overlap, or normalised Dyson orbital, directly from experimental electron momentum spectroscopy data by using a quantum-mechanically constrained statistical fitting procedure. This method is used in conjunction with the previously verified, for molecular targets, plane wave impulse approximation (PWIA) reaction model. The present procedure was applied to previously measured momentum distributions (MDs) for the 2e' and le' valence orbitals of cyclopropane, the 7ag orbital of trans 1,3-butadiene, the 2e orbital of 1,2-propadiene and the 3a1 orbital of [l.l.l]propellane. We note that this is the first extensive application of the present method to organic molecular systems. In each case the derived normalised Dyson orbital provided a superior representation of the experimental MD than did the corresponding Hartree Fock orbital. The ramifications of this result are discussed in the text.
Author
Procedures; Dyson Theory; Orbitals; Experimentation; Hartree Approximation; Valence

19990110081 Flinders Univ., Dept. of Chemistry, Adelaide, Australia
Application of DFT and EMS to the Study of Strained Organic Molecules
Adcock, W., Flinders Univ., Australia; Brunger, M. J., Flinders Univ., Australia; Michalewicz, M. T., Commonwealth Scientific

and Industrial Research Organization, Melbourne, Australia; Winkler, D. A., Commonwealth Scientific and Industrial Research Organization, Australia; Australian Journal of Physics; 1998; Volume 51, No. 4, pp. 707-728; In English; See also 19990110071; Copyright; Avail: Issuing Activity (Australian Journal of Physics, P.O. Box 1139, 150 Oxford St., Collingwood, Victoria 3066, Australia), Hardcopy, Microfiche

Electron momentum spectroscopy (EMS) studies of the valence shells of [l.l.llpropellane, 1,3-butadiene, ethylene oxide and cubane are reviewed. Binding energy spectra were measured in the energy regime of 3 5-46 5 eV over a range of different target electron momenta, so that momentum distributions (MDs) could be determined for each ion state. Each experimental electron momentum distribution is compared with those calculated in the plane wave impulse approximation (PWIA) using both a triple-(plus polarisation level self-consistent field (SCF) wave function and a further range of basis sets as calculated using density functional theory (DFT). A critical comparison between the experimental and theoretical momentum distributions allows us to determine the 'optimum' wave function for each molecule from the basis sets we studied. This 'optimum' wave function then allows us to investigate chemically or biologically significant molecular properties of these molecules. EMS-DFT also shows promise in elucidating the character of molecular orbitals and the hybridization state of atoms.

Author

Electron Spectroscopy; Momentum; Molecules; Organic Chemistry; Research; Valence; Propellant Properties

19990110299 Department of Energy, Office of Energy Research, Washington, DC USA

Experiments on the nuclear interactions of pion and electrons

Minehart, R. C., Department of Energy, USA; May 31, 1998; 39p; In English

Report No.(s): DE99-000039; DOE/ER/40390-10; No Copyright; Avail: Department of Energy Information Bridge, Microfiche

The work in this report is grouped into four categories. (1) The experiments in pion nucleus physics were primarily studies of pion absorption and scattering in light nuclei, carried out at the Los Alamos Meson Physics Facility (LAMPF). (2) The experiments on fundamental particle properties were carried out at LAMPF and at the Paul Scherrer Institute (PSI) in Switzerland, the pion-beta decay experiment is still under construction and will begin taking data in 1999. (3) The experiments in electro-nuclear physics were performed at the Stanford Linear Electron Accelerator (SLAC), at the Saclay Laboratory in France, at the LEGS facility at the Brookhaven National Laboratory, and at the Continuous Electron Beam Accelerator Facility (CEBAF) at the Jefferson Laboratory. These experiments relate mainly to the question of the role of longitudinal and transverse strength for inelastic scattering from nuclei, measurements of fundamental nuclear properties with tagged polarized photons, and to the quark structure of the nucleon and its excited states. (4) Experiments on absorption of antiprotons in heavy nuclei, were carried out by K. Ziock primarily while on a sabbatical leave in Munich, Germany.

NTIS

Nuclear Physics; Mesons; Nuclear Interactions; Particle Decay; Pions; Quarks

19990110492 Central Lab. of the Research Councils, Daresbury Lab., Warrington, UK

Molecular Modelling and Neutron Scattering Workshop: Techniques for Large-Scale Systems

Smith, W., Central Lab. of the Research Councils, UK; Gabrys, B., Central Lab. of the Research Councils, UK; Daresbury Laboratory Information Newsletter for Computer Simulation of Condensed Phases; October 1998, pp. 30-33; In English; See also 19990110489; No Copyright; Avail: CASI; A01, Hardcopy; A01, Microfiche

This workshop sought to bring together two distinct groups of researchers with much in common but hitherto had not interacted particularly strongly. With the growing complexity of the systems in which both groups are currently interested, not least systems of increasing length scale, the time was ripe for a meeting of minds. It was hoped by the organisers that the experimentalists would leave the workshop better informed about the capabilities of molecular simulation, while the simulators would better appreciate the difficulties experimentalists face in interpreting the results of neutron scattering experiments. The first speaker was Prof. Dominic Tildesley (Imperial College), who described the molecular dynamics simulation of various air/water/oil/surfactant interfaces. Experimental confirmation of these observations was available from laser reflectometry. Simulations were also undertaken to determine the microscopic origin of friction in the fabric softener dioctadecyl dimethyl ammonium chloride (DODAB). The final example of interface simulation presented was ongoing work of the DODAB/hexane interface to explore the penetration of oil into the DODAB matrix. Prof. R.W. Richards (University of Durham) spoke on the subject of coarse-grain problems and asked "is there a fine grained solution?".

Derived from text

Molecular Dynamics; Models; Neutron Scattering; Conferences; Optical Measurement; Methyl Compounds

19990110518 Department of Energy, Office of Energy Research, Washington, DC USA

Discovery of the B(sub C) meson

Singh, P., Department of Energy, USA; Jul. 31, 1998; 12p; In English; 12th; Les Recontres de Physique de la Vallee D'Aosta: Results and Perspectives in Particle Physics, USA

Report No.(s): DE98-057346; FNAL/C-98/209-E; CONF-9803100; No Copyright; Avail: Department of Energy Information Bridge, Microfiche

We report on the first observation of the bottom-charm mesons B(sub c) through the decay mode B(sub c)(+/-) yields J/(psi)l(+/-)nu in 1.8 TeV p(anti p) collisions using the CDF detector at the Fermilab Tevatron. A fit of background and signal contributions to the observed J/(psi)l mass distribution yielded 20.4(sup +6.2, sub -5.5) events from B(sub c) mesons. A fit to the same distribution with background alone was rejected at the level of 4.8 standard deviations. We measured the B(sub c)(sup +) mass to be 6.40(+-) 0.39(+-)0.13 GeV/sq c and the B(sub c)(+) lifetime to be 0.46(sup 0.18, sub -0.16)(stat.) +/- 0.03(syst.) ps. The measured production cross section times branching ratio for B(sub c)(+) yields J/(psi)l(+)(nu) relative to that for B(+) yields J/(psi)K(+) is 0.132(sup 0.041, sub -0.037) (stat.) +/- 0.031(syst.)(sup +0.032, sub -0.020)(lifetime).

NTIS

Mesons; Particle Collisions; Leptons; Particle Decay; Particle Production

19990110521 Department of Energy, Office of Energy Research, Washington, DC USA

Quantum Monte Carlo calculations for light nuclei

Wiringa, R. B., Department of Energy, USA; Dec. 31, 1998; 20p; In English; Electronuclear Physics with Internal Targets and the BLAST Detector, USA

Report No.(s): DE98-058041; ANL/PHY/CP-96990; CONF-980580; No Copyright; Avail: Department of Energy Information Bridge, Microfiche

Quantum Monte Carlo calculations of ground and low-lying excited states for nuclei with A less thanor equal 8 are made using a realistic Hamiltonian that fits NN scattering data. Results for more than 30 different j' T states, plus isobaric analogs, are obtained and the known excitation spectra are reproduced reasonably well. Various density and momentum distributions and electromagnetic form factors and moments have also been computed. These are the first microscopic calculations that directly produce nuclear shell structure from realistic NN interactions.

NTIS

Nuclear Structure; Monte Carlo Method; Hamiltonian Functions; Excitation; Form Factors; Elementary Particle Interactions

19990111472 Prairie View Agricultural and Mechanical Coll., Dept. of Electrical Engineering, TX USA

Radiation Effects on DC-DC Converters

Attia, John O., Prairie View Agricultural and Mechanical Coll., USA; Mazid, M. A., Prairie View Agricultural and Mechanical Coll., USA; Zhang, D., Prairie View Agricultural and Mechanical Coll., USA; HBCUs/OMUs Research Conference Agenda and Abstracts; August 1999, pp. 26; In English; See also 19990111455; No Copyright; Avail: Issuing Activity, Hardcopy; Abstract Only

Dc-dc converters are increasing being used in space vehicles. The natural space environment contains high-energy photons, protons and electrons that cause total-dose ionizing radiation damage. In addition, the space environment has high-energy protons and heavy ions that can introduce transient, high density charged ions through electron devices. The charged ions can interact with sensitive regions of devices to trigger catastrophic failure mechanisms. This work investigates the effects of high energy particles on dc-dc converters found in spacecraft and communication satellites. The paper reports the results of radiation studies on several dc-dc converters, undertaken to ascertain the susceptibility of total ionizing dose and single event effects. Results-to-date indicate that, of the converters simulated with total ionizing dose radiation, the performance of the Buck-Boost converter significantly degraded under radiation environment. The effects of total ionizing dose on Buck, Boost, Cuk and Flyback converters were not significant. Simulation results of the full bridge-zero voltage switching converter, under worst case single-event burnout, and single-event gate rupture conditions, show a decreasing output voltage of the converter, as increasing number of power mosfets becomes short-circuited. Under special operating conditions, the converter output voltage reduces to zero. The ongoing research work will experimentally verify the analytical results. Future efforts will be directed towards the development of converters which will reliably operate in radiation environment.

Author

Aerospace Environments; Electric Potential; Radiation Damage; Radiation Effects; Simulation; Voltage Converters (DC to DC); Power Supply Circuits

19990111504 Kinki Univ., Faculty of Engineering, Hiroshima, Japan

Investigation of Particle Tracking Velocimetry

Kojima, Tadatomo, Kinki Univ., Japan; Yang, Jinglong, Tsinghua Univ., China; Xu, Hongqing, Tsinghua Univ., China; Shimazue, Mari, Kinki Univ., Japan; Research Reports of the Faculty of Engineering, Kinki University; 1993; ISSN 0386-491X, No. 27, pp. 7-12; In Japanese; Copyright; Avail: Issuing Activity, Hardcopy, Microfiche

This paper deals with measurement of the velocity distribution of flow by means of the particle tracking velocimetry. A two-dimensional flow visualization picture is input through a TV-camera, and then by a set of image processing methods to extract the velocity distribution information from the path-lines of the particles in the picture.

Derived from text

Flow Visualization; Image Processing; Television Cameras; Two Dimensional Flow

19990111505 Kinki Univ., Faculty of Engineering, Hiroshima, Japan

Investigation of Particle Image Velocimetry

Kojima, Tadatomo, Kinki Univ., Japan; Yang, Jinglong, Tsinghua Univ., China; Xu, Hongqing, Tsinghua Univ., China; Shimazue, Mari, Kinki Univ., Japan; Research Reports of the Faculty of Engineering, Kinki University; 1993; ISSN 0386-491X, No. 27, pp. 1-5; In Japanese; Copyright; Avail: Issuing Activity, Hardcopy, Microfiche

This paper deals with measurement of the velocity distribution of flow field by means of the particle image velocimetry. On purpose to extract the displacements of particles moving with the flow, the principles of the Fourier transform, spatial autocorrelation and probability statistics methods are presented. A computer simulation has been developed to analyze the results of these methods and the velocity distribution of a converging flow has been measured by means of the Fourier transform method.

Derived from text

Particle Image Velocimetry; Fourier Transformation; Flow Distribution; Computerized Simulation; Velocity Distribution; Probability Theory

19990111741 NASA Langley Research Center, Hampton, VA USA

Accurate Universal Parameterization of Absorption Cross Sections, 3, Light Systems

Tripathi, R. K., NASA Langley Research Center, USA; Cucinotta, F. A., NASA Johnson Space Center, USA; Wilson, J. W., NASA Langley Research Center, USA; Nuclear Instruments and Methods in Physics Research B: Beam Interactions With Materials and Atoms; 1999; ISSN 0168-583X; Volume 155, pp. 349-356; In English; Copyright; Avail: Issuing Activity, Hardcopy

Our prior nuclear absorption cross sections model is extended for light systems (A less than or equal to 4) where either both projectile and target are light particles or one is light particle and the other is medium or heavy nucleus. The agreement with experiment is excellent for these cases as well. Present work in combination with our original model provides a comprehensive picture of absorption cross sections for light, medium and heavy systems. As a result the extended model can reliably be used in all studies ”where there is a need for absorption cross sections.

Author

Absorption Cross Sections; Nuclear Models; Accuracy

19990113115 NASA Goddard Inst. for Space Studies, New York, NY USA

The Density Matrix of H20 - N2 In the Coordinate Representation: A Monte Carlo Calculation of the Far-Wing Line Shape

Ma, Q., NASA Goddard Inst. for Space Studies, USA; Tipping, R. H., Alabama Univ., USA; 1999; 35p; In English

Report No.(s): GCN-99-61; No Copyright; Avail: CASI; A03, Hardcopy; A01, Microfiche

The far-wing line shape theory within the binary collision and quasistatic framework has been developed using the coordinate representation. Within this formalism, the main computational task is the evaluation of multidimensional integrals whose variables are the orientational angles needed to specify the initial and final positions of the system during transition processes. Using standard methods, one is able to evaluate the 7-dimensional integrations required for linear molecular systems, or the 7-dimensional integrations for more complicated asymmetric-top (or symmetric-top) molecular systems whose interaction potential contains cyclic coordinates. In order to obviate this latter restriction on the form of the interaction potential, a Monte Carlo method is used to evaluate the 9-dimensional integrations required for systems consisting of one asymmetric-top (or symmetric-top) and one linear molecule, such as H20-N2. Combined with techniques developed previously to deal with sophisticated potential models, one is able to implement realistic potentials for these systems and derive accurate, converged results for the far-wing line shapes and the corresponding absorption coefficients. Conversely, comparison of the far-wing

absorption with experimental data can serve as a sensitive diagnostic tool in order to obtain detailed information on the short-range anisotropic dependence of interaction potentials.
Author
Monte Carlo Method; Line Shape; Matrices (Mathematics); Algorithms; Asymmetry; Linear Systems; Mathematical Models; Molecular Structure; Molecular Collisions

73
NUCLEAR AND HIGH-ENERGY PHYSICS

Includes elementary and nuclear particles; and reactor theory. For space radiation see 93 Space Radiation.

19990107357 Sandia National Labs., Albuquerque, NM USA
Pulse Power Modulator System for Commercial High Power Ion Beam Surface Treatment Applications
Barrett, D. M.; Cockreham, B. D.; Dragt, A. J.; Ives, H. C.; Neau, E. L.; May 24, 1999; 4p; In English; 12th; International Pulsed Power Conference, 27-30 Jun. 1999, Monterey, CA, USA; Sponsored by Institute of Electrical and Electronic Engineers, USA
Report No.(s): DE00-007112; SAND98-2185C; No Copyright; Avail: Department of Energy Information Bridge, Hardcopy

The Ion Beam Surface Treatment (IBESTTM) process utilizes high energy pulsed ion beams to deposit energy onto the surface of a material allowing near instantaneous melting of the surface layer. The melted layer typically re-solidifies at a very rapid rate which forms a homogeneous, fine-grained structure on the surface of the material resulting in significantly improved surface characteristics. In order to commercialize the IBESTTM process, a reliable and easy-to-operate modulator system has been developed. The QM-I modulator is a thyratron-switched five-stage magnetic pulse compression network which drives a two-stage linear induction adder. The adder provides 400 kV, 150 ns FWHM pulses at a maximum repetition rate of 10 pps for the acceleration of the ion beam. Special emphasis has been placed upon developing the modulator system to be consistent with long-life commercial service.
NTIS
Surface Treatment; Ion Beams; Surface Layers; Deposits

19990110303 Department of Energy, Office of Energy Research, Washington, DC USA
Selected problems in nuclear/high energy physics: Experimental hypernuclear physics, muon rare decay, and development of new detector system applicable to nuclear/high energy physics experiments ***Final Report, 1 Jun . 1994 - 31 May 1997***
Tang, L., Department of Energy, USA; Aug. 31, 1998; 32p; In English
Report No.(s): DE99-000023; DOE/ER/40858-3; No Copyright; Avail: Department of Energy Information Bridge, Microfiche

Under this DOE funding, the experimental program described in this report now consists of two major approved experiments at Jlab: Investigation of the Spin Dependence of the Effective AN interaction in p Shell (E89-009) which is tentatively scheduled to be completed in the fall of 1999 and Direct measurement of the Lifetime of the Heavy (Lambda)-Hypernuclei at CEBAF (E95-002) which will be run in parasitic mode with E89-009. Also, a new experiment (E97- 008) which attempts a directly observation of the spin-orbital splitting in the higher orbits with medium heavy targets was proposed and conditionally approved by Jlab PAC-12 in 1997. The condition for this experiment is simply to run E89- 009 first and study the best possible energy resolution. The experimental group at Hampton University has played a leadership role in the development and preparation of these experiments. The Principal Investigator (PI) of this grant is spokesperson and acting program coordinator for all three experiments. Establishment of Jlab experiments is the group's main focus. In addition as originally proposed in the grant proposal, the group also contributed in completing the MEGA experiment at LAMPF. The detector development program established in the NuHEP Center has successfully constructed a large active area Lucite detector which uses a total internal reflection technique as a part of the kaon identification system for the Jlab Hall C SOS spectrometer. Its application in the first two experiments using the (e,e'K) reaction, E91-16 and E93-18 in 1996, has proved its effectiveness to reject the proton background both on-line and off-line. The author continued the program to develop new techniques and equipment associated with the Jlab experiments and possible future experiments at different national laboratories. This new work included developing: (1) a fission fragment detector with excellent timing and position resolution for the lifetime measurement of heavy hypernuclei and (2) new spectrometer systems for strangeness S = -1 or -2 hypernuclear programs at either hadronic facilities such as BNL and KEK (or JHF-50 the new Japanese 50 GeV proton accelerator) or electron facility (mainly CEBAF). The fission chamber has been built and tested by source in lab

and it is now under beam test. The optical design of the S2S spectrometer was presented in AGS-2000 Workshop (1996) and recently in JHF98 International Conference.
NTIS
Nuclear Physics; High Energy Interactions; Particle Decay; Particle Production; Hadrons; Hypernuclei; Kaons; Muons; Strangeness

19990110477 Department of Energy, Washington, DC USA
HPGe compton suppression using pulse shape analysis
Schmid, G. J., Department of Energy, USA; Beckedahl, D., Department of Energy, USA; Blair, J. J., Department of Energy, USA; Kammeraad, J. E., Department of Energy, USA; Apr. 15, 1998; 18p; In English; 9th; Radiation Measurements and Applications, USA
Report No.(s): DE98-057451; UCRL-JC-130495; No Copyright; Avail: Department of Energy Information Bridge, Microfiche
We present a new technique for High Purity Germanium (HPGe) Compton suppression using pulse shape analysis (PSA). The novel aspect of our approach involves a complete unfolding of the charge pulse shape into a discrete sum of component y-ray interactions. Using the energy and position information obtained from such an unfolding, an algorithm is then applied which favorably rejects Compton escape events. The advantage of the current PSA approach, as compared with other recent approaches, is the potential to reject not only single-site escape events, but also multiple site escape events. Here we discuss the details of our algorithm, and present experimental results from a real-time implementation on a 5 cm X 5 cm HPGe. An experimental comparison with a standard BGO suppresser is shown. We also discuss the possible improvements to the current PSA approach that could be obtained if the HPGe could be highly segmented on the outer contact.
NTIS
Germanium; Compton Effect

19990111451 Kyushu Univ., Faculty of Engineering, Fukuoka, Japan
A Study on the Catalytically Stabilized Thermal Reactor
Ono, Shinsuke, Kyushu Univ., Japan; Hirayama, Yoshinori, Kyushu Univ., Japan; Imanishi, Takahiro, Kyushu Univ., Japan; Andou, Akiji, Kyushu Univ., Japan; Technology Reports of Kyushu University; Nov. 06, 1998; Volume 71, No. 6, pp. 559-566; In Japanese; See also 19990111450; No Copyright; Avail: CASI; A02, Hardcopy; A01, Microfiche
Since a homogeneous gas-phase reaction between hydrocarbon and oxygen starts at the temperature above 600 C, by mixing a catalytical burner gas having ia moderate temperature for gas-phase reaction with it fresh combustible mixture, it is possible to constitute a thermal reactor to produce a combustion gas having higher temperature than that from the catalytic combustor. AS a fundamental study for developing the above reactor, the adiabatic reaction devices with hot air and the catalytic combustion gas supply are used for the experiment. The experimental results show that the thermal reaction is possible without a flame initiation within the mixture concentration range between 1.2 approx. 2.5% and the combustion characteristics are well correlated with the rate of energy supply of the secondary mixture.
Author
Research; Thermal Reactors; Combustion; Stabilization

74
OPTICS

Includes light phenomena; and optical devices. For lasers see 36 Lasers and Masers.

19990106565 Instituto Nacional de Pesquisas Espacias, Sao Jose dos Campos, Brazil
The Invariant Imbedding Methodology applied to the solution of the Radiative Transfer Equation in Hydrologic Optics Problems ***A Metodologia de Invariant Imbedding Aplicada a Resolucao da Equacao de Transferencia Radiativa em Problemas de Otica Hidrologica***
Stephany, Stephan, Instituto Nacional de Pesquisas Espacias, Brazil; 1999; 54p; In Portuguese
Report No.(s): INPE-7170-NTC/338; No Copyright; Avail: CASI; A04, Hardcopy; A01, Microfiche
The theory of the invariant imbedding methodology applied to the solution of the steady state, unidimensional and single wavelength radiative transfer equation in Hydrological Optics problems is presented. This study is based on C.D. Mobley's book Light and Water - Radiative Transfer in Natural Waters. The invariant imbedding methodology, models the interaction between the light and the medium by, means of transmittance, reflectance and source term operators. These operators are calculated the

integration of sets of non-linear ordinary differential equations, the Riccati differential equations, with use of standard numerical techniques.
Author
Invariant Imbeddings; Technology Transfer; Radiative Transfer; Steady State; Wavelengths

19990107377 Smithsonian Astrophysical Observatory, Cambridge, MA USA
AXAF Coordinate Transformation at XRCF
He, Helen, Smithsonian Astrophysical Observatory, USA; McDowell, Jonathan, Smithsonian Astrophysical Observatory, USA; Conroy, Maureen, Smithsonian Astrophysical Observatory, USA; [1997]; 1p; In English; No Copyright; Avail: CASI; A01, Hardcopy; A01, Microfiche; Abstract Only; Abstract Only

Coordinate transformation between focal plane and detector pixel systems must be handled carefully at the X-ray Calibration Facility (XRCF) as it will be during flight. The High Resolution Mirror Assembly (HRMA) X-ray Detection System (HXDS) stage dithers, and the five-axis mount (FAM) attachment points underwent various types of motion during testing. At the XRCF when the FAM moved, the Science Instrument Module (SIM) travel direction was not necessarily aligned with the mirror axis motion, and, in addition, an arbitrary position offset had to be calibrated. Misalignment from the mirror axis was assessed by measuring its displacement from the boresight configuration of the default FAM frame, and the HXDS stage was monitored for motion from the default FAM reference point. Mirror position, prescribed in a mirror modal coordinate system, was measured in HRMA pitch and yaw axes. Prior to corrections for dithering and FAM movement, the coordinate data at XRCF also had to be corrected for possible misalignments of the mirror mount relative to XRCF and the default FAM axes due to the movement of the FAM feet. Those misalignments were processed in terms of yaw-pitch-roll Euler angles in the mirror nodal coordinate, and in the default FAM frame, respectively.
Author
Coordinate Transformations; X Ray Astrophysics Facility; X Rays; Calibrating; Test Facilities

19990107386 NASA Goddard Space Flight Center, Greenbelt, MD USA
Broadband Interferometer for Measuring Transmitted Wavefronts of Optical Bandpass Filters for HST (ACS)
Boucarut, R. A., NASA Goddard Space Flight Center, USA; Leviton, D. B., NASA Goddard Space Flight Center, USA; 1998; 1p; In English, 26 Mar. 1998, Kona, HI, USA; Sponsored by International Society for Optical Engineering; Copyright; Avail: Issuing Activity, Hardcopy; Abstract Only

The transmitted wavefronts of optical filters for the Hubble Space Telescope (HST) Advanced Camera for Surveys (ACS) are characterized using the Wildly and Openly Modified Broadband Achromatic Twyman Green (WOMBAT) Interferometer developed in the NASA/GSFC Optics Branch's Diffraction Grating Evaluation Facility (DGEF). Because only four of thirty-three of ACS's optical bandpass filters transmit the 633 nm light of most commercial interferometers, a broadband interferometer is required to verify specified transmitted wavefront of ACS filters. WOMBAT's design is a hybrid of the BAT interferometer developed by JPL used for HST Wide Field and Planetary Camera 2 (WFPC-2) filters and a WYKO 400 phase shifting interferometer. It includes a broadband light source, monochromator, off-axis, parabolic collimating and camera mirrors, an aluminum-coated fused silica beam splitter, flat retroreflecting mirrors for the test and reference arms, and a LTV-sensitive CCD camera. An outboarded, piezo-electric phase shifter holds the flat mirror in the interferometer's reference arm. The interferometer is calibrated through interaction between the WYKO system's software and WONMAT hardware for the test wavelength of light entering the beam splitter. Phase-shifted interferograms of the filter mounted in the test arm are analyzed using WYKO's Vision' software. Filters as large as 90 mm in diameter have been measured over a wavelength range from 200 to 1100 nm with a sensitivity of lambda/200 rms at lambda = 633 nm. Results of transmitted wavefront measurements are shown for ACS fixed band pass and spatially-variable bandpass filters for a variety of wavelengths.
Author
Bandpass Filters; Broadband; CCD Cameras; Interferometers; Optical Filters; Wave Fronts

19990107387 NASA Goddard Space Flight Center, Greenbelt, MD USA
Design and Specification of Optical Bandpass Filters for Hubble Space Telescope (HST) Advanced Camera for Surveys (ACS)
Leviton, Douglas B., NASA Goddard Space Flight Center, USA; Tsevetanov, Zlatan, NASA Goddard Space Flight Center, USA; Woodruff, Bob, NASA Goddard Space Flight Center, USA; Mooney, Thomas A., NASA Goddard Space Flight Center, USA; 1998; 1p; In English, 20-28 Mar. 1998, Kona, HI, USA; Sponsored by International Society for Optical Engineering; Copyright; Avail: Issuing Activity, Hardcopy; Abstract Only

Advanced optical bandpass filters for the Hubble Space Telescope (HST) Advanced Camera for Surveys (ACS) have been developed on a filter-by-filter basis through detailed studies which take into account the instrument's science goals, available optical filter fabrication technology, and developments in ACS's charge-coupled-device (CCD) detector technology. These filters include a subset of filters for the Sloan Digital Sky Survey (SDSS) which are optimized for astronomical photometry using today's charge-coupled-devices (CCD's). In order for ACS to be truly advanced, these filters must push the state-of-the-art in performance in a number of key areas at the same time. Important requirements for these filters include outstanding transmitted wavefront, high transmittance, uniform transmittance across each filter, spectrally structure-free bandpasses, exceptionally high out of band rejection, a high degree of parfocality, and immunity to environmental degradation. These constitute a very stringent set of requirements indeed, especially for filters which are up to 90 mm in diameter. The highly successful paradigm in which final specifications for flight filters were derived through interaction amongst the ACS Science Team, the instrument designer, the lead optical engineer, and the filter designer and vendor is described. Examples of iterative design trade studies carried out in the context of science needs and budgetary and schedule constraints are presented. An overview of the final design specifications for the ACS bandpass and ramp filters is also presented.
Author
Astronomical Photometry; Cameras; Charge Coupled Devices; Design Analysis; Bandpass Filters; Optical Filters

19990109164 General Optics, Inc., Moorpark, CA USA
Technology Demonstrator for Direct Polishing of a 50cm C/SiC Ultra Light Mirror ***Final Report, 1 Oct. 1998 - 30 Jun. 1999***
Scribner, Ken, General Optics, Inc., USA; Jun. 30, 1999; 7p; In English
Contract(s)/Grant(s): NAS9-98242; No Copyright; Avail: CASI; A02, Hardcopy; A01, Microfiche

The NRSU portion of the contract was completed on schedule and within acceptable limits of the estimated cost. The lapping of the substrate started on schedule, and completed ahead of schedule. The polishing of the substrate was begun ahead of schedule, and was completed approximately one month ahead of schedule. It is our opinion that the substrate meets the requirements of "diffraction limited performance at 2 microns" over the measured 16 in. area. The final photos suggest that there may be edge roll-off beyond the 16 in. diameter. However, we cannot quantify this. It is our opinion that this material is suitable for use in lightweight optics as long as cladding of some type is used (Silicon, SiC, Sol-Gel, etc), as the bare material itself is too "porous" to obtain a high quality finish. We feel that this part was at the low limit of structural integrity required to mechanically polish to this level of figure requirement. Any lesser structural integrity would require some form of "non contact" figuring.
Derived from text
Technology Assessment; Polishing; Mirrors; Sol-Gel Processes; Proving; Cladding

19990111485 NASA Glenn Research Center, Cleveland, OH USA
Optical Imaging of Flow Pattern and Phantom
Galland, Pierre A., City Coll. of the City Univ. of New York, USA; Liang, X., City Coll. of the City Univ. of New York, USA; Wang, L., City Coll. of the City Univ. of New York, USA; Ho, P. P., City Coll. of the City Univ. of New York, USA; Alfano, R. R., City Coll. of the City Univ. of New York, USA; Breisacher, K., NASA Glenn Research Center, USA; HBCUs/OMUs Research Conference Agenda and Abstracts; August 1999, pp. 24; In English; See also 19990111455; No Copyright; Avail: Issuing Activity, Hardcopy; Abstract Only

Time-resolved optical imaging technique has been used to image the spatial distribution of small droplets and jet sprays in a highly scattering environment. The snake and ballistic components of the transmitted pulse are less scattered, and contain direct information about the sample to facilitate image formation as opposed to the diffusive components which are due to multiple collisions as a light pulse propagates through a scattering medium. In a time-gated imaging scheme, these early-arriving, image-bearing components of the incident pulse are selected by opening a gate for an ultrashort period of time and a shadowgram image is detected. Using a single shot cooled CCD camera system, the formation of water droplets is monitored as a function of time. Picosecond time-gated image of drop in scattering cells, spray droplets as a function of let speed and gas pressure, and model calcification samples consisted of calcium carbonate particles of irregular shapes ranging in size from 0. 1 to 1.5 mm affixed to a microscope slide have been measured. Formation produced by an impinging jet will be further monitored using a CCD with 1 kHz framing illuminated with pulsed light. The desired image resolution of the fuel droplets is on the 20 pm scale using early light through a highly scattering medium. A 10(exp -6)m displacement from a jet spray with a flow speed of 100 m/sec introduced by the ns grating pulse used in the imaging is negligible. Early ballistic/snake light imaging offers nondestructive and noninvasive method to observe the spatial distribution of hidden objects inside a highly scattering environment for space, biomedical, and materials applications. In this paper, the techniques we will present are time-resolved K-F transillumination imaging and time-gated scattered light imaging. With a large dynamic range and high resolution, time-gated early light imaging has the potential for improving rocket/aircraft design by determining jets shape and particle sizes. Refinements to these techniques may

enable drop size measurements in the highly scattering, optically dense region of multi-element rocket injectors. These types of measurements should greatly enhance the design of stable, and higher performing rocket engines.
Author
CCD Cameras; Drops (Liquids); Flow Distribution; Imaging Techniques; Scattering; Spatial Distribution; Sprayers; Image Processing

19990111655 NASA Marshall Space Flight Center, Huntsville, AL USA
Ultracompact High-Speed Electro-Optic Switch
Fork, Richard L., Alabama Univ., USA; Jones, Darryl K., Alabama Univ., USA; Keys, Andrew S., NASA Marshall Space Flight Center, USA; [1998]; 1p; In English, 4-9 Oct. 1998, Baltimore, MD, USA; Sponsored by Optical Society of America, USA
Contract(s)/Grant(s): RTOP 632-20-29; Copyright; Avail: Issuing Activity, Hardcopy; Abstract Only

We describe a coherent optical logic element susceptible of fabrication in an array format at optical wavelength-packing densities. The element offers large dynamic range, temporal storage of optical pulses, and precise clocking with no pulse loss or distortion. One- and two-pulse strategies and phase-control issues are examined.
Author
Electro-Optics; Optical Switching; Switching Circuits; Logic Circuits; Optical Density

19990111656 NASA Marshall Space Flight Center, Huntsville, AL USA
Micro-Laser-Based Devices Allowing Optical Wavelength-Packing Densities
Keys, Andrew S., NASA Marshall Space Flight Center, USA; Jones, Darryl K., Alabama Univ., USA; Fork, Richard L., Alabama Univ., USA; [1998]; 1p; In English, 4-9 Oct. 1998, Baltimore, MD, USA; Sponsored by Optical Society of America, USA; Copyright; Avail: Issuing Activity, Hardcopy; Abstract Only

We examine theoretically and experimentally the space-time domain properties of high-speed electro-optically switched microlaser devices susceptible of construction at optical wavelength-packing densities. We address adjustable phase and group delays with wide dynamic range, coherent logic, temporal storage and reconfiguration of pulse arrays and applications to optical phased arrays.
Author
Optical Density; Optical Switching; Electro-Optics; Lasers

19990113189 NASA Marshall Space Flight Center, Huntsville, AL USA
Three-Dimensional Displacement Measurement Using Diffractive Optic Interferometry
Gilbert, John A., Alabama Univ., USA; Cole, Helen J., NASA Marshall Space Flight Center, USA; Shepherd, Robert L., Colorado School of Mines, USA; Ashley Paul R., Army Missile Command, USA; 1999; 1p; In English
Contract(s)/Grant(s): CDDF Proj. 92-R04; Copyright; Avail: Issuing Activity; Abstract Only, Hardcopy, Microfiche

This paper introduces a powerful new optical method which utilizes diffractive optic interferometry (DOI) to measure both in-plane and out-of-plane displacement with variable sensitivity using the same optical system. Sensitivity is varied by utilizing various combinations of the different wavefronts produced by a conjugate pair of binary Optical elements; a transmission grating is used to produce several illumination beams while a reflective grating replicated on the surface of a specimen, provides the reference for the undeformed state. A derivation of the equations which govern the method is included along with a discussion of the experimental tests conducted to verify the theory. Overall, the results are excellent, with experimental data agreeing to within a few percent of the theoretical predictions.
Author
Displacement Measurement; Diffractive Optics; Interferometry

19990113196 NASA Marshall Space Flight Center, Huntsville, AL USA
Measuring In-Plane Displacements with Variable Sensitivity Using Diffractive Optic Interferometry
Shepherd, Robert L., Colorado School of Mines, USA; Gilbert, John A., Alabama Univ., USA; Cole, Helen J., NASA Marshall Space Flight Center, USA; Ashley, Paul R., Army Missile Command, USA; [1998]; 1p; In English; Experimental Mechanics, 1998, USA
Contract(s)/Grant(s): CDDF Proj. 92-R04; Copyright; Avail: Issuing Activity; Abstract Only, Hardcopy, Microfiche

This paper introduces a method called diffractive optic interferometry (DOI) which allows in-plane displacement components to be measured with variable sensitivity. DOI relies on binary optical elements fabricated as phase-type Dammann gratings which produce multiple diffraction orders of nearly equal intensity. Sensitivity is varied by combining the different wavefronts produced by a conjugate pair of these binary optical elements; a transmission element is used to produce several

illumination beams while a reflective element, replicated on the surface of a specimen, provides the reference for the undeformed state. The steps taken to design and fabricate these binary optical elements are described. The specimen grating is characterized, and tested on a disk subjected to diametrical compression. Overall, the results are excellent, with experimental data agreeing to within a few percent of the theoretical predictions.
Author
Displacement; Sensitivity; Diffractive Optics; Interferometry

75
PLASMA PHYSICS

Includes magnetohydrodynamics and plasma fusion. For ionospheric plasmas see 46 Geophysics. For space plasmas see90 Astrophysics.

19990106567 NASA Goddard Space Flight Center, Greenbelt, MD USA
Reconnection in Three Dimensions
Hesse, Michael, NASA Goddard Space Flight Center, USA; [1999]; 1p; In English; Interrelation between Plasma Experiments in Lab and Space (IPELS '99), 1999, Kreuth, Germany; No Copyright; Avail: Issuing Activity, Hardcopy; Abstract Only

Analyzing the qualitative three-dimensional magnetic structure of a plasmoid, we were led to reconsider the concept of magnetic reconnection from a general point of view. The properties of relatively simple magnetic field models provide a strong preference for one of two definitions of magnetic reconnection that exist in the literature. Any concept of magnetic reconnection defined in terms of magnetic topology seems naturally restricted to cases where the magnetic field vanishes somewhere in the nonideal (diffusion) region. The main part of this paper is concerned with magnetic reconnection in nonvanishing magnetic fields (finite-B reconnection), which has attracted less attention in the past. We show that the electric field component parallel to the magnetic field plays a crucial physical role in finite-B reconnection, and we present two theorems involving the former. The first states a necessary and sufficient condition on the parallel electric field for global reconnection to occur. Here the term "global" means the generic case where the breakdown of magnetic connection occurs for plasma elements that stay outside the nonideal region. The second theorem relates the change of magnetic helicity to the parallel electric field for cases where the electric field vanishes at large distances. That these results provide new insight into three-dimensional reconnection processes is illustrated in terms of the plasmoid configuration, which was our starting point.
Author
Magnetic Field Reconnection; Magnetic Field Configurations; Magnetic Fields; Electric Fields

19990106586 Carmel Research Center, Space Plasma Lab., Santa Monica, CA USA
Research on Orbital Plasma Electrodynamics (ROPE) ***Final Report, Aug. 1987 - 30 Sep. 1998***
Intriligator, Devrie S., Carmel Research Center, USA; November 1998; 12p; In English
Contract(s)/Grant(s): NAS8-37109
Report No.(s): NASA/CR-1999-209735; NAS 1.26:209735; No Copyright; Avail: CASI; A03, Hardcopy; A01, Microfiche

This final report summarizes some of the important scientific contributions to the Research on Orbital Plasma Electrodynamics (ROPE) investigation, to the Tethered Satellite System (TSS) mission, and to NASA that resulted from the work carried out under this contract at Carmel Research Center. These include Dr. Intriligator's participation in the PIT for the TSS-1R simulations and flight, her participation in ROPE team meetings and IWG meetings, her scientific analyses, and her writing and submitting technical papers to scientific journals. The scientific analyses concentrated on the characterization of energetic ions and their possible relation to pickup ion effects, correlation of particle and other effects (e.g., magnetic field, satellite surface), and collaboration with theorists including with ROPE co-investigators. In addition, scientific analyses were carried out of the effects due to satellite gas releases.
Author
Plasma Dynamics; Plasma Electrodes; Plasmas (Physics); Electrodynamics

19990106594 NASA Marshall Space Flight Center, Huntsville, AL USA
Magnetotail Plasma Signatures of Pseudobreakups and Substorms
Fillingim, M. O., NASA Marshall Space Flight Center, USA; Brittnacher, M. J., NASA Marshall Space Flight Center, USA; Parks, G. K., NASA Marshall Space Flight Center, USA; Chen, L. J., NASA Marshall Space Flight Center, USA; Germany, G. A., NASA Marshall Space Flight Center, USA; Spann, J. F., NASA Marshall Space Flight Center, USA; Lin, R. P., NASA Marshall Space Flight Center, USA; [1999]; 1p; In English, 13-17 Dec. 1999, San Francisco, CA, USA; Sponsored by American Geophysical

Union, USA; No Copyright; Avail: Issuing Activity, Hardcopy; Abstract Only

Using Polar/UVI global images, we have identified a period of successive minor auroral activations during which WIND was making a perigee pass through the near-Earth magnetotail. On the basis of images, these auroral brightenings are interpreted to be pseudobreakups due to the lack of significant global expansion. Large magnetic by the WIND spacecraft show a nearly one-to-one correspondence auroral intensifications. During intervals of large field auroral brightenings, energized ions have an Earthward velocity energized electrons generally remain isotropic. Closer inspection ion distribution functions indicate that the high velocity moments are not due to convective flows. Rather, the plasma is composed of a component and a stagnate cold component. We also trace the observed by WIND backwards in time to determine the source regions for the particles. Based upon these observations, we find that to zeroth order there is no difference in the behavior of the plasma during as compared to substorm expansive phase events.

Author

Plasma Spectra; Signatures; Ion Distribution; Distribution Functions; Geomagnetic Tail

19990106602 NASA Marshall Space Flight Center, Huntsville, AL USA

Global Core Plasma Model

Gallagher, Dennis L., NASA Marshall Space Flight Center, USA; Craven, Paul D., NASA Marshall Space Flight Center, USA; Comfort, Richard H., NASA Marshall Space Flight Center, USA; [1999]; 1p; In English, 13 Dec. 1999, San Francisco, CA, USA; Sponsored by American Geophysical Union, USA; No Copyright; Avail: Issuing Activity, Hardcopy; Abstract Only

Over 40 years of ground and spacecraft plasmaspheric measurements have resulted in many statistical descriptions of plasmaspheric properties. In some cases, these properties have been represented as analytical descriptions that are valid for specific regions or conditions. For the most part, what has not been done is to extend regional empirical descriptions or models to the plasmasphere as a whole. In contrast, many related investigations depend on the use of representative plasmaspheric conditions throughout the inner magnetosphere. Wave propagation, involving the transport of energy through the magnetosphere, is strongly affected by thermal plasma density and its composition. Ring current collisional and wave particle losses also strongly depend on these quantities. Plasmaspheric also plays a secondary role in influencing radio signals from the Global Positioning System satellites. The Global Core Plasma Model (GCPM) is an attempt to assimilate previous empirical evidence and regional models for plasmaspheric density into a continuous, smooth model of thermal plasma density in the inner magnetosphere. In that spirit, the International Reference Ionosphere is currently used to complete the low altitude description of density and composition in the model. The models and measurements on which the GCPM is currently based and its relationship to IRI will be discussed.

Author

Plasmas (Physics); Core Flow; Plasma Density; Plasmasphere; Thermal Plasmas

19990107332 National Inst. for Fusion Science, Toki, Japan

Gyrokinetic Field Theory

Sugama, H., National Inst. for Fusion Science, Japan; August 1999; ISSN 0915-633X; 22p; In English

Report No.(s): NIFS-609; No Copyright; Avail: CASI; A03, Hardcopy; A01, Microfiche

The Lagrangian formulation of the gyrokinetic theory is generalized in order to describe the particles' dynamics as well as the self-consistent behavior of the electromagnetic fields. The gyrokinetic equation for the particle distribution function and the gyrokinetic Maxwell's equations for the electromagnetic fields are both derived from the variational principle for the Lagrangian consisting of the parts of particles, fields, and their interaction. In this generalized Lagrangian formulation, the energy conservation property for the total nonlinear gyrokinetic system of equations is directly shown from the Noether's theorem. This formulation can be utilized in order to derive the nonlinear gyrokinetic system of equations and the rigorously conserved total energy for fluctuations with arbitrary frequencies.

Author

Electromagnetic Fields; Particle Energy; Variational Principles

19990107340 Princeton Plasma Physics Lab., Princeton, NJ USA

Nitrogen Atom Energy Distributions in a Hollow-cathode Planar Sputtering Magnetron

Ruzic, D. N.; Goeckner, M. J.; Cohen, Samuel A.; Wang, Zhehui; Jun. 01, 1999; 404p; In English

Report No.(s): DE00-008184; PPPL-3347; No Copyright; Avail: Department of Energy Information Bridge, Hardcopy

Energy distributions of N atoms in a hollow-cathode planar sputtering magnetron were obtained by use of optical emission spectroscopy. A characteristic line, N I 8216.3, well-separated from molecular nitrogen emission bands, was identified. Jansson's nonlinear spectral deconvolution method, refined by minimization of (chi);sub lt;/sub gt; sup2; , was used to obtain the optimal deconvolved spectra. These showed nitrogen atom energies from 1 eV to beyond 500 eV. Based on comparisons with VFTRIM

results, we propose that the energetic N atoms are generated from N₂< sup>+</sup> ions after these ions are accelerated through the sheath and dissociatively reflect from the cathode.
NTIS
Nitrogen; Magnetrons; Nitrogen Atoms; Spectral Energy Distribution; Energy Distribution; Nuclear Fission

19990107342 Federal Energy Technology Center, Morgantown, WV USA
Technical Progress Report for UTSI/CFFF MHD Program Completion and Related Activities ***Progress Report***
Chapman, J. N.; Muehlhauser, J. W.; Oct. 23, 1998; 8p; In English
Report No.(s): DE00-007489; DE-AC22-95PC95231-17; No Copyright; Avail: Department of Energy Information Bridge, Hardcopy

Routine preventive maintenance of the DOE Coal Fired Flow Facility (CFFF) is being performed. Modernization programs, funded under subcontract from Foster Wheeler Development Corporation by the DOE HIPPS Program, have been completed on the coal processing system, the data acquisition and control system and the control room. Late in the quarter, all work was stopped on maintenance of the CFFF at DOE instruction. Environmental restoration actions continued with monitoring of groundwater wells and holding pond effluent. Progress is reported on the approved groundwater remediation plan. Actions are underway to dispose of spent seed/ash mixtures and excess coal remaining from the MHD POC program. The status of five (5) High Temperature Superconductor (HTS) projects is reported. A summary is included of the results attained with sol-gel experiments with buffer layers and YBCO. The status of the cost/performance study of electron beam and PLD deposition is presented. A summary of work performed in diagnostics for real time control of HTS processes is presented.
NTIS
Data Acquisition; Coal; Maintenance; Ground Water; Ground Based Control; Electron Beams; Integrated Mission Control Center

19990107344 Sandia National Labs., Albuquerque, NM USA
Analysis of Z Pinch Shock Wave Experiments
Asay, J.; Budge, K. G.; Chandler, G.; Fleming, K.; Hall, C.; May 01, 1999; 74p; In English
Report No.(s): DE00-007444; SAND99-1255; No Copyright; Avail: Department of Energy Information Bridge, Hardcopy

In this paper, we report details of our computational study of two shock wave physics experiments performed on the Sandia Z machine in 1998. The novelty of these particular experiments is that they represent the first successful application of VISAR interferometry to diagnose shock waves generated in experimental payloads by the primary X-ray pulse of the machine. We use the Sandia shock-wave physics code ALEGRA to perform the simulations reported in this study. Our simulations are found to be in fair agreement with the time- resolved VISAR experimental data. However, there are also interesting and important discrepancies. We speculate as to future use of time-resolved shock wave data to diagnose details of the Z machine X-ray pulse in the future.
NTIS
Shock Waves; Experimentation; Numerical Analysis; Computation; Zeta Pinch

19990108845 National Inst. for Fusion Science, Toki, Japan
One Dimensional Simulation on Stability of Detached Plasma in a Tokamak Divertor
Nakazawa, Shinji, National Inst. for Fusion Science, Japan; Nakajima, Noriyoshi, National Inst. for Fusion Science, Japan; Okamoto, Masao, National Inst. for Fusion Science, Japan; Ohyabu, Nobuyoshi, National Inst. for Fusion Science, Japan; June 1999; ISSN 0915-633X; 18p; In English
Report No.(s): NIFS-598; No Copyright; Avail: CASI; A03, Hardcopy; A01, Microfiche

The stability of radiation front in the Scrape-Off-Layer (SOL) of a tokamak is studied with a one dimensional fluid code; the time-dependent transport equations are solved in the direction parallel to t magnetic field line. The simulation results show that stable detached solutions exist, where the plasma temperature near the divertor target is approx. 2eV. It is found that whenever such stable detached states are attained, the strong radiation front is contact with or at a small distance from the divertor target. When the energy externally injected into the SOL is decreased below a critical value, the radiation front starts to move towards the X-point, cooling the SOL plasma. In such cases, no stationary solutions such that the radiation front rests in the divertor channel are observed in our parameter space. This qualitatively corresponds to the results of tokamak divertor experiments which show tile movement of radiation front.
Author
Plasma Radiation; Time Dependence; Stability; Simulation; Magnetic Fields; Dimensional Stability

19990108846 National Inst. for Fusion Science, Toki, Japan

Effect of Energetic Ion Loss on ICRF Heating Efficiency and Energy Confinement Time in Heliotrons

Murakami, S., National Inst. for Fusion Science, Japan; Nakajima, N., National Inst. for Fusion Science, Japan; Okamoto, M., National Inst. for Fusion Science, Japan; Nuehrenberg, J., Max-Planck-Inst. fuer Plasmaphysik, Germany; June 1999; ISSN 0915-633X; 22p; In English

Report No.(s): NIFS-599; No Copyright; Avail: CASI; A03, Hardcopy; A01, Microfiche

ICRF heating efficiency and the global energy confinement time during ICRF heating are investigated including the effect of energetic ion loss in heliotrons. The approximate formula of ICRF heating efficiency is derived using the results based on Monte Carlo simulations. The global energy confinement time including energetic ion effect can be expressed in terms of ICRF heating power, plasma density, and magnetic field strength in heliotrons. Our results in the CHS plasma show the systematic decrement of the global energy confinement time due to the energetic ion loss from the assumed energy confinement scaling law, which is consistent with the experimental observations. Also we apply our model to the ICRF minority heating in tire LHD plasma in two cases of typical magnetic configurations. The clear increment of the global energy confinement time due to the stored energy of energetic tail ions is obtained in the ”orbit improved” configuration, while the decrement is observed in the ”standard” configuration.

Author

Ion Cyclotron Radiation; Radio Frequency Heating; Plasma Heating; Plasma Control; Magnetic Flux; Heliotrons

19990108847 National Inst. for Fusion Science, Toki, Japan

First ICRF Heating Experiment in the Large Helical Device

Mutoh, T., National Inst. for Fusion Science, Japan; Kumazawa, R., National Inst. for Fusion Science, Japan; Seki, T., National Inst. for Fusion Science, Japan; Saito, K., Nagoya Univ., Japan; Shimpo, F., National Inst. for Fusion Science, Japan; Nomura, G., National Inst. for Fusion Science, Japan; Watari, T., National Inst. for Fusion Science, Japan; Jikang, X., Academia Sinica, China; Cattanei, G., Max-Planck-Inst. fuer Plasmaphysik, Germany; Okada, H., Kyoto Univ., Japan; July 1999; ISSN 0915-633X; 10p; In English

Report No.(s): NIFS-602; No Copyright; Avail: CASI; A02, Hardcopy; A01, Microfiche

First ICRF heating experiment in the Large Helical Device (LHD) was carried out in the 2nd experimental campaign in the end of 1998. During the experimental series, maximum 300 kW/0.2sec of ICRF power was injected to the LHD plasma by using a pair of loop antennas. This paper reports the installation of antennas and the results of coupling and heating experiments. Target plasma was produced by 2nd harmonic ECH heating of 84 GHz gyrotrons at a magnetic field of 1.5 Tesla. Target plasma density was quite low of less than 1 x 10(exp 19)/cu m. Therefore the maximum injected power was limited by low coupling resistance of plasma. Center current strap is one strap type, therefore the parallel wave number is not regulated. The higher frequency and higher density plasma should lead to the better plasma coupling and higher heating power. In addition, another new type antenna (Folded Wave-Guide antenna) is installed and will be operated in 1999.

Derived from text

Experimentation; Heliotrons; Plasma Heating; Radio Frequency Heating; Loop Antennas; Installing

19990109156 Instituto Nacional de Pesquisas Espacias, Lab. Associado de Plasma, Sao Jose dos Campos, Brazil

Plasma Heating by Lower-Hybrid and Electron-Cycloton Waves in the ETE Low-Aspect-Ratio Tokamak

Neto, Joaquim Paulino Leite, Instituto Nacional de Pesquisas Espacias, Brazil; Shibata, Carlos, Instituto Nacional de Pesquisas Espacias, Brazil; Montes, Antonio, Instituto Nacional de Pesquisas Espacias, Brazil; 1999\; 27p; In English

Report No.(s): INPE-6972-RPQ/695; No Copyright; Avail: CASI; A03, Hardcopy; A01, Microfiche

The use of RF sources both for pre-ionization purposes and auxiliar heating of plasmas is investigated for the ETE spherical tokamak. A ray-tracing code is employed in the study of the propagation and absorption of waves in the range of electron-cyclotron and lower-hybrid frequencies. The absorption model also takes into account the damping of the waves due to electron-ion collisions. It is shown that in the high density and temperature regime the use of electron-cyclotron waves injected with a frequency of 35 GHz allows the heating of a region half way between the magnetic axis and the plasma edge (high magnetic field side). In the same regime, the use of low n(sub parallel) LH waves, which are highly desirable for current drive purposes seems to be impracticable at the plasma center for typical ETE parameters. Concerning the start-up of the ETE discharge, it has been found that both lower-hybrid waves and electron-cyclotron waves may transfer energy to the plasma column very efficiently by electron-ion collisional damping.

Author

Plasma Heating; Electron Cyclotron Resonance; Plasmas (Physics); Low Aspect Ratio; Tokamak Devices; Cyclotron Frequency; Cyclotron Radiation; Landau Damping

19990109654 National Inst. for Fusion Science, Toki, Japan

Thermonuclear Reactivity of D-T Fusion Plasma with Spin-Polarized Fuel

Takahashi, Toshihi, Gunma Univ., Japan; Nakao, Yasuyuki, Kyushu Univ., Japan; April 1999; ISSN 0915-633X; 16p; In English

Report No.(s): NIFS-592; No Copyright; Avail: CASI; A03, Hardcopy; A01, Microfiche

The thermonuclear reactivity of deuterium(D) - tritium(T) fusion plasma with spin-polarized fuel has been studied. Two mechanisms of depolarization, collisions and waves, in the high temperature fusion plasma have been considered. The binary collisions have been found not to change the nuclear spin states. The waves with a frequency of a few GHz, however, changes the spin states appreciably, when (delta)B/B(sub 0) (the ratio of the amplitude of the fluctuating magnetic field to the external field) becomes larger than 10(exp -5).

Author

Thermonuclear Reactions; Fusion (Melting); Depolarization; Fuels; Research; High Temperature Plasmas; Deuterium; Tritium

19990110298 Department of Energy, Office of Energy Research, Washington, DC USA

Nonlinear magnetohydrodynamics ***Final Report***

Montgomery, D. C., Department of Energy, USA; Dec. 31, 1998; 15p; In English

Report No.(s): DE99-000045; DOE/ER/53194-T4; No Copyright; Avail: Department of Energy Information Bridge, Microfiche

This is a final report on the research activities carried out under the above grant at Dartmouth. During the period considered, the grant was identified as being for nonlinear magnetohydrodynamics, considered as the most tractable theoretical framework in which the plasma problems associated with magnetic confinement of fusion plasmas could be studied. During the first part of the grant's lifetime, the author was associated with Los Alamos National Laboratory as a consultant and the work was motivated by the reversed-field pinch. Later, when that program was killed at Los Alamos, the problems became ones that could be motivated by their relation to tokamaks. Throughout the work, the interest was always on questions that were as fundamental as possible, compatible with those motivations. The intent was always to contribute to plasma physics as a science, as well as to the understanding of mission- oriented confined fusion plasmas. Twelve Ph.D. theses were supervised during this period and a comparable number of postdoctoral research associates were temporarily supported. Many of these have gone on to distinguished careers, though few have done so in the context of the controlled fusion program. Their work was a combination of theory and numerical computation, in gradually less and less idealized settings, moving from rectangular periodic boundary conditions in two dimensions, through periodic straight cylinders and eventually, before the grant was withdrawn, to toroids, with a gradually more prominent role for electrical and mechanical boundary conditions. The author never had access to a situation where he could initiate experiments and relate directly to the laboratory data he wanted. Computers were the laboratory. Most of the work was reported in referred publications in the open literature, copies of which were transmitted one by one to DOE at the time they appeared. The Appendix to this report is a bibliography of published work which was carried out under the partial support of this grant from the mid-1980s onward. It is this collection of papers which is considered to have been the principal product of this research support. Only the broadest-brush summary of the details of this work will be given here.

NTIS

Magnetohydrodynamics; Thermonuclear Reactions; Controlled Fusion; Plasma Control; Tokamak Devices

19990110522 Department of Energy, Office of Energy Research, Washington, DC USA

Study of material destruction during powerful plasma exposure

Belan, V. G., Department of Energy, USA; Levashov, V. F., Department of Energy, USA; Maynashev, V. S., Department of Energy, USA; Muzichenko, A. D., Department of Energy, USA; Podkovirov, V. L., Department of Energy, USA; Dec. 31, 1998; 5p; In English; 20th; Fusion Technology (SOFT '98), USA

Report No.(s): DE98-058268; ANL/TD/CP-97104; No Copyright; Avail: Department of Energy Information Bridge, Microfiche

Results of experimental research during the interaction of powerful plasma flow with aluminum and graphite targets are presented. The experiments were carried out at plasma energy density of up to 5 MJ/sq m and time duration of up to 600 micro-s. Strong damage of target materials was observed as a result of the plasma flow interaction as well as the formation and the ejection of macroscopic particles from the target surface. The ejected particle size and spatial distribution were measured as well as the velocity of these particles during the experiments. The method of laser scattering was applied for these measurements.

NTIS

Aluminum; Graphite; Magnetohydrodynamic Flow; Service Life; Reactor Materials; Erosion

19990110523 Department of Energy, Office of Energy Research, Washington, DC USA

Possible applications of powerful pulsed CO2-lasers in tokamak reactors

Nastoyashchii, A. F., Department of Energy, USA; Morozov, I. N., Department of Energy, USA; Hassanein, A., Department of

Energy, USA; Dec. 31, 1998; 5p; In English; 20th; Fusion Technology (SOFT '98), USA
Report No.(s): DE98-058269; ANL/TD/CP-97107; No Copyright; Avail: Department of Energy Information Bridge, Microfiche

Applications of powerful pulsed CO2-lasers for injection of fuel tablets or creation of a protective screen from the vapor of light elements to protect against the destruction of plasma-facing components are discussed, and the corresponding laser parameters are determined. The possibility of using CO2-lasers in modeling the phenomena of powerful and energetic plasma fluxes interaction with a wall, as in the case of a plasma disruption, is considered.

NTIS

Carbon Dioxide Lasers; Tokamak Devices; Erosion; Destruction; Plasmas (Physics); Injection; Reactor Materials

19990110524 Department of Energy, Office of Energy Research, Washington, DC USA

Disruption simulation experiments and extrapolation to reactor conditions

Hassanein, A., Department of Energy, USA; Konkashbaev, I. K., Department of Energy, USA; Dec. 31, 1998; 5p; In English; 20th; Fusion Technology (SOFT '98), USA
Report No.(s): DE98-058270; ANL/TD/CP-97106; No Copyright; Avail: Department of Energy Information Bridge, Microfiche

Laboratory experiments to simulate plasma disruptions have contributed significantly in many aspects to the understanding of the physical processes occurring during high-energy deposition on target material surfaces due to plasma instabilities. Laser light, electron beams, and plasma guns have been used worldwide to study disruption effects and erosion damage of candidate divertor materials. The differences among these simulation experiments are examined. The net power flux reaching the originally exposed surface depends on many parameters, such as type of energy deposited, target material, pulse duration, and geometrical factors. Experimental results have been evaluated and compared with theoretical predictions, and the overall relevance of simulation experiments to reactor conditions has been critically examined.

NTIS

Plasmas (Physics); Erosion; Reactor Materials; Magnetohydrodynamic Stability; Laser Outputs; Damage

19990110525 National Inst. for Fusion Science, Toki, Japan

Three-Dimensional Particle Simulation of Plasma Instabilities and Collisionless Reconnection in a Current Sheet

Horiuchi, Ritoku, National Inst. for Fusion Science, Japan; Sato, Tetsuya, National Inst. for Fusion Science, Japan; June 1999; ISSN 0915-633X; 20p; In English; Original contains color illustrations
Contract(s)/Grant(s): MOE-10680468
Report No.(s): NIFS-600; No Copyright; Avail: CASI; A03, Hardcopy; A01, Microfiche

Generation of anomalous resistivity and dynamical development of collisionless reconnection in the vicinity of a magnetically neutral sheet are investigated by means of a three-dimensional particle simulation. For no external driving source, two different types of plasma instabilities are excited in the current layer. The lower hybrid drift instability (LHDI) is observed to grow in the periphery of current layer in an early period, while a drift kink instability (DKI) is triggered at the neutral sheet in a late period as a result of the nonlinear deformation of the current sheet by the LHDI. A reconnection electric field grows at the neutral sheet in accordance with the excitation of the DKI. When an external driving field exists, the convective electric field penetrates into the current layer through the particle kinetic effect and collisionless reconnection is triggered by the convective electric field earlier than the DKI is excited. It is also found that the anisotropic ion distribution is formed through the anomalous ion heating by the DKI.

Author

Three Dimensional Models; Particle Motion; Plasma Dynamics; Computerized Simulation; Current Sheets; Excitation; Ion Distribution

19990110677 NASA Marshall Space Flight Center, Huntsville, AL USA

Effects of Convection Electric Fields on Modeled Plasmaspheric Densities and ccc Temperatures

Comfort, Richard H., NASA Marshall Space Flight Center, USA; Richards, Phil G., NASA Marshall Space Flight Center, USA; Liao, Jin–Hua, NASA Marshall Space Flight Center, USA; Craven, Paul D., NASA Marshall Space Flight Center, USA; [1998]; 1p; In English, Dec. 1998, San Francisco, CA, USA; Sponsored by American Geophysical Union, USA; Copyright; Avail: Issuing Activity, Hardcopy; Abstract Only

This paper examines the effects of convection electric fields on plasmaspheric H+, O+, He+, and N+ densities and electron and ion temperatures. These effects are studied with the aid of the Field Line Interhemispheric Plasma (FLIP) model, which has recently been extended to include the effects of ExB drifts. The FLIP model solves the continuity and momentum equations for the major ion species as well as the energy equations for ions and electrons along entire drifting flux tubes from 100 km altitude in the northern hemisphere to 100 km altitude in the southern hemisphere. Electron heating in the ionosphere and plasmasphere

is provided by the solution of two-stream equations for photoelectrons. The dawn-dusk electric field imposed by the solar wind causes changes in plasmaspheric density and temperature as the plasma drifts onto flux tubes having different volumes. In an idealized convection model, outward drifts in the afternoon cause decreases in the plasmasphere density and temperature while inward drifts in the evening cause increases in plasmasphere density and temperature. In this paper we examine the effects of convection electric fields on the rate of refilling of flux tubes and investigate the hypothesis that convection electric fields are responsible for the unusually high evening electron temperatures and the post-midnight density maxima often observed in the winter ionosphere above Millstone Hill.
Author
Convection; Electric Fields; Plasmas (Physics); Plasmasphere; Ionospheric Heating; Plasma Heating; Plasma Temperature; Plasma Drift; Plasma Density

19990110699 NASA Marshall Space Flight Center, Huntsville, AL USA
Modeling Electric Field Influences on Plasmaspheric Refilling
Liemohn, M. W., NASA Marshall Space Flight Center, USA; Kozyra, J. U., NASA Marshall Space Flight Center, USA; Khazanov, G. V., NASA Marshall Space Flight Center, USA; Craven, Paul D., NASA Marshall Space Flight Center, USA; [1998]; 1p; In English; 6th; 6th Huntsville Modeling Workshop, 26 Oct. 1998, Guntersville, AL, USA; Copyright; Avail: Issuing Activity, Hardcopy; Abstract Only

We have a new model of ion transport that we have applied to the problem of plasmaspheric flux tube refilling after a geomagnetic disturbance. This model solves the Fokker-Planck kinetic equation by applying discrete difference numerical schemes to the various operators. Features of the model include a time-varying ionospheric source, self-consistent Coulomb collisions, field-aligned electric field, hot plasma interactions, and ion cyclotron wave heating. We see refilling rates similar to those of earlier observations and models, except when the electric field is included. In this case, the refilling rates can be quite different that previously predicted. Depending on the populations included and the values of relevant parameters, trap zone densities can increase or decrease. In particular, the inclusion of hot populations near the equatorial region (specifically warm pancake distributions and ring current ions) can dramatically alter the refilling rate. Results are compared with observations as well as previous hydrodynamic and kinetic particle model simulations.
Author
Electric Fields; Plasma Interactions; Plasmasphere; Plasmas (Physics); High Temperature Plasmas; Ion Cyclotron Radiation; Plasma Radiation; Plasma Waves; Refilling

19990111492 Department of Energy, Office of Energy Research, Washington, DC USA
Perspectives gained from ICRF physics studies on TFTR
Phillips, C. K., Department of Energy, USA; Bell, M., Department of Energy, USA; Batha, S., Department of Energy, USA; Dec. 31, 1998; 4p; In English
Report No.(s): DE98-057589; PPPL-CFP-3870; No Copyright; Avail: Department of Energy Information Bridge, Microfiche

The physics of ICRF heating and current drive has been studied on TFTR for over a decade. Following the early low power coupling studies, high power experiments resulted in sawtooth stabilization, the first observation of RF-driven excitation of toroidal Alfven eigenmodes, and the discovery of a mode conversion scenario for localized off-axis electron heating. The program culminated with the first studies of high power ICRF heating and profile control in tritium-rich high performance plasmas. A significant part of the concluding experiments centered on the potential of ICRF to drive sheared flows in order to suppress turbulence in the plasma core. Initial measurements taken with a novel poloidal velocity diagnostic suggest that localized sheared poloidal flows can be driven with ion Bernstein waves excited directly or else via mode conversion from a propagating fast magnetosonic wave. In this paper, recent results from TFTR on wave-based profile control techniques will be summarized along with suggestions for future studies elsewhere.
NTIS
Radio Frequency Heating; Tokamak Devices; Ion Cyclotron Radiation; Magnetohydrodynamic Waves; Plasma Heating; Plasma Oscillations

19990113111 NASA Glenn Research Center, Cleveland, OH USA
The Conductor-Dielectric Junctions in a Low Density Plasma
Vayner, Boris, Ohio Aerospace Inst., USA; Galofaro, Joel, NASA Glenn Research Center, USA; Ferguson, Dale, NASA Glenn Research Center, USA; deGroot, Wim, DYNACS Engineering Co., Inc., USA; Thomson, Clint, Utah State Univ., USA; Dennison, J. R., Utah State Univ., USA; Davies, Robert, Utah State Univ., USA; November 1999; 30p; In English; 38th; Aerospace Sciences, 10-13 Jan. 2000, Reno, NV, USA; Sponsored by American Inst. of Aeronautics and Astronautics, USA

Contract(s)/Grant(s): RTOP 632-1A-1A
Report No.(s): NASA/TM-1999-209408; E-11938; NAS 1.15:209408; No Copyright; Avail: CASI; A03, Hardcopy; A01, Microfiche

A conductor-dielectric junction exposed to the space environment is a frequent spacecraft design feature. Due to spacecraft charging and/or solar array operation, the conductor can acquire a high potential with respect to the surrounding plasma. If this potential is positive the insulators adjacent to exposed conductors can collect current as if they were conductors themselves. This phenomenon, called snapover, results in a substantial increase in current collection, and may even result in a glow discharge if the potential is high enough. If a conductor has a negative potential, arcing can occur at the site of a junction. Both of these phenomena negatively affect spacecraft operation. To prevent negative consequences, the physical mechanisms of snapover and arc inception require investigation. In this paper, results are presented of an experimental and theoretical study of snapover, glow discharge, and arc phenomena for different materials immersed in argon or xenon plasmas. The effect of snapover is investigated for several metal-dielectric junctions: copper-teflon, copper-Kapton, copper-glass, aluminum-teflon, aluminum-Kapton, steel-teflon, anodized aluminum with pinholes, and copper-ceramics. I-V curves are measured and snapover inception voltages, essential parameters (increase in current and collection area due to secondary electrons), and glow discharge inception thresholds are determined. Optical spectra are obtained for glow discharges in both argon and xenon plasmas. These spectra provide information regarding atomic species entrapped in the glow region. Some spectral lines can be used to estimate plasma parameters in the discharge area. A video-camera and linear array were used to confirm that snapover inception is accompanied by very low intensity visible light emission. This result seems to be important for the estimate of the light pollution around spacecraft. Optical spectra (wavelengths 380-650 nm) of arcs are also obtained on a negatively biased chromic acid anodized aluminum plate immersed in low density argon and xenon plasmas. Analysis of these spectra confirms our earlier findings that aluminum atoms are ejected from the arc site. Moreover, it is found that chromium atoms are also quite abundant in the arc plasma. It is believed that the latter results contribute considerably to the understanding of processes of plasma contamination caused by arcing.
Author

Conductors; Dielectrics; Solar Arrays; Spacecraft Charging; Spacecraft Glow; Spacecraft Design; Glow Discharges; Light Emission; Line Spectra; Plasma Interactions; Plasma Jets; Plasmas (Physics)

19990113140 Swedish Inst. of Space Physics, Kiruna, Sweden
High Altitude Cusp and Magnetosheath In-situ Measurements ***Topical Report***
Eklund, U.; Dec. 1998; ISSN 0284-1703; 54p; In English
Report No.(s): PB99-174161; IRF-SR-249; No Copyright; Avail: CASI; A01, Microfiche; A04, Hardcopy

This licentiate thesis consists of an introduction together with two articles with measurements made in the high-latitude cusp and in the adjacent magnetosheath. Some conclusions, based on the measurement, are made about the plasma transfer processes into the magnetosphere.
NTIS

Plasma Physics; Magnetosheath; In Situ Measurement; Polar Cusps

76
SOLID-STATE PHYSICS

Includes superconductivity. For related information, see also 33 Electronics and Electrical Engineering and 36 Lasers and Masers.

19990106591 Universities Space Research Association, Huntsville, AL USA
Crystal Growth of ZnSe and Related Ternary Compound Semiconductors by Physical Vapor Transport ***Final Report, 1 Mar. 1993 - 30 Sep. 1997***
Cushman, Paula P., Universities Space Research Association, USA; Oct. 31, 1997; 37p; In English
Contract(s)/Grant(s): NAS8-39718
Report No.(s): NASA/CR-1999-209739; NAS 1.26:209739; No Copyright; Avail: CASI; A03, Hardcopy; A01, Microfiche

Preliminary definition of all of the necessary materials, labor, services, and facilities necessary to provide science requirement definition, initiate hardware development activities, and provide an update flight program proposal consistent with the NRA selection letter. The major tasks identified in this SOW are in the general category of science requirements determination, instrument definition, and updated flight program proposal. The Contractor shall define preliminary management, technical and integration requirements for the program, including improved cost/schedule estimates. The Contractor shall identify new

technology requirements, define experiment accommodations and operational requirements and negotiate procurement of any long lead items, if required, with the government.
Author
Crystal Growth; Vapor Deposition; Transport Theory; Ternary Alloys; Zinc Selenides; Semiconductors (Materials)

19990106597 NASA Marshall Space Flight Center, Huntsville, AL USA
First Results from a Microfocus X-Ray System for Macromolecular Crystallography
Gubarev, Mikhail, National Research Council; Ciszak, Ewa, NASA Marshall Space Flight Center, USA; Ponomarev, Igor, X-Ray Optical Systems, Inc., USA; Gibson, Walter, State Univ. of New York, USA; Joy, Marshall, NASA Marshall Space Flight Center, USA; [1999]; 1p; In English; No Copyright; Avail: Issuing Activity, Hardcopy; Abstract Only

The design and performance of a 40 Watt laboratory crystallography system optimized for the structure determination of small protein crystals are described. This system combines a microfocus x-ray generator (40 microns FWHM spot size at a power level of 40 Watts) and a short focal length (F = 2.6 mm) polycapillary collimating optic, and produces a small diameter quasi-parallel x-ray beam. Measurements of x-ray flux, divergence and spectral purity of the resulting x-ray beam are presented. The x-ray flux in a 250 microns diameter aperture produced by the microfocus system is 14.7 times higher .than that from a 3.15 kW rotating anode generator equipped with graphite monochromator. Crystallography data taken with the microfocus system are presented, and indicate that the divergence and spectral purity of the x-ray are sufficient to refine the diffraction data using a standard crystallographic software. Significant additional improvements in flux and beam divergence are possible, and plans for achieving these coals are discussed.
Author
Crystallography; Design Analysis; Proteins; Crystals; Laboratory Equipment; Collimation; Apertures

19990107347 Sandia National Labs., Livermore, CA USA
Formation of Mesostructured Nanoparticles through Self-Assembly and Aerosol Process
Brinker, C.; Fan, H.; Lu, Y.; Rieker, T.; Stump, A.; May 07, 1999; 6p; In English, 5-9 Apr. 1999, San Francisco, CA, USA; Sponsored by Materials Research Society, USA
Report No.(s): DE00-007245; SAND99-1198C; No Copyright; Avail: Department of Energy Information Bridge, Hardcopy

Silica nanoparticles exhibiting hexagonal, cubic, and vesicular mesostructures have been prepared using aerosol assisted, self-assembled process. This process begins with homogennous aerosol droplets containing silica source, water, ethanol, and surfactant, in which surfactant concentration is far below the critical micelle concentration (cmc). Solvent evaporation enriches silica and surfactant inducing interfacial self-assembly confined to a spherical aerosol droplet and results in formation of completely solid, ordered spherical particles with stable hexagonal, cubic, or vesicular mesostructures.
NTIS
Aerosols; Surfactants; Procedures; Silicon Dioxide

19990107389 NASA Marshall Space Flight Center, Huntsville, AL USA
Fluorescence Studies of Protein Crystal Nucleation
Pusey, Marc L., NASA Marshall Space Flight Center, USA; [1999]; 1p; In English, 7 Aug. 1999, Glasgow, Scotland, UK; Sponsored by IUCR General Assemby and Congress, UK; No Copyright; Avail: Issuing Activity, Hardcopy; Abstract Only

Fluorescence can be used to study protein crystal nucleation through methods such as anisotropy, quenching, and resonance energy transfer (FRET), to follow pH and ionic strength changes, and follow events occurring at the growth interface. We have postulated, based upon a range of experimental evidence that the growth unit of tetragonal hen egg white lysozyme is an octamer. Several fluorescent derivatives of chicken egg white lysozyme have been prepared. The fluorescent probes lucifer yellow (LY), cascade blue, and 5-((2-aminoethyl)aminonapthalene-1-sulfonic acid (EDANS), have been covalently attached to ASP 101. All crystallize in the characteristic tetragonal form, indicating that the bound probes are likely laying within the active site cleft. Crystals of the LY and EDANS derivatives have been found to diffract to at least 1.7 A. A second group of derivatives is to the N-terminal amine group, and these do not crystallize as this site is part of the contact region between the adjacent 43 helix chains. However derivatives at these sites would not interfere with formation of the 43 helices in solution. Preliminary FRET studies have been carried out using N-terminal bound pyrene acetic acid (Ex 340 nm, Em 376 nm) lysozyme as a donor and LY (Ex -425 nm, Em 525 nm) labeled lysozyme as an acceptor. FRET data have been obtained at pH 4.6, 0.1 M NaAC buffer, at 5 and 7% NaCl, 4 C. The corresponding Csat values are 0.471 and 0.362 mg/ml (approximately 3.3 and approximately 2.5 x 10(exp -5) M respectively). The data at both salt concentrations show a consistent trend of decreasing fluorescence intensity of the donor species (PAA) with increasing total protein concentration. This decrease is more pronounced at 7% NaCl, consistent with the expected increased intermolecular interactions at higher salt concentrations reflected in the lower solubility. The calculated average

distance between any two protein molecules at 5 x 10(exp -6) M is approximately 70nm, well beyond the range where any FRET can be expected. Results from these and ongoing studies will be presented.
Author
Fluorescence; Proteins; Crystals; Nucleation; Chickens; Eggs; Lysozyme

19990108477 NASA Marshall Space Flight Center, Huntsville, AL USA
In-Situ Partial Pressure Measurements and Visual Observation during Crystal Growth of ZnSe by Seeded Physical Vapor Transport
Su, Ching–Hua, NASA Marshall Space Flight Center, USA; Feth, Shari, Alabama Univ., USA; Lehoczky, Sandor L., NASA Marshall Space Flight Center, USA; [1999]; 1p; In English; No Copyright; Avail: Issuing Activity, Hardcopy; Abstract Only

An in-situ monitoring furnace was constructed with side windows to perform partial pressure measurements by optical absorption and visual observation of the growing crystal. A fused silica -rowth ampoule with a 4.5 cm long square tube between the source and the seed was prepared for the optical absorption measurements. A ZnSe crystal was grown by the seeded physical vapor transport (PVT) technique in the horizontal configuration. The growth temperature was 1120 C and the furnace translation rate was 3nmVday. Partial pressures of Se2, P(sub Se2), at three locations along the length of the growth ampoule were measured at 90 min intervals during the growth process. The measured P (sub Se2) were in the range of 2.0 to 6.5 x 10(exp -3) atm. The P(sub Se2) results indicated that the partial pressure profile was inconsistent with the results of the one-dimensional diffusion mass transport model and that the source composition shifted toward Se-rich during the run, i.e. the grown crystal was more Zn-rich than the source. The visual observation showed that the seed crystal first etched back, with greater thermal etching occurring along the edges of the seed crystal. Once the growth started, the crystal crew in a predominately contactless mode and facets were evident during growth. The crystal did not grow symmetrically which is believed to be due to the unintentional asymmetry of the radial thermal profile in the furnace.
Author
Pressure Measurement; Visual Observation; Crystal Growth; Zinc Selenides; Vapors; Furnaces; Fabrication; Electromagnetic Absorption

19990108578 Northeastern Univ., Chemical Engineering Dept., Boston, MA USA
Zeolite Crystal Growth (ZCG) Flight on USML-2 ***Final Report***
Sacco, Albert, Jr., Northeastern Univ., USA; Bac, Nurcan, Northeastern Univ., USA; Warzywoda, Juliusz, Northeastern Univ., USA; Guray, Ipek, Worcester Polytechnic Inst., USA; Marceau, Michelle, Worcester Polytechnic Inst., USA; Sacco, Teran L., Worcester Polytechnic Inst., USA; Whalen, Leah M., Worcester Polytechnic Inst., USA; Aug. 01, 1997; 34p; In English
Contract(s)/Grant(s): NAS8-40260
Report No.(s): NASA/CR-1999-209742; NAS 1.26:209742; No Copyright; Avail: CASI; A03, Hardcopy; A01, Microfiche

The extensive use of zeolites and their impact on the world's economy has resulted in many efforts to characterize their structure, and improve the knowledge base for nucleation and growth of these crystals. The zeolite crystal growth (ZCG) experiment on USML-2 aimed to enhance the understanding of nucleation and growth of zeolite crystals, while attempting to provide a means of controlling the defect concentration in microgravity. Zeolites A, X, Beta, and Silicalite were grown during the 16 day - USML-2 mission. The solutions where the nucleation event was controlled yielded larger and more uniform crystals of better morphology and purity than their terrestrial/control counterparts. The external surfaces of zeolite A, X, and Silicalite crystals grown in microgravity were smoother (lower surface roughness) than their terrestrial controls. Catalytic studies with zeolite Beta indicate that crystals grown in space exhibit a lower number of Lewis acid sites located in micropores. This suggests fewer structural defects for crystals grown in microgravity. Transmission electron micrographs (TEM) of zeolite Beta crystals also show that crystals grown in microgravity were free of line defects while terrestrial/controls had substantial defects.
Author
Zeolites; Crystallinity; Crystal Structure; Crystal Growth; Nucleation

19990109089 NASA Marshall Space Flight Center, Huntsville, AL USA
Static Magnetic Fields in Semiconductor Floating-Zone Growth
Croll, Arne, NASA Marshall Space Flight Center, USA; Benz, K. W., NASA Marshall Space Flight Center, USA; [1999]; 1p; In English; No Copyright; Avail: Issuing Activity, Hardcopy; Abstract Only

Heat and mass transfer in semiconductor float-zone processing are strongly influenced by convective flows in the zone, originating from sources such as buoyancy convection, thermocapillary (Marangoni) convection, differential rotation, or radio frequency heating. Because semiconductor melts are conducting, flows can be damped by the use of static magnetic fields to influence the interface shape and the segregation of dopants and impurities. An important objective is often the suppression of

time-dependent flows and the ensuing dopant striations. In RF-heated Si-FZ - crystals, fields up to O.STesla show some flattening of the interface curvature and a reduction of striation amplitudes. In radiation-heated (small-scale) SI-FZ crystals, fields of 0.2 - 0.5 Tesla already suppress the majority of the dopant striations. The uniformity of the radial segregation is often compromised by using a magnetic field, due to the directional nature of the damping. Transverse fields lead to an asymmetric interface shape and thus require crystal rotation (resulting in rotational dopant striations) to achieve a radially symmetric interface, whereas axial fields introduce a coring effect. A complete suppression of dopant striations and a reduction of the coring to insignificant values, combined with a shift of the axial segregation profile towards a more diffusion-limited case, are possible with axial static fields in excess of 1 Tesla. Strong static magnetic fields, however, can also lead to the appearance of thermoelectromagnetic convection, caused by the interaction of thermoelectric currents with the magnetic field.
Author
Magnetostatic Fields; Static Characteristics; Crystal Growth; Float Zones; Melts (Crystal Growth); Semiconductors (Materials)

19990109090 NASA Marshall Space Flight Center, Huntsville, AL USA
Measurement of Temperature Fluctuations and Microscopic Growth Rates in a Silicon Floating Zone on TEXUS36
Croell, Arne, NASA Marshall Space Flight Center, USA; Schweizer, Markus, NASA Marshall Space Flight Center, USA; Dold, P., NASA Marshall Space Flight Center, USA; Kaiser, Th., NASA Marshall Space Flight Center, USA; Lichtensteiger, M., NASA Marshall Space Flight Center, USA; Benz, K. W., NASA Marshall Space Flight Center, USA; [1999]; 1p; In English; European Space Components, 20 Mar. 2000, Noordwijk, Netherlands; No Copyright; Avail: Issuing Activity, Hardcopy; Abstract Only

Several pg experiments on sounding rockets and the Space Shuttle have shown that time-dependent thermocapillary (Marangoni) convection is the major cause for the formation of dopant striations in floating-zone grown semiconductor crystals, at least in small-scale systems not employing RF heating. to quantify this correlation, a silicon floating-zone experiment was performed during the TEXUS36 flight (February 7, 1 998) in the monoellipsoid mirror furnace TEM02-ELLI. During the experiment, temperature fluctuations in the silicon melt zone and the microscopic growth rate were simultaneously measured. Temperature fluctuations of 0.5 C - 0.7 C with main frequencies between 0.1 Hz and 0.3Hz were detectable. The microscopic growth rate fluctuated considerably around the average growth rate of 1 mm/min: rates from 4mm/min to negative values (backmelting) were observed. Dopant striations are clearly visible in the Sb-doped crystal. They were characterized by Spreading Resistance measurements and Differential Interference Contrast microscopy. The frequencies associated with the dopant inhomogeneities correspond quite well with those of the temperature fluctuations and microscopic growth rates. 3D numerical simulations were performed to predict the optimum position of the temperature sensor, to evaluate characteristic temperature amplitudes and frequencies, and to give insight into the instability mechanisms of Marangoni convection in this configuration. The simulations were in good agreement with the experimental values, showing temperature fluctuations with frequencies? 0.25 Hz and amplitudes up to 1.8 C at a position equivalent to that of the sensor tip in the experiment.
Author
Temperature Measurement; Temperature Profiles; Crystal Growth; Float Zones; Melts (Crystal Growth)

19990109134 NASA Marshall Space Flight Center, Huntsville, AL USA
Detached Growth of Germanium and Germaniumsilicon
Dold, P., Freiburg Univ., Germany; Schweizer, M., Freiburg Univ., Germany; Szofran, F., NASA Marshall Space Flight Center, USA; Benz, K. W., Freiburg Univ., Germany; [1999]; 1p; In English; 11th; ACCGE-11, 1-6 Aug. 1999, Tucson, AZ, USA; Copyright; Avail: Issuing Activity, Hardcopy; Abstract Only

Up to now, detached growth was observed mainly under microgravity, i.e. under the absence of hydrostatic pressure that hinders the formation of a free melt meniscus. the detached growth of germanium doped with gallium was obtained under 1 g conditions, the growth was performed in quartz-glass ampoule. Part of the crystal grew without wall contact, the detached growth was observed in-situ with a CCD-camera as well as after the growth process in form of growth lines and the formation of is less than 111> facets on the crystal surface. GeSi crystal (oriientation: is less than 111>, maximum silicon content: 4 at%, seed material: Ge) was grown in a pBN crucible (excluding the possibility of in-situ monitoring of the growth process). The grown crystal exhibits three growth facets, indicating also wall free growth. Surface analysis of the crystals (NDIC, SEM) and characterization of crystal segregation (EDAX, resistivity measurement) and defect structure (EPD, x-ray diffraction measurements) will be presented.
Author
Crystal Growth; Germanium; Silicon; Doped Crystals; Gallium

19990109650 NASA Marshall Space Flight Center, Huntsville, AL USA

Measurement of Temperature Fluctuations and Microscopic Growth Rates in a Silicon Floating Zone on TEXUS36

Croell, Arne, NASA Marshall Space Flight Center, USA; Schweizer, Markus, NASA Marshall Space Flight Center, USA; Dold, P., NASA Marshall Space Flight Center, USA; Kaiser, Th., NASA Marshall Space Flight Center, USA; Benz, K. W., NASA Marshall Space Flight Center, USA; Lichtensteiger, M., NASA Marshall Space Flight Center, USA; [1999]; 1p; In English; 14th, Potsdam, Germany; Sponsored by European Space Agency; No Copyright; Avail: Issuing Activity, Hardcopy; Abstract Only

Several earlier (micro)g experiments have shown that time-dependent thermocapillary (Marangoni) convection is the major cause for the formation of dopant striations in floating-zone grown semiconductor crystals, at least in small-scale systems not employing RF heating. to quantify this correlation, a silicon floating-zone experiment was performed on the TEXUS36 flight (February 7, 1 998) in the monoellipsoid mirror furnace TEM02-ELLI. During the experiment, temperature fluctuations in the silicon melt zone and the microscopic growth rate were simultaneously measured. Temperature fluctuations of 0.5 C - 0.7 C with main frequencies between 0.1 Hz and 0.3 Hz were detectable. The microscopic growth rate fluctuated considerably around the average growth rate of 1 mm/min: rates from 4mm/min to negative values (backmelting) were observed. Dopant striations are clearly visible in the Sb-doped crystal. The frequencies associated with the dopant inhomogeneities correspond quite well with those of the temperature fluctuations and microscopic growth rates. 3D numerical simulations were performed to predict the optimum position of the temperature sensor, to evaluate characteristic temperature amplitudes and frequencies, and to give insight into the instability mechanisms of Maran-goni convection in this configuration. The simulations were in good agreement with the experimental values, showing temperature fluctuations with frequencies f? 0.25 Hz and amplitudes up to 1.8 C at a position equivalent to that of the sensor tip in the experiment.

Author

Temperature Measurement; Crystal Growth; Doped Crystals; Float Zones; Melts (Crystal Growth)

19990110300 Department of Energy, Office of Energy Research, Washington, DC USA

Crystal chemistry and structural analysis of uranium oxide hydrates ***Final Report, 15 May 1995 - 31 Dec. 1997***

Miller, M. L., Department of Energy, USA; Ewing, R. C., Department of Energy, USA; Dec. 31, 1998; 8p; In English

Report No.(s): DE99-000028; DOE/ER/14540-T1; No Copyright; Avail: Department of Energy Information Bridge, Microfiche

The purpose of this research program was to develop a thorough understanding of the crystal-chemical and crystal-structural systematics of uranyl oxide hydrates which are the initial corrosion products of the UO2 in spent nuclear fuel and the principal phases in which actinides occur in the near surface environment. The scope of this program has been expanded to include all inorganic phases in which U(6+) plays a significant structural role; currently 183 phases with known crystal structures.

NTIS

Uranium Oxides; Crystal Structure; Spent Fuels; Corrosion; Physical Chemistry

19990110565 Department of Energy, Office of Financial Management and Controller, Washington, DC USA

Solvent mediated self-assembly of solids

DeYoreo, J., Department of Energy, USA; Wilson, W. D., Department of Energy, USA; Palmore, T., Department of Energy, USA; Dec. 12, 1997; 23p; In English

Report No.(s): DE98-058327; UCRL-PROP-130636; No Copyright; Avail: Department of Energy Information Bridge, Microfiche

The purpose of this proposal is to understand the interplay between solution chemistry, molecular structure, surface chemistry, and the processes of nucleation and crystal growth in solvent-mediated systems, with the goal of developing the atomic and molecular basis of a solvent-mediated self-assembly technology. We achieve this purpose by: (1) utilizing an atomic force microscopy (AFM) approach that provides in situ, real time imaging during growth from solutions, (2) by modifying kinetic Monte Carlo (KMC) models to include solution-surface kinetics, (3) by introducing quantum chemistry (QC) calculations of the potentials of the relevant chemical species and the near- surface structure of the solution, and (4) by utilizing molecular dynamics (MD) simulations to identify the minimum energy pathways to the solid state. Our work focuses on two systems chosen to address both the manometer and micron-to-millimeter length scales of assembly, the family of 2,5-diketopiperazines (X-DKPs) and the system of CaCO3 with amino acids. Using AFM, we will record the evolution of surface morphology, critical lengths, step speeds, and step-step interactions as a function of supersaturation and temperature. In addition, we measure nucleation rates and orientations of CaCO3 on polyamino acid templates. From these measurements, we extract fundamental growth parameters for input into KMC simulations whose predictions in turn are compared to the experimental observations. The KMC simulations incorporate atomic processes representing the minimum energy pathways as determined from the MD calculations. The interaction potentials of the relevant chemical species as well as the hydrated surface, including the electrochemical double layer,

used in the MD simulations are determined using coupled solutions to the Schrodinger and Poisson-Boltzmann equations which take account of electronic relaxation effects.
NTIS
Calcium Carbonates; Microstructure; Nucleation; Crystallization; Crystal Growth; Monte Carlo Method; Morphology; Quantum Chemistry; Real Time Operation; Solids; Surface Reactions

19990110696 NASA Marshall Space Flight Center, Huntsville, AL USA
A Study of Single Crystal Fatigue Failure Criteria
Sayyah, Tarek, Sverdrup Technology, Inc., USA; Swanson, Gregory R., NASA Marshall Space Flight Center, USA; Schonberg, William P., Alabama Univ., USA; 2000; 7p; In English; Space and Robotics 2000, 28 Feb. - 2 Mar. 2000, Albuquerque, NM, USA; Sponsored by American Society of Chemical Engineers, USA
Contract(s)/Grant(s): NAS8-40836; No Copyright; Avail: Issuing Activity, Hardcopy

This paper presents the results of a study whose objective was to study the applicability of different failure equations in modeling low cycle fatigue (LCF) test data for single crystal test specimens. A total of four failure criteria were considered in this study. One of the failure equations was developed by Pratt & Whitney and is based on normal and shear strains on the primary crystallographic slip planes of the single crystal material. Other failure equations considered are based on isotropic criteria. Because these failure equations were originally developed for isotropic materials such as structural steel, they were modified to be applicable to the single crystal slip systems of the LCF specimen material. by observing how closely the various equations were able to reduce the scatter in the LCF test data, the applicability of those equations in modeling the LCF test data was assessed. It is desired to subsequently use the failure equation with the highest correlation in the development of a new single crystal failure criterion for the Alternative Turbopump Development (ATD) for the space shuttle main engine (SSME) High Pressure Fuel Turbopump (HPFTP).
Author
Criteria; Crystallography; Failure; Fatigue Tests; Single Crystals; Failure Analysis; Mathematical Models; Crystal Growth

19990111596 Alabama Univ., Center for Microgravity and Materials Research, Huntsville, AL USA
A Rationale for System-Dependent Advantages and Disadvantages of Solution Crystal Growth at Low Gravity
Rosenberger, Franz, Alabama Univ., USA; Vekilov, Peter G., Alabama Univ., USA; Lin, Hong, Alabama Univ., USA; Alexander, J. Iwan D., Alabama Univ., USA; Microgravity Science and Technology; 1997; Volume 10, No. 1, pp. 29-35; In English; Sponsored in part by Alabama Supercomputer Network
Contract(s)/Grant(s): NAG8-1161; NAG8-1168; Copyright; Avail: Issuing Activity, Hardcopy, Microfiche

Protein crystallization experiments at reduced gravity have yielded crystals that, depending on the specific material, are either superior or inferior in their structural perfection compared to counterparts grown at normal gravity. A reduction of the crystals' quality due to their growth at low gravity cannot be understood from existing models. Our experimental investigations of the ground-based crystallization of the protein lysozyme have revealed pronounced unsteady growth layer dynamics and associated defect formation under steady external conditions. Through scaling analysis and numerical simulations we show that the observed fluctuations originate from the coupling of bulk transport with non-linear interface kinetics under mixed kinetics-transport control of the growth rate. The amplitude of the fluctuations is smallest when either transport or interfacial kinetics dominate the control of the crystallization process. Thus, depending on the specific system, crystal quality may be improved by either enhancing or suppressing the transport in the solution. These considerations provide, for the first time, a material-dependent rationale for the advantages, as well as the disadvantages, of reduced gravity for (protein) crystallization.
Author
Protein Crystal Growth; Microgravity

19990111652 NASA Marshall Space Flight Center, Huntsville, AL USA
Solution Growth of a Novel Nonlinear Optical Material: L-Histidine Tetrafluoroborate
Aggarwal, M. D., Alabama A & M Univ., USA; Choi, J., Alabama A & M Univ., USA; Wang, W. S., Alabama A & M Univ., USA; Bhat, K., Alabama A & M Univ., USA; Lal, R. B., Alabama A & M Univ., USA; Shields, Angela D., NASA Marshall Space Flight Center, USA; Penn, Benjamin G., NASA Marshall Space Flight Center, USA; Frazier, Donald O., NASA Marshall Space Flight Center, USA; [1998]; 1p; In English; Copyright; Avail: Issuing Activity, Hardcopy; Abstract Only

Single crystals of L-Histidine tetrafluoroborate (L-HFB), a semiorganic nonlinear optical (NLO) material have been successfully grown by the temperature lowering and evaporation methods in our laboratory. Solubility curves of L-HFB have been determined in different solvents, such as water, ethanol and acetone. The solubility of L-HFB is very low in acetone, and ethanol, therefore, it is not feasible to grow L-HFB single crystals using these solvents. Good quality single crystals of a novel nonlinear

optical material L-HFB have been grown from aqueous solution. Effects of seed orientation on morphologies of L-HFB crystals were studied. The advantages and disadvantage of both the evaporation and the temperature lowering techniques are compared. The single crystals in size 20 x 20 x 10 cubic mm were grown with deionized water as solvent in two weeks with an approximate growth rate of 1.4mm/day. The transmission range for these crystals has been found to be from 250 nm to 1500 nm.
Author
Crystals; Single Crystals; Crystal Growth; Optical Materials; Histidine

19990111654 NASA Marshall Space Flight Center, Huntsville, AL USA
Electro-Optical Effects in Thin Organic Films
Leyderman, Alexander, Puerto Rico Univ., Puerto Rico; Penn, Benjamin G., NASA Marshall Space Flight Center, USA; [1998]; 1p; In English; Copyright; Avail: Issuing Activity, Hardcopy; Abstract Only

Meta-nitroaniline (mNA) and 2-cyclo-octylamino-5-nitropyridine (COANP) single crystals were grown between two transparent fused quartz plates on which indium-tin-oxide layers were deposited. Both linear and quadratic electro-optic effects of the crystals were examined by an ac modulation method. The figures of merit for mNA and COANP are estimated to be 3.2(10-12 m/V and 4.2(10-12 m/V, respectively. It was found that the crystals were under good protection of the cells and the figure of merits of the crystals did not decrease with time. It is believed that the method adopted in the paper is applicable to electro-optic cell fabrication with other compounds if those crystals growth from melt is feasible. It is suggested that the electro-optic cells have potential fortune because of their durability and relative easy manipulation processes of crystal growth.
Author
Electro-Optical Effect; Electro-Optics; Thin Films; Organic Materials

19990111697 NASA Marshall Space Flight Center, Huntsville, AL USA
The Effect of Protein Impurities on Lysozyme Crystal Growth
Judge, Russell A., NASA Marshall Space Flight Center, USA; Forsythe, Elizabeth L., Universities Space Research Association, USA; Pusey, Marc L., NASA Marshall Space Flight Center, USA; Biotechnology and Bioengineering Journal; [1998]; In English; Copyright; Avail: Issuing Activity, Hardcopy, Microfiche

While bulk crystallization from impure solutions is used industrially as a purification step for a wide variety of materials, it is a technique that has rarely been used for proteins. Proteins have a reputation for being difficult to crystallize and high purity of the initial crystallization solution is considered paramount for success in the crystallization. Although little is written on the purifying capability of protein crystallization or of the effect of impurities on the various aspects of the crystallization process, recent published reports show that crystallization shows promise and feasibility as a purification technique for proteins. In order to further examine the issue of purity in macromolecule crystallization this study investigates the effect of the protein impurities, avidin, ovalbumin and conalbumin, at concentrations up to 50%, on the solubility, crystal face growth rates and crystal purity, of the protein lysozyme. Solubility was measured in batch experiments while a computer controlled video microscope system was used to measure the f {101} and {101} lysozyme crystal face growth rates. While little effect was observed on solubility and high crystal purity was obtained (>99.99%), the effect of the impurities on the face growth rates varied from no effect to a significant face specific effect leading to growth cessation, a phenomenon that is frequently observed in protein crystal growth. The results shed interesting light on the effect of protein impurities on protein crystal growth and strengthen the feasibility of using crystallization as a unit operation for protein purification.
Author
Impurities; Lysozyme; Protein Crystal Growth; Purification

19990113089 NASA Marshall Space Flight Center, Huntsville, AL USA
Ground Based Program for the Physical Analysis of Macromolecular Crystal Growth
Malkin, Alexander J., NASA Marshall Space Flight Center, USA; [1999]; 9p; In English
Contract(s)/Grant(s): NAG8-1408; No Copyright; Avail: CASI; A02, Hardcopy; A01, Microfiche

In a reported period in situ atomic force microscopy was utilized in our laboratory to study mechanisms of growth and kinetics of crystallization of ten protein and virus crystals. These included canavalin, thaumatin, apoferritin, lipase, catalase, t-RNA, lysozyme, xylanase, turnip yellow mosaic virus (TYMV) and satellite tobacco mosaic virus (STMV). We have also designed and constructed in our laboratory both in situ conventional two-beam Michelson and phase shift Mach-Zenhder interferometers. Computer software for the processing of the interferometric images was developed as well. Interferometric techniques were applied for studies of growth kinetics and transport phenomena in crystallization of several macromolecular crystals. As a result

of this work we have published 21 papers and have given many presentations at international and national meetings. A list of these publications and conference presentations is attached.
Author
Macromolecules; Protein Crystal Growth; Kinetics; Viruses

77
THERMODYNAMICS AND STATISTICAL PHYSICS

Includes quantum mechanics; theoretical physics; and Bose and Fermi statistics. For related information see also 25 Inorganic and Physical Chemistry and 34 Fluid Mechanics and Heat Transfer.

19990110520 Department of Energy, Office of Energy Research, Washington, DC USA
Deconfinement and hadron properties at extremes of temperature and density
Blaschke, D., Department of Energy, USA; Roberts, C. D., Department of Energy, USA; Dec. 31, 1998; 13p; In English; QCD at Finite Baryon Density, USA
Report No.(s): DE98-057948; ANL/PHY/CP-96903; CONF-980461; No Copyright; Avail: Department of Energy Information Bridge, Microfiche

After introducing essential, qualitative concepts and results, the authors discuss the application of Dyson-Schwinger equations to QCD at finite T and mu. They summarize the calculation of the critical exponents of two-light-flavor QCD using the chiral and thermal susceptibilities; and an algebraic model that elucidates the origin of an anticorrelation between the mu- and T-dependence of a range of meson properties. That model also provides an algebraic understanding of why the finite-T behavior of bulk thermodynamic properties is mirrored in their mu-dependence, and why meson masses decrease with mu even though f(sub pi) and -(anti q)q increase. The possibility of diquark condensation is canvassed. Its realization is uncertain because it is contingent upon an assumption about the quark-quark scattering kernel that is demonstrably false in some applications; e.g., it predicts the existence of colored diquarks in the strong interaction spectrum, which are not observed.
NTIS
Quantum Chromodynamics; Quarks; Chirality; Strong Interactions (Field Theory)

80
SOCIAL SCIENCES (GENERAL)

Includes educational matters.

19990111470 City Univ. of New York, Bronx, NY USA
NASA Early Learning Communities Project
Davila, Susana, City Univ. of New York, USA; HBCUs/OMUs Research Conference Agenda and Abstracts; August 1999, pp. 23; In English; See also 19990111455; No Copyright; Avail: Issuing Activity, Hardcopy; Abstract Only

The Hostos Early Learning Communities Project at Hostos Community College is located in one of the poorest congressional districts in the nation. The project serves twenty-five parents, thirty-five children and ten teaching staff members. This project has impacted the lives of children, parents and staff in the South Bronx by providing them with first time access to hands-on experience in technology. For the first time, young children, parents and teachers are exposed to computers and multimedia technology in a an educational setting. These children come from low-income families who do not have the financial resources to obtain personal computers. This exposure to technology has empowered parents and staff to encourage their children to pursue the educational opportunities of the present and future in the areas of math, science and technology. Through the use of age appropriate math and science software, young children are encouraged to pursue their curiosity and further develop their problem-solving a:nd independent thinking skills. The Hostos Early Learning Communities Project has created a new set of standards and expectations for this South Bronx community by exposing them to the power of technology and it is impact on the world.
Author
Children; Education; Instructors; Research and Development; NASA Programs

19990111478 Tennessee State Univ., Nashville, TN USA
Tennessee State University (TSU) Research Project for Increasing the Pool of Minority Engineers
Rogers, Decatur B., Tennessee State Univ., USA; HBCUs/OMUs Research Conference Agenda and Abstracts; August 1999, pp.

32; In English; See also 19990111455; No Copyright; Avail: Issuing Activity, Hardcopy; Abstract Only

The NASA Glenn Research Center funded the 1997-1998 Tennessee State University (TSU) Research Project for Increasing the Pool of Minority Engineers. The NASA/GRC-Research Project is designed to develop a cadre of engineers who have academic and research expertise in technical areas of interest to NASA, in addition to having familiarity with the mission of the: NASA/Glenn Research Center. The goal of increasing minority participation in engineering is accomplished by: (1) introducing: and exposing minority youth to engineering careers and to the required high school preparation necessary to access engineering through two campus based precollege programs: Minority Introduction to Engineering (MITE), and Engineering and Technology Preview; (2) providing financial support through scholarships for minority youth majoring in engineering disciplines of interest to NASA; (3) familiarization with the engineering profession and with NASA through field trips and summer internships at NASA/GRC; and (4) practical research exposure and experiences through research internships at NASA/GRC. A total of 75 African-American high school students participated in three MITE '98 workshops; 56% were females and 44% were males. These students came from 14 states. Each two-week MITE'98 workshop introduced the participants to aeronautics, entranced their study of algebra and trigonometry, computer science, and African- American Literature, and: provided laboratory experiences in five engineering laboratories. Field trips were taken to technology centers and to: NASA/GRC. The NASA/GRC Sponsored Research Project also provided support for three 1998 Engineering and Technology Saturday Previews with a total of 85 middle and high school students in attendance. These students were introduced to the engineering profession through laboratory experiences in each department in the College. These previews were co-sponsored by the College's Business and Industry Cluster; the Johnson City, Tennessee Chapter of Delta Sigma Theta Sorority Inc.; the First Baptist Church from Memphis, Tennessee; and NSBE Birmingham, Alabama Graduate Chapter. In addition to the precollege programs, the Research Project provided scholarships for four (4) mechanical engineering scholars. The average grade-point average for the NASA/GRC Scholars is 3.472. These four (4) scholars interned at NASA/GRC during the summer of 1998. The NASA/GRC sponsored 1997-1998 TSU Research Project of Increasing the Pool of Minority Engineers was an overwhelming success as all goals and objectives were met or exceeded. This research project provided 164 African-American: students with academic and research experiences in technical areas of interest to NASA. They gained some degree of familiarity with NASA Glenn Research Center through interactions with Glenns engineers, and through field trips and internships at Glenn. Since the inception of the NASA/GRC-TSU Research Project in 1990, 708 high school students (47% female students) have participated in MITE Precollege programs. As of 1997, 71% of MITE seniors attend college with 67% of the MITE seniors enrolled in SMET degree programs, while 31 % enrolled at TSU. NACM

Author

Engineers; Occupation; Students; Minorities; University Program

19990111484 Wilberforce Univ., OH USA

Wilberforce Power Technology in Education Program

Gordon, Edward M., Wilberforce Univ., USA; Buffinger, D. R., Wilberforce Univ., USA; Hehemann, D. G., Wilberforce Univ., USA; Breen, M. L., Wilberforce Univ., USA; Raffaelle, R. P., Wilberforce Univ., USA; HBCUs/OMUs Research Conference Agenda and Abstracts; August 1999, pp. 38; In English; See also 19990111455; No Copyright; Avail: Issuing Activity, Hardcopy; Abstract Only

The Wilberforce Power Technology in Education Program is a multipart program. Three key parts of this program will be described. They are: (1) WISE-The Wilberforce Summer Intensive Experience. This annual offering is an educational program which is designed to provide both background reinforcement and a focus on study skills to give the participants a boost in their academic performance throughout their academic careers. It is offered to entering Wilberforce students. Those students who take advantage of WISE learn to improve important skills which enable them to work at higher levels in mathematics, science and engineering courses throughout their college careers, but most notably in the first year of college study. (2) Apply technology to reaming. This is being done in several ways including creating an electronic chemistry text with hypertext links to a glossary to help the students deal with the large new vocabulary required to describe and understand chemistry. It is also being done by converting lecture materials for the Biochemistry class to PowerPoint format. Technology is also being applied to learning by exploring simulation software of scientific instrumentation. (3) Wilberforce participation in collaborative research with NASA's John H. Glenn Research Center at Lewis Field. This research has focused on two areas in the past year. The first of these is the deposition of solar cell materials. A second area involves the development of polymeric materials for incorporation into thin film batteries.

Author

Education; Students; Universities

19990111503 Kinki Univ., Faculty of Engineering, Hiroshima, Japan

Construction of The FA Education System with FMS-CAD/CAM Systems and Education of Mechanical Systems Engineering

Hayami, Takashi, Kinki Univ., Japan; Kojima, Tadatomo, Kinki Univ., Japan; Research Reports of the Faculty of Engineering, Kinki University; 1993; ISSN 0386-491X, No. 27, pp. 29-35; In Japanese; Original contains color illustrations; Copyright; Avail: Issuing Activity, Hardcopy, Microfiche

Department of Mechanical Systems Engineering of Kinki University has been started since April 1992. A full systematised FA (Factory Automation, Flexible Automation) education system is installed in this new department. The FA system has been using for development of mechanical system engineers who have the element integration (systems construction) technologies and have the mechatronic expertise on a computer managed manufacturing system. This article describes a system configuration of the FA education system and an educational policy concerning the mechanical systems engineering using developed FA system. Derived from text

Education; Mechanical Engineering; Systems Engineering; Industrial Plants; Manufacturing

81
ADMINISTRATION AND MANAGEMENT

Includes management planning and research.

19990110658 New York Academy of Sciences, New York, NY USA

Steering National Security into the Next Decade: S and T as Navigational Device

Wales, Jane, Rockefeller Brothers Fund, USA; Science, Technology, and the Economic Future; [1998], pp. 3-8; In English; ISBN 1-57331-147-2; Copyright; Avail: Issuing Activity, Hardcopy

I am going to discuss the changed security policy agenda, the forces that shape it, the logic that drives it, and the mechanisms for tying science and technology to its aims. I will then say a word about the obstacles to success. The world has changed, and with it the threats to and requirements of security. The bipolar conflict that defined the Cold War no longer dominates. And, at least three interacting and largely spontaneous trends now challenge the capacity of states to govern and of nature to provide. Derived from text

Security; Governments; International Relations

19990110715 New York Academy of Sciences, New York, NY USA

The Future of the National Laboratories: Navigating the Route to Renewal

Galvin, Robert W., Motorola, Inc., USA; Science Technology and the Economic Future; [1998], pp. 125-130; In English; Copyright; Avail: Issuing Activity, Hardcopy

For decades, one of the central elements of the nation's security system has been the system of national R&D laboratories attached to the USA Department of Energy (DOE). These institutions have become premier centers of research and technology development. They are at the cutting edge of discovery across scientific disciplines. But, with the end of the cold war, times have changed. Whereas in the past much of the DOE labs' attention was focused on critical goals of national security and military preparedness, their future promises to be much more diffuse and complex, with a shift in emphasis toward competing in the global economy.

Derived from text

Laboratories; Research and Development

19990113087 Science Applications International Corp., Huntsville, AL USA

Cost and Schedule Analytical Techniques Development: Option 2 Year ***Final Report, 1 Dec. 1996 - 30 Nov. 1997***

Dec. 01, 1997; 27p; In English

Contract(s)/Grant(s): NAS8-40431

Report No.(s): NASA/CR-1999-209745; NAS 1.26:209745; No Copyright; Avail: CASI; A03, Hardcopy; A01, Microfiche

This Final Report summarizes the activities performed by Science Applications International Corporation (SAIC) for the Option 2 Year from December 1, 1996 through November 30, 1997. The Final Report is in compliance with Paragraph 5 of Section F of the contract. This CSATD contract provides products and deliverable in the form of models, data bases, methodologies, studies and analyses for the NASA Marshall Space Flight Center's (MSFC) Engineering Cost Office (PPO3) the Program Plans and Requirements Officer (PP02), and other user organizations. Detailed Monthly Progress reports were submitted to MSFC in accordance with the contract's Statement of Work, Section TV "Reporting and Documentation". These reports spelled out each

month's specific work accomplishments, deliverables submitted, major meetings held, and other pertinent information. This Final Report will summarize these activities at higher level. During this contract Option Year, SAIC expended 29,830 man-hours in tile performance of tasks called out in the Statement of Work and reported oil in this yearly Final Report. This represents approximately 16 full-time EPs. Included are the basis Huntsville-based team, plus SAIC specialists in San Diego, Ames Research Center, Chicago, and Colorado Springs performing specific tasks for which they are uniquely qualified.
Author
Schedules; Data Bases; Costs; Models; Technology Assessment

19990113097 National Inst. of Standards and Technology, Office of Standards Services, Gaithersburg, MD USA
Directory of Federal Government Certification and Related Programs. 1999 Edition
Breitenberg, M.; Aug. 1999; 506p; In English
Report No.(s): PB99-154825; NIST/SP-739; No Copyright; Avail: CASI; A22, Hardcopy; A04, Microfiche

This directory is the fourth edition of the National Institute of Standards and Technology (NIST) directory of federal government procurement and regulatory programs which may affect products and services in the marketplace. The 1998 and 1999 editions include not only certification programs, but also other related types of federal programs which impact on the marketplace.
NTIS
Certification; Government Procurement; USA; Directories

82
DOCUMENTATION AND INFORMATION SCIENCE

Includes information management; information storage and retrieval technology; technical writing; graphic arts; and micrography. For computer documentation see 61 Computer Programming and Software.

19990107375 Lembaga Penerbangan dan Antariksa Nasional, Jakarta, Indonesia
Analysis of Scientific Journal Citations in the Aerospace Field ***Analisis Sitiran Majalah/Jurnal Ilmiah Bidang Kedirgantaraan***
Prihanto, Igif G., Lembaga Penerbangan dan Antariksa Nasional, Indonesia; Redjeki, Sri, Lembaga Penerbangan dan Antariksa Nasional, Indonesia; Rahayu, Sri, Lembaga Penerbangan dan Antariksa Nasional, Indonesia; Warta: Lembaran Tambahan Majalah LAPAN; October 1998; ISSN 0126-9754; Volume 22, No. 57, pp. 19-25; In Malay-Indonesian; No Copyright; Avail: CASI; A02, Hardcopy; A01, Microfiche

The availability of scientific magazines or journals space is of important to facilitate LAPAN's research activities and development. On the basis of this preposition, the paper aims at analyzing how frequent Scientific magazines or journals available in the agency's library were cited by LAPAN'S researchers in their work. The data collecting was carried out by documenting and revising all scientific magazines or journals space cited in the articles written by LAPAN's researchers that had been published in "Majalah LAPAN" and "Warta LAPAN". The analysis of the collected data was done by using the descriptive method. The result of the analysis shows that only a small number of LAPAN's researches who have been using scientific magazines available LAPAN's library as references in their works. On the contrary, LAPAN's researchers have been more frequent quoting foreign magazines eventhough they were not subscribed by Pusdokinfo LAPAN.
Author
Aerospace Engineering; Periodicals

19990107415 Defense Information Systems Agency, Falls Church, VA USA
Department of Defense Data Model, Version 1, FY 1999, Volume 4
Nov. 30, 1998; 203p; In English
Report No.(s): AD-A359585; No Copyright; Avail: CASI; A10, Hardcopy; A03, Microfiche

The Materiel Subject Area View identifies the data relative to equipment and supply items used by an organization or required by some enterprise without distinction as to their application for administrative or combat purposes, and which are important to the accomplishment of the DoD mission.
DTIC
Data Bases; Data Management; Management Information Systems

19990109087 NASA Goddard Space Flight Center, Greenbelt, MD USA

Information Technology Strategic Planning as a Tool for Enabling 21st Century Missions

Hughes, Peter M., NASA Goddard Space Flight Center, USA; Szczur, Martha R., NASA Goddard Space Flight Center, USA; [1999]; 6p; In English; 1999 Space Technology, 28-30 Sep 1999, Albuquerque, NM, USA; Sponsored by American Inst. of Aeronautics and Astronautics, USA

Report No.(s): AIAA Paper 99-4415; Copyright; Avail: Issuing Activity, Hardcopy

Space missions of the 21st Century will be characterized by constellations of distributed spacecraft, miniaturized sensors and satellites, increased levels of automation, intelligent onboard processing, and mission autonomy. Programmatically, these missions will be noted for dramatically decreased budgets and mission development lifecycles. to achieve these future challenges, advanced technology-especially information technology-will provide a critical role for the formulation, implementation and execution of these missions. This paper will discuss a strategic technology planning process and strategic technology program operating plan which the Information Systems Center at the Goddard Space Flight Center recently formulated and implemented. Author

Information Systems; Technological Forecasting; Space Missions; Mission Planning

19990109103 Department of Defense, Washington, DC USA

Department Defense Index of Specifications and Standards Alphabetical Listing Part I

Jul. 01, 1998; 855p; In English

Report No.(s): AD-A364656; No Copyright; Avail: CASI; A99, Hardcopy; A10, Microfiche

Part I of the Department of Defense index of specifications and standards (DODISS)in alphabetical listing is presented. DTIC

Management Information Systems; Specifications; Standardization

19990109104 Department of Defense, Washington, DC USA

Department Defense Index of Specifications and Standards Numerical Listing Part II

Jul. 01, 1998; 881p; In English

Report No.(s): AD-A364657; No Copyright; Avail: CASI; A99, Hardcopy; A10, Microfiche

Part II of the Department of Defense Index of Specifications and Standards (DODISS)in numerical listing is presented. DTIC

Management Information Systems; Specifications; Standardization

19990109107 Carnegie-Mellon Univ., Software Engineering Inst., Pittsburgh, PA USA

Survivable Network Systems: An Emerging Discipline. Revision ***Final Report***

Ellison, R. J.; Fisher, D. A.; Linger, R. C.; Lipson, H. F.; Longstaff, T.; May 1999; 48p; In English

Contract(s)/Grant(s): F19628-95-C-0003

Report No.(s): AD-A364899; CMU/SEI-97-TR-013; ESC*-TR-97-013; No Copyright; Avail: CASI; A03, Hardcopy; A01, Microfiche

Society is growing increasingly dependent upon large scale, highly distributed systems that operate in unbounded network environments. Unbounded networks, such as the Internet, have no central administrative control and no unified security policy. Furthermore, the number and nature of the nodes connected to such networks cannot be fully known. Despite the best efforts of security practitioners, no amount of system hardening can assure that a system that is connected to an unbounded network will be invulnerable to attack. The discipline of survivability can help ensure that such systems can deliver essential services and maintain essential properties such as integrity, confidentiality, and performance, despite the presence of intrusions. Unlike the traditional security measures that require central control or administration, survivability is intended to address unbounded network environments. This report describes the survivability approach to helping assure that a system that must operate in an unbounded network is robust in the presence of attack and will survive attacks that result in successful intrusions. Included are discussions of survivability as an integrated engineering framework, the current state of survivability practice, the specification of survivability requirements, strategies for achieving survivability, and techniques and processes for analyzing survivability. DTIC

Internet Resources; Data Processing Terminals; Computer Networks

19990109987 Air Force Office of Scientific Research, Bolling AFB, Washington, DC USA
AFOSR FY 97 Technology Transitions/Transfers
Dec. 1998; 35p; In English
Report No.(s): AD-A360152; No Copyright; Avail: CASI; A03, Hardcopy; A01, Microfiche
No abstract available
DTIC
Technology Transfer; Defense Program

19990110672 New York Academy of Sciences, New York, NY USA
The Policy Crisis Over Cryptography in the Information Age: Who Says Who Can Access What?
Dam, Kenneth W., Chicago Univ., USA; Science, Technology, and the Econimic Future; [1998], pp. 17-24; In English; ISBN 1-57331-147-2; Copyright; Avail: Issuing Activity, Hardcopy

As Americans we often pride ourselves on living in a free society. But we are now learning that our free and open society is a vulnerable society. Telecommunications and computer networks have increased vulnerability of both individuals and businesses, a vulnerability to which we voluntarily subject ourselves the moment we turn on the modem attached to our personal computers.
Derived from text
Cryptography; Information Systems; Information Flow; Selective Dissemination of Information

19990111483 NASA Glenn Research Center, Cleveland, OH USA
Institutional Memory Preservation at NASA Glenn Research Center
Coffey, J., University of West Florida, USA; Moreman, Douglas, Southern Univ., USA; Dyer, J., Southern Univ., USA; Hemminger, J. A., NASA Glenn Research Center, USA; HBCUs/OMUs Research Conference Agenda and Abstracts; August 1999, pp. 37; In English; See also 19990111455; No Copyright; Avail: Issuing Activity, Hardcopy; Abstract Only

In this era of downsizing and deficit reduction, the preservation of institutional memory is a widespread concern for U.S. companies and governmental agencies. The National Aeronautical and Space Administration faces the pending retirement of many of the agency's long-term, senior engineers. NASA has a marvelous long-term history of success, but the agency faces a recurring problem caused by the loss of these engineers' unique knowledge and perspectives on NASA's role in aeronautics and space exploration. The current work describes a knowledge elicitation effort aimed at demonstrating the feasibility of preserving the more personal, heuristic knowledge accumulated over the years by NASA engineers, as contrasted with the "textbook" knowledge of launch vehicles. Work on this project was performed at NASA Glenn Research Center and elsewhere, and focused on launch vehicle systems integration. The initial effort was directed toward an historic view of the Centaur upper stage which is powered by two RL-10 engines. Various experts were consulted, employing a variety of knowledge elicitation techniques, regarding the Centaur and RL-10. Their knowledge is represented in searchable Web-based multimedia presentations. This paper discusses the various approaches to knowledge elicitation and knowledge representation employed, and assesses successes and challenges in trying to perform large-scale knowledge preservation of institutional memory. It is anticipated that strategies for knowledge elicitation and representation that have been developed in this grant will be utilized to elicit knowledge in a variety of domains including the complex heuristics that underly use of simulation software packages such as that being explored in the Expert System Architecture for Rocket Engine Numerical Simulators.
Author
Engineers; Knowledge Representation; Histories; Documentation; Records

19990111601 Smithsonian Astrophysical Observatory, Cambridge, MA USA
Search and Retrieval of the AXAF Data Archive on the Web Using Java
Chary, Sumitra, Smithsonian Astrophysical Observatory, USA; Zografou, Panagoula, Smithsonian Astrophysical Observatory, USA; 1997; 1p; In English; Astronomical Data Analysis Software and Systems, 13-18 Sep. 1997, Munich, Germany
Contract(s)/Grant(s): NAS8-39073; Copyright; Avail: Issuing Activity, Hardcopy; Abstract Only

An important component of the AXAF Data Archive is the interface through the WWW. Internet applications are moving beyond delivering static content to more complex dynamic content and transaction processing. While HTML and CGI based interfaces have been possible for some time, it was not until the advent of Java database connectivity that a uniform and powerful interface to the different types of servers in the archive, with secure access of proprietary data, could become a reality. This paper will present a multi-tier architecture which integrates the data servers, web server, and an HTTP/JDBC gateway and enable data on any of the data servers in the AXAF archive to be available to clients using a Web Navigator. This Web-based solution to data browsing is currently available to browse the contents of the AXAF observing catalog and other catalogs in the archive. A Java

API for other database applications to access the data will be reviewed. Performance issues and security limitations and workarounds will be discussed.
Author
Data Retrieval; Searching; World Wide Web

19990113109 Technische Hogeschool Twente, Centre for Telematics and Information Technology, Enschede, Netherlands
Structured Information States: Raising and Resolving Issues
Hulstijn, J.; 1999; 30p; In English
Report No.(s): PB99-175861; CTIT-TR-97-18; Copyright; Avail: National Technical Information Service (NTIS), Hardcopy

This paper proposes to combine update semantics with a partition semantics of questions. The resulting update semantics with questions (USQ) models a question as a change to the information-structure of an information state. Each information state is considered to be structured by one or more issues: salient questions in need of an answer. This makes it possible to clarify the notion of relevance. An utterance U is considered relevant when it (partially) resolves one or more of the current issues. For automatic inquiry systems some ways of predicting the currently salient issue, are indicated.
NTIS
Resolution; Information

83
ECONOMICS AND COST ANALYSIS

Includes cost effectiveness studies.

19990110665 New York Academy of Sciences, New York, NY USA
The Economic Promise of Environmental Technologies
Schaefer, Mark, Office of Science and Technology Policy, USA; Science, Technology, and the Economic Future; [1998], pp. 75-84; In English; ISBN 1-57331-147-2; Copyright; Avail: Issuing Activity, Hardcopy

The facts are easy enough to understand. We live in a world of more than 5.5 billion people with finite physical and biological resources. The global population is growing rapidly, placing even greater stress on already degraded resources. What is the likely outcome? Pessimists can paint a harrowing picture: degraded waterways worldwide, unsanitary living conditions, steadily declining forested land, loss of biodiversity at accelerating rates, heavily polluted air in urban areas. It is a sorry image of failed industrialism, growth gone awry, and decrements in quality of life as a result of short-sighted economic gains. If the pessimists prevail, we will have passed along a world that non of us would want our children to live in.
Derived from text
Populations; Population Theory; Probability Theory

19990110673 New York Academy of Sciences, New York, NY USA
The Globe as the Market: The Challenge of Competitiveness for U. S. Industry
Burton, Daniel, Council on Competitiveness, USA; Science, Technology, and the Economic Future; [1998], pp. 213-219; In English; ISBN 1-57331-147-2; Copyright; Avail: Issuing Activity, Hardcopy

Where the U.S. stands in terms of global competitiveness depends, to some extent, on the indicators chosen to ascertain position and momentum. Traditional economic indicators may tell a very different story than indicators based on global technology use and diffusion. Indeed, the competitiveness debate is in the midst of transition. In the 1980s, the concern was denominated in terms of classic struggles for productivity and quality in manufacturing industries. In the 1990s and into the future, even the definition of economic products change, and so must the analysis of competitiveness.
Derived from text
Competition; USA; Manufacturing; Industries; Economics

19990110685 New York Academy of Sciences, New York, NY USA
Partnerships Linking Technology to Economic Growth: Case Experience from Around the Globe
Raymond, Susan U., New York Academy of Sciences, USA; Nichols, Rodney W., New York Academy of Sciences, USA; Science, Technology, and the Economic Future; [1998], pp. 99-112; In English; ISBN 1-57331-147-2; Copyright; Avail: Issuing Activity, Hardcopy

Experimentation with ways to link science and technology policy to plans for economic growth has been wide spread in the last decade. Policy-makers and private executives in economic regions, individual nations, and even urban areas, large and small,

have come to recognize that, as the World Bank has noted, technological progress fuels productivity and "Growing productivity is the engine of development." A key philosophy running through all successful marriages of technology and economic development is partnership among industry, universities, and public policy.
Derived from text
Economic Development; Economics; Research and Development; Technologies

19990110686 New York Academy of Sciences, New York, NY USA
Achieving Economic Growth
McConough, William J., Federal Reserve Bank of New York, USA; Science, Technology, and the Economic Future; [1998], pp. 93-98; In English; ISBN 1-57331-147-2; Copyright; Avail: Issuing Activity, Hardcopy

One of the most important underpinnings of a successful link between technology and economic development is developing and maintaining a long-term, noninflationary economic growth environment. A robust economic environment is essential both for the nation and for the New York region. There are four factors that are critical to that larger goal: a preemptive approach to monetary policy; price stability; deficit reduction; and promoting the economic and financial well-being of weaker segments of society.
Derived from text
Economic Development; Economics; Costs; Stability

84
LAW, POLITICAL SCIENCE AND SPACE POLICY

Includes NASA appropriation hearings; aviation law; space law and policy; international law; international cooperation; and patent policy.

19990107429 Lembaga Penerbangan dan Antariksa Nasional, Peneliti Bidang Analisa Sistem, Jakarta, Indonesia
Strategic Analysis of Political and Legal Developments and of Aerospace Institutions 2000-2004 ***Analisis Strategik Pembangunan Politik dan Hukum, dan Kelembagaan Kedirgantaraan 2000-2004***
Sitindjak, Alfred, Lembaga Penerbangan dan Antariksa Nasional, Indonesia; Warta: Lembaran Tambahan Majalah LAPAN; October 1998; ISSN 0126-9754; Volume 22, No. 57, pp. 1-14; In Malay-Indonesian; No Copyright; Avail: CASI; A03, Hardcopy; A01, Microfiche

In providing the firmer ground for the nation in conducting ever-increasing aerospace development, Indonesia in the First National Congress on Aerospace held in Jakarta on 3 & 4 February 1998 agreed upon outlooks and policies concerning various issues on aerospace. These outlooks and policies were then formally approved in the Second Plenary Session of the National Council of Aeronautics and Space of the Republic of Indonesia held in Jakarta on 10 December 1998. by using these outlooks and policies as guidelines, strategic analysis has been applied to define strategic plan of aerospace development during the year 2000 to 2004 especially of development of Aerospace Politics and Law, and Aerospace Institution.
Author
Strategy; Politics; Aerospace Systems

19990110657 New York Academy of Sciences, New York, NY USA
In Service to Society: Renewing the Contract Between Science and Government
Stokes, Donald E., Woodrow Wilson School at Princeton Univ., USA; Science, Technology, and the Econimic Future; [1998], pp. 9-16; In English; ISBN 1-57331-147-2; Copyright; Avail: Issuing Activity, Hardcopy

This is a period of extraordinarily rapid change, not least in federal science and technology policy. The changes in S & T policy have their roots in several background factors that are shaping the policy agenda.
Derived from text
Policies; Government/Industry Relations; Contracts

19990110660 New York Academy of Sciences, New York, NY USA
To Provide for the Common Defense: Issues in Technology and Defense Strategy for Future National Security
Thomson, James A., RAND, USA; Science, Technology, and the Economic Future; [1998], pp. 25-32; In English; ISBN 1-57331-147-2; Copyright; Avail: Issuing Activity, Hardcopy

With the end of the Cold War, there has been considerable discussion of the opportunity for shifting defense resources to domestic programs. The process of that change, however, may be longer than most observers anticipate due to the pacing of

technological change. The Department of Defense now faces a need to plan for replacing those systems that were purchased in the 1970s and 1980s, systems which are now coming to the end of their technological lives. Looking out to the year 2010, there will be a tremendous procurement need even with a smaller military force. The key question is, how do we think about such decisions? Given that there is no vital U.S. national security interest directly and immediately threatened on earth today, on what basis do we plan?
Derived from text
Defense Program; Governments; Security; Military Technology; Armed Forces (USA)

19990110667 New York Academy of Sciences, New York, NY USA
Conflicts Over World Population: Cairo and Beyond
Cohen, Joel E., Rockefeller Univ., USA; Science, Technology, and the Economic Future; [1998], pp. 65-74; In English; ISBN 1-57331-147-2; Copyright; Avail: Issuing Activity, Hardcopy

Population and prosperity will remain important issues, and will require increasing attention, for decades to come. The United Nations International Conference on Population and Development (ICPD) held September 5-12, 1994, in Cairo, Egypt, aimed to build an international consensus about these issues, and succeeded in part. In this presentation, I shall sketch the context of the Cairo conference; describe some of its main achievements; and suggest critical conflicts that remain to be resolved.
Derived from text
Conferences; Populations; Population Theory; Probability Theory

19990110671 New York Academy of Sciences, New York, NY USA
Protecting the U. S. Environment in the Wake of Regulatory Reform: The Importance of Science
Roush, G. Jon, Conservation Fund, USA; Science, Technology, and the Economic Future; [1998], pp. 35-40; In English; ISBN 1-57331-147-2; Copyright; Avail: Issuing Activity, Hardcopy

Americans have disagreed, and will no doubt continue to disagree, about the specifics of environmental policy. Under the twin banners of regulatory reform and deficit reduction, these disagreements have produced an attack on environmental laws. The preferences of the American people, however, expressed through recent elections and opinion polls, have re-emphasized the degree to which environmental protection remains a priority for the nation.
Derived from text
Environment Protection; Environmental Monitoring; Environment Management; Resources Management; USA

19990110703 New York Academy of Sciences, New York, NY USA
China Changing: Can the U. S. Support Human Rights Without Sacrificing Sino-American Relations?
Oksenberg, Michel, East-West Center, USA; Science, Technology, and the Economic Future; [1998], pp. 199-206; In English; ISBN 1-57331-147-2; Copyright; Avail: Issuing Activity, Hardcopy

The search for an intersection between steadfast support for human rights abroad and the economic and security interests of the USA is neither a new nor an easy undertaking for U.S. policy makers. In the case of China, however, finding that intersection is of critical and immediate importance. China is, and will remain, a significant, even massive, global force. Indeed, the world faces a range of issues that cannot be successfully addressed without China''s active involvement. Fortunately, there is a great deal of compatibility between the pursuit of human rights and the pursuit of many other objectives of the USA with regard to China.
Derived from text
Human Beings; Politics; Sociology; Social Isolation; China

19990110704 New York Academy of Sciences, New York, NY USA
Reforms in Russia: Emerging Trends and S and T Dimensions
Pickering, Thomas R., New York Academy of Sciences, USA; Science, Technology, and the Economic Future; [1998], pp. 191-198; In English; ISBN 1-57331-147-2; Copyright; Avail: Issuing Activity, Hardcopy

In a country with a history as rich and as deep as Russia's, it may seem premature to offer an assessment of sweeping political and economic reforms that, after all, are only three years old. Such skepticism may be particularly acute because it is barely a year since the post-reform political struggle reached its most intense and bloodiest level. In modern-day Russia, however, three years is equivalent to an era. So an assessment is appropriate and the results are positive. The process may not always be smooth and progress may be uneven, but overall, democratization and economic reforms are working in Russia.
Derived from text
Trends; Trend Analysis; Performance Prediction; Research and Development

19990110705 New York Academy of Sciences, New York, NY USA
Trade in Financial Services and Advanced Technology: Clear Issues but Elusive Policy
Hawley, F. William, Citicorp/Citibank, Iceland; Science, Technology, and the Economic Future; [1998], pp. 180-189; In English; ISBN 1-57331-147-2; Copyright; Avail: Issuing Activity, Hardcopy

The seeds of involvement in the Global Agreement on Tariffs and Trade (GATT) by financial services industries were sown many years ago.

Derived from text

International Trade; Revenue; Economics

19990110706 New York Academy of Sciences, New York, NY USA
R and D Subsidies and Countervailing Measures
Morris, Robert K., National Association of Manufacturers, USA; Science, Technology, and the Economic Future; [1998], pp. 161-170; In English; ISBN 1-57331-147-2; Copyright; Avail: Issuing Activity, Hardcopy

"Know thyself," the first inscription at Delphi should also be the first commandment for those attempt to advance U.S. interests through negotiations. In fact, for negotiators the commandment is even more difficult: "know thy country," an entity over which neither the negotiator nor the administration he or she serves can have more than the smallest illusion of control. Consequently, the knowledge required to represent U.S. national interests in international trade negotiations is more a matter of analysis and than of stewardship or vision.

Derived from text

Research and Development; Delphi Method (Forecasting)

19990110714 New York Academy of Sciences, New York, NY USA
Developments in Global Trade Negotiations: A Comprehensive Subsidy Code
Bohannon, Mark, Commerce Dept., USA; Science Technology and the Economic Future; [1998], pp. 172-178; In English; Copyright; Avail: Issuing Activity, Hardcopy

The Uruguay Round Agreement is the most comprehensive trade agreement ever. This historic agreement cuts global tariffs, protects intellectual property, disciplines agricultural and industrial subsidies, and creates an effective dispute settlement mechanism. One area that has received attention since the final round came to a close in December, 1993, is the Agreement on Subsidies and Countervailing Measures, and particularly one aspect of the code, the "green light" for certain research and development (R&D) and development activities.

Derived from text

International Trade; Economics; Revenue

85
URBAN TECHNOLOGY AND TRANSPORTATION

Includes applications of space technology to urban problems; technology transfer; technology assessment; and surface and mass transportation. For related information see also 03 Air Transportation and Safety, 16 Space Transportation, and 44 Energy Production and Conversion.

19990110659 New York Academy of Sciences, New York, NY USA
Will the U. S. Wellspring of Technology Dry Up?
Spencer, William J., SEMATECH, USA; Science, Technology, and the Economic Future; [1998], pp. 153-158; In English; ISBN 1-57331-147-2; Copyright; Avail: Issuing Activity, Hardcopy

The last decade has witnessed significant change in the organization and conduct of industrial research and development. As a result, industry is different and the current industrial profile has important implications for the USA and its global competitiveness.

Derived from text

Research and Development; Technologies; Industries

19990110682 New York Academy of Sciences, New York, NY USA
Choices Amidst Change: S and T Resource Priorities for U. S. Global Leadership
GIbbons, John H., Office of Science and Technology Policy, USA; Science, Technology, and the Economic Future; [1998], pp. 131-136; In English; ISBN 1-57331-147-2; Copyright; Avail: Issuing Activity, Hardcopy

On many aspects of the role of science and technology in the nation's future, it is possible to find broad agreement across a spectrum of policy views. Congress, the Administration, and most commentators agree that the United States has embarked on an era of great change; that science and technology bring economic rewards to society; that discovery is unpredictable and research essential; that failure to maintain a robust investment in research and development will cripple U.S. competitiveness; and, that science and technology are critical to the nation's future. Indeed, Vannevar Bush, author of a seminal work on U.S. science policy, made the very same observations fifty years ago.
Derived from text
Research and Development; Technologies; USA; Leadership

19990110683 New York Academy of Sciences, New York, NY USA
Science, Technology, and the 104th Congress ***Interim Report***
Walker, Robert S., USA House of Representatives, USA; Science, Technology, and the Economic Future; [1998], pp. 137-144; In English; ISBN 1-57331-147-2; Copyright; Avail: Issuing Activity, Hardcopy

Science and technology provide an essential foundation for the future of this nation. Just as constraints on resources require choices to be made in virtually every other area of public life, choices must also be made in our allocation of government resources to science and technology programs. Because cleverness, which in this case means the ability to manipulate information, will create the wealth of the future, we must carefully determine those priorities in science that will lead to the development of new knowledge.
Derived from text
Budgeting; Allocations; Research and Development; Technologies

19990110684 New York Academy of Sciences, New York, NY USA
Integrating the Military and Civilian Technology Base: A Long and Winding Road to---Where?
Drezner, Stephen M., RAND, USA; Science, Technology, and the Economic Future; [1998], pp. 113-122; In English; ISBN 1-57331-147-2; Copyright; Avail: Issuing Activity, Hardcopy

Dual-use technology strategies are underpinned by two important, complementary rationales. On the one hand, dual-use strategies are seen as combining the best commercial technologies and capabilities with defense systems design expertise to produce necessary military technologies more quickly and at a lower cost than has characterized defense technology R&D in the past. On the other hand, such strategies are seen as reinforcing and strengthening the link between defense research and development expenditures and the nation's overall commercial performance and economic growth. Attractive though both of these arguments are, each encounters difficulties on the road between the theory and the practice of integrating military and civilian technology development.
Derived from text
Military Technology; Defense Program; Systems Engineering; Research and Development

19990110707 New York Academy of Sciences, New York, NY USA
Civilian Technology for Economic Growth: The Changing Face of Federal R and D
Prabhakar, Arati, National Inst. of Standards and Technology, USA; Science, Technology, and the Economic Future; [1998], pp. 145-152; In English; ISBN 1-57331-147-2; Copyright; Avail: Issuing Activity, Hardcopy

Technology is the most dynamic, non-linear tool that can most fundamentally change the ground rules of economic competitiveness. Education and training, ability to market, and capital all matter. But technology is the only tool that can change the ground rules in all of these other areas.
Derived from text
Economics; Economic Development; Growth; Technologies; Research and Development

19990110716 New York Academy of Sciences, New York, NY USA
Science and Technology in Hong Kong beyond 1997: Emerging Trends and Issues
Lau, Shelley, Home Affairs, Hong Kong; Science, Technology, and the Economic Future; [1998], pp. 207-212; In English; ISBN 1-57331-147-2; Copyright; Avail: Issuing Activity, Hardcopy

Increasingly, knowledge-based development underpins Hong Kong's economic strategy. It is no secret that Hong Kong is on the brink of a new future as part of China, the largest, most populous nation on earth. Yet, even now, the Hong Kong economy supports not just the six million people in its own territory, but also another four million who are economically linked across the border with China. With the current pace of innovation and change in the world, and with the growing strength of our economic

competitors in Southeast Asia, it has become clear that the trade and manufacturing base of Hong Kong economy must make a leap of technological innovation into the future.
Derived from text
Research and Development; Technologies; Technology Utilization; China; Hong Kong

88
SPACE SCIENCES (GENERAL)

19990111715 Helsinki Univ. of Technology, Kylmaelae Finland
Metsaehovi Radio Observatory Annual Report 1998
Urpo, S.; Mujunen, A.; 1999; 58p; In English
Report No.(s): PB99-159089; HUT-KURP-15; Copyright; Avail: National Technical Information Service (NTIS), Microfiche
Contents include the following: Introduction; Research Activities; Radio Astronomical Instrumentation; Extragalactic Radio Sources; Observations with Other Facilities; VLBI Research; Solar Research; HRDL for Alpha Magnetic Spectrometer (AMS); Radio Spectroscopy; Publications; Visits to Foreign Institutes; Visiting Scientists; Teaching; Other Activities; Personnel in 1998; and List of Figures.
NTIS
Radio Observation; Radio Astronomy; Finland; Radio Spectroscopy; Remote Sensing

89
ASTRONOMY

Includes radio, gamma-ray, and infrared astronomy, and astrometry.

19990106593 NASA Goddard Space Flight Center, Greenbelt, MD USA
The Design and Performance of the Astro-E/XRS Signal Processing System
Boyce, K. R., NASA Goddard Space Flight Center, USA; Baker, R. G., NASA Goddard Space Flight Center, USA; Dumonthier, J. J., NASA Goddard Space Flight Center, USA; Kelley, R. L., NASA Goddard Space Flight Center, USA; Stahle, C. K., NASA Goddard Space Flight Center, USA; Szymkowiak, A. E., NASA Goddard Space Flight Center, USA; Winkert, G. E., NASA Goddard Space Flight Center, USA; Audley, M. D., NASA Goddard Space Flight Center, USA; Gendreau, K. C., NASA Goddard Space Flight Center, USA; Fujimoto R., Tokyo Univ., Japan; [1999]; 1p; In English, 18-23 Jul. 1999, Denver, CO, USA; Sponsored by International Society for Optical Engineering, USA; No Copyright; Avail: Issuing Activity, Hardcopy; Abstract Only
We describe the signal processing system of the Astro-E XRS instrument. The Calorimeter Analog Processor (CAP) provides bias and power for the detectors and amplifies the detector signals by a factor of 20,000. The Calorimeter Digital Processor (CDP) performs the digital processing of the calorimeter signals, detecting X-ray pulses and analyzing them by optimal filtering. We describe the operation of pulse detection, pulse height analysis, and risetime determination. We also discuss performance, including the three event grades (hi-res, mid-res, and low-res), anticoincidence detection, counting rate dependence, and noise rejection.
Author
Design Analysis; Signal Processing; Digital Systems; X Ray Analysis; Pulse Amplitude

19990106595 Smithsonian Astrophysical Observatory, Cambridge, MA USA
Chandra Interactive Analysis of Observations
Fruscione, Antonella, Smithsonian Astrophysical Observatory, USA; Siemiginowska, Aneta, Smithsonian Astrophysical Observatory, USA; [1999]; 1p; In English; 8th; XMM Science Survey Consortium Science Advisory Group Meeting, 22-31 Oct. 1999, Milan, Italy
Contract(s)/Grant(s): NAS8-39073; No Copyright; Avail: Issuing Activity, Hardcopy; Abstract Only
The Chandra X-R-ay Observatory has been launched on July 23 1999. The first public release of the Chandra data analysis system, CIAO (Chandra Interactive Analysis of Observations) will be available in the near future. The XMM Science Survey Consortium is considering the possibility of using the whole or parts of CIAO to analyse observations from the XMM satellite and during the meeting we will give presentations and demonstrations of parts of CIAO, including the new GUIs developed for

"FirstLook" analysis, data filtering and browsing; SHERPA, the multi-dimensional, multi-missions modelling and fitting application; CHIPS, the Chandra Imaging and Plotting System; generic data manipulation tools and other applications.
Author
Observatories; Data Acquisition; Systems Analysis; Imaging Techniques

19990106596 NASA Marshall Space Flight Center, Huntsville, AL USA
Pulse Profiles, Accretion Column and a flare in Gx 1+4 During a Faint State
Giles, A. B., NASA Marshall Space Flight Center, USA; Galloway, D. K., NASA Marshall Space Flight Center, USA; Greenhill, J. G., NASA Marshall Space Flight Center, USA; Storey, M. C., NASA Marshall Space Flight Center, USA; Wilson, C. A., NASA Marshall Space Flight Center, USA; [1999]; 1p; In English; No Copyright; Avail: Issuing Activity, Hardcopy; Abstract Only

The Rossi X-ray Timing Explorer (RXTE) spacecraft observed the X-ray pulsar GX 1+4 for a period of 34 hours on July 19/20 1996. The source faded from an intensity of approx. 20 mcrab to a minimum of less than or equal to 0.7 mcrab and then partially recovered towards the end of the observation. This extended minimum lasted approx. 40,000 seconds. Phase folded light curves at a barycentric rotation period of 124.36568 +/- 0.00020 seconds show that near the center of the extended minimum the source stopped pulsing in the traditional sense but retained a weak dip feature at the rotation period. Away from the extended minimum the dips are progressively narrower at higher energies and may be interpreted as obscurations or eclipses of the hot spot by the accretion column. The pulse profile changed from leading-edge bright before the extended minimum to trailing-edge bright after it. Data from the Burst and Transz'ent Source Experiment (BATSE) show that a torque reversal occurred less than 10 days after our observation. Our data indicate that the observed rotation departs from a constant period with a P/P value off approx. -5% per year at a 4.5(sigma) significance. We infer that we may have serendipitously obtained data. with high sensitivity and temporal resolution about the time of an accretion disk spin reversal. We also observed a rapid flare which had some precursor activity close to the center of the extended minimum.
Author
X Rays; Gamma Ray Bursts; High Resolution; Pulsars

19990106598 NASA Marshall Space Flight Center, Huntsville, AL USA
Polycapillary X-Ray Optics for X-Ray Astronomy
Russell, C. H., National Inst. of Standards and Technology, USA; Gubarev, M., NASA Marshall Space Flight Center, USA; Kolodziejczak, J., NASA Marshall Space Flight Center, USA; Joy, M., NASA Marshall Space Flight Center, USA; MacDonald, C. A., State Univ. of New York, USA; Gibson, W. M., State Univ. of New York, USA; [1999]; 1p; In English; No Copyright; Avail: Issuing Activity, Hardcopy; Abstract Only

High-energy x-ray spectrometry from astronomical sources is difficult due to low flux rates and high background. Polycapillary x-ray optics can be used to increase the signal-to-noise ratio by focusing photons onto a small energy dispersive detector. Two optics, both designed for x-ray astronomy, have been built and tested as collimating optics with a microfocus x-ray source for x-ray energies up to 70 keV and as focusing optics with parallel x-rays up to 50 keV. Results from these tests show that polycapillary x-ray optics have transmission efficiencies ranging from 5% to 40% and signal gains ranging from 5 to over 100 for energies up to 50 keV. Furthermore the results show that these optics have potential for use up to 100 keV. The experimental results as well as simulations for the measured and for optimized optics will be discussed.
Author
X Ray Optics; Signal to Noise Ratios; Collimation; Astronomy; X Ray Spectroscopy

19990107333 Cerro Tololo Inter-American Observatory, La Serena, Chile
A Large Local Rotational Speed for the Galaxy Found from Proper-Motions: Implications for the Mass of the Milky-way
Mendez, Rene A., Cerro Tololo Inter-American Observatory, Chile; Platais, Imants, Yale Univ., USA; Girard, Terrence M., Yale Univ., USA; Kozhurina–Platais, Vera, Yale Univ., USA; vanAltena, William F., Yale Univ., USA; September 1999; 11p; In English
Report No.(s): NOAO-Preprint-852; No Copyright; Avail: Issuing Activity, Hardcopy

Predictions from a Galactic Structure and Kinematic model are compared to the absolute proper-motions of about 30,000 randomly selected stars with 9 is less than B(sub J) is less than 19 derived from the Southern Proper-Motion Program (SPM) toward the South Galactic Pole. The absolute nature of the SPM proper-motions allow us to measure not only the relative motion of the Sun with respect to the local disk, but also, and most importantly, the overall state of rotation of the local disk with respect to galaxies. The SPM data are best fit by models having a solar peculiar motion of +5 km/s in the V-component (pointing in the direction of Galactic rotation), a large LSR speed of 270 km/s and a disk velocity ellipsoid that points towards the Galactic center. We stress, however, that these results rest crucially on the assumptions of both axisymmetry and equilibrium dynamics. The

absolute proper-motions in the U-component indicate a solar peculiar motion of 11.0 +/- 1.5 km/s, with no need for a local expansion or contraction term. The implications of the large LSR speed are discussed in terms of gravitational mass of the Galaxy inferred from the most recent and accurate determination for the proper-motion of the LMC. We find that our derived value for the LSR is consistent both with the mass of the Galaxy inferred from the motion of the Clouds (3 - 4 x 10(exp 12) solar mass to approximately 50 kpc), as well as the timing argument, based on the binary motion of M31 and the Milky Way, and Leo I and the Milky Way (> 1.2 x 10(exp 12) solar mass to approximately 200 kpc).
Author
Galactic Structure; Milky Way Galaxy; Stellar Evolution; Galactic Evolution

19990107359 NASA Marshall Space Flight Center, Huntsville, AL USA
The GLAST Mission: Using Scintillating Fibers as Both the Tracker and the Calorimeter
Fisman, Gerald J., NASA Marshall Space Flight Center, USA; [1997]; 1p; In English; SCIFI97: Scintillating and Fiber Detectors, 2-6 Nov. 1997, South Bend, IN, USA; No Copyright; Avail: CASI; A01, Hardcopy; A01, Microfiche; Abstract Only; Abstract Only

The Gamma-Ray Large Area Space Telescope (GLAST) has been identified as the next major NASA mission in gamma-ray astronomy. It will operate at energies above 20 MeV to study some of the most energetic objects in the Universe. While the baseline tracker detector for GLAST during the study phase is based on silicon strips, we believe that scintillating fibers have considerable advantages for this purpose. Among the performance advantages are: larger effective area, better angular resolution at low energies and larger field of view. Practical advantages include: lower cost, the use of a common technology for both the tracker and the calorimeter, lower power consumption, and a simplified thermal design. Several alternative readout schemes for the fibers are under study.
Author
Calorimeters; Scintillating Fibers; Silicon; Gamma Ray Telescopes; Gamma Ray Astronomy; Gamma Ray Sources (Astronomy)

19990107376 Smithsonian Astrophysical Observatory, Cambridge, MA USA
Cluster Substructure and Large Scales Filaments
Foreman, William, Smithsonian Astrophysical Observatory, USA; [1997]; 1p; In English; Galaxy Clusters as Cosmological Probes, 4-11 Oct. 1997, Munich, Germany
Contract(s)/Grant(s): NAS8-39073; No Copyright; Avail: CASI; A01, Hardcopy; A01, Microfiche; Abstract Only; Abstract Only

New results from ASCA and ROSAT will be presented showing evidence for large scale structure from X-ray observations. The talk will present observations of the Coma cluster showing the interaction between an infalling group and the ambient cluster medium. For Abell 85, large scale structure is seen, consistent with the overall supercluster in which Abell 85 resides. Both X-ray temperature and X-ray surface brightness maps show evidence for merging along a supercluster filament. The filament orientation is well defined from optical observations of the overall galaxy distribution as well as the ellipticity of the central cD galaxy. The overall optical galaxy distribution shows a very complex region of sheets both behind and in front of A85. Finally, a progress report on a cluster survey using archival ROSAT PSPC and ROSAT HRI data will be presented.
Author
Elliptical Galaxies; Galactic Clusters; Cometary Atmospheres; Cluster Analysis; Image Analysis

19990107379 NASA Marshall Space Flight Center, Huntsville, AL USA
Near Real-Time Imaging of the Galactic Plane with BATSE
Harmon, B. A., NASA Marshall Space Flight Center, USA; Zhang, S. N., NASA Marshall Space Flight Center, USA; Robinson, C. R., NASA Marshall Space Flight Center, USA; Paciesas, W. S., NASA Marshall Space Flight Center, USA; Barret, D., Harvard, USA; Grindlay, J., Harvard, USA; Bloser, P., Harvard, USA; Monnelly, C., Harvard, USA; [1997]; 1p; In English; No Copyright; Avail: CASI; A01, Hardcopy; A01, Microfiche; Abstract Only; Abstract Only

The discovery of new transient or persistent sources in the hard X-ray regime with the BATSE Earth occultation Technique has been limited previously to bright sources of about 200 mCrab or more. While monitoring known source locations is not a problem to a daily limiting sensitivity of about 75 mCrab, the lack of a reliable background model forces us to use more intensive computer techniques to find weak, previously unknown emission from hard X-ray/gamma sources. The combination of Radon transform imaging of the galactic plane in 10 by 10 degree fields and the Harvard/CFA-developed Image Search (CBIS) allows us to straightforwardly search the sky for candidate sources in a +/- 20 degree latitude band along the plane. This procedure has

been operating routinely on a weekly basis since spring 1997. We briefly describe the procedure, then concentrate on the performance aspects of the technique and candidate source results from the search.
Author
Real Time Operation; Imaging Techniques; Radio Occultation; X Ray Sources; Gamma Ray Sources (Astronomy); Radio Sources (Astronomy); Galactic Bulge

19990107385 NASA Goddard Space Flight Center, Greenbelt, MD USA
Initial Evaluation of Space Environmental Effects on the NGST Sunshield
Wooldridge, Eve M., NASA Goddard Space Flight Center, USA; Powers, Charles, NASA Goddard Space Flight Center, USA; 1998; 1p; In English; Astronomical Telescopes and Instrumentation, 20-28 Mar. 1998, Kono, HI, USA; Sponsored by International Society for Optical Engineering; Copyright; Avail: Issuing Activity, Hardcopy; Abstract Only

The "Next Generation Space Telescope" (NGST), the follow-on telescope to the Hubble Space Telescope, will carry on exploration of the early universe with a primary mirror 6-8 meters in diameter optimized to operate in the infrared. The mirror and its instruments will perform extremely deep exposures at near infra-red wavelengths (0.5-30 microns), and will operate for 5-10 years. In order to achieve the requirements, cryogenic temperatures between 30-60 Kelvin must be maintained on the telescope (OTA) and in the science module (SIM). A primary feature for passive cooling in the designs presented is that of an enormous, light-weight deployable sunshield. As a result, issues of contamination from the sunshield and space environmental effects on the sunshield itself present a critical matter: if the sunshield becomes a source of contamination, or if environmental effects damage the sunshield, the NGST mission could be compromised or could fail completely. A molecular redistribution analysis has been performed on the Goddard Space Flight Center (GSFC) design for NGST. The analysis revealed that because the shield will initially cool down faster than the OTA, the shield would not be a significant source of molecular contamination during the cooling phase. However, if the shield were ever to warm up, it would be a very large source of molecular contamination. The sunshield itself is susceptible to degradation from an external source of contamination: the space environment at L2 or at 1 x 3 AU. It is therefore necessary to design the sunshield to withstand the space environment. Thin films and coatings on the sunshield have been evaluated and testing has begun so that a suitable film and/or coating can be chosen or developed for the NGST mission. The evaluation and test results will be presented.
Author
Aerospace Environments; Coating; Extraterrestrial Environments; Spaceborne Telescopes; Astronomical Observatories; Heat Shielding; Cryogenic Cooling; Coatings

19990107390 NASA Marshall Space Flight Center, Huntsville, AL USA
Observations with the Chandra X-Ray Observatory (CXO)
Weisskopf, Martin C., NASA Marshall Space Flight Center, USA; [1999]; 1p; In English, 11-14 Apr. 1999, Charleston, SC, USA; No Copyright; Avail: Issuing Activity, Hardcopy; Abstract Only

All of us are anticipating the launch of the Chandra X-Ray Observatory (CXO), formally known as the Advanced X-Ray Astrophysics Facility (AXAF). I will describe the highlights of the test and scientific calibration program that has preceded the launch activities and give an overview of the scientific investigations that are possible with NASA's next Great Observatory.
Author
X Ray Astrophysics Facility; X Ray Astronomy; X Ray Detectors

19990108596 NASA Goddard Space Flight Center, Greenbelt, MD USA
On X-Ray Variability in Seyfert Galaxies
Turner, T. J., NASA Goddard Space Flight Center, USA; George, I. M., NASA Goddard Space Flight Center, USA; Nandra, K., NASA Goddard Space Flight Center, USA; Turcan, D., Maryland Univ., USA; [1999]; 14p; In English
Contract(s)/Grant(s): NAG5-7385; No Copyright; Avail: CASI; A03, Hardcopy; A01, Microfiche

This paper presents a quantification of the X-ray variability amplitude for 79 ASCA observations of 36 Seyfert 1 galaxies. We find that consideration of sources with the narrowest permitted lines in the optical band introduces scatter into the established correlation between X-ray variability and nuclear luminosity. Consideration of the X-ray spectral index and variability properties together shows distinct groupings in parameter space for broad and narrow-line Seyfert 1 galaxies, confirming previous studies. A strong correlation is found between hard X-ray variability and FWHM Hbeta. A range of nuclear mass and accretion rate across the Seyfert population can explain the differences observed in X-ray and optical properties. An attractive alternative model, which

does not depend on any systematic difference in central mass, is that the circumnuclear gas of NLSy1s is different to BLSy1s in temperature, optical depth, density or geometry.
Author
X Ray Sources; X Rays; Variability; X Ray Astronomy; Seyfert Galaxies; Active Galactic Nuclei

19990109127 Universities Space Research Association, Huntsville, AL USA
Coherence between QPOs in X-Ray Pulsars
Finger, Mark H., Universities Space Research Association, USA; [1999]; 1p; In English, 12-15 Apr. 1999, Charleston, SC, USA; Sponsored by American Astronomical Society, USA; Copyright; Avail: Issuing Activity, Hardcopy; Abstract Only

Rossi X-ray Timing Explorer (RXTE) observations of Cen X-3 and 4U 1626 have shown that when a low frequency (upsilon(sub qpo) approx. 50 mHz) Quazi-Periodic Oscillation (QPO) is presented in the power spectrum of these sources, smaller QPOs also appear in the upper and lower sidebands of the spin frequency upsilon(sub s), and in the sidebands of the spin frequency harmonics. This is expected if the QPO is a modulation in the accretion rate.However, the QPO in the lower sideband of the spin frequency (upsilon = upsilon(sub s) - upsilon(sub qpo)) is stronger than the QPO in the upper sideband (upsilon = upsilon(sub s) + upsilon(sub qpo)), which is not consistent with pure acretion rate modulation. I will present a method for measuring the phase coherent between the main QPO and any of the sideband QPOs, and apply this to RXTE observations. Preliminary results for Cen X-3 show that the QPO in the lower sideband of the spin frequency is highly coherent with the main QPO, while the QPO in the upper sideband is not. Implications for possible QPO mechanisms will be discussed.
Author
Coherence; Oscillations; X Ray Timing Explorer; Pulsars

19990109148 NASA Goddard Space Flight Center, Greenbelt, MD USA
Does Velocity Redistribution Really Enhance the HE 304 A Line to Observed Intensities?
Jordan, Stuart, NASA Goddard Space Flight Center, USA; Andretta, Vincenzo, NASA Goddard Space Flight Center, USA; Garcia, Adriana, Coimbra Univ., Portugal; Brosius, Jeffrey, Raytheon ITSS, USA; Behring, William, NASA Goddard Space Flight Center, USA; [1999]; 4p; In English
Contract(s)/Grant(s): NCC5-377; No Copyright; Avail: CASI; A01, Hardcopy; A01, Microfiche

Previous work by this group has demonstrated that small-scale nonthermal velocities probably play a significant role in enhancing the intensity of the He II 304 A line above values predicted by the static atmosphere NLTE theories, and more in conformity with Skylab and SOHO observations. This presentation briefly summarizes the evidence for this conclusion, emphasizing SOHO and correlated groundbased observations, of which examples are presented. However, in contrast to the previous studies, the tact taken here is more critical, asking the question ”Can velocity redistribution fully explain the observations of the 304 A line, and what counter-indications and problems remain?” The conclusion reached is that, while velocity redistribution plays a significant role in the intensity enhancement, it may not be the whole story. Some other mechanism, associated with velocity filtration, may be at work.
Author
Transition Region and Coronal Explorer; Solar Transition Region; Solar Corona; Solar Atmosphere; SOHO Mission

19990109163 NASA Marshall Space Flight Center, Huntsville, AL USA
A Survey of the 30.5 Day Cycle in LMC X-4
Scott, Matthew, Universities Space Research Association, USA; Leahy, Denis, Calgary Univ., Canada; [1998]; 1p; In English; Copyright; Avail: Issuing Activity, Hardcopy; Abstract Only

LMC X-1 is a high mass X-ray binary system with a 13.5 sec period accreting pulsar n in a 1.4 day orbit. The system displays a super-orbital cycle of X-ray intensity variations repeating every 30.5 days consisting of alternating high and low X-ray flux state . This phenomenon is believed to be caused by a tilted , precessing accretion disk similar to that in Her X-1. We present results of a study of the 30.5 day ”long” cycle of LMC X-4 using RXTE observations. The 30.5 day cycle was surveyed with a series of RXTE pointings. We present the resulting lightcurve and compare it to the average lightcurve obtained from the RXTE All SKY Monitor. We show color - color and color-intensity plots as well as representative spectra. The pulse profile evolution across the single High state of LMC X-4 is shown . there is no evidence for a second weaker high state in LMC X-4 unlike that in Her X-1. We compare the properties of the long cycle in LMC X-4 with those in Her X-1.
Author
Binary Stars; X Ray Binaries; Display Devices; Light Curve; Pulsars

19990110305 National Optical Astronomy Observatories, Tucson, AZ USA

Faint Blue Objects on the Hubble Deep Field North and South as Possible Nearby Old Halo White Dwarfs

Mendez, R. A., Cerro Tololo Inter-American Observatory, Chile; Minniti, D., Pontificia Univ. Catolica de Chile, Chile; October 1999; 13p; In English; Sponsored in part by the RFG foundation, a Chilean Fondecyt grant and DIPUC

Contract(s)/Grant(s): W-7405-eng-48; N01990440

Report No.(s): NOAO-Preprint-854; No Copyright; Avail: CASI; A03, Hardcopy; A01, Microfiche

Using data derived from the deepest and finest angular resolution images of the universe yet acquired by astronomers at optical wavelengths using the Hubble Space Telescope (HST) in two postage-stamp sections of the sky (Williams et al. 1996a,b), plus simple geometrical and scaling arguments, we demonstrate that the faint blue population of point-source objects detected on those two fields (Mendez et al. 1996) could actually be ancient halo white dwarfs at distances closer than about 2 kpc from the Sun. This finding has profound implications, as the mass density of the detected objects would account for about half of the missing dark matter in the Milky-Way, thus solving one of the most controversial issues of modern astrophysics. The existence of these faint blue objects points to a very large mass locked into ancient halo white dwarfs. Our estimate indicates that they could account for as much as half of the dark matter in our Galaxy, confirming the suggestions of the MACHO microlensing experiment. Because of the importance of this discovery, deep follow- up observations with HST within the next two years would be needed to determine more accurately the kinematics (tangential motions) for these faint blue old white dwarfs.

Author

Data Bases; Angular Resolution; White Dwarf Stars; Universe; Milky Way Galaxy; Faint Objects

19990110309 Oxford Univ., Dept. of Astrophysics, Oxford, UK

The Evolution of Classical Doubles: Clues from Complete Samples

Blundell, Katherine M., Oxford Univ., UK; Rawlings, Steve, Oxford Univ., UK; Willott, Chris J., Instituto de Astrofisica de Canarias, Spain; 1999; 12p; In English; Original contains color illustrations

Report No.(s): OUAST/99/15; No Copyright; Avail: CASI; A03, Hardcopy; A01, Microfiche

We describe the inter-dependence of four properties of classical double radio sources - spectral index, linear size, luminosity and redshift - from an extensive study based on spectroscopically- identified complete samples. We use these relationships to discuss aspects of strategies for searching radio galaxies at extreme redshifts, in the context of possible capabilities of the new generation of proposed radio telescopes.

Author

Red Shift; Luminosity; Radio Galaxies

19990110698 Smithsonian Astrophysical Observatory, Cambridge, MA USA

The CfA-ROSAT Survey of Distant Clusters of Galaxies

McNamara, Brian, Smithsonian Astrophysical Observatory, USA; [1998]; 1p; In English; 1st; 1st Science with XMM, 28 Sep. - 4 Oct. 1998, Nordwiji, Netherlands

Contract(s)/Grant(s): NAS8-39073; Copyright; Avail: Issuing Activity, Hardcopy; Abstract Only

We (Vikhlinin, McNamara, Forman, Jones, Hornstrup, Quintana) have completed a new survey of distant clusters of galaxies, which we use to to study cluster evolution over cosmological timescales. The clusters were identified as extended X-ray sources in 650 ROSAT PSPC images of high Galactic latitude fields. Our catalog of approximately 230 extended X-ray sources covers 160 square degrees on the sky. Ours is the largest of the several ROSAT serendipitous cluster surveys in progress (e.g. SHARC, ROSATi, WARPS etc.). Using V,R,I imagery obtained at several observatories, we find that greater than 90% of the X-ray sources are associated with distant clusters of galaxies. We have obtained spectroscopic redshifts for nearly 80 clusters in our catalog, and we have measured photometric redshifts for the remaining clusters. Our sample contains more than 20 clusters at z is greater than 0.5. I will discuss the logN-logS relationship for our clusters. Because our large survey area, we are able to confirm the evolution of the most luminous distant clusters first seen in the Einstein Extended Medium Sensitivity Survey. In addition, I will discuss the relationships between optical richness, core radius, and X-ray luminosity for distant, X-ray-selected clusters.

Author

Cosmology; Red Shift; Galactic Clusters; X Ray Sources; ROSAT Mission; X Ray Astronomy

19990111607 Smithsonian Astrophysical Observatory, Cambridge, MA USA

How to Piece Together Diffracted Grating Arms for AXAF Flight Data

Alexov, Anastasia, Smithsonian Astrophysical Observatory, USA; McLaughlin, Warren, TRW, Inc., USA; Huenemoeder, Dave, Massachusetts Inst. of Tech., USA; 1997; 1p; In English; Astronomical Data Analysis Software and Systems, 13-18 Sep. 1997, Munich, Germany

Contract(s)/Grant(s): NAS8-39073; Copyright; Avail: Issuing Activity, Hardcopy; Abstract Only

AXAF's high and low transmission energy gratings (HETG and LETG) disperse photons along the dispersion (r) and cross dispersion (d) directions, away from zero order. Dispersion is essentially the order*wavelength relation of each photon. The goal of the gratings data processing is to correctly identify the photons in the grating arms and to give each photon its order*wavelength coordinate (also called grating coordinates). The orientation of the grating arms on the sky plane will vary from one observation interval to another, depending on the spacecraft pointing and roll. The analysis process of calculating the grating coordinates starts with the creation of mask region files for the grating arms. These masks associate each of the sections in the image with either a grating arm, zero order, or background region. Then, the location of the aspect corrected zero order centroid is found in the sky plane. The "final" step is to calculate the grating coordinates using the zero order position, aspect solution, and instrument geometry. In this process, for each time period, every photon which falls on the detector is tagged as "on" or "off" a spectral region. If it is a diffracted grating arm photon, then its relative position to zero order in chip space is input into the coordinate transformation library which calculates the order*wavelength position of that photon, using tangent plane geometry. Finally, in the case of the ACIS instrument (10 energy resolving CCD's) used with either grating, one can also distinguish the order of the photons, which allows the separation of the order*wavelength relation to get just wavelength. AXAF grating data files are typically several hundred megabytes in size. The size of these files presents an enormous challenge in writing data analysis software which can efficiently process the data quickly and accurately. Our paper will go into the details of the analysis procedure, as well as the technical constraints we had to overcome in order to process the tasks efficiently.

Author

Gratings (Spectra); Spectral Bands; Diffraction Radiation; Photorefractivity; Dispersing; Photons

19990111693 NASA Marshall Space Flight Center, Huntsville, AL USA

On the Dramatic Spin-up/Spin-Down Torque Reversals in Accreting Pulsars

Nelson, Robert W., California Inst. of Tech., USA; Bildsten, Lars, California Univ., USA; Chakrabarty, Deepto, Massachusetts Inst. of Tech., USA; Finger, Mark H., NASA Marshall Space Flight Center, USA; Koh, Danny T., California Inst. of Tech., USA; Prince, Thomas A., California Inst. of Tech., USA; Rubin, Bradley C., NASA Marshall Space Flight Center, USA; Scott, D. Mathew, NASA Marshall Space Flight Center, USA; Vaughan, Brian A., California Inst. of Tech., USA; Wilson, Robert B., NASA Marshall Space Flight Center, USA; Astrophysical Journal; Oct. 20, 1997; Volume 488, pp. L117-L120; In English; Copyright; Avail: Issuing Activity, Hardcopy, Microfiche

Dramatic torque reversals between spin-up and spin-down have been observed in half of the persistent X-ray pulsars monitored by the Burst and Transient Space Experiment (BATSE) all-sky monitor on the Compton Gamma Ray Observatory. Theoretical models developed to explain early pulsar timing data can explain spin-down torques via a disk-magnetosphere interaction if the star nearly corotates with the inner accretion disk. to produce the observed BATSE torque reversals, however, these equilibrium models require the disk to alternate between two mass accretion rates, with M+/- producing accretion torques of similar magnitude but always of opposite sign. Moreover, in at least one pulsar (GX 1+4) undergoing secular spin-down, the neutron star spins down faster during brief (approximately 20 day) hard X-ray flares-this is opposite the correlation expected from standard theory, assuming that BATSE pulsed flux increases with mass accretion rate. The 10 day to 10 yr intervals between torque reversals in these systems are much longer than any characteristic magnetic or viscous timescale near the inner disk boundary and are more suggestive of a global disk phenomenon. We discuss possible explanations of the observed torque behavior. Despite the preferred sense of rotation defined by the binary orbit, the BATSE observations are surprisingly consistent with an earlier suggestion for GX 1+4: the disks in these systems somehow alternate between episodes of prograde and retrograde rotation. We are unaware of any mechanism that could produce a stable retrograde disk in a binary undergoing Roche lobe overflow, but such flip-flop behavior does occur in numerical simulations of wind-fed systems. One possibility is that the disks in some of these binaries are fed by an X-ray-excited wind.

Author

Torque; Accretion Disks; Pulsars; Flip-Flops; Gamma Ray Astronomy

19990111694 Smithsonian Astrophysical Observatory, Center for Astrophysics, Cambridge, MA USA

The Variability and Spectrum of NGC 4051 from Deep, Simultaneous EUVE and XTE Observations

Fruscione, Antonella, Smithsonian Astrophysical Observatory, USA; Cagnoni, Ilaria, Smithsonian Astrophysical Observatory, USA; Papadakis, Iossif, Southampton Univ., UK; McHardy, Ian, Southampton Univ., UK; 1998; In English, 5-17 Mar. 1998, Milan, Italy

Contract(s)/Grant(s): NAS8-39073; Copyright; Avail: Issuing Activity, Hardcopy, Microfiche

We present timing and spectral analysis of the data collected by the Extreme Ultraviolet Explorer Satellite (EUVE) for the Seyfert 1 galaxy NGC 4051 during 1996. NGC 4051 was observed twice in May 1996 and again in December 1996 for a total

of more than 200 ksec. The observations were always simultaneous with hard X-ray observations conducted with the X-Ray Timing Explorer (XTE). The EUVE light curves are extremely variable during each observation, with the maximum variability during May 1996 when we registered changes by a factor of 21 over 8 hours and more than a factor of 24 variations from peak to minimum. We detected signal in the EUVE spectrograph in the 75-100 Arange which is well fitted by absorbed power law models. We will illustrate the results of our spectral and detailed power spectrum analysis for the simultaneous EUVE and XTE spectra and light curves and discuss the consequences on possible emission mechanisms.
Author
Variability; X Ray Astronomy; Spectrum Analysis; Seyfert Galaxies

19990111699 Smithsonian Astrophysical Observatory, Cambridge, MA USA
Fitting and Modeling of the AXAF Data with the ASC Fitting Application
Doe, Stephen, Smithsonian Astrophysical Observatory, USA; Siemiginowski, Aneta, Smithsonian Astrophysical Observatory, USA; Ljungberg, M., Smithsonian Astrophysical Observatory, USA; Joye, W., Smithsonian Astrophysical Observatory, USA; 1997; 1p; In English; Astronomical Data Analysis Software and Systems, 13-18 Sep. 1997, Munich, Germany
Contract(s)/Grant(s): NAS8-39073; Copyright; Avail: Issuing Activity, Hardcopy; Abstract Only

The AXAF mission will provide x-ray data with unprecedented spatial and spectral resolution. Because of the high quality of these data, the AXAF Science Center (ASC) will provide a new data analysis system, part of which includes a new fitting application. Our intent is to enable users to do fitting that is too awkward with or beyond the scope of existing astronomical fitting software. Our main goals are: (1) to take advantage of the full capabilities of the AXAF, we intend to provide a more sophisticated modeling capability (i.e., models that are f(x,y,E,t), models to simulate the response of AXAF instruments, and models that enable ”Joint-mode” fitting, i.e., combined partial-spectral or spectral-temporal fitting); and (2) to provide users with a wide variety of models, optimization methods, and fit statistics. In this paper, we discuss the use of an object-oriented approach in our implementation, the current features of the fitting application, and the features scheduled to be added in the coming year of development. Current features include: an interactive, command line interface; a modeling language which allows users to build models from arithmetic combinations of base functions; a suite of optimization and fit statistics; the ability to perform fits to multiple data sets simultaneously; and an interface with SM and SAOtng to plot or image data, models, and/or residuals from a fit. We currently provide a modeling capability in one or two dimensions and have recently made an effort to perform spectral fitting in a manner similar to XSPEC. We also allow users to dynamically link the fitting application to algorithms written by users. Our goals for the coming year include: incorporating the SPEC model library as a subset of models available in the application; enabling ”joint-mode” analysis; and adding support for new algorithms.
Author
Fitting; X Ray Astrophysics Facility; Data Smoothing

19990113118 Smithsonian Astrophysical Observatory, Cambridge, MA USA
Solar-B X-ray Telescope (XRT) Concept Study Report
Golub, Leon, Smithsonian Astrophysical Observatory, USA; Oct. 29, 1999; 184p; In English
Contract(s)/Grant(s): NAS8-99099
Report No.(s): NASA/DRD-867MA-001; XRT-PM-99-002; No Copyright; Avail: CASI; A09, Hardcopy; A02, Microfiche

The X-ray observations from the Yohkoh SXT provided the greatest step forward in our understanding of the solar corona in nearly two decades. Expanding on the accomplishments of Yohkoh, we believe that the scientific objectives of the Solar-B mission are achieved with a significantly improved X-ray telescope (XRT) similar to the SXT. The Solar-B XRT will have twice the spatial resolution and a broader temperature response, while building on the knowledge gained from the successful Yohkoh mission. We present the scientific justification for this view, discuss the instrumental requirements that flow from the scientific objectives, and describe the instrumentation to meet these requirements. We then provide a detailed discussion of the design activities carried out during Phase A, noting the conclusions that were reached in terms of their implications for the detailed design activities which are now commencing. Details of the instrument that have changed as a result of the Phase A studied are specifically noted, and areas of concern going into Phase B are highlighted. XRT is a grazing-incidence (GI) modified Wolter I X-ray telescope, of 35cm inner diameter and 2.7m focal length. The 2048x2048 back-illuminated CCD (now an ISAS responsibility) has 13.5 micron pixels, corresponding to 1.0 arcsec and giving full Sun field of view. This will be the highest resolution GI X-ray telescope ever flown for Solar coronal studies, and it has been designed specifically to observe both the high and low temperature coronal plasma. A small optical telescope provides visible light images for co-alignment with the Solar-B optical and EUV instruments. The XRT science team is working in close cooperation with our Japanese colleagues in the design and construction of this instrument. All of the expertise and resources of the High Energy and Solar/Stellar Divisions of the Center for Astrophysics are being made available to this program, and our team will carry its full share of responsibility for mission

operations, data reduction and education and public outreach. All aspects of the XRT design were reviewed during Phase A. The study focussed particularly on those aspects that have the greatest affect on instrument performance and extended lifetime, on the image quality error budget, and on the camera (mechanical and electrical) interface and the instrument mounting interfaces. The present instrument design differs in some details from that originally proposed. Selection of the XRT for Phase A study was contingent upon the removal of the camera and its associated electronics, and the acceptance of a stringent cost cap. The removal of the electronics left the XRT without control electronics for the instrument mechanisms. A mechanism controller was therefore added. The removal of the camera resulted in major complications to the integration and test plan. After many discussions, it was decided that the system would be less expensive, and the risk of unacceptable performance lower, if we include a focus mechanism. The remainder of the XRT design baseline matches the proposed configuration. Data requirements for the XRT are driven by the science plans, which are based on the physical processes in the solar outer atmosphere. Discussions to date of the XRT observing plan, both alone and in conjunction with the other Solar-B instruments, shows that the XRT needs 2 Gbits of on-board storage, at least one circulating buffer of 640 Mbits, and twelve 10- minute downlinks per day in order to carry out its required programs. Derived from text

X Ray Telescopes; Solar X-Rays; Solar Corona; Systems Analysis; Optical Measuring Instruments; Extreme Ultraviolet Radiation; Image Resolution

19990113187 Smithsonian Astrophysical Observatory, Cambridge, MA USA

A Description of the Capabilities of AXAF

Fabbiano, Giuseppina, Smithsonian Astrophysical Observatory, USA; 1998; In English, 26-30 Apr. 1998, Palermo, Italy; Sponsored by Italian Astronomical Society, Italy

Contract(s)/Grant(s): NAS8-39073; Copyright; Avail: Issuing Activity, Hardcopy, Microfiche

This talk will describe the Advanced X-ray Astrophysics Facility (AXAF) scientific capabilities, including mirror characteristics, focal plane instruments and gratings. AXAF has an unparalleled subarcsecond spatial resolution, coupled with medium to high spectral resolution, and it will return a totally new picture of the X-ray sky. For the first time we will be able to image in detail complex regions such as the centers of galaxies and globular clusters, and at the same time gather information on the spectral characteristics of the X-ray emission. We will be able to obtain high resolution grating spectra of bright stars and Active Galactic Nuclei (AGN). We will be able to take the deepest look ever possible into the X-ray sky and detect sources at cosmological distances.

Author

X Ray Astrophysics Facility; Mirrors; Focal Plane Devices; Gratings (Spectra); X Ray Astronomy

90
ASTROPHYSICS

Includes cosmology; celestial mechanics; space plasmas; and interstellar and interplanetary gases and dust. For related information see also 75 Plasma Physics.

19990106592 Smithsonian Astrophysical Observatory, Cambridge, MA USA

New Results From Chandra: Abundances in Stellar Coronae

Drake, Jeremy, Smithsonian Astrophysical Observatory, USA; [1999]; 1p; In English; 11th; Cambridge Workshop: Cool Stars, Stellar Systems and the Sun, 1-10 Oct. 1999, Canary Islands, Spain

Contract(s)/Grant(s): NAS8-39073; No Copyright; Avail: Issuing Activity, Hardcopy; Abstract Only

There is considerable evidence, both solar and stellar, that the chemical compositions of stellar coronae differ from their underlying 1)hotospheres. The differences for solar-type stars appear to be related to FIP, whereas the differences for active stars are more mysterious and perhaps suggest metal depletion. Results to-date will be reviewed and new results from the Chandra X-ray Observatory based on calibration and Emission Line Project observations of late-type stellar coronae, will be presented.

Author

Stellar Coronas; Solar Corona; Chemical Composition; Data Acquisition

19990107414 Institut des Hautes Etudes Scientifiques, Bures-sur-Yvette, France

New WIMP Population in the Solar System and New Signals for Dark-Matter Detectors

Damour, T., Institut des Hautes Etudes Scientifiques, France; Krauss, L. M., Case Western Reserve Univ., USA; Jul. 10, 1998; 44p; In English

Report No.(s): PB99-122301; IHES/P/98/55; No Copyright; Avail: CASI; A03, Hardcopy; A01, Microfiche

The authors describe in detail how perturbations due to the planets can cause a subpopulation of WIMPs captured by scattering in surface layers of the Sun to evolve to have orbits which no longer intersect the Sun. The authors argue that such WIMPs, if their orbit has a semi-major axis less than 1/2 of Jupiter's, can persist in the solar system for cosmological timescales. This leads to a new, previously unanticipated WIMP population intersecting the Earth's orbit. The WIMP-nucleon cross sections required for this population to be significant are precisely those in the range predicted for SUSY dark matter, lying near the present limits obtained by direct underground dark matter searches using cyrogenic detectors. Thus, if a WIMP signal is observed in the next generation of detectors, a potentially measurable signal due to this new population must exist.
NTIS
Dark Matter; Solar System Evolution; Perturbation Theory; Nuclear Fusion; Cosmology; Perturbation

19990109649 Columbia Univ., Columbia Astrophysics Lab., New York, NY USA
Dark Matter in the Universe and in the Galaxy ***Final Report, 15 Oct. 1995 - 14 Oct. 1999***
Kamionkowski, Marc, Columbia Univ., USA; October 1999; 9p; In English
Contract(s)/Grant(s): NAG5-3091
Report No.(s): CAL-3170; No Copyright; Avail: CASI; A02, Hardcopy; A01, Microfiche

During the past four years, Prof. Kamionkowski and collaborators have made progress in research on the nature and distribution of dark-matter in the Universe and in the Galaxy, and on related topics in astrophysics and cosmology. We have made progress on research on the cosmic microwave background, large-scale structure, issues related to particle dark matter, and the gamma-ray-burst enigma. A significant fraction of the research supported by this ATP has been on the cosmic microwave background (CMB). Prof. Kamionkowski and collaborators showed how the polarization of the CMB could be used to detect long-wavelength gravitational waves, such as those produced by inflation. With Kosowsky, Prof. Kamionkowski calculated the amplitude of a stochastic gravitational-wave background that could be detected for a satellite experiment of a given sensitivity and angular resolution. They showed that polarization should improve the sensitivity oa MAP to these gravity waves, and that the Planck Surveyor should do even better. Prof. Kamionkowski, Caldwell, and a student calculated and illustrated the CMB temperature/polarization pattern produced by a single plane-wave gravitational wave. They calculated the amplitude of such a wave that would be detectable with MAP and Planck, and compared that with the sensitivity of traditional gravitational-wave detectors like LIGO and LISA. With Lue and Wang, the PI showed how parity violation from new high-energy physics could conceivably give rise to an observable signature in the CMB polarization. With Loeb, Prof. Kamionkowski showed how measurement of the polarization of CMB photons scattered by hot gas in a cluster could be used to determine the quadrupole moment of the CMB incident on that cluster. Prof. Kamionkowski and Jaffe calculated the amplitude of secondary anisotropies produced by scattering of CMB photons from reionized regions. Research has also been carried out on probing the large-scale distribution of mass in the Universe today, and on structure-formation theories. They investigated the possibility of determining the large-scale distribution of mass in the Universe via measurement of ellipticity-ellipticity correlations in the FIRST radio survey induced by weak gravitational lensing due to mass inhomogeneities along the line of sight. Dr. Summers, Prof. Kamionkowski, and a student investigated the distribution of protogalactic masses and angular momenta in an effort to understand how the luminosity function and angular-momentum distribution of disk galaxies arises from an initial power spectrum of density perturbations. Several projects related to the distribution and possible detection of dark matter in our Galactic halo were studied. The PI was involved in several projects involving the calculation of nuclear-reaction rates needed for stellar evolution and for predictions of solar-neutrino fluxes.
Derived from text
Dark Matter; Universe; Cosmology; Astrophysics; Disk Galaxies

19990110311 National Optical Astronomy Observatories, Tucson, AZ USA
Galactic Kinematics Towards the South Galactic Pole. First Results from the Yale-San Juan Southern Proper-Motion Program
Mendez, Rene A., Cerro Tololo Inter-American Observatory, Chile; Platais, Imants, Yale Univ., USA; Giarard, Terrence M., Yale Univ., USA; Kozhurina–Platais, Vera, Yale Univ., USA; vanAltena, William F., Yale Univ., USA; October 1999; 64p; In English
Report No.(s): NOAO-Preprint-885; No Copyright; Avail: CASI; A04, Hardcopy; A01, Microfiche

The predictions from a Galactic Structure and Kinematic model code are compared to the color counts and absolute proper-motions derived from the Southern Proper-Motion survey covering more than 700 sq deg toward the South Galactic Pole in the range 9 less than B(sub j) less than 19. The theoretical assumptions and associated computational procedures, the geometry for the kinematic model, and the adopted parameters are presented in detail and compared to other Galactic Kinematic models

of its kind. The data to which the model is compared consists of more than 30,000 randomly selected stars, and it is best fit by models with a solar peculiar motion of +5 km/ s in the V-component (pointing in the direction of Galactic rotation), a large LSR speed 1 of 270 km/ s, and a (disk) velocity ellipsoid that always points towards the Galactic center. The absolute proper-motions in the U-component indicate a solar peculiar motion of 11.0 +/- 1.5 km/ s, with no need for a local expansion or contraction term. The fainter absolute motions show an indication that the thick-disk must exhibit a rather steep velocity gradient of about -36 km/ s kpc with respect to the LSR. We are not able to set constraints on the overall rotation for the halo, nor on the thick-disk or halo velocity dispersions. Some substructure in the U & V proper-motions could be present in the brighter bins 10 less than B(sub j) less than 13, and it might be indicative of (disk) moving groups.
Author
Galactic Structure; Galactic Rotation; Velocity Distribution; Surveys; Computation

19990110532 California Inst. of Tech., Pasadena, CA USA
350 Micron Dust Emission from High Redshift Objects, *1992-2000*
Cox, Pierre, Paris Univ., France; Benford, Dominic J., California Inst. of Tech., USA; Omont, Alain, Centre National de la Recherche Scientifique, France; Phillips, Thomas G., California Inst. of Tech., USA; McMahon, Richard G., Institute of Astronomy, UK; 1999; 6p; In English; Supported in part from INSU (Programmes Grands Telescopes Etrangers) and PCMI
Contract(s)/Grant(s): NSF-AST-96-15025; Copyright; Avail: Issuing Activity, Hardcopy

We report observations of a sample of high redshift sources (z is approximately greater than 1.8 and approximately less than 4.7), mainly radio-quiet quasars, at 350 microns using the SHARC bolometer camera at the Caltech Submillimeter Observatory. Nine sources were detected (approximately greater than 4sigma) and upper limits were obtained for 11 with 350 micron flux density limits (3sigma) in the range 30- 125 mJy. Combining published results at other far-infrared and millimeter wavelengths with the present data, we are able to estimate the temperature of the dust, finding, relatively low values, averaging 50K. From the spectral energy distribution, we derive dust masses of a few 10(exp 8)/h(sub 100) square solar mass and luminosities of 4-33x10(exp 12)/h(sub 100) square solar lumens (uncorrected for any magnification) implying substantial star formation activity. Thus, both the temperature and dust masses are not very different from those of local ultraluminous infrared galaxies. For this redshift range, the 350 micron observations trace the 60-100 micron rest frame emission and are thus directly comparable with IRAS studies of low redshift galaxies.
Author
Galaxies; Luminosity; Millimeter Waves; Quasars; Red Shift; X Ray Astronomy; Cosmic Dust; Active Galaxies

19990110579 Oxford Univ., Oxford Astrophysics, Oxford, UK
The Hyperluminous Infrared Quasar 3C 318 and Its Implications for Interpreting Sub-MM Detections of High-Redshift Radio Galaxies
Willott, Chris J., Instituto de Astrofisica de Canarias, Spain; Rawlings, Steve, Oxford Univ., UK; Jarvis, Matt J., Oxford Univ., UK; Oct. 25, 1999; 14p; In English
Contract(s)/Grant(s): NAS5-26555; FMRX-CT96-0068
Report No.(s): OUAST/99/17; astro-ph/9910422; Copyright; Avail: Issuing Activity, Hardcopy

We present near-infrared spectroscopy and imaging of the compact steep-spectrum radio source 3C 318 which shows it to be a quasar at redshift z = 1.574 (the z = 0.752 value previously reported is incorrect). 3C 318 is an IRAS, ISO and SCUBA source so its new redshift makes it the most intrinsically luminous far-infrared (FIR) source in the 3C catalogue (there is no evidence of strong gravitational lensing effects). Its bolometric luminosity greatly exceeds the 10(exp 13) solar luminosity level above which an object is said to be hyperluminous. Its spectral energy distribution (SED) requires that the quasar heats the dust responsible for the FIR flux, as is believed to be the case in other hyperluminous galaxies, and contributes (at the greater than 10% level) to the heating of the CIA dust responsible for the sub-mm emission. We cannot determine whether a starburst makes an important contribution to the heating of the coolest dust, so evidence for a high star-formation rate is circumstantial being based on the high dust, and hence gas, C-1 mass required by its sub-mm detection. We show that the current sub-mm and FIR data available for the highest-redshift radio galaxies are consistent with SEDs similar to that of 3C 318. This indicates that at least some of this population may be detected in the sub-mm because of dust heated by the quasar nucleus, and that interpreting sub-mm detection as evidence for very high (approx. less than 1000 solar mass/yr) star-formation rates may not always be valid. We show that the 3C318 quasar is slightly reddened (A(sub v) approx. = 0.5), the most likely cause of which is SMC-type dust in the host galaxy. If very distant radio galaxies are reddened in a similar way then we show that only slightly greater amounts of dust could obscure the quasars in these sources. We speculate that the low fraction of quasars amongst the very high redshift (z approx. greater than

3) objects in low-frequency radio-selected samples is the result of such obscuration. The highest-z objects might be preferentially obscured because like 3C318 they are inevitably observed very shortly after the jet-triggering event, or because their host galaxies are richer in dust and gas at earlier cosmic epochs, or because of some combination of these two effects.
Author
Quasars; Gravitational Effects; Infrared Radiation; Interstellar Extinction; Luminescence; Radio Galaxies; Starburst Galaxies; Infrared Spectroscopy

19990110581 Oxford Univ., GEMINI Support Group, Oxford, UK
Herbig-Haro Flows Near Compact Reflection Nebulae
Aspin, Colin, Oxford Univ., UK; Reipurth, Bo, Colorado Univ., USA; [1999]; 18p; In English
Report No.(s): OUAST/99/16; No Copyright; Avail: CASI; A03, Hardcopy; A01, Microfiche

We have performed an optical CCD imaging survey of star forming regions identified through compact reflection nebulae and/or embedded IRAS sources in order to search for new Herbig-Haro (HH) flows. Here we present the discovery of hitherto unknown HH objects in 7 of these regions. A bright bow shock, HH 461, is found along the axis defined by the previously known HH 164 jet from the luminous young A-star LkH(alpha) 198. The little known cometary nebula PP 11, illuminated by the partly embedded IRAS source 03507+3801 in the Perseus clouds, contains a HH object HH 462, found along the symmetry axis of the nebula. A small jet, HH 463, emanates from the recently identified FU Orionis candidate PP 13S, while another HH flow, HH 464/HH 465 appears to originate from the nearby T Tauri star PP 13N. A group of HH objects, HH 466-468, are located around the nebulous young T Tauri binary GK Tau. A well collimated HH jet and an associated bow shock, HH 470, are found extending from the young nebulous T Tauri star Haro 4-255 in Orion, and a tiny reflection nebula and associated HH object, HH 469 is located close by the deeply embedded source Class I source Haro 4-255 FIR. In light of these new HH flows in Haro 4-255, we re-interpret existing C-12O data on this source in terms of two overlapping molecular outflows. The young star LkH(alpha) 316 and the nearby IRAS source 05451+0037 in Orion are found to be associated with a cluster of HH objects, HH 471-474. It is likely that a nearby and previously identified HH object, HH 71, also originates in this region. Finally, a chain of HH objects, HH 475, are found near the little studied compact bipolar reflection nebula PP 95 in the Cygnus clouds. The origin of this HH chain remains unclear and HH 475 may equally well be driven by one of several luminous massive young stars in the region.
Author
A Stars; Imaging Techniques; Bipolarity; Herbig-Haro Objects; Massive Stars; Nebulae; Surveys; T Tauri Stars

19990111701 NASA Marshall Space Flight Center, Huntsville, AL USA
AXAF
Elvis, Martin, NASA Marshall Space Flight Center, USA; 1997; 1p; In English; 23rd; 188th, 26-30 Sep. 1997, Kyoto, Kyoto, Japan, Japan; Sponsored by International Astronomical Union, Unknown; Copyright; Avail: Issuing Activity, Hardcopy; Abstract Only

This talk will review how AXAF will revolutionize X-ray astronomy through its radically better imaging and spectroscopic resolution. Examples from many fields of astrophysics will be given.
Author
X Ray Astrophysics Facility; X Ray Astronomy; Astrophysics

19990113088 Massachusetts Univ., Dept. of Physics and Astronomy, Amherst, MA USA
Boundary Conditions for the Paleoenvironment: Chemical and Physical Processes in Dense Interstellar Clouds: Summary of Research ***Final Report, 15 Oct. 1996 - 14 Oct. 1999***
Irvine, William M., Massachusetts Univ., USA; [1999]; 8p; In English
Contract(s)/Grant(s): NAG5-3653; No Copyright; Avail: CASI; A02, Hardcopy; A01, Microfiche

The basic theme of this program was the study of molecular complexity and evolution for the biogenic elements and compounds in interstellar clouds and in primitive solar system objects. Research included the detection and study of new interstellar and cometary molecules and investigation of reaction pathways for astrochemistry from a comparison of theory and observed molecular abundances. The latter includes studies of cold, dark clouds in which ion-molecule chemistry should predominate, searches for the effects of interchange of material between the gas and solid phases in interstellar clouds, unbiased spectral surveys of particular sources, and systematic investigation of the interlinked chemistry and physics of dense interstellar clouds. In addition, the study of comets has allowed a comparison between the chemistry of such minimally thermally processed

objects and that of interstellar clouds, shedding light on the evolution of the biogenic elements during the process of solar system formation. One PhD dissertation on this research was completed by a graduate student at the University of Massachusetts. An additional 4 graduate students at the University of Massachusetts and 5 graduate students from other institutions participated in research supported by this grant, with 6 of these thus far receiving PhD degrees from the University of Massachusetts or their home institutions. Four postdoctoral research associates at the University of Massachusetts also participated in research supported by this grant, receiving valuable training.
Author
Boundary Conditions; Chemical Analysis; Molecular Clouds; Physical Chemistry

19990113112 California Univ., San Diego, CA USA
Enstatite Meteorites and the Original Heterogeneity of Mn-53 Distribution in the Solar Nebula ***Final Report***
Lugmair, Guenter W., California Univ., USA; [1999]; 4p; In English
Contract(s)/Grant(s): NAG5-4145; No Copyright; Avail: CASI; A01, Hardcopy; A01, Microfiche

We have shown earlier that the relative abundance of radiogenic Cr-53 in bulk ordinary chondrites (approximately 0.48 epsilon) is clearly different from that in the earth-moon system (0 epsilon). The SNC parent body (Mars) is characterized by an intermediate Cr-53 excess (approximately 0.23 epsilon). We have also shown that the Mn-Cr systematics of the howardite-eucrite-diogenite parent body (HED PB, the asteroid Vesta) is consistent with the chondritic Mn/Cr ratio in the bulk HED PB and that it has a Cr-53 excess of approximately 0.5 epsilon units which is within error the same as that of chondrites. It appears that the excesses of Cr-53 in these planets are a function of their present heliocentric distance. The study of some other meteorite classes (angrites, pallasites, primitive achondrites) has shown that their Mn-CR systematics is consistent with that of the ordinary chondrites. The observed gradient in the radiogenic Cr-53 abundances can be explained by a). an early volatility controlled radial Mn/Cr fractionation in the nebula or b). an original heterogeneity of Mn-53. The first assumption, however, requires the Mn/Cr ratios of the bulk Earth and Mars to be considerably lower than the inferred model Mn/Cr ratios for these two planets. For this reason, we suggested that the observed gradient is due to an original radial Mn-53 heterogeneity in the late nebula.
Derived from text
Enstatite; Heterogeneity; Manganese Isotopes; Planetary Nebulae; SNC Meteorites

19990113202 NASA Marshall Space Flight Center, Huntsville, AL USA
Discovery of the 198 s X-Ray Pulsar GRO J2058+42
Wilson, Colleen A., NASA Marshall Space Flight Center, USA; Finger, Mark H., NASA Goddard Space Flight Center, USA; Harmon, B. Alan, NASA Marshall Space Flight Center, USA; Chakrabarty, Deepto, Massachusetts Inst. of Tech., USA; Strohmayer, Tod, Universities Space Research Association, USA; [1997]; 1p; In English; No Copyright; Avail: Issuing Activity; Abstract Only, Hardcopy, Microfiche

GRO J2058+42, a transient 198 second x-ray pulsar, was discovered by the Burst and Transient Source Experiment (BATSE) on the Compton Gamma-Ray Observatory (CGRO), during a ”giant” outburst in 1995 September-October. The total flux peaked at about 300 mCrab (20-50 keV) as measured by Earth occultation. The pulse period decreased from 198 s to 196 s during the 46-day outburst. The pulse shape evolved over the course of the outburst and exhibited energy dependent variations. BATSE observed five additional weak outbursts from GRO J2058+427 each with two week duration and peak pulsed flux of about 15 mcrab (20-50 keV), that were spaced by about 110 days. An observation of the 1996 November outburst by the Rossi X-ray Timing Explorer (RXTE) Proportional Counter Array (PCA) localized the source to within a 4’ radius error circle (90% confidence) centered on R.A. = 20 h 59 m.0, Decl. = 41 deg 43 min (J2000). Additional shorter outbursts with peak pulsed fluxes of about 8 mCrab were detected by BATSE halfway between the first four 15 mCrab outbursts. The RXTE All-Sky Monitor detected 8 weak outbursts with approximately equal durations and intensities. GRO J2058+42 is most likely a Be/X-ray binary that appears to outburst at periastron and apastron. No optical counterpart has been identified to date and no x-ray source was present in the error circle in archival ROSAT observations.
Author
Gamma Ray Observatory; Pulsars; Gamma Ray Bursts; Gamma Ray Sources (Astronomy); X Ray Astronomy; X Rays

91
LUNAR AND PLANETARY EXPLORATION

Includes planetology; and manned and unmanned flights. For spacecraft design or space stations see 18 Spacecraft Design, Testing and Performance.

19990108480 NASA Goddard Space Flight Center, Greenbelt, MD USA
Mercury's Magnetosphere
Slavin, J. A., NASA Goddard Space Flight Center, USA; Encyclopedia of Astronomy and Astrophysics; [1999]; 5p; In English; No Copyright; Avail: CASI; A01, Hardcopy; A01, Microfiche

Among the major discoveries made by the Mariner 10 mission to the inner planets was the existence of an intrinsic magnetic field at Mercury with a dipole moment of approx. 300 nT R(sup 3, sub M). This magnetic field is sufficient to stand off the solar wind at an altitude of about 1 R(sub M) (i.e. approx. 2439 km). Hence, Mercury possesses a 'magnetosphere' from which the so]ar wind plasma is largely excluded and within which the motion of charged particles is controlled by the planetary magnetic field. Despite its small size relative to the magnetospheres of the other planets, a Mercury orbiter mission is a high priority for the space physics community. The primary reason for this great interest is that Mercury unlike all the other planets visited thus far, lacks a significant atmosphere; only a vestigial exosphere is present. This results in a unique situation where the magnetosphere interacts directly with the outer layer of the planetary crust (i.e. the regolith). At all of the other planets the topmost regions of their atmospheres become ionized by solar radiation to form ionospheres. These planetary ionospheres then couple to electrodynamically to their magnetospheres or, in the case of the weakly magnetized Venus and Mars, directly to the solar wind. This magnetosphere-ionosphere coupling is mediated largely through field-aligned currents (FACs) flowing along the magnetic field lines linking the magnetosphere and the high-latitude ionosphere. Mercury is unique in that it is expected that FACS will be very short lived due to the low electrical conductivity of the regolith. Furthermore, at the earth it has been shown that the outflow of neutral atmospheric species to great altitudes is an important source of magnetospheric plasma (following ionization) whose composition may influence subsequent magnetotail dynamics. However, the dominant source of plasma for most of the terrestrial magnetosphere is the 'leakage'of solar wind across the magnetopause and more direct entry through the northern and southern cusps. Although Mariner 10 did not return plasma composition measurements, the Hermean magnetosphere should be ideal for measuring the manner and rate of solar wind plasma entry due to the lack of strong internal atmospheric sources. Finally, the solar wind conditions experienced by Mercury as it orbits the Sun at 0.31 to 0.47 AU are quite different from those typically encountered by the Earth. This may allow for new understanding of the external factors affecting the transfer of mass, momentum and energy from the solar wind to planetary magnetospheres. This article provides a brief overview of what is now known about Mercury's magnetosphere and why it is a priority target for future planetary missions.
Author
Mercury (Planet); Magnetospheres; Magnetic Fields; Solar Wind; Windpower Utilization; Wind Velocity; Wind Direction; Regolith

19990108484 NASA Marshall Space Flight Center, Huntsville, AL USA
Mars Global Reference Atmospheric Model (Mars-GRAM) Version 3.8: Users Guide
Justus, C. G., Computer Sciences Corp., USA; James, B. F., NASA Marshall Space Flight Center, USA; May 1999; 34p; In English Report No.(s): NASA/TM-1999-209629; NAS 1.15:209629; M-940; No Copyright; Avail: CASI; A03, Hardcopy; A01, Microfiche

Mars Global Reference Atmospheric Model (Mars-GRAM) Version 3.8 is presented and its new features are discussed. Mars-GRAM uses new values of planetary reference ellipsoid radii, gravity term, and rotation rate (consistent with current JPL values) and includes centrifugal effects on gravity. The model now uses NASA Ames Global Circulation Model low resolution topography. Curvature corrections are applied to winds and limits based on speed of sound are applied. Altitude of the F1 ionization peak and density scale height, including effects of change of molecular weight with altitude are computed. A check is performed to disallow temperatures below CO2 sublimination. This memorandum includes instructions on obtaining Mars-GRAM source code and data files and running the program. Sample input and output are provided. An example of incorporating Mars-GRAM as an atmospheric subroutine in a trajectory code is also given.
Author
Mars (Planet); Mars Atmosphere; Atmospheric Temperature; Atmospheric Models; Atmospheric Density

19990108848 National Academy of Sciences - National Research Council, Space Studies Board, Washington, DC USA
A Scientific Rationale for Mobility in Planetary Environments
1999; 70p; In English

Contract(s)/Grant(s): NASW-96013; ISBN 0-309-06437-6; Copyright; Avail: Issuing Activity, Hardcopy

For the last several decades, the COMmittee on Planetary and Lunar EXploration (COMPLEX) has advocated a systematic approach to exploration of the solar system; that is, the information and understanding resulting from one mission provide the scientific foundations that motivate subsequent, more elaborate investigations. COMPLEX's 1994 report, An Integrated Strategy for the Planetary Sciences: 1995-2010,1 advocated an approach to planetary studies emphasizing "hypothesizing and comprehending" rather than "cataloging and categorizing." More recently, NASA reports, including The Space Science Enterprise Strategic Plan' and, in particular, Mission to the Solar System: Exploration and Discovery-A Mission and Technology Roadmap, 3 have outlined comprehensive plans for planetary exploration during the next several decades. The missions outlined in these plans are both generally consistent with the priorities outlined in the Integrated Strategy and other NRC reports,4,5 and are replete with examples of devices embodying some degree of mobility in the form of rovers, robotic arms, and the like. Because the change in focus of planetary studies called for in the Integrated Strategy appears to require an evolutionary change in the technical means by which solar system exploration missions are conducted, the Space Studies Board charged COMPLEX to review the science that can be uniquely addressed by mobility in planetary environments. In particular, COMPLEX was asked to address the following questions: 1. What are the practical methods for achieving mobility? 2. For surface missions, what are the associated needs for sample acquisition? 3. What is the state of technology for planetary mobility in the USA and elsewhere, and what are the key requirements for technology development? 4. What terrestrial field demonstrations are required prior to spaceflight missions?

Author

Solar System; Planetary Environments; Mobility

19990110319 Michigan Univ., Dept. of Atmospheric, Oceanic and Space Sciences, Ann Arbor, MI USA

Studies for the Loss of Atomic and Molecular Species from IO ***Final Report, 1 Jul. 1998 - 30 Jun. 1999***

Combi, Michael R., Michigan Univ., USA; [1999]; 44p; In English

Contract(s)/Grant(s): NAG5-6187

Report No.(s): NRA-95-OSSA-05; No Copyright; Avail: CASI; A03, Hardcopy; A01, Microfiche

The general objective of this project has been to advance our theoretical understanding of lo's atmosphere and how various atomic and molecular species are lost from this atmosphere and are distributed in the circumplanetary environment of Jupiter. This grant has provided support for the activities of Dr. Michael Combi at the University of Michigan to serve as a small part in collaboration with a larger project awarded to Atmospheric & Environmental Research, Inc., with primary principal investigator Dr. William H. Smyth. Dr. Combi is the Principal Investigator and Project Manager for the Michigan grant NAG5-6187. This Michigan grant has provided for a continuation of a collaboration between Drs. Smyth and Combi in related efforts beginning in 1981, and with the object to develop and apply sophisticated theoretical models to interpret and to relate a number of new and exciting observations for the atmospheric gases of the satellite. The ability to interpret and then to relate through the theoretical fabric a number of these otherwise independent observations are a central strength of this program. This comprehensive approach provides a collective power, extracting more from the sum of the parts and seeing beyond various limitations that are inherent in any one observation. Although the approach is designed to unify, the program is divided into well-defined studies for the likely dominant atmospheric gases involving species of the SO2 family (SO2, SO, O2, S and O) and for the trace atmospheric gas atomic sodium and a likely escaping molecular ion NaX(+) (where Na(X) is the atmospheric molecule and X represents one or more atoms).Attachments: IO's sodium corona and spatially cloud: a consistent flux speed distribution. and Io's plasma environment during the Galileo flyby: global three-dimensional MHD modeling with adaptive mesh refinement.

Derived from text

Research; Numerical Analysis; Atmospheric Chemistry; Io; Molecular Ions; Mathematical Models; Atoms

19990111453 Lunar and Planetary Inst., Houston, TX USA

Mars Field Geology, Biology, and Paleontology Workshop: Summary and Recommendations

Budden, Nancy Ann, Editor, Lunar and Planetary Inst., USA; 1999; 86p; In English, 18-19 Nov. 1998, Houston, TX, USA; See also 19990111454 through 19990111454

Contract(s)/Grant(s): NASW-4574

Report No.(s): LPI-Contrib-968; No Copyright; Avail: CASI; A05, Hardcopy; A01, Microfiche

Current NASA planning envisions human missions to Mars as early as 2013, on a mission that would send six crew members for a 500-day stay on the surface of Mars. While our understanding of how we would get there and back is fairly mature, the planning for what the crew would do to explore while on the surface for 500 days is less detailed. Mission objectives are to understand the composition and geo- morphology of the martian surface, and to continue to investigate and sample the geologic history of Mars. Special emphasis will focus on exploring for possible biogenic signatures, past or present, and on analyzing

pre-biotic chemistry. The purpose of this workshop was to explore the strategies, desired capabilities, skills, and operational realities required to lend success to the first human missions to Mars. Current mission planning dictates that there will be considerable mobility, sampling and analytical capability available to human crews, at a site warranting long-term geologic and possibly biological interest. However, the details of specific capabilities are not yet clearly defined.
Author
Mars Missions; Mars Surface; Mission Planning; NASA Programs; Planetary Geology; Conferences; Management Planning; Mars Landing; Manned Mars Missions; Mars (Planet)

19990111454 Science Applications International Corp., Houston, TX USA
Mars Surface Reference Mission: Excerpts, Appendix 1
Hoffman, Stephen, Science Applications International Corp., USA; Mars Field Geology, Biology, and Paleontology Workshop: Summary and Recommendations; 1999, pp. 39-58; In English; See also 19990111453; No Copyright; Avail: CASI; A03, Hardcopy; A01, Microfiche

This report has five sections. Examples described in the first section point out several guidelines for surface operations and for development of surface EVA suits and the equipment used by the crews while in these suits. The second section discussed the types of surface transportation that will be available to the crew and the variety of missions on which they can be deployed. The next section discusses the key mission objectives satisfied by and the functional capabilities of a remote field camp. The next section discusses the ongoing need for the crew to evaluate the level of toxicity of potential for biological activity throughout all phases of the surface mission. The next section discusses the curatorial activities which the astronaut crews will conduct while on the Martian surface. The last section discusses the sample examination and analytical capabilities that are likely to be used on the martian surface.
CASI
Mars Missions; Mars Surface; Mars Sample Return Missions; Manned Mars Missions; Return to Earth Space Flight; Topography; Mars (Planet); Planetary Geology; Bioastronautics; Space Suits

19990111600 NASA Goddard Space Flight Center, Greenbelt, MD USA
MOLA Topography of the Crustal Dichotomy Boundary Zone, Mars
Frey, Herbert V., NASA Goddard Space Flight Center, USA; E. H., Susan, Universities Space Research Association, USA; H., James, Science Systems and Applications, Inc., USA; [1998]; 1p; In English, 26-29 Oct. 1998, Toronto, Canada; Sponsored by Geological Society of America, USA; No Copyright; Avail: Issuing Activity, Hardcopy; Abstract Only

Mars Orbiter Laser Altimeter (MOLA) profiles frequently cross the crustal dichotomy boundary where the transition zone (TZ) between cratered highland terrain (CT) and lowland smooth plains (SP) is marked by mesas and knobby terrain. The detailed topographic character of the boundary zone is longitudinally variable, as is the geomorphology of the TZ. Some portions of the boundary are associated with an outer ring of the Utopia impact basin; MOLA topography is consistent with this. The regional character of the boundary topography is a 2-4 km step function from nearly flat SP to almost as flat CT. This rise has a regional slope of 1-2 degrees, 50-100 times that of the Cr and SP away from TZ, which suggests a significant change in crustal properties (thickness, composition or both) across the TZ. The overall topography is very similar to that at some passive continent-oceanic crustal margins on the Earth, with the seafloor allowed to adjust upward after removal of the overlying water. A possible temporal constraint on the CT/SP elevation difference comes from two MOLA profiles which pass through two large (150 km diameter) craters located at the boundary in Aeolis. The N and S rims of the more degraded crater are at the same elevation; north of the N rim the topography drops by greater than 2 km to the floor of the TZ. This crater predates the elevation offset between CT and TZ floor. The better preserved crater (Gale) has a N rim 2 km lower than its S rim, and appears to have been emplaced on a pre-existing regional slope of about I degree. Gale probably post- dates the elevation difference between CT and TZ floor. Based on the stratigraphy of the units in which these craters are found, the elevation difference appears to have been in place in the Mid to Late Noachian.
Author
Mars Observer; Topography; Mars Surface; Laser Altimeters; Geomorphology; Craters

92
SOLAR PHYSICS

Includes solar activity, solar flares, solar radiation and sunspots. For related information see 93 Space Radiation.

19990106580 NASA Marshall Space Flight Center, Huntsville, AL USA
Large-Scale Coronal Heating from "Cool" Activity in the Solar Magnetic Network
Falconer, D. A., NASA Marshall Space Flight Center, USA; Moore, R. L., NASA Marshall Space Flight Center, USA; Porter, J. G., NASA Marshall Space Flight Center, USA; Hathaway, D. H., NASA Marshall Space Flight Center, USA; [1999]; 1p; In English, 13 Dec. 1999, San Francisco, CA, USA; Sponsored by American Geophysical Union, USA; No Copyright; Avail: Issuing Activity, Hardcopy; Abstract Only

In Fe XII images from SOHO/EIT, the quiet solar corona shows structure on scales ranging from sub-supergranular (i.e., bright points and coronal network) to multi-supergranular (large-scale corona). In Falconer et al 1998 (Ap.J., 501, 386) we suppressed the large-scale background and found that the network-scale features are predominantly rooted in the magnetic network lanes at the boundaries of the supergranules. Taken together, the coronal network emission and bright point emission are only about 5% of the entire quiet solar coronal Fe XII emission. Here we investigate the relationship between the large-scale corona and the network as seen in three different EIT filters (He II, Fe IX-X, and Fe XII). Using the median-brightness contour, we divide the large-scale Fe XII corona into dim and bright halves, and find that the bright-half/dim half brightness ratio is about 1.5. We also find that the bright half relative to the dim half has 10 times greater total bright point Fe XII emission, 3 times greater Fe XII network emission, 2 times greater Fe IX-X network emission, 1.3 times greater He II network emission, and has 1.5 times more magnetic flux. Also, the cooler network (He II) radiates an order of magnitude more energy than the hotter coronal network (Fe IX-X, and Fe XII). From these results we infer that: 1) The heating of the network and the heating of the large-scale corona each increase roughly linearly with the underlying magnetic flux. 2) The production of network coronal bright points and heating of the coronal network each increase nonlinearly with the magnetic flux. 3) The heating of the large-scale corona is driven by widespread cooler network activity rather than by the exceptional network activity that produces the network coronal bright points and the coronal network. 4) The large-scale corona is heated by a nonthermal process since the driver of its heating is cooler than it is. This work was funded by the Solar Physics Branch of NASA's office of Space Science through the SR&T Program and the SEC Guest Investigator Program.
Author
Solar Corona; Solar Physics; Solar Heating

19990106582 NASA Marshall Space Flight Center, Huntsville, AL USA
Solar Cycle Predictions
Hathaway, D. H., NASA Marshall Space Flight Center, USA; [1999]; 1p; In English, 15 Dec. 1999, San Francisco, CA, USA; Sponsored by American Geophysical Union, USA; No Copyright; Avail: Issuing Activity, Hardcopy; Abstract Only

We currently lack a comprehensive model for the solar dynamo which might be used for predicting solar cycle activity levels. We can, nonetheless, predict these activity levels with some skill using a variety of techniques based on correlations between activity indicators at different times. A number of the techniques currently in use for predicting solar activity on a solar cycle time-scale have been tested with historical data. Some techniques, e.g., regression and curve fitting, work well as solar activity approaches maximum and provide a month by month description of future activity, while others, e.g., geomagnetic precursors, work well near solar minimum but only provide an estimate of the amplitude of the next cycle. A synthesis of different techniques is shown to provide a more accurate and useful forecast of solar cycle activity levels. The combination of two uncorrelated geomagnetic precursor techniques provides a more accurate prediction for the amplitude of a solar activity cycle of a time well before activity minimum. A mathematical function dependent on the time of cycle initiation and the cycle amplitude can then be used to describe the level of solar activity month by month for the next cycle. As the time of cycle maximum approaches a better estimate of the cycle activity is obtained by including the fit between previous activity levels and this function. The success of the geomagnetic precursors in predicting the amplitude of the next solar cycle supports the idea of extended solar cycle in which the activity cycles overlap. While the current cycle is producing sunspots and active regions in the Sun's equatorial regions the next cycle is already actively influencing the geomagnetic field, The precise nature and source of this influence remains unclear.
Author
Dynamo Theory; Geomagnetism; Solar Convection (Astronomy); Solar Activity; Solar Activity Effects; Solar Cycles; Sunspots

19990107394 NASA Marshall Space Flight Center, Huntsville, AL USA
Microflaring in Low-Lying Core Fields and Extended Coronal Heating in the Quiet Sun
Porter, Jason G., NASA Marshall Space Flight Center, USA; Falconer, D. A., NASA Marshall Space Flight Center, USA; Moore,

Ronald L., NASA Marshall Space Flight Center, USA; [1999]; 1p; In English, 30 May - 3 Jun. 1999, Chicago, IL, USA; Sponsored by American Astronautical Society, USA; No Copyright; Avail: Issuing Activity, Hardcopy; Abstract Only

We have previously reported analyses of Yohkoh SXT data examining the relationship between the heating of extended coronal loops (both within and stemming from active regions) and microflaring in core fields lying along neutral lines near their footpoints (J. G. Porter, D. A. Falconer, and R. L. Moore 1998, in Solar Jets and Coronal Plumes, ed. T. Guyenne, ESA SP-421, and references therein). We found a surprisingly poor correlation of intensity variations in the extended loops with individual microflares in the compact heated areas at their feet, despite considerable circumstancial evidence linking the heating processes in these regions. Now, a study of Fe XII image sequences from SOHO EIT show that similar associations of core field structures with the footpoints of very extended coronal features can be found in the quiet Sun. The morphology is consistent with the finding of Wang et al. (1997, ApJ 484, L75) that polar plumes are rooted at sites of mixed polarity in the magnetic network. We find that the upstairs/downstairs intensity variations often follow the trend, identified in the active region observations, of a weak correspondence. Apparently much of the coronal heating in the extended loops is driven by a type of core field magnetic activity that is ”cooler” than the events having the coronal signature of microflares, i.e., activity that results in little heating within the core fields themselves. This work was funded by the Solar Physics Branch of NASA’s Office of Space Science through the SR&T Program and the SEC Guest Investigator Program.

Author

Coronal Loops; Solar Flares; Flare Stars; Stellar Flares; Solar Physics; Solar X-Rays; Sun; Solar Heating

19990109083 NASA Goddard Space Flight Center, Greenbelt, MD USA

The Influence of Extremely Large Solar Proton Events in a Changing Stratosphere. Stratospheric Influence of Solar Proton Events

Jackman, Charles H., NASA Goddard Space Flight Center, USA; Fleming, Eric L., NASA Goddard Space Flight Center, USA; Vitt, Francis M., Sterling Software, Inc., USA; [1999]; 50p; In English; No Copyright; Avail: CASI; A03, Hardcopy; A01, Microfiche

Two periods of extremely large solar proton events (SPEs) occurred in the past thirty years, which forced significant long-term polar stratospheric changes. The August 2-10, 1972 and October 19-27, 1989 SPEs happened in stratospheres that were quite different chemically. The stratospheric chlorine levels were relatively small in 1972 (approximately 1.2 ppbv) and were fairly substantial in 1989 at about (approximately 3 ppbv). Although these SPEs produced both HO(x) and NO(y) constituents in the mesosphere and stratosphere, only the NO(y) constituents had lifetimes long enough to affect ozone for several months to years past the events. Our recently improved two-dimensional chemistry and transport atmospheric model was used to compute the effects of these gigantic SPEs in a changing stratosphere. Significant upper stratospheric ozone depletions is greater than 10% are computed to last for a few months past these SPEs. The long-lived SPE-produced NO(y) constituents were transported to lower levels during winter after these huge SPEs and caused impacts in the middle and lower stratosphere. During periods of high halogen loading these impacts resulted in interference with the chlorine and bromine loss cycles for ozone destruction. The chemical state of the atmosphere, including the stratospheric sulfate aerosol density, substantially affected the predicted stratospheric influence of these extremely large SPEs.

Author

Solar Protons; Sage Satellite; Aerosols; Air Pollution; Ozone; Solar Activity; Solar Cycles

19990109131 NASA Marshall Space Flight Center, Huntsville, AL USA

Large-Scale Coronal Heating from the Solar Magnetic Network

Falconer, David A., NASA Marshall Space Flight Center, USA; Moore, Ronald L., NASA Marshall Space Flight Center, USA; Porter, Jason G., NASA Marshall Space Flight Center, USA; Hathaway, David H., NASA Marshall Space Flight Center, USA; [1999]; 1p; In English, 30 May 1999, Chicago, IL, USA; Sponsored by American Astronomical Society, USA; Copyright; Avail: Issuing Activity, Hardcopy; Abstract Only

In Fe 12 images from SOHO/EIT, the quiet solar corona shows structure on scales ranging from sub-supergranular (i.e., bright points and coronal network) to multi- supergranular. In Falconer et al 1998 (Ap.J., 501, 386) we suppressed the large-scale background and found that the network-scale features are predominantly rooted in the magnetic network lanes at the boundaries of the supergranules. The emission of the coronal network and bright points contribute only about 5% of the entire quiet solar coronal Fe MI emission. Here we investigate the large-scale corona, the supergranular and larger-scale structure that we had previously treated as a background, and that emits 95% of the total Fe XII emission. We compare the dim and bright halves of the large- scale corona and find that the bright half is 1.5 times brighter than the dim half, has an order of magnitude greater area of bright point coverage, has three times brighter coronal network, and has about 1.5 times more magnetic flux than the dim half These results suggest that the brightness of the large-scale corona is more closely related to the large- scale total magnetic flux

than to bright point activity. We conclude that in the quiet sun: (1) Magnetic flux is modulated (concentrated/diluted) on size scales larger than supergranules. (2) The large-scale enhanced magnetic flux gives an enhanced, more active, magnetic network and an increased incidence of network bright point formation. (3) The heating of the large-scale corona is dominated by more widespread, but weaker, network activity than that which heats the bright points. This work was funded by the Solar Physics Branch of NASA's office of Space Science through the SR&T Program and the SEC Guest Investigator Program.
Author
Solar Corona; Heating; Brightness

19990109149 NASA Goddard Space Flight Center, Greenbelt, MD USA
Coronal Dimmings and Energetic CMEs, *Apr. - May 1998*
Thompson, B. J., NASA Goddard Space Flight Center, USA; Cliver, E. W., NASA Goddard Space Flight Center, USA; Nitta, N., NASA Goddard Space Flight Center, USA; Delannee, C., NASA Goddard Space Flight Center, USA; Delaboudiniere, J.–P., NASA Goddard Space Flight Center, USA; [1999]; 18p; In English
Contract(s)/Grant(s): NAS8-40801; No Copyright; Avail: CASI; A03, Hardcopy; A01, Microfiche

We have analyzed the coronal dimmings for seven fast (> 600 km/s) coronal mass ejections (CMEs) occurring between 23 April and 9 May which were associated with flares from NOAA active region (AR) 8210. These dimming regions were identified by their strong depletion in coronal emission within a half hour of the estimated time of CME lift-off. They included areas which were as dark as quiescent coronal holes as well as other regions with weaker brightness depletions. We found that the extended dimming areas in these events generally mapped out the apparent "footprint" of the CME. In two of the seven cases, a pair of dimmings were more or less symmetrically positioned north and south of the flare site. In the five remaining cases, the dimmings were most prominent to the north of AR 8210 (approximately S15 latitude) and extended well north of the solar equator, consistent with the locations of the CMEs. We discuss the implications of these results for the sigmoid/double dimming/flux rope model of CMEs.
Author
Stellar Mass Ejection; Stellar Activity; Coronal Holes; Solar Radio Emission; Radio Astronomy

19990109150 NASA Goddard Space Flight Center, Greenbelt, MD USA
The Role of Velocity Redistribution in Enhancing the Intensity of the He II 304 A Line in the Quiet Sun Spectrum
Andretta, Vincenzo, NASA Goddard Space Flight Center, USA; Jordan, Stuart D., NASA Goddard Space Flight Center, USA; Brosius, Jeffrey W., Raytheon ITSS, USA; Davila, Joseph M., NASA Goddard Space Flight Center, USA; Thomas, Roger J., NASA Goddard Space Flight Center, USA; Behring, William E., NASA Goddard Space Flight Center, USA; Thompson, William T., SM and A Corp., USA; Garcia, Adriana, Coimbra Univ., Portugal; [1999]; 2p; In English; No Copyright; Avail: CASI; A01, Hardcopy; A01, Microfiche

We present observational evidence of the effect of small scale ("microturbulent") velocities in enhancing the intensity of the He II lambda304 line with respect to other transition region emission lines, a process we call "velocity redistribution". We first show results from the 1991 and 1993 flights of SERTS (Solar EUV Rocket Telescope and Spectrograph). The spectral resolution of the SERTS instrument was sufficient to infer that, at the spatial resolution of 5", the line profile is nearly gaussian both in the quiet Sun and in active regions. We were then able to determine, for the quiet Sun, a lower limit for the amplitude of non-thermal motions in the region of formation of the 304 A line of the order of 10 km/s. We estimated that, in the presence of the steep temperature gradients of the solar Transition Region (TR), velocities of this magnitude can significantly enhance the intensity of that line, thus at least helping to bridge the gap between calculated and observed values. We also estimated the functional dependence of such an enhancement on the relevant parameters (non-thermal velocities, temperature gradient, and pressure). We then present results from a coordinated campaign, using SOHO/CDS and H-alpha spectroheliograms from Coimbra Observatory, aimed at determining the relationship between regions of enhanced helium emission and chromospheric velocity fields and transition region emission in the quiescent atmosphere. Using these data, we examined the behavior of the He II lambda304 line in the quiet Sun supergranular network and compared it with other TR lines, in particular with O III lambda600. We also examined the association of 304 A emission with the so-called "coarse dark mottle", chromospheric structures seen in H-alpha red wing images and associated with spicules. We found that all these observations are consistent with the velocity redistribution picture.
Author
Solar Atmosphere; Chromosphere; Spicules; Transition Region and Coronal Explorer; Solar Transition Region; Solar Radiation; Sun; Emission Spectra; H Alpha Line; Helium

19990109152 NASA Goddard Space Flight Center, Greenbelt, MD USA

A Direct Comparison Between EUV Coronal Flux and Helium Resonance Line Photon Flux from SOHO/CDS Data

Andretta, V., Osservatorio Astronomico, Capodimonte, Italy; Landi, Enrico, Florence Univ., Italy; DelZanna, Giulio, University of Central Lancashire, Preston, UK; Jordan, Stuart D., NASA Goddard Space Flight Center, USA; [1999]; 4p; In English; No Copyright; Avail: CASI; A01, Hardcopy; A01, Microfiche

In the wealth of EUV spectroscopic and imaging data gathered by the SOHO and TRACE missions, a prominent role is played by the helium resonance emission. For example, He I lines are among the most intense features in CDS/NIS spectra, while the EIT 304 waveband (dominated by He II emission) is routinely employed to map the structure of the solar chromosphere and transition region. However, no 'standard' model has emerged so far that is able to interpret observed He spectra/images to a satisfactory degree of self-consistency. Recent research on the problem of the formation of the solar helium spectrum tends to rule out a dominant role of coronal radiation in exciting He resonance lines. However, while evidence for this result is strong, it is based on indirect tests. Here we present a preliminary assessment of this issue based on a more direct approach, which involves a measure with CDS/GIS of the photoionizing EUV radiation. This measure can be directly compared with the observed flux in the main He I and He II resonance lines observed with CDS/NIS2.

Author

Helium; Resonance Lines; Solar Spectra; H Lines; Chromosphere; Transition Region and Coronal Explorer; Solar Transition Region; Solar Corona; SOHO Mission

19990109965 Alabama Univ., Dept. of Physics, Huntsville, AL USA

Ion Acceleration in Solar Flares ***Final Report, 1 May 1995 - 30 Nov. 1996***

Miller, James A., Alabama Univ., USA; Weir, Sue B., Alabama Univ., USA; [1996]; 4p; In English

Contract(s)/Grant(s): NAG5-2932; No Copyright; Avail: CASI; A01, Hardcopy; A01, Microfiche

Solar flares are among the most energetic and interesting phenomena in the Solar system, releasing up to 1032 ergs of energy on timescales of several tens of seconds to several tens of minutes. Much of this energy is in the form of suprathermal electrons and ions, which remain trapped at the Sun and produce a wide variety of radiations, as well as escape into interplanetary space, where they can be directly observed. The radiation from trapped particles consists in general of (1) continuum emission; (2) narrow gamma-ray nuclear deexcitation lines; and (3) high-energy neutrons observed in space or by ground-based neutron monitors. The particles that escape into space consist of both electrons and ions, which often have compositions quite different than that of the ambient solar atmosphere. Flares thus present many diagnostics of the particle acceleration mechanism(s), the identification of which is the ultimate goal of flare research. Moreover, flares in fact offer the only opportunity in astrophysics to study the simultaneous energization of both electrons and ions. Hopefully, an understanding of flares with their wealth of diagnostic data will lead to a better understanding of particle acceleration at other sites in the Universe. It is now generally accepted that flares are roughly divided into two classes: impulsive and gradual. Gradual events are large, occur high in the corona, have long-duration soft and hard X-rays and gamma rays, are electron poor, are associated with Type II radio emission and coronal mass ejections (CMEs), and produce energetic ions with coronal abundance ratios. Impulsive events are more compact, occur lower in the corona, produce short-duration radiation, and exhibit dramatic abundance enhancements in the energetic ions. Their He-3/He-4 ratio is - 1, which is a huge increase over the coronal value of about 5 x 10(exp -4), and they also posses smaller but still significant enhancements of Ne, Mg, Si, and Fe relative to He-4, C, N, and O. Specifically, above about 1 MeV nucleon(exp -1), the ratio of Fe to O is about 8 times larger than in the corona or in gradual flares, while the ratio of Ne, Mg, and Si to O is about 3 times higher; He-4, C, N, and 0 are not enchanced with respect to each other. In addition to these elemental enhancements, Ne and Mg have isotopic enhancements as well. The general scenario that has emerged from these (and other) observations is that energetic particles in gradual events are accelerated by a CME-driven shock, while those particles in impulsive events are accelerated by another mechanism(s).

Derived from text

Helium Isotopes; Neutrons; Particle Acceleration; Solar Flares; Stellar Mass Ejection; Coronal Mass Ejection; Ions

19990110586 NASA Goddard Space Flight Center, Greenbelt, MD USA

Observations of the September 24, 1997 Coronal Flare Waves

Thompson, B. J., NASA Goddard Space Flight Center, USA; Reynolds, B., Perth Observatory, Australia; Aurass, H., Astrophysikalisches Inst., Germany; Gopalswamy, N., Catholic Univ. of America, USA; Gurman, J. B., NASA Goddard Space Flight Center, USA; Hudson, H. S., Solar Physics Research Corp., USA; Martin, S. F., Helio Research, USA; St.Cyr, O. C., Computational Physics, Inc., USA; Solar Physics; September 1999, pp. 1- 22; In English; Copyright; Avail: Issuing Activity, Hardcopy

We report the coincident observations of coronal and chromospheric ”flare wave” transients in association with a flare, large-scale coronal dimming, metric radio activity and a coronal mass ejection. The two separate eruptions occurring on 24 September 1997 originate in the same active region and display similar morphological features. The first wave transient was observed in Extreme Ultraviolet Lithography (EUV) and H alpha data, corresponding to a wave disturbance in both the chromosphere and the solar corona, ranging from 250 to approaching 1000 km/sec at different times and locations along the wavefront. The sharp wavefront had a similar extent and location in both the EUV and H alpha data. The data did not show clear evidence of a driver, however. Both events display a coronal EUV dimming which is typically used as an indicator of a coronal mass ejection in the inner corona. White light coronagraph observations indicate that the first event was accompanied by an observable coronal mass ejection while the second event did not have clear evidence of a Coronal Mass Ejection (CME). Both eruptions were accompanied by metric type II radio bursts propagating at speeds in the range of 500-750 km/sec, and neither had accompanying interplanetary type II activity. The timing and location of the flare waves appear to indicate an origin with the flaring region, but several signatures associated with coronal mass ejections indicate that the development of the CME may occur in concert with the development of the flare wave.
Author
Solar Physics; Solar Flares; Solar Corona; Solar X-Rays; Solar Observatories

19990110689 California Inst. of Tech., Solar Astronomy, Pasadena, CA USA
Variability of Solar UV Irradiance Related to Bright Magnetic Features Observed in Call K-Line: Relationship between Lyman alpha and K-line Report for UARS funding agency ***Final Report, 15 Nov. 1994 - 30 Sep. 1999***
Zirin, Harold, California Inst. of Tech., USA; Cameron, Robert, California Inst. of Tech., USA; [1999]; 9p; In English
Contract(s)/Grant(s): NAG5-2782; No Copyright; Avail: CASI; A02, Hardcopy; A01, Microfiche

In this report we comment on the relationship between the Lyman alpha and Calcium K-line emission from the Sun. We firstly examine resolved Lyman alpha images (from TRACE) and resolved K-line images. We find that the Lyman alpha emission is consistent with a linear dependence on the K-line emission. As this is in conflict with the analysis of Johannesson et al.(1995, 1998) we proceed by comparing the disk integrated Lyman alpha flux as a function of ratio between the disk integrated Mg II core and wing fluxes (Johannesson et al (1998) having previously found a linear dependence between this index and the BBSO K-line index). We find that a reasonably good fit can be obtained, however note the discrepancies which lead Johannesson et al to consider the square root relationship. We suggest an alternative interpretation of the discrepancy.
Author
Solar Radiation; K Lines; Solar Physics; Irradiance; Lyman Alpha Radiation; Variability; Light (Visible Radiation)

93
SPACE RADIATION

Includes cosmic radiation; and inner and outer earth's radiation belts. For biological effects of radiation see 52 Aerospace Medicine. For theory see 73 Nuclear and High-Energy Physics.

19990106544 NASA Marshall Space Flight Center, Huntsville, AL USA
Observations of Gamma-Ray Bursts: An Update
Fishman, Gerald J., NASA Marshall Space Flight Center, USA; [1997]; 1p; In English, 17 Oct. 1997, Columbia, MO, USA; No Copyright; Avail: CASI; A01, Hardcopy; A01, Microfiche; Abstract Only; Abstract Only

Gamma-ray bursts remain one of the greatest mysteries in astrophysics. Observations of gamma-ray bursts made by the BATSE experiment on the Compton Gamma-Ray Observatory will be described. Most workers in the field now believe that they originate from cosmological distances. This view has been reinforced by observations this year of several optical afterglow counterparts to gamma-ray bursts. A summary of these recent discoveries will be presented, along with their implications for models of the burst emission mechanism and the energy source of the bursts.
Author
Gamma Ray Bursts; Big Bang Cosmology; Gamma Ray Astronomy; Gamma Ray Sources (Astronomy); Radio Sources (Astronomy); X Ray Astronomy; X Ray Sources

19990106545 Smithsonian Astrophysical Observatory, Cambridge, MA USA
X-Ray Signatures of Low Luminosity AGN and Non-AGN Activities in Galaxies
Fabbiano, Giuseppina, Smithsonian Astrophysical Observatory, USA; [1997]; 1p; In English; Non-Sleeping Universe: From Galaxies to the Horizon, 24-30 Nov. 1997, porto, Portugal

Contract(s)/Grant(s): NAS8-39073; No Copyright; Avail: CASI; A01, Hardcopy; A01, Microfiche; Abstract Only; Abstract Only

This talk will review the present knowledge, based on x-ray observations (Einstein, ROSAT, ASCA) of low-luminosity activity in otherwise normal galaxies. These phenomena cover the x-ray emission of low-luminosity AGN and LINERs found in the nuclei of galaxies. The talk will discuss these phenomena in the context of the more general AGN phenomenon. The other type of activity, which will also be discussed, is connected with enhanced starburst activity. Starburst activity has been found linked in x-rays with hot galactic winds, and gives us direct evidence of the interplay between galaxies and the surrounding medium. The talk will conclude by discussing the opportunities offered by the upcoming launch of AXAF.

Author

Active Galactic Nuclei; Active Galaxies; Galactic Winds; Starburst Galaxies

19990106587 NASA Goddard Space Flight Center, Greenbelt, MD USA

Spin Down of Pulsations in the Cooling Tail of an X-ray Burst from 4U 1636-53

Strohmayer, Tod E., NASA Goddard Space Flight Center, USA; [1999]; 16p; In English; No Copyright; Avail: CASI; A03, Hardcopy; A01, Microfiche

We report the discovery with the proportional counter array (PCA) onboard the Rossi X-ray Timing Explorer (RXTE) of a decrease in the frequency of X-ray brightness oscillations in the cooling tail of an X-ray burst from 4U 1636-53. This is the first direct evidence for a spin down of the pulsations seen during thermonuclear bursts. We find that the spin down episode is correlated with the appearance in this burst of an extended tail of emission with a decay timescale much longer than is seen in other bursts from 4U 1636-53 in the same set of observations. We present both time resolved energy and variability spectra during this burst and compare them with results from a second burst which shows neither a spin down episode nor an extended tail. A spectral evolution study of the ”spin down” burst reveals a secondary signature of weak radius expansion, not seen in other bursts, and correlated with the spin down episode, which may indicate a secondary thermonuclear energy release. We interpret the spin down episode in the context of an angular momentum conserving shell, which is reexpanded and therefore spun down by an additional thermonuclear energy release which could also explain the extended X-ray tail.

Author

X Rays; Radio Bursts; Neutron Stars; X Ray Stars; Brightness; Stellar Luminosity

19990107782 Smithsonian Astrophysical Observatory, Cambridge, MA USA

Galaxy Surveys with Future X-Ray Missions

Fabbiano, Giuseppina, Smithsonian Astrophysical Observatory, USA; [1999]; 1p; In English; Large Scale Structure in the X-ray Universe, 16-23 Sep. 1999, Santornini, Greece; No Copyright; Avail: Issuing Activity, Hardcopy; Abstract Only

The potential of large area imaging missions with good angular resolution will be demonstrated for galaxy evolution studies. X-rays are an important band in which to study galaxies, not least because the recycling of material out of galaxies (in ’superwinds’) is an inherently X-ray subject. So the chemical evolution of the universe is profoundly affected by matter emitting in the X-ray band. Specific requirements on area, FWHM of the PSF and field-of- view will be shown. There is a need for deep imaging, some 100 times fainter than Chandra deep surveys, in order to properly explore galaxy evolution in X-rays.

Author

Galaxies; Surveys; Observation; X Rays; Chemical Evolution

19990107783 Smithsonian Astrophysical Observatory, Cambridge, MA USA

X-Ray Surveys with Chandra

Elvis, Martin, Smithsonian Astrophysical Observatory, USA; [1999]; 1p; In English; Large Scale Structure in the X-ray Universe, 16-23 Sep. 1999, Santorini, Greece; No Copyright; Avail: Issuing Activity, Hardcopy; Abstract Only

The potential of unbiased high galactic latitude surveys in X-rays with Chandra will be laid out. The specifics of the surveys approved for AO1 (GO+GTO) will be used to predict source numbers and accuracy in the very soft, ’ROSAT’, and hard X-ray bands. If Chandra flight data is available by the time of the meeting examples will be shown and actual performance compared with predictions.

Author

X Rays; Observation; Data Acquisition

19990107785 Smithsonian Astrophysical Observatory, Cambridge, MA USA

X-Ray Measured Masses for Clusters of Galaxies

Forman, William, Smithsonian Astrophysical Observatory, USA; [1999]; 1p; In English; Large Scale Structures in the X-ray Universe, 17-27 Sep. 1999, Santorini, Greece

Contract(s)/Grant(s): NAS8-39073; No Copyright; Avail: Issuing Activity, Hardcopy; Abstract Only

Results of the analysis of Chandra observations fo the gas density and temperature profiles for several clusters f galaxies will be used to determine the amount and distribution of the total mass in clusters. These results will be compared with past results from ASCA. with theoretically predicted mass profiles and with mass profiles determined from gravitational lensing.

Author

Galactic Clusters; Gas Density; Temperature Profiles

19990108481 Smithsonian Astrophysical Observatory, Cambridge, MA USA

Chandra Observations of Clusters of Galaxies

Jones, Christine, Smithsonian Astrophysical Observatory, USA; [1999]; 1p; In English; Large Scale Structure in the X-ray Universe, 17-27 Sep. 1999, Santorini, Greece

Contract(s)/Grant(s): NAS8-39073; No Copyright; Avail: Issuing Activity, Hardcopy; Abstract Only

The high spatial resolution of the Chandra X-ray telescope, along with the broad energy coverage will allow a new view of the X-ray emission from clusters of galaxies. Results from the first Chandra X-ray images, including any structure in clusters on fine scales, gas temperature distributions and heavy element abundances will be presented.

Author

X Ray Telescopes; Heavy Elements; Gas Temperature; Galactic Radiation

19990109100 New Hampshire Univ., Physics Dept., Durham, NH USA

High Energy Observations of X-Ray Binaries and Gamma-Ray Blazars ***Final Report***

Vestrand, W. Thomas, New Hampshire Univ., USA; [1999]; 9p; In English

Contract(s)/Grant(s): NAG5-3157; No Copyright; Avail: CASI; A02, Hardcopy; A01, Microfiche

The report discusses the CGRO observation of X-ray binary systems and studies of gamma-ray blasars. Numerous authors have suggested mechanisms for particle acceleration within X-Ray Binary (XRB) systems. Among the acceleration mechanisms that have been applied are pulsar acceleration, shock acceleration at an accretion shock front, shock acceleration at a pulsar wind termination shock, plasma turbulence excited by the accretion flow, and a number of electrodynamic mechanisms. There are therefore many mechanisms which are capable of generating very energetic particles in the XRB environment. If the reports of TeV/PeV gamma-ray generation in XRBs are correct, then one can show that the accelerated particles must be hadrons and that the most likely gamma-ray production mechanism is the decay of collisionally-produced (or photoproduced) neutral pions. At these ultra-high energies, the emission is so strongly beamed that the target conditions are constrained by the requirement that the column depth be large enough to efficiently generate gamma-rays, but not so large that the gamma-rays are absorbed. These constraints naturally lead to models that explain the periodic, narrow duty-cycle pulses observed at TeV/PeV energies as arising from interactions with, either, the atmosphere of the binary companion, an accretion column, or an accretion disk. The production of these TeV/PeV gamma-rays by the decay of pions from ”leading isobars” must also be accompanied by a more isotropic emission component in the EGRET energy band from the decay of slower pions (i.e. the ”pionization” component). Since the attenuation of 35 MeV-1 GeV photons by photon-photon pair production is not likely to be significant in most XRBs, the TeV/PeV reports therefore strongly suggest sporadic emission in the EGRET energy band. One of the key unresolved issues for understanding AGN is the relationship between XBLs and RBLs.To test the ”reunification” hypothesis, authors conducted a multiwavelength campaign during Cycle 7 of the CGRO observing program. The analysis of the cycle 4 through cycle 6 CGRO measurements was completed. Two previously unknown EGRET sources was discovered.

Derived from text

X Ray Binaries; Gamma Rays; Blazars; Particle Acceleration; Pulsars; Acceleration (Physics); Pair Production; Energetic Particles

19990109661 Rutherford Appleton Lab., Chilton, UK

Tri-Maximal versus Bi-Maximal Neutrino Mixing

Scott, W. G., Rutherford Appleton Lab., UK; Oct. 06, 1999; ISSN 1358-6254; 10p; In English

Report No.(s): RAL-TR-1999-066; hep-ph/9909431; Copyright; Avail: Issuing Activity, Hardcopy

It is argued that data from atmospheric and solar neutrino experiments point strongly to tri-maximal or bi-maximal lepton mixing. While (”optimized”) bi-maximal m9ixing gives an excellent alpha posteriori to the data, tri-maximal mixing is an alpha priori hypothesis, which is not excluded, taking account of terrestrial matter effects.

Author

Neutrinos; Mixing

19990110678 NASA Marshall Space Flight Center, Huntsville, AL USA

The Outbursts and Orbit of the Accreting Pulsar GS 1843-02=2S 1845-024

Finger, Mark H., Universities Space Research Association, USA; Bildsten, Lars, California Univ., USA; Chakrabarty, Deepto, Massachusetts Inst. of Tech., USA; Prince, Thomas A., California Inst. of Tech., USA; Scott, D. Matthew, Universities Space Research Association, USA; Wilson, Colleen A., NASA Marshall Space Flight Center, USA; Wilson, Robert B., NASA Marshall Space Flight Center, USA; Zhang, S. Nan, Universities Space Research Association, USA; [1998]; 1p; In English; Copyright; Avail: Issuing Activity, Hardcopy; Abstract Only

We present observations of a series of 10 transient outbursts of pulsed hard x-ray flux from the 10.6 mHz accreting pulsar GS 1843-02 using the Burst and Transient Source Experiment (BATSE) on the Compton Observatory. These outbursts occurred regularly every 242 days, coincident with the ephemeris of the periodic transient GRO J1849-03 (Zhang et al. 1996)), which has recently been identified with the the SAS 3 source 2S 1845-024 (Soffitta et al. 1998). Our pulsed detection provides the first clear identification of GS 1843-02 with 2S 1845-024. We present a pulse timing analysis which shows that the 2S 1845-024 outbursts occur near the periastron passage of a highly eccentric (e = 0.88 q 0.01) 242.18 +/- 0.01 day period binary orbit about a high mass (M(sub opt) is greater than 7 solar mass companion. The orbit and transient outburst pattern suggest a Be star/X-ray pulsar system, however the optical companion is unknown. Our observations show a long-term spin-up trend, with most of the spin-up occurring during the outbursts. From the measured spin-up rates and inferred mass accretion rates we conclude that an accretion disk is present during the outbursts.

Author

Accretion Disks; X Ray Binaries; Pulsars; Radio Astronomy; Radio Bursts

19990110681 NASA Marshall Space Flight Center, Huntsville, AL USA

Average Cosmological Invariant Parameters of Cosmic Gamma Ray Bursts

Mitrofanov, Igor G., NASA Marshall Space Flight Center, USA; Anfimov, Dimitrij S., NASA Marshall Space Flight Center, USA; Litvak, Maxim L., NASA Marshall Space Flight Center, USA; Briggs, Michael S., NASA Marshall Space Flight Center, USA; Paciesas, W. S., NASA Marshall Space Flight Center, USA; Pendleton, Geoffrey N., NASA Marshall Space Flight Center, USA; Preece, Robert D., NASA Marshall Space Flight Center, USA; Meegan, Charles, NASA Marshall Space Flight Center, USA; [1998]; 1p; In English; Copyright; Avail: Issuing Activity, Hardcopy; Abstract Only

Average cosmological invariant parameters (ACIPs) are calculated for six groups of BATSE cosmic gamma-ray bursts selected by their peak fluxes on the 1.024s timescale. The ACIPs represent the average temporal and spectral properties of these events equally in the observer frame of reference and in the co-moving frames of outbursting emitters. The parameters are determined separately for rise fronts and for back slopes of bursts, defined as the time profiles before and after the main peaks, respectively. The ACIPs for the rise fronts are found to be different for different intensity groups, while the ACIPs for the back slopes show no significant dependence on intensity. We conclude that emitters of bursts manifest standard average properties only during the back slopes of bursts.

Author

Cosmology; Astrophysics; Gamma Ray Bursts; Gamma Ray Astronomy; Gamma Ray Sources (Astronomy); Radio Sources (Astronomy); X Ray Astronomy

19990111522 NASA Marshall Space Flight Center, Huntsville, AL USA

Radio and X-Ray Observations of the 1998 Outburst of the Recurrent X-Ray Transient 4U 1630-47

Hjellming, R. M., NASA Marshall Space Flight Center, USA; Rupen, M., NASA Marshall Space Flight Center, USA; Mioduszewski, A. J., NASA Marshall Space Flight Center, USA; Kuulkers, E., NASA Marshall Space Flight Center, USA; McCollough, M. L., NASA Marshall Space Flight Center, USA; Harmon, B. Alan, NASA Marshall Space Flight Center, USA; Buxton, M., NASA Marshall Space Flight Center, USA; Sood, R., NASA Marshall Space Flight Center, USA; Tzioumis, A., NASA Marshall Space Flight Center, USA; [1998]; 1p; In English; Copyright; Avail: Issuing Activity, Hardcopy; Abstract Only

We report radio (VLA and ATCA), soft X-ray (RXTE ASM), and hard X-ray (CGRO BATSE) observations of a 1998 outburst in the recurring X-ray transient 4U 1630-47 where radio emission was detected for the first time. The radio observations identify the position of 4U 1630-47 to within 1". Because the radio emission is optically thin with a spectral index of approximately -0.6 during the rise and approximately -1 during the peak and decay of the initial radio event, the emission is probably coming from an optically thin radio jet ejected over a period of time. The 20-100 keV emission first appeared 1998 January 28 (MJD 50841), the 2-12 keV emission first appeared February 3 (MJD 50847), and the first radio emission was detected February 12.6 (MJD

50856.6). The rise of the radio emission probably began about February 7 (MJD 50851) when the X-rays were in a very hard, fluctuating hardness state, just before changing to a softer, more stable hardness state.
Author
Radio Emission; Radio Observation; X Ray Stars; Gamma Ray Bursts; Black Holes (Astronomy)

19990111695 Smithsonian Astrophysical Observatory, Center for Astrophysics, Cambridge, MA USA
Four Years of EUVE Observations of the Bursting Gamma-Ray Emitting Blazar Markarian 421
Cagnoni, Ilaria, Smithsonian Astrophysical Observatory, USA; Fruscione, Antonella, Smithsonian Astrophysical Observatory, USA; Papadakis, Iossif, Southampton Univ., UK; 1998; In English, 5-17 Mar. 1998, Milan, Italy
Contract(s)/Grant(s): NAS8-39073; Copyright; Avail: Issuing Activity, Hardcopy, Microfiche

We present spectral and timing analysis of all the data collected by the Extreme Ultraviolet Explorer Satellite (EUVE) for the bright, nearby BL Lacertae object, Markarian 421, during the four-year period 1994-1997. During these years Mrk 421 has been observed by EUVE 4 times with the Deep-Survey/Spectrograph and 2 times with the imaging telescopes for a total of approximately 1.4 7nillions seconds. From 1993 to 1996 three very bright gamma ray flares were also detected by the Whipple observatory. In 1994 Mrk 421 was observed simultaneously by EUVE (Apr 2-12) and IUE one month before the TeV flare; of the 2 EUVF, observations (Feb 4-7 and Apr 25-May 13) of 1995, the second was part of a multiwavelength campaign that mapped the evolution of the TeV flare. In 1996 we observed Mrk 421 twice simultaneously with XTE: one immediately before (Apr 17-30) and another one (May 10-11) right after the May 7 1996 TeV flare. and finally in 1997 from Feb. 7 to Feb. ll. The total light curve seems to be smoothly varying on the long time-scale while on a shorter time-scale there is evidence of an EUVE flare well correlated to the TeV energy 1995 flare. We have analysed the three spectral data set in an homogenous way using the appropriate calibration data for the off-axis observations and our analysis confirms the presence of the absorption features around approximately 70A, in the entire 1995 dataset and possibly in the 1996 data set. We also show the first power spectrum analysis of the Mrk 421 EUVE lightcurves and a comparison with the power spectra predicted by current theoretical models.
Author
Extreme Ultraviolet Explorer Satellite; Emission Spectra; Blazars; Markarian Galaxies; Gamma Ray Bursts; Gamma Ray Astronomy

99
GENERAL

19990110313 Japan Broadcasting Corp., Tokyo, Japan
NHK Science and Technical Research Laboratories *Annual Report, 1998*
1998; 72p; In English; Original contains color illustrations; No Copyright; Avail: CASI; A04, Hardcopy; A01, Microfiche

Sixty-eight years have passed since the establishment in 1930 of the NHK Science & Technical Research Laboratories. The Laboratories' R&D activities have made significant contributions to the world of broadcasting over the fiscal year 1998 in three major categories: research on new broadcasting services; research to improve conventional broadcasting services; and research into the infrastructure technology needed to support the future of the broadcasting world. The twenty-first century is now only two years away. The world is changing rapidly as we enter a new, borderless era that will see increased mutual understanding among the people of the world. The environment of broadcasting, too, is undergoing major transformations. Japan's digital satellite broadcasting, which implements long-anticipated ISDB (Integrated Services Digital Broadcasting) based on HDTV pictures, will start in December 2000. Digital terrestrial broadcasting will start experimentally in 2000 over a wide area in the Kanto region, including Tokyo. This will also be implemented in ISDB. Hi-Vision (HDTV) broadcasting itself is an everyday affair now, boasting 767,000 receiving units at the end of March 1999. HDTV-incorporating ISDB is a great present from the engineers of the twentieth century to the society of the twenty-first. The next immediate challenge for the Research Laboratories after ISDB is how to implement, with ease and skill, the production of HDTV programs that are required in large quantity. Although technically speaking ISDB is at the stage of completion, we need to expend more time and effort to bring it to maturity. It is also necessary to start developing next generation technologies that will bear fruit in the early twenty-first century. In these fields of research and development, it is vital that people involved respectively in program production and in technology fully cooperate. Human friendly broadcasting is another of our interests of great importance at present. Broadcast news transcription, automated news summarization and a speech rate converter for elderly listeners, for example, are among our recent results in this field. We have also developed an automatic video analyzer to monitor for flickering and spatially periodic patterns which may cause problems for photosensitive viewers. We intend vigorously to pursue research in this area in the future. Redevelopment of the R&D building started this year with the disassembly of the tower and two annex buildings. The tower, built in 1939 and 100

meters high, was a symbolic structure for the Laboratories because it was used in Japan's first ever, albeit experimental, TV broadcasting.
Derived from text
Research Facilities; Broadcasting; Research and Development; Television Systems

19990111455 NASA Glenn Research Center, Cleveland, OH USA
HBCUs/OMUs Research Conference Agenda and Abstracts
Dutta, Sunil, Compiler, NASA Glenn Research Center, USA; HBCUs/OMUs Research Conference Agenda and Abstracts; August 1999; 68p; In English, 14-15 Apr. 1999, Cleveland, OH, USA; See also 19990111456 through 19990111485
Contract(s)/Grant(s): RTOP 282-10-08-07
Report No.(s): NASA/CP-1999-209318; NAS 1.55:209318; E-11631; No Copyright; Avail: Issuing Activity, Hardcopy; Abstract Only

The purpose of this Historically Black Colleges and Universities (HBCUS) Research Conference was to provide an opportunity for principal investigators and their students to present research progress reports. The abstracts included in this report indicate the range and quality of research topics such as aeropropulsion, space propulsion, space power, fluid dynamics, designs, structures and materials being, funded through grants from Glenn Research Center to HBCUS. The conference generated extensive networking between students. principal investigators. Glenn technical monitors, and other Glenn researchers.
Author
Abstracts; Conferences; Students; Universities; Research; Minorities

Subject Term Index

A

A STARS, 298
ABSORBERS (MATERIALS), 224, 248
ABSORPTION CROSS SECTIONS, 194, 256
ABSTRACTS, 223, 312
ACCELERATION (PHYSICS), 224, 309
ACCEPTABILITY, 15
ACCIDENT INVESTIGATION, 5
ACCIDENT PREVENTION, 7, 176
ACCRETION DISKS, 293, 310
ACCUMULATIONS, 116
ACCURACY, 20, 256
ACID RAIN, 128
ACOUSTIC ATTENUATION, 226
ACOUSTIC EMISSION, 246
ACOUSTIC MEASUREMENT, 16, 246, 248
ACOUSTIC PROPERTIES, 10, 16, 20
ACOUSTIC SOUNDING, 18
ACOUSTICS, 244, 248
ACTIVATED SLUDGE, 122
ACTIVE CONTROL, 248
ACTIVE GALACTIC NUCLEI, 291, 308
ACTIVE GALAXIES, 297, 308
ACTS, 77
ACTUATORS, 87, 238
ADAPTIVE CONTROL, 2, 55
ADVANCED MICROWAVE SOUNDING UNIT, 144
ADVECTION, 130, 207
AERATION, 122
AEROACOUSTICS, 244
AERODYNAMIC CHARACTERISTICS, 15, 23
AERODYNAMIC FORCES, 21
AERODYNAMIC NOISE, 16, 20, 223, 245, 246, 247, 248
AERODYNAMICS, 22
AEROSOLS, 118, 120, 134, 135, 137, 138, 140, 170, 171, 185, 205, 213, 270, 304
AEROSPACE ENGINEERING, 45, 84, 279
AEROSPACE ENVIRONMENTS, 122, 255, 290
AEROSPACE MEDICINE, 217, 219, 220, 224
AEROSPACE SYSTEMS, 41, 283
AEROSPIKE ENGINES, 37, 43
AEROTHERMODYNAMICS, 46
AGE FACTOR, 224
AGRICULTURE, 109
AIR, 93, 141
AIR CARGO, 5
AIR CONDUCTIVITY, 117, 135, 136, 197
AIR FLOW, 13, 24, 99, 194
AIR INTAKES, 13
AIR JETS, 245
AIR NAVIGATION, 1, 7
AIR POLLUTION, 61, 99, 116, 122, 124, 126, 127, 128, 140, 304
AIR QUALITY, 60
AIR SAMPLING, 60, 116
AIR TRAFFIC, 3, 25, 124
AIR TRAFFIC CONTROL, 4, 9
AIR TRAFFIC CONTROLLERS (PERSONNEL), 224
AIR TRANSPORTATION, 1, 5, 6, 7
AIR WATER INTERACTIONS, 118, 130
AIRBORNE EQUIPMENT, 125, 126, 190
AIRBORNE RADAR, 74
AIRCRAFT DESIGN, 3, 30, 46, 239
AIRCRAFT ENGINES, 20
AIRCRAFT FUELS, 67
AIRCRAFT INDUSTRY, 31
AIRCRAFT LANDING, 1, 33
AIRCRAFT RELIABILITY, 3
AIRCRAFT SAFETY, 4, 181
AIRCRAFT STABILITY, 11
AIRFOILS, 21
AIRLINE OPERATIONS, 3, 4, 5, 6
AIRPORT PLANNING, 25
AIRPORTS, 1, 6, 7, 25, 26, 67
ALBEDO, 213
ALBERTA, 182
ALDEHYDES, 127
ALGEBRA, 227
ALGORITHMS, 46, 70, 74, 78, 81, 90, 102, 111, 118, 212, 232, 233, 234, 235, 249, 257
ALLOCATIONS, 286
ALLOYS, 54, 55
ALUMINUM, 266
ALUMINUM NITRIDES, 91
ALUMINUM OXIDES, 43
AMAZON REGION (SOUTH AMERICA), 108, 110
AMMONIUM PERCHLORATES, 61, 67
AMMUNITION, 63, 240
AMOUNT, 125
ANALOG TO DIGITAL CONVERTERS, 141
ANALYSIS (MATHEMATICS), 175
ANALYSIS OF VARIANCE, 171
ANGULAR RESOLUTION, 292
ANHYDRIDES, 59
ANIMALS, 220
ANNEALING, 48
ANNIHILATION REACTIONS, 38
ANNUAL VARIATIONS, 107, 118, 123, 126, 168, 170, 209
ANOMALIES, 130, 145
ANTARCTIC REGIONS, 215
ANTENNA ARRAYS, 199
ANTENNA RADIATION PATTERNS, 75, 247, 248
ANTENNAS, 177
ANTIMATTER, 38
ANTIPROTONS, 38
APERTURES, 36, 270
APPLICATIONS PROGRAMS (COMPUTERS), 23, 32, 41, 100, 124, 231, 235, 236, 237
APPROXIMATION, 242
AQUIFERS, 104
ARCHITECTURE (COMPUTERS), 27, 229, 231
ARM (ANATOMY), 224
ARMATURES, 39
ARMED FORCES, 75
ARMED FORCES (UNITED STATES), 284
ARTERIES, 219, 222
ARTIFICIAL INTELLIGENCE, 235, 238
ARTIFICIAL SATELLITES, 34
ASHES, 108
ASPECT RATIO, 87
ASSESSMENTS, 119
ASTRONAUTS, 221
ASTRONOMICAL OBSERVATORIES, 290
ASTRONOMICAL PHOTOMETRY, 260
ASTRONOMY, 288
ASTROPHYSICS, 73, 296, 298, 310
ASYMMETRY, 23, 257
ASYMPTOTIC SERIES, 227
ASYNCHRONOUS TRANSFER MODE, 79, 238
ATLANTIC OCEAN, 125, 226
ATMOSPHERIC BOUNDARY LAYER, 117, 135, 136, 137, 206

ATMOSPHERIC CHEMISTRY, 64, 105, 124, 212, 214, 301
ATMOSPHERIC CIRCULATION, 115, 123, 130, 132, 151, 206
ATMOSPHERIC COMPOSITION, 94, 105, 119, 124, 127, 142
ATMOSPHERIC CONDUCTIVITY, 135, 136, 197
ATMOSPHERIC DENSITY, 132, 300
ATMOSPHERIC DIFFUSION, 127
ATMOSPHERIC EFFECTS, 64, 163
ATMOSPHERIC ELECTRICITY, 93, 105, 117, 134, 135, 136, 137, 138, 139, 140, 141, 152, 158, 159, 192, 197
ATMOSPHERIC ENERGY SOURCES, 149
ATMOSPHERIC GENERAL CIRCULATION MODELS, 115
ATMOSPHERIC HEAT BUDGET, 213
ATMOSPHERIC HEATING, 123
ATMOSPHERIC IONIZATION, 135, 136, 138, 140, 164, 183, 194
ATMOSPHERIC MODELS, 108, 115, 118, 119, 123, 130, 131, 172, 195, 196, 200, 202, 203, 213, 300
ATMOSPHERIC MOISTURE, 130, 170, 185
ATMOSPHERIC PRESSURE, 14
ATMOSPHERIC RADIATION, 110, 197, 212, 213
ATMOSPHERIC SOUNDING, 158, 187, 211
ATMOSPHERIC TEMPERATURE, 129, 132, 133, 153, 170, 183, 300
ATMOSPHERICS, 139, 167, 170, 196
ATOMS, 252, 301
ATTENUATION, 74, 77
ATTENUATION COEFFICIENTS, 96
ATTITUDE (INCLINATION), 35, 224
ATTITUDE CONTROL, 34, 238
ATTITUDE INDICATORS, 238
ATTRACTORS (MATHEMATICS), 240
AUGMENTATION, 18, 131
AURORAL ARCS, 133
AURORAL ZONES, 133, 149
AURORAS, 144, 149, 150
AUSTRALIA, 154
AUTOMATA THEORY, 237, 238
AUTOMATIC CONTROL, 33, 84, 90, 98
AUTOMATIC LANDING CONTROL, 33
AUTOMOBILE FUELS, 99
AUTOMOBILES, 83
AUTONOMY, 27
AVALANCHE DIODES, 83
AVIONICS, 30
AXIAL FLOW, 98
AXISYMMETRIC FLOW, 19

B

B–1 AIRCRAFT, 14
BAGS, 237
BALANCE, 95, 128
BALL LIGHTNING, 171
BALLISTICS, 67
BALLOON SOUNDING, 117, 136, 139, 158, 170
BALLOON–BORNE INSTRUMENTS, 136, 177
BANDPASS FILTERS, 259, 260
BAYES THEOREM, 218
BEADS, 56
BEARINGS, 98
BIBLIOGRAPHIES, 80
BIG BANG COSMOLOGY, 307
BINARY MIXTURES, 85
BINARY PHASE SHIFT KEYING, 75
BINARY STARS, 291
BINDING ENERGY, 54, 253
BIOASTRONAUTICS, 222, 302
BIOCHEMICAL OXYGEN DEMAND, 50
BIODYNAMICS, 220, 221
BIOLOGICAL EFFECTS, 217
BIPOLAR TRANSISTORS, 84
BIPOLARITY, 155, 167, 298
BIT ERROR RATE, 75
BLACK HOLES (ASTRONOMY), 311
BLASIUS FLOW, 86
BLAZARS, 309, 311
BLOOD, 98
BLOOD FLOW, 221
BLOOD PRESSURE, 221, 222
BLOOD PUMPS, 98
BLOWDOWN WIND TUNNELS, 24
BODY TEMPERATURE, 220, 222
BODY VOLUME (BIOLOGY), 93
BOEING 747 AIRCRAFT, 116
BONE MARROW, 217
BONE MINERAL CONTENT, 224
BONES, 224
BOOSTER ROCKET ENGINES, 30
BORON NITRIDES, 59
BOUNDARY CONDITIONS, 103, 123, 299
BOUNDARY LAYER TRANSITION, 86, 90
BOUNDARY LAYERS, 2, 205
BRAIN, 218, 220
BRAZING, 53
BRIGHTNESS, 305, 308
BRIGHTNESS TEMPERATURE, 190, 208
BRINES, 54
BRITTLENESS, 53
BROADBAND, 20, 246, 259
BROADCASTING, 312
BROMINE COMPOUNDS, 126
BUCKLING, 103
BUDGETING, 286
BURNING RATE, 52, 64
BUTADIENE, 252

C

C++ (PROGRAMMING LANGUAGE), 236
CABIN ATMOSPHERES, 36
CALCIUM CARBONATES, 274
CALCIUM OXIDES, 128
CALCULUS, 243
CALIBRATING, 9, 13, 28, 95, 110, 252, 259
CALORIMETERS, 92, 289
CAMERAS, 14, 144, 260
CANTILEVER BEAMS, 102
CAPACITANCE, 172
CAPACITORS, 82
CAPILLARY FLOW, 221
CARBON, 57, 123, 213
CARBON 14, 117
CARBON COMPOUNDS, 213
CARBON DIOXIDE CONCENTRATION, 55
CARBON DIOXIDE LASERS, 267
CARBON MONOXIDE, 92
CARBONACEOUS MATERIALS, 213
CARBURETORS, 99
CARBURIZING, 55
CARDIOLOGY, 219
CARDIOVASCULAR SYSTEM, 220, 222
CARTILAGE, 224
CASUALTIES, 176
CATALYSIS, 125
CATALYTIC ACTIVITY, 24
CAVITIES, 101
CCD CAMERAS, 259, 261
CELLS, 217
CELLS (BIOLOGY), 217
CELLULOSE NITRATE, 66
CENTRAL EUROPE, 201
CENTRAL NERVOUS SYSTEM, 223
CENTRAL PROCESSING UNITS, 230
CERAMIC MATRIX COMPOSITES, 42, 45
CERAMICS, 43

CERMETS, 59
CERTIFICATION, 67, 279
CESIUM, 54
CHANNELS, 161
CHAOS, 228
CHARACTERIZATION, 106, 113, 173
CHARGE COUPLED DEVICES, 260
CHARGE DISTRIBUTION, 135, 170, 186, 187, 194
CHARGE INJECTION DEVICES, 152
CHARGE TRANSFER, 141, 183, 184, 188, 189, 191, 192
CHARGED PARTICLES, 135, 136, 138, 170, 171, 181, 183, 185, 186, 194, 243, 250
CHARTS, 7
CHECKOUT, 26, 34
CHEMICAL ANALYSIS, 97, 124, 226, 299
CHEMICAL COMPOSITION, 49, 64, 295
CHEMICAL EVOLUTION, 308
CHEMICAL PROPERTIES, 66
CHEMICAL REACTIONS, 48, 63, 70, 125
CHICKENS, 271
CHILDREN, 276
CHINA, 284, 287
CHIRALITY, 276
CHLORINATION, 65
CHLORINE FLUORIDES, 123
CHLORINE OXIDES, 126
CHROMIUM, 54, 59
CHROMIUM ALLOYS, 40, 54
CHROMOSPHERE, 305, 306
CIRCADIAN RHYTHMS, 222
CIRCUIT BOARDS, 232
CIRCUITS, 34
CIRCULATION, 148
CIVIL AVIATION, 5
CLADDING, 260
CLAYS, 106
CLEAN FUELS, 67
CLEANERS, 63, 129
CLEANING, 63
CLIENT SERVER SYSTEMS, 233
CLIMATE, 111, 115, 123, 212
CLIMATE CHANGE, 67, 108, 109, 115, 119, 123, 153
CLIMATE MODELS, 115, 123, 124, 127
CLIMATOLOGY, 105, 115, 120, 124, 132, 151, 207, 209, 212
CLOUD PHYSICS, 105, 130, 131, 135, 182, 183, 184, 185, 191, 193, 195, 202, 205, 208, 213
CLOUD SEEDING, 184
CLOUD–TO–CLOUD DISCHARGES, 134, 161, 174, 193
CLOUD–TO–GROUND DISCHARGES, 135, 152, 157, 158, 159, 160, 161, 162, 164, 165, 166, 168, 170, 173, 174, 177, 180, 182, 183, 184, 185, 188, 193, 196, 198, 202, 203
CLOUDS (METEOROLOGY), 152, 211
CLUSTER ANALYSIS, 173, 289
COAL, 264
COALESCING, 68
COATING, 82, 290
COATINGS, 57, 290
CODING, 102
COHERENCE, 291
COLD FRONTS, 210
COLLIMATION, 270, 288
COMBAT, 80
COMBUSTION, 51, 241, 258
COMBUSTION CHAMBERS, 14, 20
COMBUSTION CONTROL, 241
COMBUSTION PHYSICS, 49, 52, 241
COMBUSTION PRODUCTS, 49, 94
COMBUSTION STABILITY, 17
COMETARY ATMOSPHERES, 289
COMMAND AND CONTROL, 225
COMMERCE, 33
COMMERCE LAB, 35
COMMERCIAL AIRCRAFT, 3, 4, 5, 7
COMMERCIALIZATION, 33
COMMUNICATION, 78
COMMUNICATION EQUIPMENT, 80
COMMUNICATION NETWORKS, 76, 77, 78, 79, 178, 212
COMMUNICATION SATELLITES, 79
COMPARISON, 153
COMPARTMENTS, 95
COMPETITION, 25, 282
COMPLEX COMPOUNDS, 230
COMPLEX SYSTEMS, 241
COMPOSITE MATERIALS, 11, 46, 103
COMPOSITE PROPELLANTS, 61, 67
COMPOSITE STRUCTURES, 11, 44, 45, 103, 171
COMPRESSIBILITY, 17
COMPRESSION LOADS, 103
COMPRESSION TESTS, 55
COMPRESSIVE STRENGTH, 103
COMPTON EFFECT, 258
COMPUTATION, 46, 75, 244, 245, 249, 264, 297
COMPUTATIONAL FLUID DYNAMICS, 96, 100, 244
COMPUTATIONAL GRIDS, 241
COMPUTER AIDED DESIGN, 29, 31, 41, 51, 229, 230, 235
COMPUTER AIDED MANUFACTURING, 235
COMPUTER COMPONENTS, 229
COMPUTER DESIGN, 229
COMPUTER GRAPHICS, 223, 233, 235
COMPUTER INFORMATION SECURITY, 237
COMPUTER NETWORKS, 79, 181, 238, 280
COMPUTER PROGRAMMING, 111, 231, 233, 236, 237
COMPUTER PROGRAMS, 19, 32, 121, 234, 235
COMPUTER TECHNIQUES, 75
COMPUTERIZED SIMULATION, 24, 48, 79, 100, 156, 163, 169, 176, 182, 187, 193, 195, 200, 203, 219, 229, 230, 232, 234, 235, 238, 246, 256, 267
COMPUTERS, 73, 233
CONCENTRATORS, 114
CONCRETES, 56
CONCURRENT ENGINEERING, 41
CONDENSATES, 214
CONDENSATION NUCLEI, 125, 183, 205
CONDENSED MATTER PHYSICS, 50
CONDUCTIVE HEAT TRANSFER, 87, 100
CONDUCTORS, 70, 82, 269
CONFERENCES, 14, 83, 104, 105, 254, 284, 302, 312
CONSTELLATIONS, 105
CONSTRUCTION, 82
CONTAMINATION, 50, 106
CONTINGENCY, 119
CONTRACTS, 283
CONTRAILS, 214
CONTROL EQUIPMENT, 10, 22, 78
CONTROL SURFACES, 2
CONTROL SYSTEMS DESIGN, 41, 74, 98, 239
CONTROL THEORY, 74, 96
CONTROL VALVES, 100
CONTROLLABILITY, 11
CONTROLLED FUSION, 266
CONTROLLERS, 34, 82, 84
CONVECTION, 47, 89, 91, 130, 145, 207, 268
CONVECTION CELLS, 169, 185, 193
CONVECTION CLOUDS, 165, 184, 185
CONVECTIVE FLOW, 86, 187
CONVECTIVE HEAT TRANSFER, 91, 100
CONVERGENT–DIVERGENT NOZZLES, 17
CONVEXITY, 85
COOLERS, 23

COORDINATE TRANSFORMATIONS, 259
COPPER, 54, 84
COPPER ALLOYS, 40, 53
COPPER OXIDES, 51
CORE FLOW, 263
CORN, 109
CORONAL HOLES, 305
CORONAL LOOPS, 304
CORONAL MASS EJECTION, 306
CORROSION, 55, 273
CORROSION RESISTANCE, 55
COSMIC DUST, 297
COSMIC RAY SHOWERS, 181
COSMOLOGY, 292, 296, 310
COST REDUCTION, 28, 29, 231
COSTS, 279, 283
CRACK OPENING DISPLACEMENT, 104
CRACK PROPAGATION, 54
CRASHES, 44
CRASHWORTHINESS, 44
CRATERS, 302
CRAY COMPUTERS, 229
CRITERIA, 180, 274
CRITICAL LOADING, 41
CROSS CORRELATION, 110
CROSS FLOW, 90
CRUDE OIL, 126
CRYOGENIC COOLING, 290
CRYOGENIC EQUIPMENT, 92
CRYOGENIC TEMPERATURE, 36, 91
CRYOGENICS, 69, 92, 100
CRYPTOGRAPHY, 281
CRYSTAL GROWTH, 270, 271, 272, 273, 274, 275
CRYSTAL STRUCTURE, 271, 273
CRYSTAL SURFACES, 51
CRYSTALLINITY, 271
CRYSTALLIZATION, 58, 274
CRYSTALLOGRAPHY, 270, 274
CRYSTALS, 73, 270, 271, 275
CUMULONIMBUS CLOUDS, 157, 165, 179, 180, 181, 183, 186, 189, 191, 195, 199
CURIE TEMPERATURE, 97
CURRENT DENSITY, 172
CURRENT DISTRIBUTION, 158
CURRENT SHEETS, 267
CURVED PANELS, 103
CYBERNETICS, 98
CYCLIC LOADS, 45
CYCLONES, 196, 209, 210, 211
CYCLOTRON FREQUENCY, 265
CYCLOTRON RADIATION, 265
CYLINDRICAL BODIES, 85

D

DAMAGE, 34, 176, 267
DAMAGE ASSESSMENT, 103, 176
DAMPING, 90
DARK MATTER, 296
DATA ACQUISITION, 15, 28, 48, 77, 108, 119, 136, 144, 209, 264, 288, 295, 308
DATA BASES, 229, 230, 247, 279, 292
DATA CORRELATION, 117, 157, 159, 161, 162, 179, 185, 197, 198, 199
DATA MANAGEMENT, 279
DATA PROCESSING, 192, 208, 212, 235
DATA PROCESSING EQUIPMENT, 28
DATA PROCESSING TERMINALS, 280
DATA RECORDING, 24
DATA RETRIEVAL, 118, 210, 282
DATA SMOOTHING, 294
DATA STORAGE, 9
DATA SYSTEMS, 124, 216
DATA TRANSMISSION, 80, 238
DEBRIS, 31
DECISION THEORY, 62
DEFECTS, 43
DEFENSE PROGRAM, 281, 284, 286
DEFLECTION, 101
DEFORMATION, 103, 250
DEGRADATION, 23
DELAMINATING, 44
DELAY, 48
DELPHI METHOD (FORECASTING), 285
DEMAGNETIZATION, 36
DENSE PLASMAS, 39
DEPOLARIZATION, 266
DEPOSITION, 56, 57, 140
DEPOSITS, 257
DESERTS, 115
DESIGN ANALYSIS, 10, 15, 18, 21, 24, 26, 29, 31, 41, 68, 69, 72, 76, 93, 96, 114, 124, 229, 230, 239, 260, 270, 287
DESTRUCTION, 267
DETECTION, 13, 73, 162, 177, 178, 181, 198, 199, 200, 202, 203
DETERIORATION, 249
DETONATION, 62
DEUTERIUM, 266
DIAGNOSIS, 69, 101, 223
DIAMINES, 59
DICHROISM, 252
DIELECTRICS, 56, 269
DIESEL ENGINES, 71, 99
DIESEL FUELS, 71
DIFFERENTIAL EQUATIONS, 232
DIFFRACTION RADIATION, 293
DIFFRACTIVE OPTICS, 261, 262
DIFFUSION, 48
DIFFUSION COEFFICIENT, 47
DIFFUSION LENGTH, 48
DIFFUSION THEORY, 145
DIFFUSIVITY, 47, 194
DIGITAL SIMULATION, 33
DIGITAL SYSTEMS, 287
DIMENSIONAL MEASUREMENT, 146
DIMENSIONAL STABILITY, 264
DIMETHYLHYDRAZINES, 94
DIOPHANTINE EQUATION, 228
DIPOLE MOMENTS, 230
DIRECT NUMERICAL SIMULATION, 246
DIRECTION FINDING, 161, 162, 173, 182, 188, 248
DIRECTORIES, 279
DIRICHLET PROBLEM, 228
DISCRETE FUNCTIONS, 34
DISK GALAXIES, 296
DISPERSING, 293
DISPLACEMENT, 93, 262
DISPLACEMENT MEASUREMENT, 261
DISPLAY DEVICES, 75, 204, 232, 291
DISTRIBUTED INTERACTIVE SIMULATION, 23
DISTRIBUTED MEMORY, 229
DISTRIBUTION FUNCTIONS, 158, 263
DIURNAL VARIATIONS, 116, 137, 141, 153, 164, 168, 204, 221
DOCUMENTATION, 281
DOPED CRYSTALS, 84, 272, 273
DOPPLER EFFECT, 72
DOPPLER RADAR, 179
DOSIMETERS, 251
DRAG, 2, 72
DROP SIZE, 192, 209
DROPS (LIQUIDS), 188, 191, 193, 194, 195, 261
DRYDOCKS, 143
DUALITY THEOREM, 228
DUCTILE–BRITTLE TRANSITION, 18
DUCTILITY, 53
DURABILITY, 47
DUST, 243
DYNAMIC CHARACTERISTICS, 99, 108, 145, 231
DYNAMIC MODELS, 140, 231
DYNAMIC RESPONSE, 82, 220
DYNAMIC STABILITY, 99
DYNAMICAL SYSTEMS, 140

DYNAMO THEORY, 185, 303
DYSON THEORY, 253

E

E REGION, 134
EARTH IONOSPHERE, 117, 132, 134, 135, 139, 148, 201
EARTH MAGNETOSPHERE, 148, 149
EARTH MANTLE, 145
EARTH MOVEMENTS, 147, 148
EARTH OBSERVING SYSTEM (EOS), 107, 131
EARTH RADIATION BUDGET, 213
EARTH SCIENCES, 105, 151
EARTH SURFACE, 175
EARTHQUAKES, 147, 148
ECOLOGY, 106
ECONOMETRICS, 6
ECONOMIC ANALYSIS, 71
ECONOMIC DEVELOPMENT, 71, 283, 286
ECONOMIC IMPACT, 176
ECONOMICS, 15, 119, 282, 283, 285, 286
ECOSYSTEMS, 106, 109, 116
EDUCATION, 4, 22, 23, 114, 217, 276, 277, 278
EFFECTIVENESS, 29
EGGS, 271
EJECTORS, 15, 16, 19
EL NINO, 130, 151, 189, 200
ELASTIC PROPERTIES, 102, 104
ELECTRIC AUTOMOBILES, 83
ELECTRIC BATTERIES, 72, 83, 113
ELECTRIC CHARGE, 141, 158, 159, 161, 162, 166, 170, 172, 179, 187, 188, 189, 190, 191, 193, 195
ELECTRIC CONDUCTORS, 176
ELECTRIC CORONA, 163, 164, 191
ELECTRIC CURRENT, 136, 139, 158, 169
ELECTRIC DISCHARGES, 156, 163, 164, 171, 192, 193, 205
ELECTRIC FIELD STRENGTH, 93, 138, 162, 177, 184, 190
ELECTRIC FIELDS, 57, 105, 134, 136, 137, 138, 139, 141, 152, 159, 163, 164, 168, 170, 172, 175, 177, 179, 181, 183, 186, 187, 192, 194, 197, 205, 250, 262, 268
ELECTRIC GENERATORS, 81
ELECTRIC MOTOR VEHICLES, 83, 98
ELECTRIC POTENTIAL, 82, 117, 136, 139, 156, 177, 255
ELECTRIC PULSES, 172
ELECTRICAL IMPEDANCE, 231
ELECTRICAL MEASUREMENT, 57, 93, 136, 138, 139, 141, 158, 159, 165, 171, 190, 197
ELECTRICAL PROPERTIES, 82, 113, 135, 189, 197
ELECTRICAL RESISTIVITY, 59, 135, 138, 139, 161
ELECTRICITY, 81
ELECTRIFICATION, 105, 165, 182, 185, 186, 187, 189, 190, 191, 192, 193, 195, 205
ELECTRO–OPTICAL EFFECT, 275
ELECTRO–OPTICS, 261, 275
ELECTROCHEMICAL CORROSION, 65
ELECTRODYNAMICS, 32, 40, 137, 262
ELECTROLYTES, 193
ELECTROMAGNETIC ABSORPTION, 271
ELECTROMAGNETIC FIELDS, 263
ELECTROMAGNETIC MEASUREMENT, 173
ELECTROMAGNETIC PROPULSION, 39
ELECTROMAGNETIC PULSES, 155, 166, 175
ELECTROMAGNETIC RADIATION, 18, 73, 165
ELECTROMAGNETIC WAVE TRANSMISSION, 134, 167
ELECTROMAGNETISM, 218
ELECTRON BEAMS, 243, 252, 264
ELECTRON CYCLOTRON RESONANCE, 265
ELECTRON IMPACT, 253
ELECTRON PRECIPITATION, 131
ELECTRON SCATTERING, 252
ELECTRON SPECTROSCOPY, 49, 50, 252, 254
ELECTRON TRANSFER, 54
ELECTRONS, 54
ELEMENTARY PARTICLE INTERACTIONS, 255
ELLIPTICAL GALAXIES, 289
EMISSION, 127, 128, 129
EMISSION SPECTRA, 106, 305, 311
END EFFECTORS, 22
END–TO–END DATA SYSTEMS, 27
ENERGETIC PARTICLES, 144, 309
ENERGY ABSORPTION, 224
ENERGY BUDGETS, 110, 149
ENERGY DISSIPATION, 82, 224
ENERGY DISTRIBUTION, 264
ENERGY STORAGE, 83, 149
ENERGY TECHNOLOGY, 114
ENERGY TRANSFER, 130, 144, 249
ENGINE DESIGN, 20, 40, 41, 247, 248
ENGINE PARTS, 45, 46
ENGINE TESTS, 20, 38
ENGINEERS, 277, 281
ENSTATITE, 299
ENVIRONMENT EFFECTS, 64, 67, 116
ENVIRONMENT MANAGEMENT, 121, 124, 284
ENVIRONMENT POLLUTION, 121
ENVIRONMENT PROTECTION, 61, 124, 128, 284
ENVIRONMENTAL CLEANUP, 121
ENVIRONMENTAL MONITORING, 61, 120, 124, 284
EPOXY RESINS, 43
EQUATIONS, 221
EQUATIONS OF MOTION, 195
EQUATORIAL ELECTROJET, 76
EROSION, 42, 108, 266, 267
ERROR ANALYSIS, 10, 78, 233, 248
ERRORS, 4, 9
ESTIMATES, 126, 153, 209
ESTIMATING, 104, 211, 226
ETHYL ALCOHOL, 67
EUROPE, 143, 223
EVALUATION, 9, 12, 95, 108, 225
EVANESCENCE, 243
EVANESCENT WAVES, 243
EVAPORATION, 194
EVAPORATIVE COOLING, 86
EVEN–EVEN NUCLEI, 251
EXCITATION, 251, 255, 267
EXCITONS, 75
EXHAUST CLOUDS, 120
EXHAUST EMISSION, 71, 99, 120, 122, 125
EXHAUST GASES, 71, 99, 116, 120, 122, 125, 214
EXHAUST NOZZLES, 15, 20
EXHAUST SYSTEMS, 15, 19
EXPERIMENT DESIGN, 69
EXPERIMENTATION, 17, 20, 48, 91, 226, 251, 253, 264, 265
EXPLOSIONS, 63
EXPLOSIVES, 63
EXPLOSIVES DETECTION, 240
EXPOSURE, 64
EXTRACTION, 96
EXTRAPOLATION, 248
EXTRATERRESTRIAL ENVIRONMENTS, 290
EXTRAVEHICULAR ACTIVITY, 221
EXTREME ULTRAVIOLET EXPLORER SATELLITE, 311
EXTREME ULTRAVIOLET RADIATION, 134, 295
EXTREMELY HIGH FREQUENCIES, 77

EXTREMELY LOW FREQUENCIES, 73, 137, 172

F

F REGION, 134
FABRICATION, 9, 18, 20, 24, 36, 47, 54, 76, 84, 97, 114, 119, 251, 271
FABRY–PEROT INTERFEROMETERS, 92, 119
FACE (ANATOMY), 221
FAILURE, 34, 45, 104, 274
FAILURE ANALYSIS, 274
FAINT OBJECTS, 292
FAR FIELDS, 244
FAR INFRARED RADIATION, 210
FARADAY EFFECT, 97
FATIGUE (MATERIALS), 56
FATIGUE TESTS, 11, 45, 274
FAULT DETECTION, 81
FEASIBILITY ANALYSIS, 38
FEDERAL BUDGETS, 26
FEED SYSTEMS, 37
FEEDBACK, 3, 239
FERROELECTRICITY, 231
FIBER COMPOSITES, 44, 47
FIBER LASERS, 83
FIBER OPTICS, 97
FIBERS, 66
FIBRILLATION, 219
FIELD ALIGNED CURRENTS, 134
FIELD OF VIEW, 36
FIELD STRENGTH, 78, 146, 172
FIELD THEORY (ALGEBRA), 227
FIELD THEORY (PHYSICS), 241
FILM COOLING, 90
FILM THICKNESS, 57
FINITE DIFFERENCE THEORY, 147
FINITE ELEMENT METHOD, 44, 55, 85, 102
FINLAND, 287
FIRE PREVENTION, 72
FIRES, 72, 95
FITTING, 294
FLAME RETARDANTS, 51
FLARE STARS, 304
FLAT PLATES, 55
FLIGHT CHARACTERISTICS, 11
FLIGHT CONDITIONS, 12
FLIGHT CONTROL, 10, 12
FLIGHT CREWS, 4
FLIGHT HAZARDS, 180
FLIGHT SAFETY, 3, 4
FLIGHT SIMULATION, 8, 11, 24
FLIGHT SIMULATORS, 2, 24
FLIGHT TESTS, 2, 3, 8, 10, 12, 14, 33, 37, 247
FLIGHT TRAINING, 3, 4
FLIP–FLOPS, 18, 293
FLOAT ZONES, 86, 272, 273
FLORIDA, 138, 184, 188
FLOW CHARACTERISTICS, 13, 23
FLOW DISTRIBUTION, 18, 89, 96, 256, 261
FLOW THEORY, 90
FLOW VELOCITY, 70, 90, 99
FLOW VISUALIZATION, 14, 88, 232, 256
FLOWMETERS, 96
FLUE GASES, 125
FLUID DYNAMICS, 96
FLUID FLOW, 88, 91
FLUID MANAGEMENT, 70
FLUID MECHANICS, 47, 96
FLUID–SOLID INTERACTIONS, 90
FLUORESCENCE, 271
FLUTTER ANALYSIS, 21
FLUX (RATE), 146
FLUX QUANTIZATION, 110
FOCAL PLANE DEVICES, 295
FOG, 197, 211
FORCED CONVECTION, 168
FOREBODIES, 13
FOREST MANAGEMENT, 106
FORESTS, 108, 110
FORGING, 55
FORM FACTORS, 255
FORMING TECHNIQUES, 44, 55
FOSSILS, 117
FOURIER TRANSFORMATION, 58, 256
FRACTALS, 112, 113
FRANCE, 176
FREE CONVECTION, 91, 180, 196
FREQUENCY RANGES, 143
FRESH WATER, 218
FUEL CONTROL, 98
FUEL INJECTION, 71
FUEL PUMPS, 100
FUELS, 51, 62, 64, 266
FUNCTIONAL ANALYSIS, 227
FUNCTIONAL DESIGN SPECIFICATIONS, 74
FUNCTIONS (MATHEMATICS), 227, 228, 241
FUNGI, 129
FURNACES, 68, 69, 271
FUSION (MELTING), 266
FUZZY SYSTEMS, 84, 98

G

GALACTIC BULGE, 290
GALACTIC CLUSTERS, 289, 292, 309
GALACTIC EVOLUTION, 289
GALACTIC RADIATION, 309
GALACTIC ROTATION, 297
GALACTIC STRUCTURE, 289, 297
GALACTIC WINDS, 308
GALAXIES, 297, 308
GALERKIN METHOD, 102
GALLIUM, 272
GAMMA RAY ASTRONOMY, 289, 293, 307, 310, 311
GAMMA RAY BURSTS, 288, 299, 307, 310, 311
GAMMA RAY OBSERVATORY, 299
GAMMA RAY SOURCES (ASTRONOMY), 289, 290, 299, 307, 310
GAMMA RAY TELESCOPES, 289
GAMMA RAYS, 309
GARNETS, 97
GAS ANALYSIS, 94
GAS COMPOSITION, 94, 116
GAS DENSITY, 309
GAS DETECTORS, 37, 43, 92, 94
GAS DISSOCIATION, 26, 167
GAS HEATING, 14
GAS MIXTURES, 56, 94
GAS PRESSURE, 14
GAS TEMPERATURE, 309
GAS TURBINE ENGINES, 21
GASEOUS DIFFUSION, 127
GASES, 129
GENETIC ALGORITHMS, 111
GEODESY, 146
GEOGRAPHIC DISTRIBUTION, 153
GEOIDS, 145
GEOMAGNETIC TAIL, 144, 263
GEOMAGNETISM, 141, 146, 303
GEOMORPHOLOGY, 302
GEOPHYSICS, 146, 150
GEOSYNCHRONOUS ORBITS, 40
GERMANIUM, 258, 272
GLOBAL POSITIONING SYSTEM, 7, 8, 9, 30, 105, 112
GLOW DISCHARGES, 269
GOLD, 60
GOLD ALLOYS, 53
GOVERNMENT PROCUREMENT, 279
GOVERNMENT/INDUSTRY RELATIONS, 283
GOVERNMENTS, 278, 284
GRADIENTS, 96
GRANTS, 26

GRAPHITE, 57, 266
GRAPHS (CHARTS), 223
GRASSLANDS, 108
GRATINGS (SPECTRA), 293, 295
GRAUPEL, 178, 183, 184, 189, 190, 192, 195
GRAVITATION, 89
GRAVITATIONAL EFFECTS, 52, 298
GRAVITATIONAL PHYSIOLOGY, 217
GRAVITATIONAL WAVES, 126, 131
GRAVITY WAVES, 126, 145
GREECE, 117, 147
GREEN'S FUNCTIONS, 147, 243
GREENHOUSE EFFECT, 119, 123
GRID GENERATION (MATHEMATICS), 19, 100, 235
GROUND BASED CONTROL, 264
GROUND EFFECT (AERODYNAMICS), 10, 33
GROUND EFFECT (COMMUNICATIONS), 77
GROUND OPERATIONAL SUPPORT SYSTEM, 65, 231
GROUND STATE, 250, 251
GROUND STATIONS, 77, 78, 200
GROUND TESTS, 24, 30
GROUND TRUTH, 199
GROUND WATER, 104, 264
GROUP THEORY, 227
GROWTH, 286
GUIDANCE (MOTION), 8, 12

H

H ALPHA LINE, 305
H LINES, 306
HADRONS, 258
HAFNIUM CARBIDES, 42
HAILSTORMS, 182
HAMILTONIAN FUNCTIONS, 255
HARDENING (MATERIALS), 55
HARDWARE, 232
HARDWARE DESCRIPTION LANGUAGES, 233
HARMONIC OSCILLATION, 240
HARTREE APPROXIMATION, 250, 253
HATCHES, 221
HAZARDOUS MATERIALS, 63
HAZARDS, 72
HEAD DOWN TILT, 219, 222
HEALTH, 64
HEART, 219, 223
HEART FUNCTION, 222
HEAT EXCHANGERS, 23
HEAT FLUX, 85
HEAT RESISTANT ALLOYS, 40, 43, 82
HEAT SHIELDING, 290
HEAT TRANSFER, 69, 86, 89
HEAT TRANSFER COEFFICIENTS, 69
HEATING, 305
HEAVY ELEMENTS, 309
HEAVY IONS, 140, 231
HEAVY NUCLEI, 250, 251
HELIOTRONS, 265
HELIPORTS, 1
HELIUM, 251, 253, 305, 306
HELIUM ISOTOPES, 306
HELMETS, 226
HEMODYNAMIC RESPONSES, 222
HERBIG–HARO OBJECTS, 298
HETEROGENEITY, 61, 299
HETEROJUNCTION DEVICES, 84
HETEROJUNCTIONS, 84
HIGH ENERGY INTERACTIONS, 250, 251, 258
HIGH ENERGY OXIDIZERS, 66
HIGH PRESSURE, 85, 102, 220
HIGH RESOLUTION, 209, 288
HIGH SPEED, 20
HIGH SPEED PHOTOGRAPHY, 14
HIGH STRENGTH STEELS, 103
HIGH TEMPERATURE, 20, 69
HIGH TEMPERATURE PLASMAS, 266, 268
HIGH TEMPERATURE TESTS, 20, 45
HIGH THRUST, 247
HIGHWAYS, 56
HILBERT SPACE, 227
HIMALAYAS, 164
HISTIDINE, 275
HISTOCHEMICAL ANALYSIS, 217
HISTORIES, 7, 281
HOMOLOGY, 227
HOMOMORPHISMS, 227
HONEYCOMB STRUCTURES, 23, 24
HONG KONG, 287
HOPE AEROSPACE PLANE, 21, 33
HORIZONTAL DISTRIBUTION, 158
HOT WORKING, 55
HUMAN BEINGS, 93, 284
HUMAN BODY, 220, 223
HUMAN FACTORS ENGINEERING, 75
HUMAN PERFORMANCE, 221, 222, 224
HUMAN REACTIONS, 220
HUMAN RESOURCES, 4
HUMAN–COMPUTER INTERFACE, 29
HURRICANES, 105, 151, 160, 188, 190, 206, 207
HYDRAULIC EQUIPMENT, 100
HYDRAZINES, 50, 62, 65, 94, 95
HYDROCARBONS, 38
HYDROGEN, 53, 252
HYDROGEN EMBRITTLEMENT, 53
HYDROGEN IONS, 48
HYDROGEN PEROXIDE, 64, 66
HYDROLOGICAL CYCLE, 112, 149
HYDROLOGY, 109
HYPERGOLIC ROCKET PROPELLANTS, 66, 94
HYPERNUCLEI, 258
HYPERSONIC AIRCRAFT, 11
HYPERTENSION, 221
HYPERVELOCITY GUNS, 28
HYPOBARIC ATMOSPHERES, 217
HYPOKINESIA, 219
HYPOXIA, 217

I

ICE, 31, 73, 189, 193
ICE CLOUDS, 182, 186, 188, 189, 190, 195
ICE FORMATION, 23, 31, 183
ICE NUCLEI, 183
ICE PREVENTION, 31
IGNITERS, 49
IGNITION, 48, 95, 99
ILLUMINATING, 78
IMAGE ANALYSIS, 111, 113, 289
IMAGE CLASSIFICATION, 107, 112, 233
IMAGE PROCESSING, 49, 56, 70, 111, 112, 232, 256, 261
IMAGE RECONSTRUCTION, 111
IMAGE RESOLUTION, 242, 295
IMAGERY, 56, 75
IMAGES, 75
IMAGING TECHNIQUES, 72, 106, 111, 112, 154, 173, 201, 204, 208, 218, 261, 288, 290, 298
IMMUNE SYSTEMS, 217
IMPACT DAMAGE, 44
IMPACT VELOCITY, 186
IMPINGEMENT, 85
IMPULSES, 208
IMPURITIES, 191, 275
IN SITU MEASUREMENT, 112, 126, 131, 269
INCIDENCE, 4, 5
INCOHERENT SCATTER RADAR, 147, 150
INCOHERENT SCATTERING, 150
INCONEL (TRADEMARK), 53
INDIA, 170
INDIUM ANTIMONIDES, 97

INDIUM ARSENIDES, 97
INDOOR AIR POLLUTION, 60
INDUSTRIAL MANAGEMENT, 101
INDUSTRIAL PLANTS, 278
INDUSTRIES, 127, 282, 285
INFORMATION, 282
INFORMATION FLOW, 78, 281
INFORMATION SYSTEMS, 75, 236, 280, 281
INFORMATION TRANSFER, 78, 225
INFRARED DETECTORS, 83
INFRARED IMAGERY, 109, 211
INFRARED PHOTOGRAPHY, 105
INFRARED RADIATION, 27, 97, 109, 154, 298
INFRARED SCANNERS, 154
INFRARED SPECTRA, 58
INFRARED SPECTROSCOPY, 58, 94, 298
INFRARED TELESCOPES, 27
INJECTION, 267
INJECTORS, 85
INJURIES, 176
INLET FLOW, 13, 20
INSPECTION, 100
INSTALLING, 265
INSTRUCTORS, 276
INSTRUMENT ERRORS, 10
INTAKE SYSTEMS, 13, 248
INTEGRAL EQUATIONS, 241
INTEGRATED MISSION CONTROL CENTER, 264
INTERFEROMETERS, 214, 259
INTERFEROMETRY, 154, 155, 157, 160, 161, 166, 174, 261, 262
INTERNAL COMBUSTION ENGINES, 99
INTERNATIONAL RELATIONS, 278
INTERNATIONAL SPACE STATION, 30, 33, 34
INTERNATIONAL TRADE, 285
INTERNET RESOURCES, 280
INTERNETS, 238
INTERNUCLEAR PROPERTIES, 250
INTERPLANETARY MAGNETIC FIELDS, 132
INTERSTELLAR EXTINCTION, 298
INTRACLOUD DISCHARGES, 152, 166, 173, 185, 198, 202, 203
INVARIANT IMBEDDINGS, 259
INVESTMENT CASTING, 43
INVESTMENTS, 26
INVISCID FLOW, 2
IO, 301
ION BEAMS, 42, 257
ION CHARGE, 141, 194
ION CONCENTRATION, 132
ION CURRENTS, 194
ION CYCLOTRON RADIATION, 265, 268
ION DENSITY (CONCENTRATION), 138
ION DISTRIBUTION, 132, 263, 267
ION MOBILITY SPECTROSCOPY, 137, 140
ION MOTION, 249
ION OPTICS, 36
ION SOURCES, 52
IONIC MOBILITY, 137, 141
IONIZATION, 34, 134, 171, 252, 253
IONIZATION CROSS SECTIONS, 253
IONIZED GASES, 49
IONIZING RADIATION, 33, 232
IONOSONDES, 74
IONOSPHERIC CONDUCTIVITY, 134
IONOSPHERIC HEATING, 268
IONS, 139, 194, 306
IRON ALLOYS, 53, 54
IRRADIANCE, 307
IRRIGATION, 104
ISOLATION, 231
ISOMORPHISM, 227
ISRAEL, 179, 180, 200
ITERATION, 228

J

J INTEGRAL, 104
JAMMING, 75
JAPAN, 143, 163, 178, 179, 183
JAPANESE SPACECRAFT, 36
JAVA (PROGRAMMING LANGUAGE), 237
JET AIRCRAFT, 4
JET AIRCRAFT NOISE, 16, 17, 20, 245, 246, 247, 248
JET ENGINE FUELS, 67
JET EXHAUST, 116
JET FLOW, 18
JET MIXING FLOW, 14, 17, 245
JOINTS (JUNCTIONS), 104
JP–4 JET FUEL, 38
JP–5 JET FUEL, 38
JP–8 JET FUEL, 38

K

K LINES, 307
K–EPSILON TURBULENCE MODEL, 216, 245
KALMAN FILTERS, 216
KAOLINITE, 106
KAONS, 258
KINETIC ENERGY, 49, 207
KINETIC EQUATIONS, 249
KINETICS, 276
KNOWLEDGE REPRESENTATION, 281

L

LABOR, 6
LABORATORIES, 243, 278
LABORATORY EQUIPMENT, 270
LAGRANGE MULTIPLIERS, 237
LAMINAR BOUNDARY LAYER, 86
LAND, 173, 203
LAND SURFACE TEMPERATURE, 180
LANDAU DAMPING, 265
LANDSAT 7, 107
LANDSAT SATELLITES, 113
LAPLACE TRANSFORMATION, 243
LARGE EDDY SIMULATION, 90
LASER ALTIMETERS, 302
LASER MATERIALS, 87
LASER OUTPUTS, 97, 267
LASER PLASMAS, 161
LASER SPECTROMETERS, 94
LASER WELDING, 56
LASERS, 261
LATCH–UP, 231
LATEX, 60, 127
LATITUDE, 147
LAUNCH VEHICLES, 30
LAUNCHING, 40
LAUNCHING SITES, 120, 121
LEAD COMPOUNDS, 64
LEAD ZIRCONATE TITANATES, 58
LEADERS (METEOROLOGY), 156, 157, 159, 160, 167, 168, 171, 172
LEADERSHIP, 286
LEADING EDGES, 21
LEAKAGE, 37, 95, 103, 226
LEARNING, 22
LENGTH, 146
LEPTONS, 255
LEVEL (QUANTITY), 93
LIAPUNOV FUNCTIONS, 240
LIGHT (VISIBLE RADIATION), 307
LIGHT CURVE, 291
LIGHT EMISSION, 163, 165, 269
LIGHT IONS, 140
LIGHT TRANSMISSION, 165
LIGHTNING, 105, 124, 135, 142, 143, 152, 153, 154, 155, 156, 157, 158, 159, 160, 161, 162, 163, 164, 165, 166, 167, 168, 169, 170, 171, 172, 173, 174, 175, 176, 177, 178, 179, 180, 181, 182, 183, 184, 185, 188,

189, 190, 191, 195, 196, 197, 198, 199, 200, 201, 202, 203, 204, 205, 208, 214
LINE CURRENT, 82
LINE SHAPE, 257
LINE SPECTRA, 269
LINEAR ENERGY TRANSFER (LET), 232
LINEAR POLARIZATION, 92
LINEAR SYSTEMS, 257
LIQUEFACTION, 143
LIQUID FUELS, 65
LIQUID METALS, 47
LIQUID NITROGEN, 43
LIQUID OXIDIZERS, 66
LIQUID PHASES, 234
LIQUID PROPELLANT ROCKET ENGINES, 40, 45
LIQUID ROCKET PROPELLANTS, 62, 65, 94
LIQUID–SOLID INTERFACES, 244
LITHIUM, 113
LOADS (FORCES), 45, 70, 81, 143, 234
LOGIC CIRCUITS, 261
LOGIC DESIGN, 84
LOGIC PROGRAMMING, 233
LOGISTICS, 242
LONG DURATION EXPOSURE FACILITY, 33
LONG WAVE RADIATION, 110, 211
LONGITUDINAL CONTROL, 11
LONGITUDINAL STABILITY, 11
LOOP ANTENNAS, 265
LOSSES, 80
LOUDSPEAKERS, 249
LOW ASPECT RATIO, 265
LOW COST, 9, 28
LOW EARTH ORBITS, 40
LOW NOISE, 14, 15
LOW PASS FILTERS, 82
LOW TEMPERATURE, 180
LOW TURBULENCE, 2
LOWER ATMOSPHERE, 136, 138
LUMINESCENCE, 298
LUMINOSITY, 292, 297
LYMAN ALPHA RADIATION, 307
LYSOZYME, 271, 275

M

MACH NUMBER, 18
MACROMOLECULES, 276
MAGNESIUM, 253
MAGNETIC COILS, 33
MAGNETIC COOLING, 36, 92
MAGNETIC DISTURBANCES, 139
MAGNETIC FIELD CONFIGURATIONS, 262
MAGNETIC FIELD RECONNECTION, 262
MAGNETIC FIELDS, 36, 86, 134, 172, 220, 262, 264, 300
MAGNETIC FILMS, 97
MAGNETIC FLUX, 39, 265
MAGNETIC MEASUREMENT, 240
MAGNETIC STORMS, 144, 147, 149, 150
MAGNETO–OPTICS, 97
MAGNETOHYDRODYNAMIC FLOW, 266
MAGNETOHYDRODYNAMIC STABILITY, 267
MAGNETOHYDRODYNAMIC WAVES, 268
MAGNETOHYDRODYNAMICS, 266
MAGNETOPAUSE, 131
MAGNETOPLASMADYNAMICS, 39
MAGNETOSHEATH, 269
MAGNETOSPHERES, 300
MAGNETOSTATIC FIELDS, 272
MAGNETRON SPUTTERING, 54
MAGNETRONS, 264
MAINTENANCE, 264
MANAGEMENT, 112, 249
MANAGEMENT INFORMATION SYSTEMS, 279, 280
MANAGEMENT METHODS, 231
MANAGEMENT PLANNING, 29, 33, 302
MANDRELS, 71
MANEUVERABILITY, 154
MANGANESE ISOTOPES, 299
MANIFOLDS (MATHEMATICS), 228
MANNED MARS MISSIONS, 302
MANUFACTURING, 33, 95, 127, 278, 282
MANY BODY PROBLEM, 241
MAPPING, 111, 146, 175, 196
MARKARIAN GALAXIES, 311
MARS (PLANET), 300, 302
MARS ATMOSPHERE, 36, 74, 300
MARS ENVIRONMENT, 36
MARS EXPLORATION, 26
MARS LANDING, 302
MARS MISSIONS, 302
MARS OBSERVER, 302
MARS SAMPLE RETURN MISSIONS, 302
MARS SURFACE, 302
MARYLAND, 116
MASS DISTRIBUTION, 95, 128
MASS SPECTROMETERS, 36
MASS TRANSFER, 86, 183
MASSIVE STARS, 298
MASSIVELY PARALLEL PROCESSORS, 216
MATERIALS SCIENCE, 35
MATHEMATICAL MODELS, 2, 13, 23, 44, 47, 52, 89, 90, 101, 121, 134, 136, 137, 139, 141, 156, 160, 162, 165, 167, 169, 175, 185, 187, 189, 191, 193, 194, 218, 219, 228, 257, 274, 301
MATRICES (MATHEMATICS), 257
MEASURING INSTRUMENTS, 93, 126, 141, 206, 252
MECHANICAL ENGINEERING, 278
MECHANICAL MEASUREMENT, 70
MECHANICAL PROPERTIES, 43, 46, 47, 53
MEDIA, 244
MEDIAN (STATISTICS), 125
MELTING, 70, 89
MELTS (CRYSTAL GROWTH), 272, 273
MEMBRANES, 86
MEMORY (COMPUTERS), 73, 229, 231
MENTAL PERFORMANCE, 224
MERCURY (METAL), 116
MERCURY (PLANET), 300
MERCURY COMPOUNDS, 128
MERCURY VAPOR, 128
MEROMORPHIC FUNCTIONS, 228
MESOMETEOROLOGY, 213
MESONS, 250, 254, 255
MESOPAUSE, 133
MESOSCALE PHENOMENA, 161, 162, 169, 186, 187, 196, 206, 213, 215
MESOSPHERE, 131, 133, 134, 163, 165
METAL COMBUSTION, 49, 52
METAL FILMS, 54, 97
METAL IONS, 113
METAL OXIDES, 51, 57, 59
METAL PARTICLES, 49
METAL POLISHING, 71
METAL WORKING, 44, 55
METALORGANIC CHEMICAL VAPOR DEPOSITION, 97
METALS, 230
METEOROLOGICAL PARAMETERS, 117, 124, 137, 159, 197, 202, 210, 213
METEOROLOGICAL RADAR, 206
METEOROLOGICAL SATELLITES, 105, 111, 211
METEOROLOGICAL SERVICES, 176, 210
METEOROLOGY, 65, 105, 111, 116, 210, 211

METHANE, 127
METHYL COMPOUNDS, 254
METHYLHYDRAZINE, 94
METROLOGY, 71, 80
MICROELECTRONICS, 84
MICROGRAVITY, 35, 68, 70, 222, 274
MICROMECHANICS, 46, 47, 95
MICROMETEOROLOGY, 137, 213
MICROSCOPY, 217
MICROSTRUCTURE, 55, 87, 274
MICROWAVE IMAGERY, 108, 144, 190, 196, 208
MICROWAVE RADIOMETERS, 108, 211
MICROWAVE SCATTERING, 190
MICROWAVE SENSORS, 109
MICROWAVES, 209
MIDDLE ATMOSPHERE, 132, 163, 164, 172
MILITARY TECHNOLOGY, 38, 284, 286
MILKY WAY GALAXY, 289, 292
MILLIMETER WAVES, 297
MINERALS, 106
MINIATURIZATION, 36, 97
MINIMAX TECHNIQUE, 233
MINORITIES, 114, 277, 312
MIRRORS, 101, 260, 295
MISALIGNMENT, 249
MISSION PLANNING, 27, 35, 280, 302
MIXERS, 16, 19
MIXING, 309
MIXING RATIOS, 124, 197
MOBILE COMMUNICATION SYSTEMS, 79
MOBILITY, 136, 301
MODELS, 18, 25, 41, 109, 235, 241, 254, 279
MODULATION, 133
MOISTURE, 67
MOISTURE CONTENT, 149, 170, 189
MOISTURE RESISTANCE, 88
MOLDS, 47
MOLECULAR CLOUDS, 299
MOLECULAR CLUSTERS, 52
MOLECULAR COLLISIONS, 257
MOLECULAR DYNAMICS, 210, 234, 254
MOLECULAR EXCITATION, 250
MOLECULAR GASES, 51
MOLECULAR IONS, 135, 250, 301
MOLECULAR STRUCTURE, 257
MOLECULES, 252, 254
MOLYBDENUM ALLOYS, 54
MOMENTUM, 49, 50, 254
MOMENTUM TRANSFER, 130
MONITORS, 94
MONOMERS, 59
MONSOONS, 130, 138, 151, 209
MONTE CARLO METHOD, 48, 255, 257, 274
MORPHOLOGY, 217, 274
MOTION SICKNESS, 220, 221
MULTIDISCIPLINARY DESIGN OPTIMIZATION, 239
MULTIDISCIPLINARY RESEARCH, 239
MULTIPATH TRANSMISSION, 9
MULTIPHASE FLOW, 87
MULTIPLE ACCESS, 79
MULTIPLEXING, 97
MULTIPOLES, 234
MULTISENSOR APPLICATIONS, 169, 240
MUONS, 258
MYOCARDIUM, 220, 222

N

NACELLES, 14
NASA PROGRAMS, 27, 29, 107, 276, 302
NATIONAL AIRSPACE SYSTEM, 7
NATURAL GAS, 126
NAVIER–STOKES EQUATION, 245
NAVIGATION, 8, 12
NAVIGATION SATELLITES, 8
NAVY, 225
NEBULAE, 298
NETWORK ANALYSIS, 79
NETWORK CONTROL, 41, 78
NETWORKS, 182
NEURAL NETS, 98, 238, 239, 240
NEUROLOGY, 220, 223
NEUTRINOS, 309
NEUTRON DECAY, 251
NEUTRON SCATTERING, 234, 254
NEUTRON STARS, 308
NEUTRONS, 306
NEW MEXICO, 167
NICKEL ALLOYS, 82
NIGERIA, 166
NIGHT, 211
NIMBOSTRATUS CLOUDS, 186
NITRIC ACID, 226
NITRIC OXIDE, 203
NITROGEN, 131, 226, 264
NITROGEN ATOMS, 264
NITROGEN DIOXIDE, 126
NITROGEN OXIDES, 14, 116, 123, 124, 125, 142, 197, 201, 205
NITROGEN TETROXIDE, 65, 66
NOAA SATELLITES, 144
NOCTILUCENT CLOUDS, 133
NOISE (SOUND), 245
NOISE GENERATORS, 245
NOISE INTENSITY, 19, 222
NOISE MEASUREMENT, 24, 248
NOISE PREDICTION, 245, 246, 247
NOISE PREDICTION (AIRCRAFT), 246
NOISE REDUCTION, 10, 16, 17, 18, 19, 20, 89, 244, 247, 248
NOISE SPECTRA, 246
NONDESTRUCTIVE TESTS, 56, 100
NONINTRUSIVE MEASUREMENT, 18
NONLINEAR SYSTEMS, 140
NORTH AMERICA, 143
NORTH SEA, 226
NOZOMI MARS ORBITER, 36
NOZZLE DESIGN, 14, 15, 16, 17, 18, 19, 40, 247
NOZZLE EFFICIENCY, 14, 16, 17, 20
NOZZLE FLOW, 14
NOZZLE GEOMETRY, 16
NUCLEAR FISSION, 250, 251, 264
NUCLEAR FUSION, 251, 296
NUCLEAR INTERACTIONS, 251, 254
NUCLEAR MODELS, 256
NUCLEAR PHYSICS, 254, 258
NUCLEAR SCATTERING, 249
NUCLEAR STRUCTURE, 251, 255
NUCLEATION, 52, 137, 183, 271, 274
NUCLEONS, 250
NUMERICAL ANALYSIS, 20, 46, 55, 91, 101, 144, 216, 218, 241, 244, 246, 264, 301
NUMERICAL WEATHER FORECASTING, 212

O

OBJECT–ORIENTED PROGRAMMING, 32, 41, 236
OBSERVATION, 244, 308
OBSERVATORIES, 288
OCCUPATION, 277
OCEAN BOTTOM, 147
OCEAN CURRENTS, 216
OCEAN DATA ACQUISITIONS SYSTEMS, 181
OCEAN MODELS, 118, 216
OCEAN SURFACE, 9, 118, 248
OCEANOGRAPHY, 107, 215
OCEANS, 203, 215, 216
ODD–EVEN NUCLEI, 251
OFFGASSING, 58
ON–LINE SYSTEMS, 239
OPERATING COSTS, 5, 6
OPERATORS (MATHEMATICS), 226

OPTICAL DENSITY, 261
OPTICAL EQUIPMENT, 114, 201, 217
OPTICAL FIBERS, 83, 95
OPTICAL FILTERS, 259, 260
OPTICAL MATERIALS, 275
OPTICAL MEASUREMENT, 160, 165, 201, 254
OPTICAL MEASURING INSTRUMENTS, 295
OPTICAL PROPERTIES, 160
OPTICAL RADAR, 107, 212
OPTICAL SWITCHING, 261
OPTICAL WAVEGUIDES, 83
OPTIMIZATION, 2, 41, 82, 85, 98, 175
ORBIT DETERMINATION, 7
ORBIT TRANSFER VEHICLES, 69
ORBITAL RENDEZVOUS, 32
ORBITALS, 253
ORGANIC CHEMISTRY, 254
ORGANIC COMPOUNDS, 127
ORGANIC MATERIALS, 57, 275
ORIENTATION, 73
OSCILLATIONS, 11, 95, 291
OSCILLATORS, 70
OXIDATION, 51, 52, 99
OXIDATION RESISTANCE, 42
OXYGEN, 37, 59
OXYGEN ANALYZERS, 43
OXYGEN PRODUCTION, 26
OXYNITRIDES, 56
OZONE, 116, 118, 119, 124, 142, 226, 304
OZONE DEPLETION, 126

P

PAINTS, 60, 127
PAIR PRODUCTION, 309
PARALLEL FLOW, 249
PARALLEL PROCESSING (COMPUTERS), 75, 229
PARALLEL PROGRAMMING, 235
PARAMETERIZATION, 164, 206
PARTIAL DIFFERENTIAL EQUATIONS, 102
PARTICLE ACCELERATION, 134, 306, 309
PARTICLE ACCELERATORS, 28
PARTICLE CHARGING, 187
PARTICLE COLLISIONS, 89, 184, 186, 188, 189, 255
PARTICLE DECAY, 251, 254, 255, 258
PARTICLE ENERGY, 263
PARTICLE IMAGE VELOCIMETRY, 85, 256
PARTICLE INTERACTIONS, 49, 243, 250
PARTICLE MOTION, 144, 267
PARTICLE PRODUCTION, 255, 258
PARTICLE SIZE DISTRIBUTION, 67
PARTICLE TRAJECTORIES, 194
PARTICULATE REINFORCED COMPOSITES, 46
PARTICULATES, 116, 129, 140, 213
PASSENGER AIRCRAFT, 6
PASSENGERS, 5, 6
PATTERN METHOD (FORECASTING), 240
PAYLOADS, 29, 40
PENETRATION, 101
PERFORMANCE PREDICTION, 15, 24, 224, 284
PERFORMANCE TESTS, 15, 16, 17, 18, 30, 92, 113, 224, 226
PERIODIC VARIATIONS, 115, 142, 143, 200, 228
PERIODICALS, 70, 279
PERMEATING, 65
PERSONNEL, 231
PERSONNEL MANAGEMENT, 241
PERSONNEL SELECTION, 224
PERTURBATION, 2, 207, 296
PERTURBATION THEORY, 296
PHARMACOLOGY, 127
PHASE VELOCITY, 165
PHASED ARRAYS, 75
PHENOMENOLOGY, 152, 159
PHOTOCHEMICAL REACTIONS, 126, 142
PHOTODIODES, 83
PHOTOIONIZATION, 253
PHOTOLUMINESCENCE, 97
PHOTOMETRY, 96
PHOTONS, 293
PHOTOREFRACTIVITY, 293
PHOTOVOLTAIC CONVERSION, 77, 78
PHTHALOCYANIN, 57
PHYSICAL CHEMISTRY, 273, 299
PHYSIOLOGICAL EFFECTS, 217, 220, 222, 223
PHYSIOLOGICAL RESPONSES, 219
PIEZOELECTRICITY, 87
PILOTLESS AIRCRAFT, 12
PILOTS (PERSONNEL), 221
PIONS, 254
PIPELINES, 103
PIPELINING (COMPUTERS), 230
PISTONS, 47
PLANE STRESS, 102
PLANETARY BOUNDARY LAYER, 206
PLANETARY ENVIRONMENTS, 301
PLANETARY GEOLOGY, 302
PLANETARY IONOSPHERES, 74
PLANETARY MAGNETOTAILS, 131
PLANETARY NEBULAE, 299
PLANETARY RADIATION, 212
PLANETARY WAVES, 133, 145
PLANFORMS, 22
PLASMA ACCELERATORS, 28
PLASMA CONTROL, 265, 266
PLASMA DENSITY, 144, 263, 268
PLASMA DRIFT, 268
PLASMA DYNAMICS, 262, 267
PLASMA ELECTRODES, 262
PLASMA HEATING, 163, 265, 268
PLASMA INTERACTIONS, 268, 269
PLASMA JETS, 269
PLASMA OSCILLATIONS, 268
PLASMA PHYSICS, 269
PLASMA PROPULSION, 39
PLASMA RADIATION, 264, 268
PLASMA SPECTRA, 263
PLASMA SPRAYING, 40
PLASMA TEMPERATURE, 268
PLASMA WAVES, 73, 268
PLASMAS (PHYSICS), 39, 125, 131, 171, 262, 263, 265, 267, 268, 269
PLASMASPHERE, 144, 148, 263, 268
PLASTIC PROPERTIES, 104
PLATEAUS, 155
PLAYBACKS, 96
PLUG NOZZLES, 19
PLUMES, 18, 19, 116, 214
PLUTONIUM 239, 226
POLAR CAPS, 139
POLAR CUSPS, 134, 269
POLAR METEOROLOGY, 133
POLAR REGIONS, 133
POLARIMETRY, 182
POLARITY, 162, 183, 193
POLARIZATION (CHARGE SEPARATION), 167, 169, 172, 186, 188, 190, 193, 195
POLARIZATION (SPIN ALIGNMENT), 73
POLARIZATION CHARACTERISTICS, 252
POLARIZED LIGHT, 92
POLICIES, 6, 283
POLISHING, 70, 260
POLITICS, 283, 284
POLLEN, 117
POLLUTION CONTROL, 60, 99, 121, 122, 128
POLLUTION MONITORING, 60, 122
POLLUTION TRANSPORT, 99
POLYCARBONATES, 43

POLYCRYSTALS, 59
POLYETHYLENES, 65
POLYIMIDES, 59
POLYMER MATRIX COMPOSITES, 45
POLYMERIZATION, 58
POLYMERS, 51, 58
POLYMETHYL METHACRYLATE, 87
POLYNOMIALS, 227
POLYSILOXANES, 88
POPULATION THEORY, 282, 284
POPULATIONS, 282, 284
POSITION (LOCATION), 175, 176, 178, 182
POSITION INDICATORS, 7
POSITIVE FEEDBACK, 48
POSITIVE IONS, 36
POSITRONIUM, 251
POTENTIAL ENERGY, 207
POWDER (PARTICLES), 67
POWER LINES, 81
POWER SUPPLY CIRCUITS, 255
PRECIPITATION (METEOROLOGY), 123, 151, 206, 212
PREDICTION ANALYSIS TECHNIQUES, 148, 246
PREDICTIONS, 70, 244
PRESSURE BROADENING, 210
PRESSURE DEPENDENCE, 99
PRESSURE DROP, 87
PRESSURE EFFECTS, 57
PRESSURE MEASUREMENT, 13, 16, 271
PRESSURE PULSES, 133
PRESSURE RATIO, 87
PRESSURE SENSORS, 37, 91
PRESSURE VESSELS, 91, 102
PROBABILITY DENSITY FUNCTIONS, 158
PROBABILITY DISTRIBUTION FUNCTIONS, 118
PROBABILITY THEORY, 80, 240, 256, 282, 284
PROBE METHOD (FORECASTING), 240
PROCEDURES, 2, 58, 81, 146, 206, 253, 270
PROCESS CONTROL (INDUSTRY), 55
PRODUCTION COSTS, 29
PRODUCTIVITY, 6
PROGRAM VERIFICATION (COMPUTERS), 235
PROGRAMMABLE LOGIC DEVICES, 233
PROGRAMMING ENVIRONMENTS, 231
PROGRESS, 49
PROJECT MANAGEMENT, 231
PROJECT PLANNING, 247
PROPAGATION (EXTENSION), 156
PROPAGATION VELOCITY, 160, 165, 167, 168, 172
PROPELLANT GRAINS, 66, 67
PROPELLANT PROPERTIES, 66, 254
PROPELLANTS, 61
PROPULSION, 10, 38, 39, 40, 72
PROPULSION SYSTEM CONFIGURATIONS, 19, 37, 72, 247
PROPULSION SYSTEM PERFORMANCE, 20, 30, 40, 42, 72
PROTECTION, 81, 178
PROTEIN CRYSTAL GROWTH, 274, 275, 276
PROTEINS, 270, 271
PROTOCOL (COMPUTERS), 79, 236
PROTONS, 34
PROTOTYPES, 36, 232, 237
PROVING, 124, 260
PUBLIC HEALTH, 119
PULSARS, 288, 291, 293, 299, 309, 310
PULSE AMPLITUDE, 287
PULSE GENERATORS, 39
PULSED LASER DEPOSITION, 59
PUMPS, 100
PURGING, 43
PURIFICATION, 275
PYROLYSIS, 51

Q

QUADRATIC EQUATIONS, 227
QUANTUM CHEMISTRY, 274
QUANTUM CHROMODYNAMICS, 276
QUANTUM MECHANICS, 135, 228
QUANTUM WELL LASERS, 87
QUARKS, 254, 276
QUARTZ, 57
QUASARS, 297, 298
QUEUEING THEORY, 237, 238

R

RADAR CROSS SECTIONS, 74
RADAR DATA, 184, 185
RADAR DETECTION, 178
RADAR ECHOES, 157, 179, 180, 184, 187, 196, 202
RADAR IMAGERY, 196
RADAR MEASUREMENT, 147, 191
RADAR SCATTERING, 150, 182
RADAR TRACKING, 157, 179, 180, 182, 183, 184, 185, 187, 188, 205
RADIAL FLOW, 98
RADIANCE, 110
RADIATION ABSORPTION, 213
RADIATION DAMAGE, 255
RADIATION DISTRIBUTION, 168, 173
RADIATION DOSAGE, 34
RADIATION EFFECTS, 34, 255
RADIATION MEASUREMENT, 110, 251
RADIATION PRESSURE, 87
RADIATION PROTECTION, 226
RADIATION SHIELDING, 226
RADIATION SOURCES, 155, 248, 249
RADIATIVE HEAT TRANSFER, 52
RADIATIVE TRANSFER, 112, 118, 129, 211, 259
RADIO ASTRONOMY, 287, 305, 310
RADIO BURSTS, 308, 310
RADIO COMMUNICATION, 79, 80
RADIO DIRECTION FINDERS, 175
RADIO EMISSION, 199, 311
RADIO FREQUENCIES, 80, 152, 199, 208
RADIO FREQUENCY DISCHARGE, 154
RADIO FREQUENCY HEATING, 265, 268
RADIO FREQUENCY INTERFERENCE, 77, 78
RADIO GALAXIES, 292, 298
RADIO OBSERVATION, 287, 311
RADIO OCCULTATION, 290
RADIO RECEIVERS, 74
RADIO SOURCES (ASTRONOMY), 290, 307, 310
RADIO SPECTROSCOPY, 287
RADIO TRANSMISSION, 79, 80
RADIOACTIVE DECAY, 226, 250, 251
RADIOACTIVE MATERIALS, 54, 117
RADIOACTIVITY, 33
RADIOLYSIS, 117
RADIOMETERS, 110
RADON ISOTOPES, 135
RAIN, 77, 115, 130, 151, 153, 157, 159, 182, 196, 205, 206, 207, 209, 211, 212
RAIN GAGES, 206
RAINDROPS, 189, 192, 194, 208, 209
RANDOM ACCESS, 232
RANDOM ACCESS MEMORY, 232
RANGE SAFETY, 210
RANGEFINDING, 182
RATS, 217, 222
REACTION KINETICS, 44, 51, 63
REACTION TIME, 52
REACTIVITY, 63, 125
REACTOR MATERIALS, 266, 267
REAL TIME OPERATION, 24, 239, 249, 274, 290

RECEIVERS, 7, 8, 30
RECLAMATION, 65
RECORDING HEADS, 96
RECORDS, 281
RECOVERABILITY, 65
RECYCLING, 65
RED SHIFT, 292, 297
REENTRY VEHICLES, 21, 33
REFERENCE ATMOSPHERES, 132
REFILLING, 268
REFLECTANCE, 74, 161, 191, 202, 209
REFRACTIVITY, 114
REFRACTORY MATERIALS, 42
REFRACTORY METAL ALLOYS, 40
REFRIGERATORS, 36
REGENERATION (ENGINEERING), 65
REGOLITH, 300
REGRESSION ANALYSIS, 6
REGULATIONS, 1
REGULATORS, 4
REINFORCING FIBERS, 44
REINFORCING MATERIALS, 44
RELIABILITY, 78
RELIABILITY ANALYSIS, 102
REMOTE SENSING, 9, 74, 105, 106, 107, 108, 109, 112, 119, 120, 129, 131, 144, 150, 153, 196, 199, 211, 214, 233, 287
RENDEZVOUS GUIDANCE, 32
RENDEZVOUS SPACECRAFT, 32
RENEWABLE ENERGY, 114
RESEARCH, 24, 38, 47, 90, 152, 215, 219, 243, 253, 254, 258, 266, 301, 312
RESEARCH AIRCRAFT, 13
RESEARCH AND DEVELOPMENT, 29, 71, 79, 124, 276, 278, 283, 284, 285, 286, 287, 312
RESEARCH FACILITIES, 24, 35, 312
RESEARCH MANAGEMENT, 239
RESEARCH VEHICLES, 83
RESIDUAL STRESS, 55, 104
RESOLUTION, 282
RESONANCE LINES, 306
RESONANT FREQUENCIES, 142, 143, 200, 201, 220
RESOURCES MANAGEMENT, 112, 284
RESPIROMETERS, 122
RETRAINING, 231
RETURN TO EARTH SPACE FLIGHT, 302
REUSABLE LAUNCH VEHICLES, 29, 30
REUSE, 65
REVENUE, 6, 285
REVISIONS, 38
RHEOLOGY, 61
RING STRUCTURES, 218
RIOMETERS, 74
RISC PROCESSORS, 230
RISK, 62, 121
ROADWAY POWERED VEHICLES, 83
ROBUSTNESS (MATHEMATICS), 175, 238, 249
ROCKET ENGINE DESIGN, 41
ROCKET ENGINES, 41, 66, 67, 234, 235
ROCKET EXHAUST, 120
ROCKET LAUNCHING, 120
ROCKET LININGS, 40
ROCKET NOZZLES, 40
ROCKET OXIDIZERS, 66
ROCKET PROPELLANTS, 64
ROCKET TEST FACILITIES, 69
ROSAT MISSION, 292
ROTATIONAL STATES, 250
ROTOR DYNAMICS, 99
ROTOR SPEED, 96
ROTORS, 96
RURAL AREAS, 77

S

SAFETY, 3, 4, 61, 62, 63
SAFETY DEVICES, 178
SAFETY MANAGEMENT, 7, 62, 63
SAGE SATELLITE, 120, 304
SAPPHIRE, 57
SARCOPLASMIC RETICULUM, 222
SATELLITE COMMUNICATION, 76, 77
SATELLITE CONTROL, 78
SATELLITE IMAGERY, 113, 150, 151, 173
SATELLITE INSTRUMENTS, 173
SATELLITE OBSERVATION, 105, 111, 154, 163, 173, 174, 198, 199, 202, 203, 208, 211
SATELLITE SOUNDING, 129, 211
SATELLITE–BORNE RADAR, 199
SCALE MODELS, 33
SCANNERS, 60
SCATTERING, 261
SCATTERING CROSS SECTIONS, 49, 251, 252, 253
SCHEDULES, 6, 279
SCHUMANN–RUNGE BANDS, 143, 200
SCIENTIFIC SATELLITES, 33, 105
SCINTILLATING FIBERS, 289
SCREECH TONES, 17, 245
SCRUBBERS, 128
SEA ICE, 215
SEA SURFACE TEMPERATURE, 105, 111, 170, 215
SEARCHING, 282
SEAS, 173
SEASONS, 136
SECURITY, 278, 284
SEGMENTED MIRRORS, 71
SEISMIC WAVES, 147
SEISMOLOGY, 147, 148, 244
SELECTION, 72
SELECTIVE DISSEMINATION OF INFORMATION, 281
SEMICONDUCTOR LASERS, 94, 97
SEMICONDUCTORS (MATERIALS), 59, 270, 272
SENSITIVITY, 10, 73, 127, 262
SENSORY PERCEPTION, 224
SEQUENCING, 226
SEQUENTIAL ANALYSIS, 227
SEQUENTIAL CONTROL, 74
SERIES (MATHEMATICS), 227
SERIES EXPANSION, 227, 243
SERVICE LIFE, 70, 266
SERVICES, 4, 6
SEYFERT GALAXIES, 291, 294
SHALLOW WATER, 243
SHAPE MEMORY ALLOYS, 55
SHEAR LAYERS, 87
SHIPS, 225
SHOCK WAVES, 245, 246, 247, 264
SHORT HAUL AIRCRAFT, 6
SHOT PEENING, 55
SIGNAL DETECTION, 175, 181, 182, 196, 198
SIGNAL DETECTORS, 199
SIGNAL FADING, 77
SIGNAL GENERATORS, 8
SIGNAL MEASUREMENT, 159, 173, 196
SIGNAL PROCESSING, 9, 287
SIGNAL REFLECTION, 72
SIGNAL TO NOISE RATIOS, 288
SIGNAL TRANSMISSION, 76
SIGNATURES, 263
SILICON, 21, 50, 54, 59, 272, 289
SILICON COMPOUNDS, 88
SILICON DIOXIDE, 43, 60, 128, 270
SILICON FILMS, 60
SILICON OXIDES, 48
SILICON TRANSISTORS, 84
SILOXANES, 88
SIMULATION, 10, 19, 24, 34, 100, 145, 156, 234, 235, 244, 249, 255, 264
SIMULATORS, 23, 33, 41, 79, 234, 241
SINGLE CRYSTALS, 114, 274, 275
SINGLE EVENT UPSETS, 232

SINGULARITY (MATHEMATICS), 242
SIZE DISTRIBUTION, 49, 118, 209
SKIN TEMPERATURE (BIOLOGY), 220
SLABS, 132
SMALL SCIENTIFIC SATELLITES, 27
SNAILS, 218
SNC METEORITES, 299
SNOW, 73
SNOW COVER, 73
SNOWSTORMS, 193
SOCIAL ISOLATION, 284
SOCIOLOGY, 284
SODIUM CHLORIDES, 193
SOFTWARE DEVELOPMENT TOOLS, 32, 236
SOFTWARE ENGINEERING, 31, 32, 231, 235, 236
SOFTWARE RELIABILITY, 32
SOFTWARE REUSE, 32
SOHO MISSION, 291, 306
SOIL MOISTURE, 108, 109, 149
SOIL SAMPLING, 106, 108
SOL–GEL PROCESSES, 58, 260
SOLAR ACTIVITY, 142, 303, 304
SOLAR ACTIVITY EFFECTS, 303
SOLAR ARRAYS, 269
SOLAR ATMOSPHERE, 291, 305
SOLAR CELLS, 59
SOLAR CONVECTION (ASTRONOMY), 303
SOLAR CORONA, 291, 295, 303, 305, 306, 307
SOLAR CYCLES, 303, 304
SOLAR ELECTRIC PROPULSION, 26
SOLAR ENERGY CONVERSION, 39
SOLAR FLARES, 304, 306, 307
SOLAR GENERATORS, 39
SOLAR HEATING, 303, 304
SOLAR OBSERVATORIES, 307
SOLAR PHYSICS, 303, 304, 307
SOLAR PROTONS, 304
SOLAR RADIATION, 213, 305, 307
SOLAR RADIO EMISSION, 305
SOLAR SPECTRA, 306
SOLAR SYSTEM, 301
SOLAR SYSTEM EVOLUTION, 296
SOLAR TERRESTRIAL INTERACTIONS, 141
SOLAR THERMAL PROPULSION, 114
SOLAR TRANSITION REGION, 291, 305, 306
SOLAR WIND, 131, 133, 142, 300
SOLAR X–RAYS, 295, 304, 307
SOLDERED JOINTS, 53
SOLID PROPELLANT COMBUSTION, 64
SOLID PROPELLANT ROCKET ENGINES, 42, 61, 64
SOLID ROCKET PROPELLANTS, 61, 64, 66, 67
SOLID STATE, 92
SOLID STATE DEVICES, 83
SOLID–SOLID INTERFACES, 186
SOLIDS, 241, 274
SOLVENTS, 63
SOOT, 51
SORBENTS, 128
SOUND INTENSITY, 247
SOUND PRESSURE, 87, 244
SOUND WAVES, 18, 87, 245, 247, 249
SOUTHERN OSCILLATION, 130, 151, 200
SPACE CHARGE, 137, 140, 163
SPACE COMMERCIALIZATION, 35, 39
SPACE COMMUNICATION, 77
SPACE DEBRIS, 28
SPACE MISSIONS, 27, 280
SPACE PROGRAMS, 84
SPACE SHUTTLE PAYLOADS, 34
SPACE STATION PAYLOADS, 34
SPACE SUITS, 302
SPACE TRANSPORTATION, 1, 30
SPACE VEHICLE CHECKOUT PROGRAM, 34
SPACE WEATHER, 105
SPACEBORNE EXPERIMENTS, 33
SPACEBORNE TELESCOPES, 290
SPACECRAFT CABINS, 220
SPACECRAFT CHARGING, 269
SPACECRAFT CONFIGURATIONS, 93
SPACECRAFT CONTROL, 12
SPACECRAFT DESIGN, 269
SPACECRAFT DOCKING, 32
SPACECRAFT ELECTRONIC EQUIPMENT, 84
SPACECRAFT ENVIRONMENTS, 220, 221
SPACECRAFT GLOW, 269
SPACECRAFT LAUNCHING, 180
SPACECRAFT MANEUVERS, 154
SPACECRAFT PROPULSION, 32
SPACECRAFT TRACKING, 7
SPATIAL DISTRIBUTION, 176, 261
SPATIAL RESOLUTION, 109
SPECIFICATIONS, 23, 280
SPECTRAL BANDS, 293
SPECTRAL ENERGY DISTRIBUTION, 264
SPECTROMETERS, 97
SPECTRORADIOMETERS, 112
SPECTRUM ANALYSIS, 137, 188, 294
SPEECH RECOGNITION, 102, 238
SPENT FUELS, 273
SPHERICAL TANKS, 102
SPICULES, 305
SPIN DYNAMICS, 252
SPONTANEOUS COMBUSTION, 99
SPORES, 129
SPRAYERS, 129, 261
SPREADING, 88
SPUTTERING, 42
SR–71 AIRCRAFT, 37
STABILITY, 34, 264, 283
STABILIZATION, 34, 156, 238, 258
STACKS, 237
STANDARDIZATION, 100, 280
STANDARDS, 176
STANDING WAVES, 87
STARBURST GALAXIES, 298, 308
STARK EFFECT, 250
STATIC CHARACTERISTICS, 104, 272
STATISTICAL ANALYSIS, 124, 171, 178, 235
STATISTICAL DISTRIBUTIONS, 144, 176, 215
STATISTICAL TESTS, 110, 152
STATORS, 39, 239
STEADY STATE, 259
STEELS, 53, 55
STELLAR ACTIVITY, 305
STELLAR CORONAS, 295
STELLAR EVOLUTION, 289
STELLAR FLARES, 304
STELLAR LUMINOSITY, 308
STELLAR MASS EJECTION, 305, 306
STEPPED LEADERS, 156, 159
STEREOPHONICS, 249
STIMULATION, 221
STOCHASTIC PROCESSES, 6
STORMS, 152
STRANGENESS, 258
STRATEGY, 283
STRATOSPHERE, 118, 125, 126, 137, 139, 142, 197
STRATUS CLOUDS, 212
STRESS (PSYCHOLOGY), 222
STRESS ANALYSIS, 102, 103
STRESS CORROSION CRACKING, 54
STROKE VOLUME, 222
STRONG INTERACTIONS (FIELD THEORY), 276
STRUCTURAL ANALYSIS, 46, 47, 102, 104
STRUCTURAL ENGINEERING, 45
STRUCTURAL FAILURE, 103

STRUCTURAL STRAIN, 103
STRUCTURAL VIBRATION, 99
STRUCTURED GRIDS (MATHEMATICS), 235
STUDENTS, 277, 312
SUBMERGED BODIES, 72
SUBSONIC FLOW, 17, 85
SUBSTITUTES, 67
SUBSTRATES, 57
SULFUR DIOXIDES, 128
SULFURIC ACID, 52
SUMMER, 133, 179
SUN, 304, 305
SUNRISE, 138
SUNSPOTS, 303
SUPERCONDUCTORS (MATERIALS), 39
SUPERHIGH FREQUENCIES, 77
SUPERSONIC COMBUSTION, 24
SUPERSONIC FLOW, 87
SUPERSONIC JET FLOW, 17, 18, 19, 245, 246
SUPERSONIC NOZZLES, 247
SUPERSONIC TRANSPORTS, 19
SUPINE POSITION, 224
SUPPLYING, 242
SUPPORT SYSTEMS, 101
SUPPRESSORS, 15, 51
SURFACE DEFECTS, 51
SURFACE LAYERS, 55, 108, 257
SURFACE PROPERTIES, 192
SURFACE REACTIONS, 274
SURFACE ROUGHNESS, 2
SURFACE TREATMENT, 257
SURFACE WATER, 104
SURFACE WAVES, 248
SURFACTANTS, 88, 270
SURGES, 135
SURVEILLANCE, 12
SURVEYS, 297, 298, 308
SWEAT COOLING, 91
SWITCHING CIRCUITS, 261
SYNCHRONISM, 82, 236
SYNTHESIS (CHEMISTRY), 44
SYSTEM FAILURES, 84
SYSTEM IDENTIFICATION, 102
SYSTEMS ANALYSIS, 19, 26, 41, 84, 288, 295
SYSTEMS ENGINEERING, 30, 32, 41, 235, 236, 278, 286

T

T TAURI STARS, 298
TANTALUM CARBIDES, 42
TARGETS, 224
TATB, 44
TECHNOLOGICAL FORECASTING, 280
TECHNOLOGIES, 124, 283, 285, 286, 287
TECHNOLOGY ASSESSMENT, 14, 20, 26, 49, 87, 242, 260, 279
TECHNOLOGY TRANSFER, 39, 78, 259, 281
TECHNOLOGY UTILIZATION, 26, 36, 40, 114, 232, 287
TELECOMMUNICATION, 79
TELECONFERENCING, 76
TELECONNECTIONS (METEOROLOGY), 151
TELESCOPES, 101
TELEVISION CAMERAS, 256
TELEVISION SYSTEMS, 151, 312
TEMPERATE REGIONS, 118, 126
TEMPERATURE, 152
TEMPERATURE CONTROL, 83, 95
TEMPERATURE DEPENDENCE, 47, 97, 113, 117, 180, 210
TEMPERATURE EFFECTS, 36, 58, 59, 67, 220
TEMPERATURE GRADIENTS, 216
TEMPERATURE MEASUREMENT, 36, 216, 246, 272, 273
TEMPERATURE MEASURING INSTRUMENTS, 36
TEMPERATURE PROFILES, 129, 272, 309
TEMPORAL DISTRIBUTION, 143, 176
TEMPORAL RESOLUTION, 113
TENSILE PROPERTIES, 45, 53
TENSILE STRENGTH, 40
TENSILE TESTS, 103
TERNARY ALLOYS, 270
TEST CHAMBERS, 70
TEST FACILITIES, 24, 259
TEST STANDS, 69
TEST VEHICLES, 83
TESTING TIME, 237
TETHERING, 32, 73
TETHERLINES, 32, 73
TEXTILES, 46
TEXTURES, 112
THEMATIC MAPPING, 173
THERMAL ANALYSIS, 46, 100
THERMAL DEGRADATION, 47
THERMAL ENVIRONMENTS, 220
THERMAL EXPANSION, 46
THERMAL FATIGUE, 45
THERMAL PLASMAS, 144, 263
THERMAL PROTECTION, 31
THERMAL RADIATION, 87
THERMAL REACTORS, 258
THERMAL STRESSES, 104
THERMISTORS, 92, 95
THERMODYNAMIC PROPERTIES, 45, 66
THERMOMETERS, 95
THERMONUCLEAR REACTIONS, 266
THERMOREGULATION, 220, 222
THESES, 76
THICKNESS, 132
THIN FILMS, 57, 59, 275
THREE BODY PROBLEM, 253
THREE DIMENSIONAL MODELS, 89, 105, 124, 195, 203, 217, 267
THRUST, 10, 40
THUNDERSTORMS, 105, 143, 152, 154, 155, 156, 157, 158, 159, 163, 164, 165, 166, 167, 168, 170, 173, 174, 178, 179, 180, 182, 183, 184, 185, 186, 187, 189, 190, 191, 193, 194, 195, 196, 197, 199, 200, 201, 202, 203, 204, 205, 208, 214
TILES, 58
TIME DEPENDENCE, 34, 76, 145, 204, 245, 264
TIME SERIES ANALYSIS, 6, 241
TIN OXIDES, 51
TISSUES (BIOLOGY), 217
TITANIUM ALLOYS, 54
TITANIUM ALUMINIDES, 55
TOKAMAK DEVICES, 265, 266, 267, 268
TOLERANCES (MECHANICS), 103
TOLLMIEN–SCHLICHTING WAVES, 86
TOPOGRAPHY, 108, 113, 145, 302
TOPOLOGY, 228
TORNADOES, 105, 188, 202
TOROIDAL PLASMAS, 148
TORQUE, 293
TOWERS, 174
TOXICITY, 38, 50, 64, 104, 120, 121
TOXICOLOGY, 120
TRACE CONTAMINANTS, 191
TRACE ELEMENTS, 120
TRACKING (POSITION), 96, 161, 178
TRACKING NETWORKS, 177
TRACKING PROBLEM, 96
TRAINING ANALYSIS, 29
TRAINING DEVICES, 9, 29
TRAINING EVALUATION, 22
TRAINING SIMULATORS, 22, 23
TRANSIENT PRESSURES, 133
TRANSIENT RESPONSE, 99
TRANSITION PROBABILITIES, 241
TRANSITION REGION AND CORONAL EXPLORER, 291, 305, 306

TRANSMISSION EFFICIENCY, 78
TRANSMISSION LINES, 70, 82
TRANSMITTANCE, 211
TRANSOCEANIC FLIGHT, 7
TRANSONIC FLOW, 21
TRANSONIC SPEED, 88
TRANSPORT AIRCRAFT, 2, 116
TRANSPORT THEORY, 145, 270
TRANSPORTATION, 83
TRAVELING WAVES, 2, 243
TREND ANALYSIS, 6, 284
TRENDS, 6, 284
TRIANGULATION, 201
TRICHLOROETHYLENE, 63
TRITIUM, 266
TRMM SATELLITE, 173, 199, 201, 207, 212
TROPICAL METEOROLOGY, 207
TROPICAL REGIONS, 106, 123, 153, 166, 169, 170, 203, 206, 212
TROPICAL STORMS, 209, 211
TROPOSPHERE, 119, 142, 197
TUMORS, 217
TUNABLE LASERS, 94
TURBINE BLADES, 85
TURBINE ENGINES, 45
TURBOFAN ENGINES, 89, 248
TURBOFANS, 89
TURBULENCE, 2, 89, 215
TURBULENCE EFFECTS, 137, 197
TURBULENCE MODELS, 19, 90, 215, 216, 245
TURBULENT BOUNDARY LAYER, 86
TURBULENT DIFFUSION, 136, 197
TURBULENT FLOW, 86, 91, 216
TURBULENT JETS, 88
TURBULENT MIXING, 185
TWO DIMENSIONAL BOUNDARY LAYER, 90
TWO DIMENSIONAL FLOW, 256
TWO DIMENSIONAL MODELS, 15, 16, 145, 219, 226, 244, 247
TWO PHASE FLOW, 89

U

ULTRAHIGH FREQUENCIES, 157
ULTRASONIC TESTS, 100
ULTRAVIOLET IMAGERY, 150
UNDERWATER ACOUSTICS, 244
UNDERWATER ENGINEERING, 72
UNDERWATER PROPULSION, 72
UNITED STATES, 162, 168, 176, 188, 189, 279, 282, 284, 286
UNIVERSAL TIME, 141
UNIVERSE, 292, 296
UNIVERSITIES, 277, 312
UNIVERSITY PROGRAM, 114, 277
UNIX (OPERATING SYSTEM), 236
UNSTEADY FLOW, 20, 90
UPPER ATMOSPHERE, 163, 183
URANIUM 238, 250
URANIUM ALLOYS, 55
URANIUM OXIDES, 273
USER MANUALS (COMPUTER PROGRAMS), 237

V

VALENCE, 253, 254
VAPOR DEPOSITION, 270
VAPOR PHASES, 129
VAPORS, 58, 271
VARIABILITY, 115, 149, 291, 294, 307
VARIATIONAL PRINCIPLES, 263
VECTORS (MATHEMATICS), 35
VEGETATION, 106, 107, 109, 115, 123
VEGETATION GROWTH, 109
VEGETATIVE INDEX, 109
VELOCITY, 148
VELOCITY DISTRIBUTION, 256, 297
VELOCITY MEASUREMENT, 2, 10
VENTILATION, 194
VENTING, 69
VERTICAL AIR CURRENTS, 160, 185, 191
VERTICAL DISTRIBUTION, 126, 135, 161, 163
VERY HIGH FREQUENCIES, 155, 198
VERY LONG BASE INTERFEROMETRY, 93
VERY LONG BASELINE ARRAY (VLBA), 93
VIABILITY, 4
VIBRATION, 220
VIETNAM, 242
VIRTUAL REALITY, 29
VIRUSES, 276
VISCOSITY, 58, 68
VISIBLE INFRARED SPIN SCAN RADIOMETER, 154
VISUAL AIDS, 75
VISUAL OBSERVATION, 153, 163, 164, 271
VOICE DATA PROCESSING, 102
VOLTAGE CONVERTERS (DC TO DC), 255
VOLTAGE GENERATORS, 177
VOLUMETRIC ANALYSIS, 93
VORTICES, 2, 18
VORTICITY, 17, 88

W

WAKES, 2
WARFARE, 242
WARM FRONTS, 210
WASHING, 128
WASTE MANAGEMENT, 65
WASTE TREATMENT, 50, 122
WASTE WATER, 50, 122
WATER, 65, 88
WATER BALANCE, 108
WATER MANAGEMENT, 104
WATER POLLUTION, 50, 104
WATER RESOURCES, 104, 112
WATER TREATMENT, 50, 122
WATER VAPOR, 133
WATERPROOFING, 58
WAVE ATTENUATION, 147
WAVE DRAG, 145
WAVE EQUATIONS, 243
WAVE EXCITATION, 215
WAVE FRONTS, 259
WAVE PROPAGATION, 83, 126, 134, 147, 165, 166, 167, 168, 219, 244
WAVEFORMS, 9, 158, 170, 172, 177
WAVEGUIDES, 83
WAVELENGTHS, 259
WAVELET ANALYSIS, 242
WEAPONS, 12
WEATHER FORECASTING, 105, 115, 181, 184, 196, 208, 210, 213
WEATHER STATIONS, 105
WEIBULL DENSITY FUNCTIONS, 158
WEIGHTLESSNESS, 26, 68, 69, 221
WEIGHTLESSNESS SIMULATION, 217, 220, 222
WELDED JOINTS, 56, 100
WELDING, 100, 104
WETLANDS, 127
WETTING, 88
WHITE DWARF STARS, 292
WHITE NOISE, 78
WIDTH, 56
WIND (METEOROLOGY), 126, 206, 210, 212
WIND DIRECTION, 300
WIND EFFECTS, 139, 223
WIND MEASUREMENT, 151
WIND PRESSURE, 133
WIND TUNNEL TESTS, 21, 33
WIND TUNNELS, 223
WIND VELOCITY, 9, 126, 300
WINDPOWER UTILIZATION, 300
WINDS ALOFT, 133
WING CAMBER, 2
WING PROFILES, 21

WINTER, 163, 178, 179, 183
WIRE, 82
WIRELESS COMMUNICATION, 79, 80
WORKSTATIONS, 28, 225
WORLD WIDE WEB, 237, 282

X

X RAY ANALYSIS, 287
X RAY ASTRONOMY, 290, 291, 292, 294, 295, 297, 298, 299, 307, 310
X RAY ASTROPHYSICS FACILITY, 259, 290, 294, 295, 298
X RAY BINARIES, 291, 309, 310
X RAY DETECTORS, 290
X RAY OPTICS, 71, 288
X RAY SOURCES, 290, 291, 292, 307
X RAY SPECTROMETERS, 36, 92
X RAY SPECTROSCOPY, 288
X RAY STARS, 308, 311
X RAY TELESCOPES, 71, 295, 309
X RAY TIMING EXPLORER, 291
X RAYS, 259, 288, 291, 299, 308
X–29 AIRCRAFT, 24
X–34 REUSABLE LAUNCH VEHICLE, 31
X–38 CREW RETURN VEHICLE, 30

Z

ZEOLITES, 271
ZETA PINCH, 264
ZINC OXIDES, 57
ZINC SELENIDES, 270, 271
ZONAL FLOW (METEOROLOGY), 207

Personal Author Index

A

Abbud–Madrid, A., 52
Abdeldayem, Hossin, 57
Abe, Koki, 229, 230
Aber, Gregory S., 97
Abernathy, M. C., 54
Abernathy, R. N., 120
Acharya, Sumanta, 90
Acikel, Omer, 75
Acosta, R., 77
Acousta, R., 76
Adcock, W., 253
Adler, R. F., 207
Adler, Robert, 151, 211
Adler, Robert F., 206, 209
Adzhiev, A. Kh, 165
Ag, R. J., 108
Aggarwal, M. D., 274
Agui, Juan, 87
Agzagova, M. B., 165
Ahearne, John F., 124
Ahuja, Krish K., 17
Aikin, A. C., 131
Akers, A., 100
Akpan, U. E., 166
Alexander, J. Iwan D., 274
Alexov, Anastasia, 292
Alfano, R. R., 260
Allen, C. S., 247
Alonso, Roberto, 8
Altaratz, Orit, 179
Altemir, David A., 95
Alves, Miriam Celia Bergue, 230
Amirov, A. K., 171
Anderson, B. E., 125
Anderson, James G., 126
Anderson, John H., Jr, 25
Anderson, M. S., 93
Anderson, Mark O., 32
Anderson, R . R., 144
Ando, Yutaka, 229
Andou, Akiji, 258
Andreev, Andrei A., 117
Andreopoulos, Yiannis, 87
Andretta, V., 306
Andretta, Vincenzo, 291, 305
Andrews, Jason, 30
Anfimov, Dimitrij S., 310
Anisimov, S. V., 136, 139, 141
Anisimova, E. B., 141
Antar, Basil N., 68
Aplin, K. L., 138
Araki, Keisuke, 242
Areitio, J., 158
Areitio, J., 159
Argo, P., 152, 198
Argo, P. E., 151, 154, 199, 207
Armatys, Michael, 9
Armstrong, R. A., 163, 164
Armstrong, T. W., 33
Arnold, S. L., 65
Asay, J., 264
Ashley Paul R., 261
Ashley, Paul R., 261
Askew, J., 15
Askew, J. W., 14, 15
Aspin, Colin, 298
Aten, Laurie A., 216
Atherton, James, 29
Atkinson, L., 204
Atlas, Robert, 211
Attia, John O., 255
Audley, M. D., 35, 287
Aurass, H., 306
Avila, E. E., 184
Avila, Eldo E., 188

B

Babnik , Tadeja, 81
Bac, Nurcan, 271
Badir, Ashraf, 45
Baeten, J. C. M., 237
Bailey, J. C., 190
Bailey, Jeff C., 197
Bailey, Larry L., 8
Bakastov, S. S., 136, 141
Baker, David L., 95
Baker, Donald J., 103
Baker, M. B., 185
Baker, P. P., 3
Baker, R. G., 287
Bakic, Kresimir, 81
Bakker, D., 25
Balakrishman, A. V., 238
Ballard, J. R., Jr., 109
Banish, R. Michael, 47
Banks, Curtis E., 57
Barabash, S., 36
Barabash, V., 133
Baranski, P., 189
Barbee, T. W., 54
Barber, T. J., 19
Barlow, Janet F., 137
Barnard, Y. F., 22, 23
Barnes, Robert A., 109, 153
Barnes, W., 207
Barnes, William L., 153
Barret, D., 289
Barrett, D. M., 257
Barrick, John D., 125
Bartels, D. L., 157
Barto, Rod L., 84
Barton, J. S., 73
Baskaran, Subbiah, 239
Bateman, M. G., 190
Batha, S., 268
Battiste, R. L., 102
Bauer, Steven X. S., 21
Baumgart, C. W., 56
Beasley, W., 169
Beasley, William H., 177
Beckedahl, D., 258
Beech, Geoffrey, 31
Beeson, Harold D., 65, 94
Behring, William, 291
Behring, William E., 305
Beil, Robert J., 37
Belan, V. G., 266
Bell, M., 268
Bell, Robert A., 83
Bello, A. F., 54
Bellomy–Ezell, Jenny, 69
Bender, Matthew W., 60
Benford, Dominic J., 297
Bennett, R. R., 120
Benson, D. E., 76
Benz, K. W., 86, 271, 272, 273
Bergstra, J. A., 237
Berlinrut, D. D., 210
Berman, C., 244
Berman, Charles H., 48
Bernard, Lisa Hamet, 229
Berthelsen, Petter Andreas, 101
Bespalov, P. A., 135
Best, Steve R., 27
Betjes, P. N., 75
Bhalwankar, Rohini V., 193
Bhat, K., 274
Bhat, T. R. S., 246
Bhatia, A. K., 250

Bidwell, S. W., 74
Biefeld, R. M., 97
Biggar, Stuart F., 109
Bildsten, Lars, 293, 310
Birch, M. E., 213
Bishop, Judith, 243
Bixon, Eric R., 120
Black, Michael, 160
Black, Peter, 160
Blair, A. K., 190
Blair, J. J., 258
Blair, James, 29
Blakeslee, R. J., 190
Blakeslee, Richard J., 197, 202, 203, 204
Blanchet, P., 155, 174, 205
Blaschke, D., 276
Bloser, P., 289
Blundell, Katherine M., 292
Blyth, Alan M., 195
Bo, Liang, 221
Boccipio, Dennis, 173
Boccippio, D., 134, 204
Boccippio, D. J., 182, 203
Boccippio, Dennis, 203
Boccippio, Dennis J., 115, 202, 203, 204
Boeck, W. L., 164
Boeck, William, 173, 204
Boeck, William L., 153, 202, 203
Bohannon, Mark, 285
Boldi, Bob, 188
Boldi, R., 134, 142, 200, 214
Bolun, Tong, 220, 221
Bolvin, David, 151
Bolvin, David T., 206
Bondiou–Clergerie, A., 156, 174
Bondiou–Clergerie, Anne, 193
Borg, H., 36
Borhani, N., 91
Borisov, V. V., 134
Borovikov, Anna Y., 215
Borrer, Jerry, 12
Boucarut, R. A., 259
Boulet, J. A. M., 101
Bounoua, L., 122
Bowen, Brent D., 1
Boyce, K. R., 287
Boyd, B. F., 210
Boyd, Robert W., 60
Boyle, Robert, 92
Branch, M.C., 52
Braswell, William D., 143
Braun, Scott A., 205
Brausch, J., 15
Brausch, J. F., 16
Bray, Igor, 252
Breeding, Shawn, 69
Breeding, Shawn P., 95
Breen, M. L., 277
Breisacher, K., 260
Breitenberg, M., 279
Brekosky, R. P., 35
Breon, Susan, 92
Brickstad, B., 104
Bridges, James, 16
Briggs, Michael S., 310
Brinker, C., 270
Britt, Vicki O., 103
Brittnacher, M., 132, 149
Brittnacher, M. J., 144, 149, 150, 262
Broach, Dana M., 8
Brodie, A. W., 105
Brook, M., 164
Brooks, W. A., 174
Brosius, Jeffrey, 291
Brosius, Jeffrey W., 305
Brouwer, J., 13
Brown, John H., 5
Brown, Kenneth G., 92
Brown, Pamela R., 62, 93
Brown, Steven W., 109
Brown, T. H., 226
Brown, W. H., 16
Brucker, G. J., 251
Brunger, M. J., 253
Brunke, K. E., 125
Brunner, Dominik, 115
Brusasco, R. M., 124
Budden, Nancy Ann, 301
Budge, K. G., 264
Buechler, D. E., 189, 202
Buechler, Dennis, 187, 188
Buechler, Dennis E., 202, 203, 204
Buffinger, D. R., 114, 277
Bull, Barton, 7
Bunker, R. L., 61
Buntine, Wray L., 235
Burcham, Frank, 10
Burdisso, Ricardo A., 248
Burken, John, 10
Burton, Daniel, 282
Butler, James J., 109
Buxton, M., 310
Bychkov, Vladimir L., 171
Byerley, L. G., III, 174

C

Cagnoni, Ilaria, 293, 311
Cai, Y., 89
Cairns, Brian, 117
Caldwell, Delmar R., 216
Callahan, C. V., 98
Cameron, Robert, 307
Campbell, Chip, 8, 30
Canacci, Victor A., 23
Canavan, Ed, 92
Canuto, V. M., 214, 215, 216
Caranti, G. M., 194
Caranti, Giorgio M., 185, 188
Carey, A. B., 105
Carey, Lawrence A., 168
Carey, Lawrence D., 182
Carlson, C. W., 132
Carpenter, R. L., 38
Carpenter, Russell, 8, 30
Carroll, J. N., 99
Carvalho, A. M., 158
Carvalho, Andre M., 158, 161, 162
Carvalho, Joao Carlos, 129
Carver, T., 4
Castellano, N. E., 184
Castro, D., 134
Cattanei, G., 265
Caulder, S. M., 67
Cavanagh, S. J., 253
Cave, S. P., 56
Cazetta, A. M., 158
Cederwall, R. T., 212
Celniker, Robert, 14
Cercek, Milan, 240
Cerniglia, Mark C., 118
Cess, R. D., 212
Cezzar, Ruknet, 41, 233
Chai, Steven, 208
Chakrabarty, Deepto, 293, 299, 310
Challa, Preeli, 45
Chan, K. W., 71
Chan, L. M., 99
Chandler, G., 264
Chandler, Kristie, 31
Chandler, M. O., 132, 148
Chandler, Michael O., 131
Chang, A. T. C., 73, 207
Chang, D. –E., 196
Chang, J. –S., 169
Chang, J. C. S., 60, 129
Chang, T., 134
Chang, Yehui, 115
Chao, B. F., 105
Chapman, J. N., 264
Chapman, John J., 91
Chary, Sumitra, 281
Chauzy, S., 157, 174, 192
Chauzy, Serge, 191

Chen, B. Q., 250
Chen, L. J., 262
Chen, M., 155, 156, 167
Chen, S. S., 89
Chen, X. J., 49
Chen, Ya–Chin, 102
Chen, Yani, 224
Cheng, Y., 216
Chengwu, Shen, 220
Chi, Xu, 220
Chiappetta, L. M., 19
Chiles, Harry R., 37, 42
Chilson, P., 133
Chin, H. N. S., 212
Cho, John Y. N., 125
Choi, J., 274
Christian, H. J., 104, 170, 201, 202, 203
Christian, H. J., Jr., 164
Christian, Hugh, 173, 203
Christian, Hugh J., 202, 203, 204
Christian, Hugh J., Jr., 153, 195
Christofferson, S. S., 50
Chu, Martha I., 231
Chua, D., 132
Chuang, C. C., 212
Chuanxian, Zheng, 101
Chudin, E. E., 219
Ciszak, Ewa, 270
Clerc, H.–G., 250
Clinton, R. G., Jr., 40, 44
Cliver, E. W., 305
Clodman, Stephen, 163
Cobb, S. D., 35
Cobleigh, Brent R., 12
Cocchiaro, James E., 60, 63
Cockreham, B. D., 257
Coffey, J., 281
Coffey, Victoria N., 131
Cohen, Dorothea, 23
Cohen, Joel E., 284
Cohen, Samuel A., 263
Cohn, N., 6, 25
Colborn, B. L., 33
Cole, Helen J., 261
Collatz, G. J., 122
Combal, B., 192
Combi, Michael R., 301
Comfort, R. H., 148, 243
Comfort, Richard H., 144, 263, 267
Conforte, Jorge C., 162
Conroy, Maureen, 259
Considine, David B., 145
Content, D., 71
Cook, William, 119
Cooper, B. A., 24
Cooper, John W., 109
Cooper, K., 43
Cooray, Vernon, 168, 172
Coquillat, S., 192
Corpening, Griffin P., 37, 42
Corsetti, L., 212
Couzis, Alex, 88
Cox, D. F., 51
Cox, Pierre, 297
Cox, Timothy H., 11
Craig, L. D., 101
Cramer, J. A., 181
Craven, P. D., 132, 148
Craven, Paul D., 144, 148, 263, 267, 268
Crawford, D. E., 172
Crawford, Kevin, 29
Creutzberg, F., 149
Criminale, W. O., 85
Croell, Arne, 86, 272, 273
Croll, Arne, 271
Cronquist, B., 231
Cronquist, B. E., 232
Cuanghua, Yang, 217
Cucinotta, F. A., 256
Cummins, K. L., 174, 177, 181
Cumnock, J., 150
Cunningham, R. A., 47
Cunnold, Derek M., 126
Curran, E. Brian, 175
Curran, H. J., 98
Curtis, Scott, 151, 206
Cushman, Paula P., 269

D

D, 236
Dachev, T. P., 251
daCostaGalvao, Jose Alexandre, 110
daCostaTredinnick, Marcelo Ricardo Alves, 34
Daily, J. W., 52
Daixiu, Cui, 220
DAlessandro, F., 177, 178
Dalke, R. A., 78
Dam, Kenneth W., 281
DAmbrosia, Christine M., 92
Damour, T., 295
Darden, J. Mark, 99
Darvenzia, M., 141
Das, Kalyan, 84
Dash, J. G., 183
Dash, Sanford M., 19
Datta, Saswati, 188
Davies, Robert, 268
Davila, Joseph M., 305
Davila, Susana, 276
Davis, D., 156
Davis, D. A., 160, 172
Davis, Daniel A., 159
Davis, Dennis D., 63, 65, 94, 95
Davis, Ed, 8, 30
Davis, Edward, 8
Davis, George, 8, 30
Davis, Hubert P., 30
Davis, M., 196
Davis, Stepehen M., 159
Davydenko, S. S., 135
Dazlich, D. A., 122
De, Utpal K., 188
deAraujoTredinnick, Patricia Trindade, 33
DeArmond, Anna H., 65
deBoer, P. T., 79
DeBonis, J. R., 18
deBruin, T. F., 197
deFainchtein, Rosalinda, 234
Defer, E., 155, 191, 205
Defer, Eric, 193
deFigueiredo, Marco Aurelio, 28
Defoy, S., 157
deGroot, Wim, 268
deJeu, R., 108
DeJong, M., 250
Dekai, Sun, 101
Delaboudiniere, J.–P., 305
Delannee, C., 305
Delannoy, A., 174
Delfin, P., 104
Delgado, Rafael H., 63, 94
DelZanna, Giulio, 306
Denardini, Clezio Marcos, 76
Dennison, J. R., 268
DeSordi, S. P., 180
Devine, R. A. B., 48
deVries, S. C., 22
deWit, A., 6
DeYoreo, J., 273
DeYoung, Russell J., 83
Dhanorkar, Savita, 135
Dibb, Jack E., 225
Dilley, Arthur D., 90
Dimitrov, P. G., 251
Diniz, J. H., 158
Diniz, Jose H., 158, 161, 162
Dipirro, M. J., 35
DiPirro, Michael, 92
DiRienzi, Joseph, 251
Dixon, Andrew, 217
Dmitrev, E. M., 136
Dmitriev, E. M., 141
Doe, R. A., 149

Doe, Stephen, 294
Dold, P., 86, 272, 273
Domingues, M. O., 158
Donelson, M. J., 246
Dong, W., 156
Dong, Wansheng, 166
DOrdine, M., 231
Douglass, Anne R., 118
Dovgaluk, Ju. A., 184
Drachman, Richard J., 250, 251
Dragt, A. J., 257
Drake, Jeremy, 295
Dreizin, Edward L., 48
Drezner, Stephen M., 286
Driscoll, K., 202
Driscoll, Kevin, 190, 203
Driscoll, Kevin T., 197, 202, 203, 204
Drury, Derek, 32
Dryer, F. L., 98
Duarte, Valdete, 107
Dubovikov, M. S., 214, 215, 216
Duguet, A., 253
Dula, Arthur M., 30
Dumonthier, J. J., 287
Dunn, H. J., 239
Dupre, M. J., 228
Durand, S., 76, 77
Durbin, Steve M., 59
Dutta, Sunil, 312
Dutton, E. G., 212
Dye, J. E., 191
Dyer, J., 281

E

E. H., Susan, 302
Eack, K., 169, 199
Eack, K. B., 151, 154
Eack, Kenneth B., 177, 199
Earhart, Eric M., 99
Eastes, R., 149
Eberle, Marc H., 199
Ebneter, Arnold E., 182
Eckel, Andy, 40
Eisele, F. L., 51
Eklund, U., 269
Elfayoumy, Mahmoud, 98
Elliott, H. A., 148
Ellis, David, 39
Ellison, R. J., 280
Elvis, Martin, 298, 308
Emerson, Charles W., 112, 113
Emrich, Carol, 76, 77
Engman, E., 111
Engman, Edwin T., 108
Ennis, George, 4
Ennix, Kimberly A., 37, 42
Enos, Robert J., 8
Erickson, Ken, 84
Ermakov, V. I., 180
Espana, Martin, 1
Essers, I., 25
Estes, Robert D., 72
Estes, Robert D., 31, 40
Ethridge, Edwin, 68
Everist, S., 56
Ewing, R. C., 273
Ezcurra, A., 158, 159

F

Fabbiano, Giuseppina, 295, 307, 308
Falconer, D. A., 303
Falconer, David A., 304
Fan, H., 270
Fangzi, Wang, 220
Farley, R. D., 187, 202
Farmer, Jeff, 69
Farmer, Jeffrey T., 95
Fehr, T., 201
Feigenbaum, Harold N., 66
Fellows, Jack, 119
Fengwu, Zhang, 101
Ferebee, Melvin J., 9
Ferguson, Dale, 268
Ferritto, J. M., 143
Feth, Shari, 271
Figueiredo, Marco A., 233
Filho, Armando Cazetta, 161, 162
Filimonova, Ludmila V., 117
Fillingim, M., 132
Fillingim, M. O., 262
Finger, Mark H., 291, 293, 299, 310
Finke, U., 201
Finkelstein, M., 200
Fisher, D. A., 280
Fishman, Gerald J., 307
Fisman, Gerald J., 289
Fitzgerald, T. J., 199
Fitzgerald, Wendy S., 216
Fitzpatrick, M. E., 210
Flachbart, Robin H., 68
Fleetwood, D. M., 48
Fleischhacker, Peter R., 182
Fleming, D. L., 54
Fleming, David C., 44
Fleming, Eric L., 145, 304
Fleming, K., 264
Flowers, George T., 99
Foarde, K. K., 129
Foch, B. J., 47
Forbes, Gregory S., 184
Ford, M. J., 253
Foreman, William, 289
Forgan, B. W., 213
Fork, Richard L., 261
Forman, William, 308
Forsythe, Elizabeth L., 275
Fortmann, R., 126, 129
Fortmann, R. C., 60
Foster, J. L., 73
Fournier, G., 177
Fox, D. E., 104
Foxall, W., 148
Francis, Karen M., 216
Francois, Marianne, 100
Frandsen, J. D., 53
Frank, L. A., 144
Franks, Greg, 73
Franz, R., 152, 198
Frassanito, John, 30
Frazier, Donald O., 57, 274
Frey, Herbert V., 302
Frostemark, T., 80
Fruscione, Antonella, 287, 293, 311
Fry, Craig D., 74
Fu, Qi, 218
Fuellekrug, Martin, 201
Fujimoto R., 287
Fukao, S., 183
Fuller, Chris R., 248
Fuller, Clark W., 114
Furuhashi, Akiko, 230

G

Gabrys, B., 254
Gakumasawa, Hidetaka, 99
Gallagher, Dennis L., 131, 144, 263
Galland, Pierre A., 260
Gallanger, Dennis L., 131
Gallimberti, I., 156
Galloway, D. K., 288
Galofaro, Joel, 268
Galvan, Arturo, 172
Galvin, Robert W., 278
Gang, Liu, 222
Gann, R. G., 71
Gao, Wenyuan, 218
Garber, D. P., 213
Garcia, Adriana, 291, 305
Gardner, L., 163

Garrison, James L, 9
Garrison, James L., Jr., 72
Gates, W. L., 213
Gattaleeradapan, S., 187
Geerts, Bart, 208
Gendraau, K. C., 35
Gendreau, K. C., 287
Geogdzhayev, Igor V., 117
George, I. M., 290
George, J. S., 218
George, M. A., 57
Georgiadis, Nicholas J., 19
Georgis, J. F., 192
Gerk, T. J., 48
Gerlach, J., 204
Germany, G. A., 150
Germany, G. A., 132, 149, 150, 262
Gerrish, H. P., 38
Gezari, Daniel Y., 93
Ghorishi, B., 128
Ghorishi, S. B., 128
Ghrayeb, Ali, 78
Giarard, Terrence M., 296
Giardina, G., 250
GIbbons, John H., 285
Gibson, W. M., 288
Gibson, Walter, 270
Gilbert, John A., 261
Giles, A. B., 288
Giles, B. L., 132
Gilyard, Glenn, 1
Girard, Terrence M., 288
Glass, David E., 90
Glazebrook, J. F., 228
Glezer, A., 87
Gloersen, Per, 215
Gloster, Clay S., 233
Godines, Cody, 102
Goeckner, M. J., 263
Goetschl, Thomas, 172
Goetz, Alexander F. H., 112
Goldstein, M. E., 245
Golub, Leon, 294
Golub, R. A., 246, 247
Gomez–Knight, Sylvia J., 60
Gonda, Hiroyuki, 24
Gongdong, Yan, 220
Gonsalez, Jose C., 23
Goodman, S. J., 141, 153, 164, 182, 189, 202, 203, 214
Goodman, Steve, 173
Goodman, Steven J., 187, 188, 202, 203, 204, 208
Goodwin, Thomas J., 216
Gopalswamy, N., 306
Gordon, Edward M., 114, 277
Gordon, G., 244
Goshima, Hisashi, 161
Goswami, K., 188
Goto, Y., 163
Gourbiere, Elisabeth, 176
Grady, J. E., 20
Graves, Corey A., 233
Green, J., 152, 198
Greenhill, J. G., 288
Greenwald, R. A., 132
Greet, Bart, 209
Gregory, Don A., 60
Grgic, David, 80
Griffin, Timothy P., 37
Griffioen–Young, H. J., 74
Grindlay, J., 289
Grossman, A. S., 212
Gruemmer, F., 250
Guay, Robert, 242
Gubarev, M., 288
Gubarev, Mikhail, 270
Gubina, Ferdinand, 80, 81
Guillen, J., 198
Guillen, J. L., 152
Gullett, B. K., 128
Gumley, J. R., 177
Guo, C., 155, 156, 166, 176
Guoyin, Liu, 222
Guray, Ipek, 271
Gurman, J. B., 306
Gurnett, D. A., 144
Gvozdenovic, Slobodan, 5
Gyergyek, Tomaza, 240
Gysax, J. D., 35

H

H., James, 302
Haber, Jerold M., 62
Hack, J. J., 213
Hackenberg, P., 90
Haering, Edward A., Jr., 12
Hagler, R. A., 122
Hagstrom, Thomas, 240
Hale, Joseph P., 28
Hale, Leslie C., 171
Hall, C., 264
Hall, D. K., 73
Hall, Dorothy K., 119
Hall, Harvey, 84
Hall, John M., 202, 203, 204
Hallett, John, 194
Hamasaka, Naoji, 55
Hamed, M. M., 5
Hamlin, Susanne, 91
Hamlin, T., 167, 196
Hamlin, Timothy, 173
Handel, Peter H., 186
Hansell, William, 32
Hao, Y. L., 88
Hara, K., 137
Harari, D., 227
Harlin, J., 167, 196
Harmon, B. A., 289
Harmon, B. Alan, 299, 310
Harms, D. E., 180, 210
Harreld, Michael R., 232
Harris, D. H. R., 3
Harrison, E. F., 213
Harrison, R. G., 138
Harrison, R. Giles, 137
Hart, J. E., 91
Hart, S. J., 240
Hartley, Tom T., 242
Hashizume, Kunio, 241
Hasler, Fritz, 105, 151
Hass, Neal, 37
Hassanein, A., 266, 267
Hastings, Leon J., 68
Hatate, Minoru, 55
Hathaway, D. H., 303
Hathaway, David H., 304
Hatton, Kenneth S., 21
Hawk, Clark, 39
Hawk, Clark W., 39
Hawley, F. William, 285
Hayakawa, H., 36
Hayakawa, M., 143, 164
Hayami, Takashi, 223, 278
Hayder, M. E., 245
Haynes, M. A., 253
He, Helen, 259
Heckman, S., 134, 142, 182, 202
Heckman, Stan, 203
Hehemann, D. G., 277
Heil, Michael C., 224
Heimann, Martin, 127
Heimdal, Per, 248
Heirtzler, J. R., 146
Helsdon, J. H., 187, 202
Hemminger, J. A., 281
Henderson, D. O., 114
Hepp, Al F., 114
Hernandez, E., 67
Herrero, I., 158, 159
Hesse, Michael, 262
Hethcock, J. Donn, 103
Hetherington, D. L., 70

Heymsfield, G., 209
Heymsfield, G. M., 74
Heymsfield, Gerald M., 208
Hickman, Robert, 39
Hicks, Roslin, 57
Hilburger, Mark W., 103
Hines, Tonjua M., 28
Hinson, M. S., 180
Hirahara, M., 36, 132
Hirai, Takeo, 178
Hirayama, Yoshinori, 258
Hjellming, R. M., 310
Ho, Chih–Ming, 17
Ho, P. P., 260
Hobara, Y., 143, 164
Hodanish, S., 214
Hodanish, Stephen, 188
Hoeller, H., 201
Hoffert, Steven G., 184
Hoffman, Stephen, 302
Hoffmann, Vern K., 48
Hohsho, Yukio, 99
Hojo, J., 154
Holdeman, J. D., 13
Holden, D. N., 151, 154
Holle, Ronald L., 175
Holmes, Richard, 39
Holt, James B., 68
Hong, Ye, 153
Honma, N., 163
Horack, John M., 78
Horiuchi, Ritoku, 267
Horrak, U., 140
Horwitz, J. L., 132
Hou, A., 207
Houseman, John, 62, 93
Houser, P., 111
Houser, Paul R., 149
Houttuin, K., 225
Howard, A., 216
Howard, E., 129
Howard, J., 231
Howse, J. W., 249
Huaguang, Gu, 220
Huang, E., 134
Hubbard, Danny E., 59
Hubler, G., 191
Hudson, H. S., 306
Hudson, J. M., 121
Huenemoeder, Dave, 292
Huffines, Gary R., 162
Huffman, George, 151
Huffman, George J., 206
Hugh, Christian J., 208
Hughes, Peter M., 280
Hulstijn, J., 282
Hung, Ching–Chen, 56
Hunt, Gary R., 237
Huntrieser, H., 201
Hussein, A. M., 169
Hutcheson, Florence V., 248
Hutchings, L., 147

I

Idogaki, Toshihiro, 48
Idone, Vincent, 160
Idone, Vincent P., 159, 180
Ignatyuk, A. V., 250
Ikantiah, G. S., 89
Ikeda, H., 125
Ikeuchi, Ken, 223
Illies, G., 228
Imanishi, Takahiro, 258
Imhoff, W. L., 144
Ingalls, M. N., 99
Inokuchi, Yuzo, 24
Intriligator, Devrie S., 262
Ioannidou, E., 147
Irvine, William M., 298
Ishii, M., 154
Ishii, Norihiko, 96
Isoda, Hitoshi, 160
Israelsson, S., 139, 140, 166, 196
Ito, T., 165
Ivanhoff, A., 127
Ivanovsky, A. V., 167
Ivansson, Sven, 243, 244
Ives, H. C., 257

J

Jackman, Charles H., 145, 304
Jackson, E., 244
Jackson, Julie R., 62, 93
Jackson, Larry, 8, 30
Jackson, T. L., 85
Jacobs, S. C., 180
Jacobson, A., 198, 199, 207
Jacobson, A. R., 152, 198
Jacobson, Abram R., 198
Jaeger, S. M., 247
Jakl, Franc, 81
James, B. F., 300
Janischewskyj, W., 169
Jankowski, A. F., 59
Jansen, Bernard J., 18, 246
Jarpe, S., 147
Jarvis, Matt J., 297
Jarvis, Michele, 37, 42
Jayaratne, E. Rohan, 190, 191
Jayaratne, K. P. S. C., 139
Jeker, Dominique P., 115
Jensen, Brian J., 57
Jiabai, Rui, 101
Jiang, Jie, 70
Jianhe, Chen, 221
Jianmin, Wu, 220
Jifu, Wen, 222
Jikang, X., 265
Jing, X., 213
Jingrui, Meng, 221
Jingtai, Sun, 221
Jinhe, Wei, 219, 220
Johnson, B. Carol, 109
Johnson, D., 130
Johnson, D. L., 131
Johnson, Les, 31
Jokela, Jorma, 146
Jolly, Clifford D., 36
Jones, Christine, 309
Jones, Christopher W., 16
Jones, Darryl K., 261
Jones, Linwood, 188
Jones, Matthew R., 95
Jones, Michael G., 20
Jones, V. M., 236
Jones, William G., 73
Jonk, K. J., 79
Jordan, Stuart, 291
Jordan, Stuart D., 305, 306
Jorgensen, Catherine A., 32
Jorgensen, D. P., 186
Joshi, M. C., 87, 246
Joslin, R. D., 85
Joy, M., 288
Joy, Marshall, 270
Joye, W., 294
Jozewicz, W., 128
Ju, Liu, 223
Juang, Jer–Nan, 102
Judge, Russell A., 275
Jun, Wang, 101
Junghans, A. R., 250
Juricic, Dani, 101
Justus, C. G., 131, 300

K

Kabashkin, Igor, 1
Kaddah, Sahar, S., 41
Kaiser, Th., 86, 272, 273
Kakar, R., 207

Kalov, R. Kh., 165
Kalu, Alex, 76, 77
Kamaly, A., 226
Kami, Kouichirou, 177
Kamimura, H., 87
Kamionkowski, Marc, 296
Kamiya, Atsunori, 218
Kammeraad, J. E., 258
Kamra, A. K., 135, 193
Kanda, A., 21
Kanda, Kazufumi, 210
Kandalgaonkar, S. S., 170, 205
Kappe, B., 22
Karagozian, A. R., 48
Karniadakis, G., 244
Karplus, W. J., 219
Karplus, Walter J., 219, 232
Karpoukhin, Mikhail G., 219
Kasameyer, P., 147
Kassabova, Tzveta, 192
Katnik, Gregory N., 30
Katsu, Takeshi, 230
Katz, R. B., 232
Katz, Richard, 231, 233
Katz, Richard B., 84
Katzberg, Stephen J., 72
Kawasaki, Z., 166
Kawasaki, Z. –I., 155
Kawasaki, Z. I., 154, 183
Kawasaki, Zen, 157, 160, 173
Kawazaki, Z., 156
Keddy, C. P., 61
Kelder, H., 123
Kelley, R. L., 35, 287
Kellogg, Louise H., 144
Kelly, H. Neale, 90
Kelly, J. D., 149
Kelly, John D., 146
Kempf, W. S., 120
Kennedy, Patrick C., 184
Kepesis, J. E., 54
Keppenne, Christian L., 215
Kern, R. D., 51
Kessler, Joachim, 252
Kevin, Driscoll T., 208
Keys, Andrew S., 261
Khavaran, A., 244
Khazanov, G. V., 268
Kheifets, Anatoli S., 252
Kibens, V., 87
Kiefer, Walter S., 144
Kiehl, J. T., 213
Kielin, Erik J., 92
Kigawa, Seiichiro, 111
Killeen, Timothy, 119
Kim, C. M., 244
Kim, K.–M., 129
Kirkland, M., 198, 199, 207
Kirkwood, S., 133
Kishiba, Seigo, 242
Kishida, Keiji, 242
Kita, K., 125
Kitagawa, N., 176
Kithil, R., 176
Kittleman, S., 91
Kizhner, Semion, 8, 30
Klaver, M. H. A., 74
Klemt, V., 251
Klepeis, J. E., 53
Kleyner, I., 231
Klingo, V. V., 135
Klumov, B., 141
Knoll, A., 11
Knox, S., 198
Knupp, K., 189
Kobayashi, F., 157
Kobayashi, Fumiaki, 178
Koelfgen, Syri, 39
Kogan, B. Y., 219
Kogan, Boris, Y., 219
Koh, Danny T., 293
Koike, M., 125
Koike, Matoke, 115
Kojima, Tadatomo, 256, 278
Kolev, Staytcho I., 142
Kolodziejczak, J., 288
Kolpakov, A. V., 193
Kondo, Y., 125
Kondo, Yutaka, 115
Konkashbaev, I. K., 267
Kordi, B., 169
Korte, J. J., 239
Koshak, W. J., 175, 203
Koshak, William, 203
Koshak, William J., 202, 203, 204
Koster, R., 111
Kotaru, Raj, 239
Kozak, Steven, 181
Kozhurina–Platais, Vera, 288, 296
Kozlowski, W., 128
Kozyra, J. U., 268
Krasnitsky, Y. A., 170
Krauss, L. M., 295
Krehbiel, P., 164, 169
Krehbiel, P. R., 137, 167, 196
Krehbiel, Paul R., 173
Krewald, S., 250
Kroes, E., 25
Krol, T., 236
Krothapalli, A., 87
Kudyaev, G. A., 250
Kulda, Richard J., 75
Kumar, Adarsh, 138
Kumar, Nitin, 88
Kumar, Rajendra, 9
Kumazawa, R., 265
Kummerow, C., 207
Kummerow, Christian D., 153
Kumykov, Kh. K., 165
Kuo, Y. H., 105
Kupovykh, G. V., 136
Kurniaty, Tatty, 152
Kurtz, S. R., 97
Kustas, W., 111
Kutteh, Ramzi, 234
Kuulkers, E., 310

L

LaBarre, R. E., 19
Labrada, C., 204
Lacerda, Moacir, 158
Lacis, Andrew A., 117
Lagen, Nicholas T., 18
Lahmam–Bennani, A., 253
Lal, R. B., 274
Lalande, P., 156
Lam, Nina Siu–Ngan, 113
Lambert, H. H., 20
Landi, Enrico, 306
Lang, Timothy J., 184
Langston, James H., 237
Lao, H. C., 60, 126
Laroche, P., 155, 156, 160, 172, 191, 201, 205
Larsen, S. B., 65
Lasseigne, D. G., 85
Latham, John, 195
Lau, K.–M., 129, 206
Lau, Kenneth H., 9
Lau, Shelley, 286
Lau, William K.–M., 115
Lawrence, Tim, 40
Lawson, R. Paul, 182
Laymon, Charles A., 113
Leahy, Denis, 291
Ledley, Tamara S., 119
Lee, Joseph W., 10
Lee, K., 116
Lee, L. C., 105
Lehoczky, S. L., 57
Lehoczky, Sandor L., 271
Leighty, Bradley D., 92
Lelwala, R., 139
Leong, M. Y., 13

Leslie, F., 91, 96
Leslie, M., 234
Levashov, V. F., 266
Levin, Zev, 179
Levine, S. R., 44
Levine, Stanley R., 44
Leviton, D. B., 259
Leviton, Douglas B., 259
Lewis, C. W., 213
Leyderman, Alexander, 275
Li, Xiaofan, 206
Liang, X., 260
Liao, Jin–Hua, 267
Lichtensteiger, M., 272, 273
Liemohn, M. W., 268
Lifan, Zhang, 222
Lightsey, E. Glenn, 8, 30
Lin, Hong, 274
Lin, R. P., 262
Lindberg, S., 79
Linder, K. E., 56
Lindstroem, B., 226
Linger, R. C., 280
Linjie, Wang, 220
Linnenbank, G. R. J., 79
Lipeles, R. A., 58
Lipson, H. F., 280
Litchford, Ron, 39
Litvak, Maxim L., 310
Liu, S. C., 125
Liu, X., 155, 156, 166, 167
Liu, Xinsheng, 166, 193
Livingston, John M., 119
Ljungberg, M., 294
Lockwood, M., 169
Logan, D. T., 116
Logan, Jennifer A., 126
Lohmann, Birgit, 253
Lojou, J. Y., 174
Lomax, Curtis, 86
Long, C. N., 213
Long–Davis, M., 24
Long–Davis, Mary Jo, 14
Longstaff, T., 280
Lopez, Raul E., 175
Lorenzini, Enrico, 31
Lorenzo, Carl F., 242
Los, S. O., 122
Lu, Y., 270
Luck, William S., Jr., 83
Lue, Yvonne, 231
Lugmair, Guenter W., 299
Luijf, H. A. M., 74
Lum, B. Y., 54
Lummerzheim, D., 149, 150
Lun, Zhao, 220
Lundblad, B. L., 120
Lundin, R., 36
Luvall, Jeffrey C., 112
Lyons, J. J., III, 71
Lyons, R. M., 80
Lyons, W., 134
Lyons, W. A., 163, 164
Lyu, Cheng–Hsuan, 153

M

Ma, Q., 256
Ma, Z. Y., 250
MacCarley, C. A., 71
MacDonald, C. A., 288
MacGorman, D. R., 169, 186, 195
MacGorman, Donald R., 177
Mach, D., 164
Mach, D. M., 153
Mach, Douglas, 173
Mach, Douglas A., 204
Mach, Douglas M., 202, 203
Mackall, Dale, 23
Mackerras, D., 141
MacNeice, Peter, 234
Macosko, Robert P., 114
Madden, N., 204
Madura, J. T., 180
Maekawa, Y., 183
Magana, R., 59
Mai, A. K., 11
Maine, Trindel, 10
Malcolm, W., 38
Maldarelli, Charles, 88
Maliarova, L. V., 193
Malkin, Alexander J., 275
Man, Qiu, 220, 222
Mankbadi, R. R., 245
Manning, James C., 18
Mano, Tadaaki, 218
Manohar, G. K., 170, 205
Manyin, Mike, 151
Marceau, Michelle, 271
Marchol, Paul, 40
Marcu, Bogdan, 95
Mardiana, R., 154
Mareev, E. A., 136, 139, 185
Mareeva, O. V., 139
Margolis, J. S., 93
Marino, Jodilyn, 16
Markham, Brian L., 109
Markley, F. Landis, 35
Markson, Ralph, 117, 174
Marlais, S. M., 124
Marshall, Cheryl J., 34
Marshall, Paul W., 34
Marshall, T. C., 137, 157, 186
Martel, Hugh, 7
Martin, J. J., 38
Martin, S. F., 306
Martinez, Joe, 40
Martinez–Sanchez, Manuel, 31
Marx, W. J., 50
Mason, B. L., 183
Mason, Keith J., 6
Massey, R., 199, 207
Massey, R. S., 151, 154
Massey, Robert S., 199
Mast, Dion J., 95
Masuelli, S., 194
Matejka, T., 191
Matlin, A., 214
Matlin, Anne, 188
Matsumoto, Kentaro, 24
Matsuura, K., 154
Mattie, David R., 64
Mattson, C. B., 58
Maxwell, Daniel, 68
May, R. D., 93
Maynashev, V. S., 266
Mazid, M. A., 255
Mazur, V., 156
McBride, David, 23
McCarthy, I. E., 253
McCarthy, Ian E., 49
McCaul, E. W., 189
McCaul, Eugene W., Jr., 187
McCollough, M. L., 310
McCollum, J. L., 232
McCollum, J,, 231
McConough, William J., 283
McDonald, A. J., 120
McDonald, J. R., 240
McDowell, Jonathan, 259
McHardy, Ian, 293
McInnis, R. J. , 3
McKechnie, Timothy, 39
McLaughlin, Dennis K., 245
McLaughlin, Don, 30
McLaughlin, Warren, 292
McMahan, A. K., 53
McMahon, Richard G., 297
McManus, H. L., 47
McNamara, Brian, 292
Meegan, Charles, 310
Mehta, Amita, 211
Meijer, E. W., 123
Mendes, O., Jr., 139, 158

Mendez, R. A., 292
Mendez, Rene A., 288, 296
Meneghelli, B. J., 94
Menetrez, M. Y., 129
Mengle, V., 15
Mengle, V. G., 15
Menyuk, C. R., 82
Merritt, B. T., 124
Meurling, F., 56
Meyer, K. J., 38
Meyers, James F., 10
Michaelian, Mark, 17
Michalewicz, M. T., 253
Michimoto, K., 179
Mickler, Dave, 9
Miki, Megumu, 161
Miller, James A., 306
Miller, M. L., 273
Miller, T., 91
Min, I. A., 120
Minehart, R. C., 254
Minnis, P., 212
Minniti, D., 292
Mioduszewski, A. J., 310
Mirshams, R. A., 54
Mishchenko, Michael I., 117
Mital, Subodh K., 46
Mitchell, A. R., 43
Mitchell, L. K., 18
Mitchell, L. Kerry, 18
Mito, Ryousuke, 24
Mitra, Debasis, 235
Mitrofanov, Igor G., 310
Mitzeva, Rumjana, 192
Miura, K., 137
Miyazaki, Tadaomi, 178
Mizukami, M., 20
Mizukami, Masashi, 37
Mobarry, Clark, 234
Mobilia, J. H., 144
Mohan, Avinash, 183
Mohanty, B. P., 149
Molen, G. Vander, 100
Molenkamp, E., 236
Molinari, John E., 160
Molinie, G., 157
Momoh, James A., 41, 98
Monnelly, C., 289
Monteiro, Marcia Aparecida, 241
Montes, Antonio, 265
Montgomery, D. C., 266
Mooney, Thomas A., 259
Moore, Arlene, 26
Moore, C. B., 164
Moore, Paul K., 180
Moore, R. L., 303
Moore, Ronald L., 303, 304
Moore, T. E., 132, 148
Morales, C. A., 196
Morcrette, J.–J., 213
Moreman, Douglas, 281
Moretto, T., 133
Morgan, R. E., 61, 122
Mori, Hideo, 85
Mori, Shigeo, 224
Morosov, V. N., 162
Morozov, I. N., 266
Morrell, Peter, 6
Morris, Charles, 29
Morris, Heidi E., 177
Morris, Philip J., 245
Morris, Robert K., 285
Morrison, J. Ian, 71
Mortlock, Alan K., 10
Moskito, John, 86
Muehlhauser, J. W., 264
Mueller, Charles W., 34
Mujunen, A., 287
Mukai, T., 36
Mulder, Edwin J., 60
Munson, W. O., 65
Murakami, M., 154
Murakami, S., 249, 265
Murakami, Tsutomu, 24
Muraoka, Yoshinori, 48
Murray, Henry L., 237
Murray, Natalie, 195
Murray, W. Clifton, 182
Murthy, Pappu L. N., 46
Mushtak, V., 134, 200
Muske, K. R., 249
Mutoh, T., 265
Muzichenko, A. D., 266

N

Nagasubramanian, G., 113
Nagata, Hideki, 48
Nakae, S., 137
Nakajima, N., 249, 265
Nakajima, Noriyoshi, 264
Nakamura, K., 156, 166, 171
Nakano, M., 156, 166, 171
Nakao, Yasuyuki, 266
Nakazawa, Shinji, 264
Nakkar, Mouna, 233
Namba, Masanobu, 24, 85
Nandra, K., 290
Narita, K., 163
Nastoyashchii, A. F., 266
Nastran, Janez, 82
Nauflett, George W., 66
Ndri, Narcisse, 100
Neal, Bradford A., 37
Neau, E. L., 257
Nedeljkovic, David, 82
Neelin, J. David, 115
Nelkin, Eric, 151
Nelkin, Eric J., 206
Nelson, J., 56
Nelson, P. A., 90, 248
Nelson, Robert W., 293
Nelson, T., 134
Nelson, T. E., 163, 164
Nemeth, Michael P., 103
Neto, Joaquim Paulino Leite, 265
Newchurch, M. J., 126
Newell, Reginald E., 125
NewMeyer, David A., 25
Newton, R. L., 97
Ng, A., 126, 129
Nichols, Rodney W., 282
Nickolaenko, A. P., 143
Nicola, V. F., 79
Nicolson, R. J. F., 253
Nielsen, J. Eric, 118
Nierow, A., 181
Nihart, G. L., 17
Nilsson, H., 133
Nimmerfroh, Norbert, 66
Nitta, N., 305
Noever, David, 239
Noggle, R. C., 174
Nomura, G., 265
Norberg, O., 36
Nordholm, A. F., 38
Norrby, M., 80
Norris, G. A., 213
Northam, G. Burton, 46
Norum, T. D., 247
Nuehrenberg, J., 265
Numata, Izaya, 107
Numphas, E. F., 166
Nyden, M. R., 51

O

OConnor, Kim C., 216
Ogawa, Tetsuaki, 85
Oglesby, Donald M., 92
Ohlsen, D., 91
Ohno, Masaki, 85
Ohyabu, Nobuyoshi, 264

Oka, Masanori, 223
Okada, H., 265
Okada, N., 33
Okamoto, M., 249, 265
Okamoto, Masao, 264
Oksenberg, Michel, 284
Oladiran, E. O., 166
Olsen, S., 36
Olson, Kevin M., 234
Olson, W. S., 196
Olson, William S., 153
Omont, Alain, 297
Ono, K., 11
Ono, Shinsuke, 258
Orlov, A. V., 171
Orszag, S., 244
Orville, Richard E., 162
Orville, R. E., 141, 197
Orville, Richard E., 161, 195
Osuga, Daikichi, 230
Ota, Y., 154
Otsuyama, T., 164
Otte, T. L., 213
Overbeck, K. B., 210
Owe, M., 108

P

Paciesas, W. S., 289, 310
Packer, Charles, 234
Padula, S. L., 239
Pagoria, P. F., 43
Palmore, T., 273
Panchishkina, I. N., 135
Papadakis, Iossif, 293, 311
Parekh, D. E., 87
Park, Kwangjai, 209
Park, Nohpill, 73
Parks, C. R., 210
Parks, G. K., 132, 144, 149, 150, 262
Parrott, Tony L., 20
Parts, Tiia–Ene, 136
Paskey, Ernest M., 238
Passenier, P. O., 225
Patterson, Mark, 42
Patton, H. J., 147
Patzold, Jack D., 62
Peck, S. L., 184
Pelt, J. S., 59
Pendleton, Geoffrey N., 310
Penetrante, B. M., 124
Penn, Benjamin, 57
Penn, Benjamin G., 274, 275
Pereyra, Rodolfo, 188
Pereyra, Rodolfo G., 185
Peteet, Dorothy M., 117
Petermann, Y. F. S., 227
Peters, P., 57
Petersen, Walter A., 182
Petre, R., 71
Petrenko, I. A., 192
Petrov, A. I., 135
Petrova, G. G., 135
Pfister, L., 123
Pfister, Lenny, 115
Pham, T., 35
Philipson, L. L., 121
Phillips, C. K., 268
Phillips, J. D., 97
Phillips, Thomas G., 297
Phillips, Tom, 32
Pickering, Kenneth E., 115
Pickering, Thomas R., 284
Pierce, Harold, 211
Pierce, Harold F., 209
Pietersen, William G., 71
Ping, Hu, 217
Pinto, I. R. C. A., 139, 158
Pinto, Iara R. C. A., 158, 161
Pinto, lara R. C. A., 162
Pinto, O., Jr., 139, 158
Pinto, Osmar Jr., 161
Pinto, Osmar, Jr., 158, 162
Pitz, W. J., 98
Pizarro, Marco Antonio, 106
Plants, W. C., 232
Platais, Imants, 288, 296
Podkovirov, V. L., 266
Poindexter, E., Jr., 59
Polites, Michael E., 12
Pollock, C. L., 132
Ponomarev, Igor, 270
Ponomarev, Yu. Ph., 184
Ponton, M. K., 18
Ponton, Michael K., 18
Porter, F. S., 35
Porter, J. G., 303
Porter, Jason G., 303, 304
Posey, Joe W., 20
Postma, A., 236
Potter, G. L., 213
Poutanen, Markku, 146
Povinelli, L. A., 245
Powers, Charles, 290
Powers, William T., 91
Prabhakar, Arati, 286
Prabowo, Anondo, 152
Prather, Michael J., 123
Preece, Robert D., 310
Prewett, Tacey L., 216
Price, C., 200
Priestly, K. F., 147
Prihanto, Igif G., 279
Prince, Thomas A., 293, 310
Prior, Mike, 27
Pusey, Marc L., 270, 275
Pyle, R. B., 177

Q

Qie, X., 156, 166
Qie, Xiushu, 166
Qiulu, Xiang, 221
Quattrochi, Dale A., 112, 113

R

R., Yeti Priyati, 116
Raboin, P., 55
Radhakrishnan, Krishnan, 240
Raeisaenen, A., 79
Raffaelle, R. P., 277
Raghavan, R., 214
Rahayu, Sri, 279
Rai, Jagdish, 138
Rakar, Andrej, 101
Rakotondrasimba, Y., 226
Rakov, V. A., 165, 172
Ramachandran, N., 96
Ramachandran, Narayanan, 239
Raman, A., 54
Raman, G., 17
Ramanathan, V., 213
Rambo, K. J., 172
Ramohalli, Kumar, 26
Ramsey, M. E., 59
Ran, Duan, 220
Randall, D. A., 122
Randel, W., 197
Randel, William J., 126
Rangkuti, Alzah S., 152
Ransone, Philip O., 46
Rathgeber, K. A., 61
Ratzloff, J. M., 78
Raush, P. J., 78
Rawlings, Steve, 292, 297
Rawls, J. W., 246
Ray, Pradosh, 42
Raymond, Susan U., 282
Reagan, Shawn, 73
Reaves, Shawn, 59
Rechou, A., 133
Reddy, N.N., 246

Reddy, D., 45
Redjeki, Sri, 279
Reed, R., 231
Refaat, Tamer F., 83
Reid, Mark, 32
Reipurth, Bo, 298
Reitan, Paula J., 232
Remy, J. L., 227
Ren, W., 238
Renner, Rolf H., 66
Retalis, A. D., 116
Retalis, D. A., 116
Reuter, Gerhard, 181
Reynolds, B., 306
Rhemer, Chris, 40
Rice, E. J., 17
Rich, F., 149
Richard, P., 174
Richards, Phil G., 267
Richie, Wayne R., 26
Ricketts, Daniel, 84
Rieker, T., 270
Rienecker, Michele, 215
Riishojgaard, L. P., 124
Rind, David H., 123
Rison, W., 164, 167, 169, 196
Rison, William, 173
Ritchie, G. D., 38
Rivers, H. Kevin, 46
Rivers, Robert A., 2
Roache, N., 126, 129
Roache, N. F., 60
Roback, V. Eric, 12
Roberts, C. D., 276
Robertson, J. P., 102
Robertson, R. P., 251
Robertson, Tony, 39
Robinson, C. R., 289
Robinson, J. B., 4
Robinson, R. Craig, 21
Rodgers, Edward, 211
Rodgers, Edward B., 209
Rodriguez, D. J., 212
Roeder, W., 137
Roeder, W. P., 180
Rogers, C. B., 87
Rogers, Decatur B., 276
Rogers, John, 26
Romanenko, Fedor A., 117
Rood, Richard B., 118
Rosati, P. N., 210
Rose, M. Frank, 27
Rose–Pehrsson, S. L., 240
Rosenberg, T. J., 74
Rosenberger, Franz, 47, 274
Rosenfeld, D., 204
Rosenzweig, Cynthia, 118
Rosida, 152
Rossi, John, III, 38
Rossow, William B., 117
Rothkin, K., 142, 204
Roush, G. Jon, 284
Rousseau, Carl Q., 103
Roussel–Dupre, R. A., 162
Roux, F., 174
Roy, A. K., 54
Roy, H. Scott, 235
Rubaai, Ahmed, 84, 239
Rubin, Bradley C., 293
Ruhnke, L. H., 156
Ruhnke, Lothar, 174
Rupen, M., 310
Rusnadi, Iyus Edi, 132
Russell, C. H., 288
Russell, C. T., 198
Russo, Angela, 9
Rust, W. D., 137, 157, 169, 186
Rust, W. David, 177
Rutledge, S. A., 191
Rutledge, Steven A., 168, 184
Rutledge, Steven D., 182
Rutner, Stephen M., 5
Ruzic, D. N., 263
Ryan, Robert, 29
Ryan, William E., 75, 78

S

Saba, M. M. F., 139
Sacco, Albert, Jr., 271
Sacco, Teran L., 271
Sachs, G., 11
Saha, T., 71
Saito, K., 265
Sakai, T., 157
Sakai, Tsutomu, 177
Sakuma, Fumihiro, 109
Salas, A. O., 239
Salikuddin, M., 15
Salm, J., 140
Salomonson, Vincent V., 106
Salvail, P., 43
Samuelsen, G. S., 13
Sanders, F. H., 78
Sanders, Jim, 39
Sanger, N. T., 197
Sanmartin, Juan, 31
Sardonia, J. E., 180
Saric, William S., 2
Sarkisov, Sergei, 60
Sarkisov, Sergey, 57
Sathe, A. B., 193
Sato, K., 154
Sato, Ryuji, 96
Sato, Tetsuya, 267
Satonobu, Jun, 235
Satonobu, Toshiyuki, 235
Satori, G., 142
Satroi, G., 200
Sattari–Far, I., 104
Saunders, C. P. R., 184
Saunders, Clive, 192
Saunders, Mark, 26
Saylor, Richard, 27
Sayyah, Tarek, 274
Schaefer, D. A., 35
Schaefer, Mark, 282
Schaefer, Peter, 10
Schlager, H., 123
Schmid, G. J., 258
Schmidt, D. M., 218
Schmidt, G. R., 38
Schmidt, K.–H., 250
Schmidt, R. D., 43
Schnetzer, G. H., 172
Scholtz, M. T., 127
Schonberg, William P., 274
Schreck, Stefan, 17
Schroeder, Vicki, 185
Schryer, David R., 92
Schubert, Siegfried, 115
Schuerer, Paul, 29
Schulte, P., 123
Schultz, C. A., 147
Schutzenhofer, Luke, 29
Schwartz, Stephen, 119
Schweizer, M., 272
Schweizer, Markus, 272, 273
Scott, D. Mathew, 293
Scott, D. Matthew, 310
Scott, J. N., 19
Scott, Matthew, 291
Scott, R., 167
Scott, W. G., 309
Scribner, Ken, 260
Scuka, Viktor, 172
Sedman, C. B., 128
See, A. M., 121
Seiner, John M., 246
Seiner, J. M., 18
Seiner, John M., 18
Seki, T., 265
Self, Kennt, 40
Selkirk, Rennie B., 115

Sellers, P. J., 122
Senocak, Inanc, 100
Serlemitsos, Aristides, 92
Settle, Gray, 29
Severa, P., 228
Shackford, R. W., 72
Shaffer, R. E., 240
Shams, Qamar A., 91
Shanholtz, C. E., 63
Shao, X., 151
Shao, X. M., 154
Shao, Xuan–Min, 199
Shaoyong, Chang, 220, 222
Sharangpani, R., 56
Sharp, A. J., 178
Sharp, D., 214
Sharp, David, 188
Shauck, M. E., 67
Shchukin, G. G., 192
Shell, Elaine M., 231
Shepherd, Robert L., 261
Shepherd, T. R., 186
Shibata, Carlos, 265
Shields, Angela D., 274
Shiliang, Dai, 220
Shimabukuro, Yosio Edemir, 107
Shimazue, Mari, 256
Shimizu, K., 154
Shimpo, F., 265
Shimura, T., 157, 179
Shimura, Takatsuga, 178
Shin, H–W., 15
Shindo, Takatoshi, 157, 161
Shinjo, K., 154
Shinjo, Kazuo, 177
Shio, Hisashi, 192
Shiota, Toshio, 55
Shirakawa, Yoshishige, 111
Shivakumar, Kuwigai, 45
Shoikhet, B., 227
Shonkwiler, Brian, 45
Shostak, V., 169
Showalter, R. C., 181
Shutthanandan, V., 42
Shvarts, Ya. M., 192
Shyy, Wei, 85, 100
Siconolfi, Steven F., 93
Siddiqui, A. A., 70
Siemiginowska, Aneta, 287
Siemiginowski, Aneta, 294
Siewert, T. A., 100
Silvani, X., 192
Simms, B., 50
Simond, N., 157
Simpson, J., 207
Simpson, James, 8, 30
Sims, B. L., 121
Singer, C., 128
Singer, C. F., 128
Singh, A. K., 138
Singh, H. B., 125
Singh, Mrityunjay, 44
Singh, N., 183
Singh, P., 255
Sinkevich, A. A., 184
Sirron, Peter, 92
Sitindjak, Alfred, 283
Siu, K. Y., 238
Sizhahev, S. M., 165
Sjamsuar, Suharnis, 152
Skorobogatov, A. N., 227
Slavin, J. A., 300
Sledd, Annette M., 34
Smialek, James A., 44
Smith, D., 199
Smith, D. A., 154
Smith, David A., 199
Smith, David D., 60
Smith, G. A., 38
Smith, H. J. P., 131
Smith, J. A., 109
Smith, Jerome P., 248
Smith, P. M., 56
Smith, Richard K., 7
Smith, W., 234, 254
Smith, William Hayden, 213
Soh, W. Y., 244
Solakiewicz, R. J., 175
Solecki, William, 118
Solina, Franc, 70
Solomon, P. A., 213
Solomon, Robert, 193
Sonoi, Y., 183
Sood, R., 310
Soreq, Hermona, 223
Sorokin, Andrew E., 194
Souders, C. G., 181
Soula, S., 157
Soula, Serge, 191
Soulage, A., 174
Soule, C., 227
Spalding, R., 198
Spann, J. F., 243, 262
Spann, J. F., Jr., 149, 150
Spann, James F., Jr., 132, 144, 149
Sparling, Lynn C., 118
Spaulding, Glenn F., 216
Speers, T. M., 232
Spencer, Roy W., 143
Spencer, William J., 285
Sperber, K. R., 123
Spivey, Reggie, 69
Springintveld, J., 236
Spyak, Paul R., 109
Sree, Dave, 45, 89
Srivastava, R. K., 128
St. John, Clinton, 37
St.Cyr, O. C., 306
Stahle, C. K., 35, 287
Stajner, I., 124
Stanley, M., 164
Stanojevic, Mladen, 240
Stapleton, M. V., 172
Starobinets, B., 200
Stassinopoulos, E. G., 251
Stauffer, C. A., 251
Stavrakakis, G. N., 147
Stebel, K., 133
Steeneken, H. J. M., 226
Steenken, William G., 13
Steffen, Konrad, 112
Stein, D. J., 70
Stempel, Robert C., 83
Stepananeko, V. D., 184
Stepanenko, V. D., 199
Stephany, Stephan, 258
Stephens, J. J., 53
Stephens, Mark, 233
Stevenson, D., 204
Stewart, Christopher, 70
Stewart, Eric C., 2
Stewart, M. F., 190
Stewart, Michael F., 202, 204
Stewart, Roy, 182
Stich, R., 11
Still, K. R., 38
Stocker, E., 207
Stocker, Erich Franz, 212
Stoeckenius, T. E., 116
Stokes, Donald E., 283
Stolarski, Richard S., 126, 145
Stolzenburg, M., 137, 157, 186
Storey, M. C., 288
Stout, R. P., 210
Stozhkov, Y. I., 180
Strabley, R., 163, 164
Strack, W. C., 247
Straka, J. M., 195
Strangeway, R. J., 198
Strohmayer, Tod, 299
Strohmayer, Tod E., 308
Struminsky, V. I., 136
Strumminsky, V. I., 92
Stuever, Robert A., 2
Stump, A., 270

Su, C.–H., 57
Su, Ching–Hua, 271
Suarez, Max, 115, 215
Subasilar, B., 213
Sud, Yogesh C., 130
Sugama, H., 263
Sugita, A., 176
Sugita, T., 125
Sugiyama, Yoshiki, 218
Sui, C.–H., 206
Suito, T., 33
Sulerzhitsky, Leopold D., 117
Sumi, S., 156, 171
Sumi, Takahiro, 24
Sun, J. S., 232
Sundquist, Eric, 119
Susskind, Joel, 211
Suszcynsky, D., 198
Suszcynsky, D. M., 163, 164
Suszynsky, D., 199, 207
Suzuki, Katsuhiro, 242
Suzuki, Kazufumi, 210
Suzuki, N., 163
Suzuki, T., 179
Suzuki, Tomoyuki, 178
Swaim, K. W., 104
Swanson, Gregory R., 274
Swift, W. R., 149
Swinson, W. F., 102
Syarifudin, M., 153
Symbalisty, E. M. D., 162
Syssoev, V. S., 171
Szczur, Martha R., 280
Szofran, F., 272
Szofran, F. R., 35
Szofran, Frank, 86
Szymkowiak, A. E., 35, 287

T

Takagi, N., 155, 156, 165, 166, 167
Takahashi, S., 176
Takahashi, T., 183
Takahashi, Toshihi, 266
Takahashi, Tsutomu, 189
Takeuchi, N., 163
Takeuchi, T., 248
Talbot, Robert W., 225
Tam, Christopher K. W., 246
Tamaki, Takahiko, 96
Tammet, H., 140
Tanaka, Akinori, 48
Tanaka, Isao, 96
Tang, L., 257
Tao, Wang, 217
Tao, Wei–Kuo, 130, 205
Tao, Yong, X., 70, 88
Taouil, I., 253
Tarasov, Pavel E., 117
Tay, S. P., 56
Taylor, A., 116
Taylor, M., 163
Teal, Marion, 29
Temnikov, A. G., 171
Thery, C., 155, 174, 205
Thery, Claire, 193
Thiele, O., 207
Thomas, R., 164, 169
Thomas, R. J., 167, 196
Thomas, Roger J., 305
Thomas, Ronald J., 173, 182
Thompson, A. M., 123
Thompson, Anne M., 115
Thompson, B. J., 305, 306
Thompson, Richard C., 8
Thompson, William T., 305
Thomsen, Michelle F., 144
Thomson, Clint, 268
Thomson, Ewen M., 159
Thomson, James A., 283
Thunberg, H., 228
Thysell, D. R., 105
Tian, L., 74, 208, 209
Tiancheng, Sun, 221
Tiancheng, Zhang, 223
Ticknor, L. O., 249
Tie, X., 197
Tien, C. L., 87
Tinmaker, M. I. R., 170, 205
Tinsley, Brian A., 138
Tipping, R. H., 256
Titova, E. I., 193
Tolocka, M. P., 213
Tomov, B. T., 251
Toracinta, E. Richard, 168
Toshimitsu, Kazu, 85
Treise, Deborah, 78
Tripathi, R. K., 256
Trost, Andrej, 232
Tsevetanov, Zlatan, 259
Tsirigotis, P. E., 128
Tsuruta, Mitsutoshi, 230
Tucker, C. J., 122
Tucker, P. Kevin, 85
Tuomi, T. J., 139
Tuomi, Tapio J., 175
Turcan, D., 290
Turkel, E., 245
Turner, Matt, 39
Turner, T. J., 290
Tuttle, J. G., 35
Tuttle, James, 92
Tutty, O. R., 90
Tzioumis, A., 310

U

Udaykumar, H. S., 100
Ueda, T., 21
Uman, M. A., 165, 172
Upchurch, Billy T., 92
Urbanski, M., 228
Uribe, R. M., 114
Urpo, S., 287
Ushio, T., 166
Ushio, Tomo, 155
Ushio, Tomoo, 203
Utkin, A. B., 134
Uyeda, H., 183

V

Vaandrager, F., 236
Vaidyanathan, Rajkumar, 85
Vaisberg, Oleg L., 131
Valentino, Daniel J., 232
Van Heyst, B. J., 127
van Rooij, J. C. G. M., 22
vanAltena, William F., 288, 296
VanBuuren, T., 54
VandeGriend, A. A., 108
vander Kleij, R., 74
vanderHage, J. C. H., 197
Vanheusden, K., 48
VanOsdell, D. W., 129
vanRooij, J. C. G. M., 23
vanVelthoven, P. F. J., 123
Vardakas, M. A., 13
Vardi, I., 227
Varela, G. G. Aguirre, 184
Varela, Guillermo G. Aguirre, 185, 188
Vargas–Aburto, C., 114
Vas, Irwin, 31
Vaughan, Brian A., 293
Vayner, Boris, 268
Vekilov, Peter G., 274
Veldhuis, J., 25
Ventre, G., 76, 77
Venturini, C. C., 243
Verstegen, D. M. L., 22
Verstegen, D. M. L., 23
Vesely, E., 43
Vestrand, W. Thomas, 309

Vicroy, Dan D., 2
Viltard, Nicolas, 153
Vitt, Francis M., 304
Vogel, Daniel, 117
Vogtlin, G. E., 124
Volgers, P. T. G., 237
Vos, Maarten, 49

W

Wada, A., 157
Wada, Atsushi, 161
Wakai, Takeo, 177
Wales, Jane, 278
Walker, Robert S., 286
Wallace, Shawn, 29
Waller, J. M., 64
Walsh, Kevin R., 13
Walter, Bernadette P., 127
Walter, R. J., 53
Walyus, Keith, 27
Walzer, Egon, 66
Wang, C., 156
Wang, D., 155, 156, 165, 166, 167
Wang, F., 55
Wang, J. J., 231, 232
Wang, L., 260
Wang, W., 249
Wang, W. S., 274
Wang, Y., 130
Wang, Zhehui, 263
Ward, Jerry M., 63
Warren, W. L., 48
Warzywoda, Juliusz, 271
Watanabe, T., 155, 156, 165, 166, 167
Watari, T., 265
Weaver, Kim A., 182
Webb, Jay C., 246
Weber, M., 214
Weber, Mark, 188
Webster, C. R., 93
Weigold, Erich, 50
Weinman, J. A., 196
Weir, Sue B., 306
Weisskopf, Martin C., 290
Wells, D., 43
Wentz, F., 207
Wereczak, A., 54
Wernli, Heini, 115
Wessman, Carol, 112
Westbrook, C. K., 98
Westra, Douglas G., 68
Wetzel, Melanie, 208
Whalen, Leah M., 271
Whidborne, Richard StJ, 5
White, J. J., 99
White, Warren B., 215
Whitehouse, Paul, 92
Whiteman, J. M., 63
Whitfield, C., 15
Whitfield, C. E., 15
Whitlock, C. H., 213
Whitmore, Stephen A., 12
Wiederhold, Michael L., 218
Wieland, Chris, 182
Wiens, K. C., 154
Wiens, Kyle C., 199
Wilbur, Matthew L., 11
Willett, J. C., 156, 160
Williams, E., 134, 200, 204, 214
Williams, E. R., 141, 142, 143, 163, 197
Williams, Earle, 188
Williams, J. F., 252
Williams, J. H., 64
Williams, James H., 63
Williams, John G., 13
Willott, Chris J., 292, 297
Willshire, W. L., 247
Wilson, C. A., 288
Wilson, Colleen A., 299, 310
Wilson, J. W., 256
Wilson, Robert B., 293, 310
Wilson, W., 76, 77
Wilson, W. D., 273
Winans, Dick, 40
Winkert, G. E., 287
Winkler, D. A., 254
Winn, W. P., 182
Wirasasmita, Mulyana, 152
Wiringa, R. B., 255
Wisler, S., 15
Wolff, David B., 161
Wolter, John D., 16
Wong, Sun, 123
Wong, Wayne A., 114
Wood, C. C., 218
Wood, George M., 92
Wood, Richard M., 21
Woodruff, Bob, 259
Wooldridge, Eve M., 290
Wouk, Victor, 83
Wright, A. L., 102
Wright, G., 71
Wu, F. T., 147
Wu, Liu, 222
Wu, Y., 238
Wucherer, E. J., 50

X

Xianmin, Wang, 221
Xianyun, Shen, 221
Xiao, Q., 156
Xiao, Rongfu, 60
Xingye, Fang, 223
Xinjun, Liu, 101
Xinying, Zhang, 220
Xiufeng, Shi, 222
Xiulan, Wen, 217
Xiushu, Q., 155
Xu, Hongqing, 256
Xuejun, Yu, 220

Y

Yafu, Xu, 221
Yahr, G. T., 102
Yair, Yoav, 179
Yamagiwa, Ryutaro, 210
Yamamoto, K. J., 246
Yamamoto, Missae, 110
Yamanaka, T., 87
Yamasaki, Akira, 230
Yamasaki, Nobuhiko, 24, 85
Yamauchi, M., 36
Yamazaki, Shin–Ichi, 210
Yan, Muhong, 193
Yanagisawa, Hitoshi, 96
Yang, J. M., 11
Yang, Jinglong, 256
Yaorong, Yu, 221
Yasuda, Hiroaki, 111
Yetter, J., 14
Yi, Jose Luis Rodriques, 107
Yong, Huang, 221
Yongjun, Zhao, 221
Yoon, Howard W., 109
Yoshida, Suguru, 85
Yoshihashi, Sachi, 157, 160, 173
Young, Archie, 26
Young, D. F., 213
Yu, Kyung O., 64
Yu, Y., 166
Yuanhuai, Zhao, 221
Yukhimuk, V., 162
Yun, Yang, 223
Yuqing, Gai, 221

Z

Zadorozhny, A. M., 134
Zajac, Bard A., 168

Zajc, Baldomir, 70, 232
Zalewski, Edward F., 109
Zaman, K. B. M. Q., 17
Zaniewski, J., 71
Zanin, M. G., 67
Zawodny, Joseph M., 126
Zemva, Andrej, 232
Zeng, Ning, 115
Zhang, D., 255
Zhang, G., 156, 166
Zhang, M. H., 212
Zhang, R., 197
Zhang, S. N., 289
Zhang, S. Nan, 310
Zhang, X., 202
Zhang, Y., 156, 167
Zhang, Yijun, 193
Zhao, Y., 125
Zhenfu, Liang, 222
Zhengyuan, Hu, 222
Zhibin, Yu, 222
Zhiwen, Tang, 222
Zhong, D., 167
Zhou, L., 167
Zhou, Ruhai, 240
Zhou, Y., 213
Zhu, Jizhong, 41
Zhu, Shen, 57
Zieger, B., 142, 200
Ziegler, C. L., 195
Zipser, E. J., 168
Zipser, Edward L., 161
Zirin, Harold, 307
Zografou, Panagoula, 281
Zuelsdorf, R. S., 198